



# SFμ 2023

Du 3 au 7  
juillet 2023  
•  
**ROUEN**



## 18<sup>e</sup> colloque de la Société Française des Microscopies



L'Université de Rouen Normandie est ravie d'accueillir en 2023 le 18<sup>ème</sup> colloque de la SFμ. Les objectifs fixés par l'équipe organisatrice à l'origine de ce projet étaient nombreux : i) renouer avec un colloque 100% en présentiel après le distanciel imposé par la crise sanitaire lors du précédent colloque de Reims ; ii) limiter l'impact environnemental du colloque autant que possible ; iii) attirer à Rouen de nombreux participants enthousiastes de la microscopie mais peut-être moins de la réputation pluvieuse du climat normand.

À l'heure où ces mots sont couchés sur ce papier numérique, le pari du 100% présentiel est encore tenu et des hordes de microscopistes s'apprêtent à déferler sur la métropole rouennaise. Parmi celles-ci, on distingue 220 participants, 65 exposants et 45 membres du GN MEBA. Le groupe des utilisateurs de microscopes électroniques en balayage tiendra en effet sa réunion de printemps les mercredi 5 et jeudi 6 juillet sur le site du colloque, partageant au passage avec la communauté SFμ un symposium de sciences de la matière le mercredi. Ce seront donc plus de 330 personnes qui auront l'occasion de se retrouver et d'échanger autour de la microscopie pendant cette semaine de juillet, soleil normand ou pas.

Quid de l'impact environnemental du colloque ? Celui-ci n'est pas simple à calculer mais il demeure évident que les émissions de gaz à effet de serre (GES) liées à sa tenue, qui nous préoccupent à juste titre, seront principalement le fruit de nos déplacements. Pour évaluer ces émissions et inciter de manière ludique le choix de mobilités les moins impactantes, le challenge SFMeuh a vu le jour. Celui-ci récompensera l'équipe (plus de trois participants) ayant eu le plus faible impact en termes d'émission de GES par participant et par kilomètre parcouru. Une équipe venant en tandem 3 places depuis Toulouse a ainsi toutes ses chances. Mais si les vélos ne sont pas de mise, tous les labos pourront se disputer ce challenge. Les rouennais sont bien entendu hors concours.

Outre les objectifs précédemment listés, le principal, inhérent à tout colloque peut se résumer ainsi : échanger, faire des rencontres, proposer, faire germer des idées, entrevoir de nouvelles opportunités d'expériences, de champs de recherche, de carrière. En d'autres mots, mettre pendant une semaine les relations humaines au centre de nos recherches.

Pour faciliter cela, l'Université de Rouen Normandie a ouvert grand ses portes et mis nombre de ses équipes, services et ressources à contribution. Le LABEX EMC3 a immédiatement apporté son soutien à l'évènement ainsi que la Métropole Rouennaise. Ces soutiens institutionnels extrêmement précieux témoignent de la confiance placée dans l'équipe organisatrice, qui à son tour leur témoigne sa gratitude. L'afflux inédit des exposants est également un signal fort et au moment où ce texte trop long progresse, de belles avancées méthodologiques et technologiques promettent de nous être présentées. Par ailleurs, les participants du colloque auront la primauté de l'exposition itinérante « Patrimoine &Microscopie, regarder l'invisible en Normandie », créée par l'organisme normand Resitech.

Enfin, il nous faut dire quelques mots sur l'équipe organisatrice. Celle-ci est constituée de personnels du Groupe de Physique des Matériaux et de la plateforme d'imagerie PRIMACEN. Cette brillante et enthousiaste équipe a œuvré pendant un an et demi pour que ce colloque soit un succès et j'ai eu le plus grand plaisir d'en être le modeste animateur, qui en gardera le souvenir d'une belle aventure humaine.

Il ne reste plus qu'à vous souhaiter à toutes et tous un très bon colloque SFμ 2023. Et s'il finit par pleuvoir, on n'y peut rien.

*Williams Lefebvre-Ulrikson au nom de l'équipe organisatrice*

## Composition du conseil scientifique du colloque SFu 2023



Williams  
Lefebvre  
Président  
SDM, GPM, Rouen



Marie-Laure  
Follet-Gueye  
Vice-Présidente  
SDV, Primacen-  
Glycomec, Rouen



Xavier  
Sauvage  
SDM, GPM, Rouen



Ludovic  
Galas  
SDV, Primacen, Rouen



Zineb  
Saghi  
SDM, CEA - Grenoble



Cécile  
Hébert  
SDM, EPFL -  
Lausanne



Jean  
Michel  
SDV, INSERM, UMR-  
S1250, Reims



Sandrine  
Lecart  
SDV, I2BC – Gif sur  
Yvette



Philippe  
Boullay  
SDM, CRISMAT - Caen



Damien  
Alloyeau  
SDM, MPQ - Paris



Pierre  
Bon  
SDV, LP2N - Talence



Sophie  
Le Panse  
SDV, Merimage -  
Roscoff



Bénédicte  
Warot  
SDM, CEMES - Toulouse



Laurence  
Dubreil  
SDV, INRA/ONIRIS - Nantes

## Le comité d'organisation

Magalie BENARD

Sophie BERNARD

Delphine BUREL

Celia CASTRO

Christophe CHAMOT

Laurence CHEVALIER

Auriane ETIENNE

Marie-Laure FOLLET-GUEYE

Ludovic GALAS

Alexis LEBON

Williams LEFEBVRE-ULRIKSON

Etienne TALBOT

Simona MOLDOVAN

Cristelle PAREIGE

Lorenzo RIGUTTI

Marc ROPITAUX

Solène ROULAND

François VURPILLOT

Xavier SAUVAGE

Damien SCHAPMAN

Le comité d'organisation a été appuyé dans son travail par :

Sibylle Gilbert (administratrice du site du Madrillet)

Florent Decorde (électricien du site du Madrillet)

Hugues Aroux (maquettiste de l'UFR ST)

Isabelle MengDie Hu (Chargée de mission - Graduate School Materials & Energy Sciences)

Claire Boulogne (Trésorière de la SFμ)

Ilse Hurbain (Trésorière adjointe de la SFμ)

Jean-Pierre Lechaire (Administrateur de la SFμ)

Christophe Schwob (Société MCO Congrès)

# Programme du colloque

Lundi 3/07	Mardi 4/07	Mercredi 5/07	Jeudi 6/07	Vendredi 7/07	
8:15 8:30 8:45 9:00 9:15 9:30 9:45 10:00 10:15 10:30 10:45 11:00 11:15 11:30 11:45 12:00 12:15 12:30 12:45 13:00 13:15 13:30 13:45 14:00 14:15 14:30 14:45 15:00 15:15 15:30 15:45 16:00 16:15 16:30 16:45 17:00 17:15 17:30 17:45 18:00 18:15 18:30 18:45 19:00 19:15 19:30 19:45	Ateliers SDM  Ateliers SDV  8h15 : SDM1 Conf. JEOL Conf. Cameca 10h35 : Pause (sponsorisée par CAMECA)	8h15 : SDV1 Conf. JEOL Thermofisher 10h35 : Pause (sponsorisée par CAMECA)  11h : SC2  13h20 : Introduction	8h30 : SDM3 Conf. Oxford Conf. Gatan  GNMEBA  13h : Pause déjeuner  14h : Conférence plénière  15h : SC1  Ateliers SDM  16h15 : Pause - Exposition	8h30 : SDV3 Conf. Aberrior Conf. Gatan  GNMEBA  Expo-Pause-démos  12h30 : Pause déjeuner  14h : AG SFμ  14h15 : SDM2 & GN MEBA  15h30 : Pause - Exposition  16h15 : Pause - Exposition  16h30-19h : Session poster (sponsorisée par Gatan)  17h30 : Prix Pierre Favard  Sponsor Pierre Favard  Réunion utilisateurs Gatan & EDAX dès 18h30  18h50 : Cocktail (sponsorisé par Jeol)  Fin 20h30	8h30 : SC4  GNMEBA  10h30 : Pause  10h50 : SDM4  10h50 : SDV4  13h : Fin du colloque  SC : Symposium Commun  SDM: Sciences de la Matière  SDV: Sciences du Vivant  16h : SC3 Fin 18h  19h : Gala

## Exposition – Exhibition

Liste des exposants par ordre alphabétique :

[Abberior Instruments GmbH](#)

[Cameca – Ametek](#)

[CLS Engineering – NewTec](#)

[Clinisciences](#)

[Delta Microscopies](#)

[EDEN Instruments](#)

[Eloïse](#)

[Gatan – Ametek](#)

[JEOL](#)

[LFG distribution – Diatome](#)

[Microtonano](#)

[Milexia](#)

[Oxford Instruments](#)

[Quantum Detectors](#)

[Renishaw](#)

[Synergie 4](#)

[Tescan](#)

[ThermoFisher](#)

[VIB&TEC](#)

[Zeiss](#)



**SYNERGIE<sup>4</sup>**







- A Milexia
- B Delta Microscopies
- C MicroToNano
- D Eloïse
- E Synergie4
- F CLS Engineering - Newtec
- G Clinisciences
- H EDEN Instruments
- I Abberior Instruments GmnH
- J CAMECA
- K Gatan - Ametek
- L JEOL
- M LFG distribution - Diatome
- N Tescan
- O Oxford Instruments
- P ThermoFischer
- Q VIB&TEC
- R ZEISS
- S Quantum Detectors
- T Renischaw

## Événements organisés par les sponsors



La société [JEOL](#) sponsorise le cocktail de bienvenue du mardi 4 juillet à 19h dans le hall d'exposition du colloque.



La société [Gatan](#), sponsor de la session poster, organisera sa première réunion d'utilisateurs le mercredi dès 18h30 dans la salle de conférences du Groupe de Physique des Matériaux. Les personnes intéressées pourront se rendre au stand Gatan pour s'inscrire dès le mardi.



Pendant la session Exposition-Démonstrations du jeudi 6 juillet matin, la société [CAMECA](#) proposera une introduction ainsi qu'une démonstration sur la Sonde Atomique Tomographique LEAP 5000 XS. Les personnes intéressées sont invitées à s'inscrire sur le stand CAMECA dès le mardi 4 juillet (détails ci-dessous).

The invitation card is a white rectangular card with a red header and footer. The top section features the CAMECA and AMETEK logos. The middle section has a red banner with a white envelope icon and the word "INVITATION". Below this, the text "Jeudi 06 Juillet 11h15 - 12h45" and "Visit GPM's state-of-the-art Atom Probe Tomography lab" are displayed. The bottom section contains a portrait of Robert Ulfig, a text about the presentation by Anna Bui, and an image of the LEAP 5000 XS instrument. The footer text reads "Registration is free but limited seat. Book your seat on CAMECA booth J".

COMECA® / AMETEK®  
SCIENCE & METROLOGY SOLUTIONS

INVITATION

Jeudi 06 Juillet  
11h15 - 12h45

Visit GPM's state-of-the-art Atom Probe Tomography lab

Live demo on LEAP 5000 XS platform conducted by Robert Ulfig

La Génération 6000 : présentation des nouvelles Sondes Atomiques Tomographiques CAMECA, by Anna Bui

Registration is free but limited seat.  
Book your seat on CAMECA booth J

## Communications des exposants sur les démonstrations pendant la semaine du colloque



Tout au long du colloque et particulièrement pendant la session expo-démonstration du jeudi matin, la société MILEXIA présentera le MEB Compact analytique Hitachi FlexSEM II en fonctionnement sur son stand ainsi que des équipements de préparation d'échantillons. Si vous souhaitez une démonstration personnalisée, n'hésitez pas à vous inscrire dès votre arrivée au colloque, sur le stand de MILEXIA.



Fondée en 2012 par Stefan Hell (prix Nobel de chimie 2014) et ses collègues, Abberior Instruments se spécialise dans les microscopies confocales et de super-résolution STED, RESOLFT et MINFLUX. À l'occasion du colloque SF $\mu$ 2023, nous ferons la démonstration du STEDYCON, module confocal et STED multi-couleur, permettant la mise à jour de nombreuses bases droites ou inversées de microscopie optique. Le STEDYCON sera sur une base droite d'épiéfluorescence motorisée. Des images de cultures cellulaires fixées seront acquises en direct, en modes confocal et STED 2D.

### Cliniscience

CliniSciences is a distributor specializing in providing a comprehensive range of scientific products and laboratory solutions to researchers, healthcare professionals, and life science organizations. With a strong focus on biotechnology, molecular biology, and diagnostics, Clinisciences offers a diverse portfolio of high-quality products sourced from leading manufacturers worldwide. Clinisciences places great emphasis on quality control and ensures that all products undergo rigorous testing to maintain the highest standards. With dedicated attention to quality, innovation, and customer service, they play a vital role in supporting scientific progress and improving patient care.



Vous adaptez vos préparations et vos essais à votre équipement, CLS Engineering vous propose d'adapter votre équipement à votre besoin. Depuis 2016, notre TPE intervient sur des équipements de préparation, d'analyse ou d'essai de laboratoire. CLS Engineering apporte évolutions, améliorations ou aménagements sur votre équipement de laboratoire ou sur vos manipulations, au regard d'un besoin ou d'une mise en œuvre non conventionnelle. N'hésitez pas à venir nous rendre visite sur notre stand.



Venez visitez le stand Diatome par votre distributeur officiel en France : LFG Distribution. Vous faites de la microscopie électronique ou optique ? Tentez de gagner un véritable diamant de Joaillerie, en participant au tirage au sort sur notre stand (M).

LFG Distribution est également distributeur en France du catalogue Electron Microscopy Sciences.

# inLux™ SEM Raman interface

A universal solution for *in situ* SEM Raman analysis



**Information-rich.** Raman, photoluminescence (PL) and spectral cathodoluminescence (CL) analysis is performed simultaneously and co-located with SEM imaging.

**Universal.** The InLux Interface can be mounted on a wide range of SEMs from different manufacturers, with different chamber sizes, and without any SEM modification.

**Non-Invasive.** The InLux probe can be fully retracted with a single click. This ensures that the probe does not interfere with other SEM functions or workflows when not in use.

**Determine distribution.** Confocal Raman Images can be produced as standard thereby enabling easy measurement of sample heterogeneity.

**Sample viewing.** Large area optical imaging and montaging for visualising your sample and targeting areas of interest.

**Configurable.** Up to two different excitation laser wavelengths, plus an optional CL module.

**Automated.** One-click switching of laser wavelengths for Raman analysis of challenging samples.



[www.renishaw.com/inlux](http://www.renishaw.com/inlux)



VOTRE PARTENAIRE AU SERVICE DE LA QUALITÉ &  
LA FIABILITÉ EN IMAGERIE ET MICROSCOPIE



**TECHNOLOGIES ANTIVIBRATOIRES  
COMPENSATION & TRAITEMENTS  
ÉLECTROMAGNÉTIQUES**



Compensation  
électromagnétique  
active AC/DC



Blindage  
électromagnétique  
passif, AC/DC  
(SiFe, Mumetal...)



Systèmes  
antivibratoires  
pneumatiques et  
piézoélectriques  
pour MEB, MET,  
FIB, AFM...



Analyse  
environnementale,  
vibration,  
électromagnétique,  
acoustique



Tables  
antivibratoires et  
tables optiques  
pneumatiques



Plateaux  
antivibratoire  
pneumatiques et  
piézoélectrique  
pour microscopes,  
AFM, balances de  
précision...



Conduite complète  
des projets  
d'implantation  
des microscopes  
électroniques



Caissons  
acoustiques  
standard et sur-  
mesure pour  
applications  
scientifiques et  
industrielles

## Prix et challenge



Modalité sur :  
<http://www.sfmu.fr>  
email : [sfmu@sfmu.fr](mailto:sfmu@sfmu.fr)

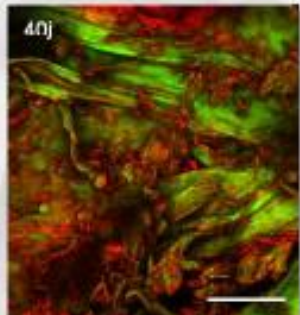
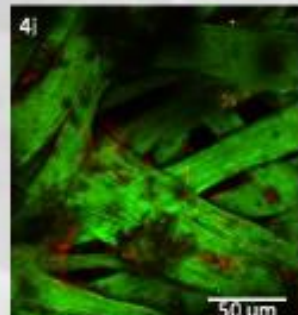
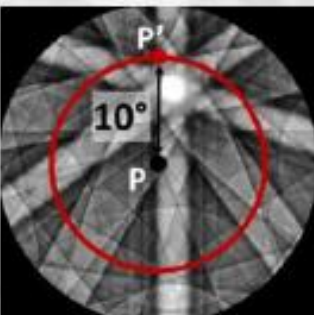
Les **prix Pierre Favard** récompensent des travaux de **recherche de grande qualité** menés à l'occasion d'une **thèse soutenue dans une université française** dans le **domaine de la microscopie** (électronique, optique, champ proche, sonde atomique tomographique, traitements des images, intelligence artificielle...).

**Remise des prix :** lors du colloque de la SFM à Rouen du 3 au 7 juillet.

Deux prix de 1000 € en Sciences du Vivant et Sciences de la Matière

**Thèses soutenues entre le 1er mars 2021 et le 28 février 2023**

Date limite de dépôt des candidatures : 15 mars 2023



Prix Favard 2021: Clément Lafond et Margaux Schmeltz

**Présidents de jurys :**

Pierre Mahou ([pierre.mahou@polytechnique.edu](mailto:pierre.mahou@polytechnique.edu)) en Sciences du Vivant  
Martien Den Hertog ([martien.den-hertog@neel.cnrs.fr](mailto:martien.den-hertog@neel.cnrs.fr)) en Sciences de la Matière

En partenariat avec :

 **Abbelight**  
NOW, WE SEE

 **TESCAN**  
PERFORMANCE IN NANOSPACE

## Prix Raymond Castaing

Ce grand prix rend hommage à Raimond Castaing (1921-1998), père de nombreuses techniques d'analyse locale, par émission de rayons X (la "microsonde de Castaing"), par émission ionique secondaire (le SIMS) avec Georges Slodzian et par filtrage des énergies en microscopie électronique avec Lucien Henry. Il fut aussi le premier président de la Société Française de Microscopie Electronique (1959-1961)".

Le Grand prix « Raimond Castaing » sera remis au cours du diner de Gala du colloque Il est décerné tous les deux ans **à deux chercheurs**, selon leur spécialité, sciences du vivant (SDV) ou sciences de la matière (SDM). Le montant du prix est de 2500 € par lauréat.

Ce prix récompense des **chercheurs(euses) confirmé(e)s sans limite d'âge, menant leurs recherches en France et ayant contribué de manière remarquable à la microscopie au sens large**, soit en instrumentation (innovation, développement remarquable...) soit dans l'utilisation innovante d'un instrument en SDV ou SDM (résultat marquant, mise en évidence d'un effet non vu auparavant). Toutes les microscopies, analytiques ou non, sont concernées (TEM, SEM, OM, STM, AFM, APT...).

### Lauréats du prix Castaing

2021

- **Pr François Vurpillot**, Groupe de Physique des Matériaux, Université de Rouen  
Prix Raimond Castaing - Sciences de la matière, 2021
- **Dr Graça Raposo**, UMR 144 Institut Curie / CNRS, Paris  
Prix Raimond Castaing - Sciences de la vie, 2021

2019

- **Pr Ovidiu Ersen**, Institut de Physique et Chimie des Matériaux de Strasbourg  
Prix Raimond Castaing - Sciences de la matière, 2019
- **Dr Emmanuel Beaurepaire**, Laboratoire d'optique et biosciences, Ecole Polytechnique Palaiseau  
Prix Raimond Castaing - Sciences de la vie, 2019

2017

- **Marcel Tencé**, LPS, Orsay  
Prix Raimond Castaing - Sciences de la matière, 2017
- **Bruno Klaholz**, IGBMC, Strasbourg  
Prix Raimond Castaing - Sciences de la vie, 2017

## Prix du meilleur poster



Les posters seront affichés durant toute la semaine du congrès (Installation possible dès le 03 juillet 2023). Le format autorisé est le A0 (largeur 80-90 cm hauteur 100-120 cm). Des pinces seront à votre disposition pour l'accrochage. La session poster avec discussions autour de vos affiches aura lieu le mercredi 5 juillet après-midi dans une ambiance conviviale.

## Concours photo

La Sfμ est là pour promouvoir vos talents artistiques avec le prix photo.

Pour participer au prix Photo du colloque Sfμ, merci de vous inscrire en envoyant un mail (**Objet** : Contribution pour le Prix Photo de la SFμ 2023) à

[lorenzo.rigutti @ univ-rouen.fr](mailto:lorenzo.rigutti@univ-rouen.fr)

en spécifiant auteur, titre, et si l'image concourt pour la catégorie Sciences de la Matière ou Sciences de la Vie.

La photo à exposer **devra être imprimée par vos soins** en format de taille inférieure ou égale à A3 (portrait ou paysage) et sera affichée dans l'espace dédié durant la durée du colloque. Le prix de 100€ sera remis le 6 juillet au début du Symposium Commun SC3.

## Challenge SFmeuh

Pourquoi Meuh ?

1. Parce que meuh ~ meut, vient du verbe mouvoir
2. Parce que Sfmeuh ~ Sfμ
3. Parce qu'en Normandie on a quand même beaucoup de vaches

*Meuh, comment on gagne ?*

Ce challenge récompensera l'équipe (laboratoire, sponsor, exposant) ayant collectivement fait le plus d'efforts côté transport pour se rendre à la



conférence. Le nombre de keCO2 par km sera calculé\* par personne et moyenné à l'échelle des participants d'une même équipe (minimum 3 personnes). Pour cela, un questionnaire sera à remplir à votre arrivée à la conférence.

*Meuh, qu'est-ce qu'on gagne ?*

Un panier (très bien) garni avec des produits du coin.

*La remise du prix du Challenge Sfmeuh est prévue pendant le diner de Gala.*

\*grâce au simulateur de la plateforme Labos 1point5  
(<https://apps.labos1point5.org/travels-simulator>)

## Soirée de Gala

### Adresse

HANGAR 10 Quai Ferdinand de Lesseps 76000 ROUEN

Début des festivités : 19h

Fin des festivités : 1h

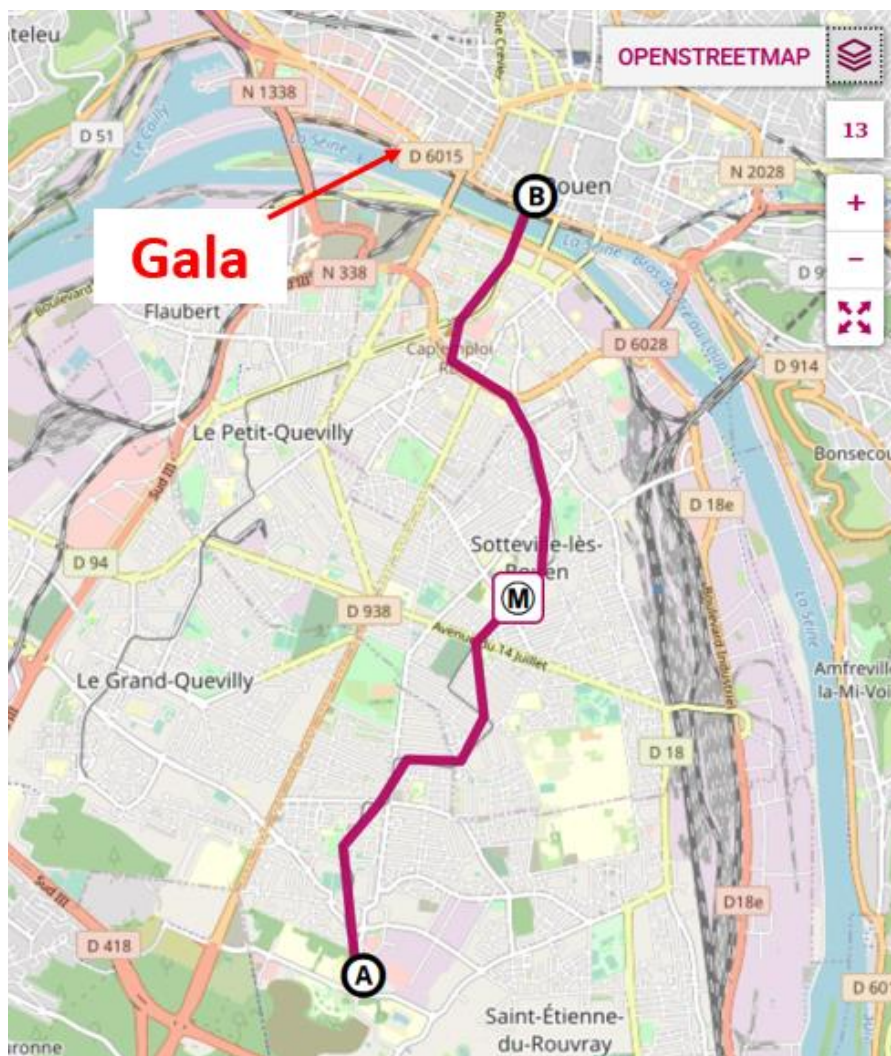
### Parking sur place



Trajet en transports en commun : Plusieurs alternatives (prévoir 45 mn)

Alternative 1 :

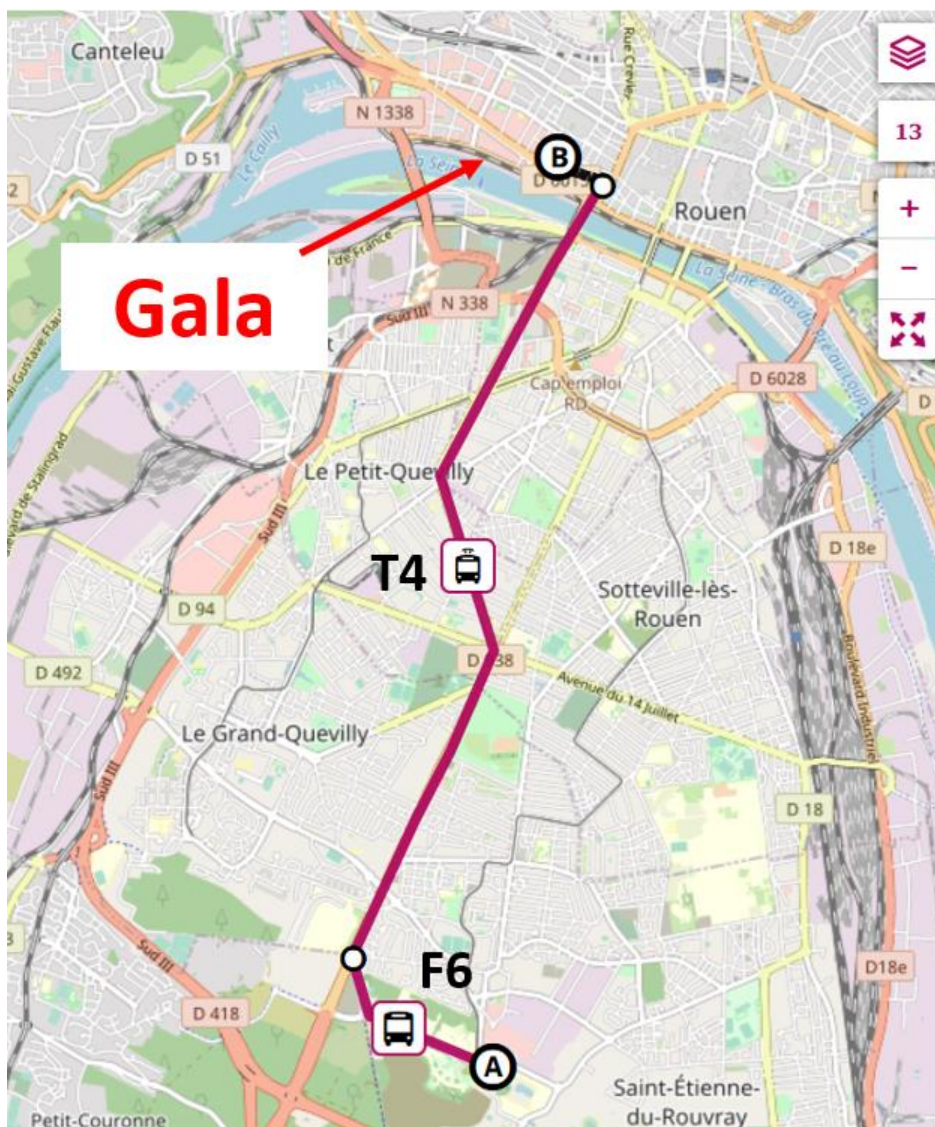
- Métro jusqu'à l'arrêt « théâtre des arts »
- Prendre TEOR (T1 ou T2 ou T3) jusqu'à l'arrêt « Pasteur » et marches sur les quais jusqu'au lieu du gala.



Alternative 2 :

- Prendre le F6 vers Les Boutières – Grand Couronne. Descendre à Zenith parc Expo.  
Ou marcher depuis la conférence jusqu'à Zenith- Parx Expo
- Prendre le T4 vers CHU Charles Nicolle et descendre à Boulevard des Belges
- Prendre T1, T2 ou T3 et descendre à Pasteur. Rejoindre les quais jusqu'au Hangar

10



## **Structure du programme scientifique**

## Symposia communs (SC)

### **SC 1 : Méthodes émergentes pour le traitement de données et l'acquisition**

*Maxime Moreaud (IFPEN, Solaize et MINES ParisTech, Fontainebleau)*

*Christophe Zimmer (Unité Imagerie et Modélisation, Institut Pasteur et UMR 3691, Paris)*

### **SC2 : Microscopie à l'interface physique et biologie**

*Guillaume Mabilleau (GEROM, Université d'Angers et Département de Pathologie Cellulaire et Tissulaire, CHU d'Angers)*

*Thierry Douillard (Matériaux ingénierie et science – MATEIS, Lyon)*

### **SC3 : Diffraction et résolution structurale**

*Wai-Li Ling (Institut de Biologie Structurale - IBS, Grenoble)*

*Stéphanie Kodjikian (Institut Néel, Grenoble)*

### **SC4 : Avancées instrumentales**

*Francisco de la Peña (Unité Matériaux et Transformations-UMET, Lille)*

*Patrick Bron (Centre de Biochimie Structurale - CBS, Montpellier)*

## Symposia de Sciences de la Matière (SDM)

### **SDM1 : Imagerie volumique, cartographie de propriétés et approches corrélatives**

*Isabelle Mouton (CEA, Saclay)*

*Karine Masenelli-Varlot (Matériaux ingénierie et science - MATEIS, Lyon)*

### **SDM2 : Microscopies In situ et Operando**

*Patricia Abellan (Institut des Matériaux de Nantes Jean Rouxel – IMN, Nantes)*

*Ileana Florea (CIMEX, Palaiseau)*

### **SDM 3 : Microscopie des matériaux et nano-matériaux**

*Carine Davoisne (Laboratoire de Réactivité et Chimies des Solides – LRCS, Amiens)*

*Michaël Texier (Matériaux Microélectronique et Nanosciences de Provence - IM2NP, Marseille)*

### **SDM4 : Spectroscopie à haute résolution, ultrarapide**

*Jaysen Nelayah (Laboratoire Matériaux et Phénomènes Quantiques - MPQ, Paris)*

*Matthieu Bugnet (Matériaux ingénierie et science - MATEIS, Lyon)*

## Symposia en Sciences du Vivant

**SDV1 : Techniques corrélatives, combinatoires ou multi-modales**

*Christel Genoud (UNIL, Université de Lausanne ; Friedrich Miescher Institute for Biomedical Research, Basel).*

*Angélina d'Orlando (Plateforme Imagerie, Biochimie et Structure – BIBS, Nantes)*

**SDV2 : Cryo-méthodes 1 : nano-objets**

*Yaser Hashem (ARNA, Pessac)*

*Marc Schmutz (Institut Charles Sadron, Strasbourg)*

**SDV3 : Cryo-méthodes 2 : cellulaire/tissulaire**

*Anna Sartori (Ultrastructural BiolImaging Core facility, Institut Pasteur- Paris)*

*Aurélie Bertin (Institut Curie, Paris)*

**SDV4 : Stratégies pour tendre vers la résolution nanométrique en microscopie photonique**

*Christine Terryn (PICT Platform, Reims)*

*Audrey Salles (UtechS Photonic BiolImaging (Imagopole) - Institut Pasteur, Paris*

## **Recueil des résumés**

### **Partie 1 : Conférences**

## **Symposium commun 1 (SC1) :**

### **Méthodes émergentes pour le traitement de données et l'acquisition**

***Animation :***

*Maxime Moreaud (IFPEN, Solaize et MINES ParisTech, Fontainebleau) & Christophe Zimmer (Unité Imagerie et Modélisation, Institut Pasteur et UMR 3691, Paris)*

**SC1-Inv****Une revue des méthodes de segmentation par apprentissage automatique.**

- **Hugues Talbot** \* (hugues.talbot@centralesupelec.fr) / CVN-INRIA, Centrale Supelec, Saclay France

Le problème de la segmentation d'image, c'est à dire celui de la reconnaissance et du détourage d'objets d'intérêt dans une image est un problème fondamental en vision par ordinateur.

Depuis 2015 environ, des nouvelles méthodes à base d'apprentissage ont été proposées et constituent l'état de l'art dans beaucoup de domaines.

Toutefois, ces méthodes ne sont pas exemptes de problèmes qui ont été identifiées petit à petit : existence de biais, faible résistance aux attaques adversaires, difficulté à étendre en 3D, nécessité disposer de de grandes bases de données annotées, etc. Dans cet exposé, nous montrons les méthodes principales de l'état de l'art, leurs limitations et nous exposons certains travaux en cours pour tenter de réduire la portée de ces problèmes.

**SC1-Oral1****L'intelligence artificielle pour la classification de nanoparticules d'or facettées observées en microscopie électronique en transmission****Deep Learning for the classification of faceted gold nanoparticles investigated with transmission electron microscopy**

- **Romain Moreau** \* (romain.moreau-ext@onera.fr) / Université Paris-Saclay, ONERA, CNRS, Laboratoire d'Étude des Microstructures, 92320 Châtillon, France
- **Hakim Amara** / Université Paris-Saclay, ONERA, CNRS, Laboratoire d'Étude des Microstructures, 92320 Châtillon, France
- **Maxime Moreaud** / IFP Énergies Nouvelles, 69360 Solaize, France
- **Jaysen Nelayah** / Université Paris Cité, CNRS, Laboratoire Matériaux et Phénomènes Quantiques (MPQ), 75013 Paris, France
- **Christian Ricolleau** / Université Paris Cité, CNRS, Laboratoire Matériaux et Phénomènes Quantiques (MPQ), 75013 Paris, France
- **Damien Alloyeau** / Université Paris Cité, CNRS, Laboratoire Matériaux et Phénomènes Quantiques (MPQ), 75013 Paris, France
- **Riccardo Gatti** / Université Paris-Saclay, ONERA, CNRS, Laboratoire d'Étude des Microstructures, 92320 Châtillon, France

\* Auteur correspondant

Nanoparticles (NPs) are usually investigated with Transmission Electron Microscopy (TEM). Recent improvements allowed high resolved views of nanoparticles, even reaching atomic resolution. However, the identification of both the crystallographic structure and 3D shape of nanoparticles turns out to be a tedious procedure. Manual post-processing can be even more challenging as experimental noise degrades the image. To overcome this constraint, we propose a Deep Learning (DL) model to automatize this task, making it reliable even with images exhibiting a low signal-to-noise ratio.

In particular, DL models based on Convolutional Neural Networks (CNN) were fed and trained with large datasets of simulated TEM images of nanoparticles that were labeled in terms of their shape, with size ranging from 4 to 8 nm. One crucial step is to generate a representative dataset. To achieve this goal and to mimic experimental conditions, NPs were rotated randomly to sample all the potential orientations, while a substrate has been simulated with realistic model of carbon membrane and noise. In this way, we have succeeded in developing an efficient and accurate frame for predicting the shape of nanoparticles investigated with High Resolution TEM (see figure 1). This model has been tested on both simulated and experimental images.

**Mots clefs** : artificial intelligence, deep learning, nanoparticle, transmission electron microscopy, atomic simulation

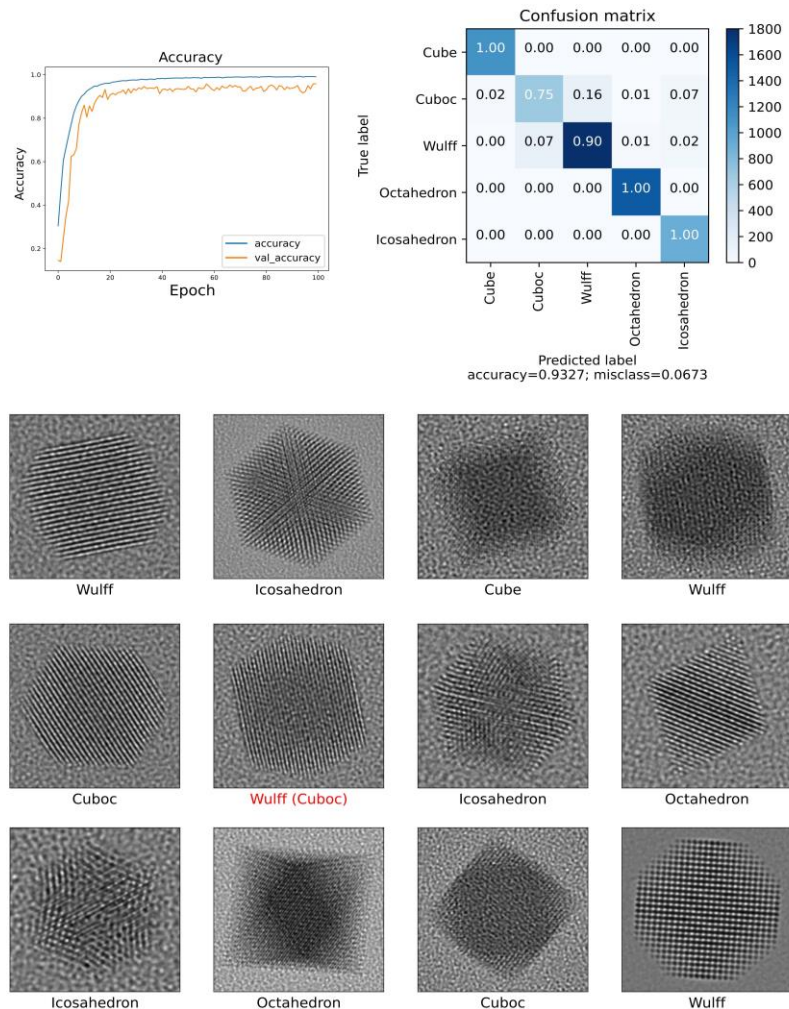


*Figure 1: Performance of the model (accuracy and confusion matrix) trained with 44,800 images for classifying 5 different shapes and some examples of 3D shape predictions on simulated TEM images.*

## SC1-Oral2

### Alignment et configuration de MET asservi par l'IA pour une meilleure acquisition de données

#### AI-driven TEM alignment and configuration for better data acquisition

- **Loïc Grossetête** \* (loic.grossetete@cemes.fr) / CEMES-CNRS
- **Cécile Marcelot** / CEMES-CNRS
- **Christophe Gatel** / CEMES-CNRS
- **Sylvain Pauchet** / ENAC
- **Martin Hytch** / CEMES-CNRS

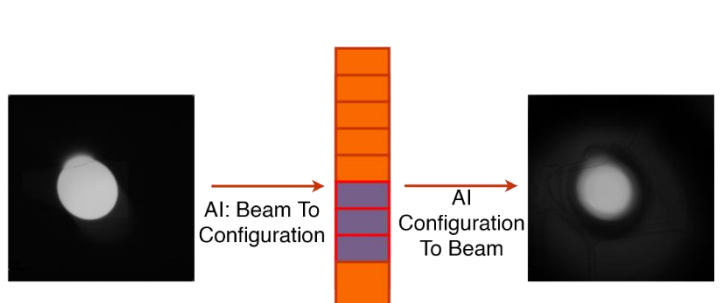
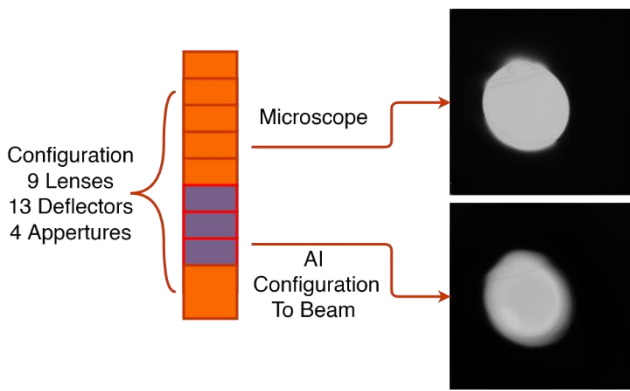
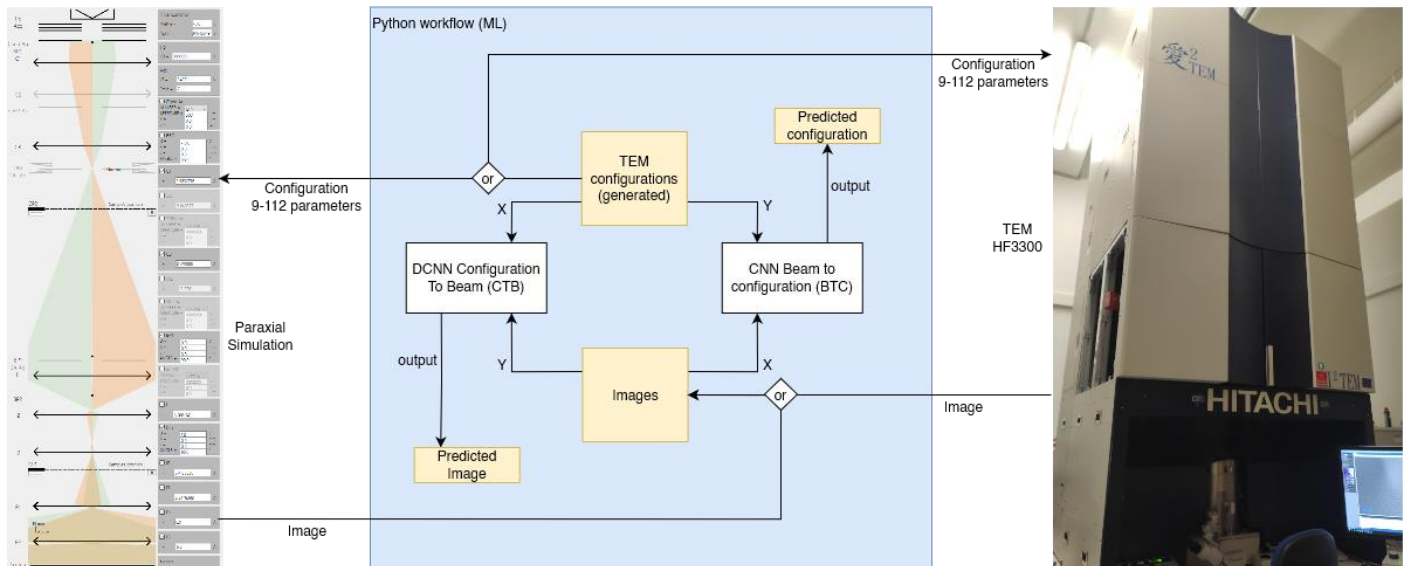
\* Auteur correspondant

Recent advances in artificial intelligence are paving the way for automating data acquisition across many scientific disciplines. In transmission electron microscopy (TEM), Deep Convolutional Neural Networks (CNN) are being used for image post-processing for feature extraction and super resolution applications. Similar methods could be used to combine real-time images and microscopist-defined goals (such as drift correction or automatic alignment) to automatically adjust the alignment and lens configurations of the TEM.

To assess the feasibility of such an endeavour, we first tested a model's ability to predict the beam shape and position based only on the information of the lenses, deflectors and apertures. For training, we used both experimental images on the I2TEM microscope and paraxial simulations developed in-house [1] (Fig. 1). Then we did the opposite experiment: we predicted a configuration from an image that would result in a microscope image similar to the given image. The ultimate goal is to be able to predict a configuration in which the resulting image meets user-defined properties such as being in-focus, centred, and properly illuminated.

As a result, a dataset containing configurations and their associated images was required. We began with a well-aligned microscope and then slightly modified all parameters while preserving a beam in the field of view. Completely randomizing those parameters would have produced too many empty images. We generated 9 datasets with 450-900 configuration/image tuples each with the TEM. The deep learning models were then trained to predict one using the other (Fig. 2). This validated the models' ability to simulate the entire microscope and reverse engineer its configuration from an image. Because direct prediction is impossible for the latter since multiple configurations produce similar images, we trained it to produce a configuration whose resulting image is similar to the given one. To address the issue of automation using user-defined goals, we are developing a workflow based on Reinforcement Learning [2] (RL) that will allow the models to train in real time by modifying the microscope configuration directly.

**Mots clefs :** TEM, AI, CNN, RL



## SC1-Oral3

### Analyse quantitative EDS assistée par l'apprentissage automatique non supervisé : Mesure des gradients chimiques dans nanoparticules d'alliage

#### Quantitative EDS Analysis supported by unsupervised machine learning: Measuring chemical gradients in alloy nanoparticles

• **Murilo Moreira** \* (murilo.moreira@univ-lyon1.fr) / Institute of Light and Matter, Université Claude Bernard Lyon

1, CNRS, UMR5306, F-69622 Villeurbanne, France / Instituto de Fisica "Gleb Wataghin", Universidade Estadual de Campinas-UNICAMP, 13083-859, Campinas - SP, Brazil

• **Matthias Hillenkamp** / Institute of Light and Matter, Université Claude Bernard Lyon 1, CNRS, UMR5306,

F-69622 Villeurbanne, France / Instituto de Fisica "Gleb Wataghin", Universidade Estadual de Campinas-UNICAMP, 13083-859, Campinas - SP, Brazil

• **Varlei Rodrigues** / Instituto de Fisica "Gleb Wataghin", Universidade Estadual de Campinas-UNICAMP, 13083-859, Campinas - SP, Brazil

• **Daniel Ugarte** / Instituto de Fisica "Gleb Wataghin", Universidade Estadual de Campinas-UNICAMP, 13083-859, Campinas - SP, Brazil

\* Auteur correspondant

The performance of Energy-dispersive X-ray Spectroscopy (EDS) combined with Scanning Transmission Electron Microscope (STEM) has been significantly enhanced, permitting the analysis of chemical composition in nanometric objects, including bimetallic nanoparticles (BNPs) with diameters less than 10 nm. This breakthrough is crucial for the extraction of quantitative information for individual particles. The properties of BNPs depend on their chemical ordering (random, gradient or core-shell, etc.), e.g. BNPs of identical size, shape and environment can display drastically different optical spectra or chemical reactivities for alloyed or segregated structures. For such very small volumes, below 10 nm, high-quality signal-to-noise ratios (SNR) are difficult to attain; besides, data acquisition and treatment methodologies, followed by rigorous error analysis, are essential. Subsequently, the results should be compared with realistic simulations [1] to generate meaningful and reproducible physical descriptors and interpretations [2]. In this context, we have measured the chemical composition variations inside AgAu BNPs using EDS-STEM in a Titan-Themis Cubed operated at 80 kV using a high solid angle X-ray detector(0.8 sr). Our results reveal size-dependent chemical compositions, with Au depletion for sizes below 4 nm[3] and likewise, chemical gradients with Ag enrichment towards the surface of the BNPs. This latter can in principle be attributed to differences in surface energy and/or the higher reactivity towards oxygen. We have used unsupervised machine learning methods (Principal Component Analysis-PCA and, Non-negative Matrix Factorization-NMF) to verify the existence of latent information on radial composition variations in our data. This analysis provides strong direct statistical verification that the estimated radial composition changes represent real information provided by the EDS spectra. Our study demonstrates the possibility of quantifying the chemical composition within bimetallic nanoparticles in the range of 3-7 nm in diameter, opening the way for further studies concerning segregation effects or chemical reactivity. These findings represent a significant improvement over the widely used qualitative chemical mapping, providing essential insights into understanding the elemental distribution inside small nanovolumes.

[1]Moreira, M. et al. Microsc. Microanal. 28 (2), 338–349 (2022)

[2]Spurgeon, S.R. et al. Nat. Mater. 20, 274–279 (2020)

[3]Moreira, M. et al. J. Phys. Chem. C, 127 (4), 1944-1954 (2023)

**Mots clefs :** EDS, Quantification, Chemical gradient, NMF, PCA, Machine Learning

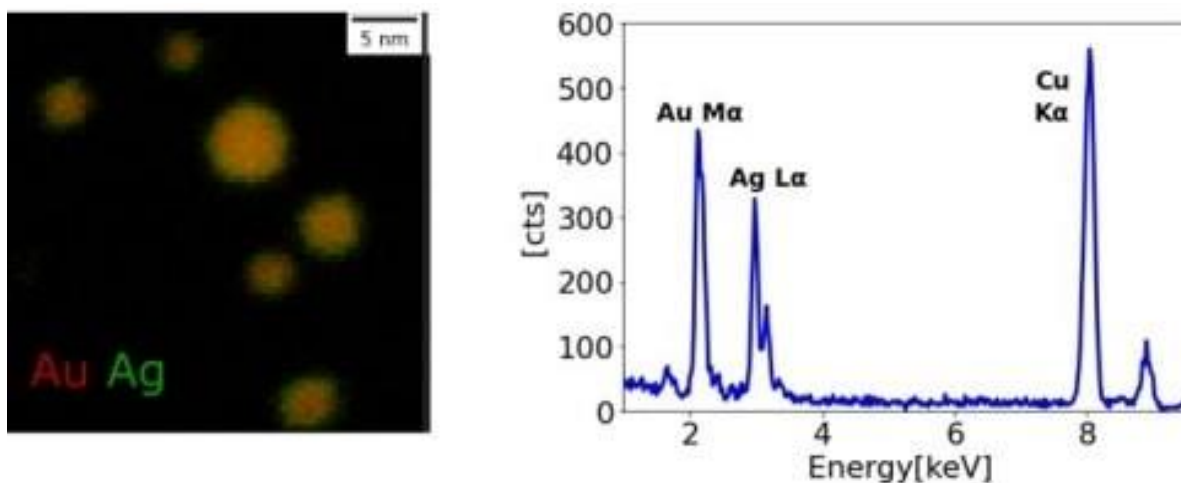


*Figure 1:* a) EDS-STEM elemental mapping of AuAg NPs. Au and Ag intensities in red and green, respectively. b) Spectrum of a single 5 nm BNP to illustrate the number of counts obtained for the measurement.

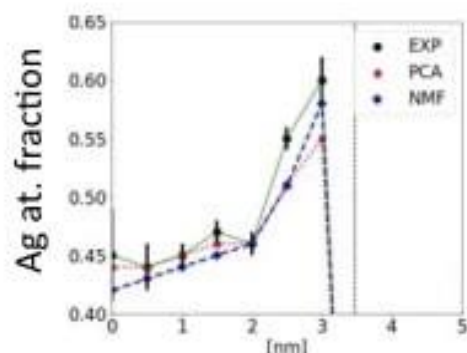


*Figure 2:* Quantitative radial chemical composition profile of a single AuAg BNP in Ag atomic fraction. In black raw experimental, in red PCA and in blue NMF reconstructed (denoised) EDS data. The center of the BNP is the zero position, and the surface is defined by the straight line derived from ADF measurements.

## SC1-Oral4

### Cartographie Élémentaire Quantitative de Nanoparticules à partir d'Images STEM-HAADF à l'Échelle Atomique

#### Quantitative Elemental Mapping Of Bimetallic Nanoparticles From Atomic Scale STEM-HAADF Images

- **Adrien MONCOMBLE** \* (adrien.moncomble@u-paris.fr) / Université Paris Cité, CNRS, Laboratoire Matériaux et Phénomènes Quantiques, 75013 Paris, France
- **Christian RICOLLEAU** / Université Paris Cité, CNRS, Laboratoire Matériaux et Phénomènes Quantiques, 75013 Paris, France
- **Damien ALLOYEAU** / Université Paris Cité, CNRS, Laboratoire Matériaux et Phénomènes Quantiques, 75013 Paris, France
- **Guillaume WANG** / Université Paris Cité, CNRS, Laboratoire Matériaux et Phénomènes Quantiques, 75013 Paris, France
- **Hakim AMARA** / Université Paris-Saclay, ONERA, CNRS, Laboratoire d'Etude des Microstructures, 92020 Chatillon, France
- **Riccardo GATTI** / Université Paris-Saclay, ONERA, CNRS, Laboratoire d'Etude des Microstructures, 92020 Chatillon, France
- **Maxime MOREAUD** / IFP Énergies Nouvelles, 69360 Solaize, France
- **Jaysen NELAYAH** / Université Paris Cité, CNRS, Laboratoire Matériaux et Phénomènes Quantiques, 75013 Paris, France

\* Auteur correspondant

The alloying of metals at the nanoscale is often used to enhance nanoparticles' physical/chemical properties and engineer new ones leading to multimetallic nanoparticles (NPs) with different chemical structures [1]. Access to composition is paramount for a fundamental understanding of nanoalloys' chemical and physical properties. Particle composition can be accessed by spectroscopic techniques such as energy-dispersive X-ray spectroscopy, but a dedicated set-up with a high-brightness electron source and wide-angle detection is required. However, when we work at atomic resolution, the signals are too weak for precise elemental quantification. Instead, a promising alternative is scanning transmission electron microscopy (STEM), high-angle annular dark field (HAADF). HAADF-STEM produces images at the atomic scale presenting a contrast depending, in particular, on the atomic number Z.

In this contribution, we propose an innovative method to quantify the composition of individual atomic columns in bimetallic NPs from their intensities in 2D HAADF-STEM images. Firstly, with multislice STEM simulations [2], the effects of the composition, the atomic configuration, and the thickness are studied to reveal their degree of intertwining on HAADF intensities in such systems. Then, from aberration-corrected STEM, we correlate HAADF intensity and composition, developing two different approaches to predict columns' composition. In the first one, we develop a straightforward procedure based on a regression-based statistical analysis of local variations of intensity to predict the columns' composition (Fig. 1). In the second approach, refined composition map is predicted by analyzing the global distribution of HAADF intensity with a convolutional neural network (CNN) trained on synthetic images, HAADF-STEM images of NPs with different sizes, shapes, and compositions (Fig. 2). The implementation of both approaches on Au-Cu random alloys will be presented and compared.

#### References:

- [1] Ferrando, Riccardo et al; Chemical Reviews, 108 (2008), p.845-910
- [2] Barthel, Juri; Ultramicroscopy, 193 (2018), p.1-11

**Mots clefs :** Bimetallic Nanoparticle, AuCu alloy, HAADF-STEM, Convolutional Neural Network, Artificial Intelligence

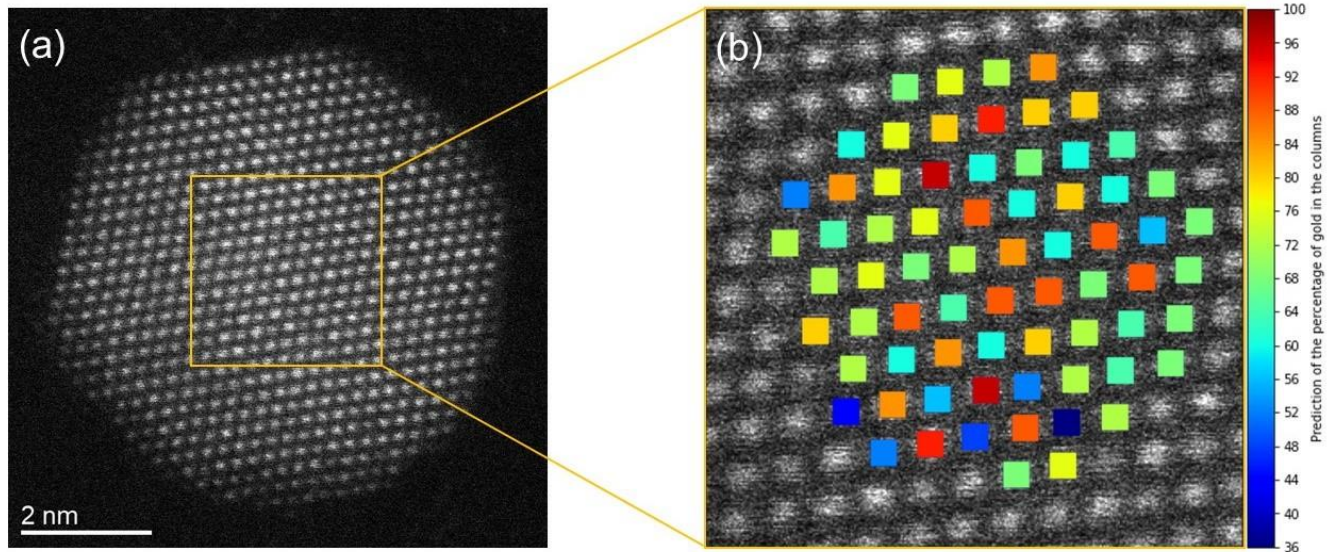


*Figure 1: (a) Experimental STEM-HAADF image of a AuCu nanoparticle; (b) Prediction of the percentage of Au atoms in the atomic columns at the center of the bimetallic nanoparticle from the image (a) using our first approach.*

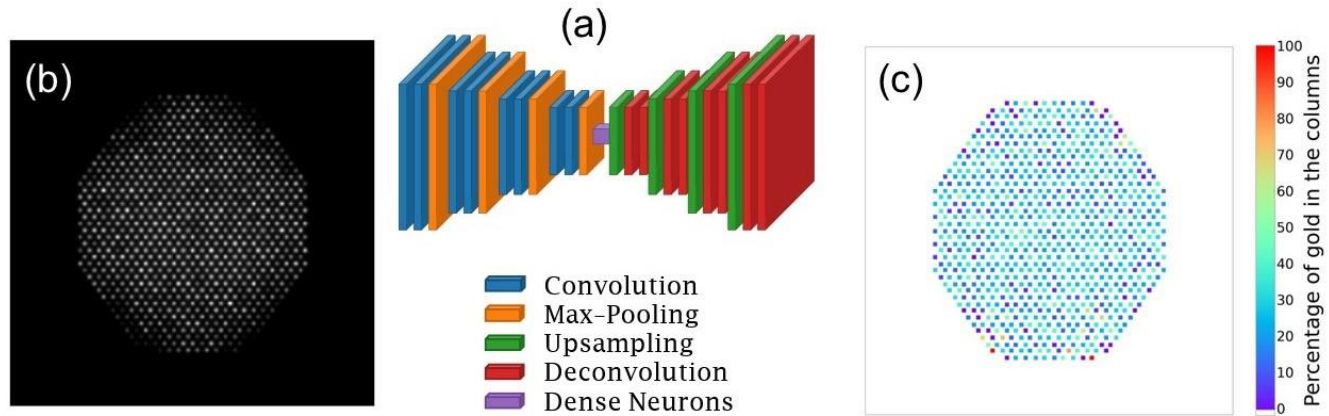


*Figure 2: (a) Representation of a convolutional neural network, an encoder followed by a decoder; (b) Input: simulated STEM-HAADF image of a AuCu<sub>3</sub> nanoparticle; (c) Output: elemental map of the proportion of Au in the columns.*

## SC1-Oral5

### Apprentissage profond pour la détection d'objets en microscopie électronique en transmission

#### Deep learning for detection in transmission electron microscopy

- **Thomas Bilyk** \* (thomas.bilyk@cea.fr) / Université Paris-Saclay, CEA, SR2C, SRMP, 91191, Gif-sur-Yvette, France
- **Mihai-Cosmin Marinica** / Université Paris-Saclay, CEA, SR2C, SRMP, 91191, Gif-sur-Yvette, France
- **Alexandra Goryaeva** / Université Paris-Saclay, CEA, SR2C, SRMP, 91191, Gif-sur-Yvette, France
- **Camille Flament** / Université Grenoble Alpes, CEA LITEN, Grenoble, France
- **Catherine Sabathier** / CEA, DES, IRESNE, DEC, Cadarache, France
- **Éric Leroy** / Université Paris-Est Creteil, CNRS, ICMPE (UMR 7182), F-94320 Thiais, France
- **Estelle Meslin** / Université Paris-Saclay, CEA, SR2C, SRMP, 91191, Gif-sur-Yvette, France

\* Auteur correspondant

La caractérisation d'objets de taille nanométrique observés, souvent en grand nombre, par microscopie électronique en transmission (MET), est essentielle pour évaluer le comportement mécanique des matériaux. Une analyse manuelle est minutieuse, répétitive, sujette à l'erreur humaine et coûteuse en temps. Au cours de la dernière décennie, des améliorations majeures de réseaux de neurones (NN) artificiels les ont rendus compétitifs à l'œil humain, ou à d'autres approches automatiques classiques, pour ces tâches de détection d'objets [1]. Plus particulièrement, le NN Mask R-CNN permet d'effectuer à la fois détection et segmentation des objets étudiés [2]. Ce type d'approche sera présenté dans un premier temps, ainsi que la problématique de la création d'une base de données d'apprentissage en MET. Une mise en application à la segmentation de boucles de dislocations sur des micrographies STEM-BF dans un alliage à haute entropie (Y3, 46%Fe16%Mn23%Ni14%Cr (%at.)) élaboré à l'école des mines de Saint Etienne (EMSE) irradié aux ions dans les plateformes Jannus Saclay et Orsay. Cette classe de matériaux métalliques est envisagée pour des applications dans le domaine du nucléaire [3], du fait d'une potentielle haute limite d'élasticité, accompagnée d'une excellente ductilité, et d'une bonne résistance sous irradiation.

Un exemple typique de micrographie STEM-BF analysé est présenté en Figure 1.a). La détection des boucles de dislocation illustrée en Figure 1.b) démontre la possibilité d'apporter une caractérisation individuelle d'un grand nombre d'objets, de façon automatisée. La fonction de distribution radiale (RDF) présentée en Figure 1.c), établit grâce à l'extraction des positions des différentes boucles, met par exemple en évidence une faible mobilité des boucles de dislocations. Enfin, l'approche étant généralisable à d'autres cas, une discussion sur des résultats préliminaires obtenus sur d'autres systèmes sera présentée.

#### Références :

- [1]C. M. Anderson et al., "Automated detection of helium bubbles in irradiated X-750", Ultramicroscopy, 217 (2020), p.113068
- [2]K. He et al., "Mask R-CNN", IEEE International Conference on Computer Vision, (2017), p.2980-2988
- [3]E. J. Pickering et al., "High-entropy alloys for advanced nuclear applications", Entropy, 23.1 (2021), p.98

**Mots clefs** : Apprentissage profond, microscopie électronique en transmission, alliages à autre entropie, segmentation

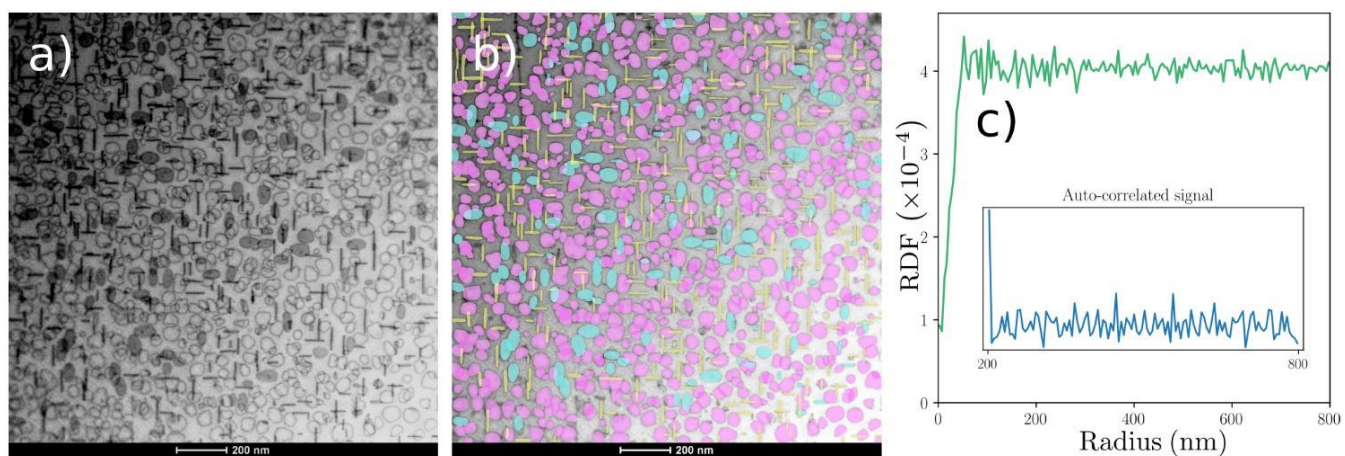


*Figure 1: a) Exemple typique d'une micrographie STEM-BF acquise après irradiation aux ions fer de l'alliage Y3. b) Illustration de la détection obtenue en utilisant un réseau de neurones Mask R-CNN, entraîné au préalable. c) Fonction de distribution radiale obtenue en analysant l'ensemble des positions des boucles de dislocation.*

## SC1-Oral6

# Une méthode puissance de simulation pour le développement de détecteurs d'électrons directs

## A Powerful Simulation Solution for Direct Electron Detectors Development

- **Olivier Marcelot \*** (o.marcelot@isae.fr) / ISAE-SUPAERO
- **Cécile Marcelot** / CEMES-CNRS
- **Franck Corbière** / ISAE-SUPAERO
- **Magali Estripeau** / ISAE-SUPAERO .**Florent Houdellier** / CEMES-CNRS
- **Sébastien Rolando** / ISAE-SUPAERO
- **Philippe Martin-gonthier** / ISAE-SUPAERO
- **Christian Pertel** / CEMES-CNRS
- **Vincent Goiffon** / ISAE-SUPAERO

\* Auteur correspondant

Direct Electron Detectors are now the most advanced devices for Transmission Electron Microscope (TEM) observations and replace hybrid detectors using a scintillator. These devices, only based on CMOS technology, offer superior performances thanks to the integration of CMOS functions, strong radiation hardness, and a much better spatial resolution due to the absence of scintillator and the optimization of the sensitive substrate. Few companies develop such detector, and the literature related to direct detector simulation and optimization is still underdeveloped. In particular, no global simulation tool focused on CMOS electron detection has been demonstrated. However, this kind of simulator is of primary importance, as the development of direct electron detector is based on compromises between signal detection efficiency and spatial resolution [1].

In this work we propose a new simulation method based on TCAD using Monte-Carlo electron distributions as an input, and a comparison between simulation and measurement of detector gain and Modulation Transfer Function (MTF). The design and material characteristics of the used CMOS detector [2] are perfectly known, allowing a good implementation in the simulator. Thus, the detector gain is simulated in 3 dimensions (3D) and the MTF is simulated thanks to 2D simulations of Line Spread Functions (LSF) operated on several pixels. In situ measurements are performed on the same CMOS detector (Fig. 1), by means of a Hitachi HF2000 microscope operated at three beam energies. A Faraday cap is used to extract the detector gain, and slanted edges are used to extract the MTF of the detector for each beam energy. Dark current and noise are also extracted for Detection Quantum Efficiency (DQE) calculation.

The comparison between measurements and simulations of the studied CMOS detector shows an acceptable agreement for the gain, and especially reproduces well the gain behavior according to the beam energy. Then, the analysis of simulated and measured MTF show an excellent agreement for all beam energies (Fig. 2). These results demonstrate that this simulation method can be used for future electron detector developments, by optimizing substrate thicknesses and pixel architecture and dimensions.

[1] O. Marcelot,Ultramicroscopy,243(2023),p.113628

[2]V.Goiffon,CAMRAD:Development of a Multi Mega gray Radiation Hard CMOS Camera for Dismantling Operations,(2018)

**Mots clefs :** MTF, gain, simulation, direct electron detector

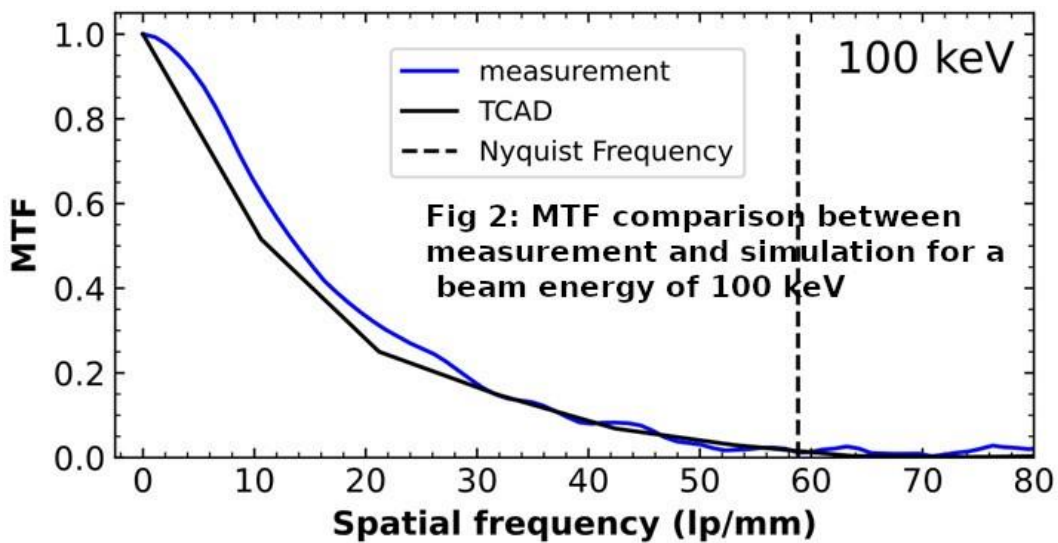
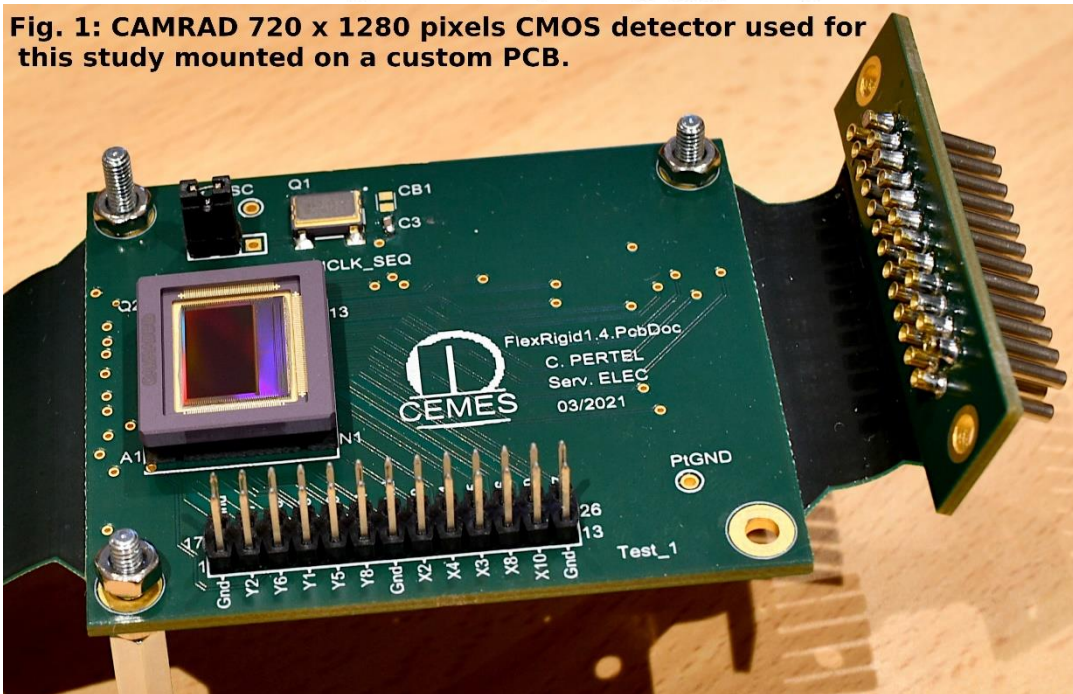


Fig. 1: CAMRAD 720 x 1280 pixels CMOS detector used for this study mounted on a custom PCB.



## **Symposium Commun 2 (SC2) : Microscopie à l'interface physique et biologie**

### ***Animation :***

*Guillaume Mabilleau (Inserm UMR\_S 1229-RMeS Equipe REGOS – Institut de Biologie en Santé – CHU)*

*Thierry Douillard (Matériaux ingénierie et science – MATEIS, Lyon)*

## SC2 - Inv1

### Brillouin microscopy : stiffness, and so much more

- **Lucie Vovard** (lucie.vovard@univ-lyon1.fr) / Institut Lumière Matière, UMR5306, Université Lyon 1-CNRS, Université de Lyon, 69622 Villeurbanne, France
- **Alexis Viel** (alexis.viel@univ-lyon1.fr) / Institut Lumière Matière, UMR5306, Université Lyon 1-CNRS, Université de Lyon, 69622 Villeurbanne, France
- **Gaëtan Jardiné** (gaetan.jardine@univ-lyon1.fr) / Institut Lumière Matière, UMR5306, Université Lyon 1-CNRS, Université de Lyon, 69622 Villeurbanne, France
- **Sylvain Monnier** (sylvain.monnier@univ-lyon1.fr) / Institut Lumière Matière, UMR5306, Université Lyon 1-CNRS, Université de Lyon, 69622 Villeurbanne, France
- **Thomas Dehoux** \* (thomas.dehoux@univ-lyon1.fr) / Institut Lumière Matière, UMR5306, Université Lyon 1-CNRS, Université de Lyon, 69622 Villeurbanne, France

\* Corresponding author

Brillouin spectroscopy uses the interaction of a laser light with picosecond timescale density fluctuations in the sample. It gives access to the mechanical properties (stiffness, viscosity...) on a sub-micrometer scale and at GHz frequencies. It has long been used in physics and material science since its discovery almost 100 years ago. Thanks to improvements in spectrometer technology, acquisition times have been reduced significantly in recent years, opening new applications in biology and medicine. Since 2015, BLS has been successfully used for mechanical phenotyping and imaging with a contrast based on the stiffness in single cells using spectroscopic and time-resolved implementations, live organisms, plant tissues and teeth. Because it is label-free, all-optical and non-destructive, BLS has gained interest in the pharmaceutical and biomedical fields as a promising tool to investigate the mechanobiology of different pathologies. However, its relevance from a physiological standpoint remains debated due to the ultrashort timescales involved. Since the probing mechanism involves coupling of photons to longitudinal phonons, variations in the scattering spectra can be interpreted as the response of the sample to an infinitesimal uniaxial compression. With a few examples and some fundamental concepts, I will give some insights on how to interpret such data in biological samples, and offer new perspectives.

**Mots-clés/Keywords:** Brillouin microscopy, biology

## SC2 – Inv2

# Vibrational microspectroscopic techniques, Bone Quality, and Fragility Fractures.

- Sonja Gamsjaeger ([sonja.gamsjaeger@osteologie.lbg.ac.at](mailto:sonja.gamsjaeger@osteologie.lbg.ac.at)) / Ludwig Boltzmann Institute of Osteology
- Eleftherios P. Paschalis\* ([eleftherios.paschalidis@osteologie.lbg.ac.at](mailto:eleftherios.paschalidis@osteologie.lbg.ac.at)) / Ludwig Boltzmann Institute of Osteology

\* Corresponding author

It is well accepted that bone strength depends on bone quantity and quality, the latter a broad term encompassing its structural and material properties.

In the clinic, a plethora of pathologies are associated with compromised bone's resistance to fracture. On the other hand, at the material level, it may be far less complicated. Bone is a hierarchically organized composite material consisting of mineral, organic matrix, and water. As such, it is expected that any pathology associated with fragility fracture occurrence, will also be associated with alterations in the quantity and / or quality of one or more of the three composite components. One of the difficulties in appreciating the contribution of material properties towards the determination of bone strength is their significant dependence not only on the patient age, but on tissue age within the same patient as well.

Vibrational spectroscopic techniques such as Fourier transform Infrared microspectroscopy (FTIRM) and Imaging (FTIRI), and Raman spectroscopy, are suitable analytical tools for the determination of bone quality as they provide simultaneous, quantitative and qualitative information on all main bone tissue components (mineral, organic matrix, tissue water), as well as tissue organization, in a spatially resolved manner. The various instruments available allow spatial resolutions at all bone hierarchical levels, from ~ 10 nm to dm. Moreover, the results of such analyses may be readily combined with the outcomes of other techniques such as histology/histomorphometry, small angle x-ray scattering, quantitative backscattered electron imaging, and nanoindentation. Of particular value is the combinatorial approach with histology/histomorphometry which allows the comparison of similar tissue ages across specimens, thus providing information on mechanisms that are independent of bone turnover rates.

The range of spatial resolutions afforded by vibrational spectroscopic techniques is pivotal in clinical cases with an abundance of fragility fracture occurrence. Bone's mechanical properties are governed by three attributes: stiffness (often measured by the elastic modulus or Young's modulus)[1]), strength (maximum stress the bone material can sustain prior to failure), and toughness (absorption of impact energy without reaching complete failure ; inversely related to stiffness) [1]. Stiffness is a non-linear average of all the local stiffness values [1], unlike strength and especially toughness which are dependent on microscopic material defects, particularly close to interfaces such as cement lines. Fragility fractures are mostly due to compromised toughness [2]. Thus vibrational spectroscopic techniques are particularly well suited to reveal the underlying mechanisms that result in fragility fractures as they can provide information anywhere from the nm to the dm scales, while precisely selecting the regions of interest to be analyzed and compared. Their unique contributions may be appreciated in instances such as idiopathic osteoporotic, and diabetes patients amongst other cases where fracture risk estimates fail to predict fracture occurrence [3-12], and in which vibrational spectroscopic outcomes strongly correlate with fracture incidence rather than risk estimated from clinical indicators such as bone mineral density by dual x-ray absorptiometry. Interestingly, in the overwhelming majority of such studies it is organic matrix quality indices that correlate the strongest with fragility occurrence, something that cannot be assessed in the clinic to date.

In summary, vibrational spectroscopic techniques afford a wealth of unique information on bone material properties and organization. One limitation of such analysis is the fact that bone tissue is required, usually in the form of an iliac crest biopsy or bone chips from surgery sites, involving invasive procedures. On the other hand, recent advances in fiber optics offer considerable promise that the existing instruments with relatively minor modifications may be employed in the routine clinical setting in the near future.

**Mots-clés/Keywords:** Bone quality, Fragility Fracture, Fourier transform infrared spectroscopy, Raman spectroscopy

- [1] W. Wagermaier, K. Klaushofer, P. Fratzl, Fragility of Bone Material Controlled by Internal Interfaces, *Calcif Tissue Int* 97(3) (2015) 201-12.
- [2] C.J. Hernandez, M.C. van der Meulen, Understanding Bone Strength Is Not Enough, *J Bone Miner Res* 32(6) (2017) 1157-1162.
- [3] S. Gourion-Arsiquaud, D. Faibis, E. Myers, L. Spevak, J. Compston, A. Hodsman, E. Shane, R.R. Recker, E.R. Boskey, A.L. Boskey, Use of FTIR spectroscopic imaging to identify parameters associated with fragility fracture, *J Bone Miner Res* 24(9) (2009) 1565-71.
- [4] H.H. Malluche, D.S. Porter, H. Mawad, M.C. Monier-Faugere, D. Pienkowski, Low-energy fractures without low T-scores characteristic of osteoporosis: a possible bone matrix disorder, *The Journal of bone and joint surgery. American volume* 95(19) (2013) e1391-6.
- [5] B.M. Misof, S. Gamsjaeger, A. Cohen, B. Hofstetter, P. Roschger, E. Stein, T.L. Nickolas, H.F. Rogers, D. Dempster, H. Zhou, R. Recker, J. Lappe, D. McMahon, E.P. Paschalis, P. Fratzl, E. Shane, K. Klaushofer, Bone material properties in premenopausal women with idiopathic osteoporosis, *J Bone Miner Res* 27(12) (2012) 2551-61.
- [6] E.P. Paschalis, E.V. Glass, D.W. Donley, E.F. Eriksen, Bone mineral and collagen quality in iliac crest biopsies of patients given teriparatide: new results from the fracture prevention trial, *The Journal of clinical endocrinology and metabolism* 90(8) (2005) 4644-9.
- [7] E.P. Paschalis, E. Shane, G. Lyritis, G. Skarantavos, R. Mendelsohn, A.L. Boskey, Bone fragility and collagen cross-links, *J Bone Miner Res* 19(12) (2004) 2000-4.
- [8] R.D. Blank, T.H. Baldini, M. Kaufman, S. Bailey, R. Gupta, Y. Yershov, A.L. Boskey, S.N. Coppersmith, P. Demant, E.P. Paschalis, Spectroscopically determined collagen Pyr/deH-DHLNL cross-link ratio and crystallinity indices differ markedly in recombinant congenic mice with divergent calculated bone tissue strength, *Connect Tissue Res* 44(3-4) (2003) 134-42.
- [9] A. Mieczkowska, S.A. Mansur, N. Irwin, P.R. Flatt, D. Chappard, G. Mabilleau, Alteration of the bone tissue material properties in type 1 diabetes mellitus: A Fourier transform infrared microspectroscopy study, *Bone* 76 (2015) 31-9.
- [10] S. Rokidi, E.P. Paschalis, K. Klaushofer, S. Vennin, A. Desyatova, J.A. Turner, P. Watson, J. Lappe, M.P. Akhter, R.R. Recker, Organic matrix quality discriminates between age- and BMD-matched fracturing versus non-fracturing post-menopausal women: A pilot study, *Bone* 127 (2019) 207-214.
- [11] E.M. McNerny, B. Gong, M.D. Morris, D.H. Kohn, Bone fracture toughness and strength correlate with collagen cross-link maturity in a dose-controlled lathyrism mouse model, *J Bone Miner Res* 30(3) (2015) 455-64.
- [12] E.P. Paschalis, D.N. Tatakis, S. Robins, P. Fratzl, I. Manjubala, R. Zoehler, S. Gamsjaeger, B. Buchinger, A. Roschger, R. Phipps, A.L. Boskey, E. Dall'Ara, P. Varga, P. Zysset, K. Klaushofer, P. Roschger, Lathyrism-induced alterations in collagen cross-links influence the mechanical properties of bone material without affecting the mineral, *Bone* 49(6) (2011) 1232-41.

## SC2 – Oral1

### Étude de la structure de biomatériaux innovants et de leurs interfaces avec les cellules et les tissus osseux durs grâce à la tomographie FIB-MEB en mode cryogénique

The study of the structure of innovative biomaterials and of their interfaces with cells and hard bone tissue using 3D cryo-FIB/SEM

- **Laura Samperisi, Aekta Upadhyay, Mouad Essani** / Nantes Université, Institut des Matériaux de Nantes Jean Rouxel (IMN), CNRS, Nantes, France
- **Pierre Weiss** / Nantes Université, INSERM, Regenerative Medicine and Skelton laboratory, F-44042 Nantes, France
- **Angélique Galvani** / Nantes Université, INSERM, Regenerative Medicine and Skelton laboratory, F-44042 Nantes, France
- **Amina Merabet, Nicolas Stephan, Jean Le Bideau** / Nantes Université, Institut des Matériaux de Nantes Jean Rouxel (IMN), CNRS, Nantes, France
- **Valérie Geoffroy** / Nantes Université, INSERM, Regenerative Medicine and Skelton laboratory, F-44042 Nantes, France
- **Baptiste Charbonnier** / Nantes Université, INSERM, Regenerative Medicine and Skelton laboratory, F-44042 Nantes, France
- **Patricia Abellan \*** (patricia.abellan@cnrs-imn.fr) / Nantes Université, Institut des Matériaux de Nantes Jean Rouxel (IMN), CNRS, Nantes, France

\* Auteur correspondant

Hydrogel-based biomaterials have shown a tremendous potential as three-dimensional (3D) scaffolds for tissue regeneration/engineering as their high permeability for oxygen and nutrients through their high-water content matrix provides an excellent environment for cell growth and tissue regeneration. To understand the phenomena of biocompatibility and improve hydrogel-based scaffold designs, it is of paramount importance to access the cell focal contacts with the substrate. Biocompatible hydrogels can be combined with calcium phosphate cements (CPCs) for the development of novel bone substitute composites. In the field of tissue engineering it is therefore crucial to characterize biomaterials' interfaces, whether it is at the material (e.g., CPC-hydrogel), cellular (e.g., cell/substrate) or tissue (e.g., tissue/substrate in implants) level. Among them, hard-soft interfaces are particularly difficult to access by microscopy techniques due to the high mismatched behaviours in terms of bio (chemical), mechanical and physical properties and require the development of specific methods of sample preparation, imaging, and analysis.

3D reconstructions of the ultrastructure of biomaterials and cells can now be produced using datasets obtained by scanning electron microscopy (SEM) combined with focused ion beam (FIB). In 3D FIB/SEM, the FIB can etch sequentially through 2D plans while serial SEM images are captured. Moreover, as per their hydrated and fragile nature, the use of cryogenic temperatures allows the analysis of samples in their native unaltered state. In this presentation, we will show cryo-FIB-SEM protocols capable of delivering 3D reconstruction and detailed interface description of mice fibroblasts grown inside hydroxypropyl methylcellulose. The images revealed porous microstructures at nanometer resolution, and offered crucial insights into material factors affecting cell proliferation at specific regions within the scaffold. Also, we will show that cryo-FIB/SEM combined with energy dispersive spectrometry (EDS) can provide the spatial distribution of the different phases (organic/inorganic) in CPC/hydrogels composites. Finally, we will discuss the challenges, propose methods of sample preparation, including the steps of cryo fixation, and show our latest results on hard-soft bone interfaces. The proposed protocols provide a unique platform for analysis of the microstructures of novel biomaterials and for exploration of their interactions with the cells and with hard bone tissue.

**Mots clefs :** hydrogels, biomaterials, interfaces, FIB/SEM, cryogenic temperatures, bone

## SC2 – Oral2

### Conception, synthèse et caractérisation d'un origami protéique basé sur l'auto-assemblage d'une paire de protéines artificielles de type brique et agrafe

**Design, synthesis, and characterization of protein origami based on self-assembly of a brick and staple artificial protein pair**

- **Cécile Marcelot** \* (cecile.marcelot@cemes.fr) / CEMES, CNRS UPR 8011, 29 rue J. Marvig, B.P. 94347, F-31055 Toulouse, France
- **Laureen Moreaud** / CEMES, CNRS UPR 8011, 29 rue J. Marvig, B.P. 94347, F-31055 Toulouse, France
- **Sébastien Viollet** / I2BC, Université Paris-Saclay, CEA, CNRS, 91198, Gif-sur-Yvette, France
- **Agathe Urvoas** / I2BC, Université Paris-Saclay, CEA, CNRS, 91198, Gif-sur-Yvette, France
- **Marie Valerio-Lepiniec** / I2BC, Université Paris-Saclay, CEA, CNRS, 91198, Gif-sur-Yvette, France
- **Inès LI DE LA SIERRA-GALLAY** / I2BC, Université Paris-Saclay, CEA, CNRS, 91198, Gif-sur-Yvette, France
- **Jessalyn Miller** / I2BC, Université Paris-Saclay, CEA, CNRS, 91198, Gif-sur-Yvette, France
- **Malika Ouldali** / I2BC, Université Paris-Saclay, CEA, CNRS, 91198, Gif-sur-Yvette, France
- **Stéphanie Balor** / METI, CBI, Université de Toulouse, CNRS, UPS, 31062, Toulouse, France
- **Vanessa Soldan** / METI, CBI, Université de Toulouse, CNRS, UPS, 31062, Toulouse, France
- **Franck Artzner** / IPR, CNRS, UMR 6251, Université de Rennes 1, F-35042 Rennes, France
- **Cristelle Meriadec** / IPR, CNRS, UMR 6251, Université de Rennes 1, F-35042 Rennes, France
- **Dujardin Erik** / ICB, CNRS UMR 6303, Université de Bourgogne, 21000 Dijon, France
- **Philippe Minard** / I2BC, Université Paris-Saclay, CEA, CNRS, 91198, Gif-sur-Yvette, France

\* Auteur correspondant

Spontaneous building of bio-inspired organization with both accurate morphologies and well-defined functions is still highly challenging. A versatile strategy to create an inducible protein assembly with predefined geometry is demonstrated.[1] The assembly is triggered by a binding protein that staples two identical protein bricks together in a predictable spatial conformation. The brick and staple proteins are designed for mutual directional affinity and engineered by directed evolution from a synthetic modular repeat protein library.[2] We design the brick protein with a semi-lock washer shape so that equimolar mixtures with the staple protein result in the sequential growth of macroscopic tubular superhelices.

Cross-examination by small-angle X-ray scattering (SAXS) and transmission electron microscopy (TEM with staining agent and cryoTEM) successfully elucidates the resulting superhelical arrangement that precisely matches the a priori intended 3D assembly. The highly ordered, macroscopic biomolecular construction sustains temperatures as high as 75°C thanks to the robust  $\beta$ -Rep building blocks. Since the  $\beta$ -helices of the brick and staple proteins are highly programmable, their design allows encoding the geometry and chemical surfaces of the final supramolecular protein architecture. This work opens new routes towards the design and fabrication of multiscale protein origami with arbitrarily programmed shapes and chemical functions.[3]

#### References :

- [1]L. Moreaud, et al., PNAS 120 (2023) e2218428120.
- [2]A. Urvoas et al., J Mol Biol 404 (2010) 307-327. A. Guellouz et al., PLoS One 8 (2013) e71512.
- [3]K. L. Gurunatha et al., ACS Nano 10 (2016) 3176. J. Prasad et al., Nanoscale, 12 (2020) 4612-4621.

**Mots-clés:** characterization of protein, tomography, cryo-microscopy

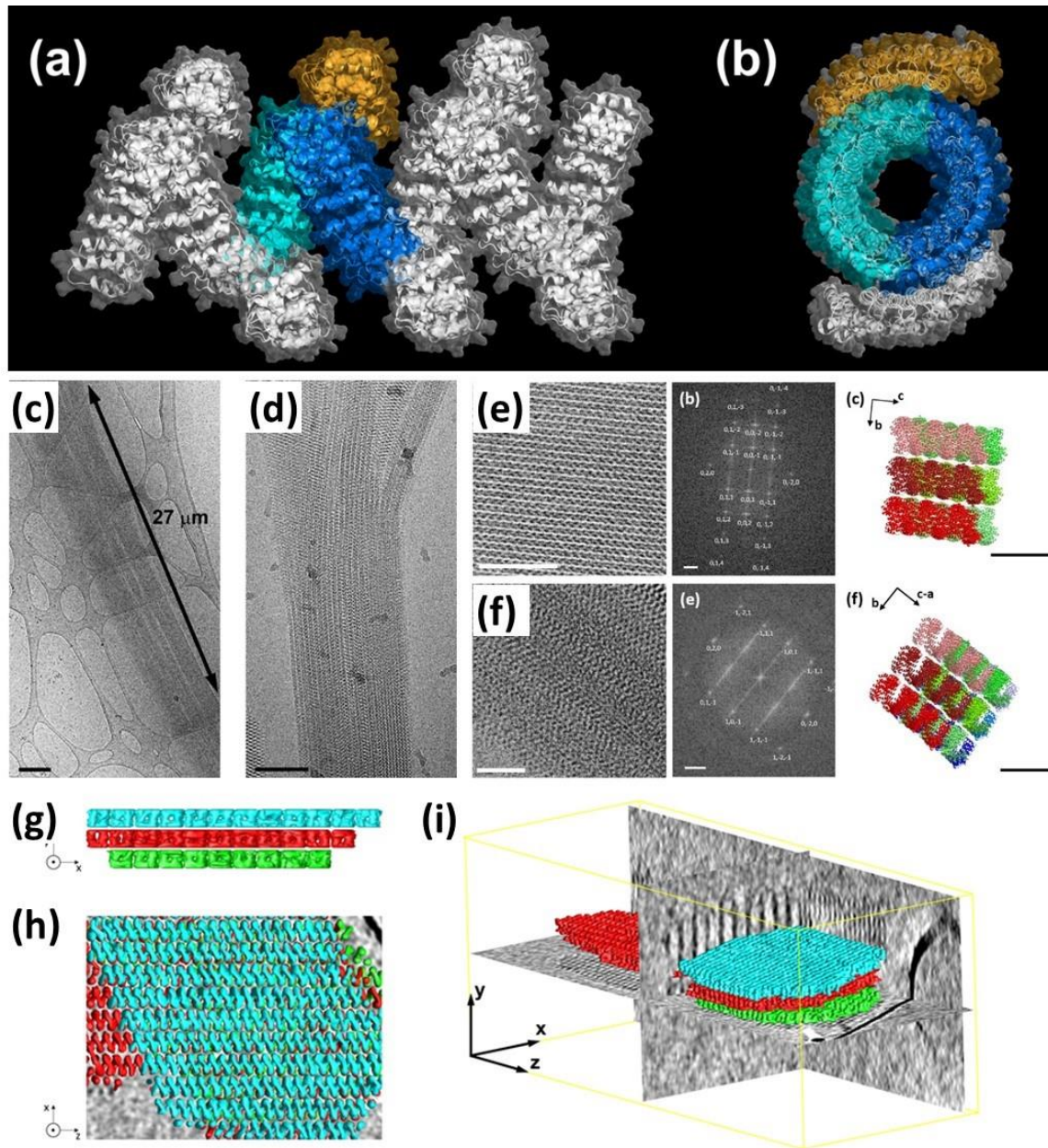


Figure 1: Design principle of self-assembling helical protein origami. (a) Side and (b) axial views of a ribbon model of the supramolecular  $\alpha$ Rep helix based on the crystallographic structure reported in (PDB Code 8AW4). The elementary assembly motif comprises two brick proteins (blue and cyan) linked by a staple protein (orange). (b,c) Wide field and zoomed cryo-TEM images of brick-bBE3 superhelix aligned into large-scale compact bundles. (e,f) Zoomed areas (left), FFT images (middle) and 3D model (right) along (e)[100] and (f) [101] zone axis. (g-i) Axial, transverse and 3D view of partially reconstructed 430x175x160 nm<sup>3</sup> tomogram (cubic pixel size 1.12 nm). [1]

## SC2 – Oral3

### Dévoilement du comportement de MoS<sub>2</sub> dans les milieux biomimétiques et biologiques : étude complémentaire *in vivo*, *in situ* et *ex vivo*

Unveiling MoS<sub>2</sub> behavior in biomimetic and biological media: In vivo, in situ and ex vivo complementary study

- **Nathaly ORTIZ PEÑA** \* (nathaly.ortiz@u-paris.fr) / Université Paris Cité, MPQ Matériaux et Phénomènes

Quantiques, CNRS, 10 rue Alice Domon et Léonie Duquet, Paris 75205 Cedex 13, France

- **Kondareddy CHERUKULA** / Université Paris Cité, MSC Matière et Systèmes Complexes, CNRS, 45 rue des Saints Pères, Paris 75006 France

• **Benjamin EVEN** / elias.fattal@universite-paris-saclay.fr

• **Ding-Kun JI** / CNRS, Immunology, Immunopathology and Therapeutic Chemistry, UPR 3572, University of Strasbourg, ISIS, 67000 Strasbourg, France

• **Sarah RAZAFINDRAKOTO** / Université Paris Cité, MSC Matière et Systèmes Complexes, CNRS, 45 rue des Saints Pères, Paris 75006 France

• **Shiyuan PENG** / CNRS, Immunology, Immunopathology and Therapeutic Chemistry, UPR 3572, University of Strasbourg, ISIS, 67000 Strasbourg, France

• **Amanda K. A. SILVA** / Université Paris Cité, MSC Matière et Systèmes Complexes, CNRS, 45 rue des Saints Pères, Paris 75006 France

• **Cécilia MÉNARD MOYON** / CNRS, Immunology, Immunopathology and Therapeutic Chemistry, UPR 3572, University of Strasbourg, ISIS, 67000 Strasbourg, France

• **Hervé HILLAIREAU** / Université Paris-Saclay, CNRS, Institut Galien Paris-Saclay, 91400 Orsay, France

• **Alberto BIANCO** / CNRS, Immunology, Immunopathology and Therapeutic Chemistry, UPR 3572, University of Strasbourg, ISIS, 67000 Strasbourg, France

• **Elias FATTAL** \* (elias.fattal@universite-paris-saclay.fr) / Université Paris-Saclay, CNRS, Institut Galien Paris-Saclay, 91400 Orsay, France

• **Damien ALLOYEAU** / Université Paris Cité, MPQ Matériaux et Phénomènes Quantiques, CNRS, 10 rue Alice Domon et Léonie Duquet, Paris 75205 Cedex 13, France

• **Florence GAZEAU** / Université Paris Cité, MSC Matière et Systèmes Complexes, CNRS, 45 rue des Saints Pères, Paris 75006 France

\* Auteur correspondant

In the booming of 2D materials for a variety of applications, transition metal dichalcogenides, in particular molybdenum disulfide, have raised as an attractive subject thanks to their exceptional electronic, optical, mechanical and chemical properties.(1) Notably, the large surface area with tunable electronic properties, the intercalable layers and the readiness for functionalization makes them good candidates for biomedical proposes such as biosensing, bioimaging, and drug delivery, among others. Furthermore, MoS<sub>2</sub> have shown to have a better biocompatibility and stability in comparison with their carbon-based analogues. Prior publications assessing the degradation products from the biotransformation of MoS<sub>2</sub> point to the oxidation of the sheets leading to the formation of free Mo<sup>4+</sup> ions and molybdenum oxides.(2) Such degradation process appears to be innocuous for the cell life. Nonetheless, additional insight in the biotransformation mechanism of exfoliated MoS<sub>2</sub> nanosheets is key in the assessment of its viability for biomedical applications. Herein, we have implemented a complementary approach by using *in situ* liquid phase transmission electron microscopy(LP-TEM) and *ex-vivo* studies to unveil a new aspect of the behavior of MoS<sub>2</sub> patches in conditions mimicking those within cells, in particular those with high concentrations of ROS and H<sub>2</sub>O<sub>2</sub>.(3) Using LP-TEM experiments, we could evidence the dynamics of

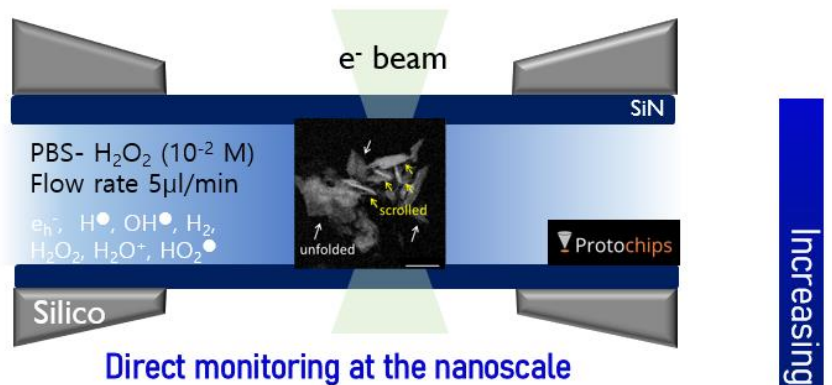
MoS<sub>2</sub> nanosheets transformation triggered by reactive oxygen species. Three main transformation mechanisms were observed directly at the nanoscale level: 1- scrolling of the dispersed sheets leading to the formation of nanoscrolls and folded patches (Figure 1a) encountered as well in ex vivo samples (Figure 1b). 2- etching releasing soluble MoO<sub>4</sub><sup>2-</sup>, and 3) oxidation generating oxidized sheet fragments. We would like to acknowledge the financial support of the French national research agency for the CYCLYS project.

#### References:

1. K. Bazaka et al., J. Phys. D. Appl. Phys. 51, (2019) 1–39.
2. R. Kurapati et al., Adv. Funct. Mater. 27, (2017) 1605176.
3. N. Ortiz Peña et al., Adv. Mater., (2023) 2209615.

#### a) In situ analysis

MoS<sub>2</sub> sheets in PBS- H<sub>2</sub>O<sub>2</sub> (10<sup>-2</sup> M)



Direct monitoring at the nanoscale

#### b) In vivo & in vitro analysis

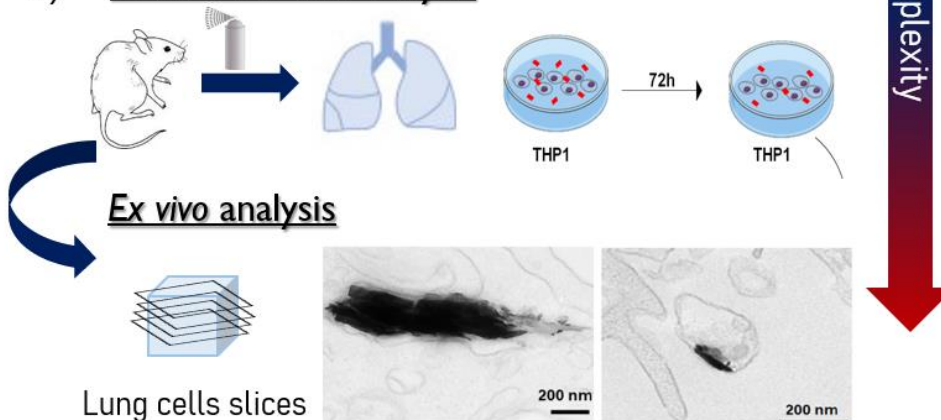


Figure 1: a) Image from in situ liquid phase recording of MoS<sub>2</sub> patch scrolling in a 5 mM H<sub>2</sub>O<sub>2</sub>-DPBS.b) Cell slices from ex vivo experiments displaying scrolled sheets imbedded within inner cellular structures after 48h. \*nathaly.ortiz@u-paris.fr  
\*damien.alloyeau@u-paris.fr  
\*florence.gazeau@u-paris.fr

**Mots clefs :** in situ liquid phase transmission electron microscopy, molybdenum disulfide, 2D materials, In vivo, complementary studies

**SC2 – Oral4****Holographies Electroniques "in-line" et "off-axis" pour l'étude des échantillons biologiques****In-line and off-axis electron holography for the study of biological specimens**

- **Elio Karim** \* (elio.karim@cemes.fr) / CEMES/CNRS et MCD-CBI; Toulouse, France
- **Bumsu Park** \* (artemist.bpark@gmail.com) / CEMES-CNRS; Toulouse, France
- **Cécile Marcelot** / CEMES-CNRS; Toulouse, France
- **Vanessa Soldan** / Meti-CBI; Toulouse, France
- **Stéphanie Balor** / Meti-CBI; Toulouse, France
- **Sara Bals** / EMAT-Université d'Antwerp, Belgique
- **Amélie Leforestier** / LPS-Université Paris-Saclay; Paris, France
- **Célia Plisson-Chastang** / MCD-CBI; Toulouse, France
- **Christophe Gatel** / CEMES-CNRS; Toulouse, France
- **Pierre-Emmanuel Gleizes** / MCD-CBI; Toulouse, France
- **Etienne Snoeck** / CEMES-CNRS; Toulouse, France

\* Auteur correspondant

3D structures of biological specimens have been studied for a long time using three main techniques: NMR, X-Ray crystallography, and cryo-electron microscopy (cryo-EM). While NMR is very challenging for proteins bigger than 50 kDa and X-Ray crystallography is exclusive to crystallizable proteins, cryo-EM has recently emerged as another powerful technique for high-resolution structural biology. Electron microscopy has however a major drawback due to the low amplitude contrast resulting from the weak electron interaction with the light elements composing biological samples. Biologists have developed methods to get around this issue, in particular the use of contrasting solutions containing heavy metals at room temperature or various types of phase plates in cryogenic conditions to enhance the TEM contrast. Herein, we analyze the performances of two electron holography techniques mostly developed for phase retrieval in material science, the focal series in-line holography and the off-axis holography techniques, to study unstained bacteriophages at room and at cryogenic temperatures. We showed that in-line holography in cryogenic conditions has great potential for imaging unstained biological specimens. In addition, thanks both to recent developments carried out at CEMES [1,2] and to the direct electron detectors performances, we show that off-axis holography enables us to retrieve the phase shift information that the electron undergoes when interacting with the low-Z biological samples. We show that these methods provide high SNR and high contrast phase images on unstained samples.

[1]C Gatel et al, Applied Physics Letters, 113 (2018), p. 13. <https://doi.org/10.1063/1.5050906>

[2]M Hÿtch & C Gatel, Microscopy, 70 (2021), p. 47. <https://doi.org/10.1093/jmicro/dfaa044>

[3]

**Mots clefs :** Electron Holography, Structural Biology, Cryo-EM, Off-Axis, In-line, Phase contrast.

## **Symposium commun 3 (SC3) : Diffraction et résolution structurale**

***Animation :***

*Wai-Li Ling (IBS, Grenoble)*

*Stéphanie Kodjikian (Institut Néel, Grenoble)*

**SC3 – Inv1****Mapping structure and electric field in two-dimensional materials using 4D-STEM**

- **Hanako Okuno** \* (hanako.okuno@cea.fr) / Univ. Grenoble Alpes, CEA-Grenoble, IRIG-MEM

\* Corresponding author

Epitaxial growth is a route to achieve large scale and well-oriented single crystalline two-dimensional (2D) materials with a great flexibility in the choice of elements and a potential in building van der Waals stacks, alloys or 2D layers doped either electrically or with magnetic elements. However, growing defect-free material remains a big challenge and the synthesized materials should be characterized as a patchwork of numerous defect structures in order to understand and control the material properties in large scale. In addition, the ability to correlate the structural configuration with their local electric properties at the atomic scale is also essential to realize the synthesis of the desired complex materials and to explore their functionalities.

High resolution scanning transmission electron microscopy (STEM) has become the most powerful technique for providing detailed local atomic structure of 2D layers such as graphene and transition metal dichalcogenides (TMDs) by Z-contrast direct imaging as well as the associated chemical information by electron energy loss spectroscopy (EELS). Recently a new STEM acquisition technique so-called four-dimensional STEM (4D-STEM) has demonstrated its great potential to fulfil information either on up-scaled structures or on local electric properties. The technique consists in recording a diffraction pattern for each scanning beam position on the sample, enabling to visualize multiple structural information in micrometer scale, such as orientation and polarity [1-2]. Analyzing the deviation of the transmitted beam position (Center of Mass: CoM) in 4D-datasets gives access to the local electric field at atomic scale, and to the electrostatic potential and the charge density through Poisson's equation [3].

In this work, we demonstrate the use of 4D-STEM to study 2D monolayers grown in both laboratory and industrial scales. First, orientation, polarity and phase maps of wafer-scale epitaxial TMDs are reconstructed at micron scale from 4D-diffraction datasets. The density and the distribution of typical domain junctions are quantitatively measured and directly correlated with their atomic structures [4]. In addition, the correlative application of different STEM techniques is demonstrated to fully study a single dopant atom incorporated into MBE grown WSe<sub>2</sub> monolayer. Single dopant atoms were localized in defective host materials by HAADF imaging and chemically identified by EELS. The local electric field around the dopant atoms was then investigated at atomic scale by CoM method. The results show the potential of 4D-STEM to construct an overview of synthesized 2D materials from large scale down to atomic scale with multiple information on structure, chemistry and electric characters.

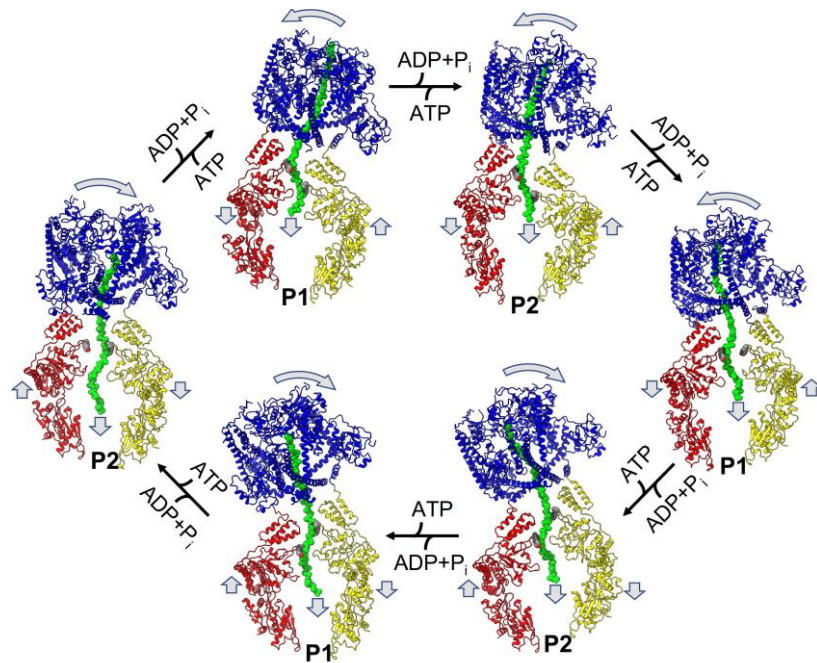
- [1] P.Dev et al., Ultramicroscopy, 215(2020)113019.
- [2] W. Caplins, D. Holm, M. White, R. Keller. Ultramicroscopy, 219 (2020) 113137.
- [3] C. Ophus, Microscopy and Microanalysis, 25 (2019) 563.
- [4] D. Dosenovic, H. Okuno et al., arXiv:2306.05505v1 (2023).

**Mots-clés/Keywords:** 4D-STEM, 2D materials

**SC3 – Inv2****Human mitochondrial Lon Protease is a molecular ratchet**

- **Jan Pieter Abrahams \*** (jp.abrahams@unibas.ch) / Biozentrum Basel, PSI Villigen, Switzerland
  - **Niko Schenck** (niko.schenck@unibas.ch) / Biozentrum Basel, Switzerland
  - **Mette Roegaard** (mette.roesgaard@unibas.ch) / Biozentrum Basel, Switzerland
  - **Min Chevalier Kwon** (min.chevalierkwon@unibas.ch) / Biozentrum Basel, Switzerland
  - **Senik Matinyan** (senik.matinyan@unibas.ch) / Biozentrum Basel, Switzerland
  - **Pavel Filipcik** (pavel.filipcik@unibas.ch) / Biozentrum Basel, Switzerland
  - **Eric van Genderen** (eric.van-genderen@psi.ch) / PSI Villigen, Switzerland
- \* Corresponding author

The human mitochondrial Lon protease homolog (LonP1) is a 600 kDa essential enzyme responsible for recognizing, unfolding, and degrading damaged proteins within the mitochondrial matrix. In our recent study, we elucidated the structure of intact wildtype LonP1 in nine distinct conformations [1]. The nucleotide content observed within its six ATP-binding sites correlated with the corresponding subunit conformations. Subsequent analysis revealed that LonP1 employs a ratchet mechanism to unfold substrate proteins, wherein ATP hydrolysis prevents partially unfolded substrates from refolding. We discuss the structural features of LonP1 that underlie this ratchet mechanism. Our conclusions are based on cryo-electron microscopy (cryo-EM) reconstructions of LonP1 captured at different stages of its threefold binding change ATPase mechanism. Unfortunately, current technologies do not permit direct observation of this binding change mechanism and the associated ratcheted unfolding of substrate proteins. To address this problem, we are developing novel approaches in single-molecule electron diffraction in the liquid state. We discuss our current advances, in the anticipation that this new technology will allow us to definitely prove the proposed enzyme mechanism of LonP1.



[1] Mohammed I, Schmitz KA, Schenck N, Balasopoulos D, Topitsch A, Maier T, Abrahams JP. Catalytic cycling of human mitochondrial Lon protease. *Structure*. 2022 Sep 1;30(9):1254-1268.e7. doi: 10.1016/j.str.2022.06.006. Epub 2022 Jul 22. PMID: 35870450.

**Keywords:** transmission EM, electron diffraction, protein, enzyme mechanism, methods development, structural biology

## SC3 – Oral1

### Étude de la dynamique de la lithiation dans des particules primaires des matériaux cathodiques par 4D-STEM et cellule liquide TEM

Study of Lithiation Dynamics in Primary Particles of Cathode Materials by 4D-STEM and in situ Electrochemical Liquid TEM

- **Kevyn GALLEGOS MONCAYO** \* (kevyn.gallegos.moncayo@u-picardie.fr) / LRCS (Laboratoire de Réactivité et Chimie des Solides), UMR 7413 CNRS-UPJV, Amiens, France
- **Justine JEAN** / LRCS (Laboratoire de Réactivité et Chimie des Solides), UMR 7413 CNRS-UPJV, Amiens, France
- **Nicolas FOLASTRE** / LRCS (Laboratoire de Réactivité et Chimie des Solides), UMR 7413 CNRS-UPJV, Amiens, France
- **Arash JAMALI** / LRCS (Laboratoire de Réactivité et Chimie des Solides), UMR 7413 CNRS-UPJV, Amiens, France
- **Ahmed YOUSFI** / LRCS (Laboratoire de Réactivité et Chimie des Solides), UMR 7413 CNRS-UPJV, Amiens, France
- **Arnaud DEMORTIERE** / LRCS (Laboratoire de Réactivité et Chimie des Solides), UMR 7413 CNRS-UPJV, Amiens, France

\* Auteur correspondant

Lithium-ion (LIB) batteries, thanks to their high energy density and capacity, have enabled the development of new technologies ranging from consumer electronics to hybrid or fully electric vehicles. However, the increasing demand for energy consumption has led to the search for new and more efficient materials to further improve the current capabilities of LIB batteries. A crucial step in the further development of LIB is to understand the behavior of lithium in the cathodic side of the battery and to study its dynamics in a realistic configuration.

To better understand the dynamics of (de)lithiation, an in-situ analysis at the primary particle scale in different cathode materials is proposed. The electrochemical liquid TEM analysis configuration [1] allows the performance of battery cycling inside the TEM for imaging at different SoC (state of charge), inducing less of perturbations during data acquisition and imaging analysis. The information obtained could reveal the behavior of lithium inside the crystallographic lattice for different compounds, as well as other phenomena that lead to battery degradation.

4D-STEM technique allows us to obtain structural information based on electron diffraction pattern collections [2-4]. Using this method, changes in lattice parameters can be detected by comparing the displacement between diffraction spots in diffraction patterns obtained during the cycle of an in-situ analysis. It is proposed to use 4DSTEM in-situ analysis on different SoC from non-cycled to failure to understand the influence of lithium behavior on the NMC cathode material and compare with literature. We developed a software suite, called ePattern, to help us to treatment 4D-STEM datasets using NMF clustering approach and registration/reconstruction strategy to optimize the ACOM result confidence.

[1]Fan Wu, Nan Yao, Nano Energy, 11 (2015), p 196-210. Doi:10.1016/j.nanoen.2014.11.004

[2]Bhatia, A., Cretu, S., Hallot, M., Folastre, N., Berthe, M., Troadec, D. Demortière, A. (2022). Small Methods, 6(2),2100891.

[3]Folastre, N., Cherednichenko, K., Cadiou, F., Bugnet, M., Rauch, E., Olchowka, J., Demortière, A. (2021). Microscopy and Microanalysis, 27(S1), 3446-3447.

[4]Gomez-Perez, A., Galanis, A., Das, P., Nicolopoulos, S., Demortière, A.(2021).Microscopy &Microanalysis,27(S1),2234-2235.

**Mots clefs :** 4D-STEM, Lithium-ion, TEM, liquid cell, electrochemistry, diffraction pattern

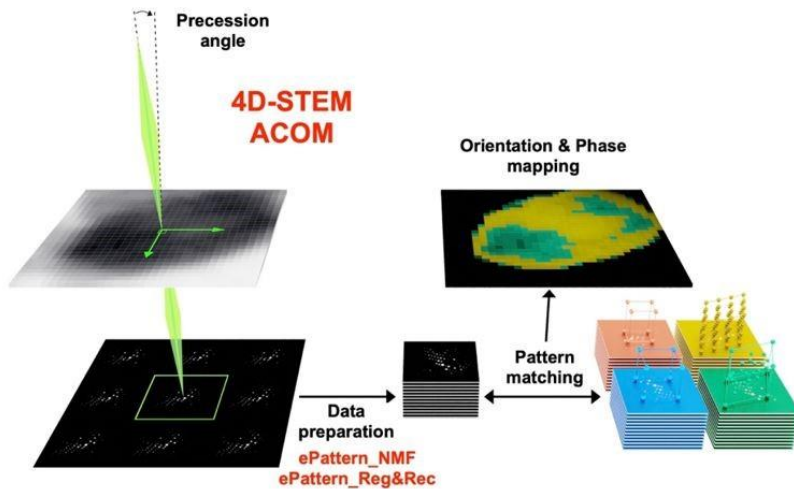


**Figure 1.** Global scheme of 4D-STEM ACOM technique using precession. The main steps are (1) the acquisition of diffraction pattern (DP) images using the Oneview CMOS camera in column (2) Data preparation (3) Pattern matching with banks of simulated DPs and (4) Orientation and phase mapping.

**SC3 – Oral2****Caractérisation 4D-STEM de matériaux sensibles : Etude de l'astéroïde Ryugu et des météorites carbonées****4D-STEM characterization of beam-sensitive materials: A case study on Hayabusa2's Ryugu asteroid samples and carbonaceous meteorites**

- **Bahae-eddine Mouloud, Damien Jacob, Francisco De la , Jean-Christophe Viennet, Sylvain Laforet**

, Université de Lille, CNRS, INRAE, Centrale Lille, UMR 8207-UMET-Unité Matériaux et Transformations, F-59000 Lille, France

- **Maya Marinova** / Université de Lille, CNRS, INRAE, Centrale Lille, Université Artois, FR 2638-IMEC-Institut Michel-Eugène Chevreul, 59000 Lille, France

- **Adrien Teurtrie** / Université de Lille, CNRS, INRAE, Centrale Lille, UMR 8207-UMET-Unité Matériaux et Transformations, F-59000 Lille, France

- **Corentin Le-Guillou** / Université de Lille, CNRS, INRAE, Centrale Lille, UMR 8207-UMET-Unité Matériaux et Transformations, F-59000 Lille, France

- **Hugues Leroux** / Université de Lille, CNRS, INRAE, Centrale Lille, UMR 8207-UMET-Unité Matériaux et Transformations, F-59000 Lille, France

- **Takaaki Noguchi** / Division of Earth and Planetary Sciences, Kyoto University; Kitashirakawaoiwake-cho, Sakyo-ku, Kyoto 606-8502, Japan

Four-dimensional scanning transmission electron microscopy (4D-STEM) has emerged as a powerful tool for the characterization of beam-sensitive materials, enabling structural analysis at the nanometer scale with minimal radiation damage. In a 4D-STEM experiment, a converging electron probe is scanned across a thin area of a sample and a 2D diffraction pattern is recorded at each scan position, yielding a four-dimensional dataset (Fig 1). 4D-STEM coupled with the new direct electron detection technology allows for the acquisition of diffraction information with unprecedented sensitivity and speed. The unique advantages of 4D-STEM make it an attractive option for studying a wide range of materials, including those that have previously been challenging for structural characterization using conventional transmission electron microscopy (TEM) techniques. Among these materials, carbonaceous meteorite and asteroid samples represent some of the most primitive specimens in our solar system, containing a wealth of information about its formation and evolution. The study of such samples is rendered particularly difficult due to the very fine scale mixing of beam sensitive phases composing their phyllosilicate matrix.

In this work, we report an application of the 4D-STEM technique to investigate the mineralogy of Ryugu asteroid samples from the Japanese mission Hayabusa2 [1] and the composition-close Orgueil carbonaceous meteorite. Experiments have been carried out on a probe corrected 60-300 kV Thermo Fisher Titan Themis (S)TEM coupled with a Medipix 3 direct electron detector (Quantum Detectors) installed behind a post-column high-resolution energy filter (Gatan Quantum ERS/966), enabling energy-filtered 4D-STEM. Data have been analyzed using the open-source Python packages py4DSTEM and HyperSpy software. We introduce an analysis protocol for mapping the different mineralogical phases in the phyllosilicate matrix of the samples (Fig 2). We find that the serpentine in Ryugu is, with a good level of confidence, present in the form of Lizardite. We also map the interplanar spacing in the smectite phase (Fig 2). We will discuss the implications of such findings.

[1] T. Nakamura et al. In: Science (Sept. 2022). issn: 0036-8075. doi: 10.1126/science.abn8671.

**Mots clefs :** 4D-STEM, Hayabusa2, Ryugu, beam-sensitive, carbonaceous meteorites, direct electron detector, Medipix3

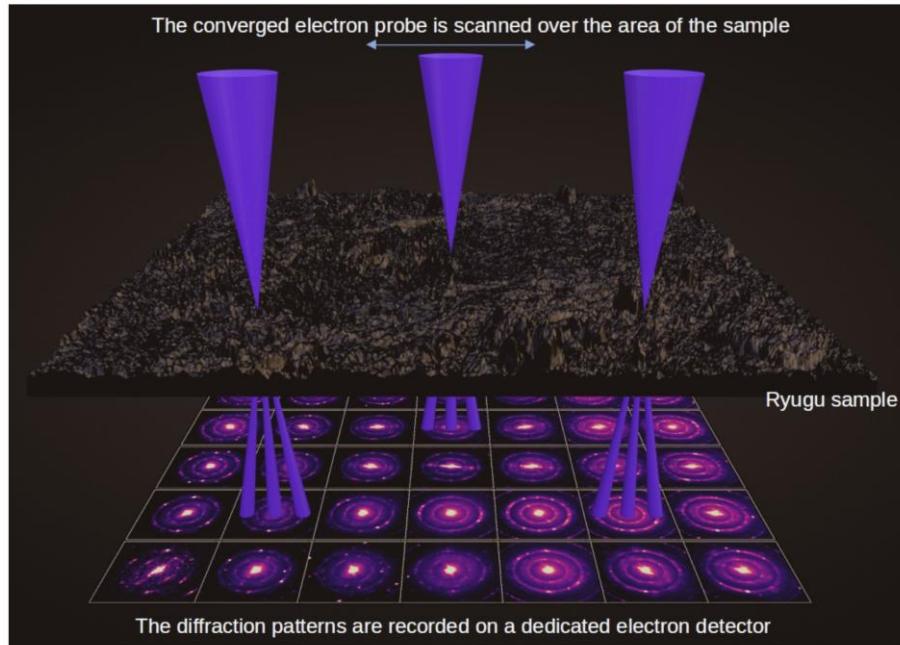


Fig. 1: Simplified schematic of a 4D-STEM experiment over an area of a Ryugu sample. The cones in blue represent the electron probe being scanned across the sample area. Each diffraction pattern in the figure is an average of  $9 \times 9$  experimental diffraction patterns recorded on a Medipix3 pixelated detector.

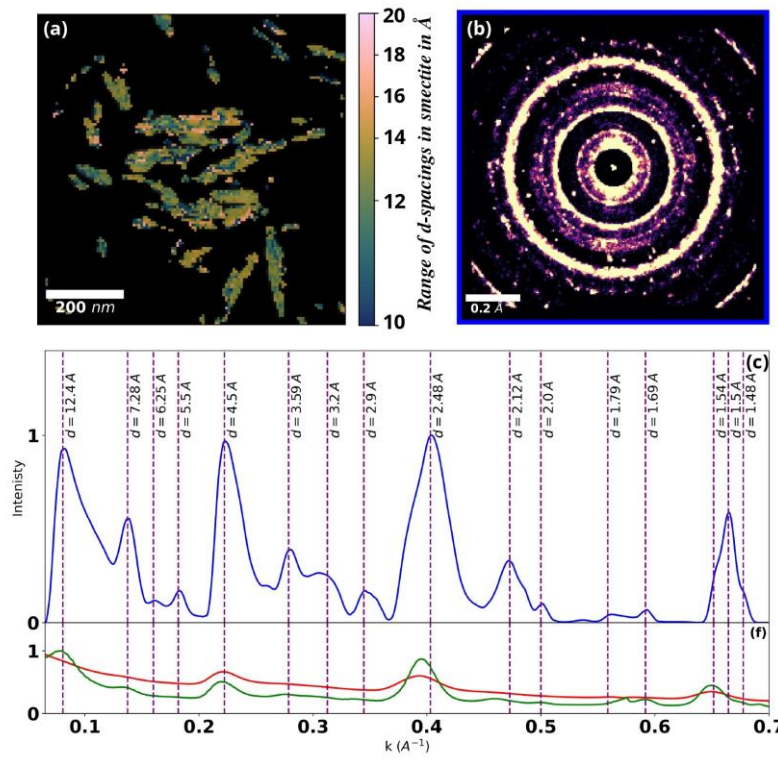


Fig. 2: (a) Dark field image of smectite with areas color coded based on the interlayer spacing of the mineral with warm colors representing larger d-spacings and cool colors indicate smaller d-spacings. (b) A Bragg Vector Map (BVM) of the 4D-STEM dataset representing a summary of all the scattering informations thereon. (c) In blue is a 1D radial profile, in a logarithmic scale, obtained by azimuthally averaging the BVM, while the red and green radial profiles correspond to the 1D profiles obtained by azimuthal integration of the mean and the variance diffraction patterns over the dataset, respectively.

**SC3 – Oral3****Tomographie par diffraction électronique de précession pour l'analyse structurelle des nanoparticules : étude de la taille minimale et des effets dynamiques associés**

**PEDT for structural analysis of nanoparticles: a study of minimal size and associated dynamical effects**

.Erica Cordero Oyonarte \* (erica.cordero-oyonarte@ensicaen.fr) / CNRS, CRISMAT

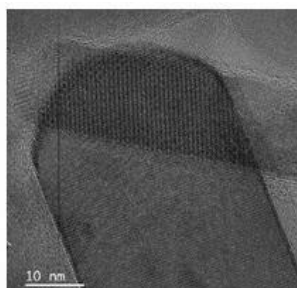
\* Auteur correspondant

The applicability of X-ray and neutron diffraction for single crystal structure analyses is often limited by the capacity to grow large enough crystals. For crystals with size below 1µm, so-called 3D electron diffraction (3D ED) methods [1] have emerged as a promising alternative. Electron diffraction results in a much stronger interaction with matter, while the electron beam can be focused to an extremely fine probe size (about 1 nm). Since early studies [2], there is little if no experimental data estimating the minimum size of individual particles that can be analyzed by 3D ED methods.

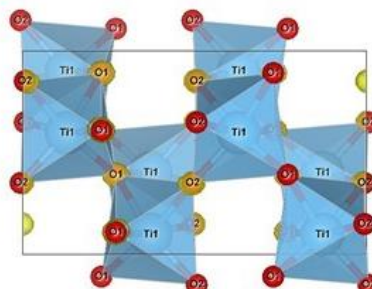
The present study aims to fill this gap by analyzing different nanoparticles with sizes down to 10 nm using Precession Electron Diffraction Tomography (PEDT) and dynamical refinements [3]. Our findings highlight the various challenges encountered during data acquisition such as the dispersion of the nanoparticles on the grid, the ratio between the beam size and the particle size, the minimum exposure time per frame or the total beam exposure time. We demonstrate here that it is possible to accurately refine the structure of individual nanoparticles down to 10nm using PEDT (Fig. 1). Interestingly, for such small nanoparticles, the R-values appear sometimes to be quite similar when comparing the results obtained from kinematical and dynamical refinements (see ITO results in Fig. 1). We will see this does not mean that we have reached the size limit, where the dynamic effect ceases to exist, but that the reason lies in the way the 3D ED data are processed for dynamical refinements. We hence show that dynamic scattering effects are still present even for such tiny crystals.

These results are obtained within the framework of European project NanED (Electron Nanocrystallography – H2020-MSCA-ITN GA956099)

**Mots clefs :** Electron diffraction, PEDT, nanoparticles

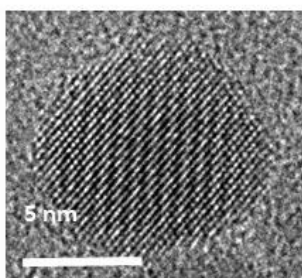


70nm largest part, 30nm narrow part

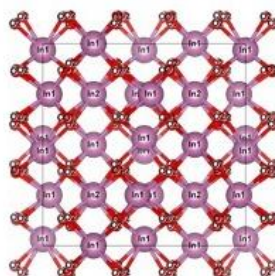
Brookite TiO<sub>2</sub>

$a = 9.1153$   $b = 5.4154$   $c = 5.1141$   
 $\alpha = \beta = \gamma = 90^\circ$   
Space group – Pbca

	All / Observed Reflections	Kinematical Refinement $R(\text{obs})$	All / Observed Reflections	Dynamical Refinement $R(\text{obs})$
Averaged	372, 300	<b>0.1708</b>	349, 316	0.0513
Not Averaged	379, 355	0.1592	1593, 1312	<b>0.0622</b>



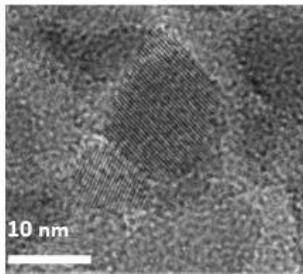
10nm



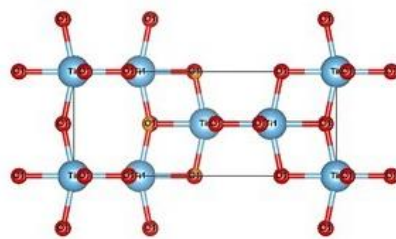
ITO

$a = 10.1432$   $b = 10.1432$   $c = 10.1433$   
 $\alpha = \beta = \gamma = 90^\circ$   
Space group – Ia-3

	All / Observed Reflections	Kinematical Refinement $R(\text{obs})$	All / Observed Reflections	Dynamical Refinement $R(\text{obs})$
Averaged	370,199	<b>0.0675</b>	369, 291	0.0443
Not Averaged	370, 321	0.1049	2502, 1412	<b>0.0688</b>



10nm

Anatase TiO<sub>2</sub>

$a = 3.8188$   $b = 3.8188$   $c = 9.4728$   
 $\alpha = \beta = \gamma = 90^\circ$   
Space group – I41/amd

	All / Observed Reflections	Kinematical Refinement $R(\text{obs})$	All / Observed Reflections	Dynamical Refinement $R(\text{obs})$
Averaged	173 / 136	<b>0.1038</b>	94 / 89	0.0305
Not Averaged	94 / 92	0.1218	666 / 492	<b>0.0387</b>

Fig 1: Visual summary of the structure analysis of Brookite TiO<sub>2</sub>, ITO and Anatase TiO<sub>2</sub> nanoparticles. A direct comparison of conventionally reported kinematical and dynamical reliabilities factors ( $R_{\text{obs}}$  values in bold) is misleading because these quantities are not calculated on the same way

## SC3 – Oral4

### Analyse structural des matériaux fonctionnels avec Scanning Precession Electron Tomography (SPET)

Structural analysis of functional materials through Scanning Precession Electron Tomography (SPET)

- **Sara Passuti** \* (sara.passuti@ensicaen.fr) / ENSICAEN, CNRS
- **Julien Varignon** / ENSICAEN, CNRS
- **Adrian David** / ENSICAEN, CNRS
- **Philippe Boullay** / ENSICAEN, CNRS

\* Auteur correspondant

Structural analysis of functional materials is the fundamental step towards the ability of tuning their physical properties as desired. For crystalline materials, 3D ED has been proven to be an effective technique to perform ab initio structure solution and refinements of crystals with size well below 1µm [1]. As the crystal or domain size reduces, the capacity to collect 3D ED data with smaller electron beams is the key to access the structure of individual embedded nanodomains. Tracking the area of interest becomes then a major issue. To circumvent this problem, we considered an alternative approach of acquiring 3D ED data by combining PEDT with a scan across the sample for each tilt angle. SPET (Scanning Precession Electron Tomography) has already been used for analysing the domains volume and orientation in known crystalline materials [2-3], relying, as 4D-STEM, on the comparison of the acquired diffraction patterns with theoretical ones taken from a reference database.

In the present work, SPET is used to acquire PEDT data over an area, extract the intensities collected at different positions and used them to obtain accurate structure refinements. As of proof-of-concept, we performed a SPET experiment on a 50 nm thick perovskite PrVO<sub>3</sub> film deposited on SrTiO<sub>3</sub> substrate using a probe size of about 10 nm. This way, it was possible to analyse small changes in the PVO structure along the film thickness from the variation of unit cell parameters to accurate atomic positions and tilt amplitude of the VO<sub>6</sub> octahedra (Fig. 1). We believe that SPET has the potential to become the standard procedure to characterize unknown films or embedded domains as small as 10 nm.

These results are obtained withing the framework of European project NanED (Electron Nanocrystallography – H2020-MSCA-ITN GA956099).

#### References:

- [1]Gemmi, M. et al. 3D electron diffraction: the nanocrystallography revolution. ACS Central Science 5(8) (2019) 1315-1329.
- [2]Eggeman, A. S et al. Scanning precession electron tomography for three-dimensional nanoscale orientationimaging and crystallographic analysis. Nature communications 6(1) (2015) 7267.
- [3]E. F. Rauch et al., New Features in Crystal Orientation and Phase Mapping for Transmission Electron Microscopy, Symmetry 13 (2021) 1675.

**Mots clefs :** SPET, 3D ED, transmission electron microscopy, functional materials

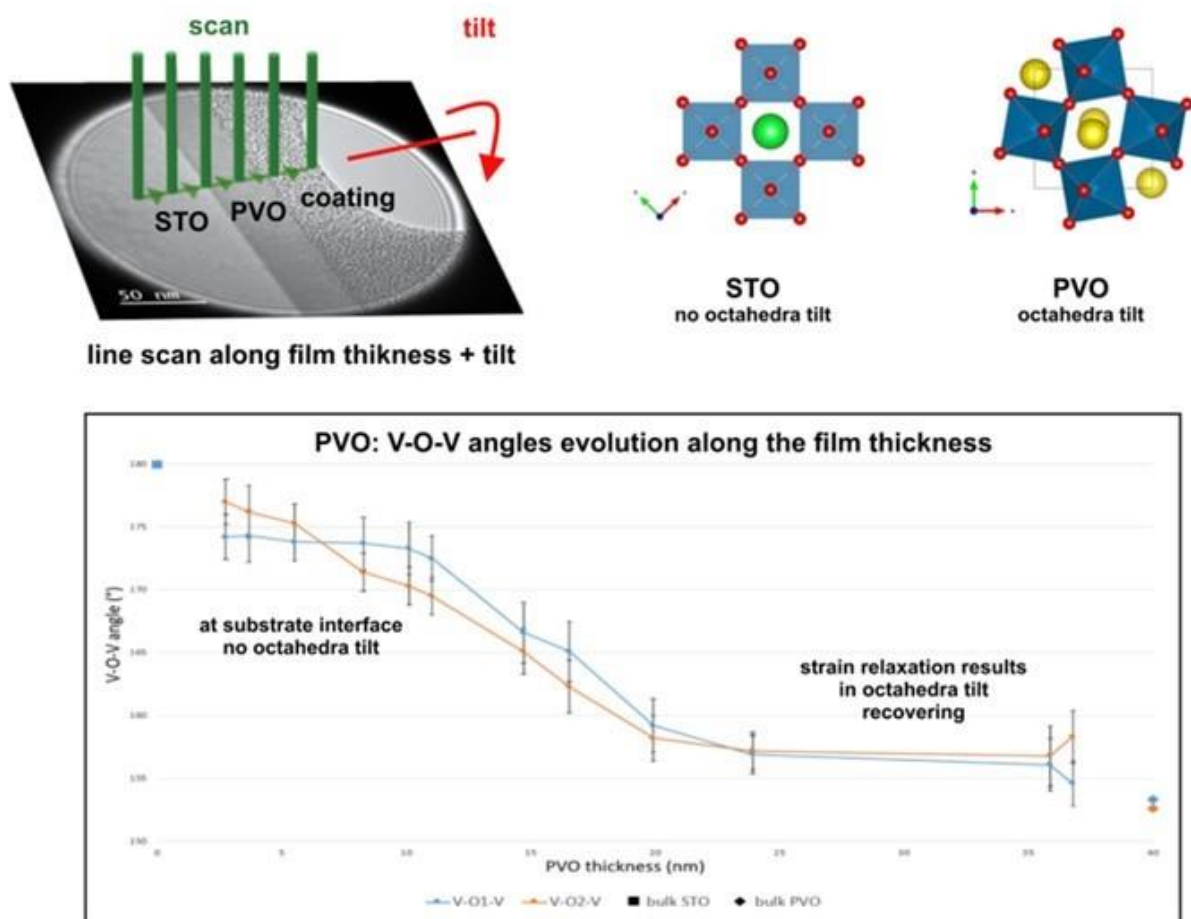


*Figure 1: Upper left: TEM image of the thin film cross section. The electron nanobeam is represented in green while scanning along the thickness of the film. Upper right: Bulk structure of STO and PVO. When clamped to STO, PVO film is expected to be strain resulting in a strong reduction of the amplitude of the  $\text{VO}_6$  octahedra. Lower part: using SPET, it is possible to analyze small changes in a structure of PVO (here octahedral tilting) along the thickness of the film with a spatial resolution about 10nm.*

## **Symposium commun 4 (SC4) : Avancées instrumentales**

***Animation :***

*Francisco de la Peña (UMET, Lille)*

*Patrick Bron (CBS, Montpellier)*

## SC4 – Inv1

### Reaching atomic resolution on biological sample by cryo-EM

- Alexandre Durand \* ([duranda@igbmc.fr](mailto:duranda@igbmc.fr)), Nils Marechal (marechan@igbmce.fr) / Integrated Structural Biology Platform- Electron Microscopy, IGBMC (Illkirch-Graffenstaden, France)
  - Corinne Crucifix ([crucifix@igbmc.fr](mailto:crucifix@igbmc.fr)) / Group of Patrick Schultz & Integrated Structural Biology Platform- Electron Microscopy, IGBMC (Illkirch-Graffenstaden, France)
- \* Corresponding author

Over the past ten years and since the beginning of the Resolution Revolution [1], the number of structures deposited in databases solved by cryo-electron microscopy (cryo-EM) has been increasing exponentially, while in parallel, the resolution that could be routinely achieved has constantly improved [2]. A few years ago, due to the latest technological development in the electron microscopes, the atomic resolution barrier has been crossed by single particle analysis (SPA) [3-4], while molecular mechanisms could be revealed directly in cells at atomic level [5].

As a national and European infrastructure, the Cryo-EM Facility of INSTRUCT Centre France1 (IGBMC) offers access to the equipment and services for structure determination by cryo-EM to the structural biology community, either by SPA or cryo-Tomography. The facility is the first one in France to house a Titan Krios G4, equipped with the latest available technologies to achieve atomic resolution on biological sample. The G4 is the first generation of Titan Krios to be equipped with a Cold-FEG, having lower energy spread, for improves signal-to-noise ratio at high resolution. It is also equipped with a more stable energy filter, the Selectris X, as well as the latest generation of direct electron detector, the Falcon 4i. This microscope is thus able to achieve atomic resolution on biological sample such as Apoferritin. The Titan Krios is setup for fringe-free illumination and aberration-free image shift, in order to maximize data acquisition rate during SPA and Tomography data collection.

While tremendous improvements in the transmission electron microscopes have been made, the sample preparation is very often the limiting factor in the workflow of structure determination by cryo-EM. Indeed, the old blot-plunging approach has been used for decades and the Vitrobot is still the vitrification standard for cryo-EM. However, this method causes interaction of the sample with the air-water interface that is formed during freezing, due to the long incubation time of the sample on the grid [6]. This leads to preferential orientation of the sample, or sample denaturation, which are both detrimental for the final reconstruction. In order to alleviate this issue, we have implemented on the facility two new approaches for sample preparation. The Chameleon is a vitrification robot which aims at limiting the time the sample is exposed to the air-water interface by a new, blot-less, fast plunging of the grid in the ethane. This approach has been shown to improve protein stability in some cases [7]. For challenging sample, or sample of low concentration, Streptavidin Affinity Grid has been developed as an on-grid capture method [8]. It allows the concentration of low abundance samples, as well as increased stability. Eventually, for cellular tomography, the facility is equipped with an Auriga 60 FIB-SEM, allowing the milling of biological material to produce thin lamellas, making possible the observation of cellular components and their contents at high resolution with the Titan Krios.

- [1] Werner Kühlbrandt ,The Resolution Revolution Science 343,1443-1444(2014). DOI:10.1126/science.1251652
- [2] Yoshiyuki Fukuda et al, Microscopy, 72(2) 135–143, 2023 <https://doi.org/10.1093/jmicro/dfac053>
- [3] Nakane, T et al. Single-particle cryo-EM at atomic resolution. Nature 587, 152–156 (2020). <https://doi.org/10.1038/s41586-020-2829-0>
- [4] Yip, K.M et al. Atomic-resolution protein structure determination by cryo-EM. Nature 587, 157–161 (2020). <https://doi.org/10.1038/s41586-020-2833-4>
- [5] Xue, L. et al. Visualizing translation dynamics at atomic detail inside a bacterial cell. Nature 610, 205–211 (2022). <https://doi.org/10.1038/s41586-022-05255-2>
- [6] Edoardo D'Imprima et al eLife 8:e42747 (2019) <https://doi.org/10.7554/eLife.42747>
- [7] Noble AJ et al.. Nat Methods. 2018 15(10):793-795. doi: 10.1038/s41592-018-0139-3
- [8] Marechal, N. et al.. Nat Commun 13, 2380 (2022). <https://doi.org/10.1038/s41467-022-30082-4>

**Mots-clés/Keywords:** TEM, Cryo-EM, Titan Krios G4, Single-Particle Analysis, Cryo-Tomography, Sample preparation

## SC4 – Inv2

# Recent developments in time-resolved spectroscopies in a continuous-gun electron microscope

- **Yves Auad** ([yves.maia-auad@universite-paris-saclay.fr](mailto:yves.maia-auad@universite-paris-saclay.fr)) / Université Paris-Saclay, CNRS, Laboratoire de Physique des Solides, Orsay, France
- **Nadezda Varkentina** / Université Paris-Saclay, CNRS, Laboratoire de Physique des Solides, Orsay, France
- **Steffi Woo** / Université Paris-Saclay, CNRS, Laboratoire de Physique des Solides, Orsay, France
- **Jean-Denis Blazit** / Université Paris-Saclay, CNRS, Laboratoire de Physique des Solides, Orsay, France
- **Xiaoyan Li** / Université Paris-Saclay, CNRS, Laboratoire de Physique des Solides, Orsay, France
- **Alberto Zobelli** / Université Paris-Saclay, CNRS, Laboratoire de Physique des Solides, Orsay, France
- **Laura Bocher** / Université Paris-Saclay, CNRS, Laboratoire de Physique des Solides, Orsay, France
- **Mike Walls** / Université Paris-Saclay, CNRS, Laboratoire de Physique des Solides, Orsay, France
- **Odile Stéphan** / Université Paris-Saclay, CNRS, Laboratoire de Physique des Solides, Orsay, France
- **Mathieu Kociak** / Université Paris-Saclay, CNRS, Laboratoire de Physique des Solides, Orsay, France
- **Luiz Tizei** / Université Paris-Saclay, CNRS, Laboratoire de Physique des Solides, Orsay, France
- **Francisco de la Peña** / Université de Lille, Unité Matériaux et Transformations, Lille, France
- **Marcel Tencé** / Université Paris-Saclay, CNRS, Laboratoire de Physique des Solides, Orsay, France

The scanning transmission electron microscope (STEM) has been profoundly transformed in the last years by the advent of a new generation of instrumental developments, such as sub-5 meV electron energy loss spectroscopy (EELS), and in photon-electron spectroscopies, such as cathodoluminescence and electron energy-gain spectroscopy. Additional STEM instrumentation is in progress, and, in particular, time-resolved experiments can be critical for accessing further physical information from the sample. In this seminar, we begin discussing the recently-developed acquisition scheme using the event-based Timepix3 direct electron detector (providing sub 5 ns temporal resolution) as our EELS detector. Besides important instrumental progress, such as readout-free hyperspectral image [1], we have also developed a new type of time-correlated experiments based on temporal coincidences between inelastic electron scattering and photon emission events. This technique, called cathodoluminescence excitation spectroscopy (CLE), is capable of unveiling the excitation pathways in the sample, circumventing one of the major limits for EELS spectroscopy, i.e., the broadband nature of the energy exchange between a fast electron and matter [2]. In the second part of the seminar, we discuss a conceptually similar experiment, time correlating inelastically scattered electrons with injected photon events. In this case, electrons can undergo a stimulated energy gain or loss of energy [3], a process primarily well-known as photon-induced near-field electron microscopy (PINEM). We show that by rastering the laser wavelength synchronized with a typical EELS acquisition, electron spectroscopy with a spectral resolution down to a few micro eVs can be successfully performed [4].

## References

- [1] Auad, Y., et al. Ultramicroscopy 239 113539 (2022)
- [2] Varkentina, N. and Auad, Y., et al. Science advances 8 40 (2022)
- [3] F. J. García de Abajo and M. Kociak. New Journal of Physics 10 073035 2008
- [4] Y. Auad, et. al. Nature Communications. In press (2023)

**SC4 – Oral1****Holographie électronique automatisée avec détection directe  
DIRECT ELECTRON DETECTION FOR AUTOMATED ELECTRON  
HOLOGRAPHY**

- **Martin HYTCH** \* (martin.hytch@cemes.fr) / CEMES-CNRS, 15 rue Jeanne Marvig, 31055 Toulouse
- **Cécile MARCELOT** / CEMES-CNRS, 15 rue Jeanne Marvig, 31055 Toulouse
- **Christophe GATEL** / CEMES-CNRS and Université de Toulouse, Toulouse

\* Auteur correspondant

Electron holography can measure electric, magnetic and strain fields. In the off-axis configuration, the phase of the electron wave interacting with the specimen is measured with respect to a reference wave passing through the undisturbed vacuum. The precision of the measurement depends on the visibility of the hologram fringes and the number of electrons contributing to the signal. We will present two ways of maximising sensitivity: acquiring holograms over very long exposure times through automation and improving the detective quantum efficiency (DQE) of the camera.

Exposure times are limited by instabilities. We have developed dynamic automation of the microscope to stabilize the position of the specimen and the hologram fringes [1]. Images from the camera are analysed continuously and in real-time using dedicated scripts running in Digital Micrograph (Gatan) (Fig. 1). Two processes run in parallel to control the specimen position and the hologram fringes independently.

To test the improvement, a series of stabilised holograms were taken, accumulating the dose over time (Fig. 2a). The standard deviation of the phase in a region of vacuum serves as our estimate of the phase error. As expected the phase precision improves over time (Fig. 2b). Holograms were acquired on a scintillator-coupled CMOS camera (OneView, Gatan) and a direct detection device (DDD) (K3, Gatan), under identical conditions. The improvement in the precision is spectacular for direct detection. The exposure time could be reduced by an order of magnitude for the same precision according to counting statistics. However, in both cases, the phase error reaches a plateau, with little improvement beyond a certain dose.

We will discuss these results in terms of the characteristics of the detectors and recent theory [2].

[1]C. Gatel, J. Dupuy, F. Houdellier, M.J. Hÿtch, Appl. Phys. Lett. 113 (2018), p. 133102.

[2]M.J. Hÿtch and C. Gatel, Microscopy 70 (2021), p. 47.

The authors thank the Conseil Régional Midi-Pyrénées and the European FEDER for financial support within the CPER program Occi'TEM. The research leading to these results has received funding from the European Union Horizon 2020 research and innovation program under Grant Agreement No. 823717-ESTEEM3.

**Mots clefs :** DIRECT DETECTION, AUTOMATISATION, ELECTRON HOLOGRAPHY

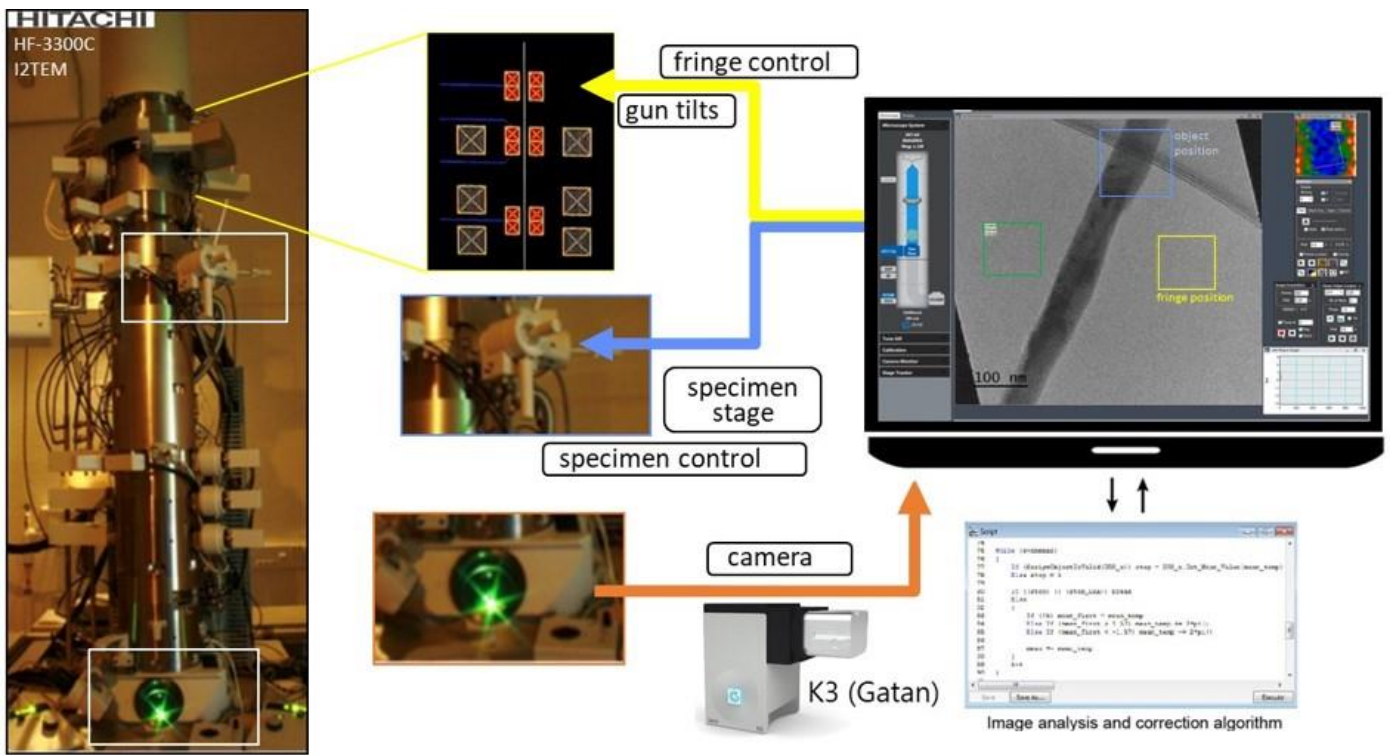


Figure 1: Automatic stabilisation of position of specimen and hologram fringes

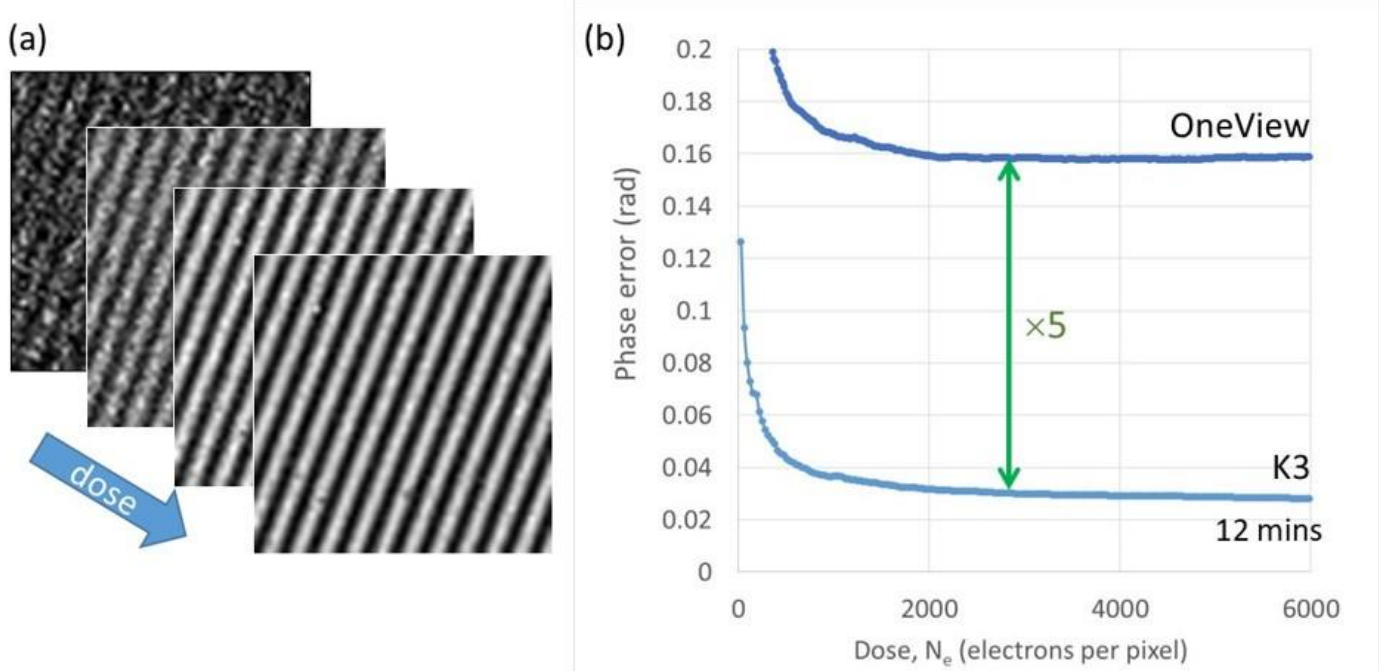


Figure 2: Measuring phase sensitivity: (a) automatically acquired hologram series; (b) phase error as a function of electron dose. Holograms were acquired on CMOS (OneView, Gatan) and DDD (K3, Gatan) cameras.

**SC4 – Oral2****Corrélation entre la structure et les propriétés optiques d'une hétérostructure complexe III-N à l'aide d'une Sonde Atomique Photonique**

**Correlating structure and optical properties of a complex III-Nitride heterostructures with A Photonic Atom Probe**

- **Eric Maximilian Weikum** \* (eric.weikum1@univ-rouen.fr) / Groupe de Physique des Matériaux, CNRS, University of Rouen Normandie, 76000 Rouen, France.
- **Abraham Diaz Damian** / Groupe de Physique des Matériaux, CNRS, University of Rouen Normandie, 76000 Rouen, France.
- **Jonathan Houard** / Groupe de Physique des Matériaux, CNRS, University of Rouen Normandie, 76000 Rouen, France.
- **Gérald Da Costa** / Groupe de Physique des Matériaux, CNRS, University of Rouen Normandie, 76000 Rouen, France.
- **Fabien Delaroche** / Groupe de Physique des Matériaux, CNRS, University of Rouen Normandie, 76000 Rouen, France.
- **Grzegorz Muziol** / Institute of High Pressure Physics of the Polish Academy of Sciences "UNIPRESS", 01-142, Warszawa, Poland.
- **Henryk Turski** / Institute of High Pressure Physics of the Polish Academy of Sciences "UNIPRESS", 01-142, Warszawa, Poland.
- **Angela Vella** / Groupe de Physique des Matériaux, CNRS, University of Rouen Normandie, 76000 Rouen, France.
- **Lorenzo Rigutti** / Groupe de Physique des Matériaux, CNRS, University of Rouen Normandie, 76000 Rouen, France.

\* Auteur correspondant

The Photonic Atom Probe (PAP)-technique [1] allows for measuring the Photoluminescence (PL) signal of a nanoscale needle-shaped specimen while it is analyzed in Laser-assisted Atom Probe Tomography (La-APT). The method exploits fs-laser pulses for both triggering the specimen's field evaporation and for generating the electron-hole pairs whose recombination causes the PL signal. The obtained data allow to correlate [2] the chemical information with near-atomic resolution with the PL spectra, which are being obtained during the tip's evaporation process.

Such a correlated measurement was performed on a relatively thick semiconductor (GaN-based) heterostructure [3] ( $\approx 2$  nm), which contains a tunnel junction (TJ) [4] and a p-i-n-junction. These two regions contain InGaN sections and doped zones.

By comparing these structural informations to the obtained PL spectra, the evolution of the measured PL signal as a function of the specimen's field evaporation progress can be obtained. The modulation of the optical signals emitted from the specimen can be traced back to the evaporation of localized emitters as well as to the development of the mechanical stress during the APT measurement [5]. A systematic correlation between the APT and PL allows discriminating the origins of the different components of the PL spectra. In particular, it becomes possible to discriminate between donor-acceptor pair (DAP) transitions occurring within the Mg-doped section and transitions taking place within the InGaN sections, even though the PL components are spectrally strongly superimposed.

#### Références/References :

- [1] J. Houard et al., Rev. of Sci. Instr., 91.8 (2020), p. 083704.
- [2] E. Di Russo et al., Nano Lett., 20 (2020), 12, pp. 8733–8738.
- [3] H. Turski, et al., ECS J. Solid State Sci. Technol., 9 (2020), p. 015018.
- [4] L. Esaki, Phys. Rev. 109 (1958), p. 603
- [5] P. Dalapati et al., Phys. Rev. Appl., 15.2 (2021), p. 024014.

**Mots clefs** : Atom Probe, Photoluminescence, Instrumentation

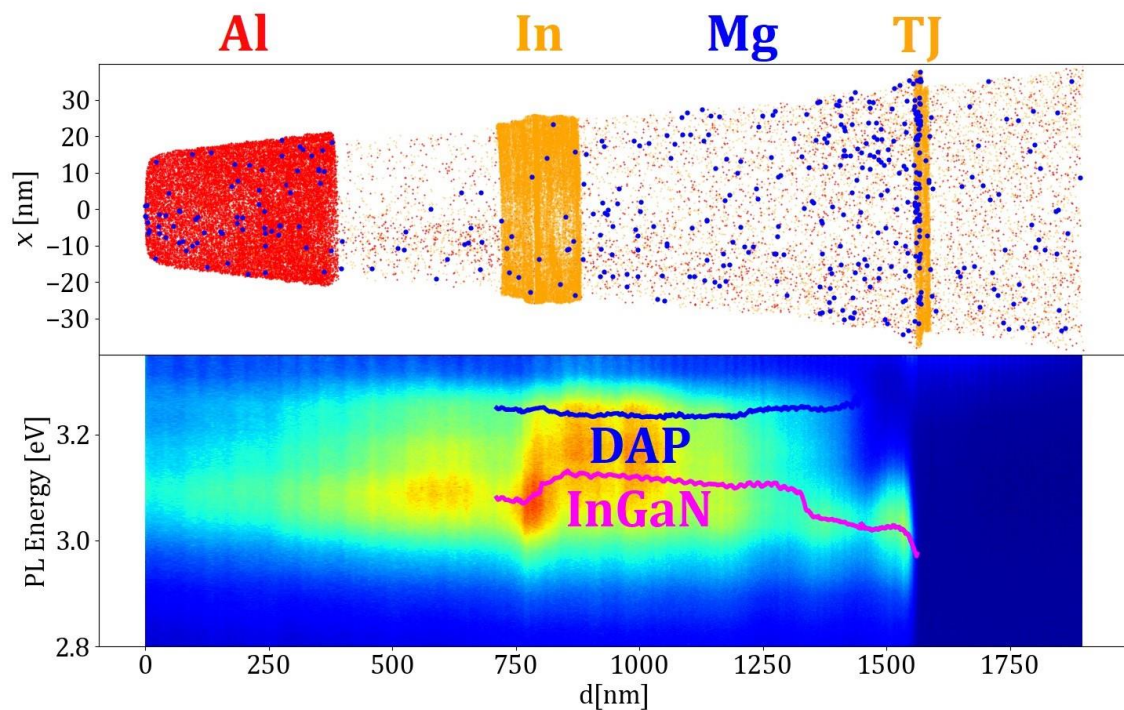


Figure 1: Correlation between the APT reconstruction and the recorded PL spectra. The PL signals shown here are emitted from donor-acceptor-pairs (DAP) as well as from the band-gap-modulation by alloying In into GaN (InGaN).

## SC4 – Oral3

### Une nouvelle méthodologie pour déterminer la chimie du rayonnement de la glace d'eau et des interfaces eau-solide en microscopie électronique

A new methodology to determine the radiation chemistry of water ice and water-solid interfaces in electron microscopy

- **Patricia Abellan \*** (patricia.abellan@cnrs-imn.fr) / Nantes University, Institut des Materiaux de Nantes Jean Rouxel (IMN), CNRS, Nantes, France
- **Eric Gautron** / Nantes University, Institut des Materiaux de Nantes Jean Rouxel (IMN), CNRS, Nantes, France
- **Jay LaVerne** / Radiation Laboratory and Department of Physics and Astronomy, University of Notre Dame, Notre Dame, Indiana, USA

\* Auteur correspondant

All transmission electron microscopes are now capable of probing hydrated samples and solid-water interfaces by using dedicated cryo- and liquid holders. However, these experiments are severely limited, and in many cases impeded by the sensitivity of the samples to the action of the electron beam. Considerable research efforts have been made toward the development of instrumentation and approaches for minimizing the electron dose used and maximizing the information content for a given dose. Despite these technical advances, many samples and processes in hydrated environments cannot currently be investigated in electron microscopes due to radiation damage.

The decomposition of water by high energy electrons is well known in the radiation chemistry community, which routinely uses this knowledge to minimize, prevent or utilize the chemical effects of irradiation in materials. Some of these approaches have been tested in the electron microscope with limited impact, thus suggesting that the radiolysis of water in electron microscopy most likely differ from what is widely accepted in conventional radiation chemistry experiments. Methods to study radiolysis in electron microscopy are needed, however determining chemical species and yields by performing ex-situ (post-mortem) analysis is not currently possible, since: 1) radical and molecular species produced in the radiolysis of water are typically short-lived, 2) the doses and dose rates used in electron microscopes are orders of magnitude larger than those possible in current electron accelerators and 3) the presence of interfaces can change production yields and chemical rates. Alternative in situ methods for the determination of radiation-induced radicals and molecular species are therefore sought. In this presentation, we will present an innovative methodology to determine in situ all radiolysis products of water ice (except for H<sub>2</sub> and •H) and apply it to the study of the radiolysis of water in the electron microscope and at water-solid interfaces. We perform dosimetry using EELS at the oxygen K-edge in ice films and interfaces with controlled thickness variation. A new high-dose reaction scheme is proposed. The significance of our results with respect to the radiolysis of water ice and for electron microscopy studies will be also discussed.

**Mots clefs :** Method development, radiation chemistry, cryo-EELS, high-dose regime, water-solid interfaces, radiation damage, dosimetry

**SC4 – Oral4****Bâtonnets magnétiques comme sondes pour la microrhéologie active : applications au cytoplasme des cellules vivantes et aux fluides corporels extracellulaires****Magnetic wires as probes for active microrheology: applications to the cytoplasm of living cells and extracellular body fluids****Jean-François Berret \*** (jean-francois.berret@u-paris.fr) / Université Paris Cité / CNRS

\* Auteur correspondant

In living environments, biological materials are often in a crowded state. Crowding has a strong impact on biological functions, as it restrains molecular motion, affects the flow and induces viscoelasticity. Here we address the question of the mechanical properties of living cells using a microrheology platform based on the video-microscopy tracking of magnetic wires. Wires are submitted to an external magnetic field of increasing frequencies. Extensive measurements performed on three cells lines confirm the viscoelastic character of the cytoplasm. With this microrheology platform, we also study on the effect of inhaled nanoparticles on extracellular body fluids, in particular on lung fluids and show that their bulk viscosity can be strongly affected by nanomaterials. The present work demonstrates the potential of this microrheology technique as an accurate tool to explore biological soft matter dynamics.

**Related References**

- J.-F. Berret, Local viscoelasticity of living cells measured by rotational magnetic spectroscopy, *Nat. Commun.*, 7 (2016) 10134  
L.-P.-A. Thai et al., Effect of Nanoparticles on the Bulk Shear Viscosity of a Lung Surfactant Fluid *ACS Nano*, 14 (2020) 466-475  
M. Radiom et al., Magnetic Wire Active Microrheology of Human Respiratory Mucus, *Soft Matter*, 17 (2021) 7585-7595.

**Mots clefs** : microrheology cytoplasm body fluids

## **SDM1 : Imagerie volumique, cartographie de propriétés et approches corrélatives**

***Animation :***

*Isabelle Mouton (SIMAP, Grenoble)*

*Karine Masenelli-Varlot (MATEIS, Lyon)*

## SDM1 – Inv1

### Towards the Re-design of interfaces in energy materials

- **Oana Cojocaru-Mirédin \*** ([oana.cojocaru-miredin@inatech.de](mailto:oana.cojocaru-miredin@inatech.de)) / INATECH, University of Freiburg, Emmy-Noether-straße 2, 79110
- **Mohit Raghuvanshi** ([raghuvanshi@physik.rwth-aachen.de](mailto:raghuvanshi@physik.rwth-aachen.de)) / I. Institute of Physics, RWTH Aachen, Sommerfeldstraße 14, 52074 Aachen
- **Yuan Yu** ([yu@physik.rwth-aachen.de](mailto:yu@physik.rwth-aachen.de)) / I. Institute of Physics, RWTH Aachen, Sommerfeldstraße 14, 52074 Aachen

\* Corresponding author: Oana Cojocaru-Mirédin

Very often the presence of internal interfaces in energy devices such as solar cells, thermoelectrics and batteries limits devices performance. Numerous studies are available in literature where the bulk properties of energy materials can be designed to meet specific properties. However, this is not easily the case for the internal interfaces. This is mainly due to the difficulty to determine the specific properties of these internal interfaces. This research gap has hindered the Re-Design of internal interfaces with outstanding properties much needed for empowered energy devices.

Atom probe tomography (APT) and correlative microscopy & techniques, i.e. a combination of atom probe tomography with other (microscopy) techniques, is making considerable progress into the nanocharacterization of these energy materials[1],[2],[3],[4]. This opens now the possibility to answer long-standing questions in material science (see example Figure 1) and to provide clear design strategies for synthesising internal interfaces with superior properties. Therefore, this presentation will show a selection of several studies including the study of grain boundaries in standard energy materials.

Finally, this talk will demonstrate how the device performance can be manipulated by the correlations between structure and property down to interface level providing a novel bottom-to-top strategy for the material design.

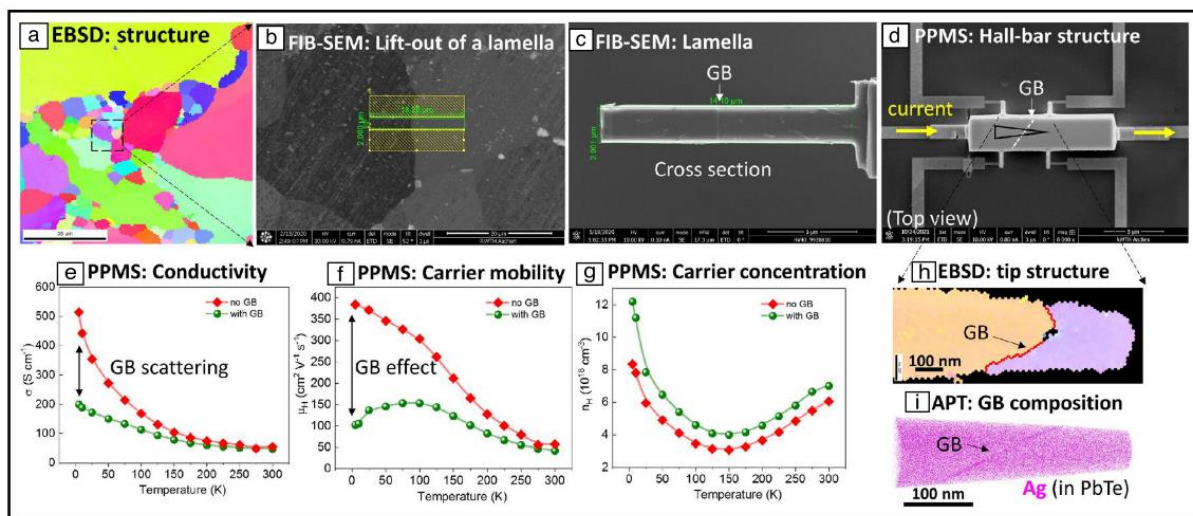


**Figure 1.** Example of a direct correlation between the grain boundary composition with their respective structure and transport in PbTe thermoelectrics. For more information consult ref.[5].

#### Bibliography:

- [1] O. Cojocaru-Mirédin, M. Raghuvanshi, R. Wuerz, and S. Sadewasser, “Grain Boundaries in Cu(In, Ga)Se<sub>2</sub>: A Review of Composition–Electronic Property Relationships by Atom Probe Tomography and Correlative Microscopy,” *Adv. Funct. Mater.*, vol. 31, no. 41, 2021, doi: 10.1002/adfm.202103119.
- [2] M. Raghuvanshi, R. Wuerz, and O. Cojocaru-Mirédin, “Interconnection between Trait, Structure, and Composition of Grain Boundaries in Cu(In,Ga)Se<sub>2</sub> Thin-Film Solar Cells,” *Adv. Funct. Mater.*, vol. 30, no. 31, pp. 1–9, 2020, doi: 10.1002/adfm.202001046.
- [3] C. H. Liebscher *et al.*, “Strain-Induced Asymmetric Line Segregation at Faceted Si Grain Boundaries,” *Phys. Rev. Lett.*, vol. 121, no. 1, pp. 1–5, 2018, doi: 10.1103/PhysRevLett.121.015702.
- [4] O. Cojocaru-Mirédin, J. Schmieg, M. Müller, A. Weber, E. Ivers-Tiffée, and D. Gerthsen, “Quantifying lithium

enrichment at grain boundaries in Li<sub>7</sub>La<sub>3</sub>Zr<sub>2</sub>O<sub>12</sub> solid electrolyte by correlative microscopy," *J. Power Sources*, vol. 539, no. January, 2022, doi: 10.1016/j.jpowsour.2022.231417.

[5] O. Cojocaru-Mirédin and A. Devaraj, "Correlative microscopy and techniques with atom probe tomography: Opportunities in materials science," *MRS Bull.*, vol. 47, no. 7, pp. 680–687, 2022, doi: 10.1557/s43577-022-00369-4.

**Mots-clés/Keywords:** energy materials, Re-Design of internal interfaces, atom probe tomography, correlative microscopy & techniques

## SDM1 – Inv2

### Dernière avancée en tomographie électronique en transmission des dislocations

#### Recent development in dislocation transmission electron tomography

Alexandre Mussi \* (alexandre.mussi@univ-lille.fr) / Univ. Lille, CNRS, INRAE, Centrale Lille, UMR 8207 - UMET –

Unité Matériaux et Transformations, F-59000 Lille, France

\* Auteur correspondant

L'imagerie de dislocations est obtenue par contraste de diffraction qui est extrêmement sensible à l'orientation. Parvenir à conserver un contraste de dislocation constant pour différentes orientations est un exercice particulièrement délicat. C'est pourquoi, il a fallu attendre 2006 pour que la première tomographie électronique en transmission de dislocations puisse être réalisée [1] alors que les premières tomographies conventionnelles datent de la fin des années 60 [2].

Nous avons récemment développé la tomographie des dislocations à faible nombre d'images à l'Université de Lille [3]. Cette technique permet d'effectuer des acquisitions tomographiques rapides nous laissant entrevoir la possibilité d'effectuer de la tomographie lors d'essais in-situ.

Dans cette étude, nous avons suivi l'évolution des microstructures 3D de dislocations d'un monocristal de MgO préalablement déformé à 1500°C sous une pression de confinement de 10 GPa. Les caractérisations par microscopie électronique en transmission ont été menées à l'aide d'un porte-objet chauffant double-tilt. L'association de la température et de l'irradiation électronique fait évoluer les géométries de dislocations en tours d'hélices.

Cette première étude 4D de dislocations [4] nous permet d'analyser les premières étapes de l'évolution en tour d'hélice des dislocations (Figure 1).

Pour aller plus loin, nous sommes actuellement en cours de développement de l'association de la tomographie électronique en transmission des dislocations à la mécanique des milieux continus.

#### Références :

- [1]Barnard, J.S., Sharp, J., Tong, J. R., Midgley, P.A., High-resolution three-dimensional imaging of dislocations, *Science*, 313 (2006), p.319.
- [2]De Rosier, D. J., Klug, A., Reconstruction of three-dimensional structures from electron micrographs, *Nature*, 217 (1968), p.130.
- [3]Mussi, A., Gallet, J., Castelnau, O., Cordier, P., Application of electron tomography of dislocations in beam-sensitive quartz to the determination of strain components, *Tectonophysics*, 803 (2021), 228754.
- [4]Mussi, A., Carrez, P., Gouriet, K., Hue, B., Cordier, P., 4D electron tomography of dislocations undergoing electron irradiation, *Comptes Rendus. Physique* 22 (2021), p. 67-81.

**Mots clefs :** Dislocation ; Tomographie électronique ; 4D ; Irradiation électronique ; MgO

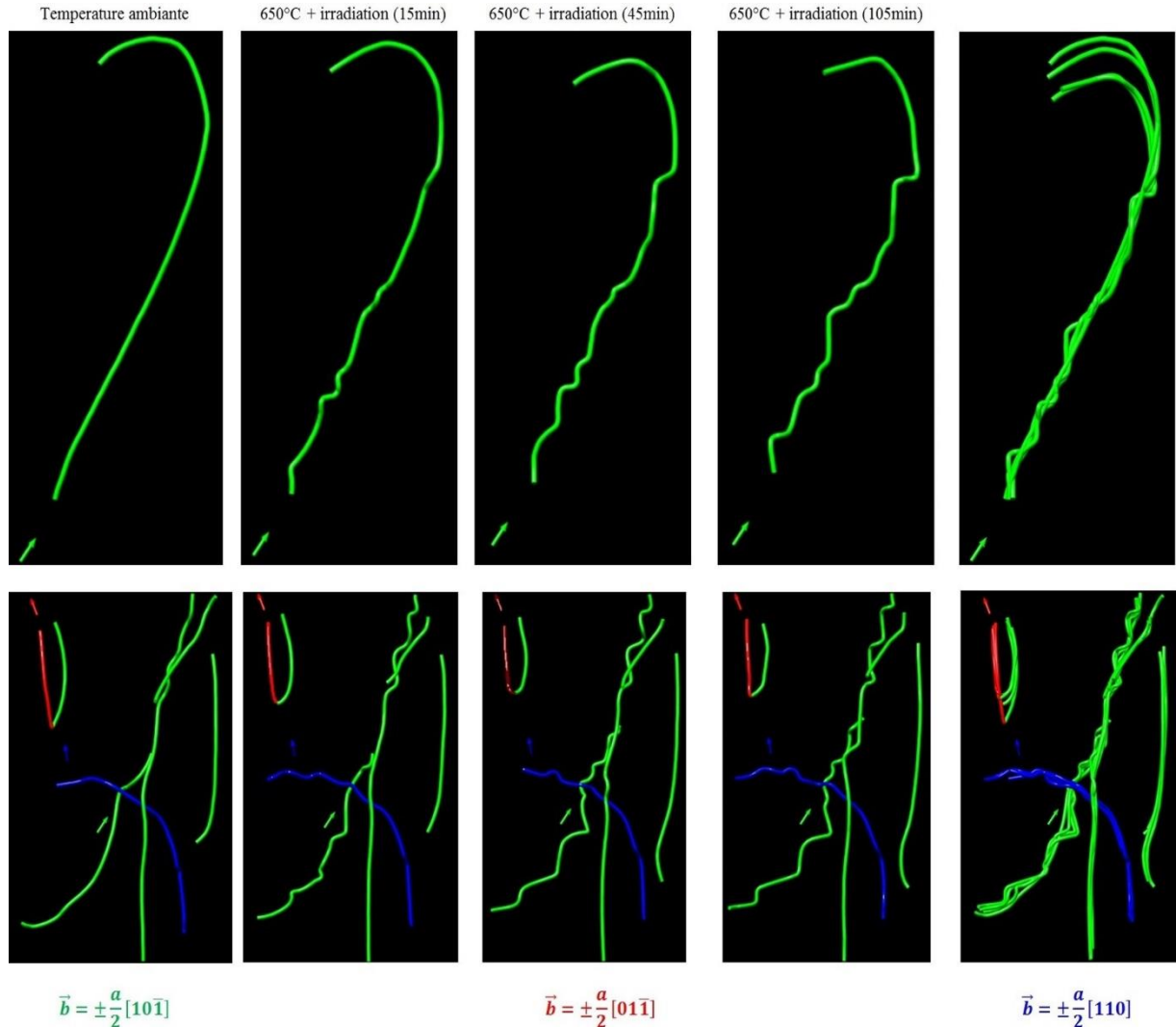


*Figure 1 : Evolution de la géométrie des dislocations par irradiation électronique pour différentes durées d'irradiation à 650°C (le code couleur fait référence aux vecteurs de Burgers).*

## SDM1 – Oral1

### Deep learning for limited-angle electron tomography

#### Deep learning for limited-angle electron tomography

- **Serge Brosset** / Univ. Grenoble Alpes, CEA, LETI, Grenoble F-38000, France
- **Guillaume Biagi** / Univ. Grenoble Alpes, CEA, LETI, Grenoble F-38000, France
- **Philippe Ciuciu** / Univ. Paris Saclay, CEA-NeuroSpin, INRIA, Parietal, Gif-sur-Yvette, F-91191, France
- **Zineb Saghi** \* (zineb.saghi@cea.fr) / Univ. Grenoble Alpes, CEA, LETI, Grenoble F-38000, France

\* Auteur correspondant

Electron tomography (ET) plays an important role in the three-dimensional (3D) characterization of nanomaterials. However, for slab-like specimen geometries, projections are often acquired within a limited angular range. In these conditions, ET reconstructions suffer from blurring and distortions (also called ‘missing wedge’ artefacts), which affect significantly the final resolution and the reliability of measurements. Compressed sensing (CS) approaches were recently introduced to overcome the limitations of classical reconstruction algorithms under limited data acquisition conditions [1]. While CS has demonstrated its superior performance for sparse-view acquisitions over the full tilt range, the reconstructions still suffer from artefacts under limited-angle conditions [2-3].

In this work, we propose a deep learning (DL) approach to improve the quality of limited-angle ET reconstructions. We chose a deep neural network with U-Net architecture composed of four convolutional layers. A highly-sampled experimental dataset, consisting of 180 STEM-HAADF projections of a needle-shaped sample [1], was used to train the model. Simultaneous iterative reconstruction technique (SIRT) was applied to generate the reference images obtained with the complete dataset (-90°:1°:90°), and the degraded ones obtained with an incomplete dataset (-60°:1°:60°). 500 2D reconstructions through the sample were used for the training of the DL model, and 50 for the validation step. The obtained DL model was then applied to improve the reconstruction of a 2D slice, unseen during training.

Figure 1(a) shows the SIRT reconstruction obtained with the full tilt range, and figure 1(b) the one affected by the missing wedge artefacts. CS with total variation minimization (CS-TV) improves slightly the quality of the reconstruction, but the blurring and feature elongation are still present (figure 1(c)). Figure 1(d) shows the restored image obtained with the DL approach. Compared to SIRT and CS, DL succeeds in retrieving fine details and correcting for the distortions of the pores and the overall needle. We also extracted the PSNR (peak signal-to-noise ratio) and SSIM (structural similarity index measure) values of the images, using the fully-sampled SIRT reconstruction (figure 1 (a)) as ground truth. A significant increase in both metrics is obtained with DL, suggesting that data-driven approaches are promising alternatives to model-based reconstruction methods.

**Mots clefs :** electron tomography, microscopy, deep learning, nanomaterials

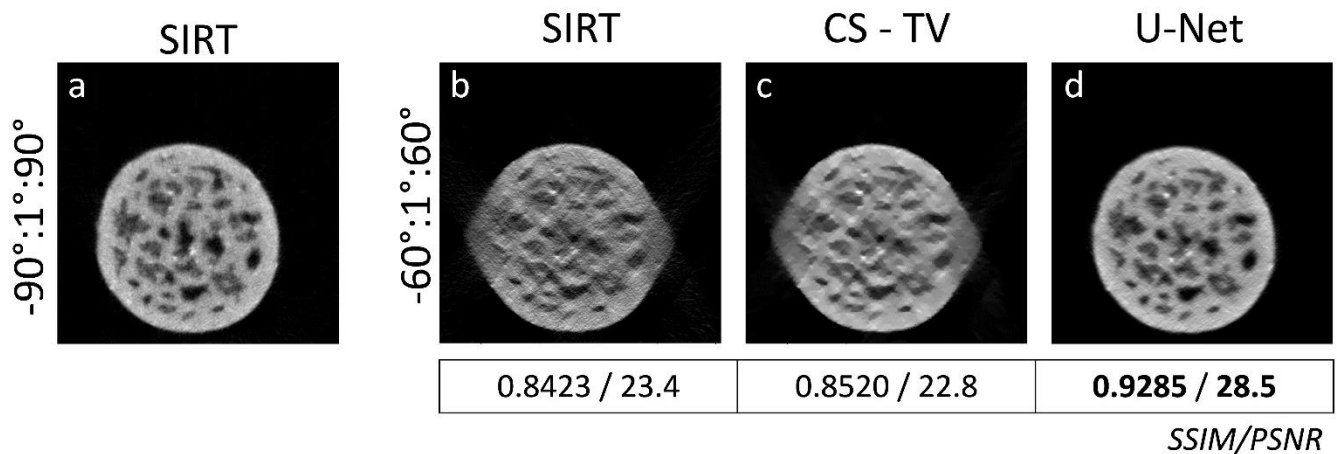


*Figure 1: (a) SIRT reconstruction of an Er-doped porous Si structure, using the full tilt range (-90°:1°:90°); (b-d) SIRT, CS-TV and DL reconstruction of the same slice using a limited tilt range (-60°:1°:60°). The SSIM and PSNR metrics are shown below each image.*

## SDM1 – Oral2

### Vers les cartographies d'orientations aux basses tensions

#### Toward low voltage orientation mapping

- **L'HÔTE Gabriel** \* (gabriel.l-hote@insa-lyon.fr) / Univ Lyon, INSA Lyon, UCBL, CNRS, MATEIS, UMR5510, 69621 Villeurbanne, France
- **Douillard Thierry** / Univ Lyon, INSA Lyon, UCBL, CNRS, MATEIS, UMR5510, 69621 Villeurbanne, France
- **Bugnet Matthieu** / Univ Lyon, INSA Lyon, UCBL, CNRS, MATEIS, UMR5510, 69621 Villeurbanne, France
- **Cazottes Sophie** / Univ Lyon, INSA Lyon, UCBL, CNRS, MATEIS, UMR5510, 69621 Villeurbanne, France
- **Maurice Claire** / Univ Lyon, Mines Saint-Etienne, CNRS, Centre SMS, Laboratoire Georges Friedel, UMR5307, 42023, St-Etienne, France
- **Langlois Cyril** / Univ Lyon, INSA Lyon, UCBL, CNRS, MATEIS, UMR5510, 69621 Villeurbanne, France

\* Auteur correspondant

Mapping of crystalline orientations obtained by scanning electron microscopy (SEM) using the Electron Back Scattered Diffraction (EBSD) technique is crucial to obtain local information on the microstructure of polycrystalline materials. However, the interaction volume of the electrons under the sample surface and the particular geometry of EBSD experiments (70° sample tilt) limits the spatial resolution. Because it is hardly possible to obtain usable information in EBSD down to 5keV electron beam energy, some submicron features of the microstructure may not appear in the EBSD maps. Actually, electron channeling contrast can still be present at much lower voltages. This contrast is the signal used by CHORD, an innovative approach to obtain orientation maps based on the variation of the backscattered electron signal during sample rotation [1]. Orientation mapping with CHORD at very low voltages has been demonstrated using a primary beam acceleration of 1kV on alumina samples [2].

The gain in spatial resolution when working at low accelerating voltage was then studied experimentally. CHORD and EBSD experiments were carried out on metallic thin films on which a low-angle wedge has been milled from the surface of the film to the monocrystalline substrate using a Focused Ion Beam, providing a surface with controlled thickness variations (see Fig. 1). For EBSD, the interaction depth under the surface was evaluated for different accelerating voltages by monitoring the substrate contribution in Kikuchi patterns for different film thicknesses along the wedge. For CHORD, orientation maps for different accelerating voltages have been acquired on the wedge surface. The quality of the orientation map with respect to the wedge position and the accelerating voltage is used as a marker to evaluate the interaction depth for the channeling contrast.

This preliminary result paves the way to the study of samples sometimes difficult to characterize by conventional EBSD due to the submicron characteristics of the microstructure (orientation gradients, fine precipitation...).

#### References:

- [1]Lafond & al. Electron CHanneling ORientation Determination (eCHORD): An original approach to crystallineorientation mapping. Ultramicroscopy, 186 (2018), p.146-149
- [2]Lafond & al. eCHORD orientation mapping of bio-inspired alumina down to 1 kV. Materialia, 20 (2021),P.101-107

**Mots clefs :** CHORD ; Orientation ; Channeling ; Low voltage

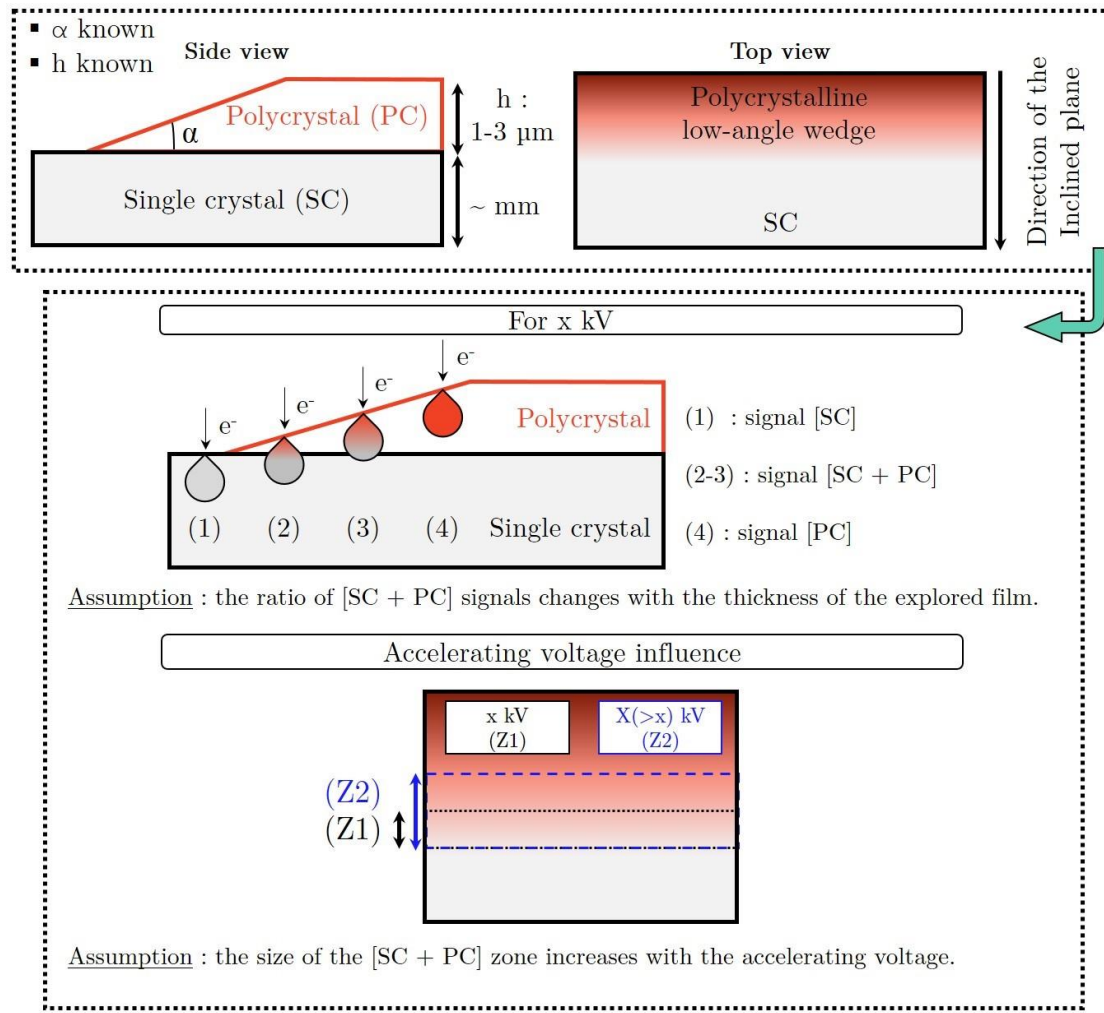


Figure 1: methodology for studying spatial resolution from an inclined plane

**SDM1 – Oral3****Magnétotaxie collective d'holobiontes microbiens révélés par cryo-SXT, STEX-XMCD et TEM****COLLECTIVE MAGNETOTAXIS OF MICROBIAL HOLOBIONTS REVEALED BY Cryo-SXT, STXM-XMCD and TEM**

- **Nicolas MENGUY** \* (Nicolas.Menguy@sorbonne-universite.fr) / IMPMC – UMR 7590 Sorbonne Université – CNRS 4, place Jussieu F-75005
- **Daniel CHEVRIER** \* (Daniel.CHEVRIER@cea.fr) / BIAM – UMR 7265 Aix-Marseille Université – CNRS – CEA / Saint-Paul-lez-Durance F-13108
- **Amélie JUHIN** / IMPMC – UMR 7590 Sorbonne Université – CNRS 4, place Jussieu F-75005
- **Christopher LEFÈVRE** / BIAM – UMR 7265 Aix-Marseille Université – CNRS – CEA / Saint-Paul-lez-Durance F-13108

\* Auteur correspondant

Over the last few decades, symbiosis and the concept of holobiont—a host entity with a population of symbionts—have gained a central role in our understanding of life functioning and diversification. Regardless of the type of partner interactions, understanding how the biophysical properties of each individual symbiont and their assembly may generate collective behaviors at the holobiont scale remains a fundamental challenge. This is particularly intriguing in the case of the newly discovered magnetotactic holobionts (MHB) whose motility relies on a collective magnetotaxis (i.e., a magnetic field-assisted motility guided by a chemoaerotaxis system) [1]. This complex behavior raises many questions regarding how magnetic properties of symbionts determine holobiont magnetism and motility. Here, a suite of light-, electron- and X-ray-based microscopy techniques reveals that symbionts optimize the motility, the ultrastructure, and the magnetic properties of MHBs from the microscale to the nanoscale [2]. The surface organization of symbionts is explicitly presented herein, depicting bacterial membrane structures that ensure longitudinal alignment of cells (figure 1). Magnetic dipole and nanocrystalline orientations of magnetosomes were also shown to be consistently oriented in the longitudinal direction, maximizing the magnetic moment of each symbiont (figure 2). In the case of these magnetic symbionts, the magnetic moment transferred to the host cell is in excess ( $\approx$  100 times stronger than free-living magnetotactic bacteria), well above the threshold for the host cell to gain a magnetotactic advantage.

**References :**

- [1]Monteil CL , Vallenet D, Menguy N, Benzerara K, Barbe V, Fouteau S, Cruaud C, Floriani M, Viollier E, AdryanczykG, Leonhardt N, Faivre D, Pignol D, Lopez-Garcia P, Weld RJ, Lefevre CT Nature Microbiology 4 (2019), p. 1088–1095
- [2]Chevrier D, Juhin A, Menguy N, Bolzoni R, Soto-Rodriguez P, Kojadinovic-Sirinelli M, Paterson G, Belkhouch R, Williams W, Skouri-Panet F, Kosta A, Le Guenno H, Pereiro E, Faivre D, Benzerara K, Monteil CL and Lefèvre CT, PNAS 120 (2023), e2216975120

**Mots clefs :** magnétotaxie, symbiose, Cryo-tomographie sur synchrotron, STXM-XMCD, approches corrélatives.

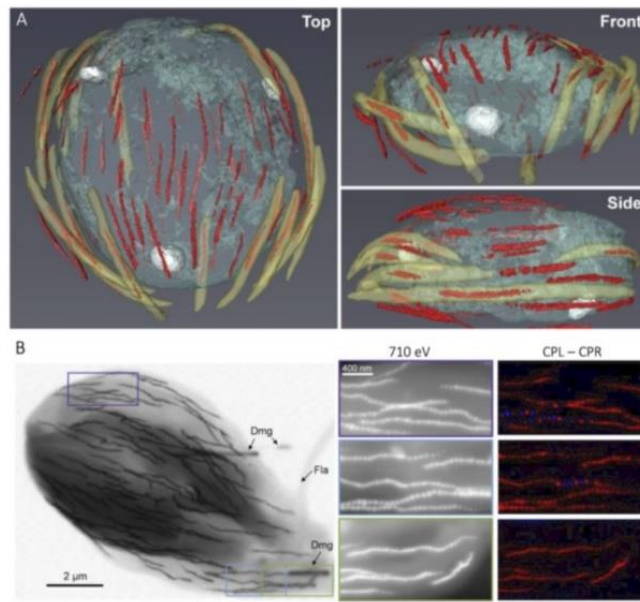


**Figure 1:** A 3-D reconstruction of vitrified MHB using cryo-SXT : magnetosome chains (red), ectosymbiotic bacteria membrane (yellow), the protistan host (cyan). B Magnetic moment orientation of magnetosomes relative to the protistan flagella using STXM-XMCD at the Fe L-edge.

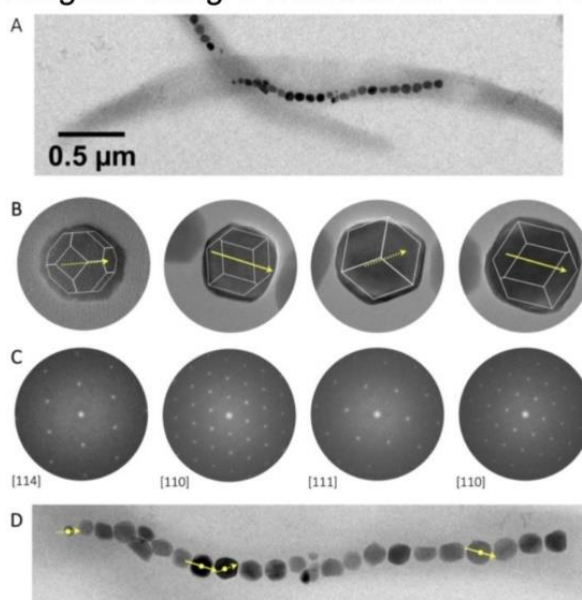


**Figure 2:** Crystallography of the prismatic/cuboctahedral magnetite particles produced by magnetic ectosymbiotic bacteria. A- TEM-BF image, B-HRTEM, C-FFT and D- the  $<111>$  direction is superimposed to the magnetosome chain (yellow arrows) showing that their easy magnetization axis.

**SDM1 – Oral4****DE L'INTÉRÊT DU COUPLAGE MET / SAT EN SCIENCES DE L'UNIVERS  
OF THE INTEREST OF THE TEM / APT COMBINATION IN THE SCIENCES OF THE UNIVERSE.**

• **Anne-Magali Seydoux-Guillaume** \* (anne.magali.seydoux@univ-st-etienne.fr) / Université Jean Monnet, CNRS, LGL-TPE, Saint Etienne, France.

• **Denis Fougerouse** / School of Earth and Planetary Sciences, Curtin University, GPO Box U1987, Perth, Australia \* Auteur correspondant

Au cours des processus géologiques variés (e.g. tectonique, altération, érosion, sédimentation, impacts), les roches (terrestres ou extraterrestres) sont affectées par des mécanismes physiques et chimiques qui laissent des traces plus ou moins visibles et durables, très souvent seulement décelables à l'échelle nanométrique, qui permettent (plus ou moins facilement) d'interpréter la dynamique planétaire. L'autre paramètre crucial, pour comprendre l'évolution planétaire et lier entre eux les événements qui ont façonné la Terre et les autres planètes, est le temps. La géochronologie, c'est à dire la datation des minéraux et par extension des roches, revêt une importance particulière, puisqu'elle permet l'accès aux durées et vitesses des différents processus en plus de l'âge absolu [1]. Pour un minéral et un système isotopique donnés, la mesure actuelle de la quantité d'élément fils produit par décroissance radioactive de l'élément père permettra de déduire l'âge de (la dernière) fermeture du système isotopique. Cette fermeture correspond le plus souvent à la cristallisation ou la transformation du minéral qui est la brique fondamentale permettant ces mesures.

A travers d'exemples choisis je montrerais comment la combinaison d'outils de pointe tels que le microscope électronique en transmission (MET), couplé à une préparation par faisceau d'ion focalisé (FIB), et la Sonde Atomique Tomographique (SAT), permet d'étudier les structures des minéraux et leurs transformations sous différentes conditions [2], les mobilités élémentaires et isotopiques, la perturbation des systèmes chronométriques [3], et ainsi préciser les mécanismes actifs à l'échelle atomique.

**Références :**

[1]Seydoux-Guillaume A.-M., et al. EPSL 595 (2019) 117727.

[2]Fougerouse D. et al. Geology 49 (4) (2021) 417–421.

[3]Turuani M.J., et al. EPSL 588 (2022) 117567

\*anne.magali.seydoux@univ-st-etienne.fr

**Mots clefs :** MET; SAT; Mineralogie; planetologie; géochronologie

## SDM2 : Microscopies *in situ, operando*

**Animation :**

*Patricia Abellan (Institut des Matériaux de Nantes Jean Rouxel – IMN, Nantes)  
Ileana Florea (CRHEA, Sophia-Antipolis)*

## SDM2 – Inv1

### Coupling *in situ/operando* TEM and simulation for a better understanding of the structure and reactivity under gas of nanomaterials

- **Jaysen Nelayah** \* (jaysen.nelayah@u-paris.fr) / Université Paris Cité, CNRS, laboratoire Matériaux et Phénomènes Quantiques
- **Abdallah Nassereddine** / Université Paris Cité, CNRS, laboratoire Matériaux et Phénomènes Quantiques (now at Institut Néel, Université Grenoble Alpes, CNRS)
- **Damien Alloyeau** / Université Paris Cité, CNRS, laboratoire Matériaux et Phénomènes Quantiques
- **Christian Ricolleau** / Université Paris Cité, CNRS, laboratoire Matériaux et Phénomènes Quantiques
- **Guillaume Wang** / Université Paris Cité, CNRS, laboratoire Matériaux et Phénomènes Quantiques
- **Laurent Delannoy** / Laboratoire de Réactivité de Surface, Sorbonne Université, CNRS
- **Catherine Louis** / Laboratoire de Réactivité de Surface, Sorbonne Université, CNRS
- **Hazar Guesmi** / ICGM, Univ. Montpellier, CNRS, ENSCM

\* Corresponding author

Catalysis by metallic nanoparticles (NPs) has been over recent years at the centre of numerous scientific and application interests. Yet, metal nanocatalysts remain substantially a 'black box' despite many efforts to understand them. In many cases, while the initial state of catalysts is known, their ever-changing atomic, electronic and chemical structures, for multimetallic NPs, in reaction conditions are elusive. Identifying the reactive structures and their reactivity at the atomic scale is critical to resolve a long-standing challenge in the field of heterogeneous catalysis - understand key structure-activity relationships for the production of more efficient catalysts beyond the trial-and-error approach. In this contribution, we will present an innovative dual experimental-numerical approach developed at MPQ laboratory aims at opening the 'black box' of heterogeneous catalysis by metals.

Our strategy combines (i) *in situ* structure tracking at the atomic scale and reactivity measurements using aberration-corrected *operando* gas TEM that couples dedicated high-pressure gas cells operating up to atmospheric pressure and/or high temperatures (< 1200 °C) with mass spectrometry, and (ii) DFT-based multiscale modelling of nanoparticle structure evolution in gas environments to identify and rationalize at the atomic scale the structural evolution and reactivity of active catalytic species. We will illustrate the unique contributions of this approach in providing fundamental atomic-scale understanding in the selective hydrogenation of 1,3-butadiene reaction by monometallic Au and bimetallic Au-Cu nanocatalysts. We will highlight the size-dependent crystal structure and morphological evolution in gold nanoparticles with loss of the face-centered cubic crystal structure of gold for particle size below 4 nm uncovered under hydrogen [1] and the unique reactivity of gold nanoparticles towards 1,3-butadiene [2]. In the hydrogenation of 1,3-butadiene by copper-gold catalysts, we will discuss the effects of gold and copper alloying on the stability and reactivity of active structures [3].

[1] A. Nassereddine et al., Small, 17(51) (2021), p.2104571

[2] A. Nassereddine et al., ChemCatChem, accepted (2023)

[2] Q. Wang et al., Faraday Discussions, 242 (2023), p.375

**Mots-clés/Keywords:** gas ETEM, operando, metal catalysts, structure, reactivity

## SDM2 – Inv2

# Quantitative electrical quantification of semiconducting (nano)materials by (S)TEM based techniques?

Bruno Cesar da Silva<sup>1</sup>, Zahra Sadre Momtaz<sup>1</sup>, Yiran Lu<sup>1</sup>, Pascale Gentile<sup>s</sup>, Eva Monroy<sup>2</sup>, David Cooper<sup>4</sup>, Jean-Luc Rouviere<sup>3</sup> and Martien I. den-Hertog<sup>1\*</sup>

1 - Univ. Grenoble Alpes, CNRS, Grenoble INP, Institut Néel, 38000 Grenoble, France

2 - Univ. Grenoble-Alpes, CEA, Grenoble INP, IRIG, PHELIQS, Grenoble, France

3 - Univ. Grenoble-Alpes, CEA-IRIG, MEM, Grenoble, France

4 - CEA, LETI, MINATEC, Grenoble, France

\* Corresponding author

Various transmission electron microscopy-based techniques have the potential for quantitative characterization of the electric properties of a material at nm length scales. For example, off axis electron holography enables measuring the phase change of the electron wave, that can be directly related to the projected electrostatic potential. Four-dimensional scanning transmission electron microscopy (4D-STEM) has gained in popularity rather recently, thanks to the development of fast pixelated detectors over the last years, enabling the assessment of internal electric fields with high spatial resolution [1,2]. However, the measurement of long range built-in electric fields present in semiconductor devices, for example p-n junctions, are typically three order of magnitude smaller than atomic electric fields, making the 4D-STEM experiments in such systems challenging. The main difficulty for both methods is that the electrical information is combined with material contrast (for example due to chemical gradients, thickness gradients or diffraction contrast) and the challenge resides in reliably separating these two. One possibility to facilitate this task it to use in-situ biasing, in order to increase (decrease) only the electrical part of the signal, and allow subtraction of a reference measurement to remove all material related contrast, see Figure 1.

In this presentation we will show recent results we obtained using 4D STEM on semiconducting lamellae as well as nanowires containing a p-n junction. We will show a study on how the quantification, sensitivity and spatial resolution of electric field mapping in a silicon p-n junction are influenced by the acquisition parameters in a momentum resolved 4D-STEM experiment [3,4]. It was observed that the electric field precision is improved decreasing the semi-convergence angle. The results were invariable even using an electron dose as low as 24 e-/Å<sup>2</sup> and a detection limit as good as 0.01 MV/cm was possible. In addition, in-situ electrical biasing coupled to momentum resolved 4D-STEM measurements were performed, see Figure 2, allowing to study the junction abruptness, to asses phenomena like dopant segregation or interdiffusion [5]. Finally, recent results on a p-n junction in a Ge nanowire will be presented.

This work paves the way for the development of advanced STEM based techniques able to provide imaging and quantification of built-in electric fields, potentials and charge densities in semiconductor devices with high spatial resolution, providing crucial feedback to improve growth/device fabrication processes.

- [1] L. Bruas, V. Boureau, A.P. Conlan, S. Martinie, J.-L. Rouviere, and D. Cooper, *J. Appl. Phys.* **127**, 205703 (2020).
- [2] A. Beyer, M.S. Munde, S. Firoozabadi, D. Heimes, T. Grieb, A. Rosenauer, K. Müller-Caspary, and K. Volz, *Nano Lett.* **21**, 2018 (2021).
- [3] S. Pöllath, F. Schwarzhuber, and J. Zweck, *Ultramicroscopy* **228**, 113342 (2021).
- [4] B.C. da Silva, Z.S. Momtaz, L. Bruas, J.-L. Rouvière, H. Okuno, D. Cooper, and M.I. den-Hertog, *Appl. Phys. Lett.* **121**, 123503 (2022).
- [5] B.C. da Silva, Z. Sadre Momtaz, E. Monroy, H. Okuno, J.-L. Rouviere, D. Cooper, and M.I. Den Hertog, *Nano Lett.* **22**, 9544 (2022).

**Mots-clés/Keywords:** Transmission electron microscopy, in-situ, 4D-STEM, direct electron detector, p-n junction, nanowire

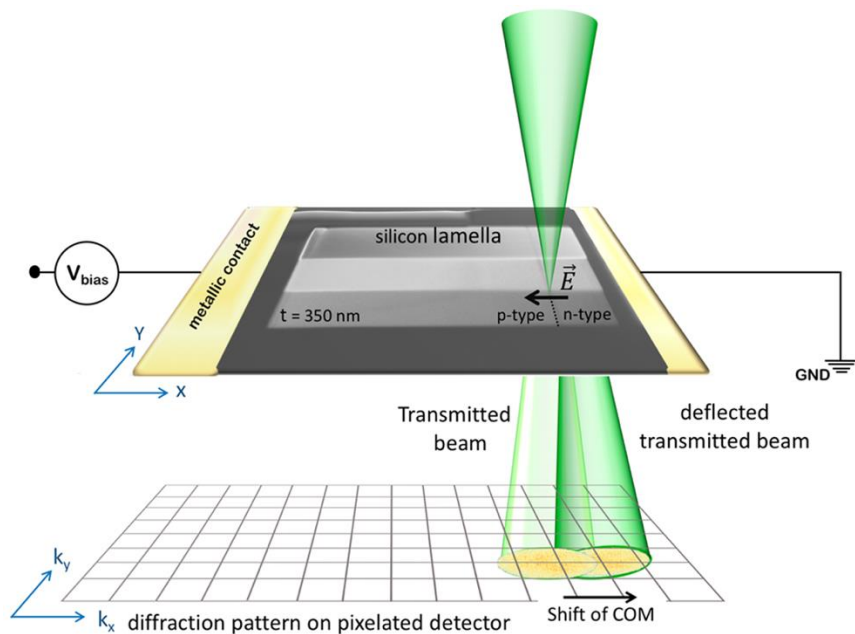


Figure 1 – Schematic of the momentum-resolved 4D-STEM experiment performed in a silicon *p-n* junction. Reverse bias is obtained by applying a negative bias ( $-V_{bias}$ ) to the *p*-side while the *n*-side is grounded [5].

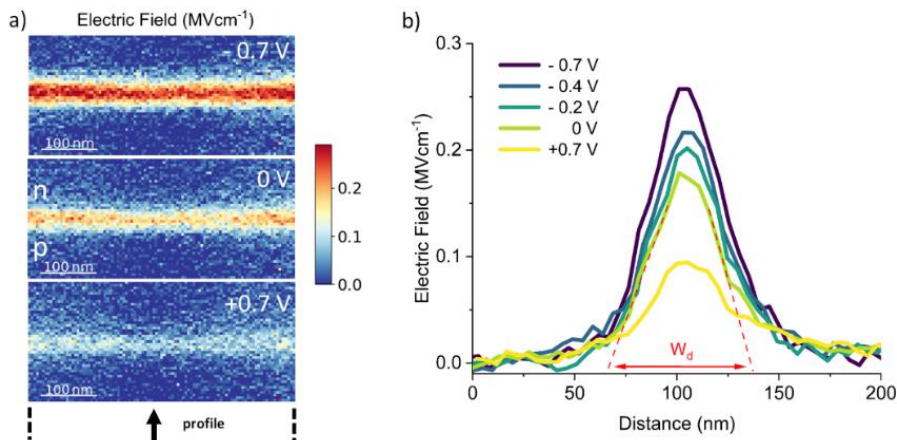


Figure 2 – In-situ biasing momentum resolved 4D-STEM electric field measurements in a silicon *p-n* junction [5].

## SDM2 – Oral1

### Spectroscopie de perte d'énergie des électrons en mode environnemental pour l'étude des interactions entre feuillets 2D de carbures de métaux de transition (MXene) et différents gaz

#### Environmental electron energy-loss spectroscopy for the investigation of 2D titanium carbide (MXene) multi-layers interactions with gases

- **Thomas Bilyk** / Université de Poitiers, ISAE-ENSMA, CNRS, PPRIME, 86073 Poitiers, France
- **Matthieu Bugnet** / Univ Lyon, CNRS, INSA Lyon, UCBL, MATEIS, UMR 5510, 69621 Villeurbanne, France
- **Clément Huot** / Université de Poitiers, ISAE-ENSMA, CNRS, PPRIME, 86073 Poitiers, France
- **Laurence Massin, Patrick Gelin, Mimoun Aouine** / Univ Lyon, Université Claude Bernard Lyon 1, CNRS, IRCELYON, F-69626 Villeurbanne, France
- **Lola Loupias** / IC2MP, Université de Poitiers, CNRS, F-86073 Poitiers, France
- **Stéphane Célérier** / IC2MP, Université de Poitiers, CNRS, F-86073 Poitiers, France
- **Jérôme Pacaud** / Université de Poitiers, ISAE-ENSMA, CNRS, PPRIME, 86073 Poitiers, France
- **Vincent Mauchamp** \* (vincent.mauchamp@univ-poitiers.fr) / Université de Poitiers, ISAE-ENSMA, CNRS, PPRIME, 86073 Poitiers, France

MXenes are a large family of 2D transition metal carbides/nitrides layers of general formula  $Mn+1XnTz$ , with M a transition metal, X standing for C or N and T being surface groups usually corresponding to O, OH, Cl and/or F (see Fig1-a for  $Ti_3C_2Tz$ , the most studied MXene). Due to their outstanding metallic conductivity, excellent mechanical strength and tunable hydrophilicity, MXenes are investigated for a very large number of applications, including gas sensors.[1] However, identifying the intrinsic mechanisms responsible for MXene multi-layers superior behavior towards gas sensing is very challenging: it involves a response at the multi-layer scale (i.e. swelling after gas insertion between the layers) and at the single-layer level with the T-groups being expected to play a pivotal role. In this context, we propose to use environmental electron energy-loss spectroscopy (EELS) in order to study in situ in the TEM the response of  $Ti_3C_2Tz$  multi-layers (Fig. 1-b) towards ethanol and water vapor, two benchmark gases. EELS is indeed a very interesting tool allowing to combine information at the single-layer level with elemental selectivity using the core losses, and at the multi-layer level using valence electrons spectra (VEELS). Experiments were conducted using a dedicated environmental TEM (FEI TITAN G2 ETEM) with vapor pressures up to few mbars. Focusing first on ethanol atmosphere, reversible modifications of the fine structure at the Cl L<sub>2,3</sub>-edge are evidenced (Fig 1-c), in contrast to the O K-edge, and highlight a key role of Cl terminations on the interactions with this gas. These variations are correlated to changes in the VEEL spectra that are interpreted in terms of swelling of the multi-layer, based on a recently developed analysis.[2] Similar experiments conducted using water vapor atmospheres give different results both in core losses and VEELS. The two distinct behaviors are analyzed making use of first principles simulations of the spectra (Fig 1-d).

METSA (FR CNRS 3507) is gratefully acknowledged for supporting the experiments performed at the Lyon-St-Etienne microscopy centre.

Références/References :

- [1]Y. Pei et al., ACS Nano, 15 (2021), p.3996
- [2]T. Bilyk et al., 2D Materials, 9 (2022), p.035017

**Mots clefs** : MXene, environmental EELS, gas, 2D material

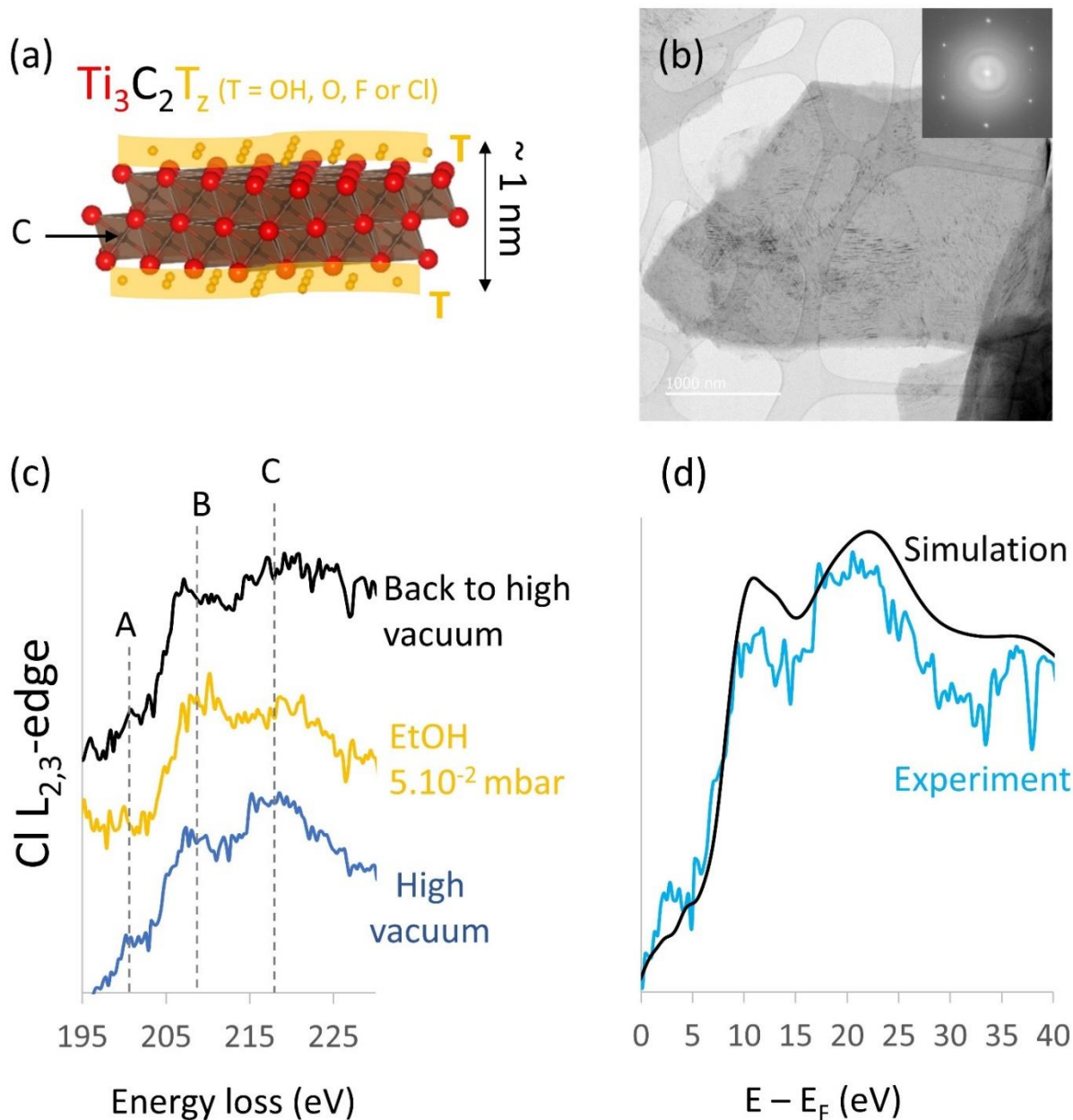


Figure 1: (a) Structural model of a  $\text{Ti}_3\text{C}_2\text{T}_z$  single-layer. (b) Typical  $\text{Ti}_3\text{C}_2\text{T}_z$  multi-layer on which were performed EELS experiments together with the corresponding FFT showing the hexagonal symmetry of the layers. (c)  $\text{Cl}\text{ L}_{2,3}$ -edge showing the disappearance of peak A and increase of peak B under ethanol (EtOH) atmosphere (yellow) as compared to the same area under high vacuum (blue). Black: spectrum recorded after coming back to high vacuum on the same flake but in a different area to minimize contamination issues. (d) Comparison between an experimental  $\text{Cl}\text{ L}_{2,3}$ -edge and the corresponding DFT simulation.

## SDM2 – Oral2

### Étude par microscopie *in situ* corrélative de photoanodes utilisées pour la photoélectrolyse de l'eau

#### Correlative *in situ* microscopy study of photoanodes for solar water splitting

- **Léon Schmidt** \* (leon.schmidt@ipcms.unistra.fr) / Institut de Physique et de Chimie des Matériaux de Strasbourg (IPCMS), CNRS, Université de Strasbourg, 23 rue du Loess, BP43, 67034 Strasbourg, France
- **Walid Baaziz** / Institut de Physique et de Chimie des Matériaux de Strasbourg (IPCMS), CNRS, Université de Strasbourg, 23 rue du Loess, BP43, 67034 Strasbourg, France
- **Dana Stanescu** / Service de Physique de l'Etat Condensé (SPEC), CEA, CNRS, Université Paris-Saclay, CEA Saclay, 91191 Gif-sur-Yvette Cedex, France
- **Stefan Stanescu** / Synchrotron SOLEIL, L'Orme des Merisiers, Départementale 128, 91190 Saint-Aubin, France
- **Ovidiu Ersen** / Institut de Physique et de Chimie des Matériaux de Strasbourg (IPCMS), CNRS, Université de Strasbourg, 23 rue du Loess, BP43, 67034 Strasbourg, France

\* Auteur correspondant

In the framework of hydrogen production as means for renewable energy storage, Ti-doped hematite photoanodes ( $Ti:\alpha\text{-Fe}_2\text{O}_3$ ) have received renewed interest, owing to their high photoelectrochemical activity, absorption spectrum compatible with sunlight, and abundance in nature, allowing cost- and resource-efficient production of hydrogen by solar water splitting [1]. A key part of the synthesis of this material is the annealing of  $Ti:\beta\text{-FeOOH}$ , obtained by ACG of a  $\text{FeCl}_3$  precursor with  $\text{TiCl}_3$  doping, to yield the final photoelectrode structure. Herein, we study this annealing step by means of correlated *in situ* gas phase transmission electron microscopy with synchrotron STXM characterization, to yield information on the morphological, structural, chemical and electronic structure of the material in real time during the annealing step. The reaction was carried out by *in situ* TEM using two MEMS chips forming a sealed environment inside the microscope to which a controlled gas atmosphere and temperature can be applied. The change in morphology and chemical composition was monitored in real time by STEM imaging and EDS mapping, and structural information was gained by electron diffraction. Furthermore, the same sample was analyzed by STXM at the HERMES beamline (Synchrotron Soleil), where information on the electronic structure of the samples was obtained. Notably, the formation of defects with varying morphology as a function of temperature was observed, which can be linked to a change in the electronic properties, possibly acting as charge recombination sites [2]. Furthermore, clusters of pseudo-brookite ( $\text{Fe}_2\text{TiO}_5$ ) was found by spectro-pytcography , which are beneficial to the photoelectrochemical activity by improving charge separation at the interface [3]. These findings provide valuable insights into the underlying mechanisms of this phase transformation, which are key to optimize the performances of hematite photoanodes.

#### Références/References :

- [1] K. Sivula, F. Le Formal, and M. Grätzel, ChemSusChem, 4 (2011), pp.432-449
- [2] A. M. Xavier, F. F. Ferreira, and F. L. Souza, RSC Adv., 4 (2014), pp.17753–17759
- [3] S. Stanescu, T. Alun, Y. Dappe, D. Ihiawakrim, O. Ersen, and D. Stanescu, Intrinsic photoanode bandengineering: enhanced solar water splitting efficiency mediated by surface segregation in Ti-doped hematite nanorods, 2023. (pre-print).

**Mots clefs** : *in situ*; electron microscopy; TEM; STXM; synchrotron; photoanodes; hematite; akaganeite

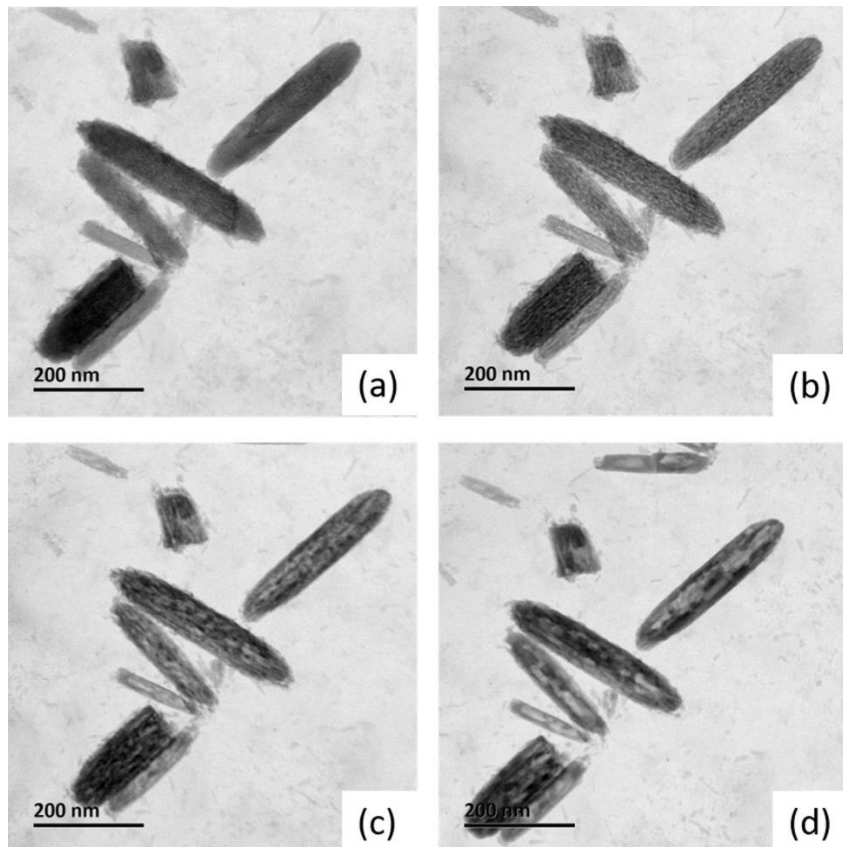


*Figure 1:* *In situ* BF-STEM images of Ti:β-FeOOH particles at (a) 200 °C, (b) 400 °C, (c) 600 °C, (d) 800 °C under N<sub>2</sub>

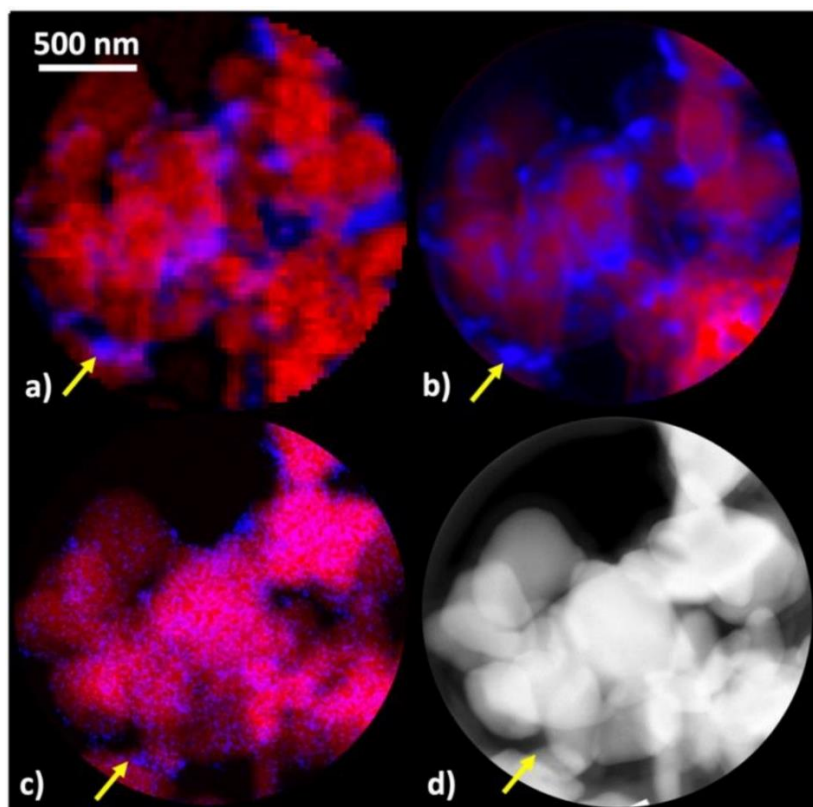


*Figure 2:* (a) STXM, (b) spectro-ptychography, (c) STEM-EDX map, (d) corresponding STEM-HAADF image of N<sub>2</sub>-annealed photoanodes. In red, bulk Ti:Fe<sub>2</sub>O<sub>3</sub>, in blue, Fe<sub>2</sub>TiO<sub>5</sub> clusters.  
Adapted from [3]

**SDM2 – Oral3****Suivi operando de la prise du plâtre par microscopie électronique en phase liquide****Operando characterization of plaster setting using Liquid-Phase Scanning Electron Microscopy**

- **Alexandre Fantou** \* (alexandre.fantou@insa-lyon.fr) / Univ Lyon, INSA Lyon, Université Claude Bernard Lyon 1, CNRS, MATEIS, UMR5510, 69621 Villeurbanne, France
  - **Anna Wozniak** / Univ Lyon, INSA Lyon, Université Claude Bernard Lyon 1, CNRS, MATEIS, UMR5510, 69621 Villeurbanne, France
  - **Annie Malchère** / Univ Lyon, INSA Lyon, Université Claude Bernard Lyon 1, CNRS, MATEIS, UMR5510, 69621 Villeurbanne, France
  - **Karine Masenelli-Varlot** / Univ Lyon, INSA Lyon, Université Claude Bernard Lyon 1, CNRS, MATEIS, UMR5510, 69621 Villeurbanne, France
  - **Sylvain Meille** / Univ Lyon, INSA Lyon, Université Claude Bernard Lyon 1, CNRS, MATEIS, UMR5510, 69621 Villeurbanne, France
  - **Solène Tadier** / Univ Lyon, INSA Lyon, Université Claude Bernard Lyon 1, CNRS, MATEIS, UMR5510, 69621 Villeurbanne, France
- \* Auteur correspondant

Gypsum has been traditionally used as a building material, but can also be a model for the development of injectable biomaterials for bone substitution. Set plaster, or gypsum ( $\text{CaSO}_4 \cdot 2\text{H}_2\text{O}$ ), is prepared by mixing dry hemihydrate powder ( $\text{CaSO}_4 \cdot 0.5\text{H}_2\text{O}$ ) with water. Its properties as a solid binder are largely influenced by the setting reaction occurring when  $\text{CaSO}_4 \cdot 0.5\text{H}_2\text{O}$  dissolve and crystals of gypsum precipitate. It is well known that the resulting solid is formed by an interlocked network of gypsum needles and platelets, but the exact setting process is not well understood yet. The objective of our study is therefore to monitor the evolution of crystals and understand the entire setting process, using operando observations [1], using Liquid-phase scanning electron microscopy. The most convenient set-up for such monitoring has found to be sealed Quantomix cells [2]. They are indeed water- and airtight, and therefore plaster evolves under the same conditions as in real use, especially in terms of water-to-plaster ratio. The influence of several experimental parameters (addition of a retardant to monitor the whole setting process, image acquisition conditions and irradiation damage, presence of a membrane) will be discussed. We will describe image processing and analysis procedures we developed to distinguish the hemihydrate particles dissolving in the mixture from the gypsum crystals growing over time (Figure 1), and therefore plot the fraction of gypsum vs time. To go into more details in the analysis of gypsum growth, we will propose an indexation of the gypsum crystal facets based on geometric information and the knowledge of the equilibrium morphologies [3]. The growth rates of the different planes will be discussed and compared with values found in the literature.

**References**

- [1] J. Seiller et al, Construction and building materials, 2021, 304, 124632.
- [2] E. Gallucci et al, Advances in Applied Ceramics 2013, 106, 319-326.
- [3] B. Madeja et al, Cement and Concrete Research, 2023, 164, 107049.

**Mots clefs :** liquide, operando, MEB, analyse d'image

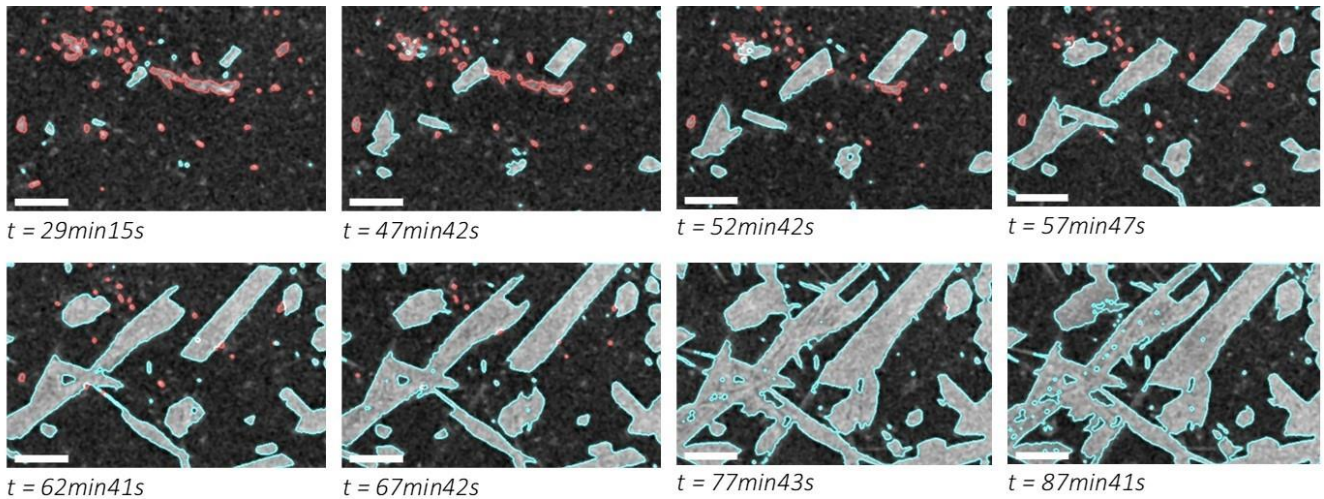


Figure 1. Evolution of hemihydrate (red) and gypsum (blue) during the hydration reaction of plaster (scale bar 10  $\mu\text{m}$ ).

## SDM2 – Oral4

### Développement d'expériences operando in-situ dans un MEB : application à l'étude des batteries

#### Development of operando experiment in situ in the SEM : application to the study of batteries

- **Neelam Yadav** \* (neelamyadavg111@gmail.com) / Laboratoire de réactivité et chimie des solides (LRCS, CNRS UMR 7314)
- **Melisa Herrman Alba** / Laboratoire de réactivité et chimie des solides (LRCS, CNRS UMR 7314)
- **Mathieu Morcrette** / Laboratoire de réactivité et chimie des solides (LRCS, CNRS UMR 7314)
- **Carine Davoisne** \* (carine.davoisne@u-picardie.fr) / Laboratoire de réactivité et chimie des solides (LRCS, CNRS UMR 7314)

\* Auteur correspondant

Dans les batteries, les réactions électrochimiques se produisent au niveau des interfaces (électrodes-electrolyte, ...) et y induisent des modifications plus ou moins réversibles. Parmi les systèmes de nouvelle génération en développement, les batteries tout solides ne font pas exception à cette règle. La compréhension des phénomènes aux interfaces entraînant un vieillissement prématûr de la batterie est donc primordiale pour comprendre et trouver des voies d'amélioration. Grâce à la naissance des techniques in-situ et operando, ces interfaces complexes en constante évolution peuvent désormais être étudiées par des observations en direct et à l'échelle de la batterie grâce à l'utilisation du MEB.

Pour réaliser ce type d'étude, nous avons développé une cellule électrochimique (Figure 1) simple qui peut être utilisée pour faire fonctionner des batteries tout solides à base lithium métal à l'intérieur du MEB. L'utilisation de lithium métal qui est un composé sensible à l'air nous a amené à fabriquer une boîte étanche permettant le transfert de la batterie entre la boîte à gants et le MEB (et inversement). Les modifications morphologiques (imagerie par électrons secondaires et rétrodiffusés) et chimiques (spectroscopie à dispersion d'énergie des rayons X) au niveau des interfaces à l'état solide ont ainsi pu être suivis en temps réel et pendant le fonctionnement de la batterie.

Ainsi, nous avons étudié et comparé l'évolution d'électrolytes solides (ES) à base de sulfure ( $\beta$ -Li<sub>3</sub>PS<sub>4</sub> (LPS) et Li<sub>6</sub>PS<sub>5</sub>Cl (LPSCl)) en gardant l'anode (lithium métal) et la cathode LiNi<sub>1</sub>/3Mn<sub>1</sub>/3Co<sub>1</sub>/3O<sub>2</sub> (NMC) constantes. Nous avons catégorisé selon trois modes les modifications observées : i) défaillance électrique par la formation de dendrites de lithium de morphologies différentes en suivant l'ES allant jusqu'au court-circuit dans le cas du LPS (Figure 2 b et d), ii) défaillance mécanique par la formation de fissures dans l'électrolyte dont la forme et la propagation dépendent fortement de la nature intrinsèque de celui-ci (Figure 2 a et c) et iii) défaillance électrochimique avec la formation d'interphases d'électrolyte solide à la surface de la matière active. Les principaux verrous pour l'utilisation du lithium métal étant lié à la propagation des dendrites de lithium et ainsi à l'instabilité mécanique des électrolytes solides.

**Mots clefs :** cellule électrochimiques, operando MEB, batteries

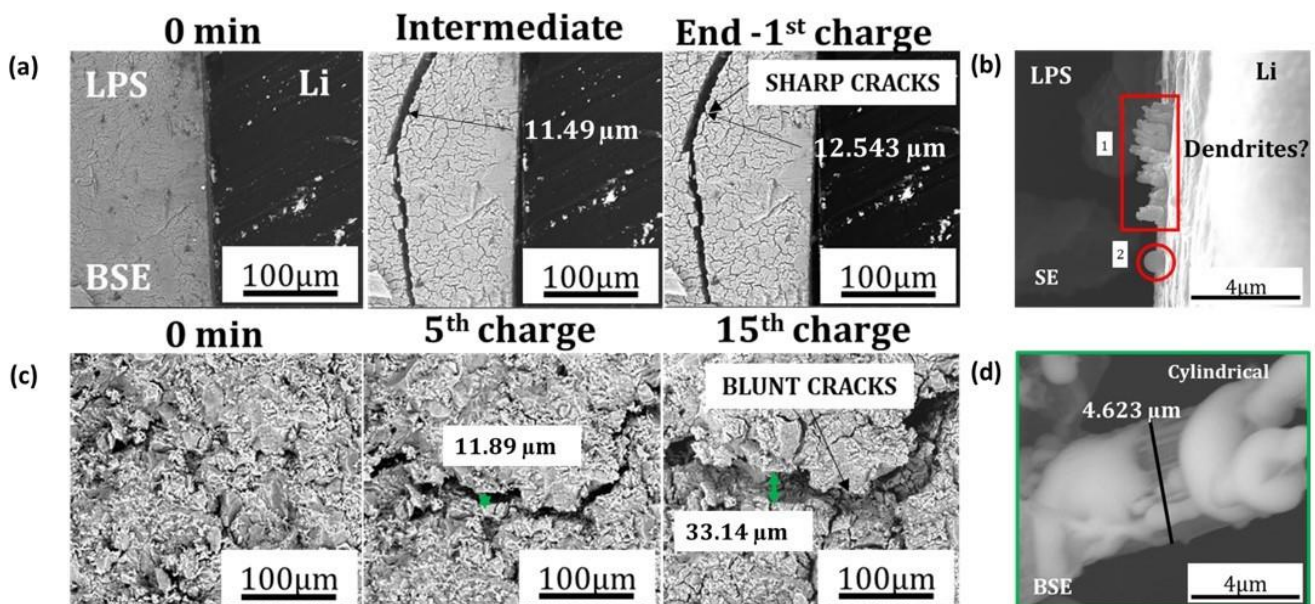
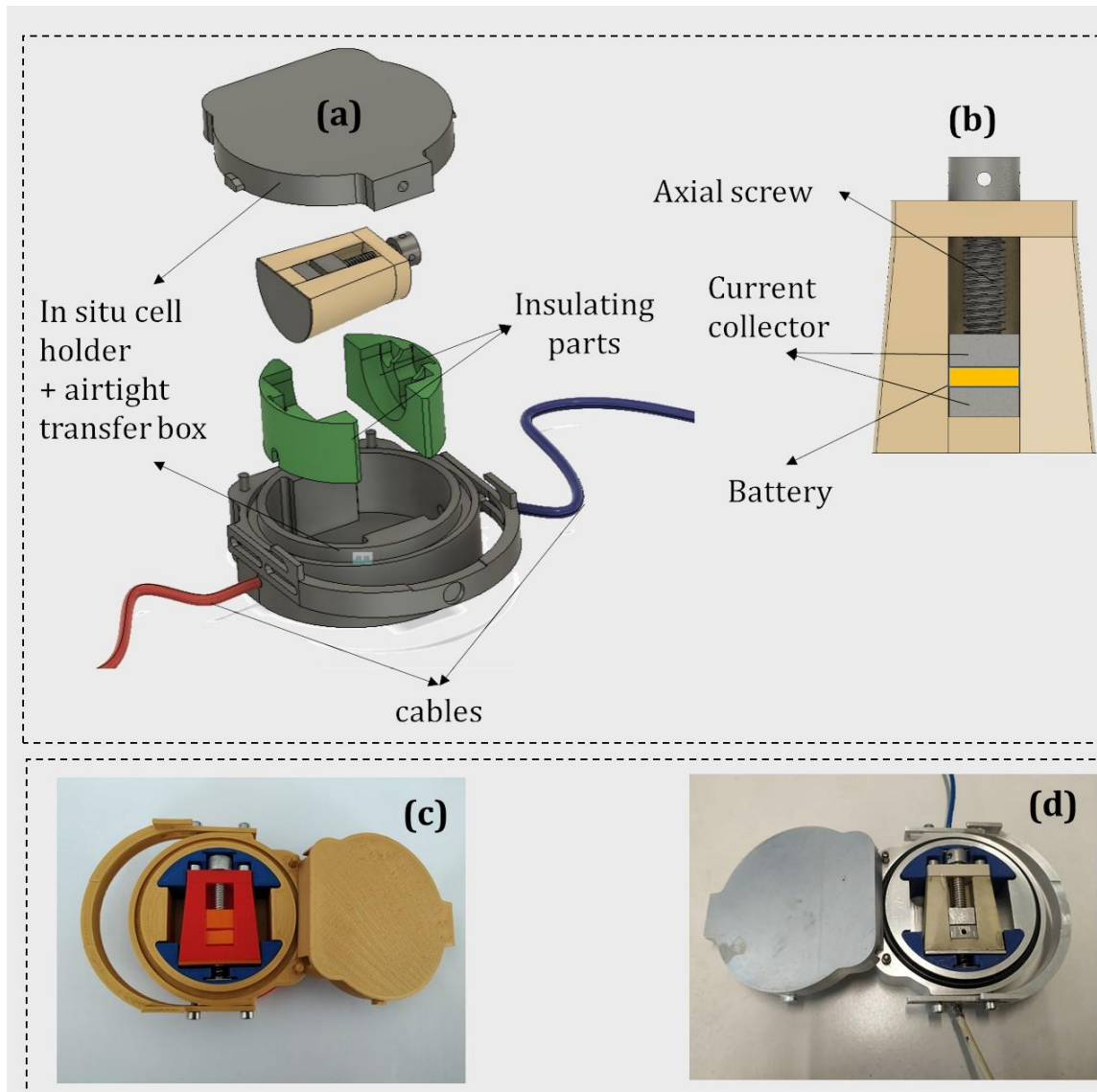


Figure 2 : a) et c) évolution des fissures dans le LPS et le LPSCl respectivement, b) et d) différentes morphologies de dendrites de lithium observées dans le LPS et le LPSCl respectivement.

## **SDM3 : Microscopie des matériaux et nano-matériaux**

***Animation :***

*Carine Davoisne (LRCS, Amiens)*

*Michaël Texier (IM2NP, Marseille)*

## SDM3 – Inv

### Croissance et optimisation de films minces comme couche sélective de capteurs solaires thermiques

- **Stéphanie BRUYERE** \* (stephanie.bruyere@univ-lorraine.fr) / IJL - UMR CNRS 7198 - UL
- **Daria KHARKHAN** (daria.kharkhan@univ-lorraine.fr) / IJL - UMR CNRS 7198 - UL
- **Joseph ANTOINE** (joseph.antoine@univ-lorraine.fr) / IJL - UMR CNRS 7198 - UL
- **Zil FERNANDEZ GUTIERREZ** (zil.fernandez-gutierrez@univ-lorraine.fr) / IJL - UMR CNRS 7198 - UL
- **Alexis GARCIA WONG** (alexis.garcia-wong@univ-lorraine.fr) / IJL - UMR CNRS 7198 - UL
- **Silvère BARRAT** (silvere.barrat@univ-lorraine.fr) / IJL - UMR CNRS 7198 - UL
- **Fabien CAPON** (fabien.capon@univ-lorraine.fr) / IJL - UMR CNRS 7198 - UL

\* Corresponding author

Les panneaux solaires thermiques sont des dispositifs conçus pour absorber les rayonnements solaires et transmettre de l'énergie thermique à un fluide caloporteur. En période de fort ensoleillement, lorsque le fluide caloporteur n'est pas en mouvement, la température du panneau peut atteindre jusqu'à 200 voire 250 °C. Par conduction thermique, le fluide caloporteur stagnant sous le panneau voit sa température augmenter et celle-ci peut alors dépasser la température critique conduisant à la dégradation progressive des propriétés du fluide. Pour conserver les capacités de production d'eau chaude sanitaire, il est alors nécessaire de changer périodiquement la totalité du fluide caloporteur. Pour limiter les coûts d'utilisation d'un panneau solaire thermique, plusieurs stratégies peuvent être mises en œuvre comme par exemple l'emploi de systèmes onéreux de recirculation du fluide en période de stagnation. Une solution plus avantageuse consiste à limiter la température de stagnation du panneau en ajoutant en surface de ce dernier une couche mince permettant d'éviter une surchauffe du panneau. Cette solution est basée sur l'utilisation d'une couche mince thermochromique, c'est-à-dire un matériau dont les propriétés optiques évoluent de manière réversible en fonction de la température. A basse température, le matériau thermochromique doit présenter une émissivité faible pour que les photons absorbés permettent le chauffage du fluide caloporteur. En revanche, au-delà d'une température critique, le matériau thermochromique doit présenter une émissivité élevée pour réduire de manière volontaire la température de surface du panneau. Parmi les différents matériaux susceptibles de répondre à ce cahier des charges, le dioxyde de vanadium ( $\text{VO}_2$ ) et les matériaux comme les pérovskites ( $\text{NdNiO}_3$ ,  $\text{LaCoO}_3$ , ...) sont particulièrement intéressants.

La caractérisation par microscopie électronique en transmission de ces films minces est déterminante pour la compréhension des phénomènes physiques liés à la formation de ces matériaux fonctionnels et donc pour le contrôle de leurs propriétés optiques.

Par exemple, des films de  $\text{LaCoO}_3$  synthétisés dans un réacteur semi-industriel [1, 2] cristallisent durant un traitement thermique par interdiffusion des atomes de La, Co et O, sans formation des oxydes binaires correspondants. D'autres films synthétisés dans un réacteur de laboratoire sont quant à eux homogènes en composition et certains présentent même une structure cubique métastable. Des films de  $\text{SmNiO}_3$  sont synthétisés en deux étapes à pression atmosphérique (dépôt + recuit). Leur cristallisation serait liée à des processus hétérogènes et homogènes impliqués dans la nucléation et la croissance des grains [3, 4]. Le dopage de couche de  $\text{VO}_2$  par de l'aluminium (8 at.%) permettrait d'augmenter l'émissivité du matériau et faire apparaître la phase cubique de  $\text{VO}_2$ . De plus, des nitrides de vanadium peuvent être utilisés comme précurseurs pour l'oxydation de  $\text{VO}_2$ , qui est un processus délicat pour éviter la formation d'oxydes parasites sans propriété thermochromique.

Les résultats de ces études démontrent l'importance de contrôler les conditions de synthèse des films minces et de post-traitement pour obtenir des films cristallisés et des propriétés optiques souhaitées.

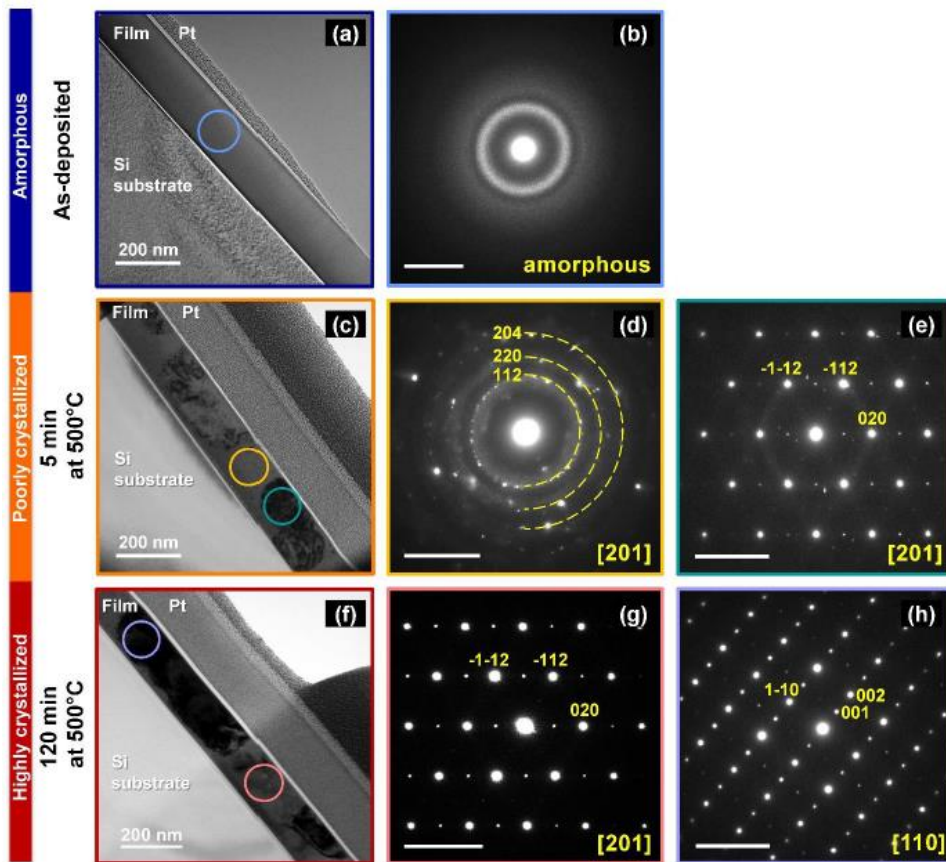


Figure 1 - évolution de la cristallisation d'un échantillon amorphe à un échantillon complètement cristallisé - première colonne : images MET en champ clair des échantillons - deuxième et troisième colonne : clichés de diffraction des zones indiquées sur les images MET de la première colonne

- [1] DN Kharkhan et al., Journal of Applied Physics 127 (1) (2020) 015304
- [2] DN Kharkhan et al., Journal of Applied Physics 127 (1), 015304 (2020)
- [3] Z Fernández-Gutiérrez et al., Journal of Alloys and Compounds 960, 170799
- [4] Z. Fernandez et al., Scripta Materialia 218 (2022) 114795
- [5] AC García-Wong et al., Solar Energy Materials and Solar Cells 210 110474 (2020)
- [6] AC García-Wong et al., Journal of Materomics 7 (4), (2021) 657-664

**Mots-clés/Keywords:** TEM, EELS, thermochromic selective layer

**SDM3 – Oral1****Caractérisation compréhensive des matériaux par EBSD****Comprehensive materials characterization by EBSD**

- **Qiwei SHI** \* (sqw@sjtu.edu.cn) / Shanghai Jiao Tong University
- **Hongru Zhong** / Shanghai Jiao Tong University
- **Dominique Loisnard** / EdF R&D, Renardières
- **Stéphane Roux** / ENS Paris-Saclay

\* Auteur correspondant

Electron Backscatter Diffraction (EBSD), a module in scanning electron microscopes, is a common technique to obtain crystallographic orientation and phase identification in crystalline samples. The high-resolution variant of EBSD (HR-EBSD) has an angular resolution of 10-4, thus can access the elastic strain and stress fields. HR-EBSD relies on full pattern matching (FPM) between diffraction image pairs, and Integrated Digital Image Correlation (IDIC) stands out among various FPM algorithms for its efficiency and precision. What's more, IDIC has a high extendibility in EBSD analyses. Whenever a physical quantity can be incorporated in the generation of a simulated diffraction pattern from pre-calculated master patterns, it can be identified via the correlation with the experimental patterns. IDIC EBSD has the potential to assess many properties:

- Geometrically necessary dislocation (GND) density (Fig.1)
- Statistically stored dislocation (SSD) density (Fig.2)
- Elastic strain (thus elastic stress)
- Optical distortion parameters
- Energy of the backscattered electrons
- Projection center coordinates of the diffraction pattern
- Topography field
- (Multiple sets of) Euler angle [1]
- Sub-surface grain boundary inclinations [2]

The polyvalent capabilities of the IDIC algorithm prove promising for characterizing crystalline samples comprehensively by EBSD solely, provided that high quality diffraction patterns can be collected.

#### References:

- [1]Q. Shi, Y. Zhou, H. Zhong, D. Loisnard, C. Dan, F. Zhang, Z. Chen, H. Wang, and S. Roux. Indexation of electrontodiffraction patterns at grain boundaries. Materials Characterization, 182:111553, 2021.  
 [2]D. Fullwood, S. Sanderson, S. Baird, J. Christensen, E. Homer and O. Johnson. Determining Grain Boundary Position and Geometry from EBSD Data: Limits of Accuracy. Microscopy and Microanalysis (2021), 1–13

**Mots clefs :** EBSD, Integrated Digital Image Correlation, Dislocation density

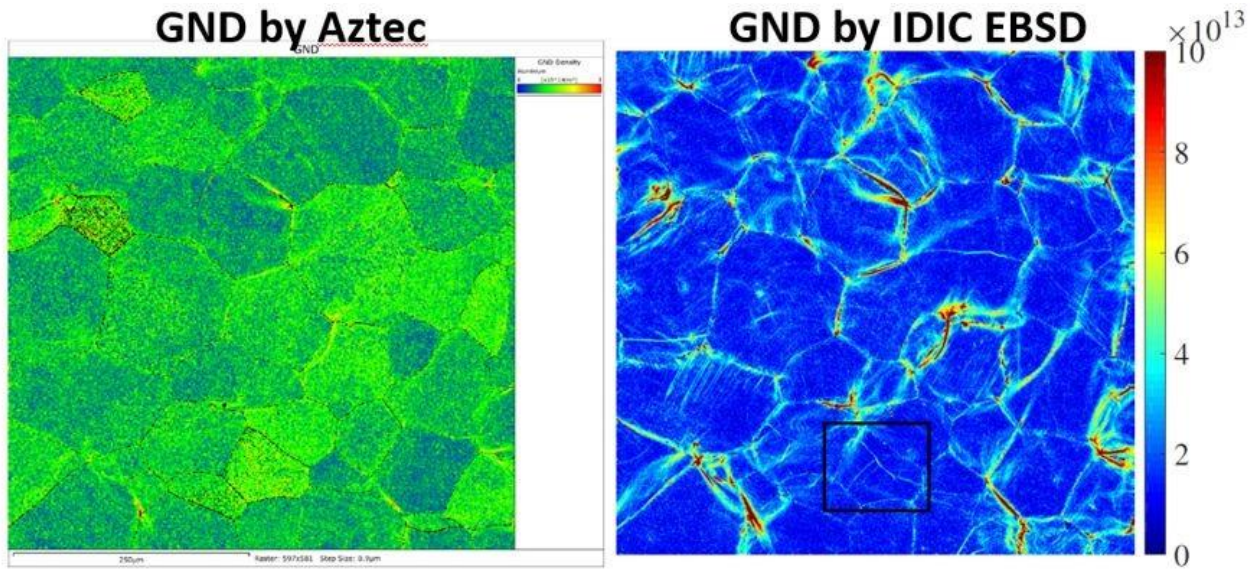


**Figure 1:** Geometrically necessary dislocation density ( $m^{-2}$ ) fields evaluated by commercial software Aztec and IDIC EBSD, based on the same diffraction patterns.

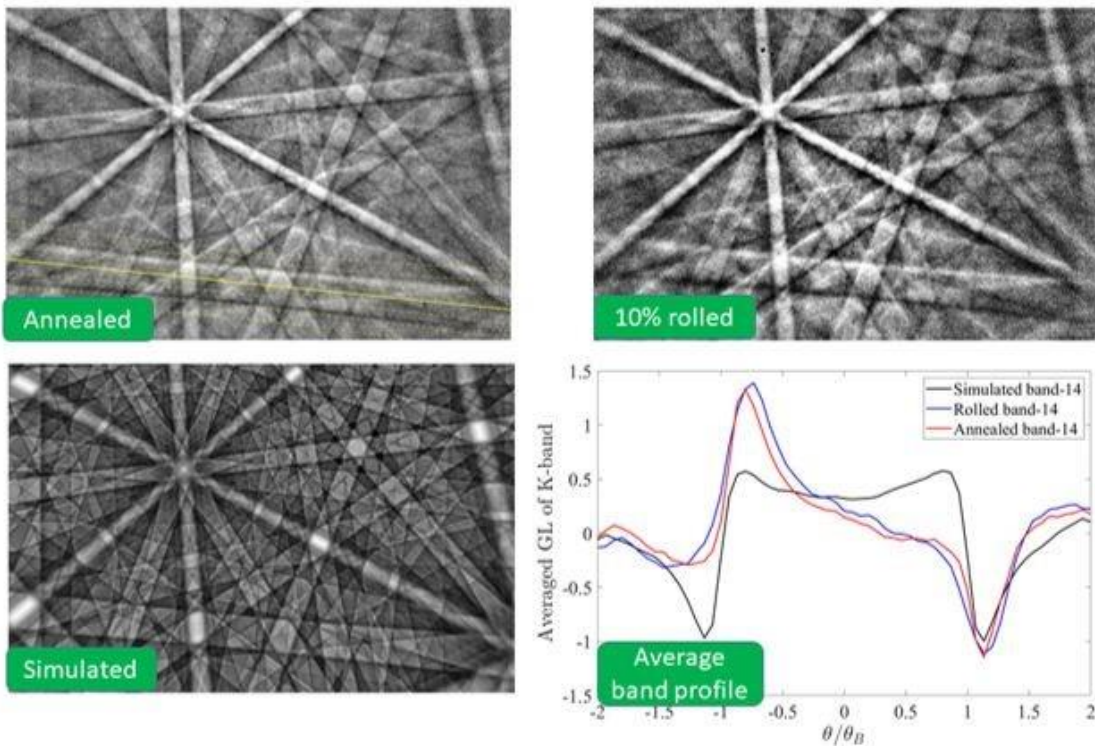


**Figure 2:** Examples of diffraction patterns from an annealed sample, 10% cold-rolled sample and from dynamical simulation. The average profiles of the same band are compared.

**SDM3 – Oral2****Resolution structurale de Ca<sub>3</sub>GaZn0.5Ge4.5O<sub>14</sub> (type langasite avec 3 cations isoélectroniques) par la quantification de cartographies 2D-EDS.**

**Structural resolution of Ca<sub>3</sub>GaZn0.5Ge4.5O<sub>14</sub>, a three isoelectronic cation langasite structure, using quantitative 2D-EDS mapping**

- **Cécile Genevois** \* (cecile.genevois@cnrs-orleans.fr) / CNRS, CEMHTI UPR3079, Univ. Orléans, F-45071 Orléans, France
- **Haytem Bazaaroui** / CNRS, CEMHTI UPR3079, Univ. Orléans, F-45071 Orléans, France
- **Dominique Massiot** / CNRS, CEMHTI UPR3079, Univ. Orléans, F-45071 Orléans, France
- **Vincent Sarou-Kanian** / CNRS, CEMHTI UPR3079, Univ. Orléans, F-45071 Orléans, France
- **Emmanuel Veron** / CNRS, CEMHTI UPR3079, Univ. Orléans, F-45071 Orléans, France
- **Sébastien Chenu** / Rennes Institute of Chemical Sciences, UMR CNRS 6226, Beaulieu Campus, 263 Av. Général Leclerc, 35042 Rennes, France
- **Michael J Pitcher** / CNRS, CEMHTI UPR3079, Univ. Orléans, F-45071 Orléans, France
- **Mathieu Allix** / CNRS, CEMHTI UPR3079, Univ. Orléans, F-45071 Orléans, France

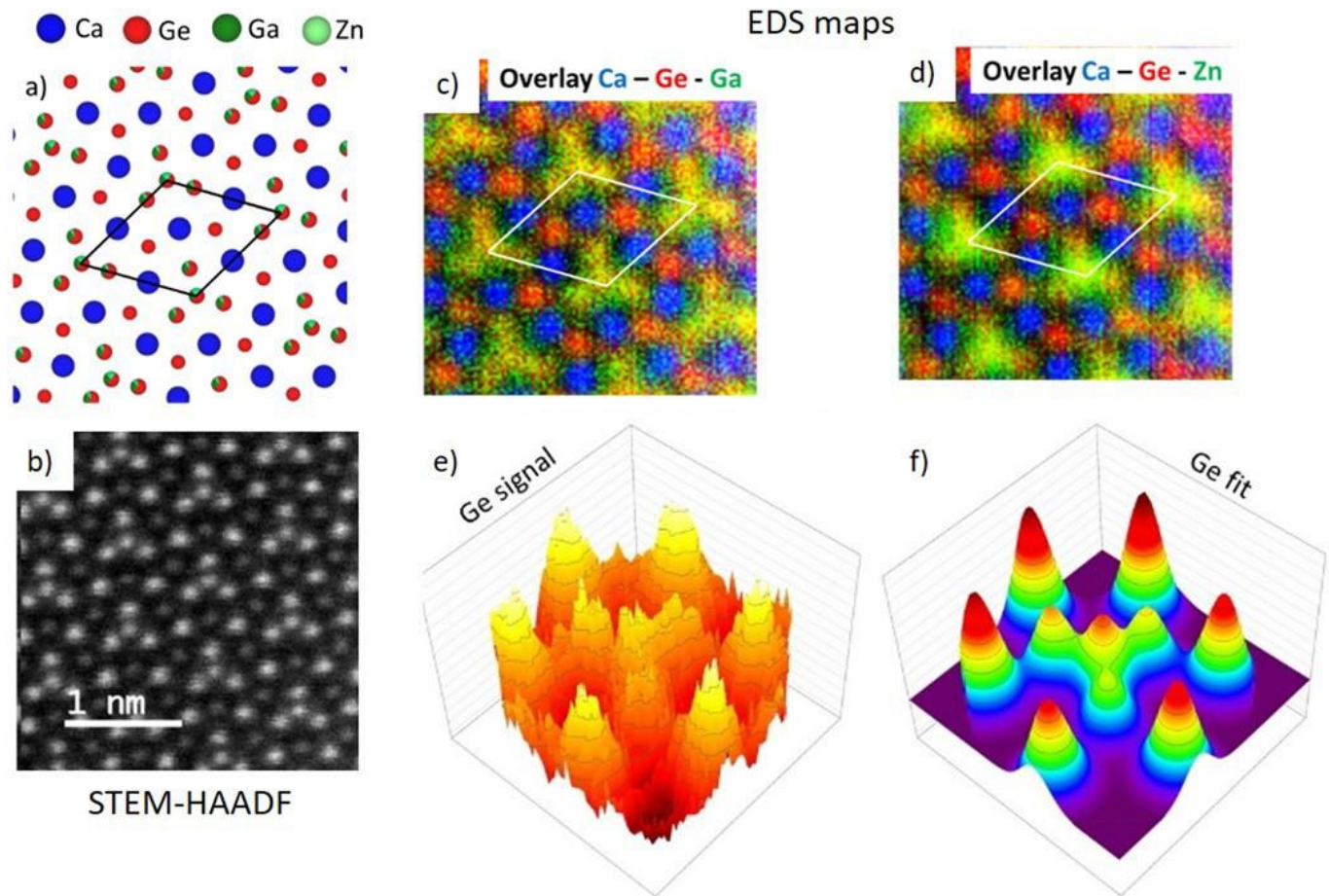
\* Auteur correspondant

Crystallisation of zinc gallogermanate glasses is of interest for the synthesis of new transparent ceramics. In this context, we were interested in the solid solution Ca<sub>3</sub>Ga<sub>2-2x</sub>ZnxGe<sub>4+x</sub>O<sub>14</sub> (0≤x≤1). Powder diffraction was used to determine that this new compound adopt the trigonal langasite structure type, offering three possible crystallographic sites for the coordination of isoelectronic Zn<sup>2+</sup>, Ga<sup>3+</sup> and Ge<sup>4+</sup>. The distribution determination through the different sites of the three isoelectronic cations for the complex intermediate member Ca<sub>3</sub>GaZn0.5Ge4.5O<sub>14</sub> is not possible using only Rietveld refinement from neutron diffraction. For this compound, we have developed an original approach using quantitative 2D analysis of atomic-resolution STEM-EDS maps.<sup>1</sup> In order to visualize the 2D structural projection of Ca<sub>3</sub>GaZn0.5Ge4.5O<sub>14</sub> the sample was imaged in STEM-HAADF at the atomic scale. However, as Ge, Ga and Zn are of similar atomic number, it is not possible to determine the distribution of these 3 cations. Consequently, EDS mapping was carried out and show that one site is composed of Ca, whilst another one contains only Ge, and the last two are mixed occupied (Ga<sup>3+</sup>/Ge<sup>4+</sup>/Zn<sup>2+</sup>). In order to gain more information and determine the cation ratio on the different sites, a 1D profile analysis was first performed by extracting an intensity profile through the sites from the EDS maps, using a Gaussian decomposition and assuming that the area under the curve is proportional to the element content. In a second time, to reduce certain limitations of this approach like a Wiener filter application on the maps, or the inability to integrate the signal through the entire sites due to the small distance between the neighboring, a two-dimensional fitting approach has been tested.<sup>2-3</sup> The results were then compared with those obtained by Rietveld refinement of NPD data whose model was built following the STEM-EDS mapping analyses. The quantitative 2D refinement of atomic-resolution STEM-EDS maps could be applicable to materials where multiple cations with poor scattering contrast are distributed over different crystallographic sites. 1 H. Bazaaroui et al., Inorg. Chem. 2022, 61, 9339-9351

2 P. Lu et al., Microsc. Microanal. 2014, 20, 1782-1790

3 P. Lu et al., Sci. Rep. 2014, 4, 3945

**Mots clefs :** resolution structurale, cartographie 2D-EDS, quantification



## SDM3 – Oral3

### Identification d'un mécanisme non conventionnel de renversement de polarisation ferroélectrique dans des films de ferrite de gallium

#### Unveiling unconventional ferroelectric switching in multiferroic gallium oxide thin films

- **Xavier DEVAUX** (xavier.devaux@univ-lorraine.fr) / Université de Lorraine, CNRS, Institut Jean Lamour (IJL), Nancy, France
- **Corinne BOUILLET** / Université de Strasbourg, CNRS, Institut de Physique et Chimie des Matériaux de Strasbourg (IPCMS), Strasbourg, France
- **Suvidyakumar HOMKAR** / Université de Strasbourg, CNRS, Institut de Physique et Chimie des Matériaux de Strasbourg (IPCMS), Strasbourg, France
- **Sylvie MIGOT** / Université de Lorraine, CNRS, Institut Jean Lamour (IJL), Nancy, France
- **Christophe LEFEVRE** / Université de Strasbourg, CNRS, Institut de Physique et Chimie des Matériaux de Strasbourg (IPCMS), Strasbourg, France
- **François ROULLAND** / Université de Strasbourg, CNRS, Institut de Physique et Chimie des Matériaux de Strasbourg (IPCMS), Strasbourg, France
- **Daniele PREZIOSI** / Université de Strasbourg, CNRS, Institut de Physique et Chimie des Matériaux de Strasbourg (IPCMS), Strasbourg, France
- **Nathalie VIART** / Université de Strasbourg, CNRS, Institut de Physique et Chimie des Matériaux de Strasbourg (IPCMS), Strasbourg, France

Le ferrite de gallium Ga<sub>0.6</sub>Fe<sub>1.4</sub>O<sub>3</sub> (GFO) est un matériau multiferroïque à température ambiante dont l'intérêt a été récemment démontré pour la spintronique frugale.[1]. Bien qu'observée par différents groupes, sa ferroélectricité est contreversée en raison de sa structure Pna21 qui ne permet pas de mécanisme centrosymétrique de renversement de polarisation comme dans les perovskites.

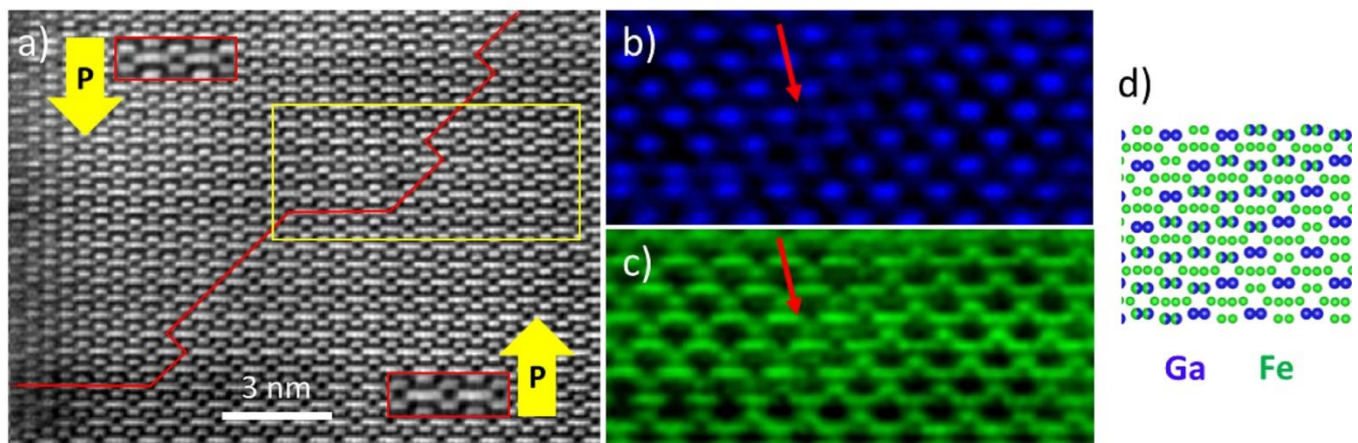
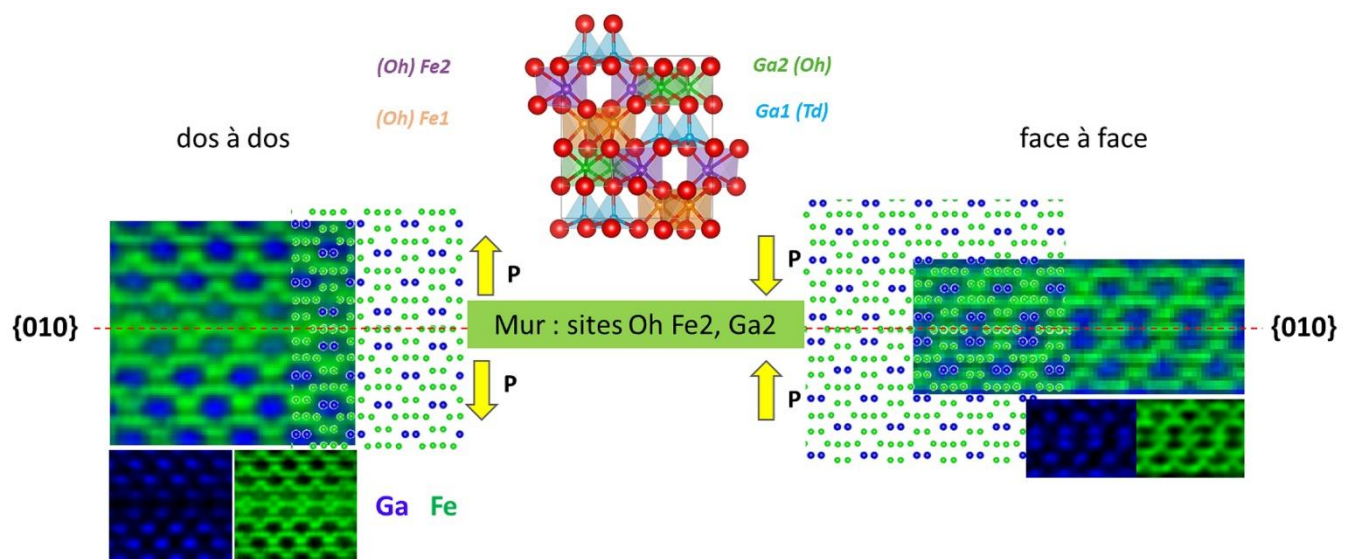
Les couches minces de GFO déposées sur STO par ablation laser pulsé présentent une microstructure texturée avec un axe de croissance parallèle à l'axe c.

La polarisation des grains est aisément identifiable par HR-STEM, comme les parois d'inversion de polarisation qui séparent deux domaines de polarisation opposées. Les murs de polarisation apparaissent traverser de nombreux grains. Ils sont en général perpendiculaires à l'axe de croissance et présentent des marches inclinées à 45°. Cependant, les images STEM ne permettent pas de comprendre la rupture de l'ordre ionique qui est nécessaire pour le maintien de la continuité structurale dans la zone d'inversion de polarisation. Les cartographies chimiques issues de spectrométrie de perte d'énergie spatialement résolue permettent de visualiser l'ordre ionique, avec le fer uniquement dans des sites octaédriques et le gallium uniquement dans des sites tétraédriques du réseau d'oxygènes. Deux différents arrangement des sites Oh and Td ont été identifiés (Fig. 1) pour des murs d'inversion de polarisations face à face ou dos à dos. Le déplacement de ces deux types de paroi d'inversion de polarisation a été initié par irradiation prolongée avec le faisceau du microscope et enregistré à l'échelle atomique en réalisant des images pour différents temps d'irradiation. Il a été observé la formation de sous-marches qui se déplacent. Les cartographies chimiques quantitatives permettent de voir un désordre chimique entre les sites Oh et Td dans la zone du mur qui se déplace, et uniquement dans cette zone (Fig. 2). La zone balayée par la paroi retrouve ensuite un arrangement normal après son passage. Ces observations suggèrent un mécanisme basé sur de la diffusion à courte distance pour expliquer le renversement de polarisation [2].

#### Références :

- [1] S. Homkar et al., ACS Appl. Electron. Mater., 3 (2021), p. 4433
- [2] A. Demchenko et al., Acta Materialia, 240 (2022), p. 118337

**Mots clefs :** HR-STEM, STEM EELS spatialement résolu, oxydes fonctionnels, ferroélectricité non conventionnelle, mobilité cationique



## SDM3 – Oral4

### Caractérisation microstructurale des cellules solaires tandem à base de CIGS/GaP/Si

#### Microstructural characterization of CIGS/GaP/Si based tandem solar cells

- **Eric Gautron** \* (eric.gautron@cnrs-imn.fr) / Nantes Université, CNRS, Institut des Matériaux de Nantes Jean Rouxel, IMN, F-44000 Nantes, France
- **Charles Cornet** / Univ Rennes, INSA Rennes, CNRS, Institut FOTON - UMR 6082, F-35000 Rennes, France
- **Maud Jullien** / Univ Rennes, INSA Rennes, CNRS, Institut FOTON - UMR 6082, F-35000 Rennes, France
- **Antoine Létoublon** / Univ Rennes, INSA Rennes, CNRS, Institut FOTON - UMR 6082, F-35000 Rennes, France
- **Rozenn GAUTHERON-BERNARD Rozenn** / Univ Rennes, INSA Rennes, CNRS, Institut FOTON - UMR 6082, F-35000 Rennes, France
- **Karine Tavernier** / Univ Rennes, INSA Rennes, CNRS, Institut FOTON - UMR 6082, F-35000 Rennes, France
- **Tony Rohel** / Univ Rennes, INSA Rennes, CNRS, Institut FOTON - UMR 6082, F-35000 Rennes, France
- **Léo Choubrac** / Nantes Université, CNRS, Institut des Matériaux de Nantes Jean Rouxel, IMN, F-44000 Nantes, France
- **Sylvie Harel** / Nantes Université, CNRS, Institut des Matériaux de Nantes Jean Rouxel, IMN, F-44000 Nantes, France
- **Ludovic Arzel** / Nantes Université, CNRS, Institut des Matériaux de Nantes Jean Rouxel, IMN, F-44000 Nantes, France
- **Alexandre Crossay** / Ecole Polytech Inst Polytech Paris, Chim Paristech PSL, UMR 9006, CNRS, Inst Photovolta Ile France, F-91120 Palaiseau, France
- **Daniel Lincot** / Ecole Polytech Inst Polytech Paris, Chim Paristech PSL, UMR 9006, CNRS, Inst Photovolta Ile France, F-91120 Palaiseau, France
- **Eugène Bertin** / Nantes Université, CNRS, Institut des Matériaux de Nantes Jean Rouxel, IMN, F-44000 Nantes, France
- **Nicolas Barreau** / Nantes Université, CNRS, Institut des Matériaux de Nantes Jean Rouxel, IMN, F-44000 Nantes, France
- **Olivier Durand** / Univ Rennes, INSA Rennes, CNRS, Institut FOTON - UMR 6082, F-35000 Rennes, France

\* Auteur correspondant

Les rendements de conversion des cellules solaires mono jonction ont atteint des valeurs proches de la limite théorique de Shockley-Queisser (~33%). Une des stratégies permettant de dépasser cette valeur est d'utiliser des cellules tandem [1] combinant une cellule « top » optimisée pour absorber le rayonnement solaire dans la gamme UV-visible avec une cellule « bottom » optimisée pour absorber dans l'IR . Dans le cadre du projet ANR EPCIS [2], nous développons ce type de cellules avec une couche de Cu(In,Ga)S<sub>2</sub> (CIGS) (band gap de 1.65-1.70 eV pour une valeur de GGI=[Ga]/([Ga]+[In]) proche de 20 %) déposée à bas coût par co-évaporation sur un substrat de Si (band gap de 1.1 eV). L'adhésion d'une couche de CIGS sur le Si est cependant très faible ; il est donc nécessaire d'ajouter une couche intermédiaire pour améliorer cette adhésion. Le matériau GaP a été choisi en raison de sa symétrie cubique de paramètre de maille proche du Si mais aussi de celui du CIGS, pour un GGI proche de 20 % (matériau chalcopyrite de symétrie quadratique pseudo-cubique avec  $c \sim 2a$ ).

La croissance épitaxiale du CIGS sur GaP/Si a été validée par diffraction électronique et STEM-HAADF (Fig. 1) avec un empilement du type CIGS[100](001)//GaP[100](001)//Si[100](001). Malgré cette croissance optimale, les cellules de CIGS épitaxié sur des pseudo-substrats GaP/Si(001) présentent des rendements de conversion faibles qui sembleraient être dus à une barrière de potentiel prévenant la collecte efficace des trous. Cette barrière a été localisée proche de la couche de GaP. Elle pourrait être

due à la présence de phases parasites néfastes. Des techniques complémentaires (HR-STEM, spectroscopies, ACOM-TEM, 4D-STEM) ont été utilisées pour mieux décrire la microstructure des couches de CIGS obtenues selon différents processus de dépôts (variation des teneurs en Cu, Ga et In au cours du dépôt) (Fig. 2). Les résultats montrent notamment la présence d'une thiospinelle  $\text{CuIn}_5\text{S}_8$  préjudiciable à l'obtention de hauts rendements.

#### Références :

- [1] F. Martinho, Challenges for the future of tandem photovoltaics on the path to terawatt levels: A technology review, (2021).
- [2] This research was supported by the French National Research Agency EPCIS Project (Grant No. ANR-20-CE05-0038)

**Mots clefs** : cellules solaires tandem, microstructure, HR-STEM, ACOM-TEM

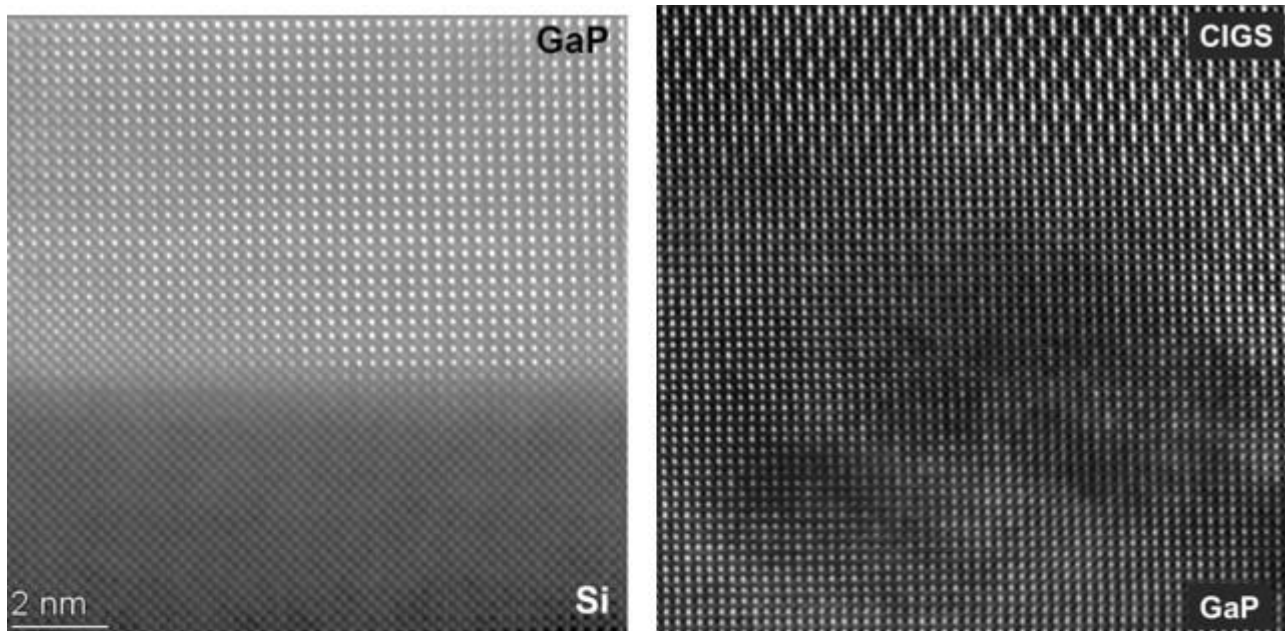
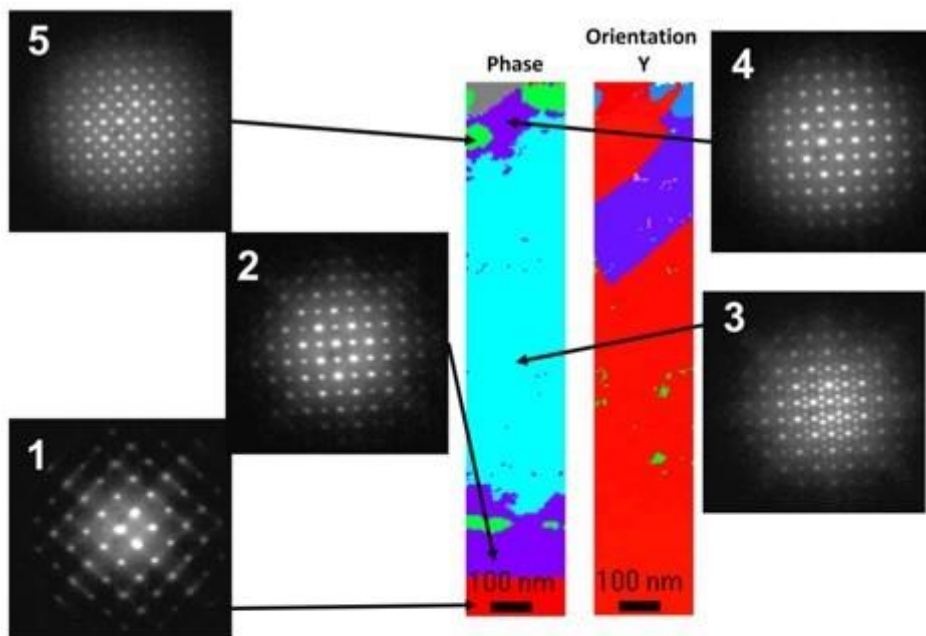


Figure 1: Images STEM-HAADF (Themis Z G3, corrigé sonde) aux interfaces GaP/Si et CIGS/GaP mettant en évidence la croissance épitaxiale du GaP sur le Si (à gauche), et du CIGS sur le GaP (à droite)



*Figure 2: Cartographies de phases et d'orientation d'un empilement CIGS/GaP/Si (ACOM-TEM). Les clichés de diffraction extraits ont été indexés avec les phases suivantes : Si (1), GaP (2), CIGS type chalcopyrite (3), CIGS type thiospinelle (4) et CIGS type zinc blende (5)*

## SDM3 – Oral5

### Études par MET d'un absorbeur solaire sélectif multicouche pour applications solaires thermodynamiques sous concentration

**Investigations by TEM of multi-layered solar selective absorber for concentrated solar power technology**

- **Florian Chabanais** \* (florian.chabanais@cnrs-imn.fr) / Nantes Université, CNRS, Institut des Matériaux de Nantes Jean Rouxel, IMN, F-44000 Nantes, France
- Mireille Richard-Plouet / Nantes Université, CNRS, Institut des Matériaux de Nantes Jean Rouxel, IMN, F-44000 Nantes, France
- **Nicolas Gautier** / Nantes Université, CNRS, Institut des Matériaux de Nantes Jean Rouxel, IMN, F-44000 Nantes, France
- **Aissatou Diop** / PROMES-CNRS UPR 8521 (Laboratory of PROcesses, Materials, Solar Energy), Rambla de la Thermodynamique 66100 Perpignan, France / 7 rue du Four Solaire 66120 Font-Romeu-Odeillo-Via, France Université de Perpignan Via Domitia, 52 Avenue Paul Alduy 66860 Per
- **Babacar Diallo** / CEMHTI-CNRS UPR 3079 (Conditions Extrêmes et Matériaux : Haute Température et Irradiation), Université d'Orléans, Site Cyclotron, 3A rue de la Férollerie 45071 Orléans, France
- **Béatrice Plujat** / PROMES-CNRS UPR 8521 (Laboratory of PROcesses, Materials, Solar Energy), Rambla de la Thermodynamique 66100 Perpignan, France / 7 rue du Four Solaire 66120 Font-Romeu-Odeillo-Via, France Université de Perpignan Via Domitia, 52 Avenue Paul Alduy 66860 Per
- **Angélique Bousquet** / Université Clermont Auvergne, CNRS, SIGMA Clermont, ICCF, 24 Avenue Blaise Pascal 63178 Aubière, France
- **Thierry Sauvage** / CEMHTI-CNRS UPR 3079 (Conditions Extrêmes et Matériaux : Haute Température et Irradiation), Université d'Orléans, Site Cyclotron, 3A rue de la Férollerie 45071 Orléans, France
- **Audrey Soum-Glaude** / PROMES-CNRS UPR 8521 (Laboratory of PROcesses, Materials, Solar Energy), Rambla de la Thermodynamique 66100 Perpignan, France / 7 rue du Four Solaire 66120 Font-Romeu-Odeillo-Via, France Université de Perpignan Via Domitia, 52 Avenue Paul Alduy 66860 Per
- **Éric Tomasella** / Université Clermont Auvergne, CNRS, SIGMA Clermont, ICCF, 24 Avenue Blaise Pascal 63178 Aubière, France
- **Laurent Thomas** / PROMES-CNRS UPR 8521 (Laboratory of PROcesses, Materials, Solar Energy), Rambla de la Thermodynamique 66100 Perpignan, France / 7 rue du Four Solaire 66120 Font-Romeu-Odeillo-Via, France Université de Perpignan Via Domitia, 52 Avenue Paul Alduy 66860 Per
- **Antoine Goulet** / Nantes Université, CNRS, Institut des Matériaux de Nantes Jean Rouxel, IMN, F-44000 Nantes, France

\* Auteur correspondant

The solar energy resource is still relatively under-exploited although it could cover most of our energy needs. Beyond the development of photovoltaics, there is a worldwide challenge to deploy large-scale concentrated solar thermal power plants. To address this issue, materials with high absorption in the visible, low emissivity and good temperature resistance are needed. To this end, multi-layered optical coatings produced by plasma processes are developed in the NANOPLAST project (nanoplast-project.cnrs.fr, ANR-19-CE08-0019).

The absorbing active layer WSiC:H is obtained by reactive magnetron sputtering of a W target in the presence of tetramethylsilane (TMS Si(CH<sub>3</sub>)<sub>4</sub>) diluted in argon. The top TaON antireflective layer is also deposited by reactive magnetron sputtering from a metallic tantalum target by controlling the oxygen and nitrogen flow rates in the plasma discharge.

TEM characterisations were carried out to get insight on the nature of the absorber and the antireflective top coating. Depending on the TMS proportion in the discharge, the quantity of Si introduced in the WSiC:H material can be tuned. In specific conditions (8% TMS), W nano-crystalites could be identified by coupling HAADF images (Figure 1), EDS mapping and High Resolution imaging (Figure 2). TEM characterisations were also performed on WSiC:H films at different TMS contents (20 and 28%).

**Mots clefs :** Concentrated Solar Power, Plasma processes, Multilayer coating, Transmission Electron Microscopy,

W-SiCH, nano-crystallites

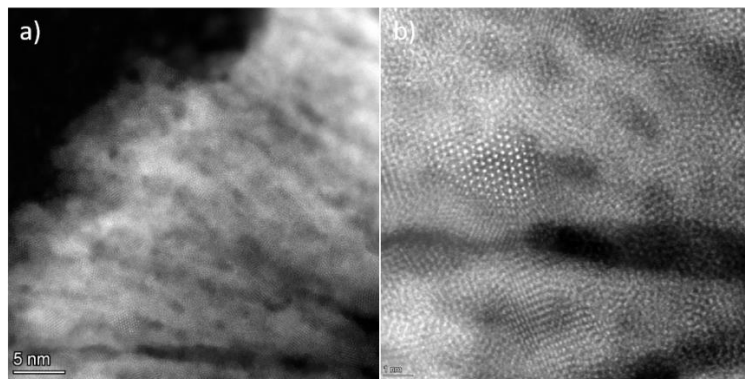


*Figure 1:* STEM-HAADF images of WSiC:H (8% TMS). Observation of multiple nano-crystalites corresponding to different orientations of bcc W metal.

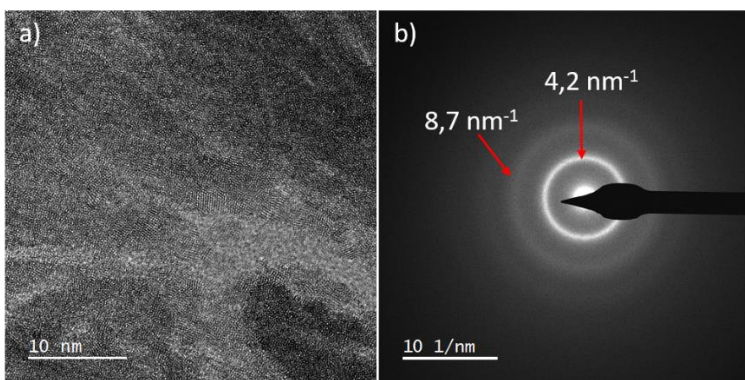


*Figure 2:* (a) HR-TEM image of WSiC:H (8% TMS), and (b) SAED pattern from the image (a).

## SDM3 – Oral6

### Étude de l'influence du laminage à froid sur la précipitation d'un alliage AA2024 industriel à l'aide de techniques de microscopie avancées

#### Investigating the Influence of Cold Rolling on Precipitation in Industrial AA2024 using Advanced Microscopy Techniques

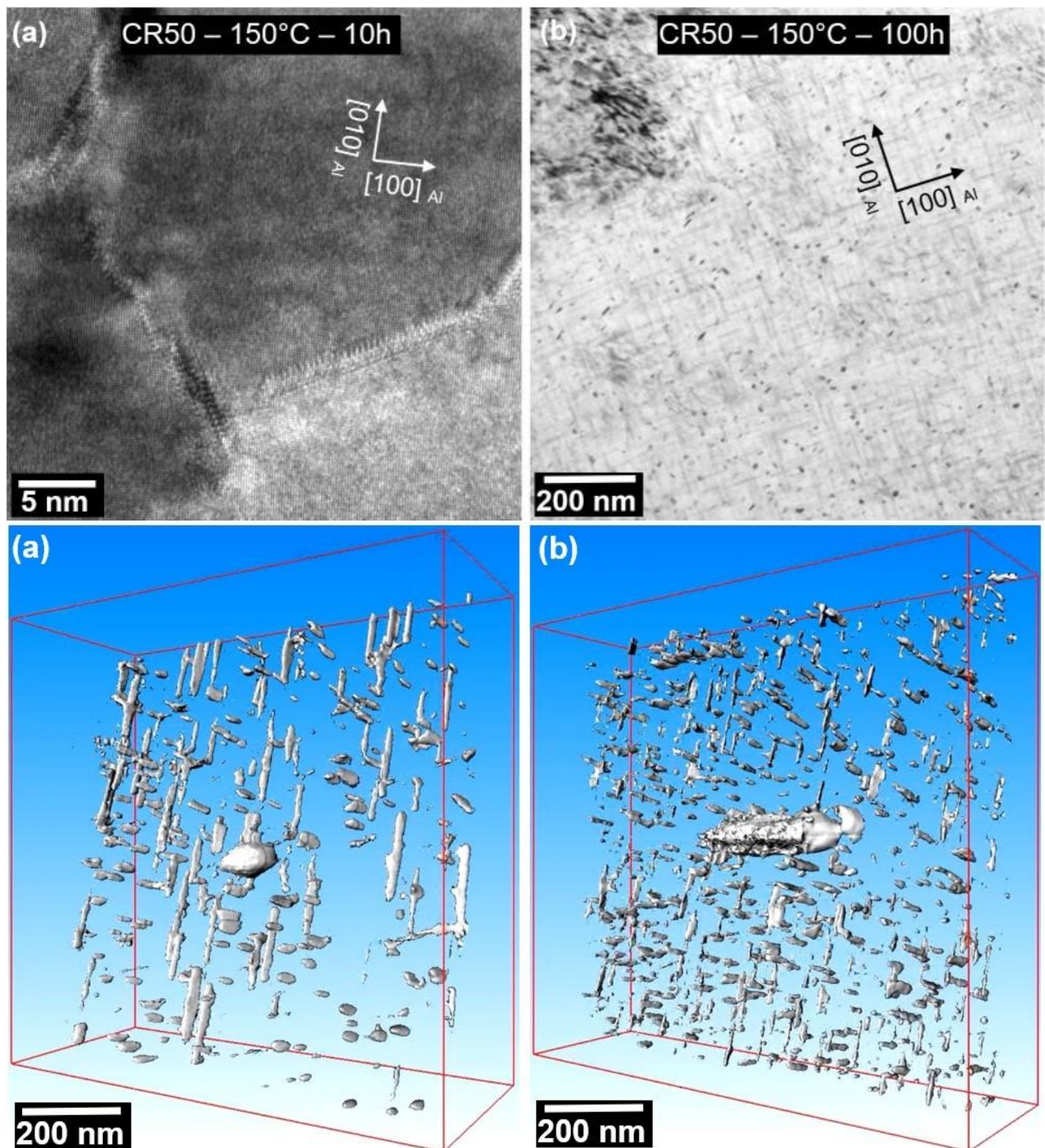
- **Daniel Irmer** \* (daniel.irmer@minesparis.psl.eu) / Mines Paris, Université PSL, Centre des Matériaux (MAT), UMR7633 CNRS, 91003 Evry, France.
- **Lisa T. Belkacemi** / Leibniz-Institute for Materials Engineering-IWT, Bremen, Germany.
- **Vladimir A. Esin** / Mines Paris, Université PSL, Centre des Matériaux (MAT), UMR7633 CNRS, 91003 Evry, France.
- **Charbel Moussa** / Mines Paris, Université PSL, Centre de Mise en Forme des Matériaux (CEMEF), UMR7635 CNRS, 06904 Sophia Antipolis, France.
- **Mohamed Sennour** / Mines Paris, Université PSL, Centre des Matériaux (MAT), UMR7633 CNRS, 91003 Evry, France.

\* Auteur correspondant

Precipitation hardened aluminium alloys are widely used for various applications due to their properties, such as low density to strength ratio and high corrosion resistance. AA2024 is a commonly used aluminium alloy in the aerospace industry with a quite simple precipitation sequence including co-cluster and Guinier-Preston-Baragyatski (GPB) zone formation during natural ageing and precipitation of the equilibrium S-phase ( $\text{Al}_2\text{CuMg}$ ) during artificial ageing [1]. This study aims to investigate the influence of pre-deformation by cold rolling (CR) on subsequent precipitation during artificial ageing in industrial AA2024. Electron backscatter diffraction (EBSD) was used to analyse the deformation microstructure focusing on the arrangement of dislocation substructures. Atom probe tomography (APT) and differential scanning calorimetry (DSC) were used to characterize co-clusters in the naturally aged AA2024-T3, and demonstrated their dissolution during cold rolling, without any further nucleation or growth during subsequent natural ageing. Precipitate evolution during artificial ageing of cold-rolled (CR) samples was investigated by transmission electron microscopy (TEM). Although heterogenous nucleation on dislocations was observed, the precipitates appear with a spacially homogeneous distribution at peak hardness (Fig. 1). Dark-field imaging and high-angle annular dark-field scanning transmission electron microscopy (HAADF-STEM) tomography were performed to study the size distribution and three-dimensional arrangement of the S-phase precipitates. A refinement of precipitates in the previously cold-rolled samples was observed (Fig. 2), connected to changes in the aspect ratio of precipitates.

The study demonstrates how advanced microscopy techniques contribute to the understanding of microstructural changes and precipitation behaviour in aluminium alloys and therefore contribute to the development of novel production processes.

**Mots clefs :** Al–Cu–Mg alloys, Precipitation hardening, Transmission electron microscopy (TEM), Atome Probe Tomographie (APT)



## **SDM4 : Spectroscopie à haute résolution, ultrarapide**

***Animation :***

*Jaysen Nelayah (MPQ, Paris)*

*Matthieu Bugnet (MATEIS, Lyon)*

**SDM4 – Inv1****Ultrafast Transmission Electron Microscopy : principle, instrumental aspects and applications**

- **Arnaud Arbouet\*, Sophie Meuret, Hugo Lourenço-Martins, Sébastien Weber, Florent Houdellier**  
CEMES-CNRS, Toulouse, France

\* Corresponding author : arbouet@cemes.fr

Ultrafast Transmission Electron Microscopes (UTEM) combining sub-picosecond temporal resolution and nanometer spatial resolution have emerged as unique tools for investigations at ultimate spatio-temporal resolution [1]. In this talk, we will report on the development of two generations of high-brightness UTEMs. First, the different approaches available to get time-resolved information in electron microscopes will be briefly reviewed. We will then discuss in details our UTEM technology which relies on femtosecond electron pulses generated from a cold field emitter by photo-emission driven by ultrashort laser pulses. The properties of the ultrafast electron beam have made possible several applications such as the acquisition of electron holograms with femtosecond electron pulses [2,3] or the measurement of the lifetime of excited states in semiconductors with a sub-wavelength spatial resolution [4].

We will discuss these applications as well as the potential of high brightness UTEMs in nano-optics and nanomechanics. The current limits of these instruments as well as the avenues for improvement that will be explored in the very near future will be presented.

[1] *Ultrafast Transmission Electron Microscopy : fundamentals, instrumentation and applications*

Arnaud Arbouet, Giuseppe M. Caruso, Florent Houdellier

Advances in Imaging and Electron Physics, Advances in Electronics and Electron Physics, 207, Elsevier, 2018, 1076-5670, **2018**

[2] *Development of a high brightness ultrafast Transmission Electron Microscope based on a laser-driven cold field emission source*

F. Houdellier, Giuseppe Mario Caruso, Sébastien Weber, Mathieu Kociak and Arnaud Arbouet  
*Ultramicroscopy*, 186, 128-138, **2018**

[3] *Optimization of off-axis electron holography performed with femtosecond electron pulses*

F. Houdellier, G. M. Caruso, S. Weber, M. J. Hÿtch, C. Gatel, A. Arbouet  
*Ultramicroscopy* 202, 26-32, **12, 2019**

[4] Time-resolved cathodoluminescence in an ultrafast transmission electron microscope

S Meuret, LHG Tizei, F Houdellier, S Weber, Y Auad, M Tencé, HC Chang, M. ociak, A. Arbouet  
*Applied Physics Letters* 119 (6), 062106, **2021**

**Mots-clés/Keywords:** Ultrafast Transmission Electron Microscopy, nano-optics, electron energy gains, acoustic vibrations

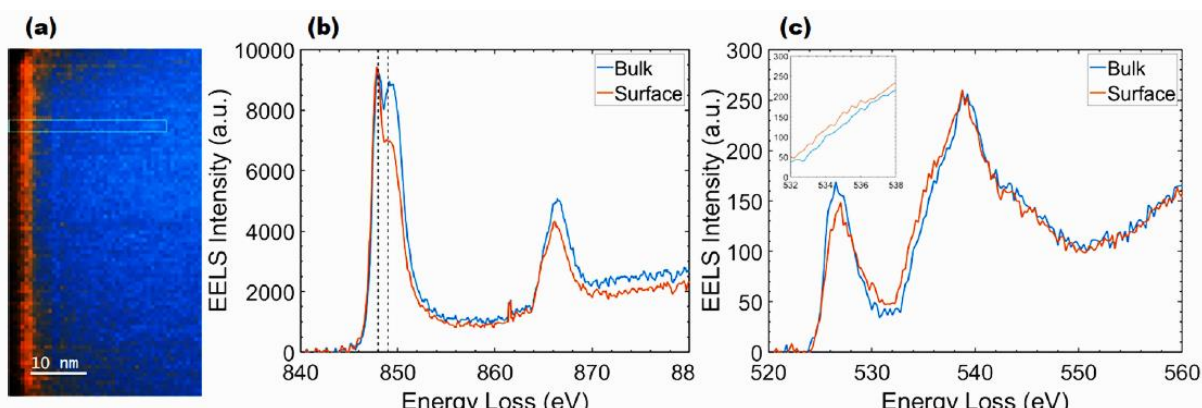
## SDM4 – Inv2

### EELS haute résolution de matériaux pour batteries : intérêts et limitations

- **Philippe Moreau** \* (Philippe.Moreau@cnrs-imn.fr) / Nantes Université, CNRS, Institut des Matériaux de Nantes Jean Rouxel, IMN, F-44000 Nantes, France
  - **Eric Gautron** (Eric.Gautron@cnrs-imn.fr) / Nantes Université, CNRS, Institut des Matériaux de Nantes Jean Rouxel, IMN, F-44000 Nantes, France
  - **Angelica.Laurita** / alors à l'IMN, désormais @BlueSolutions.
  - **Patricia Abellán** / (Patricia.Abellan@cnrs-imn.fr) / Nantes Université, CNRS, Institut des Matériaux de Nantes Jean Rouxel, IMN, F-44000 Nantes, France
- \* Corresponding author

La pertinence de l'utilisation d'un microscope monochromaté dans le contexte de l'étude de batteries (lithium, sodium, solide, organique...) se pose en raison de contraintes expérimentales particulières et également à la lumière des informations souhaitées. Une recherche autour des mots clés Monochromated/EELS/Batteries donne 3 (trois) réponses positives. En étendant le champ de la recherche, une dizaine d'articles doivent être considérés. La présence minimale dans la bibliographie de cette technique de pointe interroge. Dans un premier temps de la présentation, ces exemples seront étudiés pour en extraire la justification scientifique et percevoir les limitations.

Dans un second temps, deux études récentes à l'IMN seront exposées : un matériau oxyde NMC811 en se focalisant sur les seuils L<sub>2,3</sub> des métaux de transition [1] et un matériau phosphate LiMn<sub>x</sub>Fe<sub>1-x</sub>PO<sub>4</sub> avec une attention plus particulière sur les pertes faibles. Ils seront à nouveau l'occasion de discuter l'association mono-EELS vs batteries.



Cartographie obtenue à partir d'EELS monochromaté d'une particule primaire de NMC811 (MLLS fit) (a) utilisant les spectres L<sub>2,3</sub> du Ni (b) et K du O (c). [1]

Enfin, quelques messages seront donnés à titre personnel sur l'intérêt d'un faisceau monochromaté et ce qu'il faudrait davantage améliorer dans la (més)alliance EELS-batteries.

[1] A. Laurita et al.. ACS Appl. Mater. Interfaces 2022, **14**, 37, 41945–41956

**Mots-clés/Keywords:** monochromaté, EELS, batteries, haute resolution énergétique

## SDM4 – Oral1

### Mesures de durée de vie résolues au nanomètre et à la nanoseconde grâce aux coïncidences électron-photon

Nanometer and nanosecond resolved lifetime measurements through electron-photon coincidences

- **Jassem Baaboura** \* (jassem.baaboura@universite-paris-saclay.fr) / Université Paris-Saclay, CNRS, Laboratoire de Physique des Solides, 91405, Orsay, France
- **Yves Auad** / Université Paris-Saclay, CNRS, Laboratoire de Physique des Solides, 91405, Orsay, France
- **Elçin Akar** / Univ. Grenoble Alpes, CEA-IRIG, PHELIQS, 38000, Grenoble, France
- **Jean-Denis Blazit** / Université Paris-Saclay, CNRS, Laboratoire de Physique des Solides, 91405, Orsay, France
- **Mathieu Kociak** / Université Paris-Saclay, CNRS, Laboratoire de Physique des Solides, 91405, Orsay, France
- **Eva Monroy** / Univ. Grenoble Alpes, CEA-IRIG, PHELIQS, 38000, Grenoble, France
- **Luiz Henrique Galvao Tizei** / Université Paris-Saclay, CNRS, Laboratoire de Physique des Solides, 91405, Orsay, France

\* Auteur correspondant

III-nitride semiconductors attract interest due to their lighting technology applications. However, nitride-based light emitting devices (LEDs) suffer deleterious effects from lattice-mismatch strain. III-N heterostructured nanowires are a solution to this problem, as surfaces relax strain. As these are intrinsically small (~100 nm diameter), their characterization requires high-spatial resolution. Transmission electron microscopy and spectroscopie impacted their physics understanding [1]. For light emitters, two important quantities are excitations' lifetime and their quantum efficiency. Electron spectroscopies have also contributed here, including time-resolved cathodoluminescence, CL [2, 3, 4] and g(2)(t) measurements in CL through light bunching [5-7].

Here we consider another route to map lifetimes and relative quantum efficiency in III-nitrides using temporal coincidences between electron energy loss spectroscopy (EELS) and CL. This combination has been recently used to perform cathodoluminescence excitation (CLE) spectroscopy in diamonds and h-BN [8]. The capacity to measure lifetimes in the nanosecond range using this technique is under exploration.

GaN quantum disks (QDs) with 3.5 and 1 nm width (Figure 1a) have been grown in AlN nanowires (NW) using Molecular Beam Epitaxy, with 50 nm AlN barriers. A QDs CL-filtered map is shown in Figure 1b. The blue, orange and purple spectra (Figure 1c) correspond to the average spectra of CL from regions shown Figure 1a,b.

The 2D histogram (Figure 1d) shows the temporal evolution of electron-photon coincidence versus the position along the nanowire. The coincidence profiles (Figure 1e) decay time corresponds to the delay between the excitation and the photon emission. A significant decay time variation is observed between QDs (from 10.3 to 25.4 ns). A still to be understood small temporal profile maximum's shift occurs (2ns).

References:

- [1] L. F. Zagonel et al., APS, 93 (2016), 205410
- [2] M. Merano et al., Nature, 438 (2005), 479-482
- [3] S. Meuret et al., Ultramicroscopy, 197 (2019), 28-38
- [4] S. Meuret et al., Appl. Phys. Lett., 119 (2021), 062106
- [5] S. Meuret et al., Phys. Rev. Lett., 114 (2015), 197401
- [6] S. Meuret et al., ACS, 3 (2016), 1157-1163
- [7] S. Finot et al., ACS, 117 (2020), 221105
- [8] N. Varkentina et al., Sc. Adv., 8 (2022), 40

**Mots clefs** : cathodoluminescence, Energy electron loss spectroscopy, quantum wells, time-resolved, coincidence electron-photon

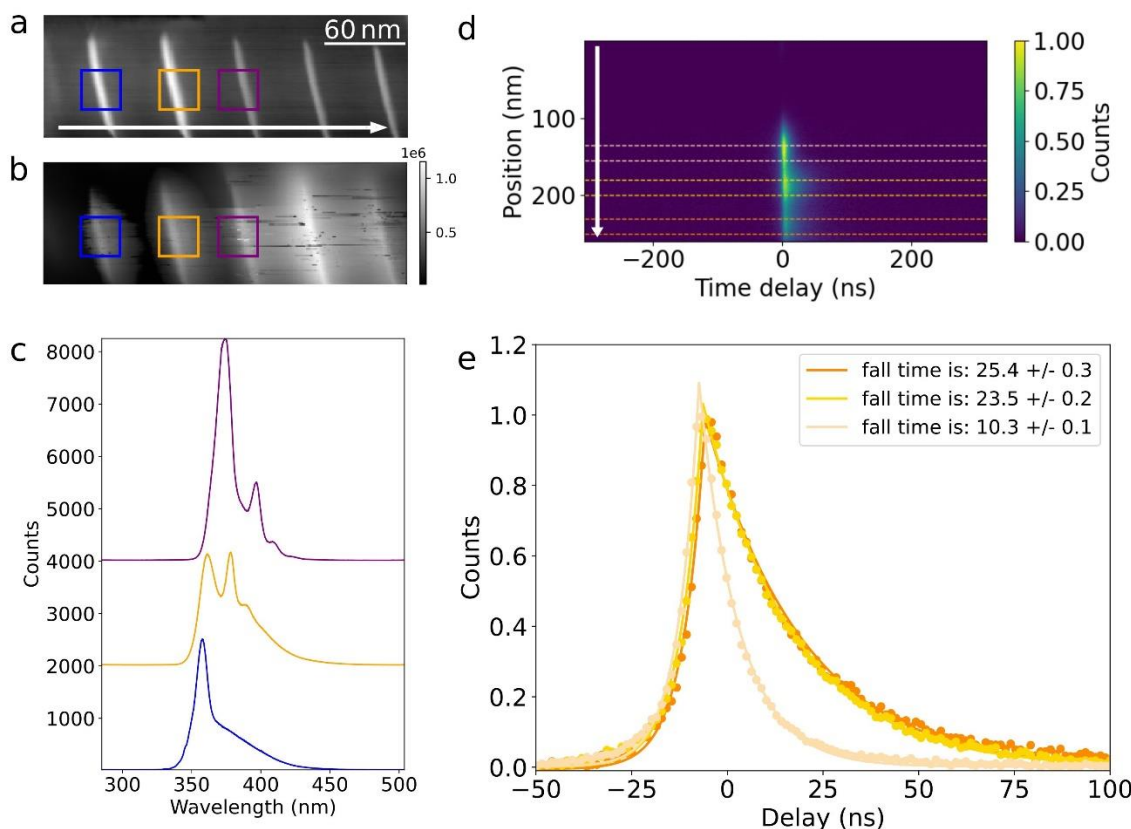


**Figure 1:** CL and lifetimes of GaN/AlN QDs: **(a-b)** HAADF image and CL filtered map. **(c)** Average CL spectrum in the squares in (a-b). **(d)** Decay profile as a function of position with an uncorrelated background set to 0 and the maximum to 1. **(e)** Average decay profile in the ROIs marked in (d). The arrows in (a) and (d) show their relative orientation.

## SDM4 – Oral2

### Microscopie électronique à transmission ultrarapide avec des impulsions électroniques nanoseconde

Time-resolved TEM and EELS of nanomaterials with nanosecond electron pulses

- **Matthieu Picher \*** ([Matthieu.Picher@ipcms.unistra.fr](mailto:Matthieu.Picher@ipcms.unistra.fr)), **Yaowei Hu, Hui Zhang, Shyam K. Sinha, Amir Khammari, François Roulland, Nathalie Viart** / Institut de Physique et Chimie des Matériaux, Université de Strasbourg, CNRS UMR 7504, Strasbourg, France
- **Marlène Palluel, Nathalie Daro, Guillaume Chastanet** / CNRS, Univ. Bordeaux, ICMCB, UPR 9048, Pessac, France
- **Ngoc Minh Tran** / Laboratoire Ondes et Matière d'Aquitaine, Talence, France
- **Eric Freysz** / Laboratoire Ondes et Matière d'Aquitaine, Talence, France
- **Ritwika Mandal, Philippe Rabiller, Maciej Lorenc** / Institut de Physique de Rennes, Université de Rennes, CNRS, Rennes, France
- **Thomas LaGrange** / Ecole Polytechnique Fédérale de Lausanne, Lausanne, Suisse
- **Florian Banhart** / Institut de Physique et Chimie des Matériaux, Université de Strasbourg, CNRS UMR 7504, Strasbourg, France

\* Auteur correspondant

Many dynamic processes at the nanoscale are not accessible by conventional TEM because they happen at shorter timescales than the millisecond. This restriction is being overcome by developing ultrafast TEMs working with short electron pulses in a pump-probe configuration.[1,2] Here, after presenting our instrumental setup working with two nanosecond lasers(Fig.1), we will present examples of recent investigations that have been carried out with the UTEM in Strasbourg.

In nanocrystalline oxides, phase transformations and chemical reactions can be induced by nanosecond laser pulses. (i) Fast phase transformations are studied in Ti<sub>3</sub>O<sub>5</sub> that can be used for photoswitches. The unique behaviour of Ti<sub>3</sub>O<sub>5</sub> under laser pulses allows us to switch in a reversible way between different phases and to measure the speed of the phase transformation in individual nanocrystals. This is undertaken in a stroboscopic approach where two electronically coupled nanosecond lasers are operated at low repetition frequency. (ii) Irreversible reactions such as the laser-induced reduction of oxide nanocrystals are studied in the single-shot approach. Electron energy-loss spectroscopy with acquisition times of nanoseconds opens a new approach to the study of fast reaction kinetics at the nanoscale.[3]

Further experiments are carried out on spin-crossover (SCO) materials which show a reversible switching between different spin states (high-spin and low-spin) under laser pulses. Due to different bond lengths in the two spin states, length changes of crystalline SCO particles are thus induced by laser pulses and can be detected by imaging and electron diffraction. A detailed study by stroboscopic UTEM shows that fast resonant oscillations between the high- and low-spin phase of SCO nanoparticles occur at the nanosecond time scale (Fig.2). This shows that SCO particles are a unique system where a resonant oscillation between two phases can be observed in a phase transformation of first order.[4]

[1]K. Bücker et al., Ultramicroscopy 171, 8 (2016)

[2]M. Picher et al., Ultramicroscopy 188, 41 (2018)

[3]S. K. Sinha et al., Nature Comm. 10, 3648 (2019)

[4]Y. Hu et al., Advanced Materials 33, 52 (2021)

Funding by the ANR (ANR-11-EQPX-0041 & ANR-22-CE09-0033-01), and METSA network are gratefully acknowledged.

**Mots clefs** : time-resolved TEM, UTEM, fast processes

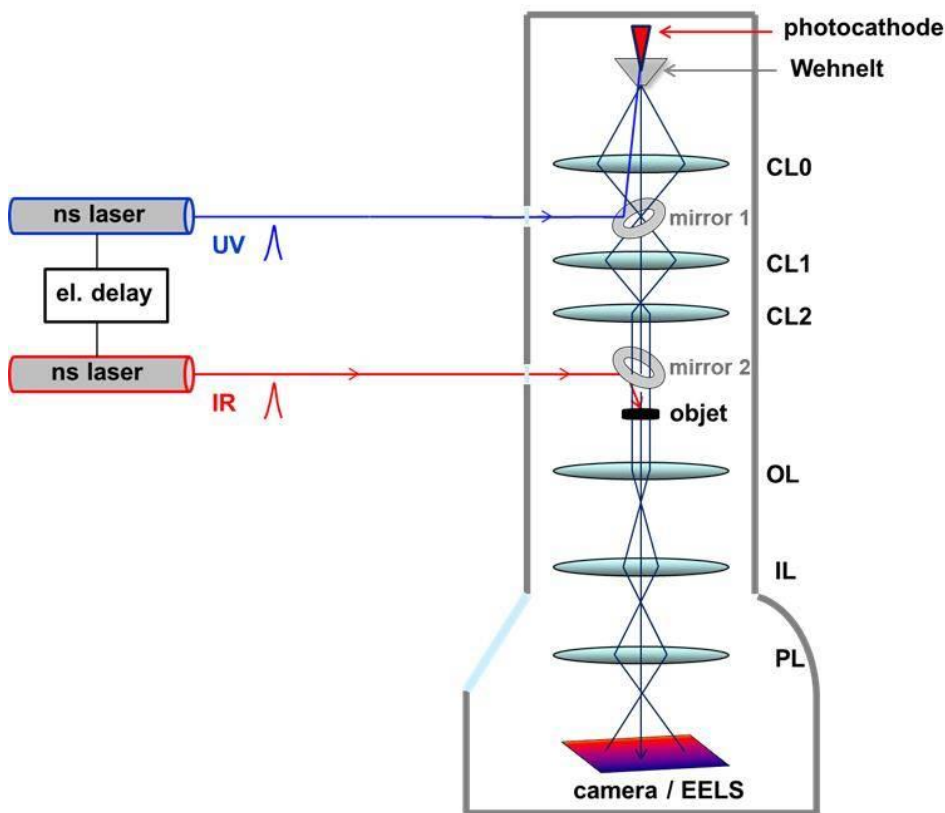


**Figure 1.** Principle of ultrafast (or dynamic) TEM. The pump and probe laser pulses reach the photocathode and the specimen, respectively, after being transmitted through windows and reflected by mirrors in the TEM column.

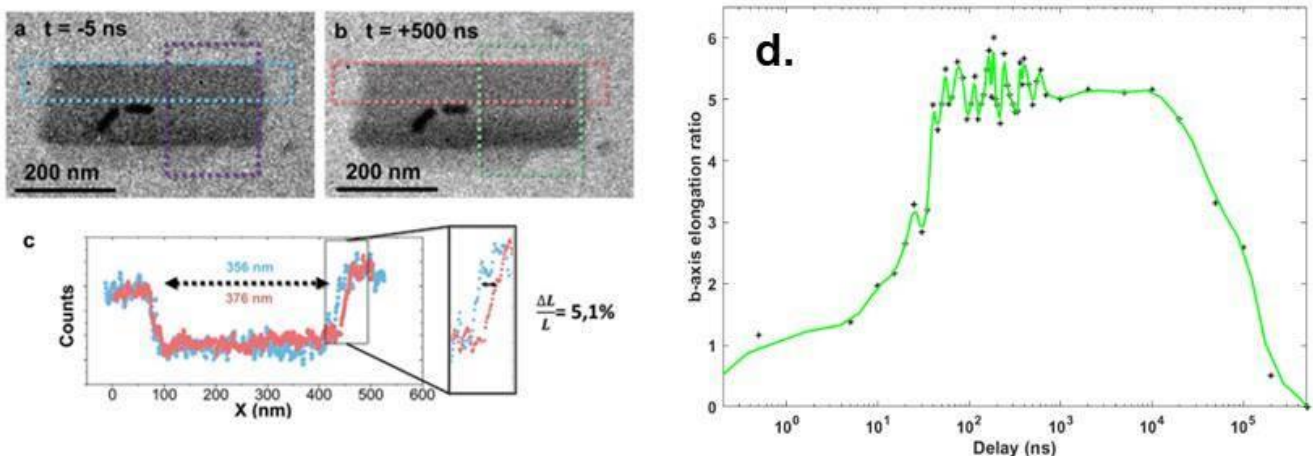


**Figure 2.** A SCO particle (encapsulating two gold nanorods) (a) before and (b) 500 ns after a 7 ns 1064 nm IR pulse. (c) The profile change shows a length variation of about 5%. (d) Time-resolved length measurements of a SCO particle showing the vibration of the SCO with a period of about 50 ns.

## SDM4 – Oral3

### Spectroscopie vibrationnelle à la nano-échelle en STEM : étude des effets d'altération spatiale sur la signature IR de l'astéroïde Ryugu

**Space weathering influence on Ryugu's IR signature: insights from nanoscale vibrational spectroscopy in the STEM**

- **Sylvain LAFORET** \* (Sylvain.Laforet@univ-lille.fr) / Université de Lille, CNRS, INRAE, Centrale Lille, UMR 8207-UMET-Unité Matériaux et Transformations, F-59000 Lille, France
- **Hugues LEROUX** / Université de Lille, CNRS, INRAE, Centrale Lille, UMR 8207-UMET-Unité Matériaux et Transformations, F-59000 Lille, France
- **Corentin LE GUILLOU** / Université de Lille, CNRS, INRAE, Centrale Lille, UMR 8207-UMET-Unité Matériaux et Transformations, F-59000 Lille, France
- **Francisco DE LA PENA** / Université de Lille, CNRS, INRAE, Centrale Lille, UMR 8207-UMET-Unité Matériaux et Transformations, F-59000 Lille, France
- **Damien JACOB** / Université de Lille, CNRS, INRAE, Centrale Lille, UMR 8207-UMET-Unité Matériaux et Transformations, F-59000 Lille, France
- **Maya MARINOVA** / Université de Lille, CNRS, INRAE, Centrale Lille, Université Artois, FR 2638-IMEC-Institut Michel-Eugène Chevreul, F-59000 Lille, France.
- **Michael WALLS** / Laboratoire de Physique des Solides, UMR CNRS 8502, Bât. 510, Université Paris-Sud, Université Paris Saclay, 91400 Orsay, France
- **TIZEI Luiz** / Laboratoire de Physique des Solides, UMR CNRS 8502, Bât. 510, Université Paris-Sud, Université Paris Saclay, 91400 Orsay, France
- **Pierre BECK** / Université de Grenoble, Laboratoire de Planétologie de Grenoble, Institut de Planétologie et d'Astrophysique de Grenoble, OSUG/CNRS, 38000 Grenoble, France
- **Van T.H. PHAN** / Université de Grenoble, Laboratoire de Planétologie de Grenoble, Institut de Planétologie et d'Astrophysique de Grenoble, OSUG/CNRS, 38000 Grenoble, France

\* Auteur correspondant

Le récent développement de microscopes électroniques monochromatés dédiés à la spectroscopie EELS à haute résolution met sur le devant de la scène la possibilité d'atteindre la gamme spectrale de l'infrarouge moyen avec, au mieux, une résolution spectrale de 40 cm<sup>-1</sup> [1]. Cette technique ouvre une porte vers des comparaisons avec des études IR à plus large échelle.

En parallèle, la mission spatiale Hayabusa2 de la JAXA a ramené, fin 2020, 5,4 g de la surface de l'astéroïde carboné Ryugu. Une partie de ces grains présentent une surface modifiée par des effets d'altération spatiale [2]. Ce phénomène est principalement dû à l'irradiation par vent solaire et aux bombardements micro-météoritiques sur la surface d'objets dépourvus d'atmosphère. L'étude de ces échantillons permet donc de mieux comprendre comment un astéroïde de type-C évolue lorsqu'il est exposé à ces sollicitations externes. Les surfaces modifiées par ces phénomènes d'altération spatiale ont été identifiées au MEB et des lames minces y ont été prélevées (FIB). La minéralogie de Ryugu est principalement constituée de phyllosilicates (silicates hydratés). Les phénomènes d'altération spatiale entraînent leur amorphisation ainsi que la formation de couches vésiculées (jusqu'à ~3 µm d'épaisseur). Nos résultats montrent qu'il est possible d'isoler les signatures spectrales IR de ces couches fondues de celles de la matrice hydratée. En particulier, nous mettons en évidence la perte des modes vibrationnels d'H<sub>2</sub>O et d'-OH dans ces couches fondues. Cela pourrait expliquer pourquoi la bande à 2.7 µm, correspondant aux groupements hydroxyles, est deux fois moins intense dans les données de NIRS3 que

dans celles des échantillons collectés [3]. Nous observons également la perte des modes liés à la matière organique dans les couches fondues, en adéquation avec les données EDS. Nous démontrons donc que l'altération spatiale peut significativement modifier les signatures IR d'astéroïdes de type-C hydratés, pouvant entraîner une sous-estimation de leur teneur en eau et en carbone lors de leur analyse à distance (ie. James Webb Space Telescope).

Références :

- [1] Colliex (2022) The European Physical Journal Applied Physics
- [2] Noguchi et al. (2022) Nature Astronomy
- [3] Nakamura et al. (2022) Science

**Mots clefs** : Vibrational Electron Energy Loss Spectroscopy - STEM - Ryugu asteroid

## SDM4 – Oral4

### Détermination par STEM-EELS de la densité atomique de Xe dans les nano-bulles de gaz de fission dans des combustibles nucléaires UO<sub>2</sub>.

STEM-EELS determination of Xe atomic density in fission gas nano-bubbles in UO<sub>2</sub> nuclear fuels.

- **Mathieu Angleraud \*** (mathieu.angleraud@cea.fr) / CEA, DES, IRESNE, DEC
- **Catherine Sabathier** / CEA, DES, IRESNE, DEC
- **Claire Onofri** / CEA, DES, IRESNE, DEC
- **David Reyes** / CEA, DES, IRESNE, DEC
- **Doris Drouan** / CEA, DES, IRESNE, DEC
- **Alain Chartier** / CEA, DES, ISAS, DPC,
- **Cécile Marcelot** / CNRS, CEMES
- **Bénédicte Warot-Fonrose** / CNRS, CEMES

\* Auteur correspondant

During its use in a nuclear reactor, the uranium dioxide fuel undergoes significant structural and physico-chemical changes. Indeed, the nuclear fission reaction leads to the formation of fission products involving the creation of defects and new chemical elements in the matrix. Among these, fission gases (FG) and their particular behaviour (precipitation, diffusion, and release) are a major issue for the lifetime of the nuclear fuel in reactor. As a result, acquiring high-fidelity FG bubbles characteristics at the nano-scale should help improving the predictivity of Pressurised Water Reactor fuel performance codes.

A challenging information is the internal pressure inside the bubbles. Indeed, some previous studies have already succeeded in obtaining such data but these have high uncertainties [1] [2]. Nevertheless, several experimental works [1]–[4] have shown that these bubbles were strongly over-pressurised and could induce high local stresses for the UO<sub>2</sub> matrix.

To complete existing literature and update fuel behaviour codes, the present work proposes a first study by STEM-EELS of the xenon atomic density of the FG nano-bubble populations in UO<sub>2</sub> fuels. Using advanced characterization technologies and procedures proven on other materials [5] [6], the ultimate goal is to obtain xenon induce pressure in the nano-bubbles present in the UO<sub>2</sub> matrix, as a function of their size.

To achieve this goal, TEM characterizations were done in the LECA-STAR hot laboratory at the CEA Cadarache in France using a TALOS F-200X G2 and a Continuum GATAN Imaging Filter system. Thanks to optimization of TEM imagery conditions coupled with Dual-EELS acquisition, this study allows us to achieve a fine characterization of FG bubbles at the nano-scale on a Xe implanted fresh fuel and on a reactor-irradiated fuel.

#### Références/References :

- [1] Thomas, Fundamental Aspects of Inert Gases in Solids (1991), p. 431
- [2] Nogita and Une, NIMB (1998), vol. 141, p. 481–486
- [3] Garcia et al., JNM (2006), vol. 352, p. 136–143
- [4] Martin et al., NIMB (2008), vol. 266, p. 2887–2891
- [5] Walsh et al., Philosophical Magazine A (2000), vol. 80, p. 1507–1543
- [6] B. Evin et al., JAC (2021), vol. 878, 160267

**Mots clefs :** STEM-EELS / Xe bubbles / UO<sub>2</sub> / Nuclear fuel / Atomic density

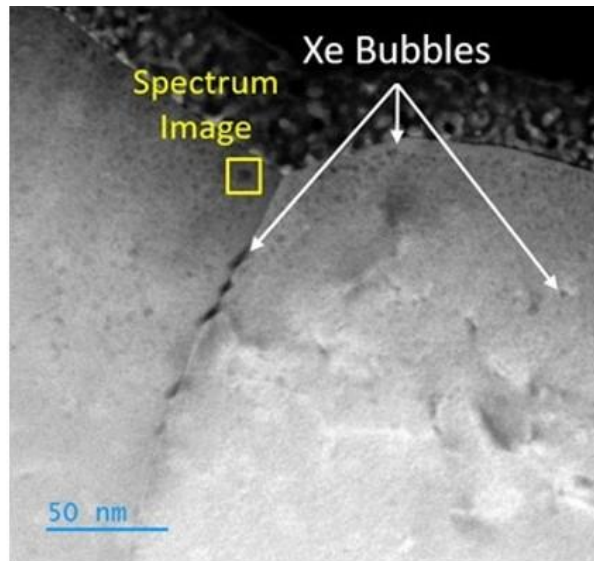


Figure 1: HAADF (95 - 200 mrad) image of a Xe implanted  $\text{UO}_2$  fresh fuel after annealing  $1300^\circ\text{C}-1\text{h}$

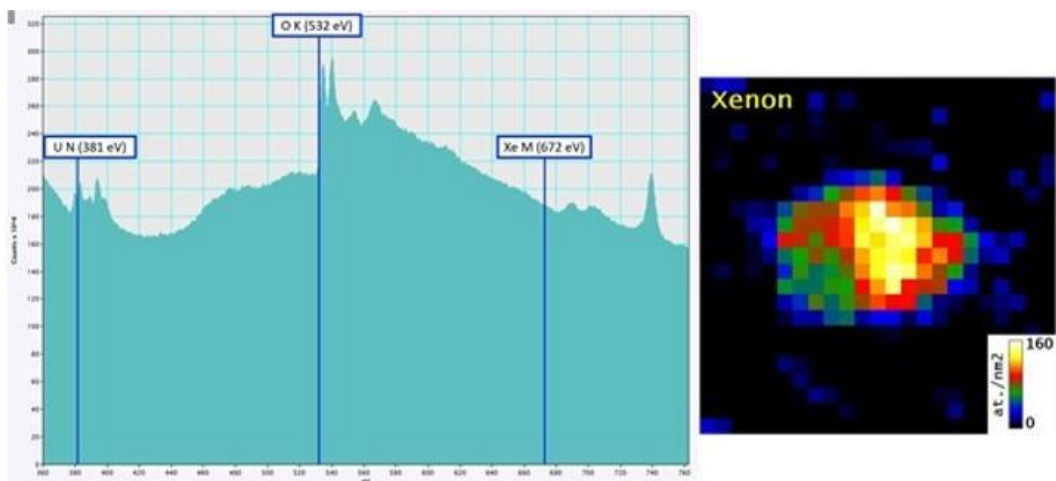


Figure 2: (a) Spectrum extracted from a SI of a Xe bubble (b) Xe atomic density map in atom/ $\text{nm}^2$

## **SDV1 : Techniques corrélatives, combinatoires ou multi-modales**

### ***Animation :***

*Christel Genoud (UNIL, Université de Lausanne ; Friedrich Miescher Institute for Biomedical Research, Basel)*

*Angélina d'Orlando (Plateforme Imagerie, Biochimie et Structure – BIBS, Nantes)*

## SDV1-Inv1

### Différentes approches de Microscopie Corrélatrice

- **Etienne Gontier** \* (etienne.gontier@u-bordeaux.fr) / Bordeaux Imaging Center, Univ. Bordeaux, CNRS, INSERM, UAR 3420, US 4, F-33000 Bordeaux, France
- **Lysiane Brocard** (lysiane.brocard@u-bordeaux.fr) / Bordeaux Imaging Center, Univ. Bordeaux, CNRS, INSERM, UAR 3420, US 4, F-33000 Bordeaux, France
- **Mónica Fernández-Monreal** (monica.fernandez-monreal@u-bordeaux.fr) / Bordeaux Imaging Center, Univ. Bordeaux, CNRS, INSERM, UAR 3420, US 4, F-33000 Bordeaux, France
- **Melina Petrel** (melina.petrel@u-bordeaux.fr) / Bordeaux Imaging Center, Univ. Bordeaux, CNRS, INSERM, UAR 3420, US 4, F-33000 Bordeaux, France

\* Corresponding author

Qu'est-ce que la microscopie corrélative ? La microscopie corrélative est une technique permettant de repérer des événements rares mais également compiler des informations complémentaires comme imager à différentes échelles, mais également obtenir à la fois des informations structurales et analytiques. Plusieurs techniques de microscopie corrélative existent comme par exemple : imagerie médicale et microscopie électronique ; microscopie électronique et NanoSIMS ; etc... Mais la plus connue reste la microscopie photonique versus microscopie électronique : la CLEM

La CLEM est utilisée pour étudier exactement la même région à la fois en microscopie optique et microscopie électronique (ME) afin d'ajouter des informations ultra structurales à un signal de fluorescence. Au fil des années, un certain nombre de méthodes de CLEM ont été développé. Malgré ces avancées, la capacité de relocaliser avec précision et fiabilité un élément d'intérêt reste techniquement difficile particulièrement sur des tissus biologiques. Par conséquent, de nouveaux développements sont nécessaires. Cet exposé aura pour but de présenter 4 projets autour de la CLEM qui sont actuellement en cours au Bordeaux Imaging Center, plateforme d'imagerie en photonique et électronique pour la biologie.

Nos thématiques scientifiques s'étendent du monde végétal au monde animal permettant l'exploitation de plusieurs approches de CLEM. Ainsi, dans un premier temps, sera présenté des méthodes mettant en jeu le principe de conservation de la fluorescence. Tout d'abord au travers de la technique d'**« In resin Fluorescence (IRF) »** [1] dont l'objectif est de conserver un signal fluorescent après inclusion en résine. Dans ce même esprit d'IRF, la technique d'**« Array-Tomography »** [2] permet non seulement d'exploiter potentiellement la conservation de la fluorescence mais surtout d'exploiter la 3D en microscopie électronique à balayage (3D MEB). Cette méthode est basée sur des coupes fines séries, l'immunomarquage et l'acquisition d'images de fluorescence et de ME de tissus inclus en résine, suivi d'une reconstruction de volume 3D. Ensuite, dans la volonté notamment d'améliorer la préservation des structures d'intérêts et la précision de leur localisation, la technique de **« cryoCLEM »** [3], aujourd'hui en pleine essor, sera présentée. L'objectif est de conserver le signal de fluorescence dans un échantillon cryofixé pour être observé en condition cryogénique à la fois en microscopie photonique mais également en cryo-MET voir cryo-tomo. Enfin, sera présenté une autre approche de repérage de la région d'intérêt. En effet, par l'utilisation de la technique des marques lasers « **Near-Infrared Branding** » (NIRB) [4], il est alors possible d'avoir accès à des événements rares dans un tissu épais non seulement en 2D mais surtout en 3D MEB et particulièrement par serial block face Imaging par ultramicrotomie in situ (SBF) [5].

[1] W. Kukulski et al., Methods Cell Biol, 111 (2012), p: 235-257. [doi.org/10.1016/B978-0-12-416026-2.00013-3](https://doi.org/10.1016/B978-0-12-416026-2.00013-3)

- [2] K.D. Micheva and S.J. Smith, *Neuron*, 55 (2007), p.25-36. doi.org/10.1016/j.neuron.2007.06.014
- [3] Y-W. Chang et al, *Nature Methods*, 11 (2014) p. 737–739. doi.org/10.1038/nmeth.2961
- [4] D. Bishop et al., *Nature Methods*, 8 (2011), p. 568–570. doi.org/10.1038/nmeth.1622 [5] W. Denk.  
*PLOS Biology*, 2 (2004) p. e329. doi.org/10.1371/journal.pbio.0020329

**Mots-clés/Keywords:** CLEM, in resin fluorescence, cryoCLEM, CLEM 3D

## SDV1-Inv2

### Correlative multi and hyperspectral imaging analysis for mapping cell wall composition in plants”

- **Fabienne Guillon** \* (fabienne.guillon@inrae.fr) / INRAE Nantes, UR1268 BIA, F-44300 Nantes
  - **Marie-Françoise Devaux\*** (marie-francoise.devaux@inrae.fr) / INRAE Nantes, UR1268 BIA, F-44300 Nantes
- \* Corresponding authors

Plants are heterogeneous materials that present a multiscale organization (organs, tissues, cell types, subcellular compartments). Tissues and enclosed cell types are highly specialised and differ from other by structural features. Cell walls whose composition and properties vary according to cell types are of major interest as they are involved in many end-use properties of plant biomass. Histological studies are therefore of major importance for evaluating the quality of plant material. Histology includes measuring morphological information about cells and tissues and investigating the composition of cell walls according to cell types. Spectral imaging is used to reveal variability in the biochemical composition at the cellular level without any labelling of the samples. However, single techniques generally provide a partial characterisation of the plant polymers. More complete information can be obtained by combining several spectral imaging methods [1].

Relating histological measures to end use properties is not an easy task because end-use properties are generally evaluated at a macroscopic scale including plant variability. The need to compare multiple plant samples brings additional constraints. All these multiple sets of images generate large and complex image collections that require the development of adapted methods to analyse them.

The objective of the presentation is to show the development of a multiscale and multimodal strategy to map the heterogeneity of cell wall composition in plant organs (Figure1).

[1] F. Allouche, M. Hanafi, F. Jamme, P. Robert, C. Barron, F. Guillon, M.F. Devaux. Chemometrics and Intelligent Laboratory Systems **117**, 200 (2012)

**Keywords:** Multispectral imaging, chemical mapping, plant tissues.

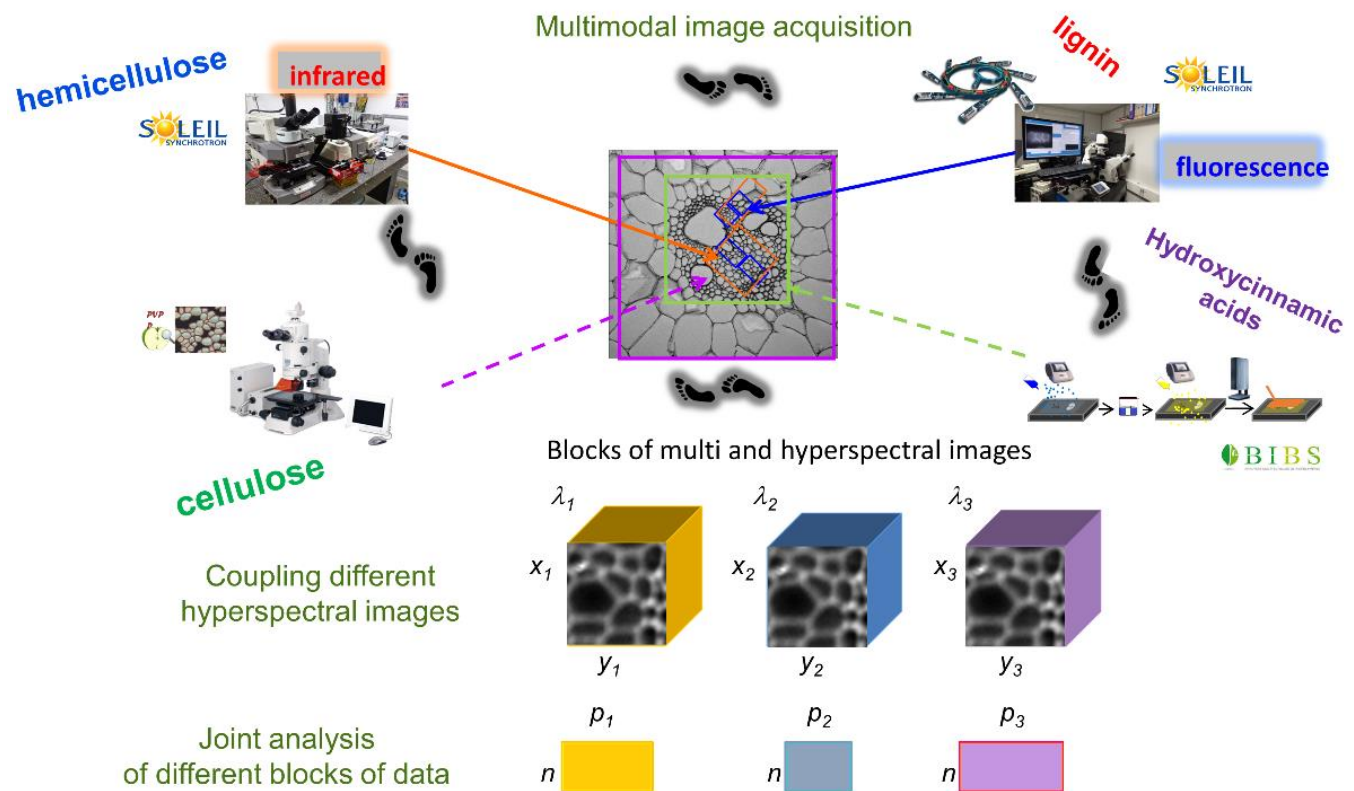


Figure 1: Workflow from multimodal image acquisition to joint data analysis

## SDV1-Oral1

### Fusion de données IRM et MALDI pour étudier le développement du grain de blé

#### Fusion of MRI and MALDI data for the study of wheat grain development

- Florent Grélard / Université de Bordeaux
- David Legland \* (david.legland@inrae.fr) / INRAE
- Loïc Foucat / INRAE
- Mathieu Fanuel / INRAE
- Hélène Rogniaux / INRAE

\* Auteur correspondant

L'eau et les polysaccharides des parois sont deux composantes qui impactent fortement les propriétés technologiques ou d'usage des produits agronomiques tels que le grain de blé. Nous avons utilisé l'imagerie par spectrométrie de masse (MSI) pour cartographier la composition chimique des échantillons, et l'imagerie par résonance magnétique (IRM) pour décrire l'anatomie des organes et leur état d'hydratation. Obtenir une vision complète de l'échantillon nécessite de pouvoir comparer et fusionner les informations obtenues par ces deux modalités. Les difficultés concernent la différence de résolution des images, et les déformations induites par la MSI lors de la préparation des échantillons.

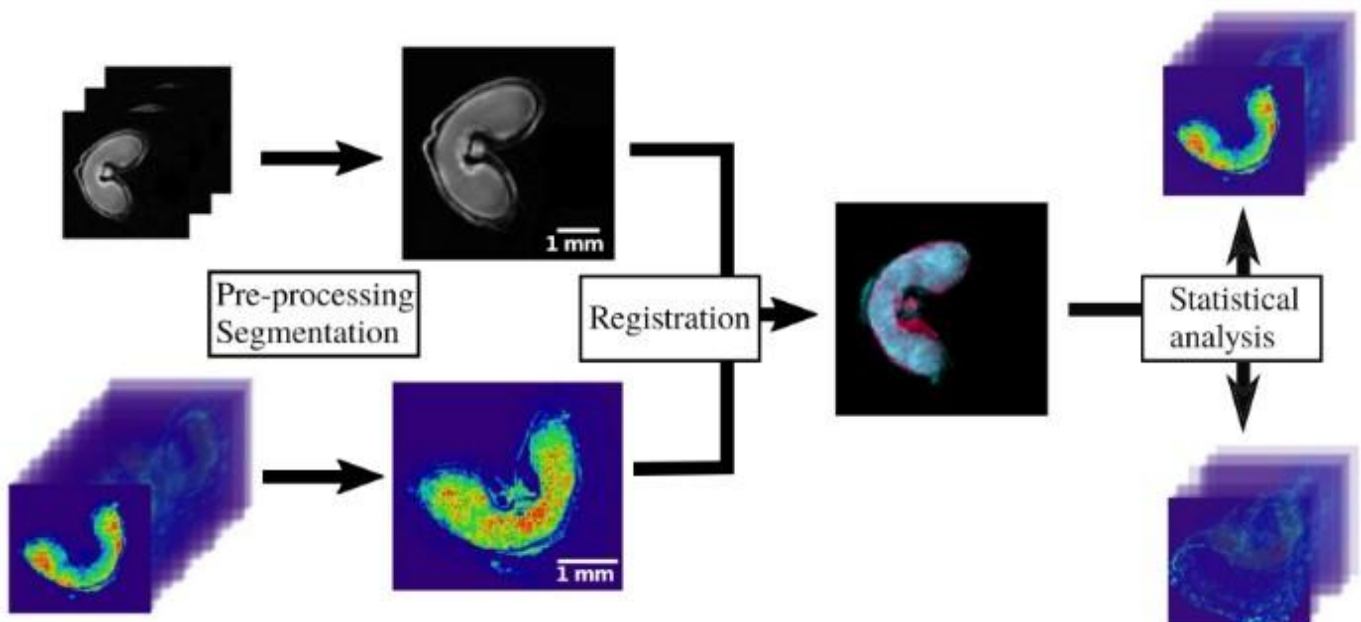
Nous avons développé une chaîne de traitement d'images qui comprend les étapes de pré-traitement spécifiques à chaque modalité, le recalage des images (par méthodes variationnelles) pour corriger les déformations et mettre les informations en correspondance spatiale, et une étape de réduction de dimension (NMF) pour simplifier les données. La superposition des informations permet de mettre en correspondance la mobilité de l'eau et la composition chimique.

La méthode permet de relier la nature de l'hydratation des parois du grain à celle du degré de substitution et d'acétylation des polysaccharides non cellulosaques. En particulier, la colocalisation des xylanes les plus substitués et/ou fortement acétylés dans les régions les plus hydratées suggère une plus grande porosité des parois liée à la modification des xylanes. Après avoir validé la méthode sur des coupes 2D, nous nous intéressons aux variations de ces corrélations dans le grain 3D à différents stades de développement.

#### Références/References :

- [1]Grélard F. et al. Esmraldi: efficient methods for the fusion of mass spectrometry and magnetic resonance images. BMC Bioinformatics (2021) <https://doi.org/10.1186/s12859-020-03954-z>.
- [2]Fanuel, M. et al. Spatial correlation of water distribution and fine structure of arabinoxylans in the developing wheat grain. Carbohydrate Polymers, <https://doi.org/10.1016/j.carbpol.2022.119738> (2022), p.294

**Mots clefs** : Correlative imaging, image registration, image data fusion, MRI, MALDI, multi-modal imaging



## SDV1-Oral2

# ELECTRON MICROSCOPY METHODS TO ASSAY THE ULTRASTRUCTURAL ORGANIZATION, MEMBRANE RESHAPING AND CURVATURE SENSITIVITY BEHAVIOR OF IN-VITRO SEPTINS NETWORK

- **Brieuc Chauvin** / Laboratoire Physico Chimie Curie, Institut Curie, PSL Research University, Sorbonne Université, CNRS UMR168, 75005, Paris, France
- **Koyomi Nakazawa** / Laboratoire Physico Chimie Curie, Institut Curie, PSL Research University, Sorbonne Université, CNRS UMR168, 75005, Paris, France
- **Alexandre Beber** / Laboratoire Physico Chimie Curie, Institut Curie, PSL Research University, Sorbonne Université, CNRS UMR168, 75005, Paris, France
- **Aurélie Di Cicco** / Laboratoire Physico Chimie Curie, Institut Curie, PSL Research University, Sorbonne Université, CNRS UMR168, 75005, Paris, France
- **Bassam Hajj** / Laboratoire Physico Chimie Curie, Institut Curie, PSL Research University, Sorbonne Université, CNRS UMR168, 75005, Paris, France
- **François Iv** / Institut Fresnel, CNRS UMR7249, Aix Marseille Univ, Centrale Marseille, 13013 Marseille, France
- **Manos Mavrakis** / Institut Fresnel, CNRS UMR7249, Aix Marseille Univ, Centrale Marseille, 13013 Marseille, France
- **Gijsje Koenderink** / Department of Bionanoscience, Kavli Institute of Nanoscience Delft, Delft University of Technology, Van der Maasweg 9, 2629 HZ Delft, The Netherlands
- **João Cabral** / Department of Chemical Engineering, Imperial College London, London SW7 2AZ, UK
- **Michaël Trichet** \* (michael.trichet@sorbonne-universite.fr) / Sorbonne Université, CNRS, Institut de Biologie Paris-Seine (IBPS), Service de microscopie électronique (IBPS-SME), F-75005, Paris
- **Stéphanie Mangenot** / Laboratoire Matière et Systèmes Complexes (MSC), Université Paris Cité, CNRS UMR 7057, 75006 Paris, France
- **Aurélie Bertin** \* (aurelie.bertin@curie.fr) / Laboratoire Physico Chimie Curie, Institut Curie, PSL Research University, Sorbonne Université, CNRS UMR168, 75005, Paris, France

\* Auteur correspondant

Septins are essential and ubiquitous cytoskeletal proteins that interact with the plasma membrane. They are implicated in various cellular functions where they interact and organize at membranes to subsequently sense specific underlying curvatures and induce membrane deformations.

Various protocols have been developed in electron microscopy in order to analyze protein structures and their assembly. Among them, techniques like rotary shadowing [1], or deep freeze-etching [2], to cite two “historic” techniques, present several drawbacks for our questioning. They necessitate specific apparatus, and they are limited as they rely on the analysis of replicas without the underlying material, making it difficult to draw associations between protein patterns and the curvatures of the support. Thus, we used cryo-transmission electron tomography (cryo-TET) to perform the analysis of the 3D network of septin filaments bound to lipid vesicles and high-resolution scanning electron microscopy (SEM) to study the septin curvature sensitivity to lipid bilayers deposited on wavy substrates of variable curvatures.

Here, we will present the complementarity between these two methods, and our optimized protocols [3] that offers the advantage of preserving the 3D organization of septin filaments, in their native states (cryo-

TET) or using a fixation protocol (derived from Svitkina's method for cytoskeleton) that is easy to implement [4] and compatible with high-resolution SEM observations.

#### References:

- [1]Sherratt, M.J., and coll., 2009. Extracellular Matrix Protocols, Methods in Molecular Biology. Humana Press, Totowa, NJ, pp. 175–181. [https://doi.org/10.1007/978-1-59745-413-1\\_11](https://doi.org/10.1007/978-1-59745-413-1_11)
- [2]Heuser, J., 2000. Traffic 1, 545–552. <https://doi.org/10.1034/j.1600-0854.2000.010704.x>
- [3]Chauvin, B., and coll., 2022. JoVE e63889. <https://doi.org/10.3791/63889>
- [4]Svitkina, T.M., Borisy, G.G., 1998. Methods in enzymology. 298, 570–592, [https://doi.org/10.1016/s0076-6879\(98\)98045-4](https://doi.org/10.1016/s0076-6879(98)98045-4)

**Mots clefs :** Cryo-Electron Tomography, High-resolution Scanning Electron Microscopy, sample preparation

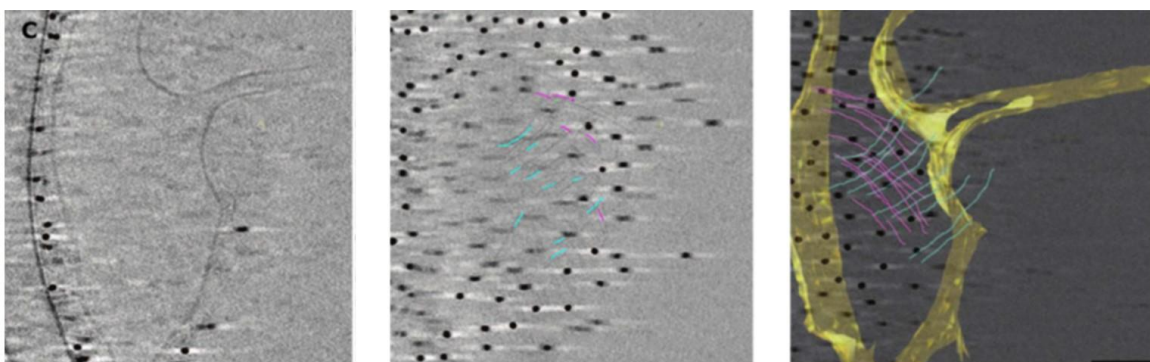


Figure 1: Cryo-EM images of (Left) septin filaments bound to a lipid vesicle and (Middle) segmented according to their orientations (green or pink). (Right) 3D model obtained after segmentation of tilted series with lipids (yellow) and orientated septins filaments (pink and green). Dark dots are gold fiducials, to align series, scale bar 100 nm.

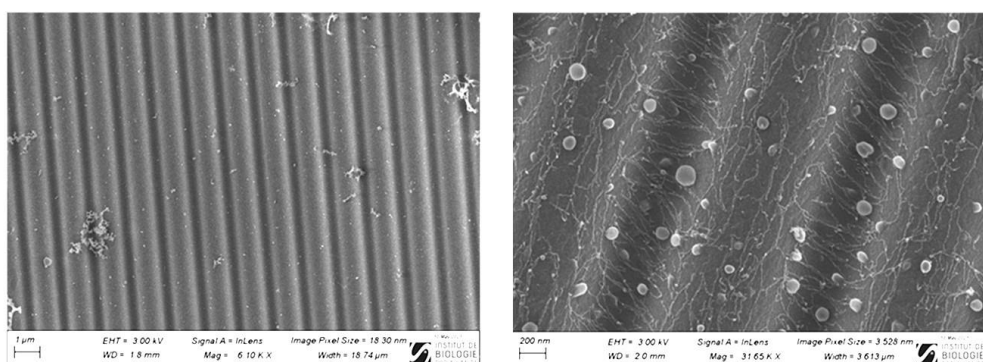


Figure 2: SEM figures of (Left) the wavy pattern of the PDMS substrate and of (Right) septins filaments orientated according to the positive or negative curvatures. Round-shape particles correspond to lipidic vesicles.

## SDV1-Oral3

### Imagerie corrélative MET/NanoSIMS pour localiser des nanoparticules de TiO<sub>2</sub> dans la peau humaine

TEM/NanoSIMS correlative imaging to localize TiO<sub>2</sub> nanoparticles in human skin

- M. Janin M., A. Delaune\*([anthony.delaune@univ-rouen.fr](mailto:anthony.delaune@univ-rouen.fr)), D. Gibouin, F. Delaroche, A. Etienne, B. Klaes, A. Cabin-Flaman, GPM Université Rouen Normandie

\* Auteur correspondant

Les nanoparticules (NPs) de dioxyde de titane (TiO<sub>2</sub>) font l'objet de nombreux travaux et controverses sur les risques qu'elles pourraient engendrer dans l'environnement et sur la santé humaine. Abondantes dans les crèmes solaires (pour leurs propriétés de filtres anti-UV), elles constituent un bon matériel d'étude pour la mise au point de la corrélation de l'imagerie par Microscopie Electronique à Transmission (MET) et par NanoSIMS parce qu'elles sont denses aux électrons et possèdent une signature chimique détectable au NanoSIMS.

Comme la MET utilise des électrons et le NanoSIMS des ions il a fallu définir un protocole de préparation d'échantillon de crème solaire appliquée sur la peau humaine, adapté aux deux instruments pour la détection, la caractérisation et la localisation d'objets de quelques nanomètres dans des coupes de quelques dizaines de nanomètres d'épaisseur. Les données obtenues et traitées ont permis de mettre au point la superposition des images MET et NanoSIMS d'une part et de conduire à une reconstruction 3D d'objets de taille inférieure à l'épaisseur de la coupe d'autre part. Cette approche a permis de montrer que la corrélation MET/NanoSIMS complète, renforce et apporte davantage d'informations que ce que fournit chaque instrument isolément. Appliquée à la peau, la corrélation permet d'approcher la distribution des NPs isolées ou agrégées à proximité des cornéocytes.

**Mots clefs :** corrélation MET NanoSIMS TiO<sub>2</sub> peau

## SDV1-Oral4

### Synchrotron deep ultraviolet radiation combined with histological staining to improve phenotyping of dystrophic muscle and assess efficacy of cell-based therapeutic strategies

- Laurence Dubreil \* ([laurence.dubreil@oniris-nantes.fr](mailto:laurence.dubreil@oniris-nantes.fr)), Norredine Damane, Romain Fleurisson, Marine Charrier, Julien Pichon, Isabelle Leroux, Cindy Schléder, Mireille Ledevin, Thibaut Larcher / Oniris, INRAE, PAnTher, 44300 Nantes, France
- Frédéric Jamme / IMT Atlantique, Lab-STICC, UMR CNRS 6285, Brest, F-29238, France
- John Puentes / Synchrotron SOLEIL, BP48, L'Orme des Merisiers, F-91120 Gif-sur-Yvette, France
- Karl Rouger / Oniris, INRAE, PAnTher, 44300 Nantes, France

\* Auteur correspondant

Duchenne muscular dystrophy (DMD) is the most common form of muscular dystrophy, affecting 1 per 3,500–5,500 male newborns. This fatal genetic muscle disease is caused by mutations in the dystrophin gene, leading to a lack of a functional protein essential to maintain muscle fiber integrity. It is characterized by a progressive replacement of fibers by fibrotic and adipose tissues. Histological characterization of dystrophic muscle provides important information on disease pathophysiology, and is a key tool used to evaluate the effects of novel therapeutic strategies. However, autofluorescence of bio- macromolecules as observed using Synchrotron deep ultraviolet (DUV) radiation may constitute an additional useful marker for ultrastructural characterization of different animal tissue and for monitoring muscle fiber typing and metabolic status [1].

In the present study, skeletal muscle samples from dystrophic Golden retriever muscular dystrophy (GRMD) dogs, a clinically relevant animal model of DMD, were subjected to Synchrotron DUV radiation and the resulting autofluorescence compared with that from healthy Golden retriever (GR) and GRMD dogs that have undergone adult stem cell (MuStem cells) transplantation (GRMDT), a recently identified therapeutic candidate for DMD [2]. Our findings show that measurement of Synchrotron DUV radiation on dystrophic muscle represents a sensitive tool to complete the classical histomorphometry approaches and facilitate both the characterization of dystrophic muscle and the evaluation of cell-based therapeutic proposal.

#### References:

- [1] Jamme et al.. Biol. Cell 105, 277–288 (2013)
- [2] Rouger K et al., Am J Pathol. 179, 2501–2518 (2011)

#### Acknowledgements

The authors thank the staff of Boisbonne Center (Oniris Nantes, France) and the APEX platform (Center of Excellence Nikon Nantes, labelled IBISA and Biogenouest) at INRAE/Oniris PAnTher UMR 0703 (Oniris, Nantes France), Synchrotron SOLEIL for their assistance with the use of the DISCO beamline (proposal 20170283).

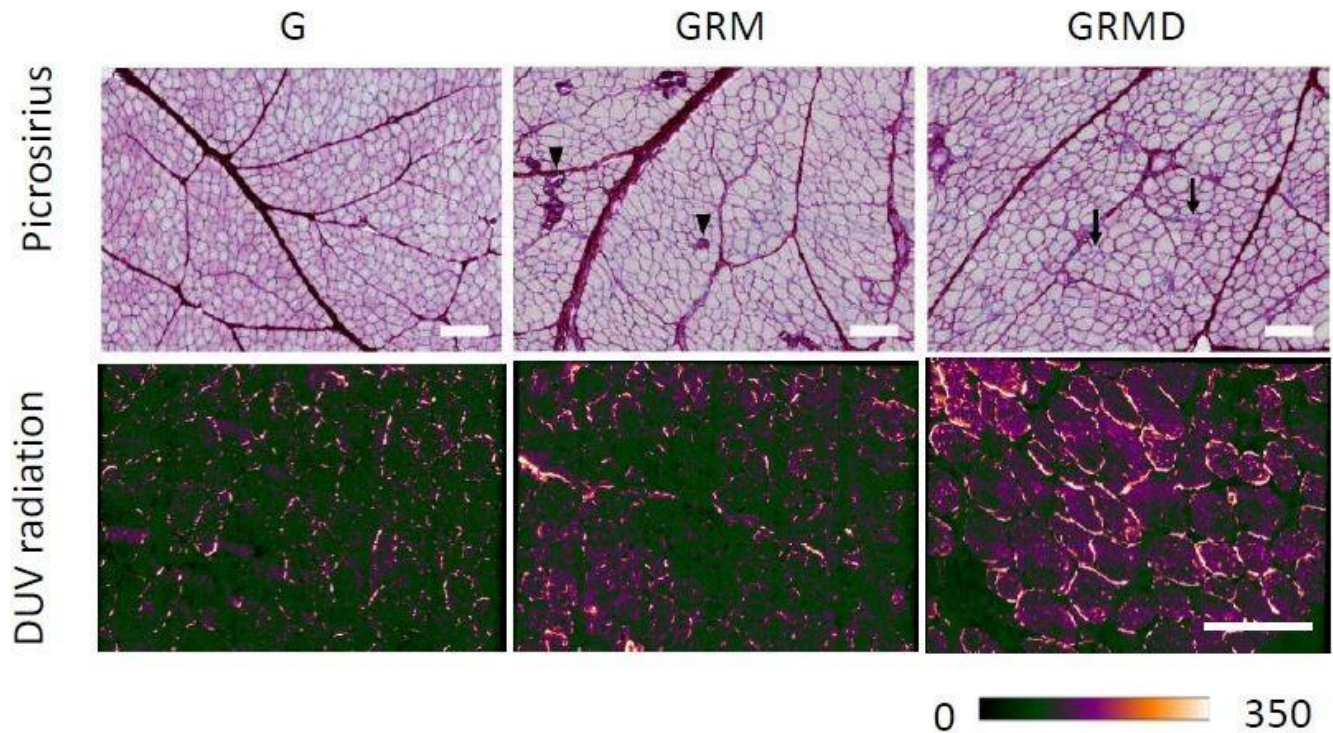


**Figure 1 :** Transverse sections from dog **Biceps femoris** muscle. from healthy (Golden Retriever; GR), dystrophic (Golden Retriever Muscular Dystrophy; GRMD) and MuStem cell-treated dystrophic GRMD (GRMDT) dogs stained with picosirius (top). investigate by synchrotron deep ultraviolet radiation (280 nm) using emission filters between 420 nm and 480 nm. (bottom). Scale bar 100µm.

## **SDV2 : Cryo-méthodes 1 : nano-objets**

### ***Animation :***

*Yaser Hashem (ARNA, Pessac)*

*Marc Schmutz (Institut Charles Sadron, Strasbourg)*

## SDV2-Inv1

# Data analysis methods based on molecular dynamics simulation for studying continuous conformational variability

• Slavica Jonic\* ([slavica.jonic@upmc.fr](mailto:slavica.jonic@upmc.fr)) / IMPMC - UMR 7590 CNRS, Sorbonne Université, MNHN, Paris, France

\* Corresponding author

The elucidation of different conformations of biomolecular complexes is the key to understand the molecular mechanisms behind the biological functions of the complexes and the key to novel drug discovery. Single-particle cryo electron microscopy (cryo-EM) allows 3D reconstruction of multiple conformations of purified biomolecular complexes from their 2D images. Cryo electron tomography (cryo-ET) allows obtaining information on the conformational variability of the complexes in their cellular environment. We are developing hybrid methods for studying continuous conformational changes of biomolecules, which integrate molecular dynamics simulations and deep learning approaches into cryo-EM [1-3] and cryo-ET data analysis [4-5]. The software and the synthetic data used for testing the methods are available via our open-source ContinuousFlex software package [6] and Zenodo [7], respectively. Also, ContinuousFlex is a plugin of Scipion [8], software platform largely used in the cryo-EM/ET field. In this talk, I will present the current and future works regarding these methods.

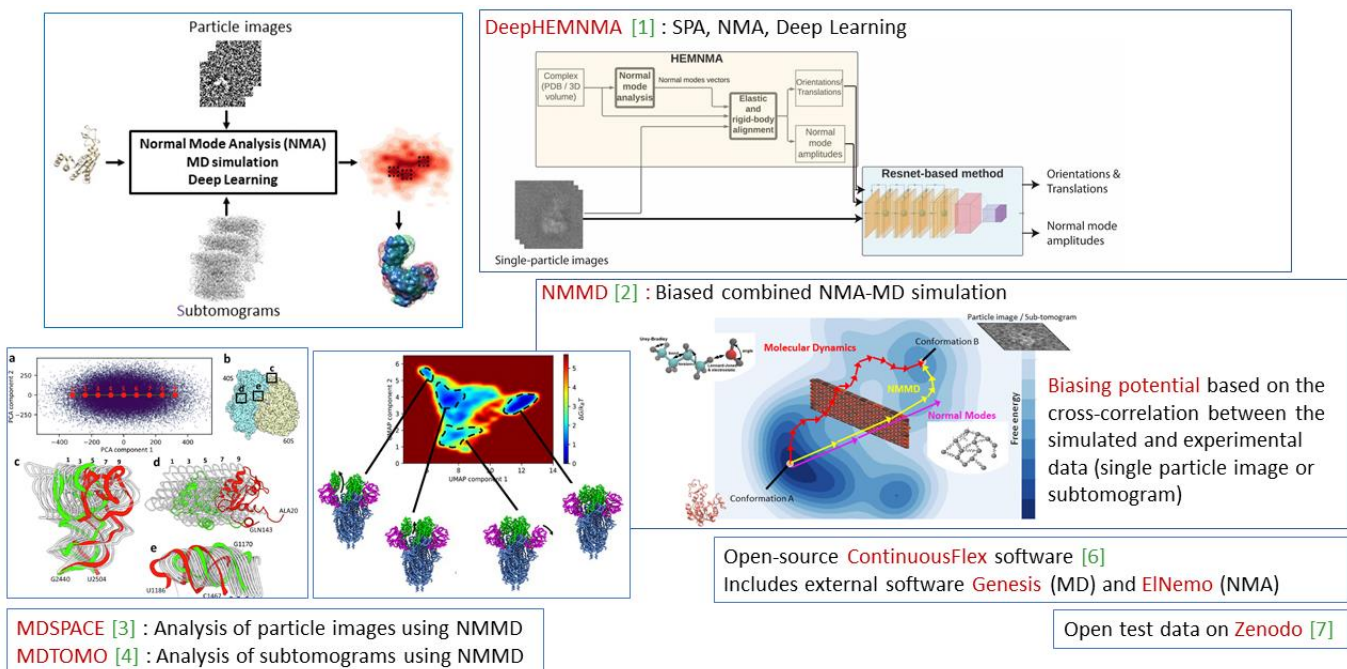


**Figure 1:** Hybrid methods for studying biomolecular conformational dynamics, which combine molecular dynamics simulation and deep learning with cryo-EM and cryo-ET data processing.

## References

- [1] Hamitouche I, Jonic S (2022) DeepHEMNMA: ResNet-based hybrid analysis of continuous conformational heterogeneity in cryo-EM single particle images. *Front Mol Biosci* 9:965645. doi: 10.3389/fmolb.2022.965645 [Open](#)

[2] Vuillemot R, Miyashita O, Tama F, Rouiller I, Jonic S (2022) NMMD: Efficient Cryo-EM Flexible Fitting Based on Simultaneous Normal Mode and Molecular Dynamics atomic displacements. *J Mol Biol* 434:167483. doi: 10.1016/j.jmb.2022.167483. [HAL](#)

[3] Vuillemot R, Mirzaei A, Harastani M, Hamitouche I, Frechin L, Klaholz BP, Miyashita O, Tama F, Rouiller I, Jonic S (2023) MDSPACE: Extracting continuous conformational landscapes from cryo-EM single particle datasets using 3D-to-2D flexible fitting based on Molecular Dynamics simulation. *J Mol Biol*: 167951. doi: 10.1016/j.jmb.2023.167951. [HAL](#)

[4] Vuillemot R., Rouiller I., Jonic, S. (2023) MDTOMO: Continuous conformational variability analysis in cryo electron subtomogram data using flexible fitting based on Molecular Dynamics simulations. *BioRxiv* [Open](#)

[5] Harastani M, Eltsov M, Leforestier A, Jonic, S (2021) HEMNMA-3D: Cryo Electron Tomography Method Based on Normal Mode Analysis to Study Continuous Conformational Variability of Macromolecular Complexes. *Frontiers Mol Biosci* 8:663121. [Open](#)

[6] Harastani M, Vuillemot R, Hamitouche I, Moghadam NB, Jonic S (2022) ContinuousFlex: Software package for analyzing continuous conformational variability of macromolecules in cryo electron microscopy and tomography data. *J Struct Biol* 214:107906. doi: 10.1016/j.jsb.2022.107906. [HAL](#)

[7] doi: 10.5281/zenodo.7415104; 10.5281/zenodo.7051222; 10.5281/zenodo.5718820

[8] <https://scipion.i2pc.es>

**Keywords:** Cryo-EM, cryo-ET, biomolecular flexibility, continuous conformational heterogeneity, MD simulation, Normal Mode Analysis, conformational landscapes, free energy

## SDV2-Inv2

### Generalized 3D localization of macromolecules in cryo-electron tomograms with TomoTwin

- Thorsten Wagner<sup>1</sup> ([thorsten.wagner@mpi-dortmund.mpg.de](mailto:thorsten.wagner@mpi-dortmund.mpg.de))
- Gavin Rice<sup>1</sup>
- Markus Stabrin<sup>1</sup>
- Oled Sitsel<sup>1</sup>
- Daniel Prumboam<sup>1</sup>
- Stefan Raunser<sup>1</sup> ([stefan.raunser@mpi-dortmund.mpg.de](mailto:stefan.raunser@mpi-dortmund.mpg.de)) \*

<sup>1</sup> Department of Structural Biochemistry, Max Planck Institute of Molecular Physiology, Dortmund, Germany.

\* Corresponding author

Cryoelectron tomography opens up the possibility of visualizing cellular environments with extraordinary detail where individual macromolecules can be resolved. However, analysis of the densely packed volumes in these tomograms lacks effective tools to fully exploit the wealth of information contained within. In particular, detailed analysis of macromolecules by subtomogram averaging requires initial localization of particles within the tomogram volume - a difficult task due to factors such as low signal-to-noise ratio and cellular space crowding. Existing methods for particle selection are error-prone or require extensive manual annotation of training data. To address this crucial step, we present TomoTwin [1]: a robust particle selection model for cryo-electron tomograms based on deep metric learning.

TomoTwin uses deep metric learning to calculate high-dimensional embeddings of tomogram subvolumes. During training, the loss function penalizes the placement of molecules from different protein classes close to each other and rewards the proximity of molecules from the same protein class. This technique promotes clustering of similar proteins and facilitates de novo identification of new proteins in the embedding space. As metric learning is adept at generalizing, it allowed us to pre-train TomoTwin on simulated data only. This pre-trained model is able to locate unseen proteins in experimental cellular tomograms and therefore circumvent the any manual training by the user.

We provide two workflows for macromolecular localization using TomoTwin: a reference-based workflow, where a single molecule is selected for each protein of interest and used as a target, and a napari-based [2] interactive de novo clustering workflow, where macromolecular structures of interest are identified on a 2D manifold.

TomoTwin is an open source software package available at <https://readthedocs.org/projects/tomotwin-cryoet/>

[1] Rice, G., Wagner, T., Stabrin, M. et al. TomoTwin: generalized 3D localization of macromolecules in cryo-electron tomograms with structural data mining. *Nat Methods* **20**, 871–880 (2023). <https://doi.org/10.1038/s41592-023-01878-z>

[2] napari contributors (2019). napari: a multi-dimensional image viewer for python. [doi:10.5281/zenodo.3555620](https://doi.org/10.5281/zenodo.3555620)

**Keywords:** cryo-em, particle picking, deep learning

## SDV2-Oral1

### Utilisation de la congélation haute pression et du cryo-microtome pour préparer des échantillons pour la microED

High pressure freezing and cryo-sectioning as a new approach to prepare protein nano-crystals for microED experiments

- Christine MORISCOT / Univ. Grenoble Alpes, CNRS, CEA, ISBG, IBS, F-38000 Grenoble, France
- Guy SCHOEHN / Univ. Grenoble Alpes, CNRS, CEA, IBS, F-38000 Grenoble, France
- Dominique HOUSSET \* (dominique.housset@ibs.fr) / Univ. Grenoble Alpes, CNRS, CEA, IBS, F-38000 Grenoble, France

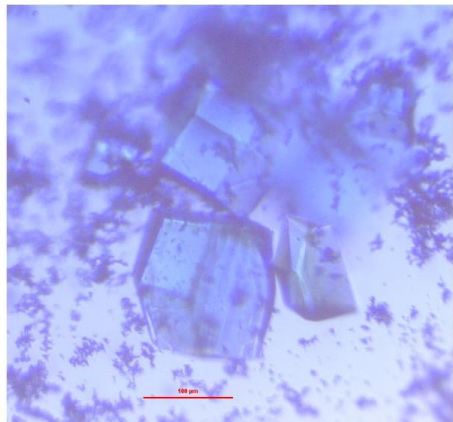
\* Auteur correspondant

Electron diffraction of 3D nanometer sized crystals, most commonly named microED, has recently emerged as a new technique to solve the structure of both small organic molecules and proteins [1–3]. MicroED is clearly a promising technique in structural biology, both quite easy to implement and very complementary to X-ray crystallography and single particle cryo-EM. Electrons are actually a very interesting probe for small samples as they strongly interact with matter, and more importantly, they deposit much less energy than X-rays per diffracted particle [4]. Sub-atomic resolution data can routinely be collected for small organic compounds and data up to 0.9 Å resolution have been obtained from protein crystals [5]. However, a quick look at the Protein Data Bank shows that among the ~70 protein structures determined so far by microED, only 10 are not model proteins, indicating that microED is still far from routinely used in structural biology. The major bottleneck of the technique when applied to protein samples is to produce nano-crystals that do not exceed 200 to 300 nm in at least one dimension and to deposit them on a grid while keeping the minimum amount of solvent around them. Here, we present a new approach that uses cryo-sectioning after high pressure freezing of dextran embedded protein crystals. 150 to 200 nm thick cryo-sections of hen egg white lysozyme tetragonal crystals were used for electron diffraction experiments. Complete diffraction data up to 2.9 Å resolution were collected and the lysozyme structure was solved by molecular replacement and refined against these data. Our data demonstrate that cryo-sectioning can preserve protein structure at high resolution and can be used as a new sample preparation technique for 3D electron diffraction experiments of protein crystals.

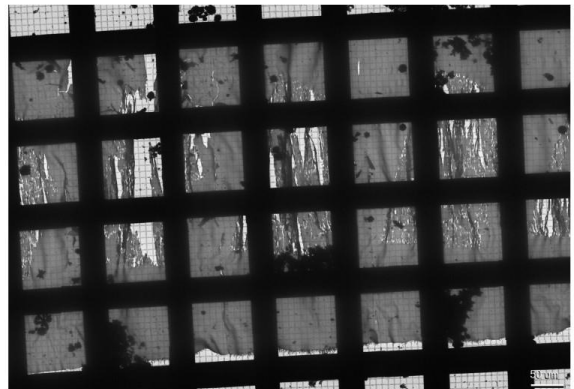
Références/References :

- [1] M.T.B. Clabbers et al., *Acta Cryst D.* 73 (2017) 738–748.
- [2] M. Gemmi et al., *ACS Cent Sci.* 5 (2019) 1315–1329.
- [3] T. Gruene et al., *Angew Chem Int Ed Engl.* 57 (2018) 16313–16317.
- [4] R. Henderson, *Q. Rev. Biophys.* 28 (1995) 171–193.
- [5] M.W. Martynowycz et al., *Nat Methods.* 19 (2022) 724–729.

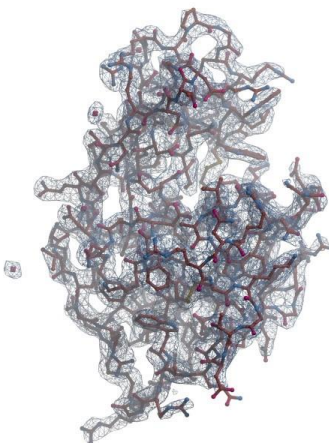
**Mots clefs :** Electron diffraction, 3D protein crystals, cryo-sectioning, CEMOVIS, 3D structure



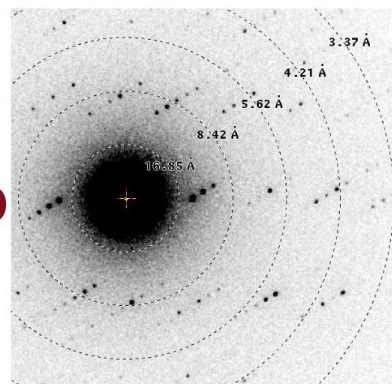
Tetragonal lysozyme crystal



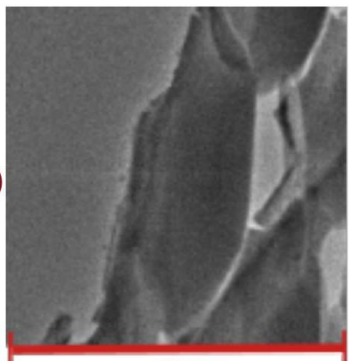
200 nm thick cryo-section of a lysozyme crystal (the cracked regions are those containing the crystal)



Refined lysozyme structure



Electron diffraction data



Single crystal fragment



## SDV2-Oral2

### La cryo-microcopie électronique révèle les liens entre corrélations entre hélices et conformation de la double hélice d'ADN

Cryo electron microscopy reveals how electrostatic zipper tunes the DNA double helix conformation in toroidal condensates

- **Kahina Vertchik** \* (kahina.vertchik@universite-paris-saclay.fr) / Université Paris-Saclay, CNRS, Laboratoire de Physique des Solides, Orsay, France
- **Sylwan Bony** / Université Paris-Saclay, CNRS, Laboratoire de Physique des Solides, Orsay, France
- **Amélie Leforestier** / Université Paris-Saclay, CNRS, Laboratoire de Physique des Solides, Orsay, France

France \* Auteur correspondant

Interactions between DNA double helices at high density are involved in packing of chromosomes in cells and viruses, but also in a number of biological reactions such as homologous pairing.

We use cryo electron microscopy to shed light on the conformation and interactions between tightly packed and curved helices found in DNA toroids spontaneously folded *in vitro* in the presence of condensing agents such as spermine 4+. In toroids, DNA double strands locally align in parallel with lateral hexagonal order [1-3] and longitudinal phasing of helices [2, 3]. The spacing between DNA helices depends on the local curvature, consistent with a mathematical model based on the competition between electrostatic interactions and the bending rigidity of DNA. This phenomenon is associated with a change in the longitudinal phasing of DNA double helices. In addition, maintaining these helical correlations within a curved architecture results in buckling into an alternation of low and high curvature leading to polygonal shaping of the toroid, and/or structural adaptation of the DNA conformation with progressive decrease of the helical pitch of the molecule with increasing curvature.

Altogether our results suggest that the electrostatic zipper mechanism [4] plays a major role DNA condensation, tuning the double helix conformation [4] and the global shape of the condensate.

#### References

- [1] N.V. Hud, K.H. Downing, Proc. Natl. Acad. Sci. USA, 98, 121 (2001).
- [2] A. Leforestier, F. Livolant, Proc. Natl. Acad. Sci. USA, 106, 57 (2009).
- [3] L. Barberi, et al., Nucleic Acid Research, 49, 12 (2021).
- [4] Kornyshev A.A, Lee D.J., Wynveen A. Rev. Mod. Phys. 79, 943 (2007).

## SDV2-Oral3

### Etude de l'auto-assemblage de nano-cylindres supramoléculaires en solution : complémentarité de la Cryo-MET et de la diffusion de la lumière

#### Study of self-assembly of supramolecular nanocylinders in solution : complementarity between Cryo-TEM & Light Scattering

- **Frederick Niepceron \*** ([frederick.niepceron@univ-lemans.fr](mailto:frederick.niepceron@univ-lemans.fr)), **Erwan Nicol, Thomas Choisnet, Olivier Colombani** / Institut des Molécules et Matériaux du Mans (IMMM) UMR CNRS 6283, Le Mans Université Avenue Olivier Messiaen, 72085 Le Mans Cedex 9, France.
- **Laurent Bouteiller** / Sorbonne Université, CNRS, IPCM, Equipe Chimie des Polymères, F-75005 Paris, France
- **Shuaiyuan Han, Sandrine Pensec** / Sorbonne Université, CNRS, IPCM, Equipe Chimie des Polymères, F-75005 Paris, France
- **David Canevet** / Laboratoire MOLTECH-Anjou, UNIV Angers, SFR MATRIX, UMR CNRS 6200, 49045 Angers Cedex, France
- **Marc Sallé** / Laboratoire MOLTECH-Anjou, UNIV Angers, SFR MATRIX, UMR CNRS 6200, 49045 Angers Cedex, France

\* Auteur correspondant

Supramolecular nanocylinders formed by self-assembly in water are promising nanoparticles for numerous application fields, like in optics, magnetism, catalysis, surface nanopatterning, or interface stabilization.

We have recently designed polymers able to self-assemble in solution[1,2]. By self-assembly of specific polymers, we can create nanoparticles of different shapes, like spherical micelles or nanocylinders, depending on the preparation method. To understand what controls the shape of these nanoparticles, they were characterized by light scattering and Cryo-TEM techniques.

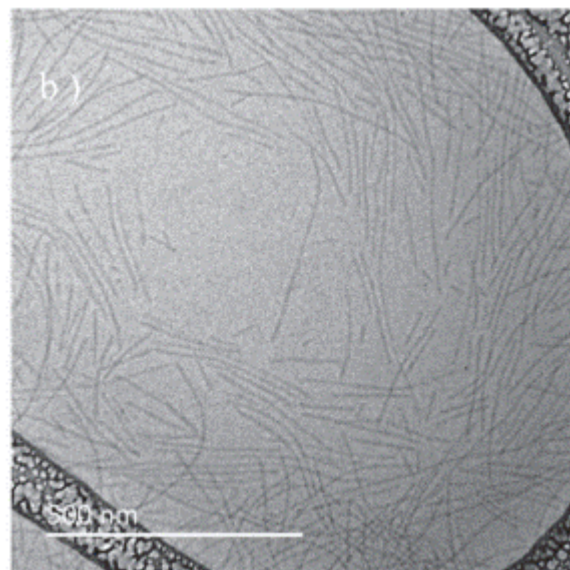
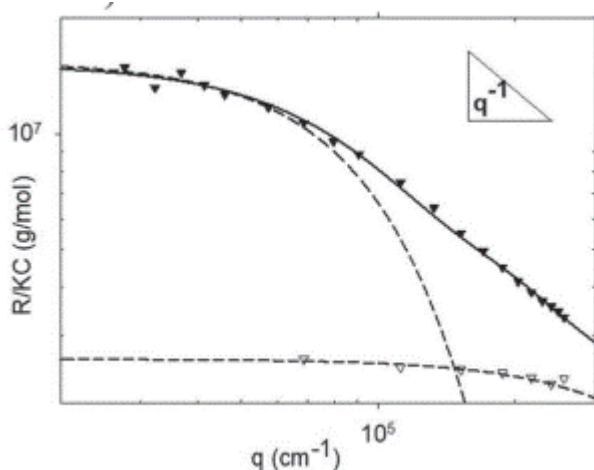
Light scattering (Fig. 1) indicated that the particles formed were strongly aggregated and exhibited a  $q^{-1}$  dependency of the scattered light intensity, revealing the formation of long and rigid rods. Cryo-TEM observation (Fig.2) confirmed this interpretation.

Beyond confirming the light scattering results by direct observation of nanoparticles, cryo-TEM observations could give access to complementary information about the characteristics of these nanocylinders. The main objective of this presentation is to demonstrate the limits of each technique and to highlight the interest of combining both techniques to characterize more completely the self-assemblies.

#### References :

- [1] Han, Shuaiyuan, et al., Macromolecular Rapid Communications, 40.3 (2019), 1800698. [2] Choisnet, Thomas, et al., ACS nano, 15.2 (2021), 2569-2577.

**Mots clefs :** Cryo-TEM, Light Scattering, nanocylinders, self-assembly



## SDV2-Oral4

### Resolution à l'échelle moléculaire de la structure de nanofibres de peptides courts par reconstruction d'images cryo-TEM

Molecular-scale resolution of the structure of short peptides-based nanofiber by cryo-electron microscopy image reconstruction

- **Alexis BIGO--SIMON** \* (abigosimon@unistra.fr) / Université de Strasbourg
- **Alain CHAUMONT** / Université de Strasbourg
- **Pierre SCHAAF** / INSERM - Institut Charles Sadron
- **Rachel SCHURHAMMER** / Université de Strasbourg
- **Loïc JIERRY** / Institut Charles Sadron
- **Marc SCHMUTZ** / Institut Charles Sadron

\* Auteur correspondant

Cryo-electronic microscopy reconstruction techniques are tremendously used to resolve the structure of viruses or even smaller entities such as proteins. Very recently, these approaches have also been successfully applied to elucidate the spatial organisation of nanostructures based on oligo or polypeptides assemblies[1]. Following this line, the next challenge would be to elucidate the molecular scale organization of nanostructures based on very short peptides assemblies (i.e. peptides containing up to three residues) since this kind of building blocks displays no secondary structures such as  $\alpha$ -helix or  $\beta$ -sheet organization for which the outcome prediction of their assembly is not obvious. In addition, these very short peptide assemblies have recently been shown as particularly appealing for bioimaging, anticancer therapy, theranostic strategy or drug delivery:[2] the understanding of their molecular scale structure would be highly interesting for the optimization of peptides sequence for various biomedical applications. Using high resolution of cryo-TEM images and tools such as RELION and crYOLO, we have obtained a density map of 3.8 Å of resolution from a tripeptide-assembled nanofiber (tripeptide sequence: Fmoc-FFY), as shown in Figure 1. Thus, a suitable correlation between this map and the molecular structure of the tripeptide resulted in the determination of the nanofiber structure at the molecular scale. The fitted model was used as a starting situation for molecular dynamics (MD) investigations highlighting the interactions ensuring the cohesion of the supramolecular architecture. Informations obtained from experimental studies (IR, CD, SAXS, Fluorescence) are in full agreement with our so-resolved nanofiber structure. In this presentation, the reconstruction, the MD simulations and the comparison with experimental data will be shown and discussed.

**Mots clefs :** self-assembly, peptides, molecular dynamics, crYOLO, RELION

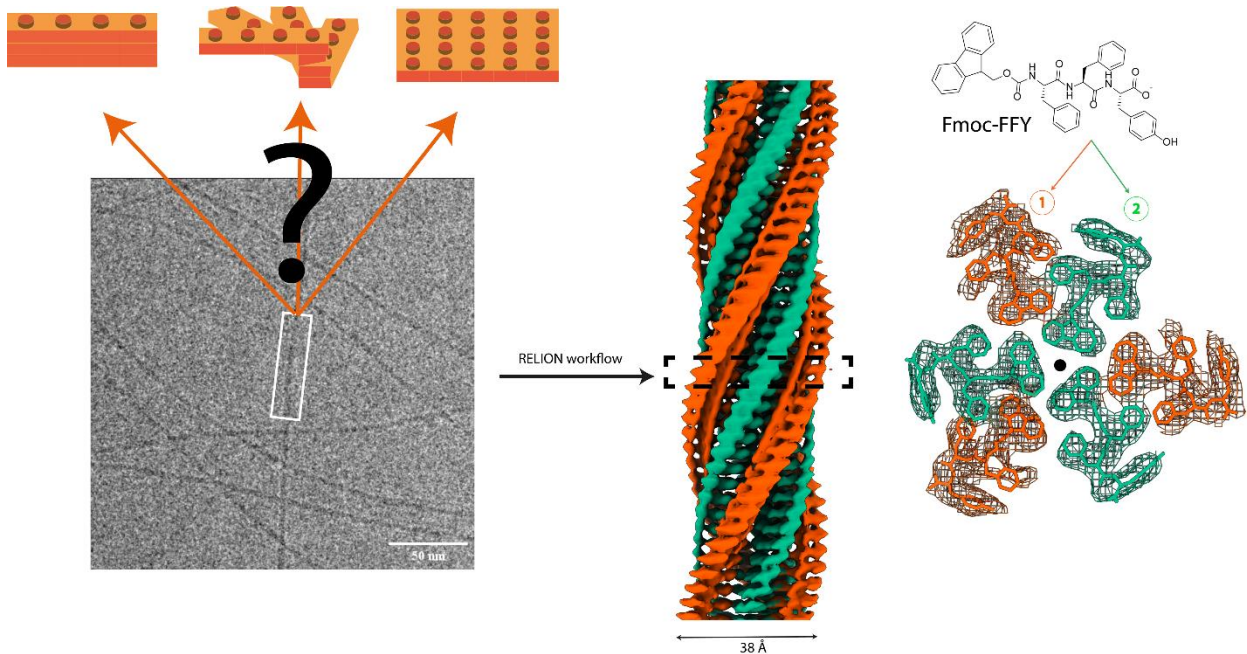


Figure 1: Micrograph of nanofibers seen in cryo-TEM resulting from the self-assembly of Fmoc-FFY in water along with the density map at 3.8 Å and the molecular model from a slice of the helix

## **SDV3 : Cryo-méthodes 2 : cellulaire/tissulaire**

**Animation :**

*Anna Sartori (Institut Pasteur- Paris)*

*Aurélie Bertin (Institut Curie, Paris)*

**SDV3-Inv1****CHROMATIN LANDSCAPE *IN SITU* REVEALED BY CRYO-ELECTRON TOMOGRAPHY OF VITREOUS SECTIONS**

**Amélie Leforestier<sup>1\*</sup>, Fadwa Fatmaoui<sup>2</sup>, Pascal Carrivain<sup>3</sup>, Fatima Taiki<sup>1</sup>, Diana Grewe<sup>4</sup>, Jean-Marc Victor<sup>3\*</sup>, Mikhail Eltsov<sup>2\*</sup>**

- 1Laboratoire de Physique des Solides (LPS), CNRS, Université Paris-Saclay Orsay, France
- 2Centre for Integrative Biology (CBI), Department of Integrated Structural Biology, IGBMC, CNRS, Inserm, Université de Strasbourg, Illkirch, France
- 3Laboratoire de Physique Théorique de la Matière Condensée (LPTMC), CNRS, Sorbonne Université, Paris, France
- 4Buchmann Institute for Molecular Life Sciences, Goethe University, Frankfurt am Main, Germany

Wrapping 145–147 DNA base pairs (bp) around a histone octamer organizes eukaryotic genomes into quasiperiodic arrays of nucleosomes connected by a DNA linker. The folding of nucleosome chains influences DNA availability for functional interactions necessary to the regulation of transcription, DNA replication and repair. Despite models based on *in vitro* studies, the nucleosome chain geometry within the crowded cell nucleus remains elusive. Using Volta Phase Plate cryo electron tomography and deep learning-based denoising, we directly observed the path of nucleosomal and linker DNA *in situ* in unstained flash-frozen Drosophila embryos. We quantified linker length and curvature characterizing a disordered zig-zag chromatin folding motif, with a low degree of linker bending. Additionally, nucleosome conformational variability with non-canonical structures and sub-nucleosomal particles were seen as individual objects, without structure averaging, highlighting the high structural heterogeneity of native chromatin [1].

**Reference**

[1] Fatmaoui F. et al, BioRxiv (2022), doi.org/10.1101/2022.08.16.502515

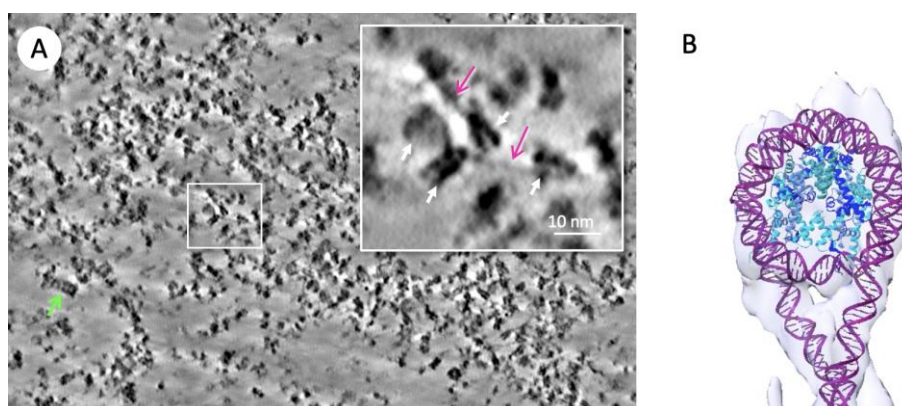


*Figure. (A)* One voxel (4.25 Å) thick tomographic slice of a cryo-tomogram after deep learning denoising. Nucleosomes and linker DNA (magnified in insert, respectively white and magenta arrows) as well as other macromolecular complexes such as proteasomes (green arrow) are well identified. *(B)* Visualization of the complete wrapping of DNA around the histone core. The crystallographic model of the Drosophila nucleosome (pdb:2PYO) is fitted.

## SDV3-Inv2

### Architecture of cellular membrane-based protein assemblies by cryo-electron tomography

- Vladan Lucic (vladan@biochem.mpg.de / Max Planck Institute of Biochemistry)

Most cellular processes are carried out by molecular complexes forming functional modules, with many biochemical pathways requiring a distinctly non-random spatial organization of their components. Arguably, the composition, precise localization and the immediate cellular environment of individual complexes, as well as the organization of large molecular assemblies that comprise multiple species of molecular complexes, determine cellular function. Of particular interest are membrane-bound complexes and assemblies because they are essential for many types of cellular processes and are targeted by more than two thirds of all approved medical drugs. In order to elucidate the organization and composition of protein complexes and assemblies *in situ*, we use cryo-electron tomography (cryo-ET). This method provides a three-dimensional, molecular-level visualization of unstained cellular compartments and is uniquely suited for simultaneous, label-free imaging of protein complexes and lipids at single nanometer resolution in their native environment.

The crowded nature of cellular compartments and the large number of protein species present in cryo-ET images made the development of novel image processing methods essential. We developed software for comprehensive, template-free detection and classification of pleomorphic, membrane bound complexes in cryo-ET datasets, as well as for their morphological, topological, statistical and spatial pattern analysis [1, 2]. These tools use advanced algorithms and machine learning techniques not previously used in cryo-ET (Morse theory, Affinity propagation clustering, Ripley's functions). Cryo-ET imaging and analysis of wild-type and genetically and pharmacologically manipulated neuronal synapses showed that the precise distance of synaptic vesicles to the presynaptic plasma membrane characterize sequential states of vesicle progression towards fusion [3]. Furthermore, synaptic vesicle tethers, short pleomorphic filaments that link synaptic vesicles to the presynaptic plasma membrane, control these states. This, together with the characterization of molecular bridges that interlink vesicles, allowed us to build a structural and molecular model of synaptic vesicle tethering and priming.

Applications of our image processing software allowed us to obtain *de novo* average structures of a range of complexes in their physiological composition, within their native environment of interacting proteins and lipids, outperforming both template-free and template-based approaches currently available in the field [2, 4]. Furthermore, we detected and characterized tripartite trans-synaptic complexes, which provide a structural link between synaptic vesicles and postsynaptic receptors. This finding might answer the long-standing question about the mechanism of the precise alignment between neurotransmitter release sites and neuroreceptors, which is required for efficient synaptic transmission. These developments provide a framework applicable to membrane-associated complexes and signaling pathways of other biological systems.

- [1] V. Lucic et al, Journal of structural biology 196 (2016), p. 503-514
- [2] A. Martinez-Sanchez et all, Nature methods 17, (2020) p 209-216
- [3] C. Papantoniou, U. Laugks et al, Science Advances (2023) in press
- [4] A. Martinez-Sanchez et al, Science advances 7 (2021), eabe6204

**Mots-clés/Keywords:** Cryo-electron tomography, Image processing, synaptic transmission

## SDV3-Oral1

### Getting closer to the native state safely: Hybrid methods for Electron Tomography of viruses

#### Getting closer to the native state safely: Hybrid methods for Electron Tomography of viruses

- **Anastasia Gazi** \* (agazi@pasteur.fr) / Ultrastructural BiolImaging Unit, Institut Pasteur, 75015, Paris, France
- **Marcia Folly-Kian** / Ultrastructural BiolImaging Unit, Institut Pasteur, 75015, Paris, France
- **Diana Baquero** / Archaeal Virology Unit, Department of Microbiology, Institut Pasteur, 75015 Paris, France
- **Esthel Penard** / Ultrastructural BiolImaging Unit, Institut Pasteur, 75015, Paris, France
- **Mart Krupovic** / Archaeal Virology Unit, Department of Microbiology, Institut Pasteur, 75015 Paris, France
- **Martin Sachse** / Ultrastructural Bio-Imaging Unit, Institut Pasteur, 75015, Paris, France
- **Jacomina Krijnse-Locker** / Ultrastructural Bio-Imaging Unit, Institut Pasteur, 75015, Paris, France & Electron Microscopy of Pathogens, Paul Ehrlich Institute, 63225, Langen, Germany

\* Auteur correspondant

Transmission Electron Microscopy (TEM), with its various imaging modes and capabilities, is an indispensable tool to peek inside the eukaryotic cell, describe cellular ultrastructure, identify new viruses, classify new microorganisms. During most of its history the conventional preparation methods contributed substantial knowledge. However, in these preparations the biological samples are fixed, dried, and embedded to supporting matrices in order to survive the vacuum needed for imaging, thus compromising the structural integrity of the sample. In recent years, with the development of cryogenic electron microscopy and the new advancements in imaging and data analysis tools, a complete turn towards high resolution imaging of samples close to their native state has been achieved.

With rapidly evolving emerging infectious diseases however, fixation is employed for a vital reason: to render the pathogenic factors safe for imaging at numerous BSL1 level labs worldwide. Hybrid preparation methods, involving cryogenic steps like the High Pressure Freezing and Freeze substitution method [1,2], have been described in the past as beneficial for structural preservation. On the other hand, Tokuyasu cryo-sectioning is mostly used conventionally for gold immunolabelling [1]. Can the existent methods be optimized further to produce hybrid solutions for (Cryo-) ET level data production and analysis? Two viral cases based on two different hybrid preparation methods will be presented and discussed [3,4].

#### Références/References :

- [1] Hurbain I & Sachse M, The future is cold: cryo-preparation methods for transmission electron microscopy of cells, *Biology of the cell*, 103;9 (2011), p.405-420
- [2] Mourer T, Sachse M, Gazi AD, d'Enfert C, Bachellier-Bassi S, A protocol for ultrastructural study of *Candida albicans* biofilm using transmission electron microscopy, *STAR Protoc.*, 16;3 (2022), p.101514
- [3] Baquero DP, Gazi AD, Sachse M, Liu J, Schmitt C, Moya-Nilges M, Schouten S, Prangishvili D, Krupovic M, A filamentous archaeal virus is enveloped inside the cell and released through pyramidal portals, *PNAS*, 118;32 (2021), p. e2105540118.

[4] Tonnemacher S, Folly-Klan  M, Gazi  AD, Sch fer S, P nard E, Eberle R, Kunz R, Walther P, Krijnse Locker J, Vaccinia virus H7-protein is required for the organization of the viral scaffold protein into hexamers, *Scientific Reports*, 12 (2022), p. 13007

**Mots clefs** : Vitrification of Sections, CryoET, dual-axis electron tomography, Image Processing, Vaccinia virus

## SDV3-Oral2

### Révéler l'ultrastructure des complexes synaptiques avec la cryo-CLEM

#### Revealing hub synapses ultrastructure with cryo-CLEM

- **Paul Lapios** \* (paul.lapios@u-bordeaux.fr) / Univ. Bordeaux, CNRS, Interdisciplinary Institute for Neuroscience, IINS, UMR 5297, Bordeaux, France
- **Robin Anger** / Univ. Bordeaux, European Institute for Chemistry and Biology, IECB, F-33000, Bordeaux, France
- **Etienne Herzog** / Univ. Bordeaux, CNRS, Interdisciplinary Institute for Neuroscience, IINS, UMR 5297, Bordeaux, France
- **Rémi Fronzes** / Univ. Bordeaux, European Institute for Chemistry and Biology, IECB, F-33000, Bordeaux, France
- **David Perrais** / Univ. Bordeaux, CNRS, Interdisciplinary Institute for Neuroscience, IINS, UMR 5297, Bordeaux, France

\* Auteur correspondant

Dopamine is an essential brain neuromodulator involved in reward and motor control which are altered in Parkinson's disease and addiction. Dopamine contained in vesicles is released by axons and binds to metabotropic receptors to modulate neuronal activity onto Spiny Projection Neurons (SPNs). However, the basic features of dopamine release sites, e.g. their location relative to receptors and other neuronal processes, are still largely unknown. We have shown recently with fluorescent tagging of dopaminergic neurons, sorting of synaptosomes with flow cytometry (FASS) and quantitative analysis with immunocytochemistry [1], that a vast proportion of dopaminergic varicosities contact specifically cortico-striatal glutamatergic terminals, which are themselves contacting the SPNs. We named these multipartite structures Dopamine Hub synapses [2].

Here, our goal is to characterize the ultrastructure of cortico-striatal hub synapses. To do that, we are using cryo-correlative light electron microscopy (cryo-CLEM) [3] and cryo-electron tomography applied to synaptosomes [4]. Therefore, we are able to label and compare synaptosomes containing glutamate or dopamine. By quantifying fundamental parameters like vesicle size and density (fig. 1) we show clear differences between those two. Moreover, using a double labelling approach, we can target dopamine hub synapses and interactions between the partners (fig. 2). With this workflow we are making a first step towards the characterization of multipartite synapses and their implication in synaptic plasticity. These findings will help to understand the basic mechanisms of dopaminergic modulation and related pathologies in the basal ganglia.

[1] Luquet et al. Purification of synaptosome populations using FASS. Methods in molecular biology, 1538 (2017) p.121-134

[2] Paget-Blanc, V. et al. A synaptomic analysis reveals dopamine hub synapses in the mouse striatum. Nat Commun 13 (2022) p. 3102

[3] Sartori et al. Correlative microscopy: Bridging the gap between fluorescence light microscopy and cryo-electron tomography. Journal of Structural Biology, 160 (2007) p.135-145

[4] Fernandez-Busnadio et al. Quantitative analysis of the native presynaptic cytomatrix by cryo-electron tomography. The Journal of Cell Biology, 188 (2010) p.145-156

**Mots clefs :** cryo-CLEM - Dopamine - Synapses - Plasticity - Ultrastructure

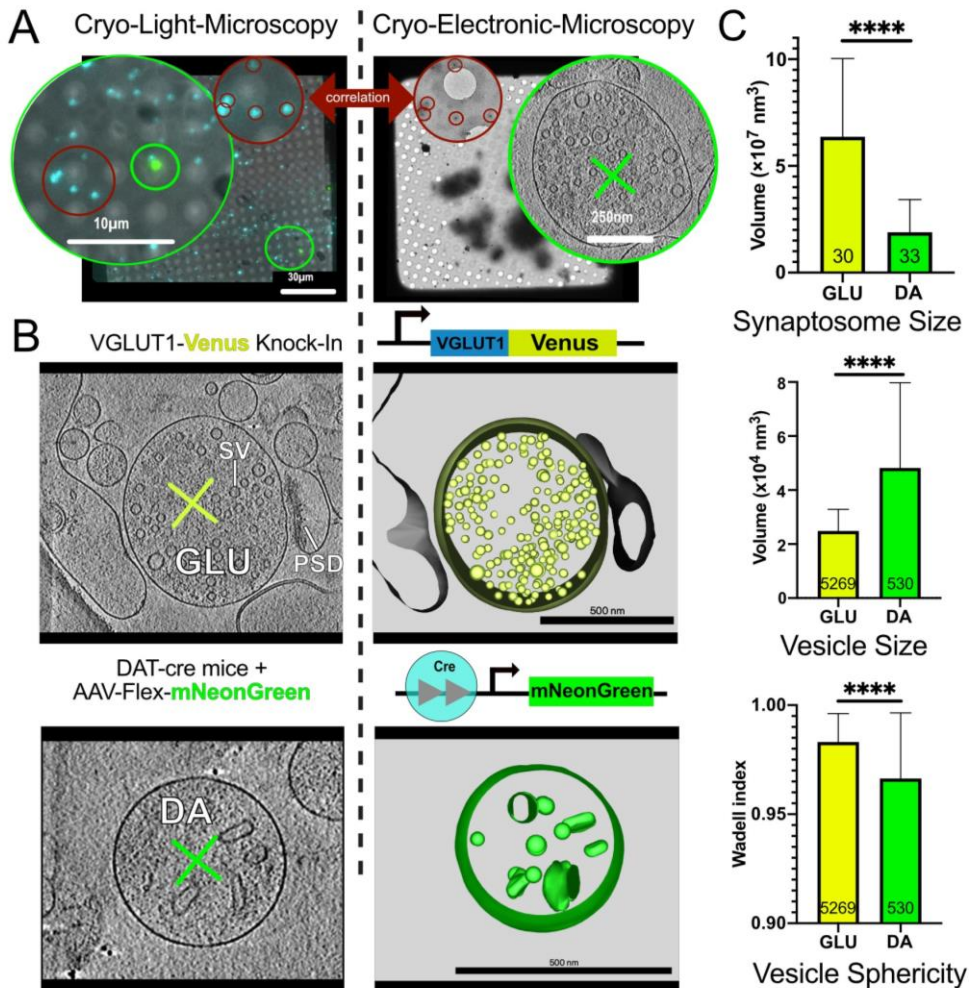


**Figure1: Ultrastructural comparison of GLU and DA synaptosomes using cryo-CLEM.**

- A. Correlation between light and electron microscopy using fiducial beads results in precise targeting of synaptosomes
- B. Tomogram of a glutamatergic synaptosome identified using VGLUT1-venus fusion protein and a dopaminergic synaptosome using a cre-dependant mNeonGreen sequence expressed in DAT+ neurons (dopamine transporter).
- C. Quantitative comparison between glutamatergic (GLU) or Dopaminergic (DA) synaptosomes shows differences in size and shapes of the synaptic vesicles.

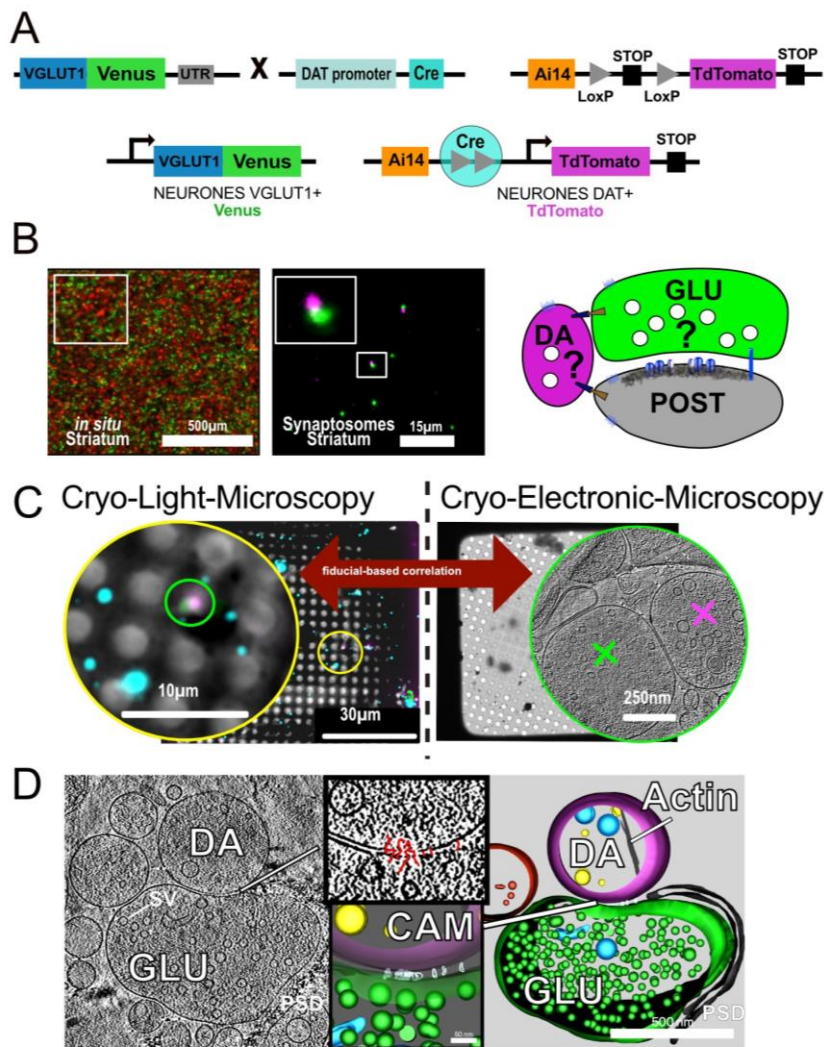


**Figure2: Ultrastructure of the striatal dopamine hub synapse identified with a double labelling.**  
**A.** Double labelling of VGLUT1+ and DAT+ neurons by crossing VGLUT1-venus KI mice with DAT-cre-Ai14-TdTomato line.  
**B.** Example of confocal images for VGLUT1 and TdTomato signal in a brain slice (*in situ*) or after synaptosome preparation.  
**C.** Cryo-CLEM workflow for targeting DHS.  
**D.** Example of a DHS and the corresponding 3D model revealing physical interaction between GLU and DA.

## SDV3-Oral3

### Réorganisation du cytoskelette d'actine dans les protrusions de membrane induites par mouillage 1D au cours de l'infection par Nm

#### F-actin reorganization within bacteria-induced 1D wetting-mediated membrane protrusions

- **Margot Sahnine \*** (margot.sahnine@pasteur.fr) / Institut Pasteur, Université de Paris, INSERM U1225, Pathogenesis of Vascular Infections Unit, 75015 Paris, France
  - **Stéphane Tachon** / Institut Pasteur, Université de Paris, CNRS UMR3528, NanolImaging Core, 75015 Paris, France
  - **Anna Sartori-Rupp** / Institut Pasteur, Université de Paris, CNRS UMR3528, NanolImaging Core, 75015 Paris, France
  - **Esthel Penard, Cyril Scandola** / Institut Pasteur, Université de Paris, Ultrastructural BioImaging Platform, 75015 Paris, France
  - **Daria Bonazzi, Guillaume Duménil, Dorian Obino** / Institut Pasteur, Université de Paris, INSERM U1225, Pathogenesis of Vascular Infections Unit, 75015 Paris, France
- Correspondence: guillaume.dumenil@pasteur.fr & dorian.obino@pasteur.fr

Plasma membrane deformations play critical roles in regulating a wide range of physiological processes, including cell migration, adhesion, and microenvironment probing. Such deformations can also be induced by pathogens upon interactions with the host-cell plasma membrane, as illustrated by the extracellular bacterium *Neisseria meningitidis* (Nm). Nm triggers the formation of filopodia-shaped plasma membrane protrusions upon adhesion to the surface of both endothelial and epithelial cells. In sharp contrast to prototypic filopodia, Nm-induced protrusions are formed independently of actin cytoskeleton reorganization, which only occurs seconds after membrane remodeling and stabilizes the nascent protrusions. We have recently shown that their formation is rather mediated by a physical process we called one-dimensional (1D) wetting driven by the interaction of the plasma membrane with bacterial adhesive nanofibers, known as type 4 pili. Beyond infection, adhesive nanofibers are also found in the extracellular matrix, suggesting a broader role for 1D wetting-mediated membrane protrusions in regulating physio-pathological processes. However, the molecular mechanisms coordinating 1D wetting-mediated membrane deformations to the subsequent actin cytoskeleton remodeling are still unknown. To address this question, we combined the use of live cell imaging, high resolution photonic and electronic microscopy approaches to genetic and drug perturbations on Nm-infected endothelial and epithelial cells. Unexpectedly, using SEM and FIB-SEM on Nm-infected cells, we highlighted morphological differences between both cell types, with thicker and wavier protrusions in endothelial cells. We next used cryo-electron tomography to characterize the ultrastructural organization of the actin cytoskeleton in Nm-induced protrusions in both endothelial and epithelial cells. Strikingly, while endothelial-derived protrusions were filled up by an Arp2/3-dependent branched actin network, Nm-induced protrusions in epithelial cells were enriched in linear actin filaments. These data suggest that the formation of plasma membrane protrusions by 1D wetting induces the local reorganization of the cell-type specific cortical actin network present underneath the infection site. Taken together, our data shed light on the molecular mechanisms coordinating plasma membrane deformations and cortical actin reorganization.

- [1] M. Soyer et al., *Cell Microbiol* (2014)
- [2] D. Bonazzi et al., *Cell*, (2018)
- [3] A. Charles-Orszag et al., *Nat Commun*, (2018)

**Mots clefs :** membrane deformation; actin cytoskeleton; host/pathogen interaction

## SDV3-Oral4

### Des microenvironnements contrôlés permettent l'étude des jonctions cellulaires à l'échelle nanométrique

**Morphological control enables nanometer-scale dissection of cell-cell signaling complexes**

.Cécile SAUVANET \* (cecile.sauvanet@pasteur.fr) / Institut Pasteur, Université de Paris, CNRS UMR3528,

Structural Studies of Macromolecular Machines in Cellulo Unit and Structural Image Analysis Unit, Paris, France

\* Auteur correspondant

Protein micropatterning enables robust control of cell positioning on electron microscopy substrates for cryogenic electron tomography (cryo-ET). However, the combination of regulated cell boundaries and the underlying electron-microscopy substrate (EM-grids) provides a poorly understood microenvironment for cell biology. Because substrate stiffness and morphology affect cellular behavior, we devised protocols to characterize the nanometer-scale details of the protein micropatterns on EM-grids by combining cryo-ET, atomic force microscopy, and scanning electron microscopy. Measuring force displacement characteristics of holey carbon EM-grids, we found that their effective spring constant is similar to physiological values expected from skin tissues. Despite their apparent smoothness at light microscopy resolution, spatial boundaries of the protein micropatterns are irregular at nanometer scale. Our workflow serves as the foundation for studying the fundamental structural changes governing cell-cell signaling [1].

[1] Dow, L.P., Gaietta, G., Kaufman, Y. et al. Morphological control enables nanometer-scale dissection of cell-cell signaling complexes. Nat Commun 13, 7831 (2022). <https://doi.org/10.1038/s41467-022-35409-9>

**Mots clefs :** CryoET, micropatterning, cell-cell contact

## **SDV4 : Stratégies pour tendre vers la résolution nanométrique en microscopie photonique**

***Animation :***

*Christine Terryn (PICT Platform, Reims)*

*Audrey Salles (Institut Pasteur, Paris)*

## SDV4-Inv1

### Visualizing cellular life - from single cell imaging to in vivo single-molecule biophysics & biochemistry and structural (micro-)biology

- Ulrike Endesfelder \*(endesfelder@uni-bonn.de) / Institute for Microbiology and Biotechnology, University of Bonn, Germany

Microbes as unicellular organisms are important model systems for studying cellular mechanisms and functions. In the last decade, immense progress has been made in our understanding of the life and inner workings of bacteria with the help of modern fluorescence microscopy techniques. By visualising single molecules and the molecular architecture of subcellular structures in living cells, we can now look at bacteria based on their molecular interactions and assemblies with molecular resolution.

In particular, we can generate detailed, quantitative, spatially and temporally resolved molecular maps and decipher dynamic heterogeneity and subpopulations at the subcellular level. Here, we will present some examples from our work and give an insight into our visions for the future.

## SDV4-Inv2

### Toward revealing the molecular architecture of the cell using expansion microscopy U-ExM, Cryo-ExM, and iU-ExM.

• **Paul Guichard** (paul.guichard@unige.ch) / Centriole Lab, University of Geneva

Expansion microscopy is a recently developed technique that physically magnifies biological samples, allowing for super-resolution visualization of cells using a standard microscope. I will present the advancements made by our laboratory in optimizing this method. By combining Ultrastructure Expansion Microscopy U-ExM with cryo-tomography, we are able to explore the molecular structure of the centriole, leading to a better understanding of retinal degeneration diseases. Additionally, I will discuss two recent breakthroughs: cryo-ExM, which allows visualization of cells in a near-native state, and iU-ExM, which achieves nanoscale resolution comparable to SMLM (single-molecule localization microscopy) using a conventional widefield microscope.

**Mots-clés/Keywords:** Nanoscopy, Structural Biology, Expansion Microscopy

## SDV4-Oral1

### Une nouvelle approche pour l'exploration en 3D de la vascularisation du muscle dystrophique : Marquage avec une lectine de tomate fluorescente suivi d'une transparisation iDISCO+/CUBIC

**iDISCO+/CUBIC clearing methods combined with fluorescent tomato lectin staining, a new approach for 3D quantitative analysis of dystrophic muscle vascularization**

- **Ibrahim Hassani** \* (ibrahim.hassani@oniris-nantes.fr) / Oniris, INRAE, PAnTher, 44300 Nantes, France & Nikon Europe BV, Nikon France, Champigny-sur-Marne, France
- **Mireille Ledevin** / Oniris, INRAE, PAnTher, 44300 Nantes, France
- **Tony Fiore** / Nikon Europe BV, Nikon France, Champigny-sur-Marne, France
- **Marie-Anne Colle** / Oniris, INRAE, PAnTher, 44300 Nantes, France
- **Karl Rouger** / Oniris, INRAE, PAnTher, 44300 Nantes, France
- **Laurence Dubreil** / Oniris, INRAE, PAnTher, 44300 Nantes, France

\* Auteur correspondant

Duchenne muscular dystrophy (DMD) is the most common and devastating form of muscular dystrophy. It is characterized by a progressive loss of muscle mass and function, resulting in muscle weakness and reduced motility. Among the pathogenic mechanisms identified, a progressive replacement of muscle by fibrous and adipose tissues is noted [1]. A pronounced alteration of angiogenesis, characterized by a loss of vascular density and abnormalities in the structure and function of the vessels, is also listed. Here, we employed methods for fluorescent staining of vessels and optical tissue clearing prior to 3D microscopy to visualise and quantify in depth the muscle microvasculature in healthy and dystrophic muscle of Rat. Post-mortem muscle tissue prefixed in formalin were stained with fluorescent Lycopersicon esculentum agglutinin (Tomato lectin) dehydrated and cleared using a combination between iDISCO+ and CUBIC clearing methods to visualise the vascular endothelium. Tissue was imaged with confocal and multiphotonic microscopy from Nikon and reconstructed in 3D with NIS software. We developed a workflow for ex vivo imaging of optically cleared dystrophic muscle and subsequent computational modeling. This workflow was used for quantification of the microvasculature in relation with density and branching of vessels in healthy and dystrophic muscle. Thanks to this work, we demonstrate that iDISCO+/CUBIC-cleared muscle can be imaged up to at least 1 mm depth at subcellular resolution. In addition, fluorescent Tomato lectin staining in cleared muscle allows detailed 3D visualization of the vasculature and reveals different patterns in healthy and dystrophic muscle. Overall, this new method represents a promising avenue to 3D microscopic analysis of vasculature in dystrophic context and therefore to improve both the knowledge on DMD pathophysiology and the impact of MuStem cell transplantation [2] on dystrophic tissue remodeling.

#### References:

- [1] Podkalicka P et al. Cell Mol Life Sci. 2019 Apr;76(8):1507-1528. doi:0.1007/s00018-019-03006-7. [2] Rouger K et al. Am J Pathol. 2011 Nov;179(5):2501-18. doi:10.1016/j.ajpath.2011.07.022.

**Mots clefs :** Muscle, Duchenne muscular dystrophy, vasculature, 3D, iDISCO, CUBIC

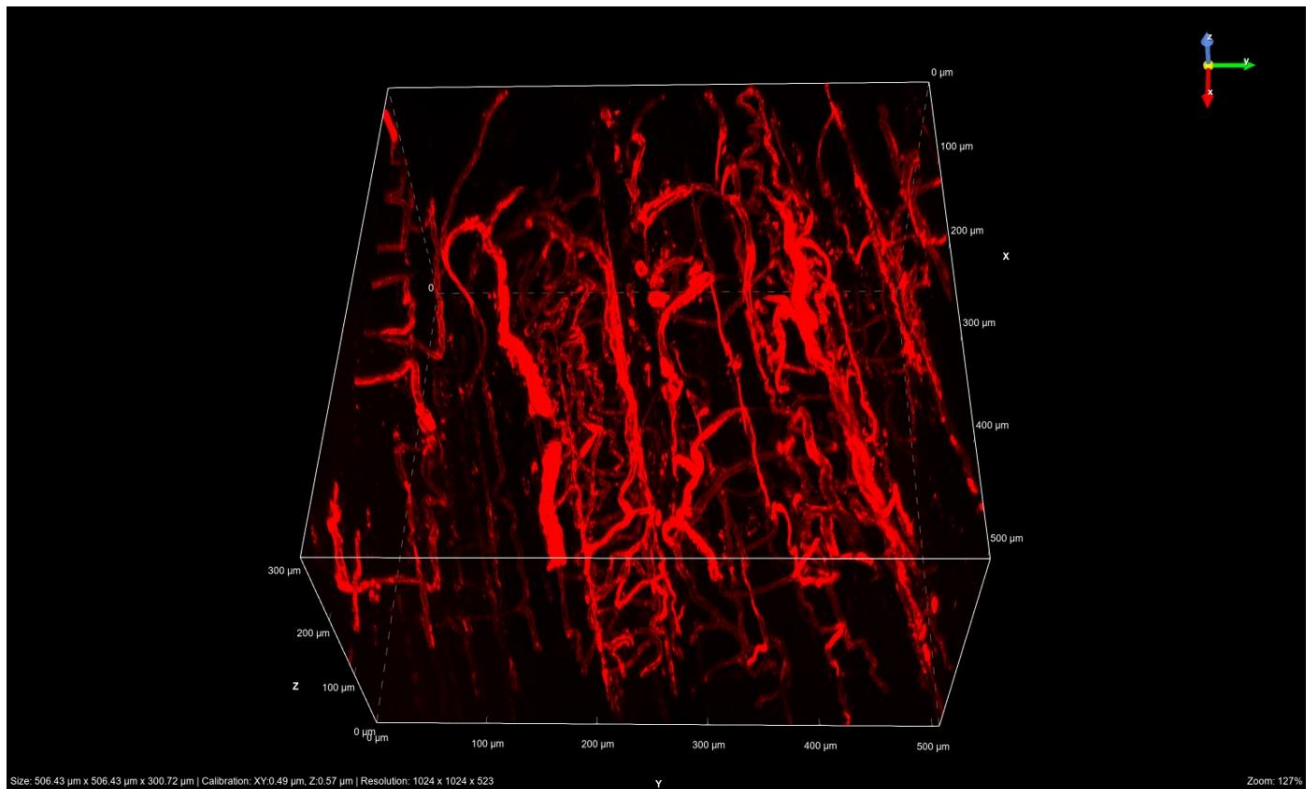


**Figure 1** 3D vasculature of dystrophic muscle tissue cleared with IDISCO+ combined with CUBIC protocol. The sample was acquired with a Nikon C2 inverted laser scanning confocal microscope using a plan Apo Lambda S 25XC Silicone objective. Pixel size  $0.49 * 0.49 \mu\text{m}^2$ , Bit Depth 12 bits, image size  $1024*1024$ , depth in Z  $300 \mu\text{m}$

## SDV4-Oral2

### Super-resolution expansion microscopy applied at tissue scale in plants

#### Super-resolution expansion microscopy applied at tissue scale in plants

- **Magali Grison** \* (magali.grison@u-bordeaux.fr) / CNRS
- **Monica Fernandez-Monreal** \* (monica.fernandez-monreal@u-bordeaux.fr) / CNRS

\* Auteur correspondant

Plants are multi-cellular organisms capable of reacting and adapting rapidly to their environment. This flexibility is largely due to their ability to modulate the pattern of their bodies and generate new organs throughout their lives. At the subcellular level, the highly compartmentalized intracellular membrane system of eukaryotic cells allows multicellular organisms to differentiate functions within a tissue and build organs in a coordinated manner.

Studying these subcellular mechanisms requires super-resolution both in space and time. However, imaging in plant cells presents some difficulties such as the pecto-cellulosic cell wall that is a hydrophobic barrier relatively impermeable to externally applied molecules. Additionally, the auto-fluorescent background can be a problem in plant tissues. The plant model is both challenging and compelling since it allows to track cell lineage and tissue differentiation in a whole organ without dissection, more particularly in the root which is a thin organ. In this work, we have developed an expansion protocol adapted to the *Arabidopsis* root model. Expansion microscopy (ExM) is a relatively new super-resolution method based on the isotropic dilation of biological samples in order to overcome the diffraction limit of conventional microscopy [1, 2, 3]. This protocol allowed us to expand the whole root tip up to 4 times and, coupled with an immunostaining of markers of the division plane [4], to visualize the membrane fenestrated sheet composing the division plane during cell division. These structures are usually visible only using electron microscopy, thus ExM allows to access membrane structures at high-resolution in a cost-and accessible-effective manner.

#### Références/References :

- [1] Tillberg et al, Nat biotechnol, 34(9): 987–992 (2016)
- [2] Chozinsky et al, Nat Methods, 13(6): 485–488 (2016)
- [3] Kao and Nodine, Methods in cell biology, 161 (2021)
- [4] Lauber et al, J of cell biol, 139(6):1485-93 (1997)

**Mots clefs** : *arabidopsis*, expansion, microscopy

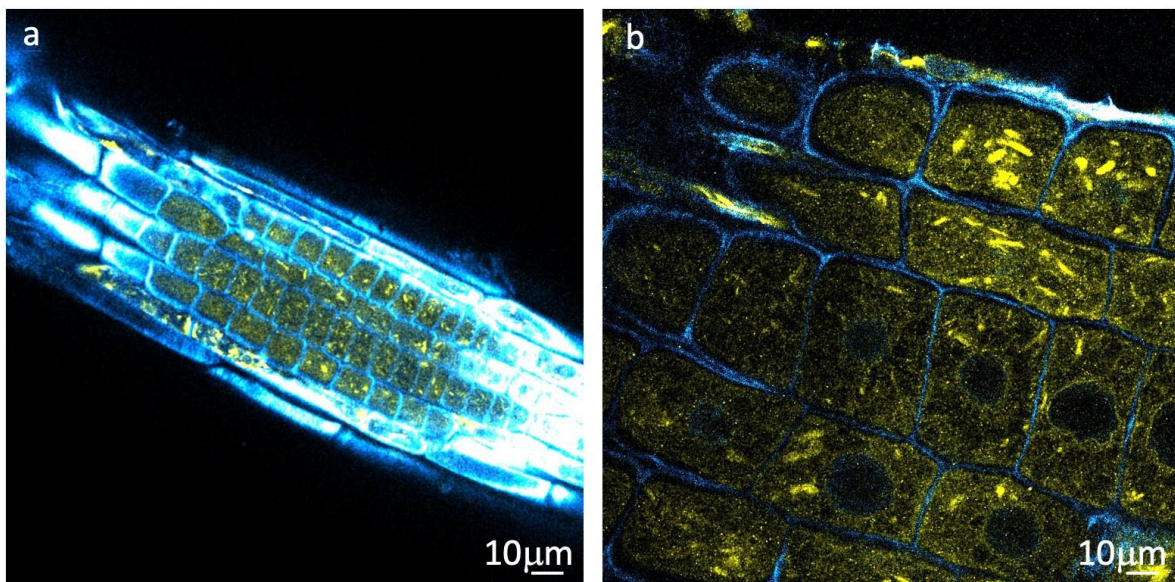


**Figure 1:** (a-b) *Arabidopsis thaliana* root tip before (a) and after (b) expansion using the same magnification (obj 40W 1,2NA zoom 1).  
Expansion factor x4,5 cyan: Cell Wall, yellow: HDEL-YFP bar= 10μm

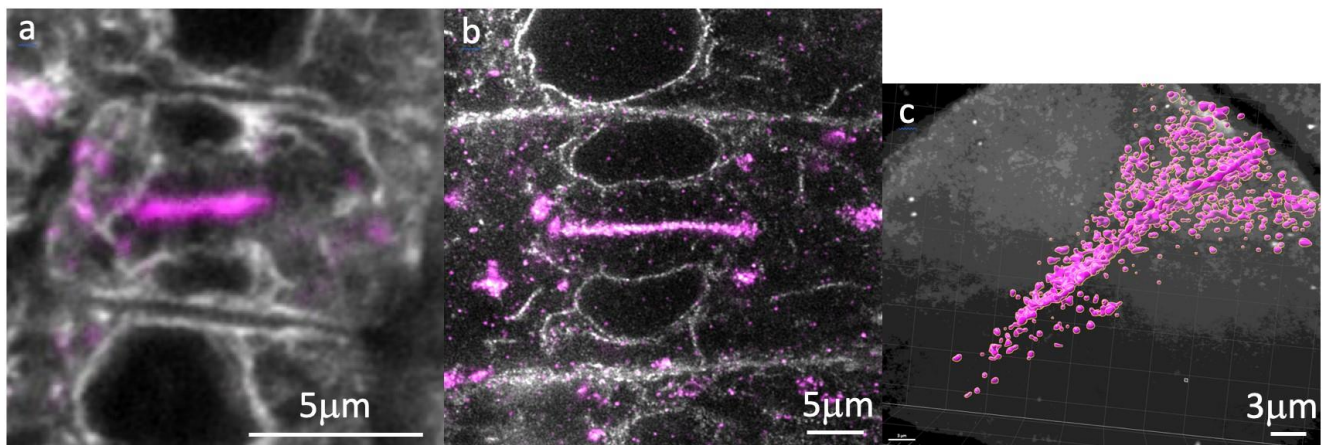


**Figure 2:** (a, b) representative image of a dividing cell in *Arabidopsis thaliana* root tip before (a) and after (b) expansion using Airyscan microscopy. (c) 3D reconstruction of an expanded dividing cell using Lattice Light Sheet acquisition and IMARIS.

magenta: Cell Plate, grey in (a, b): HDEL-YFP, grey in (c): Cell Wall

## Recueil des résumés

### Partie 2 : Posters

## Liste des Posters

### Symposia communs

#### SC1 : Méthodes émergentes pour le traitement de données et l'acquisition

##### **SC1-P1 Cédric Messaoudi (Institut Curie)**

*MIC-MAQ un plugin Fiji pour la microscopie de fluorescence à haut-débit*

##### **SC1-P2 Sebastian Cozma (EPFL, Lausanne)**

*Amélioration de l'analyse des données STEM-EDX assistée par machine learning grâce à l'utilisation de données synthétiques*

##### **SC1-P3 Jean-Luc Rouviere(CEA, Grenoble)**

*Explication simple de la ptychographie électronique*

#### SC 2 : Microscopie à l'interface physique et biologie

##### **SC2-P1 Nathaly ORTIZ PEÑA (MPQ, Paris)**

*Analyse *in situ* des mécanismes de nucléation et de croissance des nanoparticules d'or sur le virus de la mosaïque du tabac*

##### **SC2-P2 Matteo De Tullio (GPM, Rouen)**

*Analyse d'une matrice de silice en sonde atomique tomographique assistée par laser UV et THz pour l'incorporation de biomolécules*

##### **SC2-P3 Carlos Alexandre Henrique Fernandes (IMPMC, Paris)**

*Structure en cryo-microscopie électronique du canal potassique Kir2.1 humain lié à l'activateur PIP2 révèle son mécanisme d'ouverture*

##### **SC2-P4 Tom Roussel (CINAM, Marseilles)**

*Auto-assemblage modulaire et adaptatif de dendrimères amphiphiles étudié par microscopie électronique en mode standard, cryo et liquide *in situ**

##### **SC2-P5 Marta De Frutos (CNRS, Univ. Paris Saclay)**

*Analyse par STEM-EELS monochromaté de la structure et composition de la calcite biogénique*

## SC 3 : Diffraction et résolution structurale

### SC3-P1 Philippe Boullay (CRISMAT, Caen)

*Un point sur les approches 3D ED en 2023*

### SC3-P2 Nicolas Gautier (IMN, Nantes)

*Résolution structurale d'un matériau de batterie organique par diffraction électronique en mode tomographie*

### SC3-P3 Emre Yörük (Institut Neel, Grenoble)

*La synergie entre les sciences de la vie et les sciences des matériaux dans la diffraction électronique réveille les cadres magnétiques métal-organique*

## SC 4 : Avancées instrumentales

### SC4-P1 Lorenzo Rigutti (GPM, Rouen)

*La sonde atomique "photonique" pour l'étude de la physique de l'émission ionique par effet de champ*

### SC4-P2 Lorenzo Rigutti (GPM, Rouen)

*Microscopie corrélative avec une sonde atomique "photonique"*

### SC4-P3 Matus Krajinak (Quantum Detectors)

*MerlinEM, détecteur hybride de comptage d'électrons à pixels pour la microscopie électronique à transmission*

### SC4-P4 Jean-Baptiste MAILLET (GPM, Rouen)

*Une nouvelle méthode d'implantation *in-situ* et de caractérisation de l'hydrogène en Sonde Atomique Tomographique*

### SC4-P5 Francisco José CADETE SANTOS AIRES (Ircelyon)

*Étude en ETEM *in situ* de la condensation / évaporation de l'eau et du comportement hygroscopique des aérosols à l'aide d'un porte-échantillons refroidi par un micro-élément Peltier*

### SC4-P6 Christian Bacchi (GPM, Rouen)

*Développement d'un détecteur sensible en position et en énergie pour la Sonde Atomique Tomographique*

### SC4-P7 Samba Ndiaye (GPM, Rouen)

*Métrologie avancée de la composition du carbure de silicium en sonde atomique tomographie*

### SC4-P8 Malo Bezard (LPS, Orsay)

*Cathodoluminescence Polarisée et Résolue Spectralement en STEM*

**SC4-P9 Gozde Oney (ICMCB, Bordeaux)**

*Comprendre l'étendue de l'ordre dans le spinelle  $LiNi0.5Mn1.5O4$  par 4D-STEM en utilisant l'outil ASTAR*

## **Symposia en sciences de la matière**

### **SDM1 : Imagerie volumique, cartographie de propriétés et approches corrélatives**

**SDM1-P1 Chih-Ying Hsu (EPFL, Lausanne)**

*Quantification précise de la ségrégation intergranulaire du phosphore dans le fer par STEM-EDX*

**SDM1-P2 Jesus Canas (CEA, Grenoble)**

*Microscopie corrélative des grains 3D sur AlGaN QDs pour des émetteurs UV pompés par les électrons*

**SDM1-P3 Aissatou DIAGNE (GPM, Rouen)**

*Étude de la réaction de l'hydrogène et des hydrures en Sonde Atomique Tomographique des semi-conducteurs III-N*

**SDM1-P4 Pavel Komarov (Nenovision)**

*True Correlative Microscopy Using AFM-in-SEM*

### **SDM2 : Microscopies in situ, operando**

**SDM2-P1 Giuseppe De Salvo (Nanogune)**

*Calculs de radiolyse pour les régimes d'irradiation fondamentaux de microscopie électronique en phase liquide.*

*Radiolysis calculations for fundamental irradiation regimes for liquid phase TEM.*

**SDM2-P2 Sadia Traore (IPCMS, Strasbourg)**

*Etude operando par XAS et TEM des mécanismes d'activation des catalyseurs bimétalliques Fe et Sb*

**SDM2-P3 Matthieu Bugnet (MATEIS, Lyon)**

*Vers l'Analyse Operando de Piles à Combustible à Oxyde Solide en Microscopie Electronique en Transmission Environnementale*

**SDM2-P4 Jean-Luc Maurice (LPCIM, Paris) Changement de phase déclenché in situ par un plasma d'hydrogène**

*H<sub>2</sub> plasma triggers nanoparticle phase change in situ*

**SDM2-P5 Yevgeniy Pivak (Dens Solutions)**

*Développement d'un système de polarisation in situ cryogénique stable pour la résolution atomique (S)TEM*

**SDM2-P6 Karine Masenelli-Varlot (MATEIS, Lyon)**

*Essais de compression in situ en microscopie électronique en transmission sur des particules individuelles*

**SDM2-P7 Dris Ihiawakrim (IPCMS, Strasbourg)**

*Suivi en direct de la nucléation et de la croissance des nanoparticules d'oxyde de zinc par microscopie électronique à transmission liquide in situ*

**SDM2-P8 Louis-Marie Lebas (MATEIS, Lyon)**

*Caractérisation des matériaux sensibles aux électrons à l'aide de la tomographie STEM en phase liquide multi-échelles dans l'ESEM et l'ETEM*

**SDM2-P9 Francisco José CADETE SANTOS AIRES (Ircelyon)**

*Formation et évolution de catalyseurs modèles AuxPd<sub>1-x</sub> sous environnements gazeux et en température variable dans un ETEM*

**SDM2-P10 Leifeng ZHANG (CEMES, Toulouse)**

*Étude de la charge d'interface dans les empilements diélectriques tri-couches par des expériences d'holographie électronique operando*

**SDM2-P11 Nathaly ORTIZ PEÑA (MPQ, Paris)**

*Etude corrélative multi-microscopies de nano-assemblages de Pt électrodeposités comme plateformes de précipitation pour Ni(OH)<sub>2</sub>*

**SDM2-P12 Syrine KROUNA (MPQ, Paris)**

*Stabilité thermique des nanoparticules d'alliage à haute entropie étudiée par microscopie électronique en transmission in-situ*

**SDM2-P13 Juan Macchi (GPM, Rouen)**

*Les nouvelles opportunités offertes par la combinaison de la sonde atomique tomographique et du MET en un seul instrument pour la caractérisation des métaux et alliages*

**SDM2-P14 Maxime Vallet (Centrale Supelec)**

*In situ STEM monitoring of ferroelectric phase transitions of antiferroelectric PbZrO<sub>3</sub> thin films*

**SDM2-P15 Mohammad Dolatabadi (IMN, Nantes)**

*Étude des technologies émergentes par microscopie électronique operando avancée*

*Advanced operando electron microscopy for emerging technologies*

**SDM2-P16 Kilian Gruel (CEMES, Toulouse)**

*Étude de l'accumulation de charges dans les condensateurs bicouches par holographie électronique operando et modélisation*

**SDM2-P17 Josephine Rezkallah (GPM, Rouen)**

*Microscopie électronique en transmission *in situ* et *operando* pour l'étude de l'hydrogénéation catalytique du CO<sub>2</sub>*

**SDM2-P18 Juliana Guimarães (Univ. Strasbourg)**

*La bionanomagnétite : un aperçu des applications et des perspectives d'avenir*

## **SDM3 : Microscopie des matériaux et nano-matériaux**

**SDM3-P1 Frédéric Fossard (LEM CNRS ONERA, Châtillon)**

*Silicide precipitation in aged quasi- $\alpha$  Ti alloys*

**SDM3-P2 Loïc Patout (IM2NP, Marseilles)**

*Polymorphisme et structures d'intercroissance dans le système nanostructure Pr-Co: Pr<sub>2</sub>Co<sub>7</sub> et Pr<sub>5</sub>Co<sub>19</sub>*

**SDM3-P3 Cathy Vang (CEA)**

*Profilage de dopage pour Si:P hautement dopés par TEM avancé*

**SDM3-P4 Eric Gautron (IMN, Nantes)**

*Observations des faces cristallines de TiO<sub>2</sub> rutile et anatase en présence de H<sub>2</sub>PO<sub>4</sub><sup>-</sup>*

**SDM3-P5 Frédéric Pailloux (PPrime, Poitiers)**

*Sur l'insensibilité du molybdène à l'oxydation à température ambiante*

**SDM3-P6 Frédéric Pailloux (PPrime, Poitiers)**

*Analyses de nanoparticules Pt/Terres rares par MET*

*TEM investigations of Pt-REM nanocatalysts*

**SDM3-P7 Michaël Walls (LPS, Orsay)**

*Imagerie par STEM-EELS de nanoparticules cœur-coquille en super-réseaux*

**SDM3-P8 Jerome Pacaud (PPrime, Poitiers)**

*Détermination de l'architecture d'un empilement de quelques feuillets de MXENE Ti<sub>3</sub>C<sub>2</sub>Tx par VEELS*

**SDM3-P9 Benjamin Klaes (GPM, Rouen)**

*Etude de la météorite Santa Catharina par microscopie ionique à effet de champ analytique*

**SDM3-P10 Maxandre Caroff (LRCS, Amiens)**

*Etude des phénomènes de réactivité et de dégradation des batteries organiques par microscopie électronique*

**SDM3-P11 Agathe Duclos (CEMES, Toulouse)**

*Comparaison du taux de dislocations dans des alliages d'aluminium corroyés (famille 2xxx) par microscopie électronique à transmission et par diffraction des rayons X*

**SDM3-P12 Mimoun Aouine (Ircelyon)**

*Résoudre la structure de l'oxyde de bronze TiNbO<sub>x</sub> par STEM atomique et STEM-EDX*

**SDM3-P13 Florian Chabanais (IMN, Nantes)**

*Études par MET d'un absorbeur solaire sélectif multicouche pour applications solaires thermodynamiques sous concentration*

**SDM3-P14 Solène COMBY-DASSONNEVILLE (IM2NP, Marseilles)**

*Matériau à changement de phase Ge-Sb-Te : étude de la cristallisation par TEM haute résolution *in situ* et spectroscopie X à dispersion d'énergie*

**SDM3-P15 Mariana Timm (ICGM, ENSCM, Montpellier)**

*Etude des propriétés physiques des films minces amorphes CrSi<sub>2</sub> modifiés par implantation ionique*

**SDM3-P16 Jeoffrey Renaux (GPM, Rouen)**

*Influence de l'austénite sur le vieillissement de la ferrite des aciers inoxydables austénoferritiques*

**SDM3-P17 Priscille Cuvillier (EDF DI, CNPE Chinon)**

*Etude MET d'une vis fissurée de cloison-renfort d'un réacteur REP du parc français et irradiée jusqu'à 37 dpa*

*TEM investigations of a cracked baffle-former bolt coming from a French PWR and irradiated up to 37 dpa*

**SDM3-P18 Omar BOUKIR (GPM, Rouen)**

*Études par MET de l'influence de l'hydrogène et de la déformation sur la précipitation d'un alliage Al-Cu.*

**SDM3-P19 Laëtitia Rapenne (LMGP, Grenoble)**

*Caractérisation TEM d' hétéro-interfaces  $La0.75Sr0.25Cr0.5Mn0.5O3-Ce0.8Sm0.2O2$  nanostructurées comme couches fonctionnelles entièrement céramiques pour les piles à combustible à oxyde solide*

**SDM3-P20 Baptiste BOULET (GPM, Rouen)**

*Mesure des contraintes résiduelles par imagerie MEB-FIB combinée à une technique de mesure de champs*

**SDM3-P21 Valérie BRIEN (IMN, Nantes)**

*Influence de la préparation d'échantillon sur l'analyse MET de films minces Al-N-O-Cu synthétisés par pulvérisation magnétron*

**SDM3-P22 Maeva Chaupard (LPS, Orsay)**

*STEM-EELS Monochromatée à Faible Dose et à Températures Cryogéniques pour les Nanomatériaux Sensibles aux Rayonnements*

## SDM4 : Spectroscopie à haute résolution, ultrarapide

**SDM4-P1 Mario Pelaez Fernandez (UMET, Lille – Univ. Saragosse, Esp.)**

Analyses EELS des pics ELNES du seuil Si-L<sub>2,3</sub> dans des échantillons provenant de l'astéroïde Ryugu

**SDM4-P2 Ayoub Benmoumen (IMN, Nantes)**

Fonctionnalisation et modifications structurelles induites par l'irradiation ionique de films minces de carbure de métaux de transition 2D (MXène), étudiées par STEM-EELS

**SDM4-P3 Onkar Bhorade (GPM, Rouen)**

Source d'électrons lumineuse et ultrarapide en nanopointe LaB<sub>6</sub>

**SDM4-P4 Estève Drouillas (STMicroelectronics, Crolles)**

Caractérisation avancée par spectroscopie EELS de matériaux semiconducteurs dédiés à la microélectronique

## Symposia de sciences du vivant

### SDV1 : Techniques corrélatives, combinatoires ou multi-modales

#### SDV1-P1 Aurélie Bertin (Institut Curie)

*Septines: remodelage membranaire induit par des filaments sensibles à la courbe*

### SDV2 : Cryo-méthodes 1 : nano-objets

#### SDV2-1 Aurélie Bertin (Institut Curie)

*Observation directe des conformations de la formine au bout des brins barbés d'actine.*

#### SDV2-2 Eric Gautron (IMN, Nantes)

*Peut on faire de la cryo SPA sans TEM cryo dédié ?*

#### SDV2-3 Amélie Leforestier (LPS, Orsay)

*Corrélation entre propriétés physico-chimiques de solutions de tensio-actifs et formation de films minces pour la cryo-microscopie*

#### SDV2-4 Jéril Degrouard (LPS, Orsay)

*Influence des modulateurs d'assemblage sur la structure et la cinétique d'assemblage de la capsid du virus de l'hépatite B*

### SDV3 : Cryo-méthodes 2 : cellulaire/tissulaire

#### SDV3-P1 Camille Keck (Institut Pasteur)

*Décrypter le mode de vie intracellulaire de *Mycobacterium tuberculosis* dans les macrophages infectés par des approches de biologie structurale *in situ*.*

#### SDV3-P2 Fatima Taiki (Univ. Paris Saclay)

*Optimisation de la cryo-tomographie de sections vitreuses pour l'imagerie de cellules et tissus*

#### SDV3-P3 Marc Ropitaux (PRIMACEN, GlycoMEV, Rouen)

*Localisation subcellulaire des N-glycoprotéines portant un noyau bêta(1,2)-xylose chez la microalgue verte *Chlamydomonas reinhardtii**

## SDV4 : Stratégies pour tendre vers la résolution nanométrique en microscopie photonique

### SDV4-P1 Ludovic Galas (Primacen, Rouen)

Amélioration concomitante de la résolution spatiale et de la préservation de l'échantillon en utilisant des stratégies de durée de vie de fluorescence pour l'imagerie des cellules vivantes.

## SC1-P1

### MIC-MAQ un plugin Fiji pour la microscopie de fluorescence à haut-débit

#### MIC-MAQ a Fiji plugin for High-content fluorescence microscopy

- **Laetitia Besse** / Institut Curie, Université PSL, CNRS UAR2016, Inserm US43, Université Paris-Saclay, Multimodal Imaging Center, 91400 Orsay, France.
- **Camille Rabier** / Institut Curie, Université PSL, CNRS UAR2016, Inserm US43, Université Paris-Saclay, Multimodal Imaging Center, 91400 Orsay, France.
- **Typhaine Rumiac** / Institut Curie, Université PSL, CNRS UMR3348, Orsay, France. Université Paris-Saclay, CNRS UMR3348, Orsay, France. Equipe Labélisée Ligue Nationale Contre Le Cancer, 91400 Orsay, France
- **Anne Reynaud-Angelin** / Institut Curie, Université PSL, CNRS UMR3348, Orsay, France. Université Paris-Saclay, CNRS UMR3348, Orsay, France. Equipe Labélisée Ligue Nationale Contre Le Cancer, 91400 Orsay, France
- **Christine Walczak** / Institut Curie, Université PSL, CNRS UAR2016, Inserm US43, Université Paris-Saclay, Multimodal Imaging Center, 91400 Orsay, France.
- **Marie-Noelle Soler** / Institut Curie, Université PSL, CNRS UAR2016, Inserm US43, Université Paris-Saclay, Multimodal Imaging Center, 91400 Orsay, France.
- **Vincent Pennaneach** / Institut Curie, Université PSL, CNRS UMR3348, Orsay, France. Université Paris-Saclay, CNRS UMR3348, Orsay, France. Equipe Labélisée Ligue Nationale Contre Le Cancer, 91400 Orsay, France
- **Sarah A E Lambert** / Institut Curie, Université PSL, CNRS UMR3348, Orsay, France. Université Paris-Saclay, CNRS UMR3348, Orsay, France. Equipe Labélisée Ligue Nationale Contre Le Cancer, 91400 Orsay, France
- **Frederic Coquelle** / Institut Curie, Université PSL, CNRS UAR2016, Inserm US43, Université Paris-Saclay, Multimodal Imaging Center, 91400 Orsay, France.
- **Cédric Messaoudi** \* (cedric.messaoudi@curie.fr) / Institut Curie, Université PSL, CNRS UAR2016, Inserm US43, Université Paris-Saclay, Multimodal Imaging Center, 91400 Orsay, France.

\* Auteur correspondant

Immunofluorescence microscopy analysis is extensively used to monitor various cellular processes and in particular the DNA Damage Response. Here, we present an in-house developed Fiji plugin, called MIC-MAQ for Microscopy Images of Cells-Multi Analysis and Quantifications, which allows analysis of high content fluorescence microscopy images. This plugin is designed to automatically segment nuclei and/or cells using deep-learning approaches (Cellpose [1]), it then performs measurements on all available channels for each individual cell compartments detected: nucleus, cell and cytoplasm (when both nuclei and cells channels are provided). In addition to measurements based on pixel intensity and object morphology, spot detection is provided.

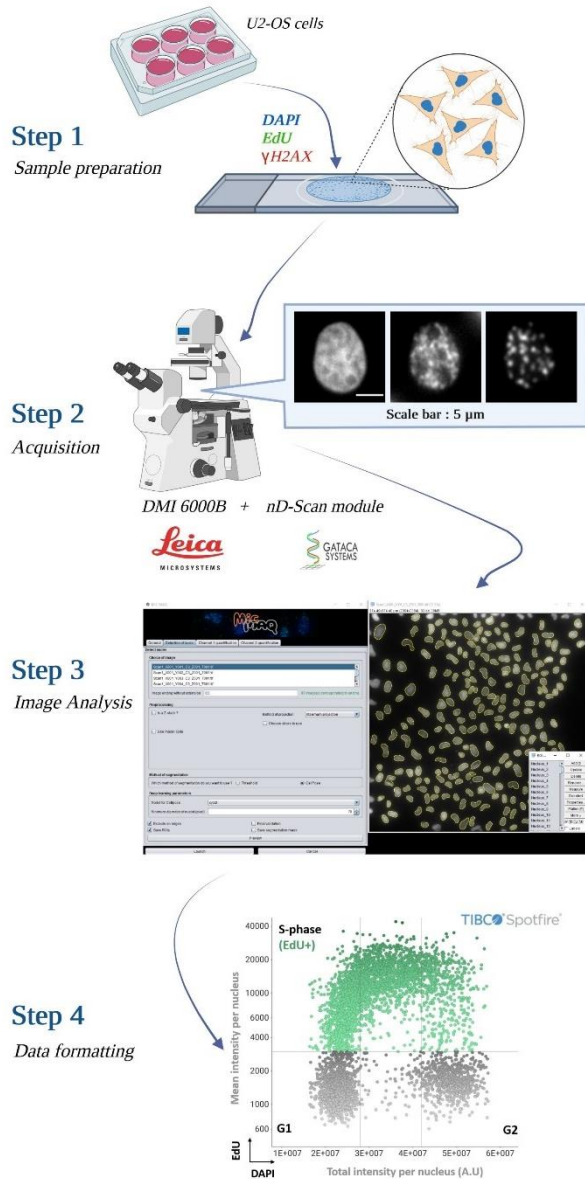
MIC-MAQ is applied in the example of a multivariate Quantitative Image-Based Cytometry (QIBC) approach [2]. This experiment determines the cell-cycle stage for each cell in a large asynchronously growing population. In parallel, the nuclear signal intensity and the counting of nuclear protein foci of a protein of interest are measured. The QIBC protocol was developed on U-2 OS cells. The cells were immunolabelled for nuclear proteins, de novo DNA synthesis in S-phase was detected by EdU labeling and DNA staining with DAPI was performed. The images were acquired automatically using a widefield

microscope. MIC-MAQ is then used to extract measurements from nuclei and examples of multiparametric data visualization will be presented.

## References

- [1] Stringer, Carsen, et al. « Cellpose: A Generalist Algorithm for Cellular Segmentation ». *Nature Methods*, vol. 18, no 1, 1, janvier 2021, p. 100-06. www.nature.com, <https://doi.org/10.1038/s41592-020-01018-x>.
- [2] Roukos, Vassilis, et al. « Cell Cycle Staging of Individual Cells by Fluorescence Microscopy ». *Nature Protocols*, vol. 10, no 2, février 2015, p. 334-48. www.nature.com, <https://doi.org/10.1038/nprot.2015.016>.

**Mots clefs :** Plugin, Cellpose, High content fluorescence microscopy, Quantitative Image-Based Cytometry (QIBC), Automatic image analysis; DNA-damage response



## SC1-P2

### Amélioration de l'analyse des données STEM-EDX assistée par machine learning grâce à l'utilisation de données synthétiques

Improving machine learning-assisted STEM-EDX data analysis through the use of synthetic data

- **Sebastian Cozma** \* (sebastian.cozma@epfl.ch) / Electron Spectrometry and Microscopy Laboratory (LSME), Institute of Physics (IPHYS), École Polytechnique Fédérale de Lausanne (EPFL), 1015 Lausanne, Switzerland
- **Hui Chen** / Electron Spectrometry and Microscopy Laboratory (LSME), Institute of Physics (IPHYS), École Polytechnique Fédérale de Lausanne (EPFL), 1015 Lausanne, Switzerland
- **Duncan T.L. Alexander** / Electron Spectrometry and Microscopy Laboratory (LSME), Institute of Physics (IPHYS), École Polytechnique Fédérale de Lausanne (EPFL), 1015 Lausanne, Switzerland
- **Cécile Hébert** / Electron Spectrometry and Microscopy Laboratory (LSME), Institute of Physics (IPHYS), École Polytechnique Fédérale de Lausanne (EPFL), 1015 Lausanne, Switzerland

\* Auteur correspondant

Machine learning algorithms such as PCA (Principal Component Analysis), NMF (Non-Negative Matrix Factorisation and BSS (Blind Source Separation) have recently become popular for analysing STEM-EDX (Scanning Transmission Electron Microscopy-Energy Dispersive X-ray spectrum image data. This derives from their potential for denoising the datasets and/or helping to retrieve meaningful components from them. These aspects are in turn becoming more vital as instrumental developments increase the volume of data that we acquire, both in terms of the size of datasets and the acquisition speed. Given the importance of machine learning algorithms to the electron microscopy community, evaluating their respective strengths and weaknesses is helpful. To this end, here we explore the capacity of selected tools (PCA, NMF and some of their newly developed derivatives) to decompose datasets from a diverse range of materials samples (meteoritic material, synthetic minerals and solid oxide fuel cells).

In order to make the evaluation as quantitative as possible, we use an open-source Python package, espm[1], which can simulate extremely realistic synthetic STEM-EDX datasets with chosen noise levels, as based on a defined ideal ground truth (datacube without noise). This package is used within the HyperSpy[2] toolbox, and was recently developed in our lab. Each synthetic dataset is based on experimental data from the three families of materials being studied. They are then used to assess the machine learning algorithm by comparing the results of the decomposition with the ground truth. We show that this approach can be used to determine the capabilities of the algorithms, for instance in terms of x-ray count statistics, size or relative volume of the different constituent phases. After testing the algorithms on synthetic datasets, we aim to apply suitably-optimised parameters to experimental datasets from our three families of samples; in pursuit of the holy grail of decomposition in which we identify only the relevant noise-free components, resulting in an ideal representation of the different pure phases of the sample material.

**Mots clefs :** STEM-EDX, NMF, espm, HyperSpy

## SC1-P3

### Explication simple de la ptychographie électronique

A simple description of electron ptychography - focus on algorithms -

- **jean-luc Rouviere** \* (jean-luc.rouviere@cea.fr) / CEA-UGA IRIG/MEM/LEMMA
- **Matthew Bryan** / CEA-UGA LETI
- **Yiran LU** / NEEL
- **Martien Den Hertog** / NEEL
- **Hanako OKUNO** / CEA-UGA IRIG/MEM/LEMMA
- **Kshipra Sharma** \* (Kshipra.sharma@cea.fr) / CEA-UGA IRIG/MEM/LEMMA

\* Auteur correspondant

La ptychographie électronique (PE) est actuellement la technique de microscopie qui a obtenu la meilleure résolution atomique (Muller).

Cette techniqu 'propos e' th oriquement par Hoppe en 1970 n'a donn  des premiers r sultats exp rimentaux timides que plusieurs ann es plus tard, mais dans le domaine des rayons X cette technique PX (Ptychographie avec des rayons X) a connu un grand succ s et de grands d veloppements. Actuellement, suivant mes connaissances parcellaires, Grenoble est la seule ville en France qui cherche  d velopper cette technique car elle est souvent jug  trop compliqu e. Dans cette expos , je voudrais montrer (1) que la th orie derri re la PE n'est pas si compliqu e que cela et (2) quelques r sultats pr liminaires obtenus  Grenoble.

**Mots clefs** : electron diffraction maps, 4D-STEM, ptychography, phase retrieval

## SC2-P1

### Analyse *in situ* des mécanismes de nucléation et de croissance des nanoparticules d'or sur le virus de la mosaïque du tabac

**In situ insights into the nucleation and growth mechanisms of gold nanoparticles on Tobacco mosaic virus**

- **Cora Moreira Da Silva** / Université Paris Cité, ITODYS, CNRS, UMR 7086, 15 rue J-A de Baif, F-75013 Paris, France
- **Nathaly Ortiz Pena** \* (nathaly.ortiz@u-paris.fr) / Université Paris Cité, CNRS, Laboratoire Matériaux et Phénomènes Quantiques, 75013 Paris, France
- **Leila Boubekeur-Lecaque** / Université Paris Cité, ITODYS, CNRS, UMR 7086, 15 rue J-A de Baïf, F-75013 Paris, France
- **Jakub Dušek** / Institute of Experimental Botany of the Czech Academy of Sciences, Rozvojová 263, Prague 6, 160 00, Czech Republic
- **Tomas Moravec** / Institute of Experimental Botany of the Czech Academy of Sciences, Rozvojová 263, Prague 6, 160 00, Czech Republic
- **Damien Alloyeau** \* (damien.alloyeau@u-paris.fr) / Université Paris Cité, CNRS, Laboratoire Matériaux et Phénomènes Quantiques, 75013 Paris, France
- **Nguyet-Thanh Ha-Duong** / Université Paris Cité, ITODYS, CNRS, UMR 7086, 15 rue J-A de Baïf, F-75013 Paris, France

\* Auteur correspondant

Biotemplated syntheses have emerged as an efficient strategy to control the assembly of metal nanoparticles (NPs) and generate original plasmonic properties. [1] However, understanding the nucleation and growth mechanisms of metallic nanostructures on biological species is an essential prerequisite to developing well-controlled nanotechnologies. Here, we used *in situ* liquid-phase transmission electron microscopy (LP-TEM) to reveal how the formation kinetics of gold NPs on the Tobacco Mosaic Virus (TMV) affects their size and density. Direct *in situ* LP-TEM observations at the single virus level revealed how the reaction kinetics affects the nucleation and growth rates of NPs. This enhanced comprehension of the kinetics allows to improve in the design of synthesis protocols with reduction cycles of different intensities in order to enhance the density of NPs on TMV. Therefore, *in situ* insights are used as a guideline to optimize bench-scale synthesis with the possibility to homogenize the coverage rate and tune the density of gold NPs. In line with *in situ* LP-TEM observations, fluorescence spectroscopy analysis confirmed that the nucleation of NPs occurs on the virus capsid rather than in solution. The proximity of gold NPs on TMV allows shifting the plasmonic resonance of the assembly in biological window.

#### Références/References :

[1] (a) Capek, I. *Adv Colloid Interface Sci.* 222 (2015), 119-134. (b) Culver, J.N. et al. *Virology* 479-480(2015), 200-212. (c) Li, F. & Wang, Q. *Small* 10 (2014), 230-245. (d) Liu, Z. et al. *Chem Soc Rev* 41(2012) 6178-6194.

**Mots clefs :** *In situ* liquid phase transmission electron microscopy, Tobacco mosaic virus, biotemplating, gold nanoparticles, plasmonic resonance

## SC2-P2

### Analyse d'une matrice de silice en sonde atomique tomographique assistée par laser UV et THz pour l'incorporation de biomolécules

UV and THz laser assisted APT analysis of a silica matrix for bio-particles embedding

- **Matteo De Tullio** \* (matteo.de-tullio@univ-rouen.fr) / Laboratoire GPM (Groupe Physique des matériaux)  
– UMR CNRS INSA 6634, Université de Rouen Normandie, Avenue de l'Université, Saint-Etienne-du-Rouvray, France.
- **Angela Vella** / Laboratoire GPM (Groupe Physique des matériaux) – UMR CNRS INSA 6634, Université de Rouen Normandie, Avenue de l'Université, Saint-Etienne-du-Rouvray, France.
- **Ivan Blum** / Laboratoire GPM (Groupe Physique des matériaux) – UMR CNRS INSA 6634, Université de Rouen Normandie, Avenue de l'Université, Saint-Etienne-du-Rouvray, France.
- **Emmanuel Cadel** / Laboratoire GPM (Groupe Physique des matériaux) – UMR CNRS INSA 6634, Université de Rouen Normandie, Avenue de l'Université, Saint-Etienne-du-Rouvray, France.
- **Laurence Chevalier** / Laboratoire GPM (Groupe Physique des matériaux) – UMR CNRS INSA 6634, Université de Rouen Normandie, Avenue de l'Université, Saint-Etienne-du-Rouvray, France.
- **Jonathan Houard** / Laboratoire GPM (Groupe Physique des matériaux) – UMR CNRS INSA 6634, Université de Rouen Normandie, Avenue de l'Université, Saint-Etienne-du-Rouvray, France.
- **Marc Ropitaux** \* (marc.ropitaux1@univ-rouen.fr) / Laboratoire Glyco-MEV (Glycobiologie et Matrice Extracellulaire Végétale) – UR 4358, Université de Rouen Normandie, Rue Lucien Tesnière, Mont-Saint-Aignan, France.
- **Martin Andersson** \* (martin.andersson@chalmers.se) / Department of Chemistry and Chemical Engineering Chalmers University of Technology, Gothenburg 41296, Sweden.
- **Gustav Eriksson** \* (gustav.eriksson@chalmers.se) / Department of Chemistry and Chemical Engineering Chalmers University of Technology, Gothenburg 41296, Sweden.

\* Auteur correspondant

Unravelling the 3D structure and composition of biological macromolecules at nanoscale sheds light on their functions and interactions with other molecules. In such a context, Atom Probe Tomography (APT) is lately arousing interest because it provides three-dimensional compositional mapping with sub-nanometre resolution, adding high chemical sensitivity throughout the whole periodic table of elements [1].

The development of the laser-assisted APT (La-APT) has extended the APT analysis from metallic materials to dielectric materials by combining the actions of a high DC field and an ultrashort laser pulse [2]. Recently, it has been shown that bio-molecules can be embedded in dielectric materials such as silica and analysed by La-APT [3].

In this work, we focus on the APT analysis of amorphous silica matrix samples, synthesized via a sol-gel process, a promising candidate for the development of an effective bio-particles embedding method, providing an aqueous-like environment for biomolecules, as demonstrated in previous works [3].

The specimen was analysed using two different APT setups, both operating under ultravacuum cryogenic conditions, but differing for laser illumination configurations: a La-APT shining UV radiation at  $\lambda=343$  nm and a Terahertz-assisted APT, where the UV laser is replaced by a high field THz mono-cycle

( $\lambda=1-0.1\text{mm}$ ,  $200\text{kV/cm}$  amplitude,  $500\text{fs}$  duration). Our objective is to find the optimal parameters (laser power, THz amplitude, DC field) to improve the accuracy of compositional analyses, thus to increase the signal to noise ratio and the mass resolution power of the mass spectra reported in Fig. 1 and Fig.2, for the La-APT and the THz-APT, respectively.

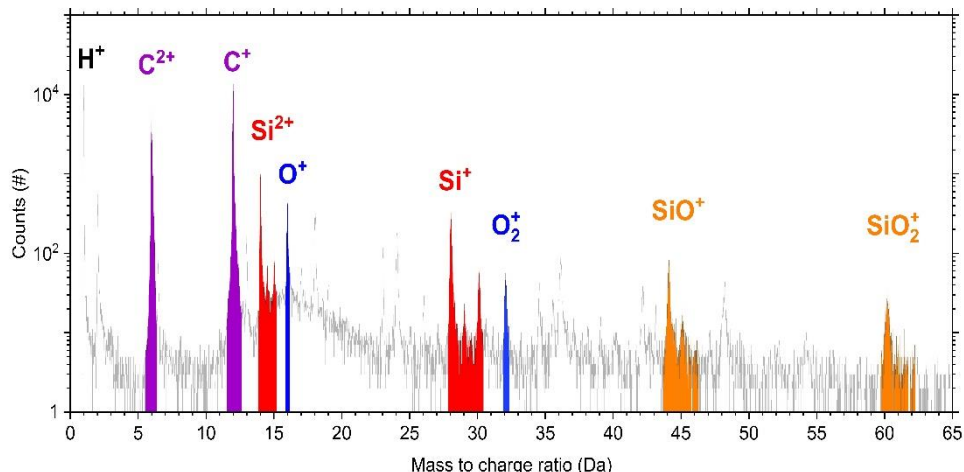
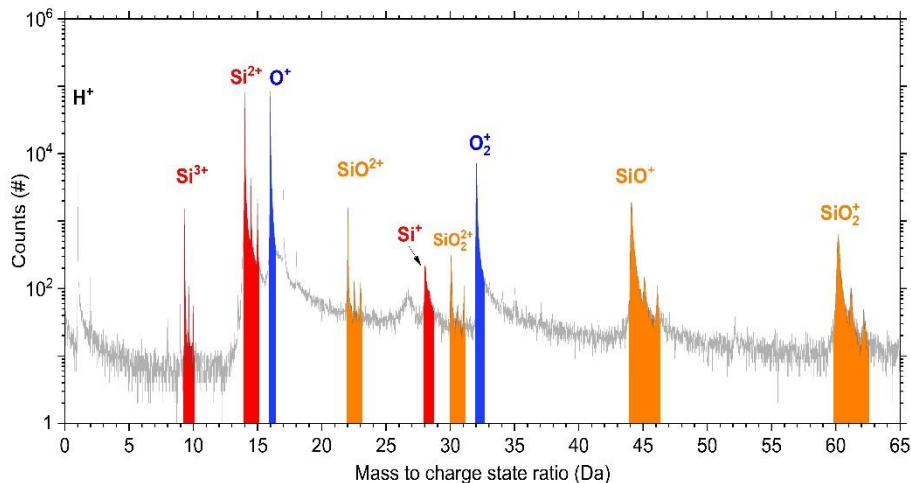
#### References:

- [1] B. Gault, et al., Nat Rev Methods Primers 1, 51 (2021).
- [2] A. Vella, Ultramicroscopy, Volume 132, Pages 5-18, ISSN 0304-3991 (2013). [3] G. Sundell, et al., Small 15, 1900316, (2019).

Figure 1: collection of  $1.8 \times 10^6$  ions in a LAWATAP, temperature  $T = 80\text{K}$ , UV laser energy  $E_{bias} = 32\text{nJ}$ , applied bias VDC range  $5-8\text{ kV}$ , detection rate  $\phi = 7.0 \times 10^{-4}$  ions/pulse.

Figure 2: collection of  $3.7 \times 10^5$  ions in a THz-assisted APT, temperature  $T = 50\text{K}$ , VDC range  $5-10\text{ kV}$ , detection rate  $\phi = 1.2 \times 10^{-1}$  ions/pulse.

**Mots clefs :** atom probe tomography, terahertz, silica, bio-molecules embedding



## SC2-P3

### Structure en cryo-microscopie électronique du canal potassique Kir2.1 humain lié à l'activateur PIP2 révèle son mécanisme d'ouverture

Cryo-electron microscopy structure of human Kir2.1 potassium channel bound to the activator PIP2 reveals its gating mechanism

- **Carlos FERNANDES** \* (carlos.henrique\_fernandes@sorbonne-universite.fr) / Institut de Minéralogie, Physique des Matériaux et de Cosmochimie, IMPMC, Sorbonne Université, CNRS, UMR7590, Paris, France
- **Dania ZUNIGA** / Institut de Minéralogie, Physique des Matériaux et de Cosmochimie, IMPMC, Sorbonne Université, CNRS, UMR7590, Paris, France
- **Andreas ZOUMPOULAKIS** / Institut de Minéralogie, Physique des Matériaux et de Cosmochimie, IMPMC, Sorbonne Université, CNRS, UMR7590, Paris, France
- **Rafael VELOSO** / Institut de Minéralogie, Physique des Matériaux et de Cosmochimie, IMPMC, Sorbonne Université, CNRS, UMR7590, Paris, France
- **Renaud WAGNER** / IMPReSs Facility, Biotechnology and Cell Signaling, CNRS, UMR7242, University of Strasbourg, Illkirch, France.
- **Catherine VENIEN-BRYAN** \* (catherine.venien-bryan@sorbonne-universite.fr) / Institut de Minéralogie, Physique des Matériaux et de Cosmochimie, IMPMC, Sorbonne Université, CNRS, UMR7590, Paris, France

\* Auteur correspondant

Kir2.1 channels are strongly inward-rectifying potassium channels that play a key role in maintaining resting membrane potential. Genetically inherited defects in Kir2.1 channels are responsible for several rare human diseases, including Andersen's syndrome [1]. Their gating (opening and closing mechanism) is modulated by phosphatidylinositol 4,5-bisphosphate (PIP2). Moreover, the Kir2.1 sensitivity to PIP2 is enhanced by the binding of a bulk of anionic lipids to a secondary anionic binding site [2]. However, the gating mechanism is not completely understood because so far there are only a Kir2.1 structure available in the closed state [3]. Here we present the preliminary cryo-EM structure of the human Kir2.1 channel complexed to PIP2 in the open state (Fig. 1). A total of 9944 micrographs were collected on a Titan Krios G4 microscope operated at 300 kV equipped with Falcon 4 direct detector and Selectris X image filter. After a visual inspection to remove poor-quality micrographs, 6961 micrographs were selected for further cryo-EM data processing. The movies were motion-corrected and dose-weighted using MotionCor2 and contrast function parameters were estimated using CTFFIND4. A total of 781,076 particles were automated picked using SPHIRE-crYOLO. The extracted particles were subject to one round of 2D and 3D classifications using RELION. A map containing 187,153 particles were subjected to 3D Auto-Refine, CTF-refinement and particle polishing. The polished particles were submitted to a 3D non-uniform refinement using cryoSPARC and provided the final cryo-EM map of the Kir2.1/PIP2 complex at 3.4 Å resolution. Preliminary atomic structure of Kir2.1/PIP2 complex was build from the cryo-EM map and revealed the PIP2 binding site. Comparative structural analysis of the Kir2.1/PIP2 complex (open state) with apo-Kir2.1 (closed state) reveals the structural changes that lead to channel opening. Moreover, the structure of the Kir2.1/PIP2 complex highlights the role of secondary anionic binding site for channel opening. These data reveal the gating mechanism of Kir2.1 channels and can help to understand the pathological mechanisms associated with these channels.

**Mots clefs :** cryo-EM, protein structure, single particle analysis, potassium channel, ion channel

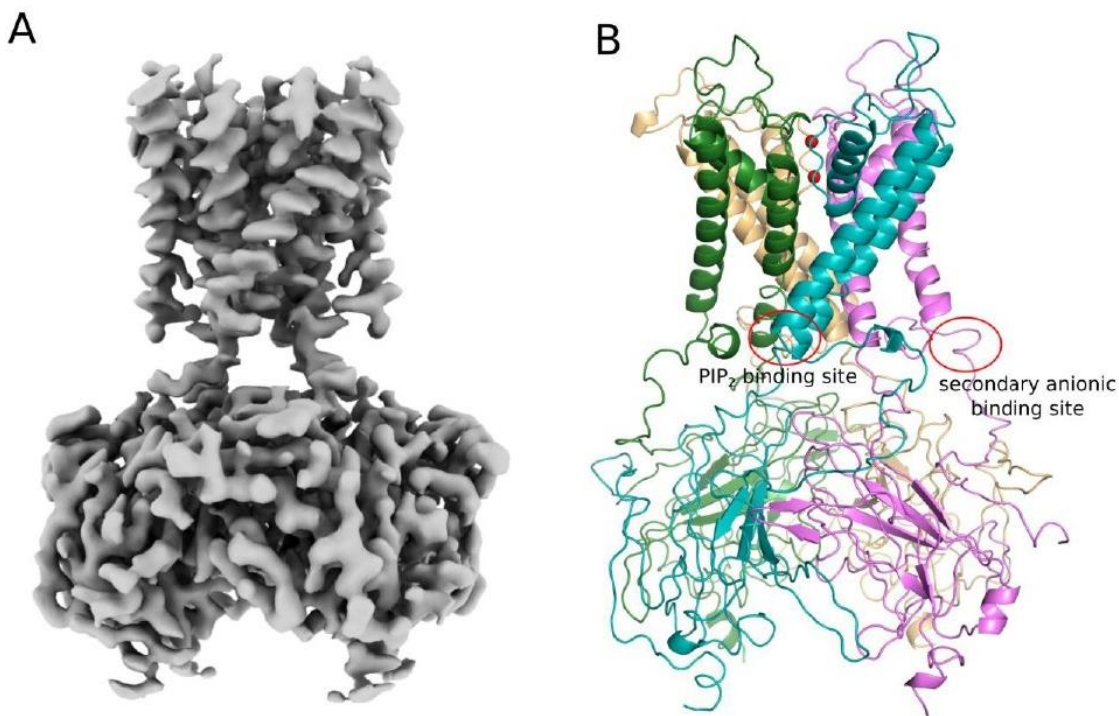


**Figure 1:** Final cryo-EM map and preliminary atomic structure of human Kir2.1 channel in the presence of lipid activator PIP<sub>2</sub>. (A) Sharpened cryo-EM map of human Kir2.1/PIP<sub>2</sub> complex obtained at 3.4 Å resolution. (B) Side view of the preliminary atomic structure of human Kir2.1/PIP<sub>2</sub> complex. The PIP<sub>2</sub> and secondary anionic binding sites are highlighted within red circles. Potassium ions are represented as red spheres.

## SC2-P4

### Auto-assemblage modulaire et adaptatif de dendrimères amphiphiles étudié par microscopie électronique en mode standard, cryo et liquide in situ

**Modular and adaptive self-assembly of amphiphilic dendrimers investigated by standard, cryo and in situ liquid TEM**

- **Tom ROUSSEL** \* (tom.roussel@univ-amu.fr) / Centre Interdisciplinaire de Nanoscience de Marseille (CINaM)
- **Ling Peng** / Centre Interdisciplinaire de Nanoscience de Marseille (CINaM)
- **Suzanne Giorgio** / Centre Interdisciplinaire de Nanoscience de Marseille (CINaM)

\* Auteur correspondant

Inspired from nature, amphiphilic molecules capable of self-assembly offer a unique way to construct powerful materials for biomedical application. Self-assembly of amphiphilic dendrimers has attracted great attention due to their well-defined structure and multivalence functionalities. However, the controllable design of supramolecular architecture still remains a challenging objective. The key to achieving this goal is the proper design of corresponding amphiphilic building blocks, because the supramolecular assembly is encoded in the molecular structure. Here we proposed controllable self-assembling amphiphilic dendrimers whose size and self-assembly depends on surface modification. The dendrimer bearing amine terminals self-assemble in particle with a size around 100 nm, while that with tertiary amine terminals in small nanomicelle of 15 nm. The initial TEM and DLS results lead us to think that the amine-terminated dendrimer self-assemble in vesicle with one bilayer (Figure 1) [1],[2]. However, detailed studies using cryo and in situ liquid TEM suggest that the amine-terminated dendrimer assemble in aggregate of micelles rather than vesicles. Cryo-TEM images show aggregation of several micelles and no bilayer was observed, consistent with in situ liquid TEM displaying particle of 100 nm with dense inner core (Figure 2A). Concerning the tertiary-amine terminated dendrimer, all three TEM techniques gave the similar results for the formation of nanomicelles with a size of 15 nm (Figure 2B). The methyl groups in the tertiary-amine terminated dendrimer bring repulsion and repel the aggregation of multiple micelles together, which explains this difference of assembly. This study highlights that combination of several electron microscopies provide information about the real size and morphology of the particles in solution, which is crucial for biomedical application.

#### References :

- [1] Liu X, et al. Adaptive amphiphilic dendrimer-based nanoassemblies as robust and versatile siRNA deliverysystems. *Angew. Chem.* 53, (2014), 11822 –11827
- [2] Y. Xiong et al. Small Activating RNA Modulation of the G Protein-Coupled Receptor for Cancer Treatment. *Adv. Sci.* 26, (2022), 2200562

**Mots clefs** : Amphiphilic dendrimers / Self-assembly / Cryo and in situ liquid TEM

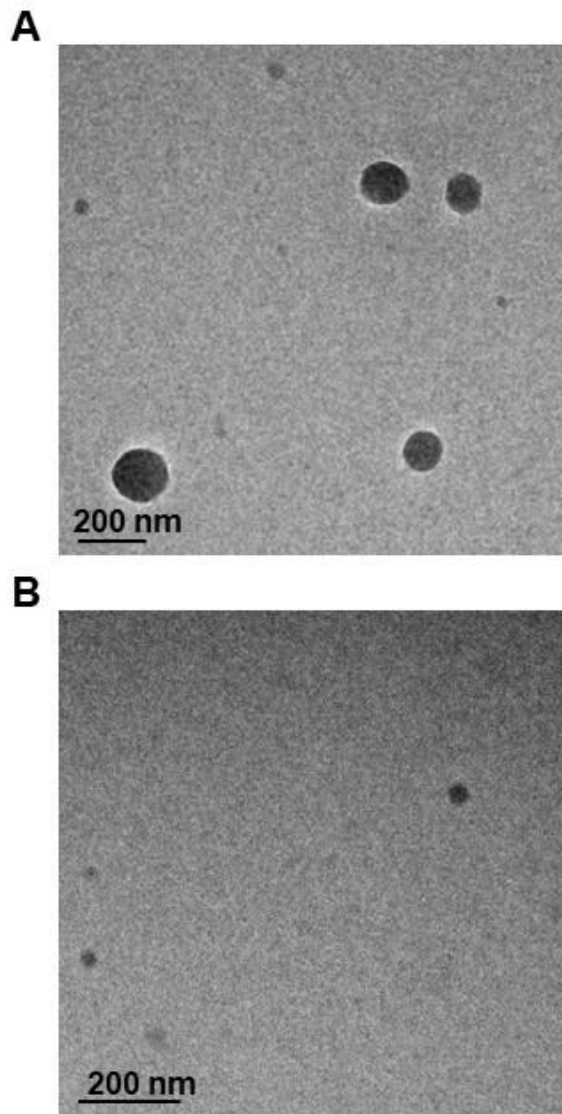


*Figure 1:* *in situ* TEM imaged in a protochips liquid sample holder of amine terminated dendrimer (upper row) A and tertiary amine terminated dendrimer (lower row) B in water, with a thickness between the  $\text{Si}_3\text{N}_4$  chips of 150 nm

## SC2-P5

### Analyse par STEM-EELS monochromaté de la structure et composition de la calcite biogénique

Monochromated STEM-EELS analysis of the structure and composition of biogenic calcite reveals the biomineral growth pattern

- **Marta de Frutos \*** (marta.de-frutos@universite-paris-saclay.fr) / CNRS Université Paris-Saclay
- **Alejandro B. Rodríguez-Navarro** / Departamento de Mineralogía y Petrología, Universidad de Granada, Spain .**Xiaoyan Li** / CNRS Université Paris-Saclay
- **Antonio Checa** / Departamento de Estratigrafía y Paleontología, Universidad de Granada and Instituto Andaluz de Ciencias de la Tierra, Spain

\* Auteur correspondant

The vast majority of calcium carbonate biocrystals differ from inorganic crystals in that they display a patent nanoroughness consisting of lumps of crystalline material (calcite/aragonite) surrounded by amorphous pellicles. Understanding of this organization and its formation mechanisms implies to unveil the chemical composition and structure at the nanoscale. Of particular relevance is the characterization of the organo-mineral interface to understand how the organic fraction regulates the calcification and direct the crystal growth. Compared to other spectroscopic approaches, STEM-EELS (scanning transmission electron microscopy coupled with Electron Energy Loss Spectroscopy) offers the advantage of an outstanding spatial resolution (at the nanometer scale) in both chemical analysis and imaging. Moreover the use of a latest-generation STEM microscope equipped with an electron monochromator and a direct-detection camera offers the possibility to detect very weak signals with a spectral resolution down to 7 meV, close to those obtained from X-ray based approaches. This high spectral resolution gives access to the crystallinity of calcium carbonate phases through the measure of the crystal field splitting (CFS) on Calcium L23-edge.

In the present study, STEM-EELS was used to map chemically and structurally the calcite secreted by a barnacle. The material is composed of irregular lumps of calcite (up to two hundred nm in diameter) surrounded by relatively continuous cortices (up to 20 nm thick) of amorphous calcium carbonate (ACC) and/or nanocalcite plus biomolecules, with a surplus of calcium relative to carbonate. Based on EELS results, we develop a model by which the separation of the crystalline and amorphous phases takes place upon crystallization of the calcite from a precursor ACC. The organic biomolecules are expelled from the crystal lattice and concentrate in the form of pellicles, where they stabilize minor amounts of ACC/nanocalcite. In this way, we change the previously established conception of biomineral structure and growth.

#### References:

- [1] Colliex, C. Eur. Phys. J. Appl. Phys. 97 (2022) p1-47.
- [2] de Frutos M., Rodríguez-Navarro A. B., Li X., and Checa A. G., ACS Nano 17 (2023) p 2829-2839

**Mots clefs :** STEM, EELS, biomineralisation, calcite

**SC3-P1****Un point sur les approches 3D ED en 2023****3D ED approaches in 2023**

.Philippe Boullay \* (philippe.boullay@ensicaen.fr) / Normandie Université, ENSICAEN, UNICAEN, CNRS, CRISMAT,Caen France

\* Auteur correspondant

La cristallographie structurale a connu une révolution au cours des dix dernières années, grâce à l'introduction de protocoles d'acquisition (ADT, PEDT, cRED, microED ...) et d'analyse des données de diffraction d'électrons en faisceau parallèle (Figure 1). Ces approches, réunies sous la dénomination générique 3D ED [1], visent toutes à reconstruire le réseau réciproque (en 3D) d'un composé cristallin en collectant, à différents angles d'inclinaison du porte objet, des diagrammes de diffraction électronique (ED) sur des monocristaux de taille beaucoup plus petite que ceux utilisables en diffraction des rayons X.

Cette présentation vise à expliciter les 2 approches actuellement les plus utilisées au CRISMAT et leurs applications. Nous commencerons, chronologiquement, par la Precession-assisted Electron Diffraction Tomography (PEDT) [2] qui permet de résoudre des structures complexes et d'obtenir des affinements fiables et précis pour des composés « stables » typiquement en sciences des matériaux. Nous parlerons ensuite de la continuous Rotation Electron Diffraction (cRED) [3] qui permet d'acquérir des données 3D ED avec des temps de collecte inférieurs à la minute pour des composés « fragiles » typiquement certains matériaux poreux, en pharmacologie et en science de la vie. Nous aborderons enfin les développements récents visant à rendre cet outil encore plus performant, notamment pour l'analyse de domaines cristallins de taille nanométrique dans les matériaux fonctionnels.

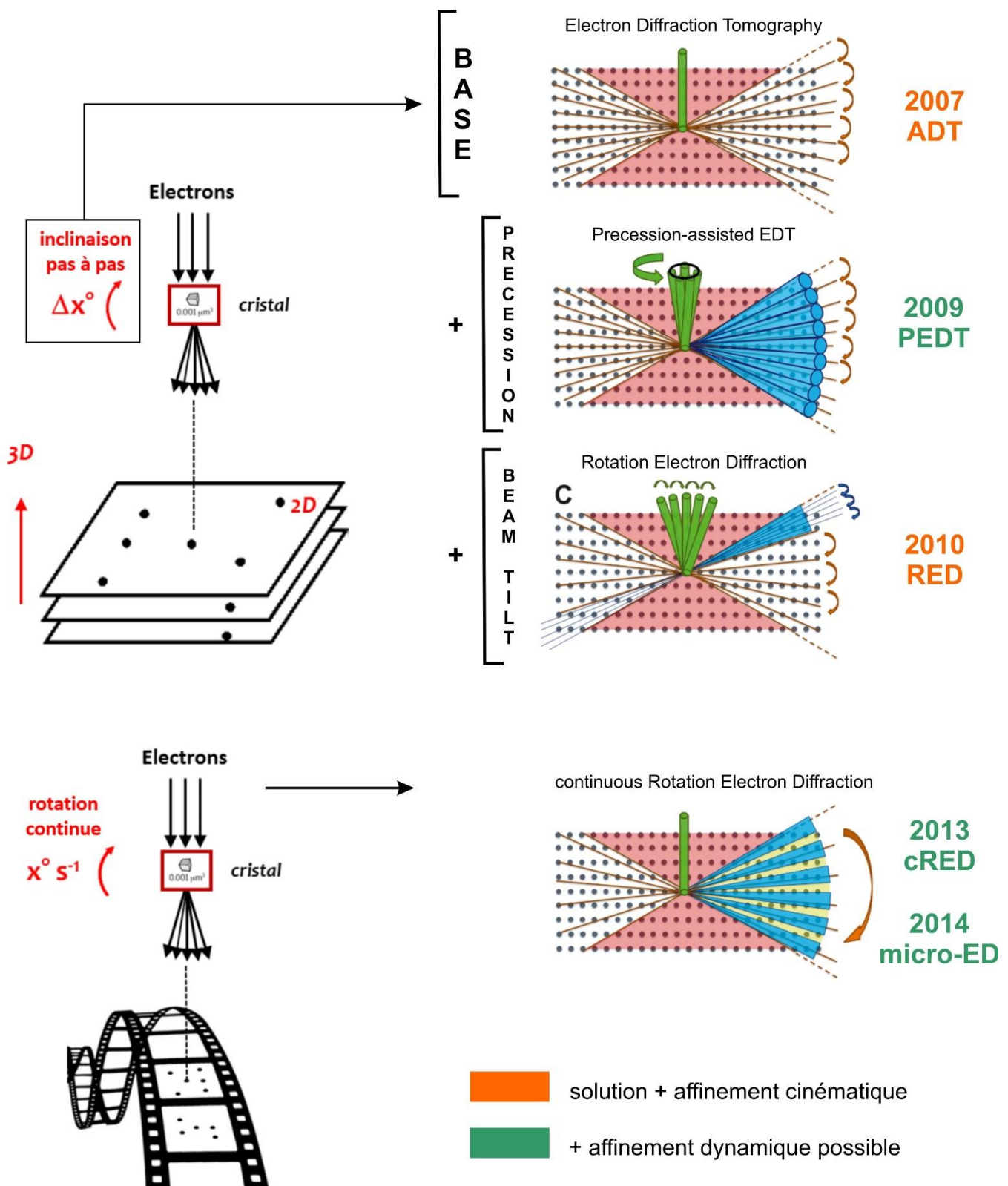
Une partie des résultats présentés ont été obtenus dans le cadre du projet européen NanED (Electron Nanocrystallography – H2020-MSCA-ITN GA956099). L'expertise du CRISMAT dans le domaine de la 3D ED est accessible par l'intermédiaire du réseau national CNRS-CEA METSA.

**Références:**

- [1]M. Gemmi et al., ACS Central Science, 5 (2019) 1315-1329.
- [2]E. Mugnaioli et al., Ultramicroscopy 109 (2009) 758–765.
- [3]I. Nederlof et al., Acta Crystallogr. D 69 (2013) 1223–1230.

Figure 1: Résumé graphique des principales approches 3D ED. Acquisition en pas à pas sans et avec précession par le groupe de U. Kolb (DE) puis avec tilt faisceau par le groupe de X. Zou (SE). Acquisition en rotation continue par le groupe de J.P. Abrahams (CH), repris par le groupe de T. Gonen (US). Voir revue [1] pour toutes les références sur le sujet.

**Mots clefs :** diffraction en faisceau parallèle; cristallographie



## SC3-P2

### Résolution structurale d'un matériau de batterie organique par diffraction électronique en mode tomographie

#### Structural resolution of an organic battery material using electron diffraction tomography

- **Nicolas Gautier** \* (Nicolas.Gautier@cnrs-imn.fr) / Nantes Université, CNRS, Institut des Matériaux de Nantes Jean Rouxel, IMN, Nantes F-44000, France
- **Éric Quarez** / Nantes Université, CNRS, Institut des Matériaux de Nantes Jean Rouxel, IMN, Nantes F-44000, France
- **Nicolas Dupré** / Nantes Université, CNRS, Institut des Matériaux de Nantes Jean Rouxel, IMN, Nantes F-44000, France
- **Alia Jouhara** / Nantes Université, CNRS, Institut des Matériaux de Nantes Jean Rouxel, IMN, Nantes F-44000, France
- **Philippe Poizot** / Nantes Université, CNRS, Institut des Matériaux de Nantes Jean Rouxel, IMN, Nantes F-44000, France

\* Auteur correspondant

La demande croissante en dispositifs de stockage électrochimique de l'énergie nécessite des batteries plus performantes mais aussi moins impactantes en termes d'empreinte environnementale. Le recours à des matériaux d'électrode organiques offre ainsi de nouvelles opportunités. Récemment, notre groupe a synthétisé un matériau d'insertion organique lithié prometteur, le (2,5-dilithium-oxy)-téraphthalate de magnésium ( $Mg(Li_2)$ -p-DHT). Ce matériau est capable de fonctionner électrochimiquement par désinsertion/insertion de  $Li^+$  à un potentiel équivalent à celui du composé inorganique LiFePO<sub>4</sub> [1]. Afin de mieux comprendre les propriétés de ce composé et d'améliorer encore ses performances, le point clé fut la détermination de sa structure. La diffraction des rayons X sur monocristal, en raison de cristallites de trop petites tailles (<1µm), n'était pas adaptée. Nous avons donc fait le choix de la diffraction électronique en mode tomographie (ED3D) dont le développement s'est fortement accéléré depuis une dizaine d'années [2].

Malheureusement les techniques classiques de ED 3D sont difficilement applicables à ce type de composés organiques, très sensibles au faisceau d'électrons. Des conditions d'acquisition spécifiques doivent être mises en œuvre pour limiter le courant du faisceau d'électrons (« low dose ») et augmenter la vitesse d'acquisition pour limiter le temps d'exposition. C'est ce que permet le script "Continuous Rotation movie acquisition" (CRmov) intégré au programme libre SerialEM [3].

Nous avons ainsi pu acquérir une série importante de clichés de diffraction par sélection d'aire (SAED). La plage d'acquisition était de 120° (+60° / -60°) et le temps d'acquisition total d'environ 300 s. Nous avons réussi à extraire une maille ainsi que les intensités des taches de diffraction qui ont pu être intégrées. À l'aide d'un logiciel de résolution structurale, la structure cristalline de ce composé très prometteur a pu être résolue.

#### Références :

- [1] Jouhara et al., Nat Commun 9, 4401 (2018)
- [2] Gemmi et al., ACS Central Science, 5 (8), (2019) p.1315– 1329
- [3] De la Cruz et al., Ultramicroscopy, 201 (2019), 77-80

**Mots clefs :** Résolution structurale Matériau organique Diffraction électronique Tomographie TEM

## SC3-P3

### La synergie entre les sciences de la vie et les sciences des matériaux dans la diffraction électronique réveille les cadres magnétiques métal-organique

**Synergy between life science and materials science in electron diffraction wakes up magnetic metal-organic frameworks**

- **Emre Yörük** \* (yoruk@fzu.cz) / Université Grenoble Alpes and CNRS, Institut Néel, Grenoble, France
- **Dominique Housset** / Université Grenoble Alpes, CEA, CNRS, IBS, Grenoble, France
- **Stéphanie Kodjikian** / Université Grenoble Alpes and CNRS, Institut Néel, Grenoble, France
- **Holger Klein** / Université Grenoble Alpes and CNRS, Institut Néel, Grenoble, France
- **Wai-Li Ling** / Université Grenoble Alpes, CEA, CNRS, IBS, Grenoble, France
- **Constance Lecourt** / Université Claude Bernard Lyon 1, LMI (UMR 5615), 69622, Villeurbanne, France
- **Yuuta Izumi** / Department of Chemistry, Hiroshima University, Hiroshima, 739-8526, Japan
- **Katsuya Inoue** / Department of Chemistry, Hiroshima University, Hiroshima, 739-8526, Japan
- **Kseniya Maryunina** / Department of Chemistry, Hiroshima University, Hiroshima, 739-8526, Japan, International  
Tomography Center SB RAS, 3A Institutskaya Street, Novosibirsk 630090, Russia
- **Evgeny Tretyakov** / N. D. Zelinsky Institute of Organic Chemistry, Moscow 119991, Russia
- **Cédric Desroches** / Université Claude Bernard Lyon 1, LMI (UMR 5615), 69622, Villeurbanne, France
- **Dominique Luneau** / Université Claude Bernard Lyon 1, LMI (UMR 5615), 69622, Villeurbanne, France

\* Auteur correspondant

Development of magnetic metal-organic frameworks (MOFs) as smart materials requires their structural characterization [1]. However, large enough single crystal MOFs suitable for X-ray diffraction are notoriously difficult to grow hampering structure determination and discouraging research in the field.

To address this obstacle we show here that the structure of two novel magnetic MOFs (Figure 1) could be successfully determined from nanocrystals by combining recent developments in TEM [2,3] with electron crystallography data processing methods designed for protein crystals [4]. Diffraction data were collected using a low-dose technique on a Tecnai F20 TEM operated at 200 kV. Samples were continuously rotated while recording diffraction patterns with a Medipix3RX hybrid pixel detector (Figure 2). Crystal structure solution was achieved by molecular replacement [5].

These results open new prospects for development of molecule-based magnets and contribute to push forwards the structural studies of MOFs.

**Mots clefs :** metal organic frameworks, electron diffraction, crystallography, TEM

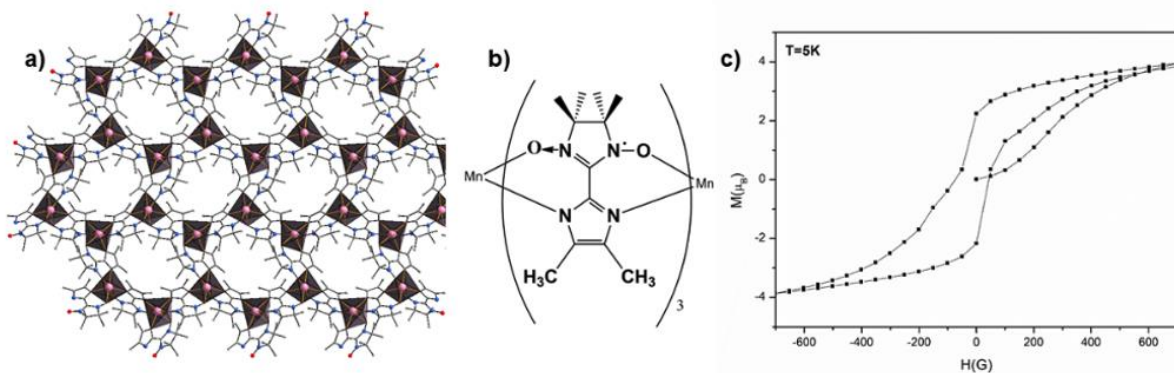


**Figure 1:** Magnetic metal-organic framework. (a) Structure of the 2D metal-organic framework resolved by electron crystallography and molecular replacement. (b)  $Mn^{2+}$  ion coordinated by bridging nitronyl nitroxide radical. (c) Hysteresis loop at 5 K showing the magnetic behavior of the sample.

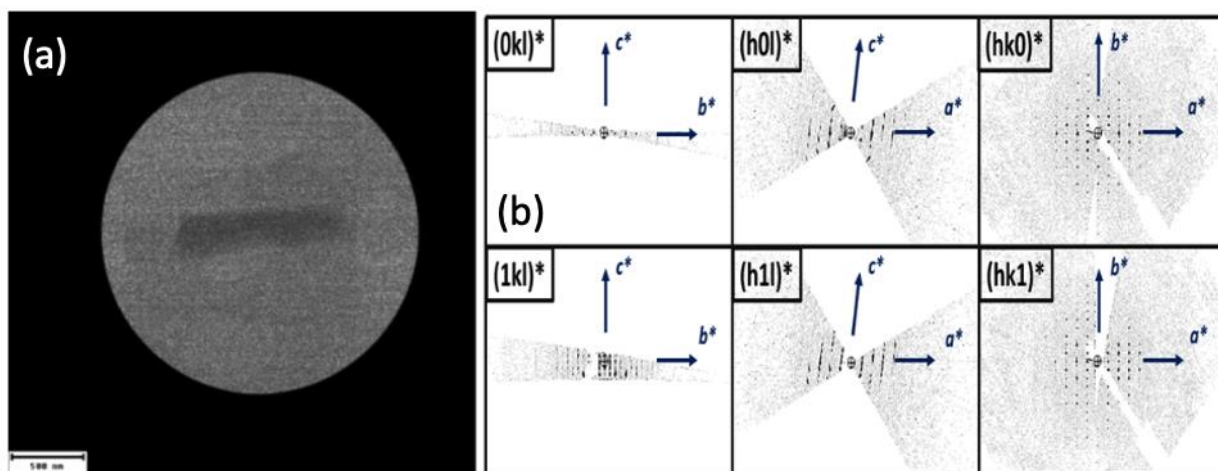


**Figure 2:** (a) TEM image of a representative particle. The lateral dimensions are estimated to be  $3\mu m \times 200 nm$ . The low contrast indicates a very low thickness, in the order of tens of nm. (b)  $hkl$  sections obtained after data processing

## SC4-P1

### La sonde atomique "photonique" pour l'étude de la physique de l'émission ionique par effet de champ

#### Field Emission Physics within a Photonic Atom Probe

- **Lorenzo Rigutti** \* ([lorenzo.rigutti@univ-rouen.fr](mailto:lorenzo.rigutti@univ-rouen.fr)), **Eric Weikum, Enrico Di Russo, Georges Beainy, Jonathan Houard, Pradip Dalapati** / Groupe de Physique des Matériaux, Université de Rouen Normandie
- **Jean-Michel Chauveau** / GEMAC, Université St Quentin Versailles / Paris Saclay
- **Maxime Hugues** / Centre de Recherches sur l'HétéroEpitaxie et ses Applications, CNRS, Université Côte d'Azur
- **Angela Vella** / Groupe de Physique des Matériaux, Université de Rouen Normandie
- **François Vurpillot** / Groupe de Physique des Matériaux, Université de Rouen Normandie

\* Auteur correspondant

The Photonic Atom Probe (PAP) allows for simultaneous collection of photoluminescence (PL) spectra from a field emission tip specimen and for its analysis in standard laser-assisted atom probe tomography (APT) [1],[2]. The particular conditions in which the optical signatures of localized light emitters are collected open intriguing possibilities for the study of field ion emission under high field and under laser illumination [3]. The PL spectral shift allows measuring the stress induced by the application of a strong electric field at the tip apex and its spatial propagation. This has been evidenced through the study of the quantum well (QW) emission in a ZnO/(Mg,Zn)O system [4], allowing measuring stress levels ~1 GPa. Time-resolved measurements evidence the role of non-radiative recombination as the tip surface progressively approach a localized emitter. The evolution of the tip shape and the accumulation of free carriers at the tip surface may have an effect on the absorption pattern of the laser light within the tip and on the far-field pattern of the emitted PL [5].

Stress-induced PL shift in a ZnO/(Mg,Zn)O QW within a photonic atom probe. (a) Reconstructed position of the Mg atoms. The emitting quantum well (QW) is the one at roughly 50 nm from the ZnO substrate/(Mg,Zn)O interface (set at 0). (b) Complete set of PL spectra acquired during the APT acquisition. (c) Calculation of the distribution of the stress-induced bandgap shift within the tip at two different evaporation stages. (d) Comparison between the experimental and calculated trends of the QW PL energy as a function of the applied voltage before evaporation and as a function of the apex position during the evaporation.

[1]J. Houard et al., Review of Scientific Instruments, vol. 91, no. 8, p. 083704, Aug. 2020, doi: 10.1063/5.0012359.

[2]E. Di Russo et al., Nano Lett., vol. 20, no. 12, pp. 8733–8738, Dec. 2020, doi: 10.1021/acs.nanolett.0c03584.

[3]E. Di Russo and L. Rigutti, MRS Bulletin, vol. 47, no. 7, pp. 727–735, Jul. 2022, doi: 10.1557/s43577-022-00367-6.

[4]P. Dalapati et al., Phys. Rev. Applied, vol. 15, no. 2, p. 024014, Feb. 2021, doi: 10.1103/PhysRevApplied.15.024014.

[5]E. Weikum, Submitted.

**Mots clefs** : sonde atomique, spectroscopie optique, émission par effet de champ, photoluminescence

## SC4-P2

### Microscopie corrélative avec une sonde atomique "photonique"

#### Correlative Microscopy within a Photonic Atom Probe

- **Lorenzo Rigutti** \* (lorenzo.rigutti@univ-rouen.fr) / Groupe de Physique des Matériaux, Université de Rouen Normandie
- **Jonathan Houard** / Groupe de Physique des Matériaux, Université de Rouen Normandie
- **Enrico Di Russo** / Groupe de Physique des Matériaux, Université de Rouen Normandie
- **Georges Beainy** / Groupe de Physique des Matériaux, Université de Rouen Normandie
- **Pradip Dalapati** / Groupe de Physique des Matériaux, Université de Rouen Normandie
- **Jean-Michel Chauveau** / GEMAC, Université St Quentin Versailles / Paris Saclay
- **Maxime Hugues** / Centre de Recherches sur l'HétéroEpitaxie et ses Applications, CNRS, Université Côte d'Azur
- **Ioanna Dimkou** / CEA-IRIG Université Grenoble Alpes
- **Eva Monroy** / CEA-IRIG Université Grenoble Alpes

\* Auteur correspondant

The laser pulses controlling the ion evaporation in Laser-assisted Atom Probe Tomography (La-APT) can simultaneously excite photoluminescence (PL) in semiconductor or insulating specimens. An atom probe equipped with appropriate focalization and collection optics can thus be coupled with an in-situ micro-PL bench [1] that can be operated even during APT analysis. Such a Photonic Atom Probe (PAP) has been applied to the study of the optical properties of nanoscale emitters in an in-situ correlative microscopy approach. The PAP discloses new possibilities for the correlative microscopy of nanoscale light emitters, as the evolution of the PL spectra can be directly correlated with the chemical 3D distribution obtained by APT. As a result, PAP can distinguish the optical signatures of separate QWs distant as few as 20 nm – well below the diffraction limit of the laser [2]. It can furthermore be applied to the study of quantum dots, in order to assess the relationship between their 3D morphology and their optical signature[3], and to the study of the interplay between the presence of structural or point defects and the possibility of radiative recombination of carriers [4].

[Figure] In-situ analysis of a field emission tip containing a set of ZnO quantum wells embedded in MgZnO barriers: (a) sequence of  $\mu$ PL spectra generated by the specimen during its evaporation (b) differential  $\mu$ PL spectra, highlighting the spectral variations during evaporation; the blue circles highlight the spectral signature of single quantum wells (c) 3D reconstruction of the positions of the Mg atoms – the red dotted lines indicate the position of the tip surface during the acquisition of the i-th spectrum.

[1]J. Houard et al., Review of Scientific Instruments, vol. 91, no. 8, p. 083704, Aug. 2020, doi: 10.1063/5.0012359.

[2]E. Di Russo et al., Nano Lett., vol. 20, no. 12, pp. 8733–8738, Dec. 2020, doi: 10.1021/acs.nanolett.0c03584.

[3]I. Dimkou et al., ACS Appl. Nano Mater., vol. 3, no. 10, pp. 10133–10143, Oct. 2020, doi: 10.1021/acsanm.0c02106.

[4]Ioanna Dimkou et al., Microscopy and Microanalysis, Volume 29, Issue 2, April 2023, Pages 451–458, <https://doi.org/10.1093/micmic/ozac051>

**Mots clefs :** semiconducteurs, instrumentation, sonde atomique, microscopie in situ

## SC4-P3

### MerlinEM, détecteur hybride de comptage d'électrons à pixels pour la microscopie électronique à transmission

**MerlinEM, Hybrid Pixel Electron Counting Detector for Transmission Electron Microscopy**

.Matus Krajinak \* (matus@quantumdetectors.com) / Quantum Detectors Ltd

\* Auteur correspondant

Electron microscopy experiments with hybrid pixelated counting detectors started with a Medipix2 detector [1]. The next generation of the detector, Medipix3 was commercialised as a MerlinEM detector by a collaboration between the University of Glasgow and Quantum Detectors Ltd. The MerlinEM can acquire micrographs with framerates more than two orders of magnitude faster than conventional CCD cameras. Moreover, this is possible without any dead time and readout noise which is very advantageous in transmission electron microscopy. This paper will demonstrate the capabilities of the MerlinEM detector in STEM, diffraction, and EELS.

The distribution of electrons for each point of scan in STEM contains a wealth of information that can be used to enhance established techniques like differential phase contrast (DPC) [2] but also to enable techniques like ptychography [3] or symmetry-STEM [4]. As an example of an enhancement for the DPC, Fig. 1(a) shows a comparison of conventional quadrant detector collected data and MerlinEM data. The diffraction contrast dominates the conventional method, whereas the post-processed 4D-STEM data reveals the quantitative magnetic information even in a complex multilayer sample [2].

The applications in diffraction and EELS utilise the exceptional dynamic range of the MerlinEM detector. As Fig. 1(b) demonstrates, it is possible to image the central diffraction peak with up to 24-bit dynamic range and still retain single electron sensitivity towards the edge of the diffraction pattern. Additionally in EELS, the absence of readout noise enables acquisitions of high core-loss information with the MerlinEELS detector. To demonstrate this, Fig. 1(c) shows an atomically sharp interface in LMO/STO sample by mapping Ti-K (5 keV) and a La-L3 (5.5 kV) EELS edges [5].

- [1]G. McMullan et al., Ultramicroscopy 107.4-5 (2007): 401-413.
- [2]K. Fallon et al., Physical Review B 100.21 (2019): 214431.
- [3]A. Strauch et al., Microscopy and Microanalysis 27.5 (2021): 1078-1092.
- [4]M. Krajinak and J. Etheridge, Proceedings of the National Academy of Sciences 117.45 (2020): 27805-27810 [5] M. Gibert et al., Nano letters 15.11 (2015): 7355-7361.

**Mots clefs :** 4DSTEM, EELS, Diffraction, Direct Detection, Electron Counting

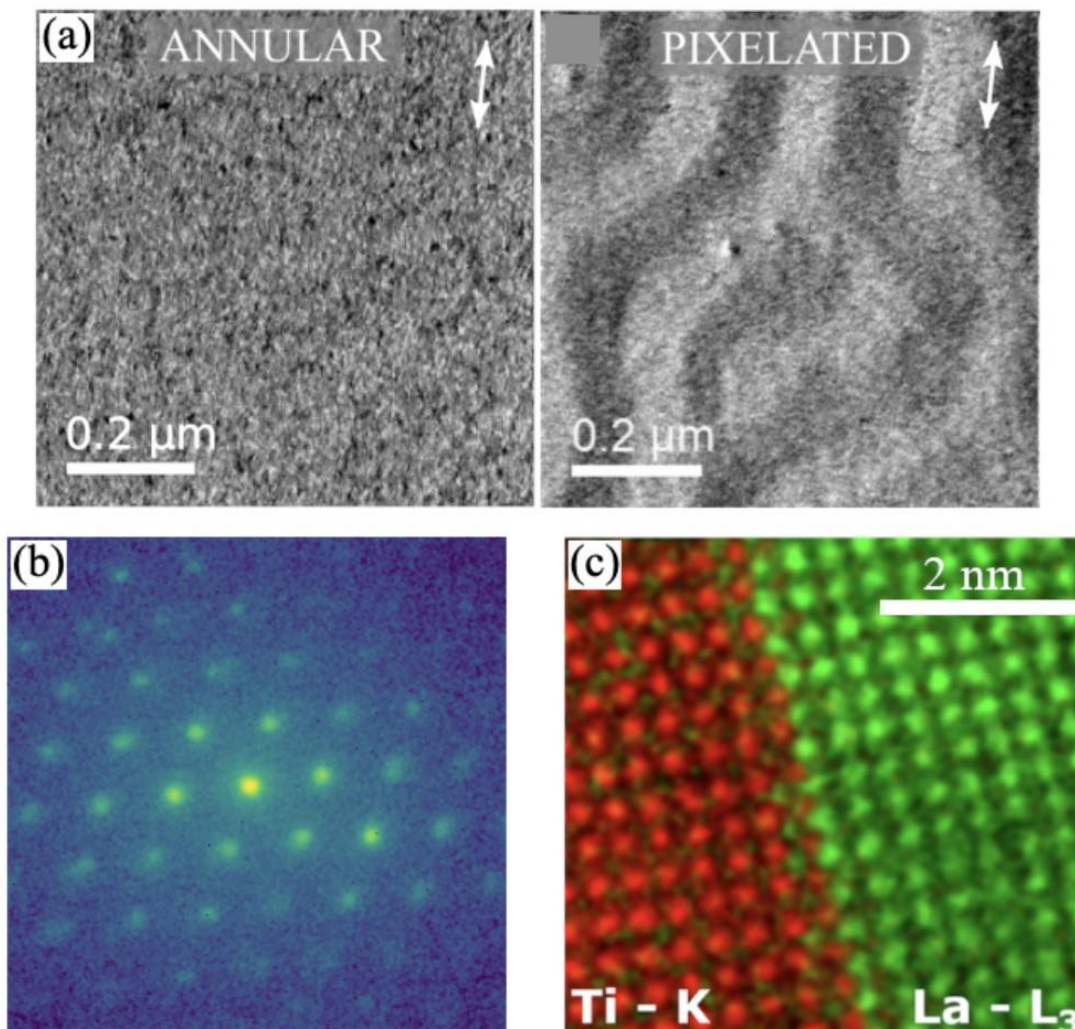


**Figure 1.** (a) annular quadrant and pixelated detector acquired DPC images of the same area. The maps of integrated magnetic induction in a complex multilayer polycrystalline sample demonstrate significant signal-to-noise enhancement using a pixelated detector (From [2] under CC 4.0 licence). (b) precession diffraction example acquired with MerlinEM detector, logarithmic scale demonstrating a high dynamic range of the detector [6]. (c) MerlinEELS example showing atomically sharp interface in LMO/STO interface for high kV core-loss EELS imaging. The author acknowledges Joaquim Portillo of NanoMegas SPRL for the precession diffraction dataset in Fig. 1(b), and Alexandre Gloter and Marcel Tencé of Université Paris-Saclay for the EELS dataset in Fig. 1(c).

## SC4-P4

### Une nouvelle méthode d'implantation in-situ et de caractérisation de l'hydrogène en Sonde Atomique Tomographique

#### A method for in-situ implantation and characterization of hydrogen in Atom Probe Tomography

- **Jean-Baptiste Maillet** \* (jean-baptiste.maillet@univ-rouen.fr) / Normandie Université, UNIROUEN, INSA Rouen, CNRS, Groupe de Physique des Matériaux, 76000 Rouen, France
- **Gerald Da Costa** / Normandie Université, UNIROUEN, INSA Rouen, CNRS, Groupe de Physique des Matériaux, 76000 Rouen, France
- **François Vurpillot** / Normandie Université, UNIROUEN, INSA Rouen, CNRS, Groupe de Physique des Matériaux, 76000 Rouen, France

\* Auteur correspondant

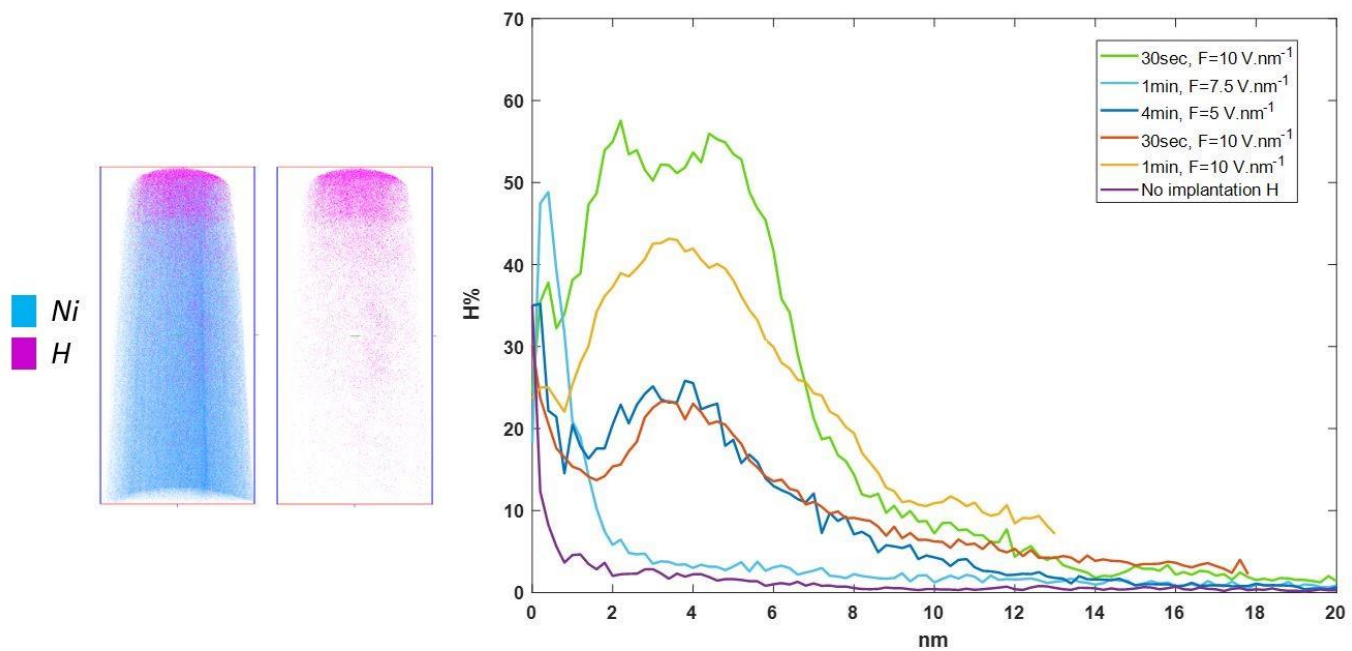
The study of hydrogen in Atom Probe Tomography is still a relevant challenge. Its low mass, high diffusion coefficient and presence as a residual gas in vacuum chambers generate multiple complications for APT investigation. Different solutions were proposed in literature like ex-situ charging and cryopreparation and cryotransfer [1] or using a separate chamber connected to the APT where hydrogen charging is performed at high temperature [2]. In this paper, we propose an alternative route for in-situ H-charging in materials. This method is derived from the work of O.V. Dudka, who proposed in 2013 [3] an in-situ low energies (140-150eV) helium ions implantation directly in a FIM chamber. The basic idea is to apply a negative voltage to the APT sample under a low pressure of H<sub>2</sub> (~10<sup>-5</sup> mbar). Under the electron bombardment, some ionized gas atoms (positive ions) are accelerated to the apex of the sample (negative polarization).

In this study we have developed a method that can implant hydrogen at a higher implantation energy (~200-900eV), and dose (~5000-100000at). The DC voltage application is replaced by controlled ns negative pulse on the emitter. Using electrodynamical simulations, it is shown that implantation energy can be increased to about 1 keV without destroying the specimen of interest. An APT chamber was modified to enable direct negative pulse application with controlled gas pressure, pulse repetition rate and pulse amplitude. A theoretical depth of implantation was predicted and compared to experiments. We found implantation depths between 2 and 12 nm for modest -1kV of pulse amplitude. It is shown that this implantation can reach a high concentration of hydrogen in nickel (up to 60%H in the sub surface), see Figure 1.

#### References :

- [1]Yi-Sheng Chen et al. Cryo Atom Probe: Freezing atoms in place for 3D mapping. Nano Today 37 (2021).
- [2]J. Takahashi et al. Origin of hydrogen trapping site in vanadium carbide precipitation strengthening steel. ActaMaterialia 153, p 193-204 (2018).
- [3]O. V. Dudka et al. Formation of Interstitial Atoms in Surface Layers of Helium Implanted Tungsten. TechnicalPhysics Letters, Vol. 39, p 960-963 (2013).

**Mots clefs :** Tomography, Hydrogen,



## SC4-P5

### Étude en ETEM *in situ* de la condensation / évaporation de l'eau et du comportement hygroscopique des aérosols à l'aide d'un porte-échantillons refroidi par un micro-élément Peltier

**In situ ETEM study of water condensation / evaporation and the hygroscopic behavior of aerosols using a Peltier micro-device cooled holder tip**

- **Thierry EPICIER** \* (thierry.epicier@ircelyon.univ-lyon1.fr) / Université Lyon, Université Claude Bernard Lyon 1, CNRS, IRCELYON, UMR 5526, 69626 Villeurbanne, France
- **Francisco José CADETE SANTOS AIRES** \* (francisco.aires@ircelyon.univ-lyon1.fr) / Université Lyon, Université Claude Bernard Lyon 1, CNRS, IRCELYON, UMR 5526, 69626 Villeurbanne, France
- **Eric EHRET** / Université Lyon, Université Claude Bernard Lyon 1, CNRS, IRCELYON, UMR 5526, 69626 Villeurbanne, France
- **Mimoun AOUINE** / Université Lyon, Université Claude Bernard Lyon 1, CNRS, IRCELYON, UMR 5526, 69626 Villeurbanne, France
- **Joseph VAS** / MajuLab, International Joint Research (UMI 3654, CNRS), F and NTU, Singapore, and Lab. for in-situ and operando Nanoscopy, NTU, Singapore.
- **Martial DUCHAMP** / MajuLab, International Joint Research (UMI 3654, CNRS), F and NTU, Singapore, and Lab. for in-situ and operando Nanoscopy, NTU, Singapore.

\* Auteur correspondant

The constant development of atmospheric closed cells since a few decades permits today a wide range of *in situ* studies of nanomaterials in liquids, or liquids themselves in a Transmission Electron Microscope (TEM). However, Liquid Cell TEM fails to properly study liquid-vapor reactions of utmost importance in many societal subjects especially concerning water interactions with nanosystems, such as in atmospheric chemistry (see e.g. [1]) or in pharmaceutical sciences [2]. Such domains can fortunately be tackled in a dedicated Environmental TEM (FEI Titan ETEM), where the absence of sealing membranes around the sample allows direct exchanges between the vapor (gas) introduced into the microscope and a solid. Several studies exist of the hygroscopic behaviour of model or atmospheric aerosols in such ETEMs, e.g.[3]. A cryo-holder is used to cool down the specimen (typically in the range 0 to 18 °C) in order to reach the vapor-liquid equilibrium in the pressure range eligible in an ETEM (below 20 mbar).

A new approach is reported, where the sample is cooled by means of a micro-Peltier stage mounted on the type of a commercial MEMS-based 'heating holder' from DENNsolutionsTM, see Fig. 1a). This montage [4] offers a bunch of advantages as compared to the above ETEM approach. One being its rapidity to reach a given relative humidity (linked to the temperature-pressure conditions), which allows to study accurately the first stages of deliquescence (dissolution) or efflorescence (recrystallisation) of soluble solids, such as NaCl nanocubes as illustrated in Fig. 1 b-d). Transient states just before the deliquescence (efflorescence) of the crystals will be described, such as shape oscillations attributed to local dissolution / reprecipitation events, see Fig. 2 [5].

#### References:

- [1] A.G. Tereshchenko. J. of Pharmaceutical Sciences, 104 (2015), 3639.
- [2] Y-L. Pan et al., J. of Aerosol Science, 155 (2021), 105767.
- [3] M.E. Wise et al., Aerosol Science and Technology, 42 (2008), 281.
- [4] J.V. Vas et al., Microsc. Microanal. 28, S1 (2022), 818.

[5] Thanks are due to CLYM ([www.clym.fr](http://www.clym.fr)) for the access to the microscope. This study is supported by the French National Research Agency (ANR) under the 'WATEM' project n° ANR-20-CE42-0008.

**Mots clefs** : micro-Peltier-based sample holder Environmental TEM, water condensation/evaporation, hygroscopic behavior of aerosols, NaCl,

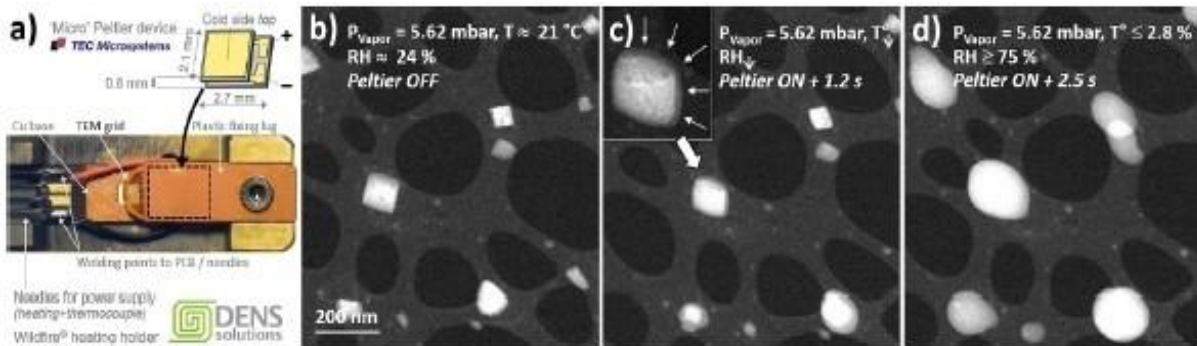


*Figure 1: A micro-Peltier stage cooled sample holder tip to study the hygroscopic behavior of aerosols in a Titan ETEM. a): montage of the tip (to be detailed during the conference). b)-d): illustration of a deliquescence sequence of NaCl nanocubes (STEM imaging, 300 kV). Note the appearance of a water layer (arrows) around crystals in c). The vapor pressure, temperature (not measured but estimated, Relative Humidity (RH, estimated but partly dictated by the behavior of the NaCl-water system – deliquescence of NaCl is known to occur at RH = 75 % –). The labels Peltier ON / OFF indicate whether the stage is powered or not; time is also reported in seconds.*

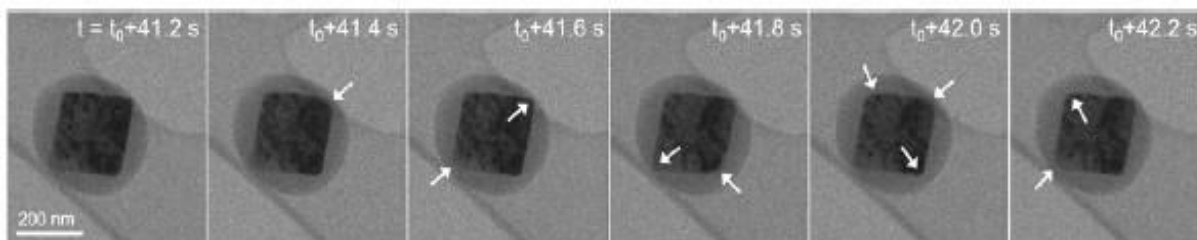


*Figure 2: oscillations of the shape of a NaCl nanocube during water condensation under constant thermodynamic conditions (1.4°C and 6.77 mbar of water vapor; ETEM bright field, 300 kV). A water layer surrounds the particle. Arrows indicate shape variations: rounding or 'reconstruction' of edges (arrows outside or inside the particle respectively).*

## SC4-P6

### Développement d'un détecteur sensible en position et en énergie pour la Sonde Atomique Tomographique

#### Towards a Position-Energy-Sensitive Detector for the Atom Probe Tomography

- **Christian Bacchi** \* (christian.bacchi1@univ-rouen.fr) / Univ Rouen Normandie, INSA Rouen Normandie, CNRS, Groupe de Physique des Matériaux UMR 6634, F-76000 Rouen, France
- **Gérald Da Costa** / Univ Rouen Normandie, INSA Rouen Normandie, CNRS, Groupe de Physique des Matériaux UMR 6634, F-76000 Rouen, France
- **François Vurpillot** / Univ Rouen Normandie, INSA Rouen Normandie, CNRS, Groupe de Physique des Matériaux  
UMR 6634, F-76000 Rouen, France

\* Auteur correspondant

It is now more than 30 years that the Atom Probe Tomography (APT) turns out to be one the best analytical techniques that is able to both visualize nano-features in 3D and determine their local compositions. However, since the invention of the technique [1], APT instruments are still not fully recognized as a reliable tool for the analysis of some elements. Indeed, the fact that the identification of atoms is performed through a Time-of-Flight Mass Spectrometry (TOFMS) technique, it is possible that some materials introduce some elements having almost equal mass-to-charge ratios. That is the case, for instance for nitrogen and silicon in TiSiN systems [2], or titanium and carbon in cemented carbide materials [3]. Thus, materials made of different elements having near or equal mass-to charge ratios may be subjected to uncertainties on the estimation of their fraction in the analysed material. Given that in most cases mass peak overlaps concern elements with different charge states (e.g., Fe<sup>{2+}</sup> and N<sub>2</sub><sup>{+}</sup> at 28 Da and Si<sup>{2+}</sup> and N<sup>{+}</sup> at 14 Da), it could be possible to partly overcome this limitation through the measurement of ions charge state.

In the case of this study, charge states are indirectly measured through ions energy. Therfore, this study introduce the development of a new APT detector that is able to partly resolve mass peak overlaps through the measurement of ions energy (Fig.1). Through the energy-sensitivity of this detector, quantitative and qualitative improvements could be considered for critical materials introducing mass peak overlaps (Figure 2).

#### References:

- [1]A. Cerezo et al., Review of Scientific Instruments, 59(6):862–866, 6 1988.
- [2]David L.J. Engberg et al., Ultramicroscopy, 184:51–60, 1 2018.
- [3]M. Thuvander et al., Ultramicroscopy, 111(6):604–608, 5 2011.

**Mots clefs :** atom probe tomography, carbon foil, mass peak overlaps, position-energy-sensitive detector

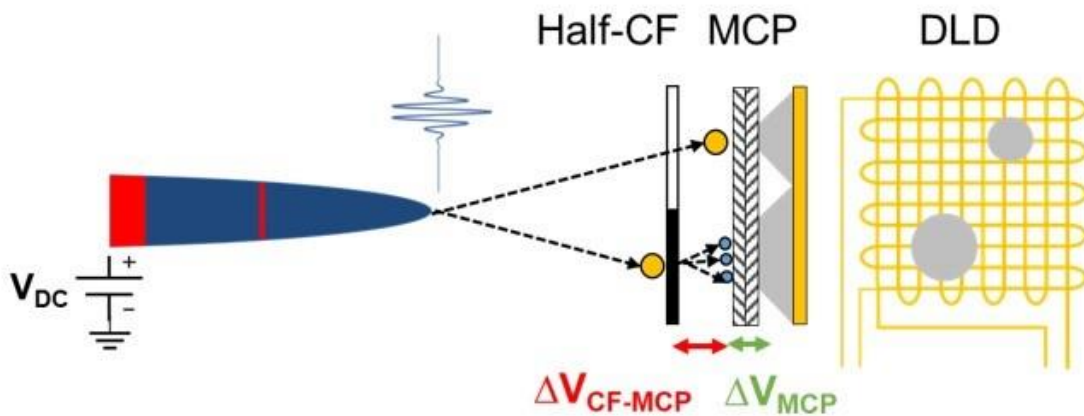


*Figure 1: Setup of the dedicated Carbon Foil detector workbench.*

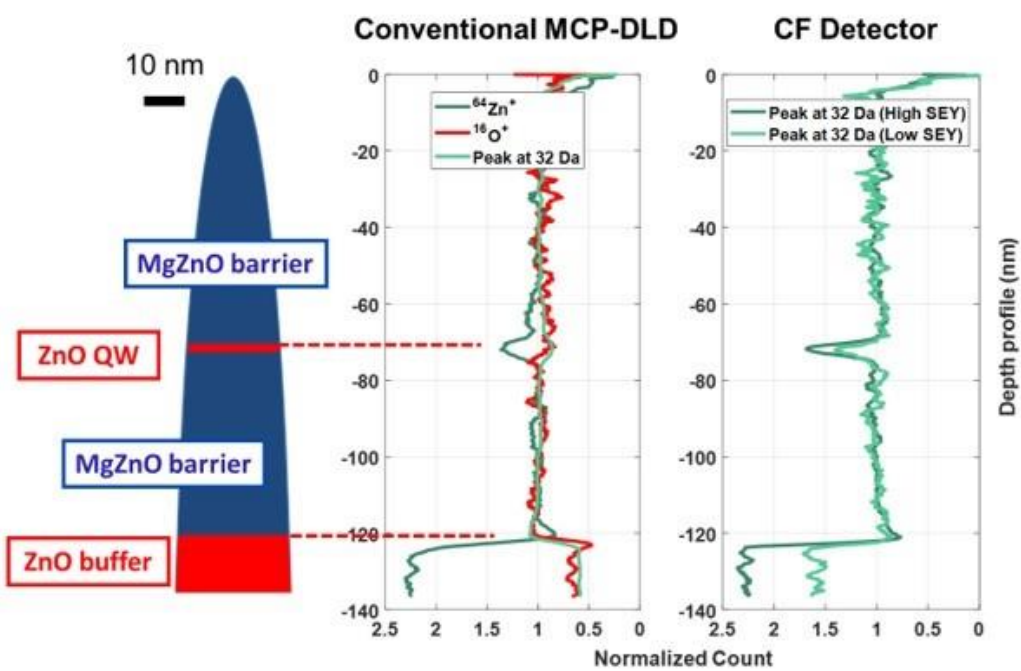


*Figure 2: Normalized depth profiles comparison from the developed detector. The outburst of  $^{64}\text{Zn}^{2+}$  that could not be observed at the QW position on the conventional MCP-DLD detector can now be observed through the pseudo-energy sensitivity of the CF detector.*

## SC4-P7

### Métrie avancée de la composition du carbure de silicium en sonde atomique tomographie

#### Advanced compositional metrology of Silicon Carbide in Atom Probe Tomography

- **Samba Ndiaye** \* (samba.ndiaye@univ-rouen.fr) / UNIROUEN, CNRS, Groupe de Physique des Matériaux, Normandie Université, 76801 St Etienne du Rouvray, France
- **Christian Bacchi** / UNIROUEN, CNRS, Groupe de Physique des Matériaux, Normandie Université, 76801 St Etienne du Rouvray, France
- **Benjamin Klaes** / UNIROUEN, CNRS, Groupe de Physique des Matériaux, Normandie Université, 76801 St Etienne du Rouvray, France
- **Mariaconcetta Canino** / CNR-IMM, I-40129 Bologna, Italy
- **François Vurpillot** / UNIROUEN, CNRS, Groupe de Physique des Matériaux, Normandie Université, 76801 St Etienne du Rouvray, France
- **Lorenzo Rigutti** / UNIROUEN, CNRS, Groupe de Physique des Matériaux, Normandie Université, 76801 St Etienne du Rouvray, France

\* Auteur correspondant

Atom Probe Tomography (APT) of compound semiconductors may present specific biases in the determination of chemical compositions because of the different behavior of different elements with respect to field evaporation [1], [2]. Silicon carbide (SiC) may be considered as a model system for the study of field ion evaporation of carbides, which must be understood in order to obtain accurate analyses of these systems by atom probe tomography (APT). As for other wide bandgap semiconductors, the measurement of composition of SiC by APT presents biases depending on the experimental parameters. Unlike silicon, carbon is characterized by a complex surface behavior, including formation of molecules and the tendency to produce correlated evaporation. Furthermore, the spatial precision of 3D reconstructions is strongly degraded in the direction parallel to the sample surface, which points out to a strong roughening or dynamic degradation of the surface. This is confirmed by field ion microscopy (FIM) analysis which reveals that atoms may move on the sample surface under the influence of the high electric field. This complex surface behavior eventually translates into hidden detection events and, therefore, to errors in the measurement of composition.

#### References

- [1] L. Mancini et al., J. Phys. Chem. C, vol. 118, no. 41, Oct. 2014, pp. 24136–24151.
- [2] E. Di Russo et al., J. Phys. Chem. C, vol. 122, no. 29, Jul. 2018, pp. 16704–16714.

\*samba.ndaye@univ-rouen.fr

**Mots clefs** : atom probe tomography (APT), composition, metrology, special resolution

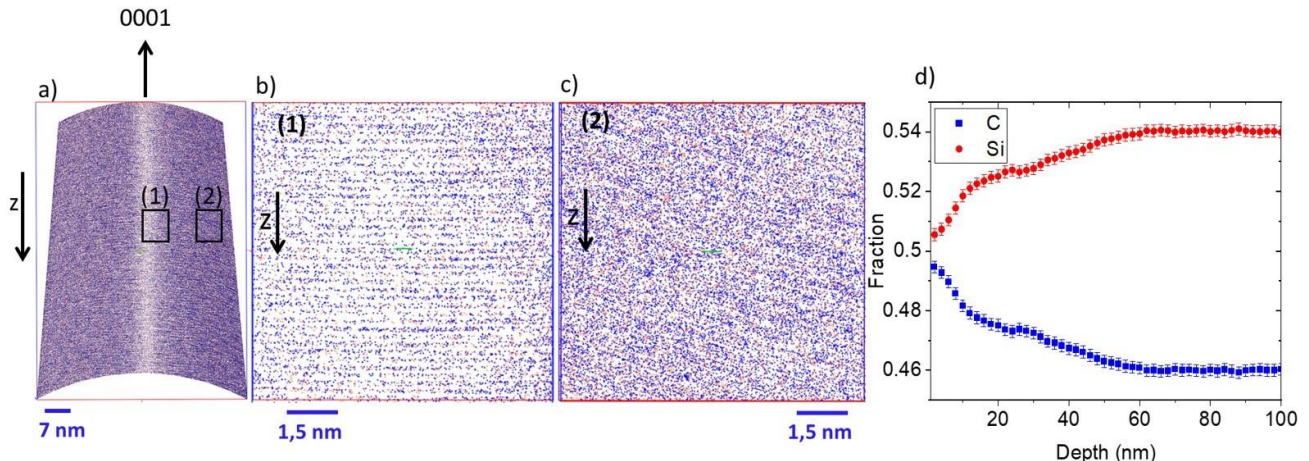


Figure1: (a) Cross section of a reconstructed volume from a 6H-SiC tip highlighting the [0001] pole along z direction (depth). (b) Reconstruction showing the atomic planes along the [0001] axis of SiC of hexagonal structure at the pole (ROI (1) in (a)), (c) Atomic positions within the ROI (2), far from the crystallographic pole, (d) Variation of the atomic fraction of Si and C as a function of the depth coordinate of the reconstructed volume.

## SC4-P8

### Cathodoluminescence Polarisée et Résolue Spectralement en STEM

#### Spectrally-Resolved Polarized Cathodoluminescence in STEM

- **Malo Bézard** \* (malo.bezard@universite-paris-saclay.fr) / Université Paris-Saclay, CNRS, Laboratoire de Physique des Solides, 91400 Orsay, France
- **Yves Auad** / Université Paris-Saclay, CNRS, Laboratoire de Physique des Solides, 91400 Orsay, France
- **Davy Gérard** / Univ. Technologique de Troyes, CNRS, Light nanomaterials nanotechnologies (L2n), 10000 Troyes, France
- **Jérémie Béal** / Univ. Technologique de Troyes, CNRS, Light nanomaterials nanotechnologies (L2n), 10000 Troyes, France
- **Jérôme Martin** / Univ. Technologique de Troyes, CNRS, Light nanomaterials nanotechnologies (L2n), 10000 Troyes, France
- **Mathieu Kociak** / Université Paris-Saclay, CNRS, Laboratoire de Physique des Solides, 91400 Orsay, France \* Auteur correspondant

Far-field optical methods are hindered by the optical diffraction limit. This is probably one of the reason of the success of electron-based optical spectroscopies available in a Scanning Transmission Electron Microscopy (STEM) such as Electron Energy Loss Spectroscopy (EELS) and Cathodoluminescence (CL), among others. One objective of the last decades is to unveil information about the electric field polarization of various excitations (plasmons, excitons, phonons, etc.) using Electron Microscopy, and measure the linear and the circular dichroism as it can be achieved in Optics. A first method to access this information is to measure, in EELS, the Orbital Angular Momentum transfers between the electron beam and the excitations to probe the near-field polarization. A second way to access the polarization measurement in the far-field, is to study the polarization of photons emitted by the sample after having been exited by the electron beam using CL. Some experiments have already combined the use of energy-filtered and polarized light and Scanning Electron Microscope to study achiral and chiral objects [1-3]. One object of interest is a well-known system called a Born-Kuhn System (BKS). This complex nanoparticle exhibits two plasmonic modes which have opposite circular polarizations (see Figure). This property already has been studied in optics on BKS networks [4] but has never been observed on a single nanoparticle. In this seminar, we discuss the way to perform such an experiment on BKS using a STEM, what are the limitations we can face of and what are the considered solutions to overcome them.

#### References

- [1] N. Yamamoto, K. Araya and F. J. Garcia de Abajo, Physical Review B, 64 205419 (2001)
- [2] C. I. Osorio, et. al., ACS Photonics, 3 147-154 (2016)
- [3] S. Zu, et. al., Nano Letter, 19, 775-780 (2019)
- [4] L. Gui, et. al., ACS Photonics, 6, 3306-3314 (2019)

**Mots clefs :** STEM, Cathodoluminescence, Polarization, Chirality

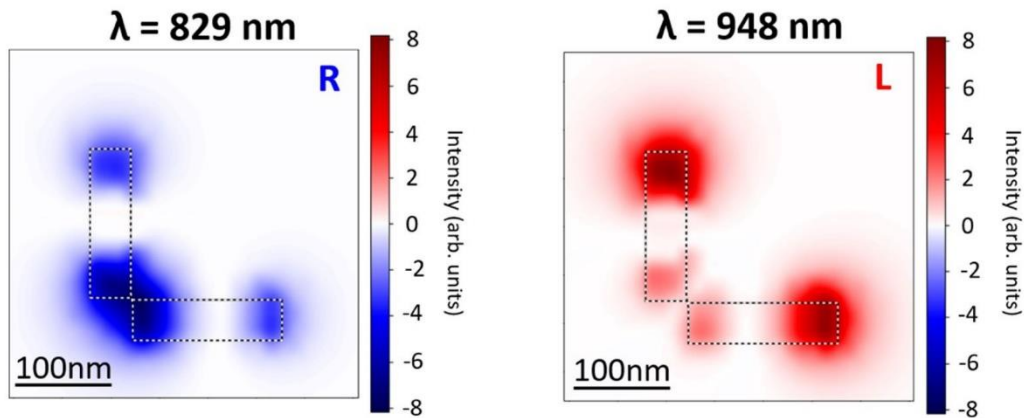


**Figure :** Simulated Right (R)-handed, and Left (L)-handed polarized cathodoluminescence on a gold BKS structure. Each arm of the structure has a length of 150 nm and a width of 50 nm. (pyGDM2)

**SC4-P9****Comprendre l'étendue de l'ordre dans le spinelle LiNi<sub>0.5</sub>Mn<sub>1.5</sub>O<sub>4</sub> par 4D-STEM en utilisant l'outil ASTAR**

**Understanding the transition metal order in spinel LiNi<sub>0.5</sub>Mn<sub>1.5</sub>O<sub>4</sub> by 4D-STEM using ASTAR system**

- **Gozde Oney** \* (gozde.oney@icmcb.cnrs.fr) / CNRS, Univ. Bordeaux, Bordeaux INP, ICMCB UMR CNRS #5026, F-33600, Pessac & France Laboratoire de Réactivité et de Chimie des Solides, Université de Picardie Jules Verne, CNRS-UMR 7314, F-80039 Amiens Cedex 1, France
- **François Weill** / CNRS, Univ. Bordeaux, Bordeaux INP, ICMCB UMR CNRS #5026, F-33600, Pessac, France
- **Chunyang Zhang** / SIMAP Laboratory, CNRS-Grenoble INP, BP 46 101 rue de la Physique, 38402 Saint Martin d'Hères, France
- **Jacob Olchowka** / CNRS, Univ. Bordeaux, Bordeaux INP, ICMCB UMR CNRS #5026, F-33600, Pessac, France
- **Christian Masquelier** / Laboratoire de Réactivité et de Chimie des Solides, Université de Picardie Jules Verne, CNRS-UMR 7314, F-80039 Amiens Cedex 1, France
- **Edgar Rauch** / SIMAP Laboratory, CNRS-Grenoble INP, BP 46 101 rue de la Physique, 38402 Saint Martin d'Hères, France
- **Muriel Véron** / SIMAP Laboratory, CNRS-Grenoble INP, BP 46 101 rue de la Physique, 38402 Saint Martin d'Hères, France
- **Laurence Croguennec** / CNRS, Univ. Bordeaux, Bordeaux INP, ICMCB UMR CNRS #5026, F-33600, Pessac, France
- **Arnaud Demortière** / Laboratoire de Réactivité et de Chimie des Solides, Université de Picardie Jules Verne,  
CNRS-UMR 7314, F-80039 Amiens Cedex 1, France

\* Auteur correspondant

The spinel LiNi<sub>0.5</sub>Mn<sub>1.5</sub>O<sub>4</sub> (LNMO) is one of the most promising candidates as a cobalt-free positive electrode material for Li-ion batteries, with its theoretical capacity of 147 mAh.g<sup>-1</sup>, achieving an attractive energy density of 650 Wh/kg. LNMO crystallizes in two different spinel structures described in P4332 and Fd-3m space groups, whether the Ni and Mn Atoms are ordered or not, respectively. The extent of the transition metal order is one the most crucial parameters which affect the electrochemical behavior and can be modulated by post-annealings. An averaged transition metal order information can be obtained by X-Ray and neutron diffraction or spectroscopy techniques; however, the local information on the process of ordering within the crystal and the homogeneity of the order at the particle scale remains to be discovered.

Transition metal order can easily be differentiated by electron diffraction because of the lowered symmetry of the ordered lattice (Fig.1). To achieve transparency to electrons, LNMO particles were prepared with platelet morphology and a homogenous thickness of 180 nm by the molten salt synthetic route. Different extents of transition metal order were obtained by post-annealings. All samples were analyzed by scanning transmission electron microscopy coupled with the ASTAR System (Nanomegas [1]). With this equipment, an electron diffraction pattern for each pixel of the acquired images is collected (4D-STEM). Then the acquired diffraction patterns are compared with the theoretic ones (generated for both lattice symmetries)

based on the position and intensity of the spots. This allowed us, even for non-zone axis patterns, to map (dis)ordered zones at the particle scale with a spatial resolution of 10 nm (Fig.2). Additionally, the intensity diffraction spots gave us information about how many ordered lattices are stacked along the thickness of the platelets, making it possible for us to generate maps of homogeneity on transition metal order in the spinel LNMO material for the first time, thus allowing us to propose the mechanism involved throughout the post-annealing process.

[1] Rauch, E. F.; Véron, M. Automated Crystal Orientation and Phase Mapping in TEM. Mater. Charact. 2014, 98, 1–9.

**Mots clefs :** ASTAR, Electron diffraction, 4D-STEM

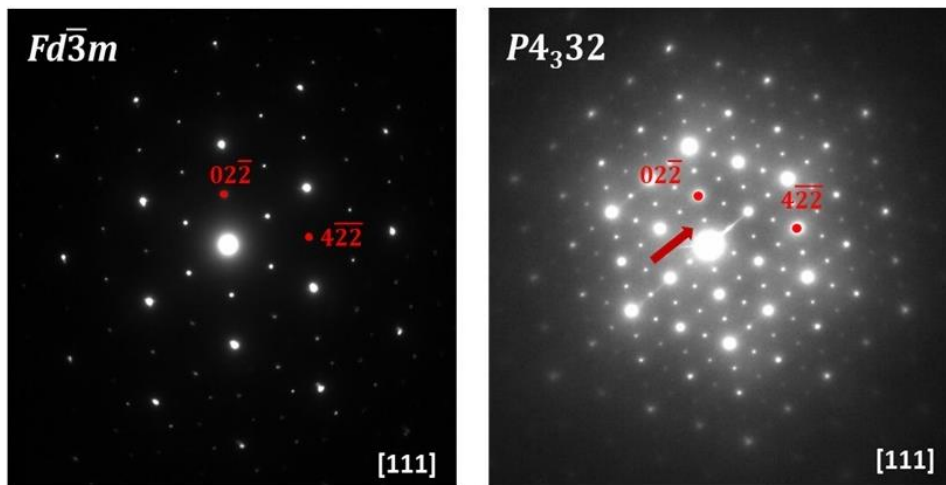


*Figure 1: Electron diffraction patterns of spinel  $\text{LiNi}_{0.5}\text{Mn}_{1.5}\text{O}_4$ : disordered (left), ordered (right), and showing extra diffraction spots.*

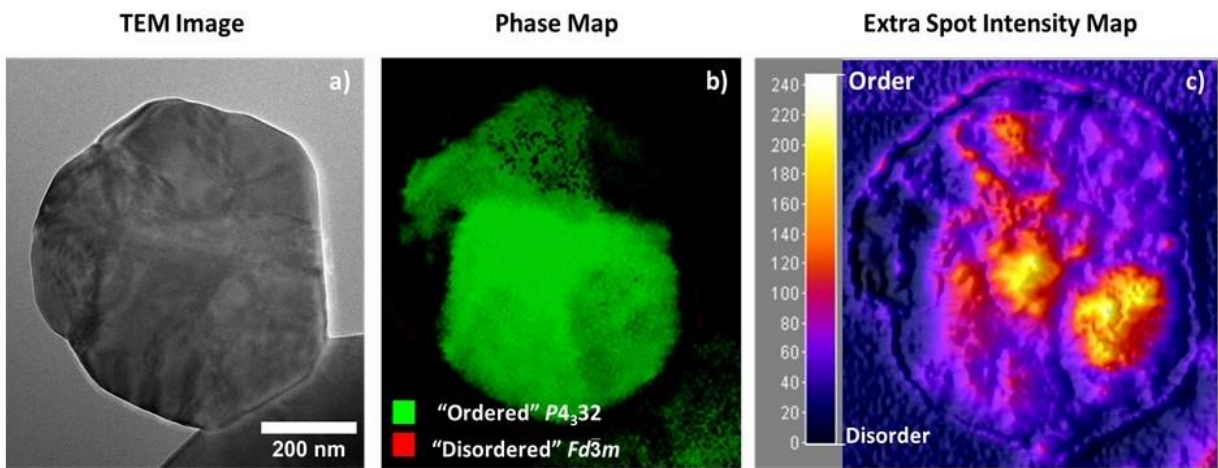


*Figure 2: (a) TEM image of platelet  $\text{LiNi}_{0.5}\text{Mn}_{1.5}\text{O}_4$  annealed at 700°C for 4h under air (x2) (b) Phase map generated by ASTAR when theoretical patterns of (dis)ordered phases are provided (c) Extra spot intensity map generated using virtual dark field image obtained from only extra spots observed on an ordered region showing transition metal order heterogeneity on the particle*

**SDM1-P1****Quantification précise de la ségrégation intergranulaire du phosphore dans le fer par STEM-EDX****Accurate quantification of phosphorus intergranular segregation in iron by STEM-EDX**

• **Chih-Ying Hsu** \* (chihyinghsu81@gmail.com) / Electron Spectrometry and Microscopy Laboratory (LSME),

Institute of Physics (IPHYS), Ecole Polytechnique Fédérale de Lausanne (EPFL) CH-1015 Lausanne; EDF R&D, MMC

Department, F-77250 Ecuelles, France; Mines Saint-Etienne, Univ Lyon, CMRS, UMR 5307 LGF

• **Julien Stodolna** / EDF R&D, MMC Department, F-77250 Ecuelles, France

• **Patrick Todeschini** / EDF R&D, MMC Department, F-77250 Ecuelles, France

• **Frederic Delabrouille** / EDF R&D, MMC Department, F-77250 Ecuelles, France

• **Bertrand Radiguet** / Normandie Université, UNIROUEN, INSA Rouen, CNRS, Groupe de Physique des Matériaux, 76000 Rouen, France

• **Frédéric Christien** / Mines Saint-Etienne, Univ Lyon, CMRS, UMR 5307 LGF, Centre SMS, F-42023 Saint-Etienne, France

\* Auteur correspondant

Phosphorus intergranular segregation is known to influence the fracture properties of steels by decreasing grain boundary cohesion and induce intergranular fracture [1]. The most common technique for grain boundary segregation identification and quantification is Auger Electron Spectroscopy [2], which only has access to embrittled enough grain boundaries. Other techniques such as Atom Probe Tomography (APT) and Energy Dispersive X-ray Spectroscopy on Scanning Transmission Electron Microscope (STEM-EDX) have also been used to study segregation especially when intergranular fracture is not seen [3]–[5].

A new way to quantify phosphorus grain boundary segregation by STEM-EDX is illustrated in this work. A “box-type method” is proposed to remove the long-discussed problem of interaction volume. The proposed methodology also introduces a novel way to subtract spectrum background that removes influences by coherent Bremsstrahlung and spurious peaks. A Fe-P model alloy is used to compare the box method to the quantification results previously obtained by APT on two high angle grain boundaries [3]. The results are specifically reported in surface concentration (atom/nm<sup>2</sup>) so that no additional hypothesis is needed and that results between the two techniques can be compared directly. The measurements show that the box-type method can accurately measure phosphorus intergranular segregation in iron.

## References :

- [1]C. A. English et al, “Review of Phosphorus Segregation and Intergranular Embrittlement in Reactor PressureVessel Steels”, doi: 10.1520/STP10531S.
- [2]P. Lejcek, Grain boundary segregation in metals. in Springer Series in Materials Science, no. 136. Berlin: Springer-Verlag, 2010.
- [3]A. Akhatova et al., “Investigation of the dependence of phosphorus segregation on grain boundary structure inFe-P-C alloy: cross comparison between Atom Probe Tomography and Auger Electron Spectroscopy,” Appl. Surf. Sci., vol. 463, pp. 203–210, Jan. 2019, doi: 10.1016/j.apsusc.2018.08.085.

[4] V. J. Keast et al, "Grain boundary chemistry," Curr. Opin. Solid State Mater. Sci., vol. 5, no. 1, pp. 23–30, Jan.2001, doi: 10.1016/S1359-0286(00)00029-2.

[5] T. Walther et al, "A Novel Method of Analytical Transmission Electron Microscopy for Measuring HighlyAccurately Segregation to Special Grain Boundaries or Planar Interfaces," Microchim. Acta, vol. 155, no. 1–2, pp. 313–318, Sep. 2006, doi: 10.1007/s00604-006-0562-5.

**Mots clefs :** Scanning transmission electron microscopy, energy dispersive X-ray analysis, quantification, intergranular segregation, phosphorus, grain boundary

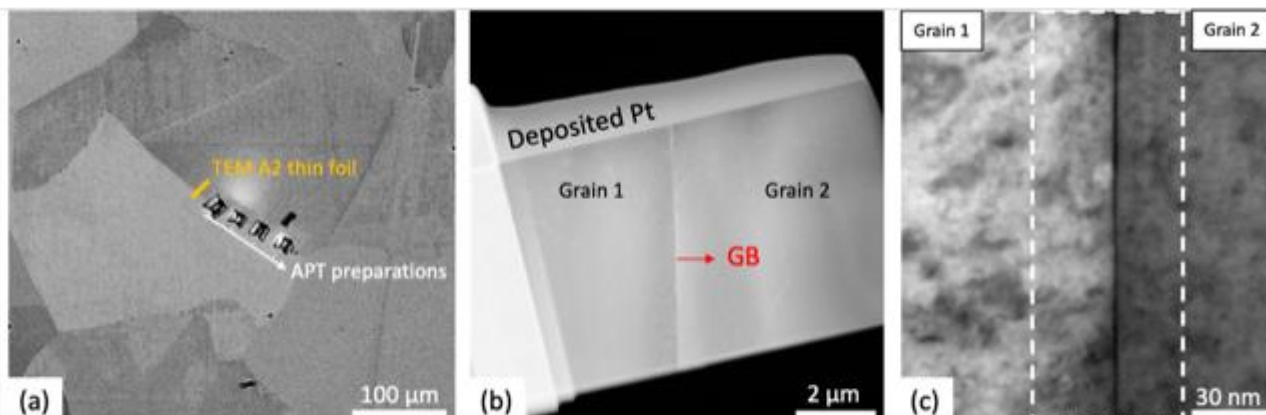


Figure 1: TEM thin foil preparation from the Fe-P model alloy: (a) SEM micrograph of a grain boundary showing four preparation sites for APT tips, the TEM thin foil was extracted close to these sites, marked in yellow, (b) STEM-HAADFimage of the full thin foil where the grain boundary is straight and close to the center of the sample, (c) STEM BF image of the thin foil with the EDX acquisition zone marked in white.

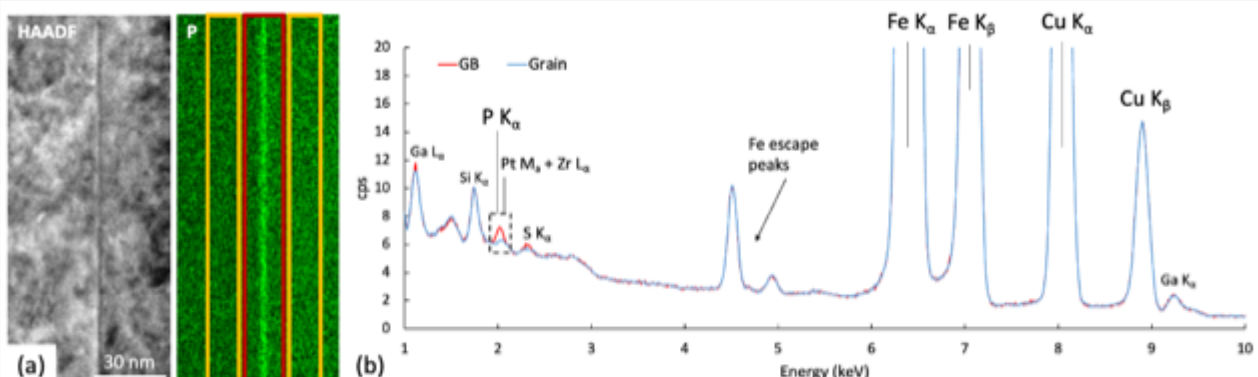


Figure 2: Example of STEM-EDX acquisition on a grain boundary of Fe-P model alloy: (a) HAADF image and EDX qualitative P K<sub>α</sub> map, the red and yellow boxes indicate the zones considered for spectrum extraction during data treatment, (b) superposed GB spectrum (corresponding to the red box in fig. 2(a)) and grain spectrum (corresponding to two yellow boxes in fig. 2(a)).

## SDM1-P2

### Microscopie corrélative des grains 3D sur AlGaN QDs pour des émetteurs UV pompés par les électrons

#### Correlative microscopy of 3D grain structures on AlGaN QDs for electron-pumped UV-emitters

- **Jesus Cañas** \* (jesus.canasfernandez@cea.fr) / Univ. Grenoble-Alpes, CEA, Grenoble INP, IRIG, PHELIQS, 38000 Grenoble, France
- **Névine Rochat** / Univ. Grenoble Alpes, CEA, LETI, 38000 Grenoble, France
- **Adeline Grenier** / Univ. Grenoble Alpes, CEA, LETI, 38000 Grenoble, France
- **Edith Bellet-Amalric** / Univ. Grenoble-Alpes, CEA, Grenoble INP, IRIG, PHELIQS, 38000 Grenoble, France
- **Anjali Harikumar** / Univ. Grenoble-Alpes, CEA, Grenoble INP, IRIG, PHELIQS, 38000 Grenoble, France
- **Audrey Jannaud** / Univ. Grenoble Alpes, CEA, LETI, 38000 Grenoble, France
- **Zineb Saghi** / Univ. Grenoble Alpes, CEA, LETI, 38000 Grenoble, France
- **Samba Ndiaye** / UNIROUEN, CNRS, Groupe de Physique des Matériaux, Normandie Université, 76000 Rouen, France
- **Catherine Bougerol** / Univ. Grenoble-Alpes, CNRS, Grenoble INP, Institut Néel, 38000 Grenoble, France
- **Lorenzo Rigutti** / UNIROUEN, CNRS, Groupe de Physique des Matériaux, Normandie Université, 76000 Rouen, France
- **Eva Monroy** / Univ. Grenoble-Alpes, CEA, Grenoble INP, IRIG, PHELIQS, 38000 Grenoble, France \*

Auteur correspondant

Much effort has been devoted to extending the LED technology towards the UV region for disinfection. However, LEDs efficiencies drop dramatically for emission wavelengths below 350 nm due to the immature status of AlGaN technology. One alternative to the particular challenges of AlGaN LEDs is the use of electron-beam pumped lamps based quantum dot (QD) superlattices (SLs). These devices consist of a semiconductor dice terminated with an AlGaN QD-SL mounted in a vacuum tube, in which a cold cathode pumps high-energy electrons generating multiple excitons that recombine in the QDs.[1] It has the benefit of avoiding the challenging p-type doping and contacts of AlGaN while providing a large active volume. Our group demonstrated AlGaN UV-B and UV-C QD-SLs grown by plasma-assisted molecular beam epitaxy emitting with internal quantum efficiency in the range of 50%. [2] However, samples often present spatial inhomogeneities, large emission lines and multi-peak structure.

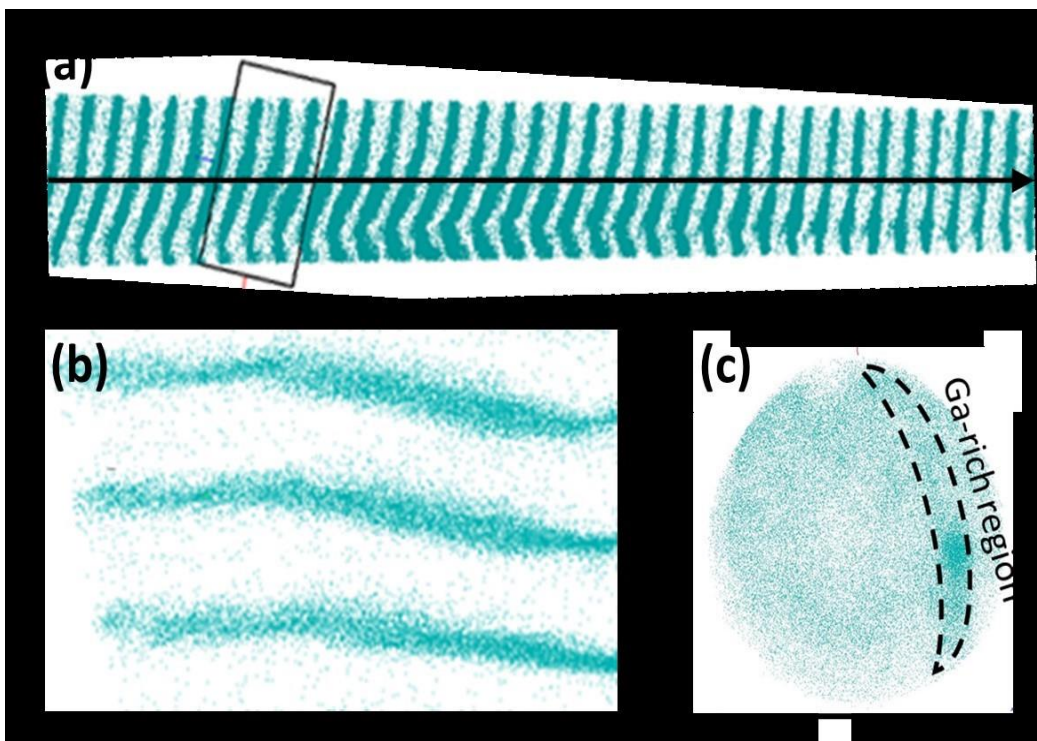
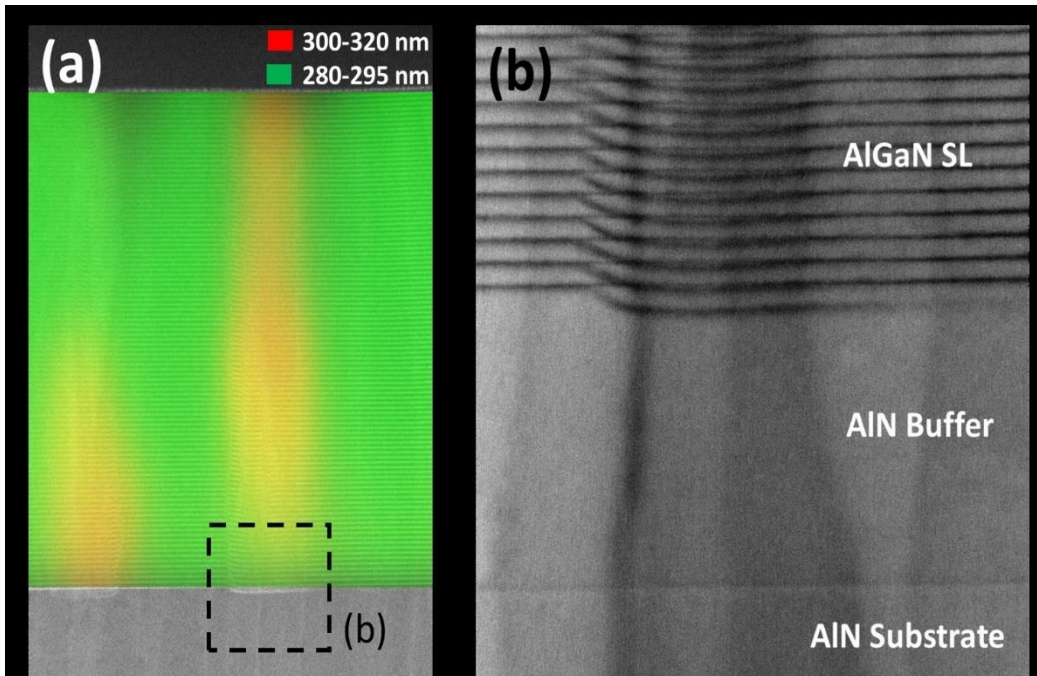
To tackle this issue, we investigate an Al<sub>0.14</sub>Ga<sub>0.86</sub>N/AlN QD-SLs using top and cross-section cathodoluminescence (CL), scanning transmission electron microscopy (STEM) and atomic probe tomography (APT). The top-view CL presents a predominant line at 290 nm and a secondary emission at 305 nm. Transversal CL performed on a TEM-lamella confirms a predominant emission at shorter wavelengths with distinct spatial regions emitting at a longer wavelength [see figure 1(a)]. STEM images allow the identification of 3D grain structures originating from the AlN buffer layer as the source of the secondary emission [see figure 1(b)]. To gain access to the QDs planes structural and chemical composition, the sample is prepared as a micro needle-shaped tip and studied by APT. The APT Ga atoms maps in figures 2(a), (b) and (c) show that the twist of the QDs planes in the grain boundary is accompanied

by a Ga-enrichment. We demonstrate theoretically that the morphology and composition of the grain justifies the spectral shift producing the secondary emission.

#### References:

- [1] S. Cuesta, et al., Journal of Physics D: Applied Physics 55, 273003 (2022). [2] A. Harikumar, et al., Nanotechnology 31, 505205 (2020).

**Mots clefs :** AlGaN/QDs/UV/Correlative microscopy



## SDM1-P3

### Étude de la réaction de l'hydrogène et des hydrures en Sonde Atomique Tomographique des semi-conducteurs III-N

#### Investigation of the reaction of hydrogen and hydrides in Atom Probe Tomography of III-N semiconductors

- **Aissatou Diagne** \* (aissatou.diagne1@univ-rouen.fr) / Univ Rouen Normandie, INSA Rouen Normandie, CNRS, Groupe de Physique des Matériaux UMR 6634, F-76000 Rouen, France
- **Samba Ndiaye** / Univ Rouen Normandie, INSA Rouen Normandie, CNRS, Groupe de Physique des Matériaux UMR 6634, F-76000 Rouen, France
- **Noelle Gogneau** / Centre de Nanosciences et de Nanotechnologies, CNRS UMR 9001, Univ. Paris-Sud, Université Paris-Saclay, C2N – Orsay, 91405 Orsay Cedex, France
- **Jonathan Houard** / Univ Rouen Normandie, INSA Rouen Normandie, CNRS, Groupe de Physique des Matériaux UMR 6634, F-76000 Rouen, France
- **Lorenzo Rigutti** / Univ Rouen Normandie, INSA Rouen Normandie, CNRS, Groupe de Physique des Matériaux  
UMR 6634, F-76000 Rouen, France

\* Auteur correspondant

We investigate the microscopic behaviour of hydrogen-containing species formed on the surface of III-N semiconductor samples by the residual hydrogen in the analysis chamber in laser-assisted atom probe tomography (APT). APT is based on the field evaporation of atoms on the surface of a nanometric tip. The formation of H-containing species occurs at field strengths between 22 and 26 V/nm and is independent of the analysed samples. The results highlight the strong dependence of the relative abundances of the ionic species H<sup>+</sup>, H<sub>2</sub><sup>+</sup>, H<sub>3</sub><sup>+</sup> and hydrides on the surface field of the samples [1]. The relative abundances of the hydrides decrease when the surface field increases due to the evolution of the tip shape or the different evaporation behaviour of the different layers. The 3D APT reconstruction makes it possible to map the evolution of the surface behaviour of these species issued by chemical reactions. This, together with the analysis of multiple, correlated evaporation events in the detector space, opens the way to a spatially resolved microscopy of single-molecule chemical reactions based on APT.

#### References:

- [1] L. Rigutti et al., « Surface Microscopy of Atomic and Molecular Hydrogen from Field-Evaporating Semiconductors », J. Phys. Chem. C, vol. 125, no 31, p. 17078-17087, août 2021, doi: 10.1021/acs.jpcc.1c04778.

## SDM1-P4

### True Correlative Microscopy Using AFM-in-SEM

#### True Correlative Microscopy Using AFM-in-SEM

- **Pavel Komarov** \* (pavel.komarov@nenovision.com) / Dr.
- **Veronika Hegrova** / Mrs.
- **Radek Dao** / Mr.
- **Jan Neuman** / Dr.

\* Auteur correspondant

Atomic force microscope (AFM) and scanning electron microscopy (SEM) are two of the most commonly used techniques for analysing nano-sized structures and topography features today. However, when used separately, both techniques have several drawbacks. To address these concerns, we propose incorporating the AFM into the SEM. The combination of AFM-in-SEM opens new possibilities for nanomaterial characterisation in Materials Science, Nanotechnology, Semiconductors, and Life Science.

NanoVision developed LiteScope, a unique and compact AFM that can be easily integrated into most SEMs. Using LiteScope and our Correlative Probe and Electron Microscopy (CPEM) technology, we can effectively combine the advantages of AFM (analysis of 3D topography, mechanical, electrical, and magnetic properties) and SEM (precise imaging with high resolution, chemical analysis and surface modification). It yields a 3D multi-channel in-situ analysis with true data from the analysed sample.

We would like to present an investigation of MoS<sub>2</sub> chemical vapor deposited (CVD) 2D flakes as an example of the benefits of the AFM-in-SEM combination. Because of its unique combination of mechanical and electrical properties, MoS<sub>2</sub> was found to be useful in a wide range of applications in the automotive and semiconductor fields. The AFM-in-SEM was used to (i) perform a complex set of analyses on topography, structure, and elemental distribution from AFM, SEM, and EDX signals, resulting in a 3D CPEM illustration; (ii) perform all analyses at the same time, place, and conditions; and (iii) enable quick and easy navigation to the region of interest.

**Mots clefs :** AFM-in-SEM, CPEM, Correlative Microscopy, Materials Science, 2D materials

**SDM2-P1****CALCULS DE RADIOLYSE POUR LES RÉGIMES D'IRRADIATION FONDAMENTAUX DE MICROSCOPIE ELECTRONIQUE EN PHASE LIQUIDE.****RADIOLYSIS CALCULATIONS FOR FUNDAMENTAL IRRADIATION REGIMES IN LIQUID PHASE-TEM.**

- **Giuseppe De Salvo / \*** (g.salvo@nanogune.eu) / Electron-Microscopy Laboratory, CIC nanoGUNE BRTA, Tolosa Hiribidea 76, 20018 Donostia, Spain;
- **Stefan Merkens** / Electron-Microscopy Laboratory, CIC nanoGUNE BRTA, Tolosa Hiribidea 76, 20018 Donostia, Spain;
- **Andrey Chuvalin** / Electron-Microscopy Laboratory, CIC nanoGUNE BRTA, Tolosa Hiribidea 76, 20018 Donostia, Spain; Ikerbasque, Basque Foundation for Science, 48013 Bilbao, Spain.

\* Auteur correspondant

Liquid Phase TEM (LP-TEM) is a promising technique to image nanoscale processes in native liquid sample environment. However, *in situ* observations suffer from numerous artefacts, with radiolysis being the most relevant in aqueous solutions. Radiolytic processes involve the excitation of water molecules upon irradiation with the electron beam, leading to the generation of highly reactive molecular and radical species. Thus the necessity of finding instruments to accurately quantify the chemistry evolution is crucial to discard the effect of the beam from the investigated process itself. Numeric modelling of reaction kinetics and mass transport dynamics was a breakthrough in understanding radiolysis. [1,2] Current numeric LP-TEM models are founded on works on nuclear power reactors, reflecting irradiation scenarios drastically different regarding the dimensions of the experimental setup and the properties of the ionizing radiation. Moreover, models tend to simplify reality, due to the spatio-temporal complexity of the phenomena. One key assumption is the constant homogeneous generation of radiolytic species in the irradiated volume; however, it has been barely validated for LP-TEM where most irradiation scenarios correspond to excitation events occurring localized in space and arbitrarily in time.

The ideal model would thus utilize discrete and random space-time generation [3] in a three-dimensional geometry during microsecond regimes at nanosecond time-stepping, posing monstrous challenges to any computational infrastructure. Here, we report major advances towards such implementation solving high concentration gradients at (sub-)nm spatial and (sub-)ns temporal resolution. An explorative study of preliminary results indicates non-uniform concentration distributions at microsecond timescales challenging the fundamental assumptions behind current radiolysis models in LP-TEM.

**Références/References :**

- [1] Schneider Nicholas M. et al., Electron-water interactions and implications in the radiolysis of water, *The Journal of Physical Chemistry C*, 118.38 (2014), 22373-22382
- [2] De Salvo G., Merkens, S. and Chuvalin, A., The effect of flow on radiolysis in liquid phase-TEM flow cells, *NanoExpress*, 3, (2022), 045006.
- [3] Hill M. A. and F. A. Smith, Calculation of initial and primary yields in the radiolysis of water, *Radiation Physics and Chemistry*, 43.3, (1994), 265-280

**Mots clefs :** LIQUID PHASE TRANSMISSION ELECTRON MICROSCOPY, RADIOLYSIS, NUMERICAL MODELLING

## SDM2-P2

### Etude operando par XAS et TEM des mécanismes d'activation des catalyseurs bimétalliques Fe et Sb

Operando study by XAS and TEM of the activation mechanisms of Fe and Sb bimetallic catalysts

.Aliou Sadia TRAORE \* (aliou-sadia.traore@ipcms.unistra.fr) / Institut de Physique et Chimie des Matériaux de

Strasbourg (IPCMS)

\* Auteur correspondant

The synthesis of light olefins from carbon monoxide via the Fischer-Tropsch reaction is a highly researched topic in heterogeneous catalysis, with iron-based catalysts being the reference system [1]. Promoters have been added to improve the stability and catalytic performance of these catalysts, with iron carbide being identified as the active phase for the reaction [2]. In this study, we focus on bimetallic catalysts based on Fe and Sb nanoparticles supported on SiO<sub>2</sub>, and investigate their behavior during activation and reaction using in-situ TEM and XAS techniques.

In the first part of the study, the species formed as a function of the temperature during a TPR (Temperature Programmed Reduction) experiment under 5%H<sub>2</sub> were identified. The analysis by MCR-ALS (Multivariate Curve Resolution with Alternating Least Square Fitting) of the Quick-XAS spectra (Figure 1 A) which we acquired in situ, during the TPR, revealed the presence of three intermediate phases before the formation of the metallic NPs at 950°C: Fe<sub>3</sub>O<sub>4</sub> at 400°C, FeO at 500°C and a phase whose structural features combine metallic Fe and iron oxide at 700°C. The in-situ TEM analysis carried out at the temperatures previously identified by XAS-MCR-ALS confirms the nature of the mentioned phases and highlights the presence at 700°C of a FeOx-Fe core-shell structure (Figure 1). Depending on the order of impregnation of iron and antimony, we observed different structural behaviour of the catalysts during activation under CO. The carbide forms more easily at 350°C on the Fe catalysts promoted with Sb, as compared to the pure Fe/SiO<sub>2</sub> catalyst. In addition, this analysis allowed us to observe that the activation of the Fe/SiO<sub>2</sub> catalyst is accompanied by the formation of hollow particles, mechanism which can be assigned to the Kirkendall effect. From a more general perspective, this study demonstrates that such an in situ TEM and XAS combination is a powerful tool for the characterisation of the catalysts during the catalytic process.

**Mots clefs :** Operando, TEM, XAS, Catalysts

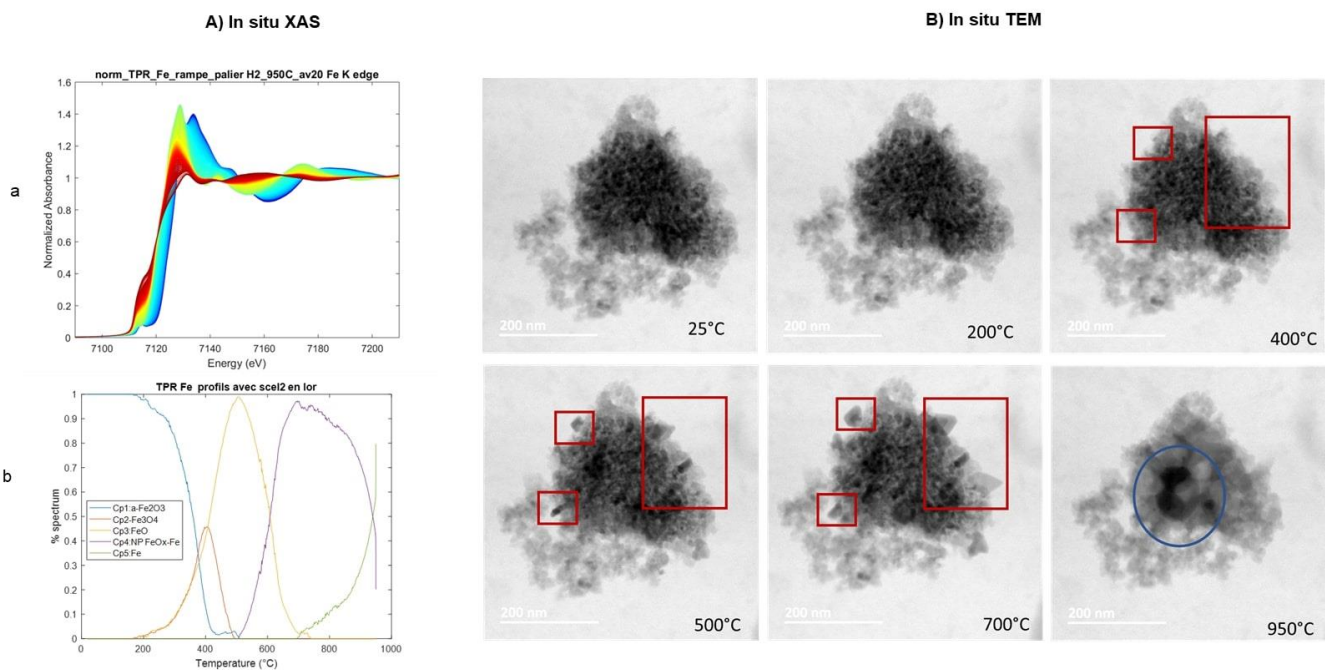


**Figure 1:** H<sub>2</sub>-TPR of the Fe/SiO<sub>2</sub> catalyst with a temperature variation from 25°C to 950°C under 5% H<sub>2</sub> A) 1) In situ XAS spectrum of the Fe/SiO<sub>2</sub> TPR, 2) determination and evolution of the relative percentages of the different species as a function of temperature by multivariate resolution analysis of the curves with alternating least squares fit. B) In situ TEM images of the Fe/SiO<sub>2</sub> TPR correlated with in situ XAS information.

## SDM2-P3

### Vers l'Analyse Operando de Piles à Combustible à Oxyde Solide en Microscopie Electronique en Transmission Environnementale

#### Towards the Operando Analysis of SOFC Devices in Environmental Transmission Electron Microscopy

- **Quentin Jeangros** / Photovoltaics and Thin Film Electronics Laboratory, Ecole Polytechnique Fédérale de Lausanne, Neuchâtel, Switzerland
- **Matthieu Bugnet** \* (matthieu.bugnet@insa-lyon.fr) / Univ Lyon, CNRS, INSA Lyon, UCBL, MATEIS, UMR 5510, 69621 Villeurbanne, France
- **Thierry Epicier** / Univ Lyon, Université Claude Bernard Lyon 1, CNRS, IRCELYON, F-69626, Villeurbanne, France
- **Cedric Frantz, Stefan Diethelm** / Group of Energy Materials, Ecole Polytechnique Fédérale de Lausanne, Sion, Switzerland
- **Dario Montinaro** / SOLIDpower SpA, Yverdon-les-bains, Switzerland
- **Elyzaveta Tyukalova** / Laboratory for In Situ & Operando Electron Nanoscopy, School of Materials Science, Nanyang Technological University, Singapore, Singapore
- **Yevgeny Pivak** / DENSSolutions, Delft, The Netherlands
- **Jan Van-Herle** / Group of Energy Materials, Ecole Polytechnique Fédérale de Lausanne, Sion, Switzerland
- **Aïsha Hessler-Wyser** / Photovoltaics and Thin Film Electronics Laboratory, Ecole Polytechnique Fédérale de Lausanne, Neuchâtel, Switzerland
- **Martial Duchamp** / Laboratory for In Situ & Operando Electron Nanoscopy, School of Materials Science, Nanyang Technological University, Singapore, Singapore

\* Auteur correspondant

Solid oxide fuel cells (SOFC) are a class of solid-state electrochemical conversion devices that produce electricity directly by oxidizing a fuel gas. They consist in an anode-cathode duet separated by a solid electrolyte conducting oxygen ions. The anode is fed with hydrogen or other fuels whereas the cathode is in contact with air. Overall, a SOFC operates from the combined action of two external stimuli: a gaseous environment and temperature. Owing to recent advances of in situ and operando transmission electron microscopy, we set up an experiment to operate a SOFC inside an environmental TEM (ETEM) to identify how the device microstructure determines its electrical properties [1]. An elementary anode(NiO)–electrolyte(yttria-stabilized zirconia)–cathode(Sr-doped lanthanum manganite) sandwich was prepared by focused ion beam and mounted on a heating/biasing MEMS-based specimen holder (DENSSolutions, Fig. 1) and inserted in a dedicated ETEM (FEI Titan).

Due to the difference in catalytic activity between the electrodes, O<sub>2</sub> should reduce at the cathode, while H<sub>2</sub> should oxidize at the anode, thus leading to a voltage difference. The reduction of NiO was first performed under a forming gas N<sub>2</sub>:H<sub>2</sub> (ratio 20:1) under 15 mbar up to 750°C. The O<sub>2</sub> to H<sub>2</sub> ratio was then increased to trigger the SOFC operation, leading to a total pressure of 16 mbar at 600°C. At this point, the variation of voltage between the anode and cathode was correlated to gas composition and anode microstructure (Fig. 2). The latter was analyzed by means of conventional and high-resolution imaging, diffraction, and EELS. The system was cycled several times by decreasing and re-increasing the O<sub>2</sub> concentration in the gas flow, and correlations between microstructure, gas composition, and SOFC voltage were established. Results were further confirmed by macroscopic ex situ tests. Such operando experiments open numerous perspectives to investigate the root cause of failure pathways affecting SOFCs, like poisoning of active sites or coarsening of the Ni catalyst [2].

[1]Q. Jeangros et al., under review; arXiv <https://doi.org/10.48550/arXiv.2302.12514>.

[2]The authors acknowledge the METSA network, the France-Singapore MERLION program (INSTANT project), and the start-up grant M4081924 at NTU.

**Mots clefs** : in situ, operando, energy materials, SOFC, environmental TEM

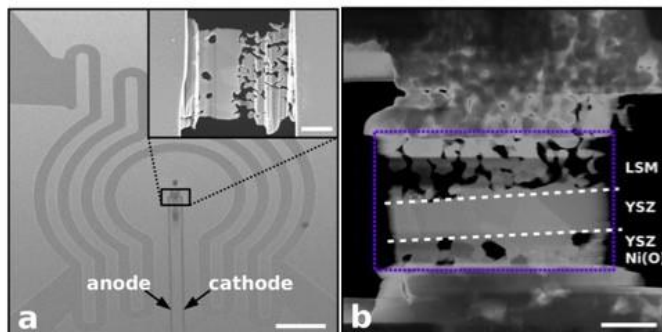


*Figure 1: a) Secondary electrons SEM image of a biasing and annealing MEMS chip (DENSSolutions) for operando TEM, where the anode and cathode of the SOFC lamella (inset) are electrically connected to the biasing electrodes of the chip. Scale bar: 50  $\mu\text{m}$ . b) STEM ADF of the electrically connected SOFC sample. Scale bar: 2  $\mu\text{m}$ .*

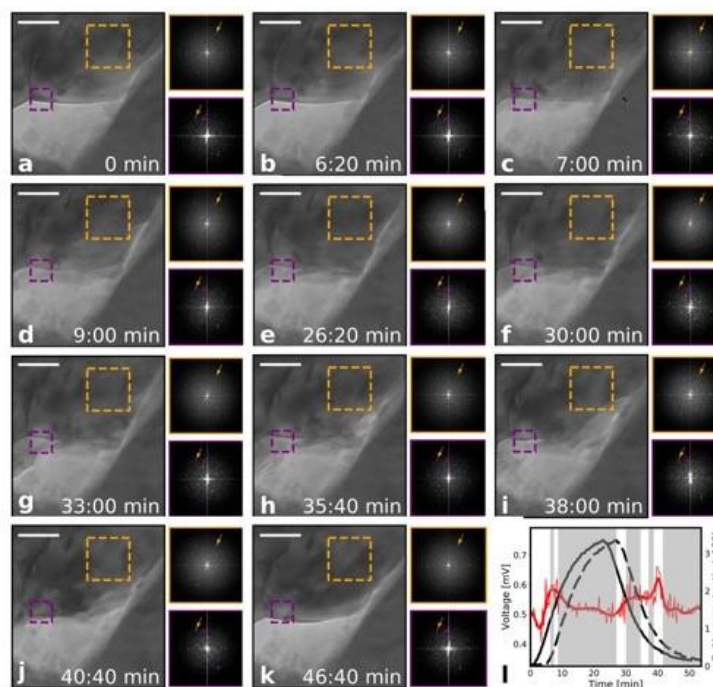


*Figure 2: a-k) Bright field TEM around the edge of a Ni grain at the critical steps of the reoxidation and reduction processes. The time corresponds to the white/grey areas in i). Scale bars: 20 nm. i) RGA O<sub>2</sub>-to-H<sub>2</sub> ratio (raw data, black full line, and shifted forward in time by 180 seconds, black dashed line), and voltage measured between the anode and cathode (raw and Gaussian-filtered data, red lines).*

**SDM2-P4****Changement de phase déclenché in situ par un plasma d'hydrogène****H2 plasma triggers nanoparticle phase change in situ**

- **Jean-Luc MAURICE** \* (jean-luc.maurice@polytechnique.edu) / École polytechnique, IP Paris, LPICM, CNRS UMR7647
- **Weixi WANG** / École polytechnique, IP Paris, LPICM, CNRS UMR7647
- **Erik V. JOHNSON** / École polytechnique, IP Paris, LPICM, CNRS UMR7647
- **Cyril JADAUD** / École polytechnique, IP Paris, LPICM, CNRS UMR7647
- **Pavel BULKIN** / École polytechnique, IP Paris, LPICM, CNRS UMR7647

\* Auteur correspondant

We report observations of plasma-assisted phase changes performed in situ in the NanoMAX environmental TEM. The plasma is produced in an electron-cyclotron-resonance plasma source (Aurawave from SAIREM). The objects are Sn-Cu nanoparticles used as catalysts in liquid-assisted vapour-solid-solid (LAVSS [1,2]) Si nanowire (NW) growth. This type of growth delivers 2H hexagonal silicon (a metastable structure that should have interesting optical properties [3]). The goal of our present in-situ study is to understand how the pre-treatment in H<sub>2</sub> plasma at 200°C allows one to transform wetting dispersed metal puddles into quasi-spherical catalyst spheres.

The H atoms generated by the plasma have the effects of reducing the Sn native oxide and changing the surface energy balance between particles and substrate. Sn, which has a low surface energy [4] tends to wet the substrate upon deposition and does not form the ball-shaped particles necessary for the growth of Si NWs [1,2,5]. Raising the temperature to 200°C and introducing H<sub>2</sub> in the TEM does not change this (Fig. 1a). Switching on the plasma (Fig. 1b) has the immediate effect of forming nanoballs (Figs. 1c and 2c). The phases present at 200°C consist of a core of a Cu-rich compound (Figs. 2a & d) and a wetting shell of amorphous Sn. Igniting the H<sub>2</sub> plasma finally results in the mixing of the two components in an alloy richer in Sn. Upon increasing temperature to 400°C and introducing SiH<sub>4</sub>, the latter will, in turn, change itself into Cu<sub>3</sub>Si and liquid Sn to drive the crystallisation of the metastable 2H phase [1,2]. (not shown here.)

Acknowledgements: we are indebted to CIMEX for the access to the TEMs at École polytechnique. This activity is partially funded through the TotalEnergies-LPICM ANR Industrial Chair "PISTOL" (Contract No. ANR-17-CHIN-0002-01).

**References :**

- [1] É. Ngo, et al., *J. Phys. Chem. C*, 125 (2021), p. 19773.
- [2] W. Wang, et al., *ACS Omega*, 6 (2021), p. 26381.
- [3] M. Amato, et al., *Nano Lett.*, 16 (2016), p. 5694.
- [4] C.T. Campbell, *Surf. Sci. Rep.*, 27 (1997), p. 1.
- [5] J.-L. Maurice, et al., *Euro. Phys. J. Appl. Phys.*, 97 (2022), p. 7.

**Mots clefs :** in situ TEM, environmental TEM, in situ plasma

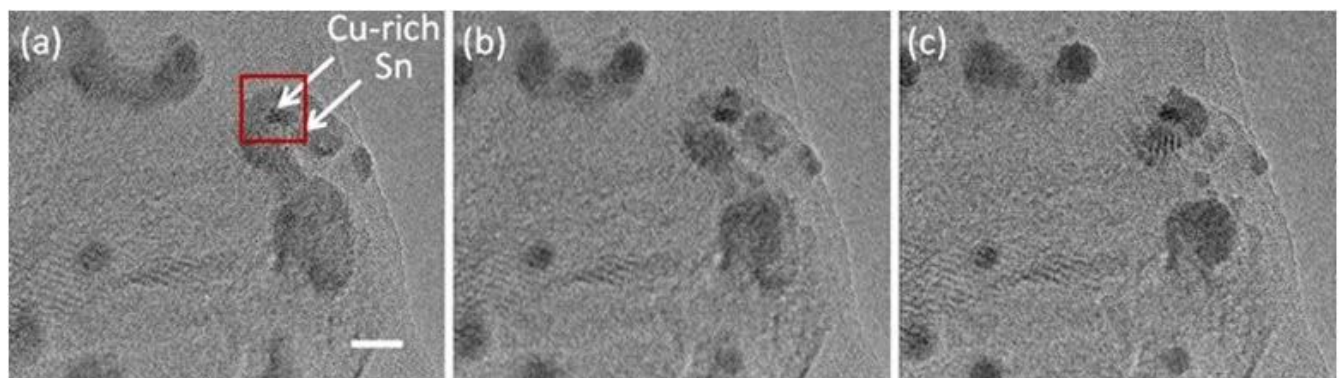


**Figure 1:** TEM images (extracted from a movie) of 1-nm of Sn deposited on 0.5-nm Cu (nominal thickness): a) before  $H_2$ -plasma ignition (no changes with time), b), at plasma ignition and c) 1 s after plasma ignition.  $H_2$  pressure  $3 \times 10^{-3}$  mbar; ECR plasma power 50 W; scale bar 10 nm. See enlarged view of red squared area in Fig. 2.

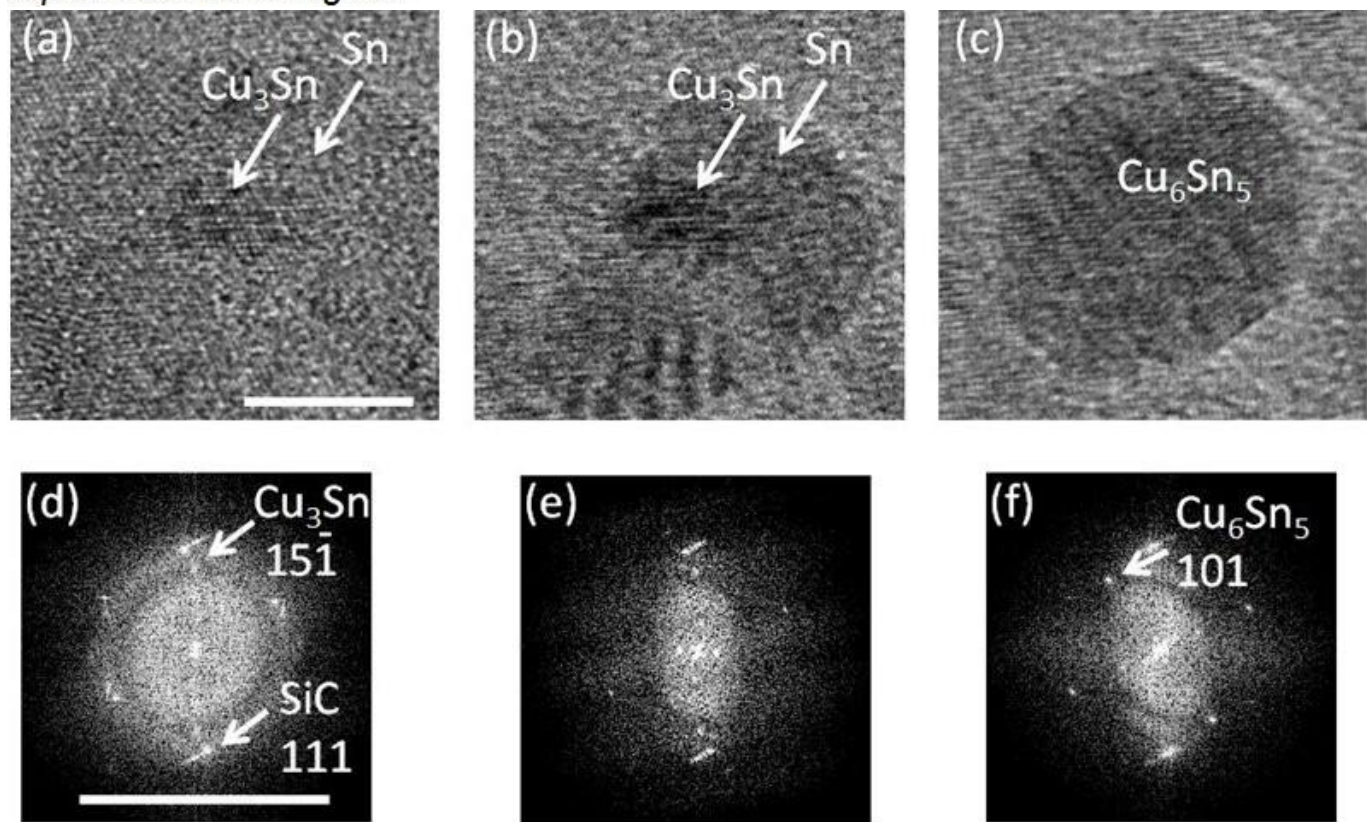


**Figure 2:** Enlarged view of squared area in Fig. 1, as a function of time: a) before plasma ignition; b) 1 s after plasma ignition; c) 10 s after plasma ignition, scale bar 5 nm. d,e,f) power spectra of respectively (a,b,c), showing the apparition of new phase due to  $H_2$  plasma, scale bar  $10 \text{ nm}^{-1}$ .

## SDM2-P5

### Développement d'un système de polarisation *in situ* cryogénique stable pour la résolution atomique (S)TEM

#### Development of a stable cryogenic *in situ* biasing system for atomic resolution (S)TEM

- **Yevheniy Pivak** \* (yevheniy.pivak@denssolutions.com) / DENSSolutions
- **Hongyu Sun** / DENSSolutions
- **Michelle Conroy** / Department of Materials, Faculty of Engineering, Imperial College London
- **Leopoldo Molina-Luna** / Advanced Electron Microscopy Division (AEM), TU Darmstadt

\* Auteur correspondant

The application of cryogenic TEM (cryo-TEM) methods to Materials Science and energy-related fields are mainly limited to beam sensitive materials like lithium-ion batteries, organic semiconductors, perovskite-based solar cells, polymers, Metal Organic Frameworks (MOFs), etc. Most low-temperature *in situ* experiments are carried-out using cryogenic holders based on liquid nitrogen and using 3mm sized TEM-grids. Despite their widespread use, grid-based cryogenic systems suffer from poor stability, making it challenging to obtain adequate atomic-resolution imaging conditions and, are time-consuming [1]. Additionally, these systems often have the inability to set intermediate temperatures, which limits the experiments to be performed at either liquid nitrogen temperature or room temperature. Furthermore, such systems are limited in applications when understanding the structure, electronic and transport properties of materials under an applied electrical stimuli at low temperatures is of interest. For such applications, a system with low sample drift that combines liquid nitrogen cooling with an external voltage bias is needed. Such a development would enable a vast range of applications in the field of quantum materials [2], magnetic materials and nanostructures, ferroelectrics [2], topological insulators, metal-to-insulator transitions, superconductors and would be extremely valuable in the *in situ* TEM community.

In this talk, we will share our latest developments with respect of a combined *in situ* cooling, biasing and heating system. The system includes a novel double-tilt cryogenic MEMS-chips based holder and uses liquid nitrogen for cooling. It has multiple electrical contacts that enables the setting of any intermediate temperature between LN2 and RT. Without the presence of the cooling agent, it is also possible to perform *in situ* heating experiments up to 800°C. By exploiting the high stability of this system and its double tilt capability, we will demonstrate how atomic resolution imaging at various temperatures could be achieved and present several application examples, including ferroelectric focused ion beam (FIB) lamellas.

#### References

- [1] E. Toutanova, J. V. Vas, R. Ignatis, A. D. Mueller, R. Medwal, M. Imamura, H. Asada, Y. Fukuma, R. S. Rawat, V. Tileli, M. Duchamp, Accounts of Chemical Research 54(16), 3125 (2021).
- [2] J.L. Hart, J.J. Cha, Nano Lett. 21, 5449 (2021)

**Mots clefs :** *in situ* TEM, cryogenic, biasing, atomic resolution

## SDM2-P6

### Suivi operando de la prise du plâtre par microscopie électronique en phase liquide

#### Operando characterization of plaster setting using Liquid-Phase Scanning Electron Microscopy

- **Alexandre Fantou** \* (alexandre.fantou@insa-lyon.fr) / Univ Lyon, INSA Lyon, Université Claude Bernard Lyon 1, CNRS, MATEIS, UMR5510, 69621 Villeurbanne, France
- **Anna Wozniak** / Univ Lyon, INSA Lyon, Université Claude Bernard Lyon 1, CNRS, MATEIS, UMR5510, 69621 Villeurbanne, France
- **Annie Malchère** / Univ Lyon, INSA Lyon, Université Claude Bernard Lyon 1, CNRS, MATEIS, UMR5510, 69621 Villeurbanne, France
- **Karine Masenelli-Varlot** / Univ Lyon, INSA Lyon, Université Claude Bernard Lyon 1, CNRS, MATEIS, UMR5510, 69621 Villeurbanne, France
- **Sylvain Meille** / Univ Lyon, INSA Lyon, Université Claude Bernard Lyon 1, CNRS, MATEIS, UMR5510, 69621 Villeurbanne, France
- **Solène Tadier** / Univ Lyon, INSA Lyon, Université Claude Bernard Lyon 1, CNRS, MATEIS, UMR5510, 69621 Villeurbanne, France

\* Auteur correspondant

Gypsum has been traditionally used as a building material, but can also be a model for the development of injectable biomaterials for bone substitution. Set plaster, or gypsum ( $\text{CaSO}_4 \cdot 2\text{H}_2\text{O}$ ), is prepared by mixing dry hemihydrate powder ( $\text{CaSO}_4 \cdot 0.5\text{H}_2\text{O}$ ) with water. Its properties as a solid binder are largely influenced by the setting reaction occurring when  $\text{CaSO}_4 \cdot 0.5\text{H}_2\text{O}$  dissolve and crystals of gypsum precipitate. It is well known that the resulting solid is formed by an interlocked network of gypsum needles and platelets, but the exact setting process is not well understood yet. The objective of our study is therefore to monitor the evolution of crystals and understand the entire setting process, using operando observations [1], using Liquid-phase scanning electron microscopy.

The most convenient set-up for such monitoring has found to be sealed Quantomix cells [2]. They are indeed water- and airtight, and therefore plaster evolves under the same conditions as in real use, especially in terms of water-to-plaster ratio. The influence of several experimental parameters (addition of a retardant to monitor the whole setting process, image acquisition conditions and irradiation damage, presence of a membrane) will be discussed. We will describe image processing and analysis procedures we developed to distinguish the hemihydrate particles dissolving in the mixture from the gypsum crystals growing over time (Figure 1), and therefore plot the fraction of gypsum vs time. To go into more details in the analysis of gypsum growth, we will propose an indexation of the gypsum crystal facets based on geometric information and the knowledge of the equilibrium morphologies [3]. The growth rates of the different planes will be discussed and compared with values found in the literature.

#### References

- [1] J. Seiller et al, Construction and building materials, 2021, 304, 124632.
- [2] E. Gallucci et al, Advances in Applied Ceramics 2013, 106, 319-326.
- [3] B. Madeja et al, Cement and Concrete Research, 2023, 164, 107049.

**Mots clefs :** liquide, operando, MEB, analyse d'image

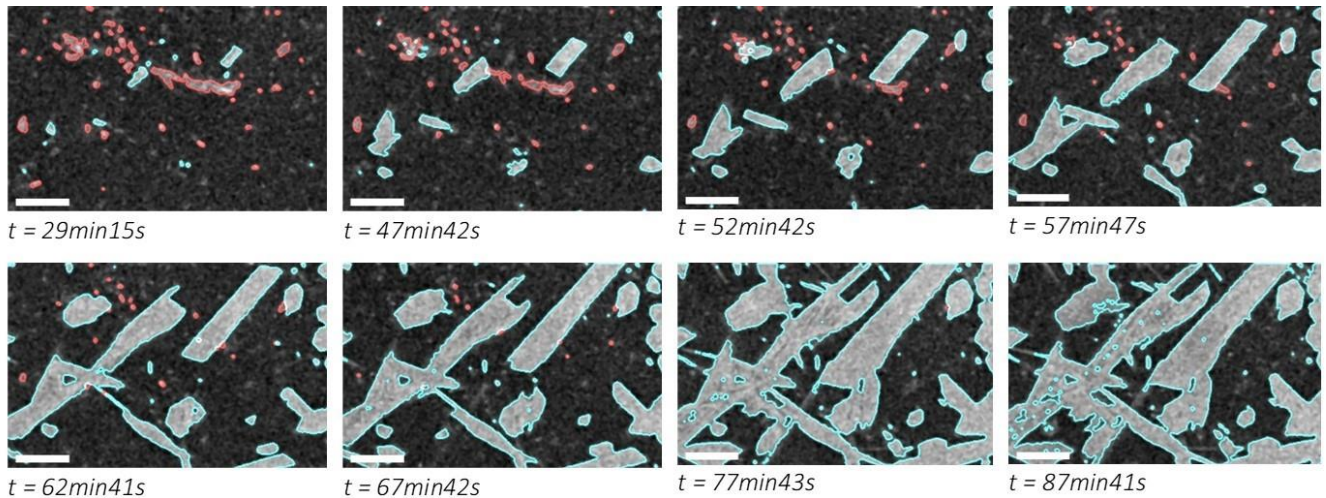


Figure 1. Evolution of hemihydrate (red) and gypsum (blue) during the hydration reaction of plaster (scale bar  $10 \mu\text{m}$ ).

## SDM2-P7

### **Suivi en direct de la nucléation et de la croissance des nanoparticules d'oxyde de zinc par microscopie électronique à transmission liquide in situ**

**Direct monitoring of the nucleation and growth of Zinc oxide nanoparticles by in situ liquid transmission electron microscopy**

- **Dris Ihiawakrim** \* (dris.ihiawakrim@ipcms.unistra.fr) / Institut de Physique et Chimie des Matériaux de Strasbourg CNRS-Université de Strasbourg
- **Ovidiu Ersen** \* (ovidiu.ersen@ipcms.unistra.fr) / Institut de Physique et Chimie des Matériaux de Strasbourg (IPCMS) CNRS-Université de Strasbourg
- **Stéphane Daniel** \* (stephane.daniele@univ-lyon1.fr) / Laboratoire de Catalyse, Polymérisation, Procédés et Matériaux (CP2M), CNRS – Université de Lyon
- **Fabien GRASSET** \* (fabien.grasset@univ-rennes1.fr) / Institut des Sciences Chimiques de Rennes (ISCR), CNRS – Université de Rennes1

\* Auteur correspondant

The recent development of liquid phase TEM (LP-TEM) allows the direct monitoring of dynamic processes in well controlled environments and opens the way for new time resolved analyses, in order to provide real time insight into the reaction mechanisms that involve processes such as aggregation or nanostructuring [1].

This work reports on the LP-TEM in situ (S)TEM analysis of the processes of nucleation and growth of ZnO nanoparticles in conditions as close as possible to the real ones, in a chemical reactor, by minimizing the influence of the electron beam on the reaction medium [1]. We performed and compared two reactions based on the same precursor AcOZn dispersed in ethanol with two different bases LiOH and KOH dispersed in ethanol as well [2]. The reaction mixture is done just before the observation zone on the silicon nitride membrane of a “Protochips” (Poseidon) liquid cell (Figure a). The in situ monitoring was performed on a JEOL 2100F/Cs (S)TEM microscope operating at 200 kV by using continuous acquisition mode (in TEM and STEM) in order to acquire dynamic events at different process steps [3]. The direct observation, in the real space, of the nucleation step sheds new light on the co-precipitation method. Using LiOH, we observed an Ostwald ripening type mechanism which provides anisotropic nanoparticles (figure 1c). With KOH, a LaMer type mechanism was evidenced which led to isotropic nanoparticles (figure 1d). By following step by step the evolution of the typical structures in the areas of interest, we demonstrated that the nucleation step plays a crucial role in determining the final shape of the nanoparticles. Finally, we use artificial intelligence to track the various stages of the processes in order to learn about the important steps, the different kinetics, and the applied mechanisms.

#### Références/References :

- [1]. James E. Evans et al. Nano Lett. 2011, 11, 2809–2813.
- [2]. Rajendra C. Pawar et al. Current Applied Physics 14 (2014) 621e629.
- 3. Ting Wang et al. The Journal of Physical Chemistry C 2020 124 (28), 15533-15540.

**Mots clefs** : LP- (S)TEM in situ, nucleation, growth, dynamic, real-time, heating, ZnO nanoparticles

## SDM2-P8

### Caractérisation des matériaux sensibles aux électrons à l'aide de la tomographie STEM en phase liquide multi-échelles dans l'ESEM et l'ETEM

#### Characterizing electron sensitive materials using multiscale Liquid-Phase STEM Tomography in ESEM and ETEM

- **Louis-Marie Lebas** \* (louis-marie.lebas@insa-lyon.fr) / Univ Lyon, INSA Lyon, UCBL, CNRS, MATEIS, UMR5510, 69621 Villeurbanne, France
- **Lucian Roiban** / Univ Lyon, INSA Lyon, UCBL, CNRS, MATEIS, UMR5510, 69621 Villeurbanne, France
- **Victor Trillaud** / Univ Lyon, INSA Lyon, UCBL, CNRS, MATEIS, UMR5510, 69621 Villeurbanne, France
- **Mimoun Aouine** / Institut de recherches sur la catalyse et l'environnement de Lyon (IRCELYON), UMR 5256  
CNRS & Université Lyon 1, 2 avenue Albert Einstein, F-69626 Villeurbanne, France
- **Karine Masenelli-Varlot** / Univ Lyon, INSA Lyon, UCBL, CNRS, MATEIS, UMR5510, 69621 Villeurbanne, France \* Auteur correspondant

For both biology and materials science applications, samples in hydrated state are really worthwhile to study in 3D at the nanometre scale, because interesting phenomena only occur in such native state. Environmental tomography addresses this issue by enabling the creation of 3D models through the acquisition of tilt series, under partial gas pressure [1, 2]. In addition, STEM mode provides chemical and structural information and a dose lower than that required in conventional TEM can be used in STEM [1]. A new protocol has been developed to overcome at the same time two major issues: time resolution and dose control, necessary for the analysis of beam-sensitive organic materials. The solution consists mainly of acquiring automatically a tilt series with a large field of view, within in a few minutes. During this time range, the sample stays in its hydrated state, and the deposited dose is quantified.

The protocol has been implemented on a QuattroS ESEM and a Titan ETEM, to take advantage of the different acceleration voltages and corresponding spatial resolutions. A dedicated stage controls the sample temperature while the microscope regulates the pressure. The whole system is automated through a software we coded. It provides automatic eucentric set-up, dynamical drift correction and other helpful tools. Post-processing and 3D reconstruction are made offline with ImageJ, TomoJ and 3D Slicer. We will present results that validated the protocol and the software specifications with reference materials. We will also show various studies on hydroxide wet gel suspensions and amphiphilic block copolymer nanorods, with antigenic gold-labelling. The tomograms exhibit a resolution from about 10 nm in ESEM to 1 nm in ETEM, showing the possibility of quantifying quickly the sample structure at the nanometer scale while in liquid state. Furthermore, the electron dose is quantified and kept below the degradation threshold.

#### References:

- [1]S. Koneti et al, Fast electron tomography: Applications to beam sensitive samples and in situ TEM or operandoenvironmental TEM studies. Materials Characterization 151, 2019.
- [2]X. Jiao et al, Electron tomography on latex particles suspended in water using environmental scanning electronmicroscopy, Micron, 2019, 117.

**Mots clefs :** Liquid, 3D, Electron, Microscopy, In situ

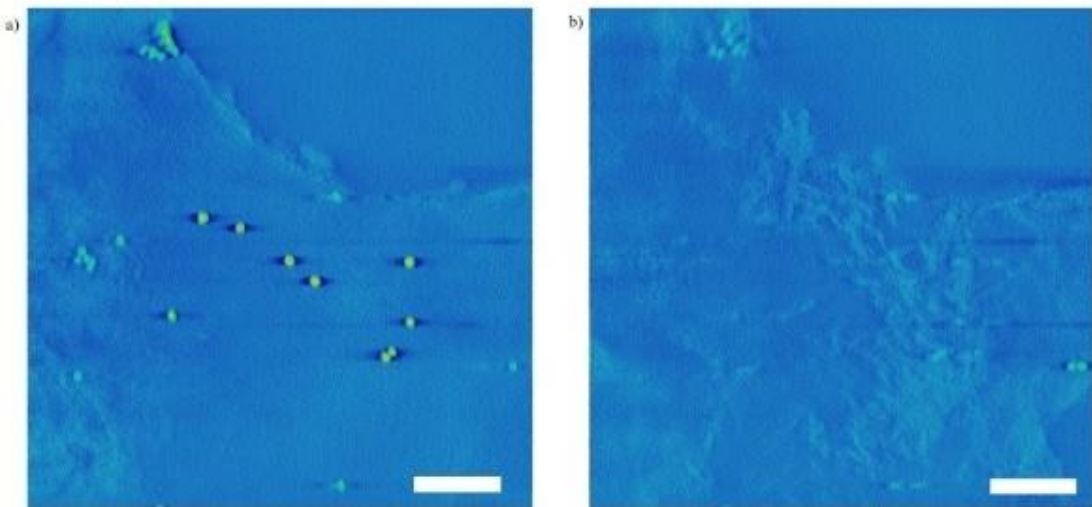


Figure 1: Two slices of a AIOOH reconstructed tomogram at different z values. a) is centered on gold nanoparticles as fiducial beads, and b) shows the nanoporous structure of the material (scale bars 150 nm).

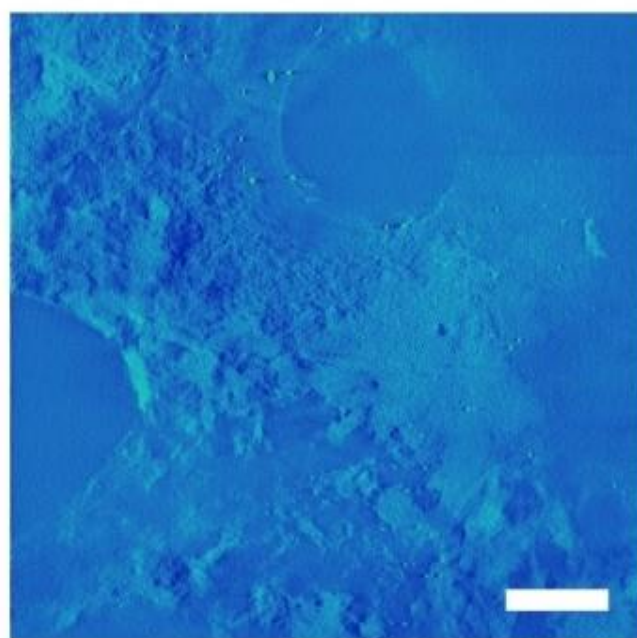


Figure 2: Slice of a AIOOH reconstructed tomogram. Some gold nanoparticles are visible, as is the nanoporous structure of the material (scale bar 600 nm).

## SDM2-P9

### Formation et évolution de catalyseurs modèles AuxPd<sub>1-x</sub> sous environnements gazeux et en température variable dans un ETEM

Formation and evolution of AuxPd<sub>1-x</sub> model catalysts under gaseous environments and variable temperature within an ETEM

- **Francisco José CADETE SANTOS AIRES** \* (francisco.aires@ircelyon.univ-lyon1.fr) / Université de Lyon, UCB Lyon1, UMR CNRS 5256, IRCELYON. Villeurbanne, France.
- **Eric EHRET** / Université de Lyon, UCB Lyon1, UMR CNRS 5256, IRCELYON. Villeurbanne, France.
- **Bruno DOMENICHINI** / Université de Bourgogne Franche-Comté, UB, UTBM, UMR CNRS 6303, ICB, Dijon, France.
- **Laurence BUREL** / Université de Lyon, UCB Lyon1, UMR CNRS 5256, IRCELYON. Villeurbanne, France.
- **Thierry EPICIER** / Université de Lyon, UCB Lyon1, UMR CNRS 5256, IRCELYON. Villeurbanne, France.

\* Auteur correspondant

Networks of nanoparticles (NPs) with well-controlled characteristics (size, composition, inter-distance) can be obtained by the di-block copolymer approach; an amphiphilic di-block copolymer dissolved in toluene yields a system of inverse micelles whose core can be charged with metallic precursors to yield such networks. The latter can be used as model catalysts when transferred to flat surfaces. The formation of individual NPs within the cores and the stability of the networks with increasing temperature under reactive gases have yet to be investigated. To do so we used an Environmental TEM (Titan ETEM/G2, TFS) operated at 300kV, under gas pressures upto 10 mbar during heating under oxygen and CO, together with a WildFire sample-holder with dedicated heating MEMS-microchips (DENSSolutions).

We used PS-b-P2VP di-block copolymer micelles metallized with HAuCl<sub>4</sub> and Pd(CH<sub>3</sub>COO)<sub>2</sub> precursors to obtain Au-rich and Pd-rich AuxPd<sub>1-x</sub> systems. The precursors selectively bind with N-functions in the P2VP cores to form bimetallic seeds as it was previously established in the case of PdAg NPs [1]. Monolayers of controlled AuxPd<sub>1-x</sub> core-metallized micellar solutions were deposited by spin-coating on the microchips. Safe illumination conditions were deduced from preliminary irradiation tests to minimize electron-beam influence during the observations.

In the case of Au<sub>80</sub>Pd<sub>20</sub>, the bimetallic seeds within the P2VP cores (Fig.1) begin to sinter around 350°C and unique NPs are eventually formed around 500°C, under oxygen; this is consistent with the decomposition temperature range of the PS-b-P2VP copolymer [2]. The NPs network is stable upto 900°C. Approaching the gold melting temperature (1064°C) the NPs begin to decompose without affecting the network frame. Regarding Au<sub>20</sub>Pd<sub>80</sub>, under oxygen, the seeds begin to sinter around 300°C and, at 450°C, NPs demixing is observed leading to Janus NPs (Au-rich/PdO; Fig.2); the latter are readily reduced upon CO exposure and bimetallic NPs reform. The stability of the bimetallic NPs networks seems to be driven by the intrinsic properties of the metals composing them.

We thank the METSA network for support and the CLYM for access to the ETEM.

#### References:

[1] E. Ehret et al., *Nanoscale*, 7 (2015), p.13239

[2] T. Orhan Lekesiz et al., *J. Anal. Appl. Pyrolysis*, 106 (2014), p.81

**Mots clefs :** di-block copolymer micelles, AuPd nanoparticle networks, stability under variable gas pressure and temperature, Janus nanoparticles, Environmental TEM

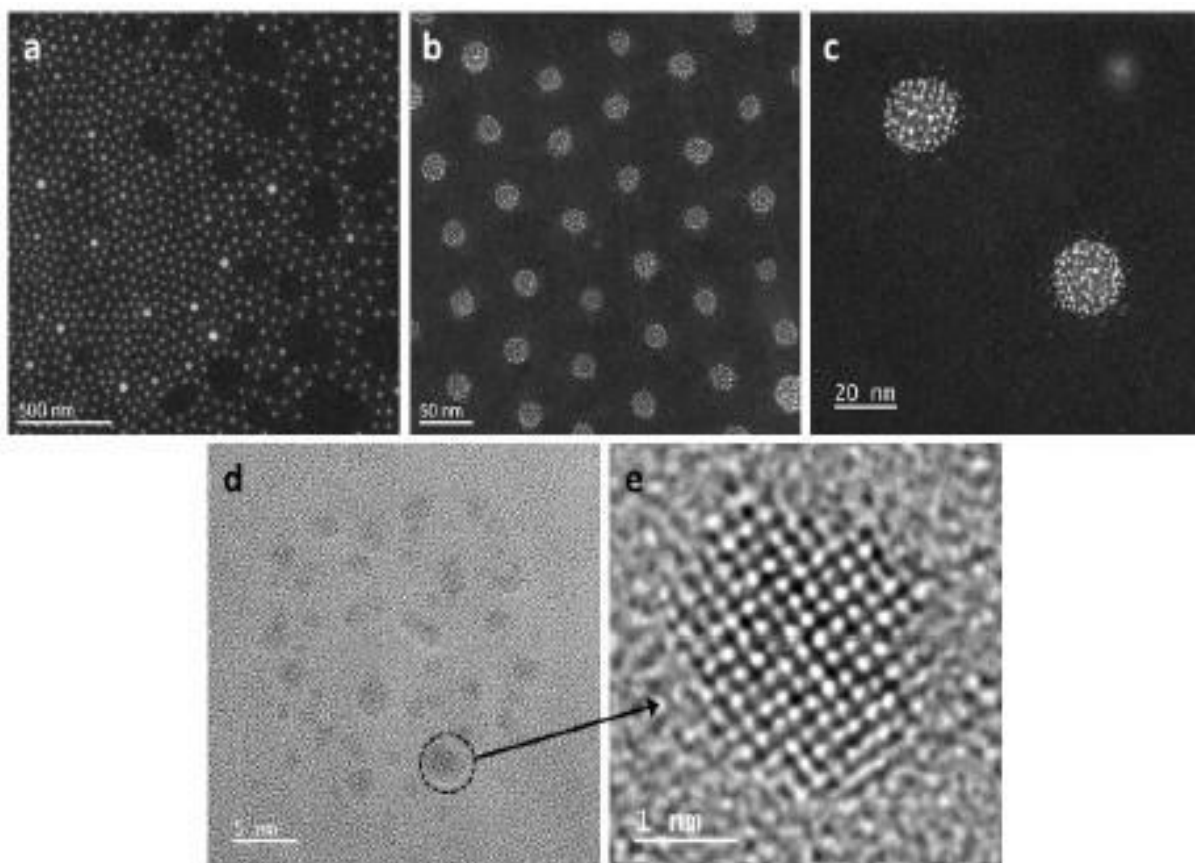


*Figure 1: Au-rich system ( $Au_{80}Pd_{20}$ ): (a-c) STEM-ADF images of the network of metallized micelles' cores at different scales; (d) BF image of an individual metallized core showing the presence of multiple 1-3 nm crystalline seeds; (e) HR image of a  $<100>$ -oriented seed.*

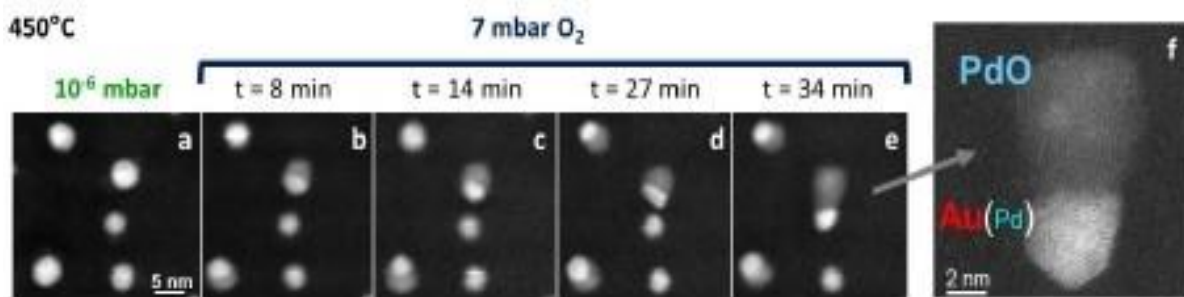


*Figure 2: Pd-rich system ( $Au_{20}Pd_{80}$ ): (a) NPs under vacuum; (b-c) formation of the Janus NPs (Au-rich/PdO) under oxygen at  $450^\circ C$ ; (f) HR image of a Janus NP.*

## SDM2-P10

### Étude de la charge d'interface dans les empilements diélectriques tri-couches par des expériences d'holographie électronique operando

Investigation of interface charging in tri-layer dielectric stacks by operando electron holography experiments

- **Leifeng ZHANG** \* (leifeng.zhang@cemes.fr) / CEMES-CNRS, 31055 Toulouse cedex, France
- **Kilian GRUEL** / CEMES-CNRS, 31055 Toulouse cedex, France
- **Muhammad Hamid RAZA** / Helmholtz-Zentrum Berlin für Materialien und Energie, Hahn-Meitner-Platz 1, Berlin 14109, Germany
- **Catherine DUBOURDIEU** / Helmholtz-Zentrum Berlin für Materialien und Energie, Hahn-Meitner-Platz 1, Berlin 14109, Germany; Freie Universität Berlin, Physical Chemistry, Arnimallee 22, Berlin 14195, Germany
- **Martin HYTCH** / CEMES-CNRS, 31055 Toulouse cedex, France
- **Christophe GATEL** / CEMES-CNRS, 31055 Toulouse cedex, France; Université Paul Sabatier, 31062 Toulouse cedex, France

\* Auteur correspondant

Resistive random access memory (RRAM) containing high-k dielectric tri-layer stacks of HfO<sub>2</sub> and Al<sub>2</sub>O<sub>3</sub> could be promising candidates for the synaptic devices in neuromorphic computing [1, 2]. However, the mechanism behind the trapping behaviour remains unclear, since traditionally, it is impossible to observe experimentally the electrical potential distribution within such devices upon biasing. We have shown recently that operando electron holography can be used for such purposes [3], the hologram phase being proportional to the electrical potential. Here, we apply the technique to thin HfO<sub>2</sub>/Al<sub>2</sub>O<sub>3</sub>/HfO<sub>2</sub> (HT-1) and Al<sub>2</sub>O<sub>3</sub>/HfO<sub>2</sub>/Al<sub>2</sub>O<sub>3</sub> (HT-2) dielectric stacks.

Thin films were fabricated by atomic layer deposition (ALD). As shown in Fig. 1(a) & (b), both tri-layer HT-1 and HT-2 structures, were successfully prepared. Each HfO<sub>2</sub> or Al<sub>2</sub>O<sub>3</sub> layer has a nominal thickness of 20 nm. TiN serves as both top and bottom electrodes during electrical biasing. Specimens for operando experiments were prepared by focused ion beam (FIB), for a Hummingbird chip-based biasing holder on the I2TEM microscope operating at 300kV.

The phase profiles of HT-1 and HT-2 are presented in Fig. 1(c) & (d), respectively. In both cases, the measured phase change across the stack, increases with the increased bias, as expected. However, the potential distributions as well as the measured electrical fields are quite different from those expected theoretically. Considering a relative permittivity of 7-8 for Al<sub>2</sub>O<sub>3</sub> and 20-22 for HfO<sub>2</sub>, the electrical field should be 2-3 times higher in Al<sub>2</sub>O<sub>3</sub> than HfO<sub>2</sub>, which consequently results in a 2-3 times higher potential drop in Al<sub>2</sub>O<sub>3</sub>. In contrast, the experimental profiles give an equivalent phase distribution in both layers for both HT-1 and HT-2. According to finite element modelling (FEM) simulations using COMSOL software, two charged interface layers, with a surface charge density of ~1.5 µC/cm<sup>2</sup> (positive or negative), are required to fit the phase profiles. For HT-1 and HT-2, a comparison of phase distributions between experiments and simulations at 6V are made in Fig. 1(e) and (f).

#### References:

- [1]C. Mahata, et al., Nanomaterials, 10(2020), 2069
- [2]E. A. Khera, et al., RSC advances, 12(2022), 11649
- [3]C. Gatel, et al., Physical Review Letters, 129(2022), 137701

**Mots clefs :** RRAM; charge trapping; operando electron holography; FIB

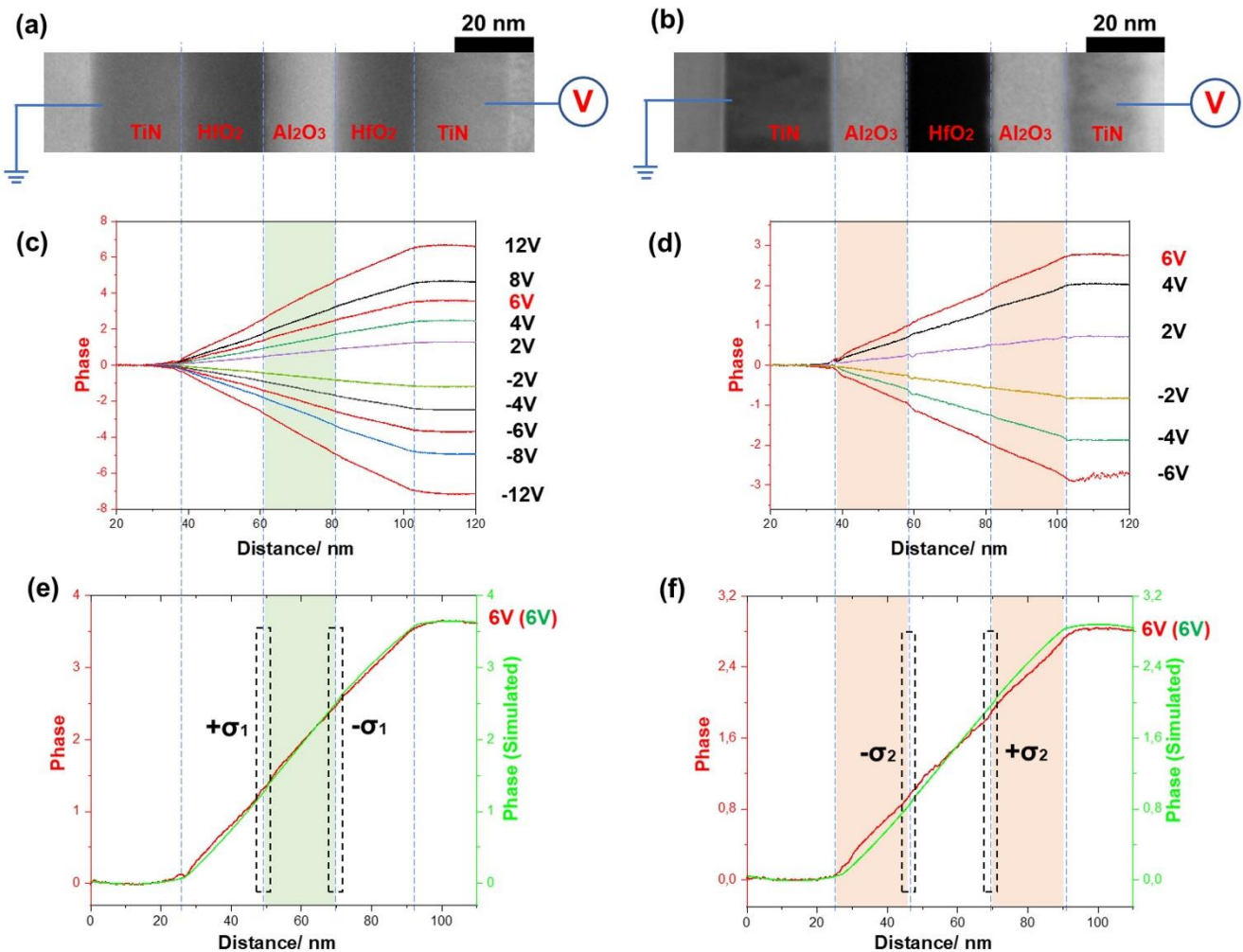


Figure 1: Operando electron holography experiments: (a) – (b) TEM images showing the tri-layer capacitors (a) HT-1: HfO<sub>2</sub>/Al<sub>2</sub>O<sub>3</sub>/HfO<sub>2</sub> and (b) HT-2: Al<sub>2</sub>O<sub>3</sub>/HfO<sub>2</sub>/Al<sub>2</sub>O<sub>3</sub>; (c) – (d) phase profiles as a function of applied bias for (c) HT-1 and (d) HT-2; (e) – (f) Comparison between experiments and FEM simulations at 6V for (e) HT-1 and (f) HT-2. In (e) and (f),  $\sigma_1$  and  $\sigma_2$  represent the charge densities at the interfaces of HT-1 and HT-2, respectively.

**SDM2-P11****Etude corrélative multi-microscopies de nano-assemblages de Pt électrodeposités comme plateformes de précipitation pour Ni(OH)2****Correlative multi-microscopies study of electrodeposited Pt nano-assemblies as precipitation platforms for Ni(OH)2**

• **Nathaly Ortiz Peña** \* (nathaly.ortiz@u-paris.fr) / Université Paris Cité, CNRS, Laboratoire Matériaux et Phénomènes Quantiques, 75013 Paris, France

• **Louis Godeffroy** / Université de Paris, ITODYS, CNRS UMR 7086, 15 rue J.A. de Baïf, F-75013 Paris, France

• **Jean-François Lemineur** / Université de Paris, ITODYS, CNRS UMR 7086, 15 rue J.A. de Baïf, F-75013 Paris, France

• **Frédéric Kanoufi** / Université de Paris, ITODYS, CNRS UMR 7086, 15 rue J.A. de Baïf, F-75013 Paris, France

• **Damien Alloyeau** / Université Paris Cité, CNRS, Laboratoire Matériaux et Phénomènes Quantiques, 75013 Paris, France

• **Jean-Marc Noël** / Université de Paris, ITODYS, CNRS UMR 7086, 15 rue J.A. de Baïf, F-75013 Paris,

France \* Auteur correspondant

Nanoscience involving nanoparticles (NPs) is a key element in the development of the next generation of efficient and safe systems enabling the conversion or storage of renewable energy. NPs being intrinsically heterogeneous in size, shape or composition, it is of prime importance to develop strategies able to investigate chemical processes at the single entity level or even at the sub-entity level. This will allow identifying structure-activity relationships that is fundamental to predict and control the activity of the NPs. Herein, we have harnessed the controlled monitoring of individual NPs electrodeposited on micrometric conductive surfaces to visualize operando by electrochemical transmission electron microscopy (EC-TEM) and post-mortem high resolution TEM (HR-TEM) their electrocatalytic activity. It is exemplified herein by tracking the electrodeposition of platinum nano-assemblies (Pt-NA) and their modification by Ni(OH)2. This electrochemical decoration of Pt nanostructures with metal hydroxides like Ni(OH)2 is of great interest for the enhancement of hydrogen evolution reaction efficiency in alkaline media.<sup>1</sup> In this sense, we have been able to analyze the morphologies of the electrodeposited Pt-NA post-mortem by HR-TEM depending on the electrodeposition strategy, whereas the precipitation of Ni(OH)2 was followed operando by EC-TEM. Complementary post-mortem analysis the structure by energy dispersive spectroscopy (EDS) and HR-TEM allowed determining the structure of the bifunctional material. Finally the reactivity of the Ni(OH)2/Pt for the hydrogen evolution reaction was investigated by EC-TEM.

**References**

1. Liu, Q. et al. Optimizing Platinum Location on Nickel Hydroxide Nanosheets to Accelerate the Hydrogen Evolution Reaction. *ACS Appl. Mater. Interfaces* 12(2020), 24683–24692.

**Mots clefs :** Correlative multi-microscopies, optical microscopy, in situ electrochemical transmission electron microscopy, Pt nano-assemblies, Ni(OH)2 precipitation

## SDM2-12

### Stabilité thermique des nanoparticules d'alliage à haute entropie étudiée par microscopie électronique en transmission in-situ

#### Thermal stability of High Entropy Alloy Nanoparticles studied by in-situ Transmission Electron Microscopy

- **Syrine KROUNA** \* (syrine.krouna@u-paris.fr) / Université Paris Cité, CNRS, Laboratoire Matériaux et Phénomènes Quantiques, 75013 Paris, France
  - **Jaysen Nelayah** / Université Paris Cité, CNRS, Laboratoire Matériaux et Phénomènes Quantiques, 75013 Paris, France
  - **Christian Ricolleau** / Université Paris Cité, CNRS, Laboratoire Matériaux et Phénomènes Quantiques, 75013 Paris, France
  - **Guillaume Wang** / Université Paris Cité, CNRS, Laboratoire Matériaux et Phénomènes Quantiques, 75013 Paris, France
  - **Hakim Amara** / Laboratoire d'Etude des Microstructures, ONERA – CNRS, Chatillon, France et Université Paris Cité, CNRS, Laboratoire Matériaux et Phénomènes Quantiques, 75013 Paris, France
  - **Damien Alloyeau** / Université Paris Cité, CNRS, Laboratoire Matériaux et Phénomènes Quantiques, 75013 Paris, France
- \* Auteur correspondant

Since their first report in 2004, high entropy alloys (HEAs) in bulk form have triggered significant research interests owing to their highly tunable chemical composition and enhanced physical and chemical properties. At the nanoscale, the physico-chemical properties of HEA nanoparticles (NPs) are even more enhanced, making them interesting candidates for several catalyzed reactions. Among these, many are conducted at high temperatures. Consequently, studying the thermal stability of these nanomaterials is required to understand their reactivity at high temperatures. In this contribution, we report the synthesis and in situ atomic-scale investigation of the structural and chemical evolution of single CoNiCuPtAu NPs between 200 and 700°C.

The HEA NPs were synthesised on silicon nitride (SiN) substrate using pulsed laser deposition, allowing control of both particle composition and size[1]. In situ TEM heating experiments combining atomic-scale STEM imaging with single nanoparticle chemical analysis by STEM-EDS were performed in an aberration-corrected JEOL ARM 200F TEM, using a Protochips Atmosphere gas/heating holder. In situ visualization reveals the coarsening of the HEA NPs upon annealing as from 400°C, mainly driven by thermo-activated coalescence phenomena (figure 1a). These phenomena generate large-sized NPs presenting several crystalline defects, mostly with twinned and multi-twinned structures (figure 1b). Furthermore, as shown in figure 2a NPs stay well alloyed, aside from Au segregation effects occasionally observed in some NPs (figure 2b). Nevertheless, figure 1c shows that at very approaching high temperature (700°C), a composition change was measured due to the sublimation of copper and gold from the NPs, which remain crystalline.

These results showcase the difficulty to control the size and composition of HEA NPs at high temperature, a peculiar behaviours to consider and study, in order to get a better and efficient uses of HEA NPs.

#### References:

[1] Andrea Barbero et al., Faraday Discuss., vol. 242, pp. 129–143, 2022.

**Mots clefs :** High Entropy Nanoalloys, in-situ heating TEM, High Resolution STEM, STEM-EDX Mapping, growth mechanism, sublimation

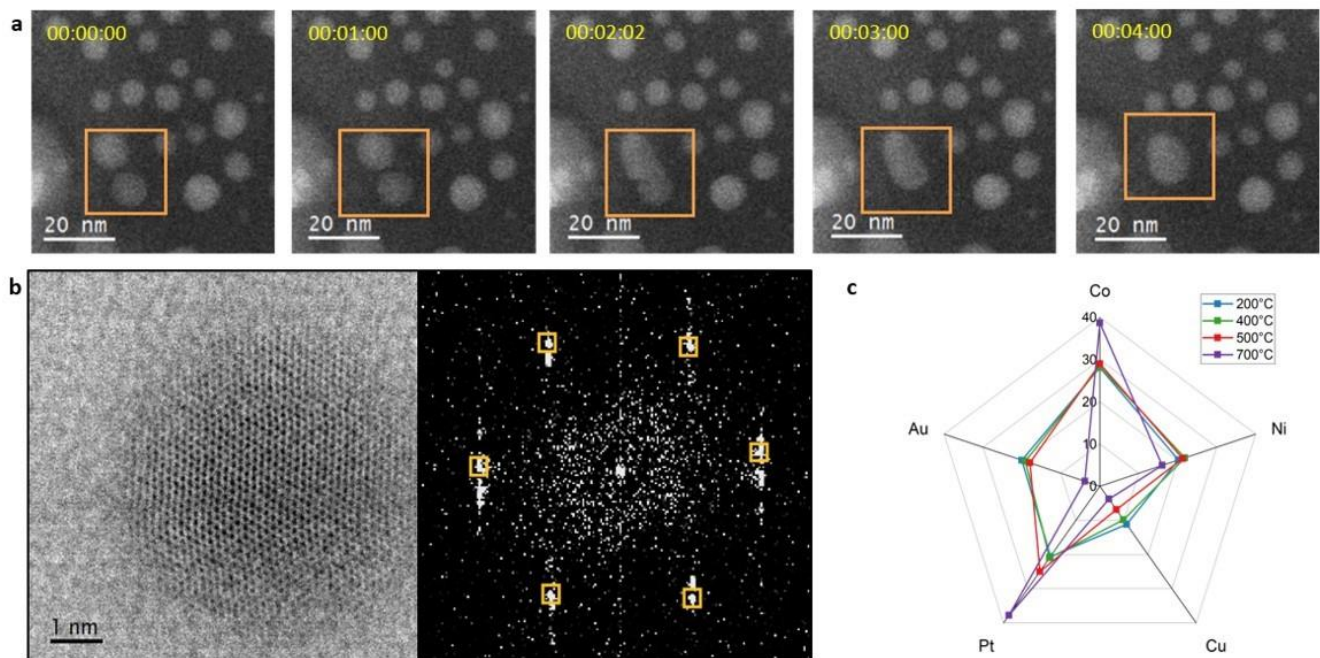


*Figure 1. (a) Coalescence event of NPs recorded in real time by STEM HAADF at 700°C. The acquisition time is indicated in the top left corner of each image. (b) Atomic scale STEM BF image of a twinned CoNiCuPtAu NP with the corresponding FFT, [220] patterns are shown in orange. (c) The evolution of the mean composition of individual NPs measured STEM-EDX analyses at single particle level.*

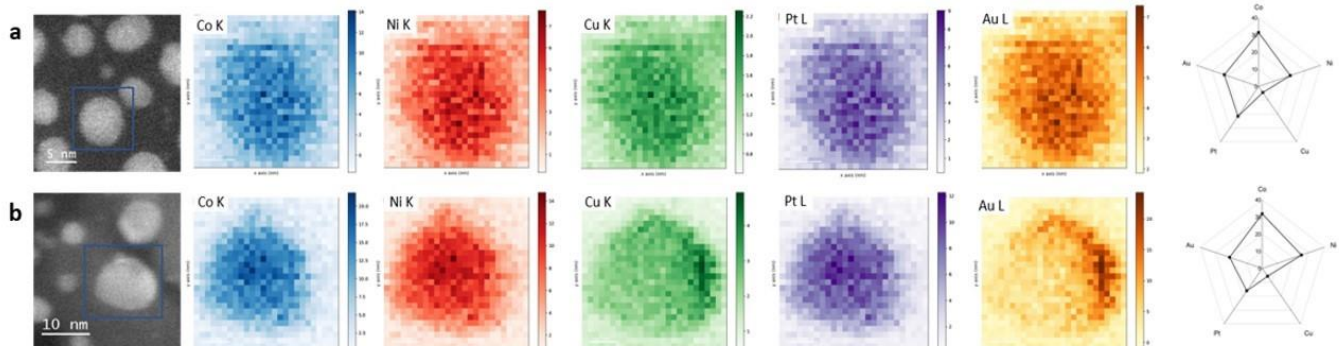


*Figure 2. STEM HAADF images and EDS elemental maps of CoNiCuPtAu NPs on SiN at 500°C with the corresponding composition showing (a) a well alloyed NP and (b) a segregated NP with gold and copper segregated at the surface*

## SDM2-P13

### Les nouvelles opportunités offertes par la combinaison de la sonde atomique tomographique et du MET en un seul instrument pour la caractérisation des métaux et alliages

New operando APT-TEM: new possibilities for atomic scale characterization of metals and alloys

- **Olha Nakonechna** \* (olha.nakonechna@univ-rouen.fr) / Univ Rouen Normandie, INSA Rouen Normandie, CNRS, Groupe de Physique des Matériaux UMR 6634, F-76000 Rouen, France
- **Macchi Juan** / Univ Rouen Normandie, INSA Rouen Normandie, CNRS, Groupe de Physique des Matériaux UMR 6634, F-76000 Rouen, France
- **Castro Celia** / Univ Rouen Normandie, INSA Rouen Normandie, CNRS, Groupe de Physique des Matériaux UMR 6634, F-76000 Rouen, France
- **Da Costa Gérald** / Univ Rouen Normandie, INSA Rouen Normandie, CNRS, Groupe de Physique des Matériaux UMR 6634, F-76000 Rouen, France
- **Vurpillot François** / Univ Rouen Normandie, INSA Rouen Normandie, CNRS, Groupe de Physique des Matériaux UMR 6634, F-76000 Rouen, France
- **Lefebvre Williams** / Univ Rouen Normandie, INSA Rouen Normandie, CNRS, Groupe de Physique des Matériaux  
UMR 6634, F-76000 Rouen,

France \* Auteur correspondant

With Atom Probe Tomography (APT), composition fields and chemical segregations can be identified in a 3D space. However, two main limitations of this unique tool can be enounced: i) first, due to limited knowledge of the APT specimen geometry during its field evaporation in APT, room exists to improve APT reconstruction and ii) second, the presence and nature of crystal defects cannot be determined with enough accuracy. Both points can be at least partially overcome by combining APT with Scanning Transmission Electron Microscopy (STEM). In the present study, a new APT-TEM instrument is presented. This instrument will allow to relate the chemical nature of the segregation to the nature of the crystal defect as well as to create better 3D reconstructions.

In the new adapted STEM, operando APT-4DSTEM experiments will be possible thanks to a coupling with an event-based nanosecond-resolution camera. As a consequence, some innovating characterization will be accessible as mapping the electric field around a sample tip. Follow the evolution of the electric field during the tip evaporation can give some insight of the electro-magnetic properties of the sample matrix as well as of some second phases which may be present. This work presents the first steps towards the combination of STEM and APT, with special emphasis of field mapping in STEM applied to polarized APT specimens.

Acknowledgement – The Normandy Region is acknowledged for the funding of project RIN Tremplin Fusion SATMET.

**Mots clefs :** APT; TEM; in operando

## SDM2-P14

### In situ STEM monitoring of ferroelectric phase transitions of antiferroelectric PbZrO<sub>3</sub> thin films

**In situ STEM monitoring of ferroelectric phase transitions of antiferroelectric PbZrO<sub>3</sub> thin films**

.Maxime Vallet \* (maxime.vallet@centralesupelec.fr) / Université Paris-Saclay, CentraleSupélec, CNRS, Laboratoire SPMS et LMPS, 91190, Gif-sur-Yvette, France

\* Auteur correspondant

The archetypical antiferroelectric, PbZrO<sub>3</sub>, is currently attracting a lot of interest but no consensus can be clearly established on the nature of his ground state as well as on the influence of external stimuli over its physical properties.

Here, a 45-nm-thick epitaxial thin films of PbZrO<sub>3</sub> and its behavior in temperature from 300 K (RT) to 570 K has been studied by coupling electron diffraction and atomically-resolved HAADF-STEM. Samples have been prepared by focused ion beam (FIB) on a thermal chips provided by Protochips®. The structural characterization has been performed on a FEI Titan3 G2 80-300 microscope, operated at 300 kV, equipped with a Cs probe corrector and by using the Fusion Select Protochips® TEM holder.

First, the antiferroelectric state has been established by observing the structural periodicity of antiparallel dipoles. Temperature-dependent measurements revealed a transition from the antiferroelectric state to a ferroelectric-like state before reaching a disordered phase at 570 K. When cooling the specimen down to 300 K, dipoles rearrange in the form of antiparallel stripes, as observed for the initial state. These transitions were further confirmed by electrical measurements and atomistic simulations.

**Mots clefs :** In situ, temperature, oxyde, phase transition

**SDM2-P15****ÉTUDE DES TECHNOLOGIES ÉMERGENTES PAR MICROSCOPIE  
ÉLECTRONIQUE OPERANDO AVANCÉE****STUDY OF EMERGING TECHNOLOGIES BY ADVANCED OPERANDO ELECTRON  
MICROSCOPY**

- **Mohammad DOLATABADI** \* (Seyed-Mohammad.Dolatabadi-Hamed@cnrs-imn.fr) / Nantes Université, CNRS, Institut des Matériaux de Nantes Jean Rouxel, IMN, F-44000 Nantes, France
- **Eric GAUTRON** / Nantes Université, CNRS, Institut des Matériaux de Nantes Jean Rouxel, IMN, F-44000 Nantes, France
- **Etienne JANOD** / Nantes Université, CNRS, Institut des Matériaux de Nantes Jean Rouxel, IMN, F-44000 Nantes, France
- **Philippe MOREAU** / Nantes Université, CNRS, Institut des Matériaux de Nantes Jean Rouxel, IMN, F-44000 Nantes, France

\* Auteur correspondant

Most of the pivotal high-level technologies nowadays rely on the application of electric current and involve mechanisms in sub-micrometer or even sub-nanometer scale, such as batteries and microelectronic devices. Thanks to the recent advances in transmission electron microscopy (TEM), now operating characterization (operando) of these systems at nano scale is feasible. In this regard, we have developed operando experiments in two different areas by using a dedicated operando sample holder equipped with a tungsten STM tip for electrical contacts. Firstly, it enabled us to set up an open cell configuration (figure.1) to simulate the working conditions of FePO<sub>4</sub> as a cathode material for sodium-ion batteries. The sodiation process in olivine FePO<sub>4</sub> is a two step process with Na<sub>0.7</sub>FePO<sub>4</sub> intermediate phase [1]. In this intermediate phase, the periodicity of sodium atoms along the b axis is two occupied sites followed by one empty site. This study is the first step towards operando investigation of the intercalation mechanism of sodium ions in FePO<sub>4</sub>. Secondly, the above-mentioned sample holder can be exploited to induce in-situ insulator to metal transition in (V<sub>1-x</sub>Crx)O<sub>3</sub> Mott insulators by the application of an electric pulse inside the microscope, and then to probe the lattice response to this stimulus. The schematic view of this experiment is illustrated in figure 2.a. Electric pulse-induced transition in insulating phase of this family of materials leads to creation of a metallic filament inside an insulator matrix, resulting in two switching resistance states. The low resistance state can be maintained by applying an electric field above a threshold value. This state can reverse back to the initial high resistance state by applying consecutive electric pulses [2]. This feature makes Mott insulators interesting for new generation of memories and other micro-electronic devices. Based on electron energy loss spectroscopy (EELS) in the low loss region (figure 2.b), we have defined a criterion to distinguish between the metallic and insulating phase of (V<sub>1-x</sub>Crx)O<sub>3</sub>.

**References:**

- [1] P. Moreau et al. Chem. Mater. 22 (2010), p.4126-4128
- [2] M. Querre et al. Physica B: Condensed Matter, 536 (2018), p.327-330

**Mots clefs :** Operando, Transmission electron microscopy, Sodium-ion batteries, Mott insulators

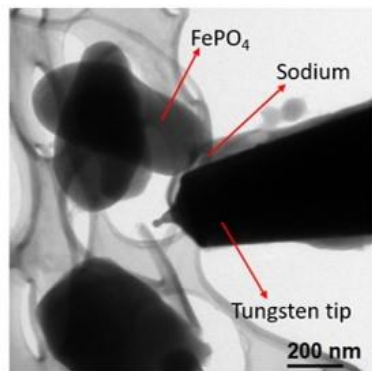


*Figure 1:* The TEM image of the operando experiment to simulate the working conditions of FePO<sub>4</sub> cathode in Na-ion batteries.

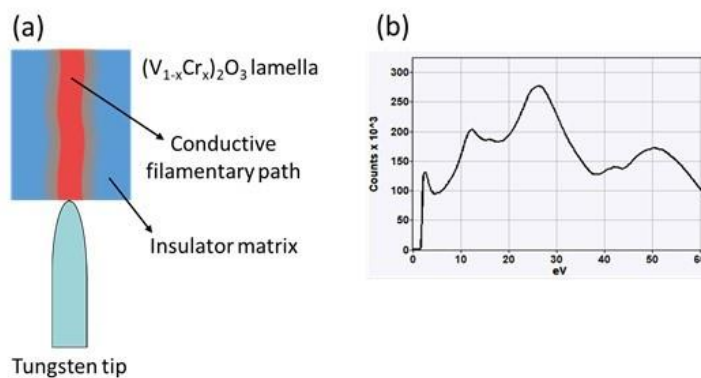


*Figure 2:* (a): Schematic representation of the strategy aiming at inducing a non-volatile metallic filament in a Mott insulator. (b): Electron energy loss spectrum of V<sub>2</sub>O<sub>3</sub> in the low loss region showing a pronounced plasmon peak chosen for the analysis around 27 eV.

## SDM2-P16

### Étude de l'accumulation de charges dans les condensateurs bicouches par holographie électronique operando et modélisation

Studying charge accumulation in bilayer capacitors by operando electron holography and modeling

- Kilian Gruel \* (kilian.gruel@cemes.fr) / CEMES-CNRS, Toulouse, France
- Raphaël SERRA / CEMES-CNRS, Toulouse, France
- Aurélien MASSEBOEUF / CEA, Grenoble, France
- Christophe GATEL / CEMES-CNRS, Toulouse, France/Université de Toulouse, Toulouse, France
- Martin J. HYTCH / CEMES-CNRS, Toulouse, France

\* Auteur correspondant

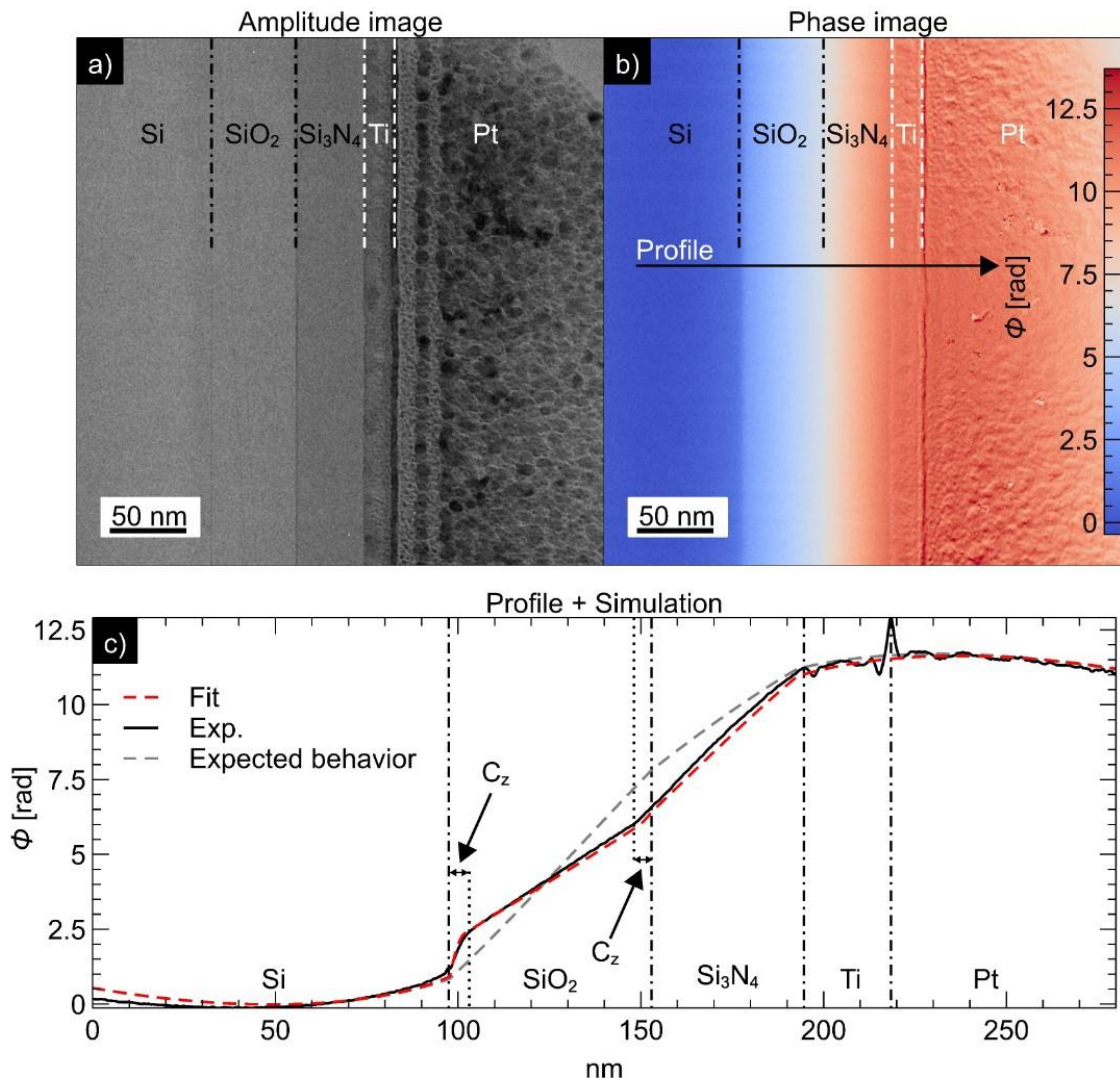
Understanding the behaviour of charges inside microelectronics devices is often essential to their development and improvement. Within dielectric stacks, for example, unwanted charging can occur at interfaces, particularly as the size of the electronic components decreases. Operando electron holography can be used to study such phenomena [1].

Here we study a model bilayer capacitor composed with 55-nm-length SiO<sub>2</sub> ( $\epsilon_4 = 3.9$ ) and 40-nm-length Si<sub>3</sub>N<sub>4</sub> ( $\epsilon_4 = 7.2$ ) in series, grown on highly p-doped Si substrate and topped with a Ti electrode. The TEM foil after FIB preparation was 70 nm thick. The sample is observed *in situ* with electron holography on the I2TEM microscope (Hitachi HF3300-C) operating at 300 kV. Figures (a,b) show the amplitude and associated phase of a 10V biased sample.

To extract quantitative data from phase image, we first need to compare the recorded experimental phase to simulations [2]. Finite element method (FEM) was used to model the electrostatic potential (COMSOL Multiphysics). At first sight, we would expect the electric field (given by the slope of the phase) to be larger in the layer with a lower dielectric constant (SiO<sub>2</sub>) (see dashed line on Figure (c)). There is indeed a point of inflection at the interface between the SiO<sub>2</sub> and Si<sub>3</sub>N<sub>4</sub> but it is positive rather than negative. The only way we can explain this is by introducing charge layers at the interphases of the SiO<sub>2</sub> with opposite charges. Parameters were then adjusted to produce an excellent fit with the experimentally measured phase shift (red dashed line on Figure c). The curvature of the phase in the electrodes is well reproduced and is caused by the stray field around the sample. This new model highlights charges layers that were unexpected in a straightforward device that we previously thought to be well known, revealing new insights.

The research leading to these results has received funding from the European Union Horizon 2020 research and innovation program under grant agreement No. 823717 – ESTEEM3.

**Mots clefs :** Electric fields, Electron holography, Modeling, Operando, Finit elements method



Figures: The amplitude image depicts the structure of the sample Si-SiO<sub>2</sub>-Si<sub>3</sub>N<sub>4</sub>-Ti a), whereas the phase profile in the same area depicts the phase acquired by electrons passing through the capacitor bias under 10 V b). A profile on the phase image then allows for a more in-depth analysis of the phase c).

**SDM2-P17****Microscopie électronique en transmission in situ et operando pour l'étude de l'hydrogénéation catalytique du CO<sub>2</sub>****In-situ and operando Transmission Electron Microscopy for CO<sub>2</sub> catalytic hydrogenation investigation**

- **Joséphine REZKALLAH** \* (josephine.rezkallah@univ-rouen.fr) / GPM Laboratory, CNRS UMR 6634, Rouen University, Normandy
- **Bernhard WITULSKI** / LCMT Laboratory, CNRS UMR 6507, ENSICAEN & Caen University, Normandy
- **Xavier SAUVAGE** / GPM Laboratory, CNRS UMR 6634, Rouen University, Normandy
- **Simona MOLDOVAN** / GPM Laboratory, CNRS UMR 6634, Rouen University, Normandy

\* Auteur correspondant

To mitigate the rising CO<sub>2</sub> levels, researchers are exploring the CO<sub>2</sub> hydrogenation into useful compounds using renewable energy. This reaction requires a catalyst to overcome the high activation energy barrier associated with it. Pt nanoparticles (NPs) are good catalysts for this process due to their high activity and selectivity. Several studies have reported that Pt NPs can efficiently catalyze the hydrogenation of CO<sub>2</sub> into both formic acid and methanol under mild conditions [1,2]. This study uses an environmental cell (E-cell) TEM holder to investigate the microstructure of nanocatalysts in a controlled gaseous environment, high temperature, and pressure. The goal is to gain a better understanding of the material behavior and its relation to catalytic reaction response. Pt-based hollow nanospheres (HNS) with an average outer diameter of 15 nm±2 nm and a shell thickness of 2-3 nm (fig1a,1b) were synthesized using a precise ratio of H<sub>2</sub>PtCl<sub>6</sub> and Co NPs as precursors. Electron tomography showed that the HNS have a complex 3D structure with a shell of locally interconnected NPs of about 2 nm. The pores in the shell are perpendicular to the outer surface of the spheres, facilitating the access to their inner surface and increasing the active surface area (fig 1c). The catalyst's morphology was monitored in an E-cell (Protobips: Atmosphere) while heating at a rate of 0.4°C/s, using a CO<sub>2</sub> and H<sub>2</sub> mixture with an H<sub>2</sub>/CO<sub>2</sub> input ratio of 4. Meanwhile, the evolution of reaction products (HCO<sub>2</sub>H, CH<sub>3</sub>OH, and H<sub>2</sub>O) was simultaneously tracked. This study identified the growth of shell NPs through the Ostwald ripening mechanism, resulting in the formation of a continuous shell at 240°C (fig 2). Despite the blockage of access to the inner surface, the reaction continued on the outer surface of the nanospheres until 450°C. At higher temperatures, the microstructure of the nanospheres began to collapse, leading to an increase in the reaction products. This indicates that some of the reaction products were trapped within the inner volume of the HNS and released upon their collapse.

[1] Wang et al., Chem. Soc, 7 (2011), 3703

[2] Men et al., Chem Eng Sci, 200 (2019), 167

**Mots clefs :** In situ, Operando, TEM, electron tomography, hydrogenation of CO<sub>2</sub>, catalyst, hollow nanospheres

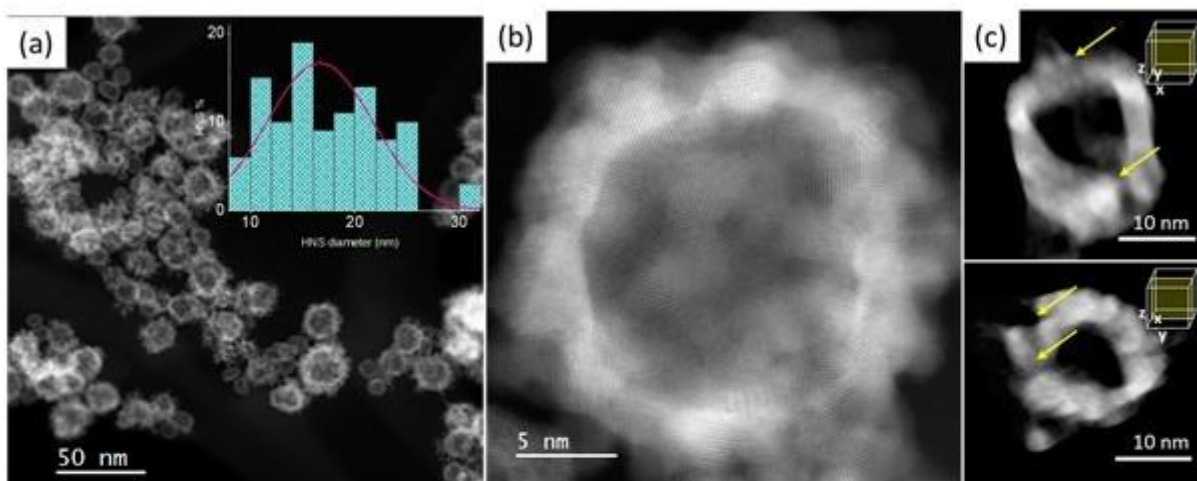


Figure 1: (a) HAADF-STEM micrograph of Pt-Co hollow nanospheres with their diameter distribution histogram as inset, (b) High-resolution HAADF-STEM micrograph of a single hollow nanosphere with the shell formed by interconnected NPs, (c) Slices of (xz) and (yz) directions redrawn from the reconstructed volume with yellow arrows pointing at the channels leading to the inner surface of the shell.

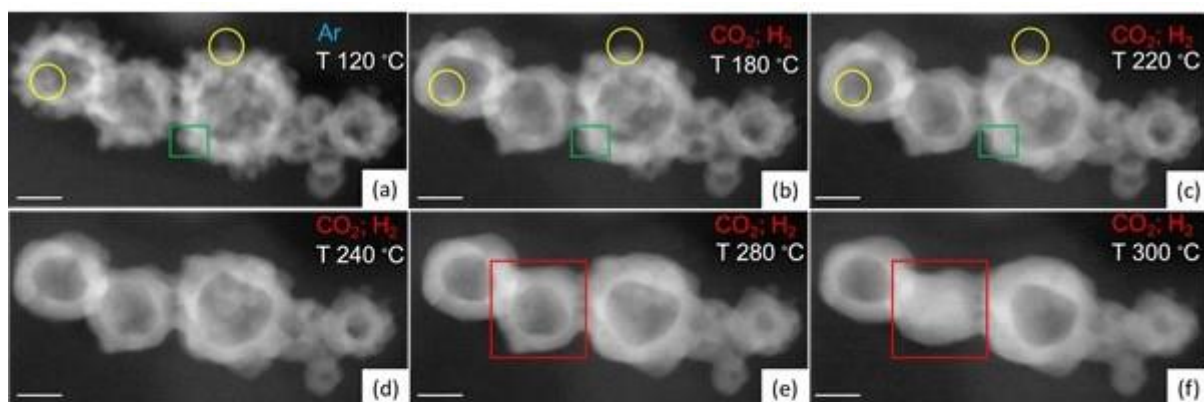


Figure 2: HAADF-STEM images of the Pt-Co catalysts: (a) in their initial state, (b-d) coalescence upon heating the specimen from 120°C to 300°C under (CO<sub>2</sub>; H<sub>2</sub>) mixture: growth of some NPs forming the shell (green rectangle) and shrinkage of others (yellow circles), (e-f) collapsing (red square). Scalebar 10 nm.

## SDM2-P18

# La bionanomagnétite : un aperçu des applications et des perspectives d'avenir

### Bionanomagnetite: an overview of applications and future perspectives

- **Juliana Guimarães** \* (julianaguimaraes@micro.ufrj.br) / Université de Strasbourg, France
- **Rogerio Presciliiano** / Universidade Federal do Rio de Janeiro
- **Vinavadini Ramnarain** / Université Paris Cité
- **Igor Taveira** / Universidade Federal do Rio de Janeiro
- **Júlia de Castro** / Universidade Federal do Rio de Janeiro
- **Beatriz Vessalli** / Universidade Federal do Rio de Janeiro
- **Dris Ihiaawakrim** / Université de Strasbourg
- **Ovidiu Ersen** / Université de Strasbourg
- **Fernanda Abreu** / Universidade Federal do Rio de Janeiro

\* Auteur correspondant

Magnetotactic bacteria (MTB) comprise a group of Gram-negative aquatic and flagellated microorganisms able to synthesize magnetosomes [1], which are magnetic nanocrystals composed of magnetite ( $\text{Fe}_3\text{O}_4$ ) or greigite ( $\text{Fe}_3\text{S}_4$ ) and surrounded by a biological membrane [2]. Magnetosomes have several advantages for application in Biotechnological approaches, such as biocompatibility, crystallographical perfection, high chemical purity, and thermal resistance. Hence, an enveloping biological membrane with several anchorage sites is helpful for functionalizing molecules.

Although chemically synthesized magnetite nanoparticles usually have a lower production cost, coating these structures is expensive. Therefore, because MTB produces magnetosomes with a natural biocompatibility coat, they are considered potential bio-based products to be applied in several Nanotechnology approaches. Currently, we are using meta-analysis to compare the performance of synthetic magnetite nanoparticles and magnetosomes in Biotechnology. Our goal is to predict the correlation between magnetite nanoparticles features and the cost/efficiency of processes in the literature.

One of the main areas in which magnetite nanoparticles have been applied recently is Nanomedicine. Since new approaches to treat antibiotic-resistant infections are currently in the spotlight, we are developing a nanoformulation based on magnetosomes (Fig. 1), using poly-L-lysine as a cross-linking agent, ampicillin, a  $\beta$ -lactam antibiotic, and clavulanate, a  $\beta$ -lactamase inhibitor. Conventional transmission electron microscopy (FEI Morgani, 80 kV) showed that the magnetosome membrane thickened after the functionalization process (Fig. 2). Functionalization with ampicillin and clavulanate resulted in very similar thicknesses, mean thicknesses of  $5.28 \pm 1.54$  nm and  $5.17 \pm 1.88$  nm respectively, while treatment with poly-L-lysine alone showed greater thickness, with a mean thickness of  $6.9 \pm 2.15$  nm, which may be due to its ability to form polymers, creating chain linkage of multiple units of the molecule. Furthermore, preliminary assays against a *Staphylococcus aureus* strain susceptible to  $\beta$ -lactams indicated that the nanoformulation inhibited cell growth more than the soluble antibiotic.

### Références/References :

- [1] Blakemore, R., Science, vol. 190 (1975), p. 377.
- [2] Bazylinski, D.A. and Frankel, R.B., Nat. Rev. Microbiol, vol. 2 (2004), p. 217. [3] Vargas, G. et al., Molecules, vol. 10 (2018), p. 2438.

**Mots clefs :** Biotechnology, magnetite, magnetotactic bacteria, nanoparticles, magnetic nanoparticles, magnetosomes, drug delivery, functionalization

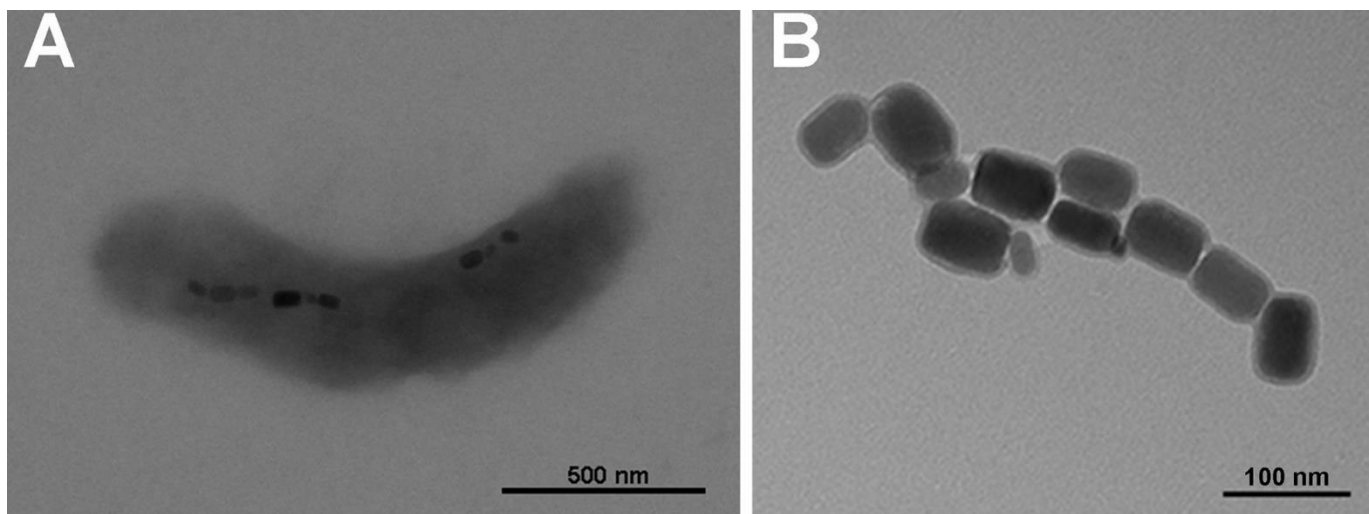


Figure 1: *Magnetovibrio blakemorei* strain MV-1 cell and purified magnetosomes. A. Transmission electron microscopy of the bacterium showing a single chain of prismatic magnetosomes within the cytoplasm. B. Transmission electron microscopy of purified magnetosomes. Note the presence of the membrane (an electronluscious layer) around each magnetite crystal.

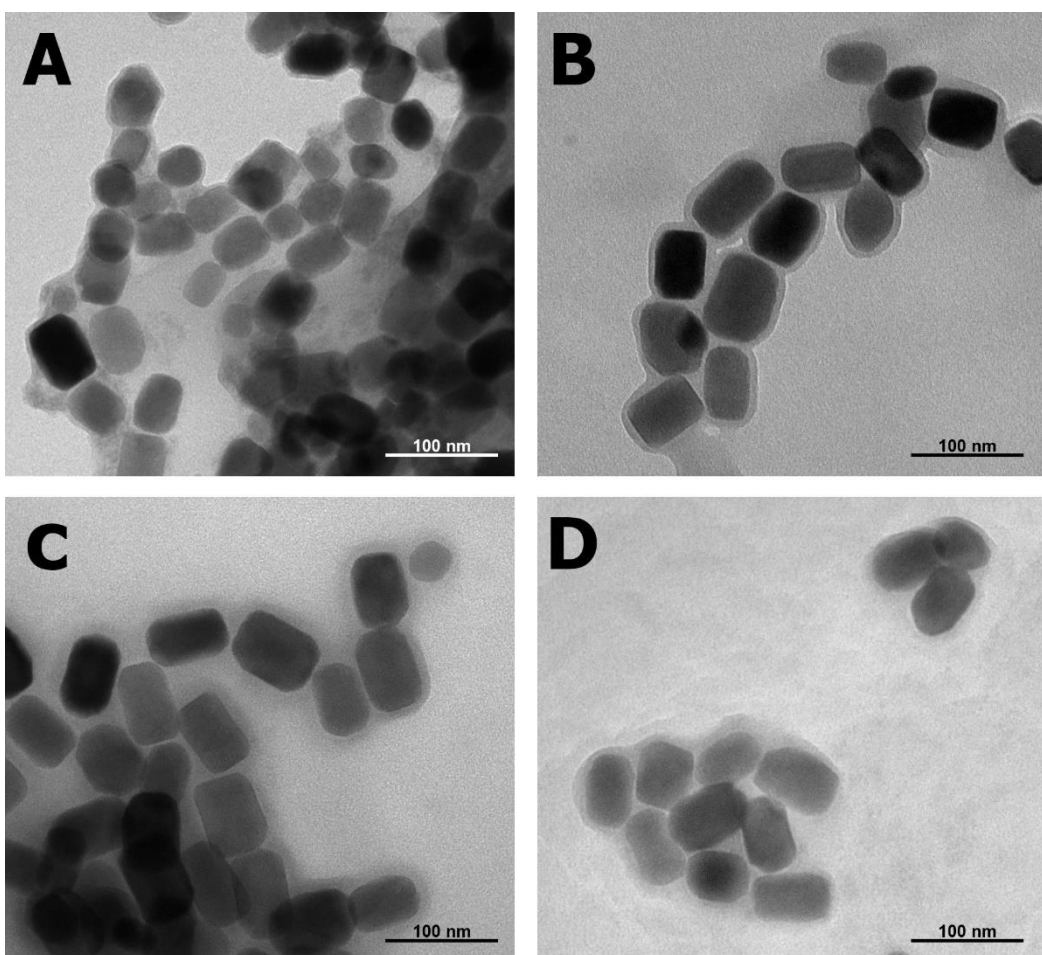


Figure 2. Transmission electron microscopy images of magnetosomes from *Magnetovibrio blakemorei* strain MV-1 species. Scale bar indicates 100 nm. A. Pure. B. Functionalized with poly-L-lysine only. C. Functionalized with ampicillin. D. Functionalized with clavulanate.

## SDM3-P1

### Silicide precipitation in aged quasi- $\alpha$ Ti alloys

- **Frédéric FOSSARD** (\*frédéric.fossard@onera.fr), Université Paris-Saclay, ONERA, CNRS, LEM, 92322, Châtillon, France
- **Thibaut ARMANNI**, Université Paris Saclay, ONERA, Matériaux et Structures, 92322, Châtillon, France
- **Thierry DOUILLARD**, INSA Lyon, Université de Lyon, MATEIS, UMR CNRS 5510, F69621 Villeurbanne, France
- **Jean-Sébastien MEROT**, Université Paris-Saclay, ONERA, CNRS, LEM, 92322, Châtillon, France
- **Benoît APPOLAIRE**, Université de Lorraine, CNRS, Institut Jean Lamour, Nancy, France

Increasing temperature properties of materials is a major strategic challenge for the aviation industry. Titanium alloys offer excellent specific mechanical strength and good corrosion resistance up to temperatures of around 550°C. The emblematic titanium alloy traditionally used is the so-called Ti6242. Nevertheless, these quasi- $\alpha$  alloys are very sensitive to fatigue-creep type stresses at room temperature, commonly known as the "dwell effect" [1] which is known to be associated with the microstructure and micro texture of the  $\alpha$  phase in the alloy [2]. To reduce the dwell effect, Mo content can be increased. However, it will alter the mechanical properties at high temperature. In order to counteract this decrease, the addition of silicon is preferred [3]. However, the strengthening mechanism of silicon is still under discussion. During aging, silicon leads to the precipitation of silicides [4].

The results obtained in this study seem to show that they would increase mechanical properties. To corroborate this relationship between silicides and properties, we have characterized the microstructures by electron microscopies and related techniques. We performed 3D reconstructions of the microstructure by SEM/FIB (Figure 1) on the alloys in the aged state to get statistical informations on the dimensions, the shape and the organisation of the silicides. In addition, TEM observations have allowed to highlight the nature of the silicide/ $\alpha$  interfaces and analysis (Figure 2) revealed small zirconium enriched precipitates of the  $(\text{Ti}, \text{Zr})_2\text{Si}$  type with specific orientation relationship with the Ti matrix.

#### Acknowledgments

The authors are grateful to financial support from the French METSA network (FR3507) for SEM/FIB experiments at CLYM. Authors would like to thank ALTITUDE ANR project.

#### References :

- [1]. W. J. Evans et al., Metallurgical Transactions A, 10(12), pp. 1837-1846(1979).
- [2]. M. Bache, International Journal of Fatigue, 25 (9-11), pp. 1079–1087 (2003).
- [3]. Paton, N.E. et al.(1976), Metallurgical Transactions A, 7(11), pp. 1685–1694.
- [4]. Banerjee, D. et al. (2013), Acta Materialia, 61(3), pp. 844–879.

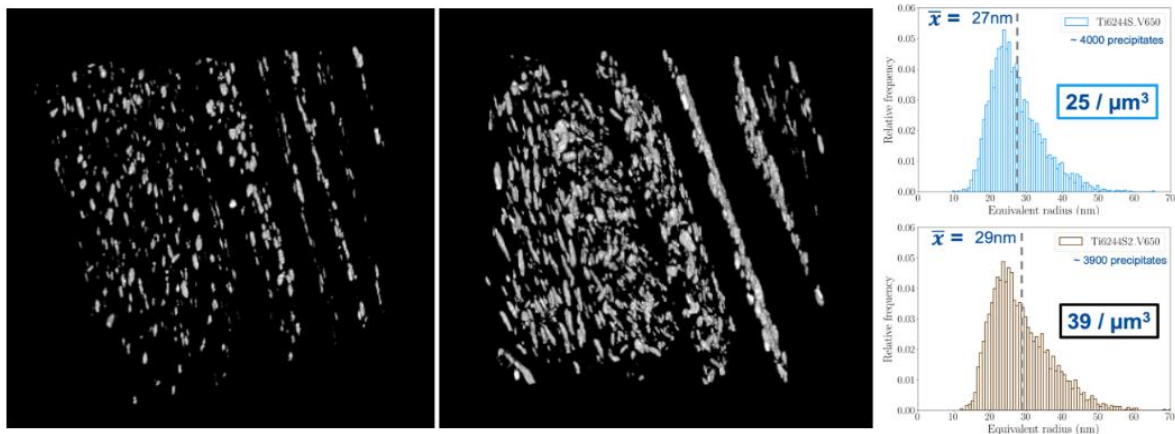


Figure 1: 3D organisation of silicides in Ti6244S (left), and Ti6244S2 (right). Precipitate size distribution in Ti6244S (blue) and Ti6244S2 (brown)

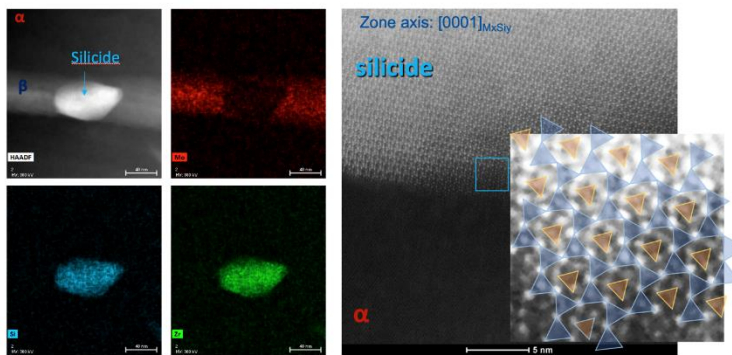


Figure 2: (Left) silicide STEM/EDS elemental maps ; (right) HRSTEM image of silicide in [0001] zone axis. Inset displays the superimposed atomic model of (Ti,Zr)<sub>2</sub>Si structure.

## SDM3-P2

### Polymorphisme et structures d'intercroissance dans le système nanostructure Pr-Co: Pr<sub>2</sub>Co<sub>7</sub> et Pr<sub>5</sub>Co<sub>19</sub>

Polymorphism and intergrowth structures in the nanostructured Pr-Co system: Pr<sub>2</sub>Co<sub>7</sub> and Pr<sub>5</sub>Co<sub>19</sub>

- **Loïc Patout** \* (loic.patout@im2np.fr) / Aix-Marseille Université, CNRS, Université de Toulon, IM2NP - Campus de St Jérôme, UMR7334, 13397 Marseille cedex 20, France
- **Farah Chafai** / Université de Tunis El Manar, Faculté des Sciences de Tunis, Laboratoire Matériaux Organisation et Propriétés (LR99ES17), 2092, Tunis, Tunisia
- **Marion Descoins** / Aix-Marseille Université, CNRS, Université de Toulon, IM2NP - Campus de St Jérôme, UMR7334, 13397 Marseille cedex 20, France
- **Khalid Hoummada** / Aix-Marseille Université, CNRS, Université de Toulon, IM2NP - Campus de St Jérôme, UMR7334, 13397 Marseille cedex 20, France
- **Lotfi Bessais** / Université Paris-Est Créteil, CNRS, ICMPE, UMR7182, F-94320, Thiais, France
- **Najeh Mliki** / Université de Tunis El Manar, Faculté des Sciences de Tunis, Laboratoire Matériaux Organisation et Propriétés (LR99ES17), 2092, Tunis, Tunisia
- **Ahmed Charaï** / Aix-Marseille Université, CNRS, Université de Toulon, IM2NP - Campus de St Jérôme, UMR7334, 13397 Marseille cedex 20, France

\* Auteur correspondant

Une poudre nanocristalline a été préparée de façon à obtenir la phase rhomboédrique Pr<sub>5</sub>Co<sub>19</sub>-3R par fusion à arc et broyage par billes à haute énergie. Des images en champ clair montrent un matériau caractérisé par des bandes de contraste nanométriques avec, dans certains cas, des décalages d'empilements de plans atomiques. Des calculs d'images HREM montrent que ces caractéristiques sont partiellement intrinsèques à ce type de structure et peuvent apparaître quand des projections sont déviées d'un axe de zone (Fig. 1). Des analyses DRX et des mesures magnétiques M(H) ont montré des caractéristiques d'une poudre contenant une monophase magnétique dure identifiée comme la structure Pr<sub>5</sub>Co<sub>19</sub>-3R. Dans l'étude présente, une analyse MET des réflections FOLZ dans les spectres de puissance FFT révèlent sans ambiguïté l'existence de nanograins de structure polytype hexagonal Pr<sub>2</sub>Co<sub>7</sub>-2H. Des domaines d'intercroissance Pr<sub>2</sub>Co<sub>7</sub>-Pr<sub>5</sub>Co<sub>19</sub> sont aussi présents dans l'empilement des sous-unités, qui pourraient s'expliquer par une transition structurale à partir de la phase Pr<sub>5</sub>Co<sub>19</sub>-3R stable à haute température (Fig. 2). L'élimination de ces défauts microstructuraux semblent difficile à cause de la gamme de solubilité solide très limitée de la phase Pr<sub>5</sub>Co<sub>19</sub> dans le système binaire Pr-Co, les énergies libres de formation très proches pour les structures 2H et 3R, ainsi que les instabilités structurales dues aux microcontraintes entre les couches de sous-unité [AB<sub>5</sub>] et [A<sub>2</sub>B<sub>4</sub>].

Référence:

L. Patout et al. Materials Characterization 196 (2023) 112621

**Mots clefs :** polymorphisme, inter-croissance, nanostructuration, magnétisme

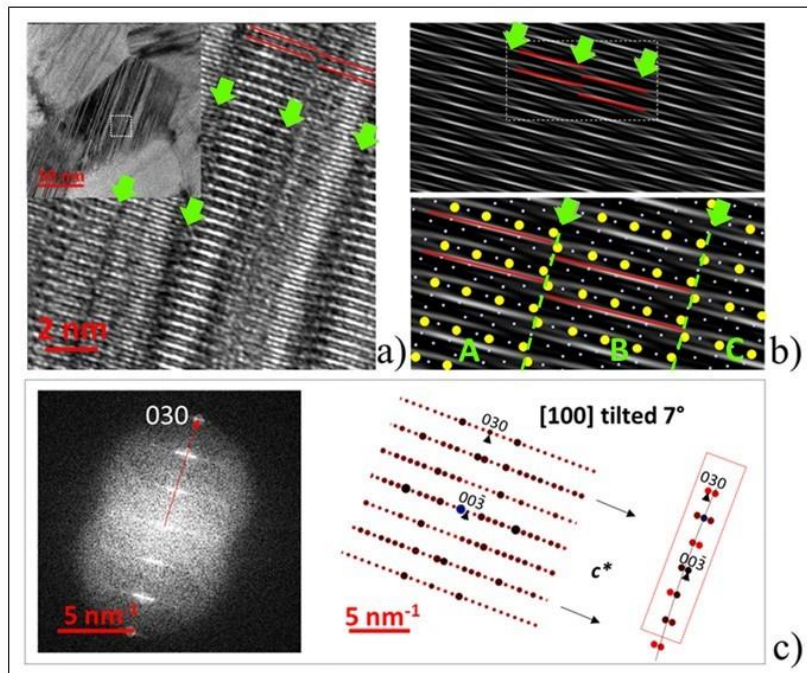


**Figure 1:** Image à fort grossissement enregistrée dans une zone du grain définie en encadrement. Les lignes rouges montrent les décalages d'empilement. Les flèches vertes pointent vers les lignes de contraste sombres a). Image calculée pour une orientation [100] tournée de  $7^\circ$  le long de  $c^*$ . L'encadrement blanc a été zoomé; les atomes Pr (jaune) ont été renforcés de façon à visualiser les empilements des couches de blocs A-B-C b). FFT expérimentale de l'image (gauche); Clichés ED calculés pour les orientations [100] et [100] tilité  $7^\circ$  (droite).

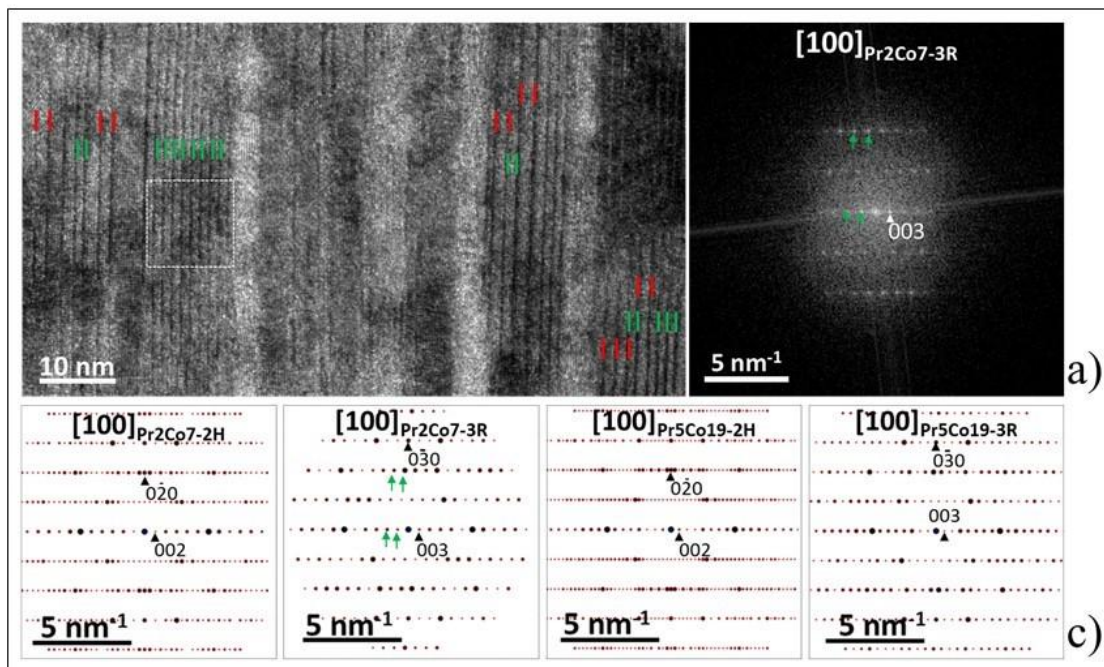


**Figure 2:** Image HREM à faible grossissement en axe de zone [100] montrant des espacements différents de franges de maille dus à la co-existence désordonnée des membres  $\text{Pr}_2\text{Co}_7$  (vert –  $d = 1.2 \text{ nm}$ ) et  $\text{Pr}_5\text{Co}_{19}$  (rouge –  $d = 1.6 \text{ nm}$ ) a). FFT expérimentale b) enregistrée dans un nanodomaine délimité en a). Calculs ED pour chaque polytype c)

## SDM3-P3

### Profilage de dopage pour Si:P hautement dopés par TEM avancé

Dopant profiling of very highly doped specimens by advanced transmission electron microscopy

- **Cathy VANG** \* (cathy.vang2@cea.fr) / Univ. Grenoble Alpes, CEA, LETI, 38000 Grenoble, France
- **joel kanyandekwe** / Univ. Grenoble Alpes, CEA, LETI, 38000 Grenoble, France
- **jean-michel Hartmann** / Univ. Grenoble Alpes, CEA, LETI, 38000 Grenoble, France
- **Nicolas Bernier** / Univ. Grenoble Alpes, CEA, LETI, 38000 Grenoble, France
- **David Cooper** / Univ. Grenoble Alpes, CEA, LETI, 38000 Grenoble, France

\* Auteur correspondant

Todays, microelectronics require high performance semiconductors devices containing complex 3D architectures. CEA-LETI has focused on 10 nm transistors grown on FD-SOI. To assess the effectiveness of different doping processes in advanced CMOS research, the challenge is the ability to develop a quantitative, high sensitivity analysis of active dopants. Here we study highly doped Si:P samples grown by low temperature cyclic deposition/etch process, to obtain smoothness, uniformity and good crystallinity [1]. To understand better their properties, we combined complementary characterization techniques by TEM. For measuring the dopant's activity we used off-axis electron holography, for measuring the substitutional dopant concentration of the dopants we used strain mapping by precession diffraction (PED) and Geometrical Phase Analysis (GPA) . Finally for measuring the total chemical concentration of dopant atoms, we used EDX.

Figure 1 shows HAADF STEM images for different specimens containing nominal P contents of 1, 4 and 8 %. A sharp interface between the substrate and the layers, and a high-crystalline quality is observed.

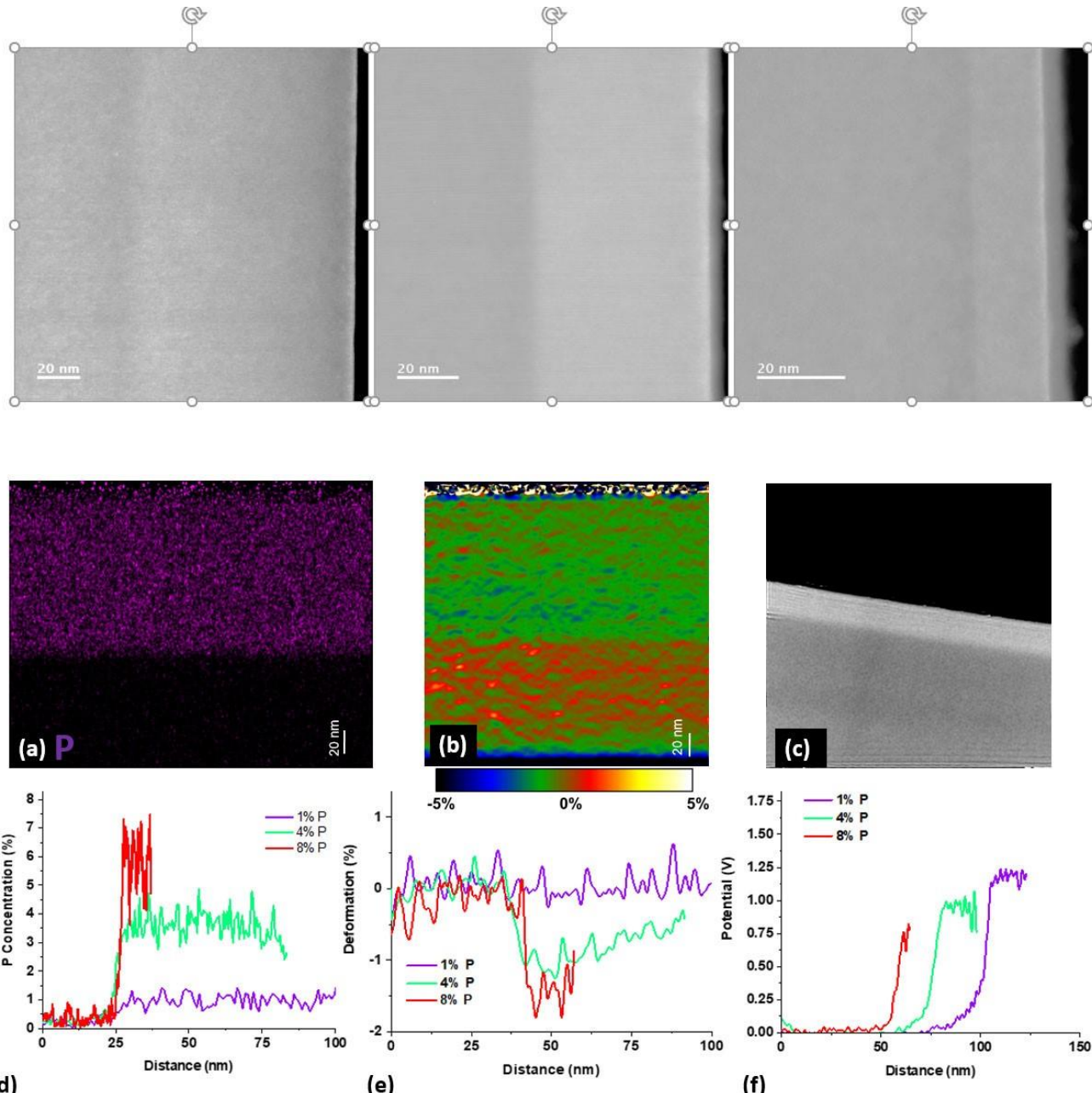
Figure 2(a) shows an EDX map for the specimen with 4% dopant concentration. The corresponding deformation map for the growth direction calculated using GPA is shown in (b) and the potential map measured by holography in (c). The quantitative composition for all of the samples examined are shown in Figure 2(d). The strain in the growth direction is shown in Figure 2(e). We would expect the lattice parameter to be contracted in the growth direction due to the presence of P dopants to an extent that would be proportional to the concentration of substitutional dopant atoms. However, we observe a similar amount of strain for samples with nominal 4 and 8% dopants. Dopants' activity can be observed in Figure 2(f) where the highest step in potential for sample corresponds to the lowest dopant concentration.

This presentation will show how several advanced TEM techniques can be combined to obtain complementary information from the same sample, in order to obtain a more complete materials' understanding.

References :

[1] J.M. Hartmann, J. Kanyandekwe Journal of Crystal Growth 582 (2022) 126549

**Mots clefs** : TEM, EDX, STEM-HAADF, Holographie, PED, Semi-conduteur, profilage



## SDM3-P4

### Observations des faces cristallines de TiO<sub>2</sub> rutile et anatase en présence de H<sub>2</sub>PO<sub>4</sub><sup>-</sup>

#### Crystal facets observation over anatase and rutile TiO<sub>2</sub> in presence of H<sub>2</sub>PO<sub>4</sub><sup>-</sup>

- Rémi BERARD / DRF/IRAMIS/NIMBE, UMR 3685, CEA-Saclay, 91191 Gif-Sur-Yvette, France
- Patricia BERTONCINI / Nantes Université, CNRS, Institut des Matériaux de Nantes Jean Rouxel, IMN, F-44000 Nantes, France
- Eric Gautron / Nantes Université, CNRS, Institut des Matériaux de Nantes Jean Rouxel, IMN, F-44000 Nantes, France
- Sophie Cassaignon / LCMCP, UMR7574, Sorbonne Universités, UPMC Univ Paris, CNRS, Collège de France, 4 place Jussieu, 75005 Paris, France
- Bernard Humbert / Nantes Université, CNRS, Institut des Matériaux de Nantes Jean Rouxel, IMN, F-44000 Nantes, France
- Hélène Terrisse / Nantes Université, CNRS, Institut des Matériaux de Nantes Jean Rouxel, IMN, F-44000 Nantes, France
- Sophie Le Caer / DRF/IRAMIS/NIMBE, UMR 3685, CEA-Saclay, 91191 Gif-Sur-Yvette, France
- Philippe Moreau \* (philippe.moreau@cnrs-imn.fr) / Nantes Université, CNRS, Institut des Matériaux de Nantes Jean Rouxel, IMN, F-44000 Nantes, France

\* Auteur correspondant

The large use of TiO<sub>2</sub> nanoparticles raise concerns about their probable carcinogenic effect [1]. Their ability to produce radical oxydative species under light can cause damage to cell's organites or DNA. The cell membrane phospholipids may play a primordial role on the adsorption of the nanoparticles through their phosphate group [2]. This adsorption may be dependent on their shape and on their type of crystalline facets also.

In order to address this issue, rutile and anatase TiO<sub>2</sub> nanoparticles with different shapes were allowed to interact with H<sub>2</sub>PO<sub>4</sub><sup>-</sup> phosphate ions in an aqueous solution at pH 2 (pH known to ensure the maximum of adsorption) (for example, see Figure 1 and 2). They were characterized using scanning transmission electron microscopy (STEM) working in two modes (high angle annular dark field-STEM measurements and differential phase contrast imaging). This permits to determine the size, morphology and crystal facets of the synthesized nanoparticles. The interactions between surface hydroxyls and phosphate ions were investigated by infrared spectroscopy.

#### Acknowledgements

Funding by the French Contrat Plan État-Région and the European Regional Development Fund of Pays de la Loire, the CIMEN Electron Microscopy Center in Nantes is greatly acknowledged.

Funding from the Agence Nationale de la Recherche (ANR ACETONE N° ANR-20-CE09-0010-01) is gratefully acknowledged.

References :

[1] ANSES-Saisine N°2019-SA-0036

[2] Q.-C. Le et al. Colloids and Surfaces B: Biointerfaces 123 (2014) 150-157

**Mots clefs :** HAADF, iDPC, crystal facets, TiO<sub>2</sub>

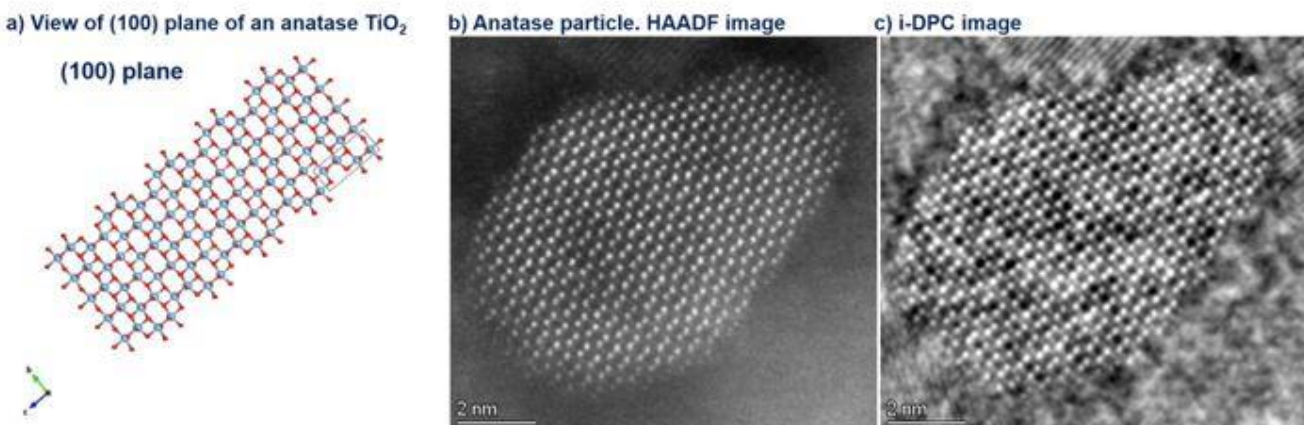


Figure 1: Anatase particle.

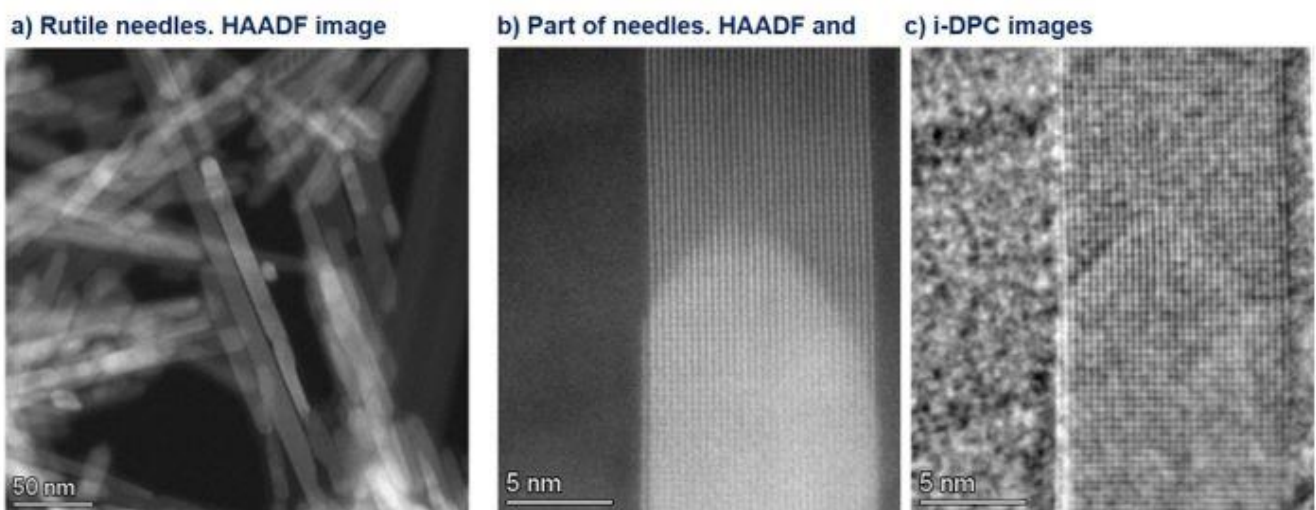


Figure 2: Rutile needles.

## SDM3-P5

### Sur l'insensibilité du molybdène à l'oxydation à température ambiante

#### Revisiting the insensitivity of Mo to oxidation at room temperature

- **Frédéric Pailloux \*** (frederic.pailloux@univ-poitiers.fr) / Institut Pprime CNRS-Université de Poitiers
- **Shuhel Altaf Husain** / Institut Pprime CNRS-Université de Poitiers
- **Hadi Bahsoun** / Institut Pprime CNRS-Université de Poitiers
- **Pierre-Olivier Renault** / Institut Pprime CNRS-Université de Poitiers
- **Damien Faurie** / LSPM, CNRS – Université Sorbonne Paris Nord, Villetaneuse
- **Megan J. Cordill** / Erich Schmid Institute of Materials Science, Austrian Academy of Sciences, Leoben

\* Auteur correspondant

With the development of flexible electronics, attention has been focused on the mechanical behavior of metallic thin films on polymeric substrates, and the in situ characterization of the fracture behavior of metal films is of great technological interest for many applications. Within this work, cracking mechanisms of a trilayer architecture composed of materials that are alternatively brittle/ductile/brittle were studied during biaxial straining. The Polyimide/Cr-100nm/Cu-100nm/Mo-100nm triple layer architecture has been elaborated by ion beam sputtering. Mo has been chosen because it plays an important role in many electronic applications ranging from back contact electrodes in solar cells or diffusion barriers in microelectronics, and because it has high thermal stability and chemical inertness, as well as low electrical resistance. Noteworthy Molybdenum was chosen as a third layer in the architecture because of its insensitivity to oxidation at temperatures below 300°C. However, 5 months after carrying out the biaxial straining, observation under an optical microscope reveals the presence of a colour gradient (fig.1). This colour film is attributed to the unexpected oxidation of Mo at room temperature. Interestingly, this change of colour does not induce any qualitative modification of the X-ray diffractograms. In this poster, we show the contribution of electron microscopy (HAADF-STEM, SAED, EDXS and EELS) to get insight into the transition from the initial Mo-layer to this Mo-oxide over-layer.

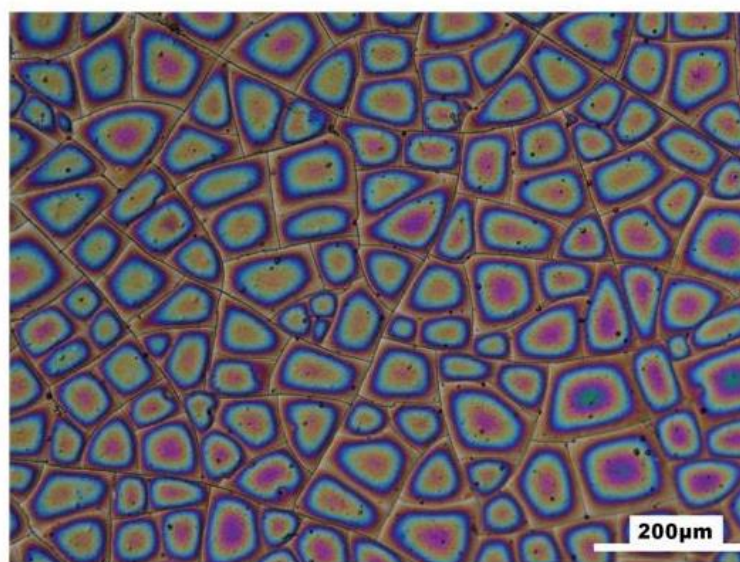


Figure 1: optical micrograph of the Mo surface after the biaxial straining and a five monthes exposure to air at room temperature

## SDM3-P6

### Analyses de nanoparticules Pt/Terres rares par MET

#### TEM investigations of Pt-REM nanocatalysts

- **Frédéric Pailloux \*** (frédéric.pailloux@univ-poitiers.fr) / CNRS Institut Pprime Poitiers
- **Carlos A. Campos-Roldan** / ICGM Montpellier
- **Pierre-Yves Blanchard** / ICGM Montpellier
- **Jacques Rozière** / ICGM Montpellier
- **Deborah Jones** / ICGM Montpellier .**Sara Cavaliere** / ICGM Montpellier

\* Auteur correspondant

In the context of proton-exchange membrane fuel cells (PEMFCs) improvement, Pt-rare earth metal (Pt-REM) alloys have been proposed as a high active and stable electrocatalysts for the sluggish oxygen reduction reaction (ORR). Previous theoretical works suggest a high stability of the PT-REM alloys due to the negative energy formation of these alloys and experimental evidences of a Pt-REM core protected by a Pt-rich overlayer in unsupported bulk sputter-cleaned nanoparticles. We have synthesized several Pt-REM (REM=Gd, Nd, Ce, Y) nanocatalysts using the carbodiimide route [1-3]. The morphology and the microstructure of the samples have been investigated by coupling high resolution transmission electron microscopy (HR-TEM) and high-angle annular dark-field scanning transmission electron microscopy (HAADF-STEM) imaging in a 200 keV schottky-FEG (S)-TEM electron microscope fitted with an in-column omega filter. Various morphological features such as dense, sponge-like, Pt-rich overlayer or even or hollow core nanoparticles have been evidenced. The distribution of the REM in the nanoparticles has been investigated by means of energy dispersive X-ray (EDX) and electron energy-loss (EEL) spectroscopies (fig. 1). The benefit of EDXS and EELS will be discussed in regard of the sensitivity of such nanomaterials to the electron beam.

#### References:

- [1]C. A. Campos-Roldan et al., ACS Catal. 2021, 11, 13519
- [2]C. A. Campos-Roldan et al., Nanoscale Adv. 2022, 4, 26-29
- [3]C.A. Campos-Roldan et al., ACS Appl. Energy. Mater. 2022, 5, 3319-3328

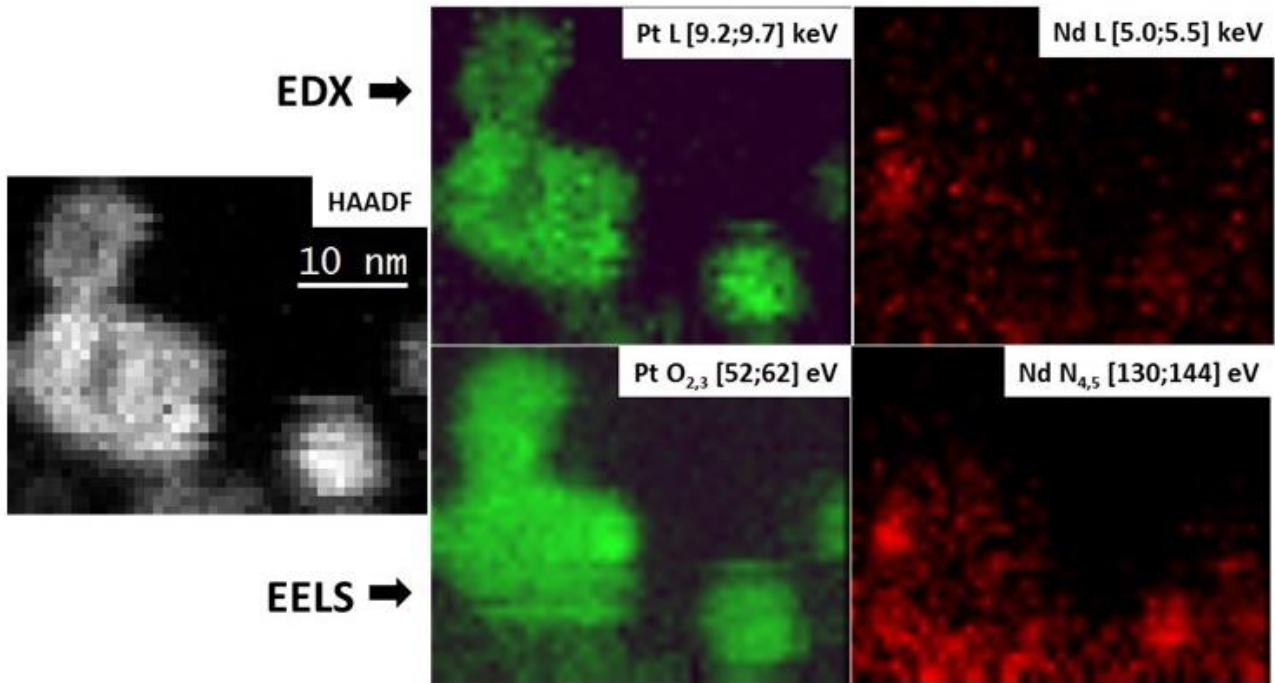


Figure 1: left, HAADF micrograph of a group of PtNd nanoparticles; center, EDXS (top) and EELS (bottom) mapping of Pt in PtNd nanocatalysts; the Nd spatial distribution is displayed on the right hand side.

## SDM3-P7

### Imagerie par STEM-EELS de nanoparticules cœur-coquille en superréseaux

#### STEM-EELS IMAGING OF CORE-SHELL NANOPARTICLE SUPERCRYSTALS

- **Michael WALLS** \* (michael.walls@u-psud.fr) / Laboratoire de Physique des Solides, CNRS Université Paris-Saclay, 91405 Orsay, France
- **Yinan FAN** / Sorbonne Université, MONARIS, CNRS-UMR 8233, 75005 Paris, France
- **Alexa COURTY** / Sorbonne Université, MONARIS, CNRS-UMR 8233, 75005 Paris, France
- **Caroline SALZEMANN** / Sorbonne Université, MONARIS, CNRS-UMR 8233, 75005 Paris, France
- **Adrien GIRARD** / Sorbonne Université, MONARIS, CNRS-UMR 8233, 75005 Paris, France

\* Auteur correspondant

Bimetallic nanocatalysts (NCs) are promising as high performance catalysts based on synergistic effects. Here, building on an initial study [1], Ag@Pt core-shell NPs were synthesized and fully characterized. Then their performance for the photocatalytic hydrogen evolution (HER) reaction was evaluated. The Ag core was chosen for its efficient plasmonic light-harvesting properties, while the Pt shell will confer both corrosion resistance and catalytic properties.

The structural changes in the SCs associated with the photocatalytic reaction were probed through via multiscale imaging. First, sub-microscale analysis is provided by a correlative (identical location) optical and SEM approach (Fig.1). The core-shell architecture and the integrity of the Pt layer were then analyzed by HAADF-STEM, and using EELS for chemical mapping. Figures 1c and 1e show typical HAADF images of Ag@Pt NPs with Ag core and Pt shell in a dark and bright contrast respectively. This is verified by the corresponding EELS maps with Ag core in yellow and Pt shell in blue.

The EELS mapping reveals discontinuities in the Pt shell and pitting that could indeed explain that the Ag core, not fully protected by the Pt layer, may corrode. The arrows in Figure 1d also highlight a very thin atomic layer of silver deposited on the Pt shell for a few NPs in a discontinuous manner. The outer Ag layer may be attributed to the possible competition of Pt ion reduction during the NP synthesis. The direct reduction of Pt ions at the Ag NP by the oleylamine ligand used in the synthesis may compete with galvanic replacement of the Ag metal (producing Ag<sup>+</sup> ions and Pt metal deposit). The dissolved Ag<sup>+</sup> may then be subsequently reduced by oleylamine during the synthesis step, causing local deposition of Ag at the NP surface. The resulting structure is detrimental during the photocatalytic HER as it will promote access to the Ag NP core, thus accelerating the overall corrosion of the NP. However, the results overall show the potential of these particles for applications in plasmonic catalysis

#### Références/References :

[1] Y.Fan et al. ACS Applied Nano Materials 6 (2023) p. 1193-1202

**Mots clefs** : nanoparticules, EELS STEM

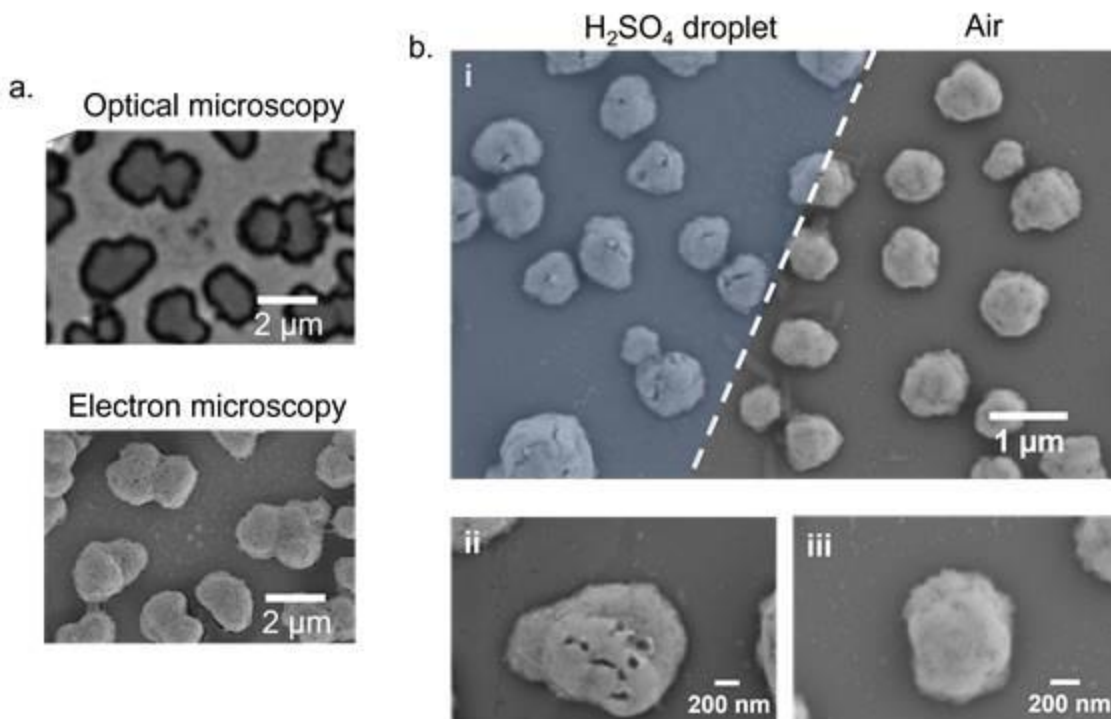


**Figure 1:** (a) Identical location optical and electron microscopy images of SCs immobilized on an ITO coverslip. (b) SEM image (i) recorded at the border (dashed line) of the droplet cell confining the photo-catalytic reaction and zoom over two single crystals inside (ii) and outside (iii) of the cell.

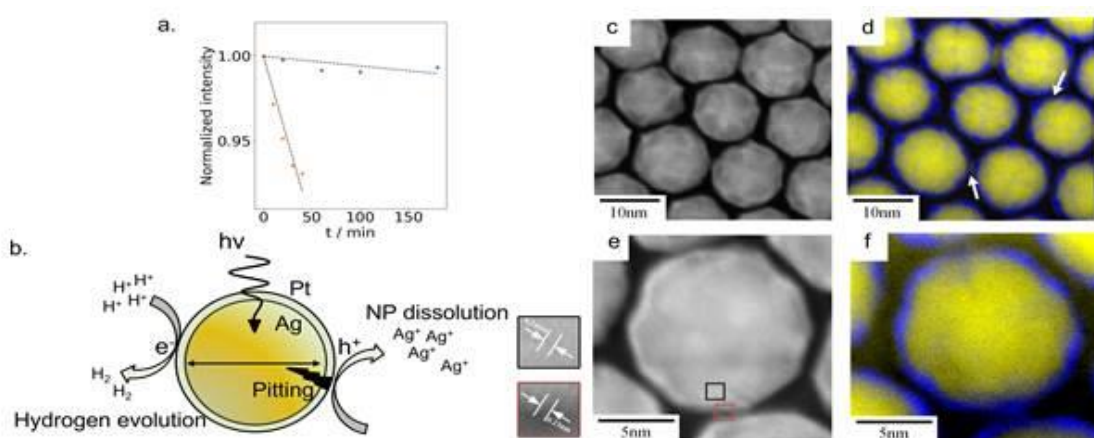


**Figure 2:** (a) Fluctuation of the maximum intensity of the plasmonic band as a function of time for Ag NPs (blue dots) and Ag@Pt NPs dispersed in sulphuric acid (orange dots). (b) the redox process occurring at the NP surface. (c, e) HAADF and (d,f) EELS maps of Ag@Pt NPs, highlighting the discontinuity of the Pt (blue) shell and the presence of silver (yellow) at the Pt outer surface

## SDM3-P8

### DETERMINATION DE L'ARCHITECTURE D'UN EMPILEMENT DE QUELQUES FEUILLETS DE MXENE PAR VEELS

#### DETERMINATION OF Ti<sub>3</sub>C<sub>2</sub>T<sub>x</sub> MXENE FEW-LAYER STACKS ARCHITECTURE USING VALENCE EELS

- **Thomas Bilyk** / Institut Pprime – UPR 3346 – CNRS, Université de Poitiers, 11 Bd M et P Curie, TSA 41123, 86073 Poitiers cedex 9
- **Haw-Wen Hsiao** / Department of Materials Science and Engineering, University of Illinois at Urbana-Champaign, Urbana, Illinois 61801, USA
- **Renliang Yuan** / Department of Materials Science and Engineering, University of Illinois at Urbana-Champaign, Urbana, Illinois 61801, USA
- **Stephane Celerier** / IC2MP – UMR 7285 – CNRS, Université de Poitiers, 4 rue Michel Brunet, TSA 51106, 86073 Poitiers cedex 9
- **Jian-Min Zuo** / Department of Materials Science and Engineering, University of Illinois at Urbana-Champaign, Urbana, Illinois 61801, USA
- **Jerome Pacaud** / Institut Pprime – UPR 3346 – CNRS, Université de Poitiers, 11 Bd M et P Curie, TSA 41123, 86073 Poitiers cedex 9
- **Vincent Mauchamp** \* (vincent.mauchamp@univ-poitiers.fr) / Institut Pprime – UPR 3346 – CNRS, Université de Poitiers, 11 Bd M et P Curie, TSA 41123, 86073 Poitiers cedex 9

\* Auteur correspondant

The properties of two-dimensional (2D) materials generally depend on their architecture, e.g. the number of layers in a stack, the interlayer distance or the layer functionalization. Focusing on the most studied MXene compound to date, i.e. Ti<sub>3</sub>C<sub>2</sub>T<sub>x</sub> 2D layers (where T-groups usually correspond to O, OH, F and/or Cl surface terminations inherited from the synthesis process), it has been shown that physical properties have a significant dependence on the number of layers in few-layer stacks. Beyond their thickness, MXene properties are also very sensitive to the interlayer distance which can be increased by intercalation of ions and/or molecules, or reduced by removing the interlayer intercalated water. In order to evidence the thickness/properties interplay in this rich family of 2D materials, one thus needs to precisely determine the architecture of a given MXene few-layer stack during TEM experiments. In this context, we show that valence EELS (VEELS) which corresponds to the excitation of the materials valence electrons, combined to density functional theory (DFT) simulations, provides a direct way to quantify (i) the number of layers in Ti<sub>3</sub>C<sub>2</sub>T<sub>x</sub> few layer stacks for thicknesses up to ~10 layers, and (ii) the average inter-layer distance. [1]

Figure 1 shows a comparison between experimental VEEL spectra recorded on different Ti<sub>3</sub>C<sub>2</sub>T<sub>x</sub> multilayers and the spectra simulated for different numbers of layers. To push the comparison quantitatively the mean squared error between experiments and simulations has been plotted, allowing to determine the exact number of layers in the thinnest samples.

Thickness of a sample can also be obtained through diffraction measurements and intensity profiles STEM-HAADF analysis. Therefore in order to validate the thickness measurements obtained by the VEELS method, position averaged CBED (PACBED) patterns and STEM-HAADF images were recorded on the very same areas of the Ti<sub>3</sub>C<sub>2</sub>T<sub>x</sub> MXenes. Different families of reflections exhibit different behavior of their pendellösung allowing to determine the sample thickness by comparison between experimental

and simulated intensity ratios (Figure 2). PACBED and STEM-HAADF analysis confirm the outcomes of the VEEL spectra analysis. ANR is acknowledged through MXENE-CAT project.

References :

- [1] T. Bilyk et al., 2D Materials, 9 (2022), p.035017

**Mots clefs** : 2D-materials, Valence-EELS, Diffraction

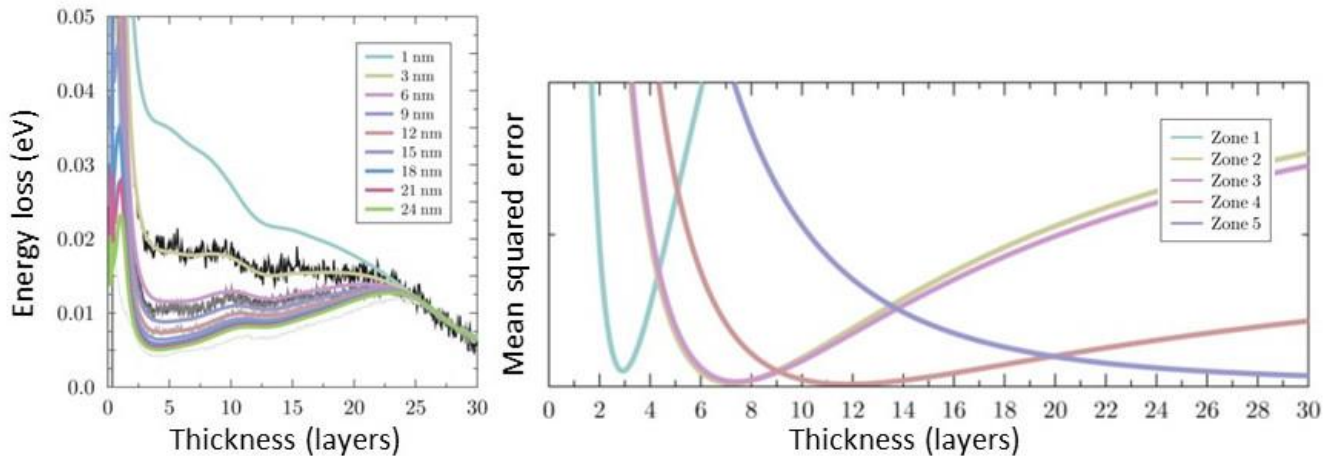


*Figure 1: (Left) Comparison between experimental VEEL spectra (black and grey curves) and DFT simulations considering thickness effects with the Kröger formula (color curves). Spectra were recorded on a FEI Themis Z microscope, equipped with a monochromator and operated at 80 kV. (Right) Mean squared error between experimental curves and simulations. It shows the very good precision on thickness determination for very thin samples.*

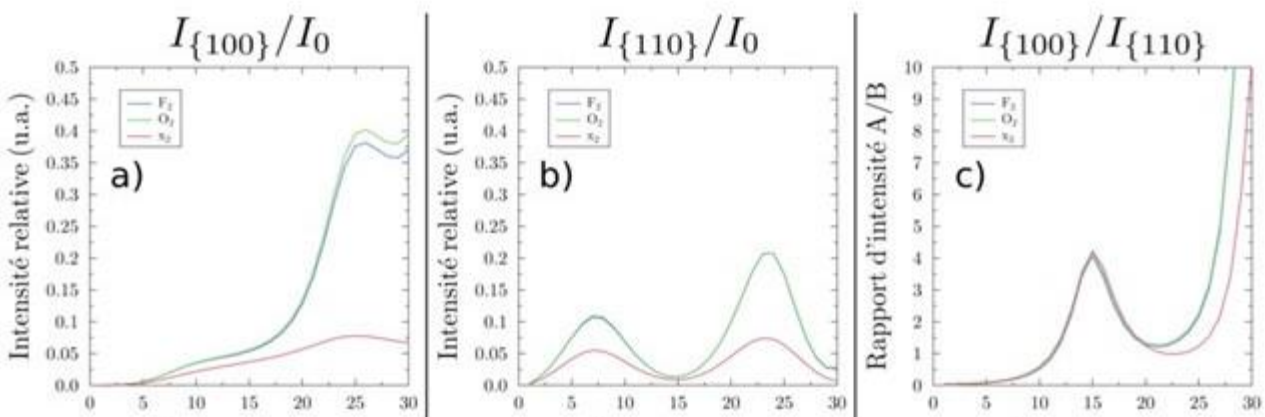


*Figure 2: Pendellösung of the 100 and 110 reflections in the [001] zone axis and intensity ratio between the reflections as a function of thickness.*

## SDM3-P9

### Etude de la météorite Santa Catharina par microscopie ionique à effet de champ analytique

Study of the Santa Catharina meteorite by analytical three-dimensional field ion microscope

- **Benjamin Klaes** \* (benjamin.klaes1@univ-rouen.fr) / Normandie Université, UNIROUEN, INSA Rouen, CNRS, Groupe de Physique des Matériaux, 76000 Rouen, France.
- **Frédéric Danoix** / Normandie Université, UNIROUEN, INSA Rouen, CNRS, Groupe de Physique des Matériaux, 76000 Rouen, France.
- **Fabien Delaroche** / Normandie Université, UNIROUEN, INSA Rouen, CNRS, Groupe de Physique des Matériaux, 76000 Rouen, France.
- **Rodrigue Lardé** / Normandie Université, UNIROUEN, INSA Rouen, CNRS, Groupe de Physique des Matériaux, 76000 Rouen, France.
- **François Vurpillot** / Normandie Université, UNIROUEN, INSA Rouen, CNRS, Groupe de Physique des Matériaux, 76000 Rouen, France.

\* Auteur correspondant

The Santa Catharina is a metallic meteorite discovered in 1875 on the island of São Francisco in Brazil [1]. The study of this meteorite allows us to have a better understanding of the primordial solar system as well as the Earth. This meteorite has a high Ni concentration (> 35%) and is composed of two phases, an ordered phase L10 (tetraenite) and a face-centered cubic disordered phase (taenite) [2,3]. Tetraenite can be formed due to the extremely slow cooling in the interplanetary medium towards the state of thermodynamic equilibrium. Tetraenite is composed of an alternance of Fe and Ni layers and form a superlattice with magnetic properties.

The latest advances in 3D Field ion microscopy (3D FIM) [4] was used to characterize the ordered phase and determine the orientation of the superlattice throughout the meteorite. Fig.(1c) shows a slice inside the reconstruction. Only Ni planes are reconstructed due to the contrast between Ni and Fe planes in FIM images (Fig.(1a)). The superlattice orientation was characterized with the Stereographic Fourier Transform [5]. This is the same orientation in several samples taken out at few 100µm. Antiphase boundary (APB) are also present in this ordered phase in Fig.(1d, 1e). This shift can also be observed in Fig.(1b) on FIM images. These results help to the understanding of the magnetic properties of this meteorite.

#### References :

- [1]Buchwald, V.F., 1975. Handbook of iron meteorites. Their history, distribution, composition and structure.
- [2]Miller, M.K. et al., 1992. An APFIM investigation of a weathered region of the Santa Catharina meteorite. Surf.Sci. 266, 441–445.
- [3]Miller, M.K., et al., 1989. AN ATOM PROBE FIELD-ION MICROSCOPY STUDY OF PHASE SEPARATION IN THE TWINCITY AND SANTA CATHARINA METEORITES. J. Phys. Colloq. 50, C8-413-C8-418.
- [4]Klaes, B., et al., 2021b. Analytical Three-Dimensional Field Ion Microscopy of an Amorphous Glass FeBSi. Microsc. Microanal. 1–9.

[5] Klaes, B., et al., 2021a. Development of Wide Field of View Three-Dimensional Field Ion Microscopy and High-Fidelity Reconstruction Algorithms to the Study of Defects in Nuclear Materials. *Microsc Microanal*.

**Mots clefs** : Meteorite, Field Ion Microscope, Tetrataenite

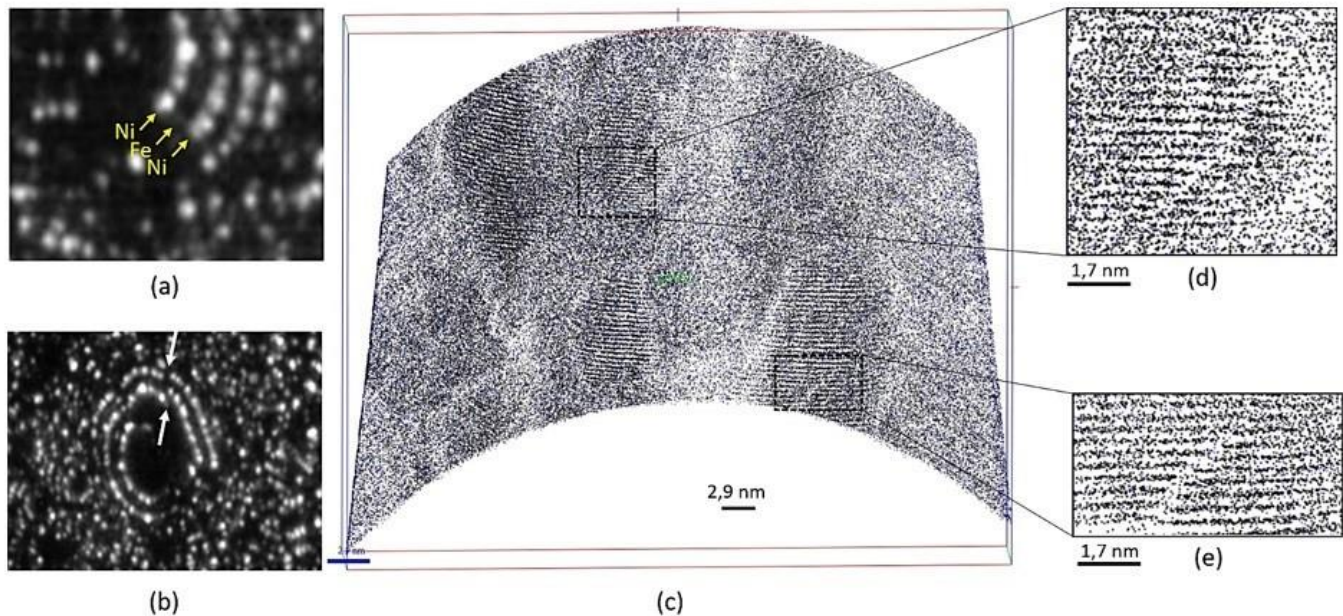


**Figure 1 :** Santa Catharina tip analyzed at 65K with Ne gaz. (a) In the ordered phase it has a very low brightness, they are not identified in the reconstruction and only Ni planes are reconstructed. (b) Discontinuities in Ni planes (white arrow) on FIM images, a bright plane (Ni) is cut and continues with a dark plane (Fe), characteristic of an APB. (c) Slice (4nm) inside the reconstruction, only Ni plane are reconstructed in the precipitates. (d,e) Zoom on area with a discontinuity in Ni planes that correspond to APB. Area (e) corresponds to a vertical slice on (b).

## SDM3-P10

### Etude des phénomènes de réactivité et de dégradation des batteries organiques par microscopie électronique

Study of degradation and reactivity mechanisms in organic batteries by electron microscopy

• **Maxandre Caroff** \* (maxandre.caroff@u-picardie.fr) / Laboratoire de Réactivité et Chimie des Solides (LRCS),

UMR CNRS 7314, Université de Picardie Jules Verne, Hub de l'Energie, 15, rue Baudelocque, 80039 Amiens Cedex, France

• **Matthieu Becuwe** / Laboratoire de Réactivité et Chimie des Solides (LRCS), UMR CNRS 7314, Université de

Picardie Jules Verne, Hub de l'Energie, 15, rue Baudelocque, 80039 Amiens Cedex, France

• **Carine Davoisne** / Laboratoire de Réactivité et Chimie des Solides (LRCS), UMR CNRS 7314, Université de

Picardie Jules Verne, Hub de l'Energie, 15, rue Baudelocque, 80039 Amiens Cedex, France

\* Auteur correspondant

Le besoin croissant en batterie électrique pose de nombreux défis notamment celui de l'extraction de métaux critiques pour les matériaux d'électrodes. L'utilisation de matériaux organiques d'électrodes pourraient permettre de limiter la demande en métaux en plus d'être facilement recyclable et d'avoir des structures chimiques adaptables[1]. Parmi ces matériaux, le naphtalène dicarboxylate de sodium (Na<sub>2</sub>-NDC) est un matériau intéressant en tant qu'électrode négative pour des applications de batteries [2]. Cependant, les phénomènes de réactivité et de dégradation du Na<sub>2</sub>-NDC pendant les charges et décharges restent mal connus. Nous proposons d'étudier ces phénomènes à l'aide des microscopies électroniques et techniques associées (MEB, MET, EELS).

Des particules de Na<sub>2</sub>-NDC de différentes tailles et morphologies ont été obtenues par précipitation dans différents solvants et caractérisées par MEB (Figure 1 et 2 ; FEI quanta-200 F). Les premiers tests de charge-décharge de batteries réalisés sur les différents matériaux ainsi obtenus, montrent que la morphologie du matériau impacte sensiblement les propriétés électrochimiques du matériau.

Pour mieux comprendre les modifications microstructurales, structurales de ce matériau, il sera suivi par MET (FEI Tecnai F20-S-TWIN, 200kV) à différents stades de charges et décharges. Les évolutions chimiques seront étudiées par infrarouge et par EELS (GIF Tridiem Gatan) notamment pour déterminer la nature des couches de passivations des particules. Les matériaux organiques étant sensibles au rayon électronique, il est nécessaire de contrôler la dose électronique reçue par le matériau afin de limiter sa dégradation sous le faisceau électronique pendant sa caractérisation. Le mode low-dose ainsi qu'un porte-objet cryogénique sont utilisés.

[1]Opportunities and Challenges for Organic Electrodes in Electrochemical Energy Storage, Philippe Poizot, Joël Gaubicher, Stéven Renault, Lionel Dubois, Yanliang Liang, and Yan Yao, Chemical Reviews 2020 120 (14), 6490-6557

[2]J.M. Cabañero, V. Pimenta, K.C. Cannon, R.E. Morris, A.R. Armstrong, Sodium Naphthalene-2,6-dicarboxylate: An Anode for Sodium Batteries, ChemSusChem. 12 (2019) 4522–4528

**Mots clefs** : matériaux organiques, cryomicroscopie électronique / organic materials, cryo-electron microscopy

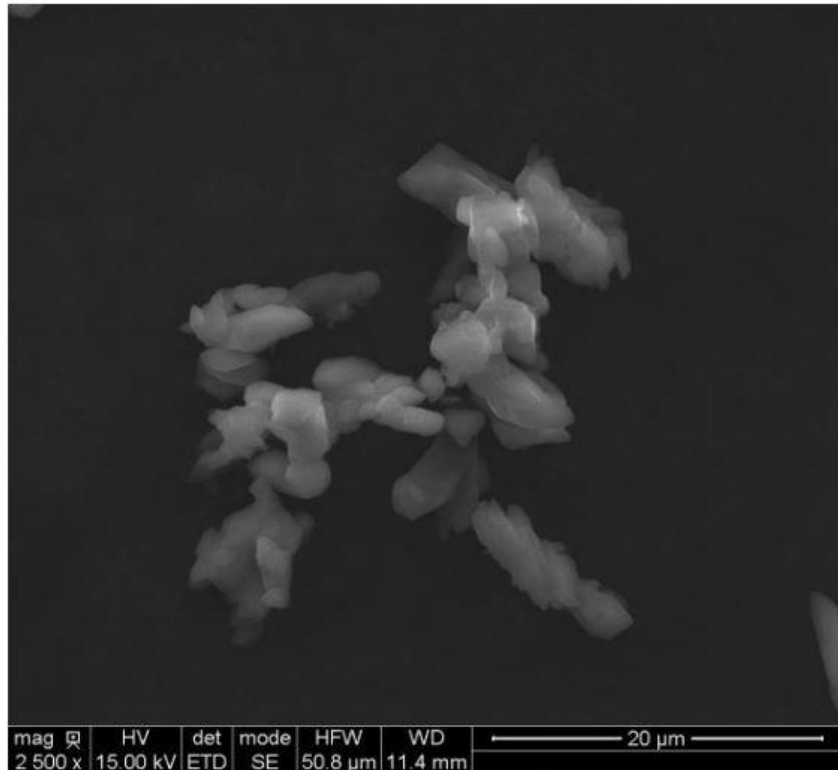


Figure 1: Photo MEB de particules de disodium naphthalene carboxylate cristallisées dans du méthanol, Morphologie “plaquette”

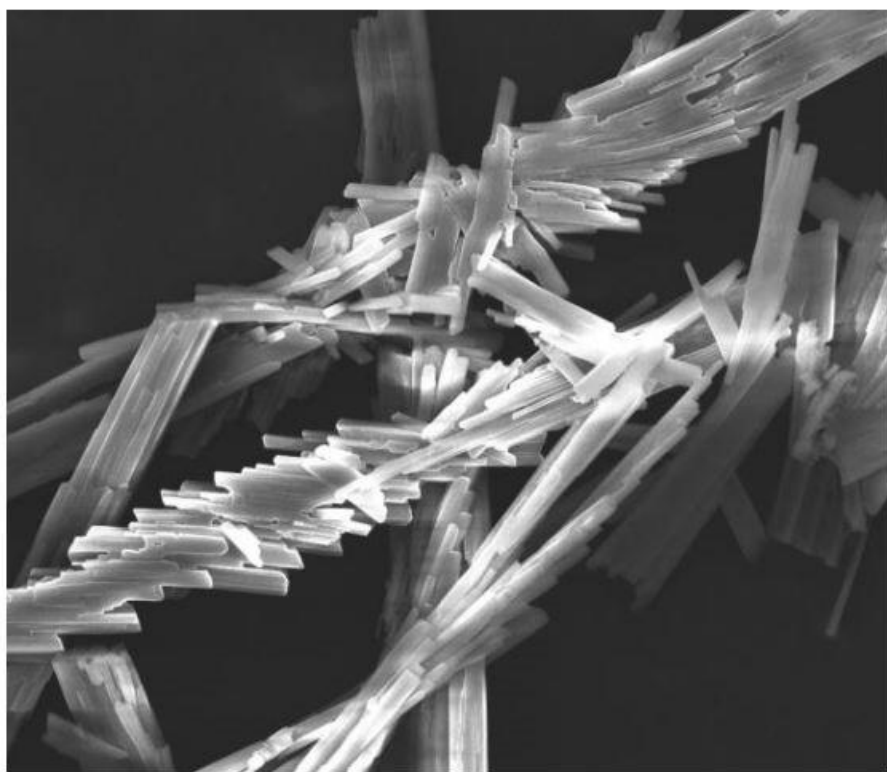


Figure 2: Photo MEB de particules de disodium naphthalene carboxylate cristallisées dans de l'acétonitrile, Morphologie “aiguille”

## SDM3-P11

### Comparaison du taux de dislocations dans des alliages d'aluminium corroyés (famille 2xxx) par microscopie électronique à transmission et par diffraction des rayons X

Comparison of dislocation rate in wrought aluminum alloys (2xxx family) by transmission electron microscopy and X-ray diffraction

- **Agathe Duclos** \* (agathe.duclos@cemes.fr) / 8011 CEMES-CNRS / 5085 CIRIMAT-CNRS-INPT-ENSIACET-UPS
- **Magali Brunet** / 8011 CEMES-CNRS
- **Benoît Malard** / 5085 CIRIMAT-CNRS-INPT-ENSIACET-UPS

\* Auteur correspondant

L'étude d'alliages d'aluminium de type Al-Cu-Mg-Si issus du patrimoine aéronautique de la Seconde Guerre mondiale vise une meilleure compréhension des propriétés mécaniques des alliages d'aluminium industriels actuels. Il est notamment intéressant de comprendre les mécanismes de durcissement des premiers alliages d'aluminium à durcissement structural (duralumin, super-duralumin) par l'analyse de leur microstructure. Certains traitements thermo-mécaniques appliqués à ce type d'alliage (T3) entraînent des mécanismes de nucléation de précipités nanométriques dépendant de dislocations provoquées par lesdits traitements. Les précipitations induites par déformation plastique, ou par piégeage d'atomes de Mg par des lacunes issues de la trempe participent au durcissement [1, 2]. Il est donc important de connaître le taux de dislocations pour le corrélérer à une densité et/ou une morphologie de précipités et évaluer l'impact de la précipitation sur les propriétés mécaniques.

Pour cela, différentes méthodes de mesure sont mises en place. Des observations en microscopie électronique à transmission (MET) sont d'abord menées pour estimer le nombre de dislocations [3]. Les taux de dislocations sont également estimés par diffraction des rayons X (DRX) sur des échantillons déformés plastiquement [4].

Un MET conventionnel JEOL-JEM-2010 (200kV) est utilisé pour les observations de dislocations. Des images sont sélectionnées sur un même grain selon plusieurs orientations pour obtenir une estimation statistique de leur nombre. La figure 1 présente un exemple d'image collectée. Un diffractomètre Bruker D8 Advance à source Cu(K $\alpha$ 1) est utilisé pour l'acquisition des diffractogrammes RX. Le logiciel TOPAS permet grâce à la méthode de Rietveld d'obtenir une estimation des tailles de cristallites et des taux de microdéformations (figure 2) tandis que la relation de Williamson-Smallman permet d'évaluer la densité de dislocations. La densité de dislocations ainsi évaluée par DRX augmente en fonction de la déformation plastique imposée et est de l'ordre de 0,1 à 1,5e15 m(-2). L'erreur maximale obtenue est d'environ 11%.

#### Références :

- [1] Nagai, Y., et al., Acta Materialia, 49 (2001) 913–920
- [2] García-Hernández, J.L., et al., Journal of Material Research and Technology, 8(6) (2019), 5471–5475
- [3] Karri, M., et al., Materials Science and Engineering A, 700 (2017), 75-81
- [4] Oger, L., et al., Materials and Design, 180 (2019)

**Mots clefs :** Aluminium / Durcissement structural / Microscopie électronique à transmission / Diffraction des rayons X / Dislocations

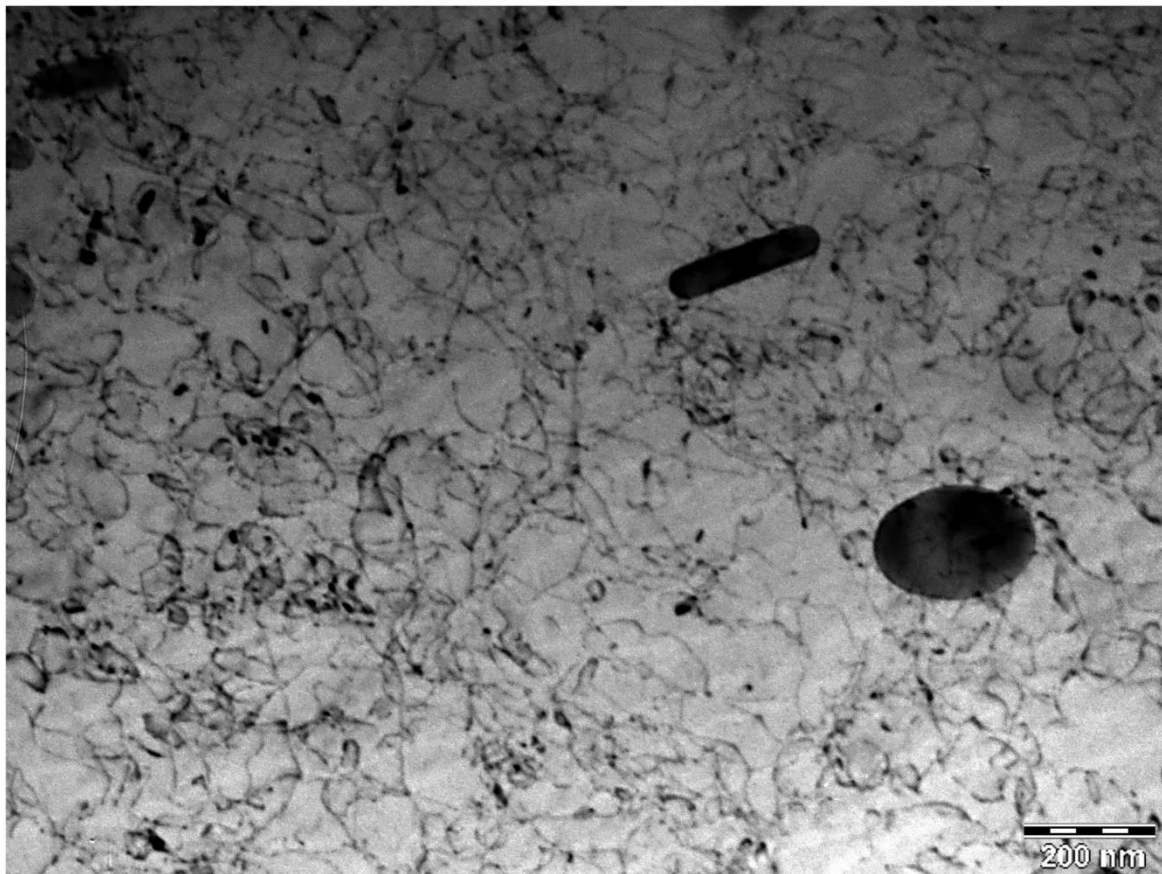


Figure 1 : Vue au MET d'un alliage 2017A-T4 brut de laminage

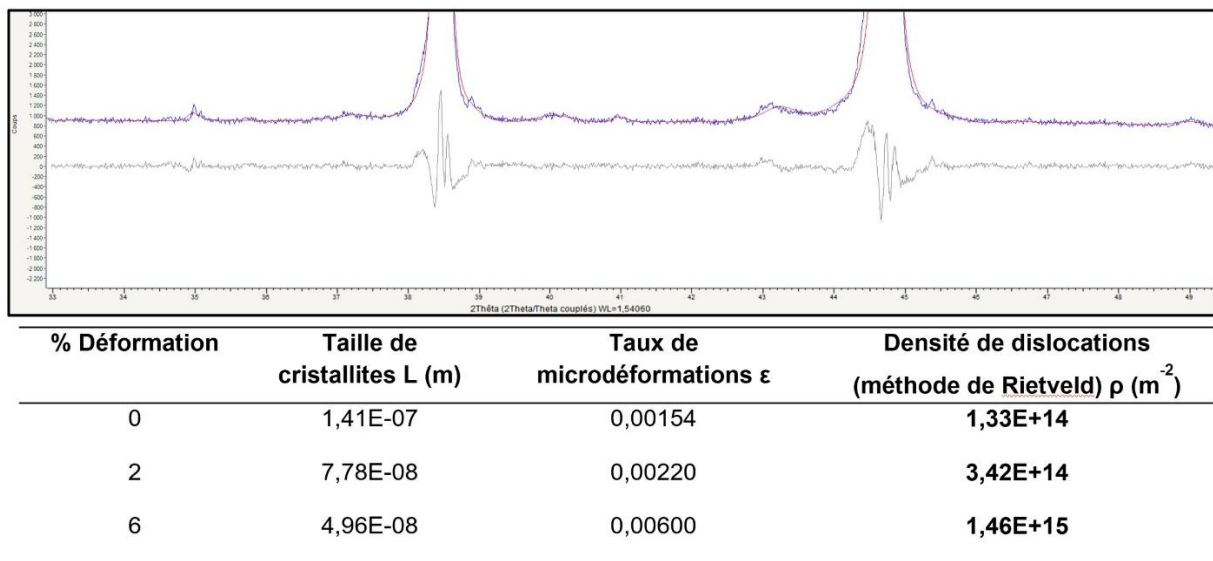


Figure 2 : Diffractogramme d'un alliage AA2024-T3 brut de laminage (bleu) et courbe d'affinement par méthode de Rietveld (rouge) (a) ; Estimation de densités de dislocations à partir des paramètres obtenus par méthode de Rietveld (b)

**SDM3-P12****Résoudre la structure de l'oxyde de bronze TiNbO<sub>x</sub> par STEM atomique et STEM-EDX****Unraveling the structure of TiNbO<sub>x</sub> bronze oxide by atomic STEM and STEM-EDX**

.**Mimoun Aouine** \* (mimoun.aouine@ircelyon.univ-lyon1.fr) / IRCELYON, Institut de recherches sur la catalyse et l'environnement de Lyon, UMR5256, 2 avenue Albert Einstein, 69626 Villeurbanne cedex

\* Auteur correspondant

**Unraveling the structure of TiNbO<sub>x</sub> bronze oxide by atomic STEM and STEM-EDX**

Mimoun AOUINE<sup>1</sup>, Thi Minh Nha LE<sup>1</sup>, Yaya LEFKIR<sup>2</sup>, Stéphanie REYNAUD<sup>2</sup>, Jean-Marc MILLET<sup>1</sup>, Thierry EPICIER<sup>1\*</sup> 1 Université Lyon, Université Claude Bernard Lyon 1, CNRS, IRCELYON, UMR 5526, 69626 Villeurbanne, France. 2 Université de Lyon, UJM-Saint-Etienne, CNRS, Institut d'Optique Graduate School, Laboratoire Hubert Curien, UMR 5516, 42023 Saint-Etienne, France.

The best catalyst for the ammoxidation of propane is presently based on a crystalline Mo-V-Nb mixed oxide, called M1 phase, with a complex bronze-type structure [1]. In addition to vanadium and molybdenum, it contains systematically a lone pair electrons element. In the structure of the M1 phase Mo, V and Nb are hexacoordinated forming corner-sharing Mo(V,Nb)O<sub>6</sub> octahedra that delimits hexagonal and heptagonal channels aligned in the 001 direction. The search for similar phases showed that rubidium or thallium niobate with compatible framework could be good candidates. In the present work, such new compounds were successfully synthesized using a microwave-assisted hydrothermal method. Among these new compounds, a new niobate with a similar structure was obtained, thallium niobate, Ti<sub>7</sub>Nb<sub>39</sub>O<sub>101</sub>, which to the best of our knowledge had never been detected before. Its relatively complex structure was determined by X-ray diffraction on the basis of precious information obtained by advanced transmission electron microscopy work, e.g. STEM imaging (300 kV FEI/TFS Titan ETEM), aberration-corrected STEM imaging and STEM-EDX atomic mapping (200 kV JEOL Neo ARM equipped with a Centurio Large Angle SDD-EDS detector). In particular, ADF, e-ABF [2] and BF micrographs were suitably combined in order to produce bright-field type atomic images revealing the location of oxygen positions and possibly required Nb interstitials cations insuring the electroneutrality of the solid. Figure 1 illustrates the results still under analysis in order to complete the structural investigation through a combined TEM / DRX Riteveld refinement approach [3].

**Références/References :**

- [1]J.L. Dubois, G.S. Patience, J.M.M. Millet, B. Sels, M. van de Voorde (Ed.), Wiley-VCH, Weinheim, (2017) 503.
- [2]S.D. Findlay, Y. Kohno, L.A. Cardamone, Y. Ikuhara, N. Shibata, Ultramicroscopy 136 (2014) 41.
- [3] Thanks are due to the CLYM ([www.clym.fr](http://www.clym.fr)) for the access to the microscopes.

**Mots clefs :** Catalyse, ammoxydation, résolution structurale, mapping atomique, STEM

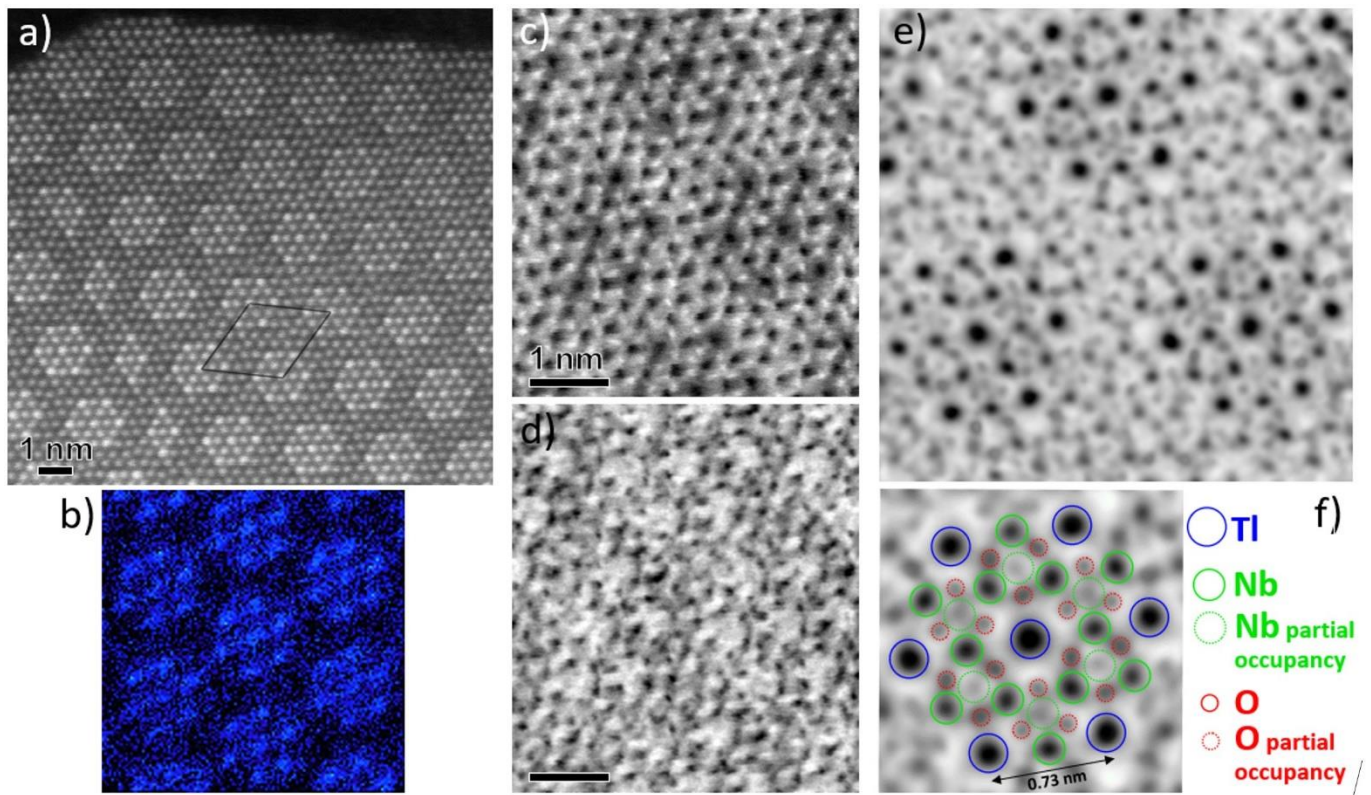


Figure 1: advanced TEM study of the thallium niobate  $Tl_7Nb_{39}O_{101}$ . a): Near High Angle Annular Dark Field image showing the cationic ( $Tl, Nb$ ) sublattice at relatively low mag (ETEM, 300 kV). Note the presence of defects, e.g. incomplete hexagonal motifs. The complete hexagonal cell ( $a = 23.94 \text{ \AA}$  and  $c = 3.96 \text{ \AA}$ ) is shown. b): atomic EDX map resolving the Tl atomic columns (Neos ARM, 200 kV). c: high mag Bright Field image and d) Annular Bright Field image of the same area. e): Averaged linear combination of images c) and d) after application of a  $P3$  symmetry. f) Enlargement of one hexagonal motif enabling to postulate the position of oxygen atoms as well as sites with a partial occupancy.

## SDM3-P13

### STEM-EELS Monochromatée à Faible Dose et à Températures Cryogéniques pour les Nanomatériaux Sensibles aux Rayonnements

Low-dose Monochromated STEM-EELS at Cryogenic Temperatures for Radiation-Sensitive Nanomaterials

• **Maeva Chaupard** \* (maeva.chaupard@universite-paris-saclay.fr) / Laboratoire de Physique des Solides, CNRS

UMR 8502, Université Paris-Saclay, France; Institut des Sciences Moléculaires d'Orsay, CNRS UMR 8214, Université Paris-Saclay, France

• **Xiaoyan Li** / Laboratoire de Physique des Solides, CNRS UMR 8502, Université Paris-Saclay, France

• **Odile Stéphan** / Laboratoire de Physique des Solides, CNRS UMR 8502, Université Paris-Saclay, France

• **Mathieu Kociak** / Laboratoire de Physique des Solides, CNRS UMR 8502, Université Paris-Saclay, France

• **Ruxandra Gref** / Institut des Sciences Moléculaires d'Orsay, CNRS UMR 8214, Université Paris-Saclay, France

• **Marta De Frutos** / Laboratoire de Physique des Solides, CNRS UMR 8502, Université Paris-Saclay,

France \* Auteur correspondant

Coupling Scanning Transmission Electron Microscopy with Electron Energy Loss Spectroscopy (STEM-EELS) provides an in-depth and local analysis of nanomaterials. By measuring the electron-matter interactions, it allows the identification of complex chemical structures with high resolution, down to the atomic scale.<sup>1</sup>

The use of a monochromated electron probe enables a wide energy range to be exploited, from the infrared to the soft X-rays. Based on this multimodality, such a technique provides, in a single experiment, spectral signatures that are comparable to the corresponding photon-based spectroscopies.<sup>1</sup> This “all-in-one” feature, combined with high spatial resolution, makes STEM-EELS a powerful approach to address questions concerning nanomaterials properties.

However, the electron probe causes radiation damage to sensitive specimens. Mainly due to radiolysis, biological, organic and organic-inorganic nanomaterials are irreversibly distorted and suffer structural and chemical losses.<sup>2</sup>

Here, we have developed a new method to obtain damage-free signatures of organic-inorganic nanoparticles. Using cryogenic temperatures and low-electron doses ( $10 \text{ e}/\text{\AA}^2$ ), we identified intact functional groups in the three spectral ranges and mapped their distribution at the nanoscale (< 10nm). By carefully controlling the electron dose, we monitored the beam-induced degradation effect to demonstrate the possibility of deciphering complex chemical reactions (Figure 1).<sup>3</sup>

In the following, we aim to use this method to study the behaviour of organic-inorganic nanomaterials in physiological media. STEM-EELS will provide more insight into the complex interactions that occur between nanoparticles and biomolecules.

## References:

- [1] Colliex, C. The European Physical Journal Applied Physics, 97, (2022), p.38.
- [2] Egerton, R. F. Micron, 119, (2019), p.72–87.
- [3] Chaupard, M.; Degrouard, J.; Li, X.; Stéphan, O.; Kociak, M.; Gref, R.; de Frutos, M. ACS Nano, 17, (2023), p.3452–3464.

**Mots clefs :** Low-dose EELS, radiation-sensitive nanomaterials, multimodal

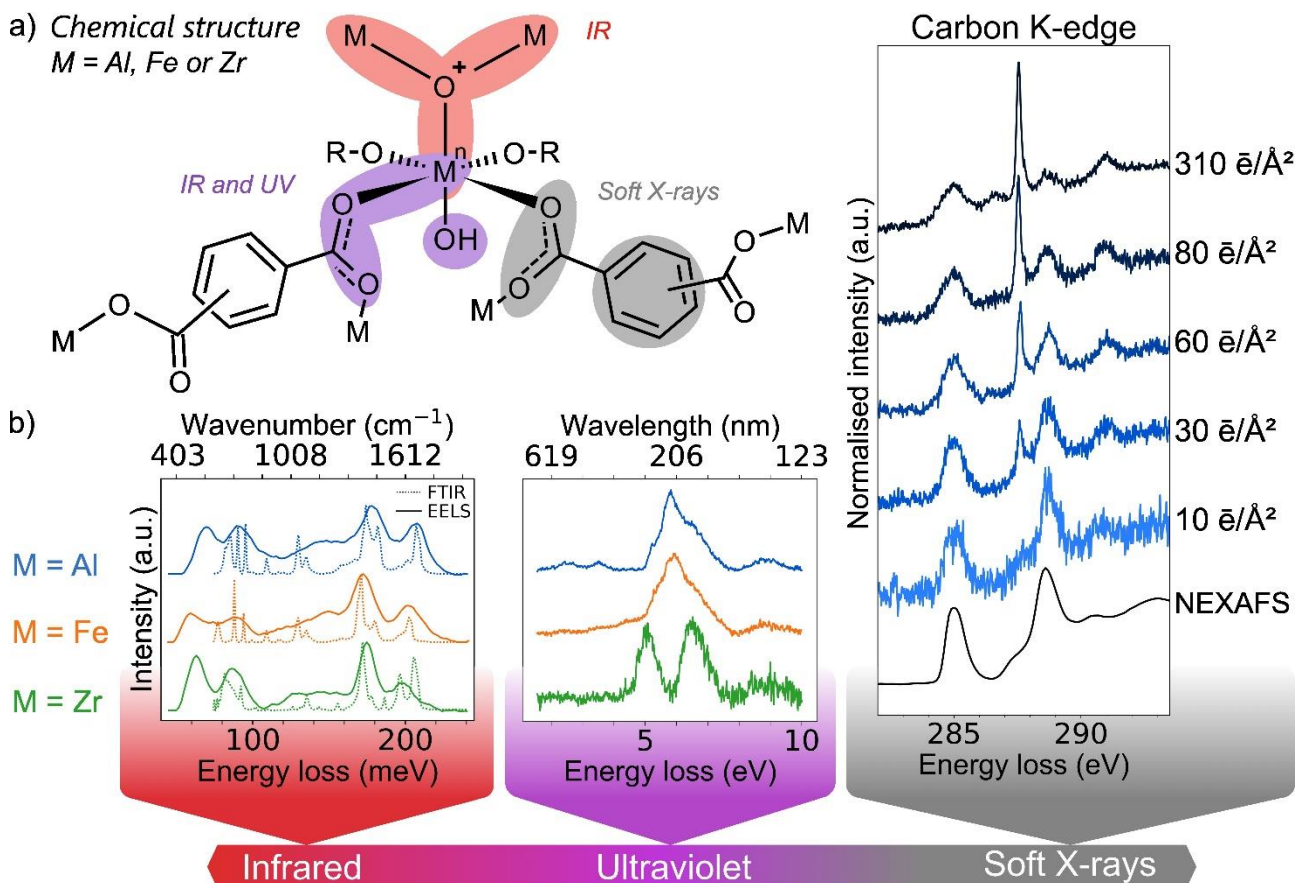


*Figure 1: a) Chemical structure of organic-inorganic nanomaterials, namely metal-organic frameworks. b) Their functional groups have been identified by EELS in the infrared, ultraviolet and soft X-ray energy scales. The carbon K-edge depicts the chemical reaction occurring under irradiation.*

## SDM3-P14

### Matériaux à changement de phase Ge-Sb-Te : étude de la cristallisation par TEM haute résolution *in situ* et spectroscopie X à dispersion d'énergie

Ge-Sb-Te phase change material: investigation of the crystallization by *in situ* high resolution TEM and Energy-dispersive X-ray spectroscopy

- **Solène Comby-Dassonneville** \* (solene.dassonneville@univ-amu.fr) / Aix Marseille Univ, Université de Toulon, CNRS, IM2NP, Marseille, France
- **Michael Texier** \* (michael.texier@univ-amu.fr) / Aix Marseille Univ, Université de Toulon, CNRS, IM2NP, Marseille, France
- **Thomas Fernandes** / Aix Marseille Univ, Université de Toulon, CNRS, IM2NP, Marseille, France
- **Philippe Hans** / Aix Marseille Univ, Université de Toulon, CNRS, IM2NP, Marseille, France
- **Thomas Cornelius** / Aix Marseille Univ, Université de Toulon, CNRS, IM2NP, Marseille, France
- **Roberto Simola** / STMicroelectronics, Crolles, France
- **Yannick Le Friez** / STMicroelectronics, Crolles, France
- **Simon Jeannot** / STMicroelectronics, Crolles, France
- **Martin Rosenthal** / European Synchrotron Radiation Facility, Grenoble F-38043, France
- **Olivier Uteza** / Aix Marseille Univ., CNRS, LP3, UMR7341, Marseille, 13288 France
- **Olivier Thomas** / Aix Marseille Univ, Université de Toulon, CNRS, IM2NP, Marseille, France \* Auteur correspondant

Phase Change Materials (PCMs) have the property to reversibly switch, through controlled and local heating, between an amorphous and a crystalline phase. These two phases exhibit a large contrast both in electrical and optical properties making PCMs very interesting for storing information. Indeed, they have been used for a long time in ReWritable Compact Disks (where writing is performed by laser heating, and reading by low power laser optical reflectivity measurement). More recently it has been realized that writing and reading can be performed using an electrical current, thus opening the path to Phase Change Random Access Memories (PCRAM) [1]. Their key advantages are their speed (in the 10's of ns), their scalability, and their intrinsic compatibility with embedded memories processes. One of the most studied PCM is Ge<sub>2</sub>Sb<sub>2</sub>Te<sub>5</sub> (commonly named GST in the literature), which has a crystallization temperature close to 150–170 °C. This temperature is too low for long-enough data retention in many applications (e.g. automotive). To address this issue, compositionally optimized Ge-rich GST (GGST) has been developed by STMicroelectronics [2] having a crystallization temperature of about 350°C. However, the exact mechanisms for crystallization of this multiphase material still need investigation and many fundamental questions remain. In this work, the crystallization of encapsulated GGST samples is followed *in situ* thanks to high resolution transmission electron microscope observations during heating, in order to assess the crystallization kinetics, the nature of the crystallized phases and their spatial distribution. Chemical segregation prior and during crystallization is discussed based on Energy-dispersive X-ray spectroscopy. In perspective, the effect of femtosecond laser irradiation on the crystallization and amorphization of a GST sample is evaluated, opening the way to the real-time study of the reversible crystallization/amorphous transformation of PCMs.

IPCEI/Nano 2022 program is acknowledged for partial funding of this work. We would like to thank ESRF for allocating beamtime on ID16B beamline.

[1] G.W. Burr et al., IBM J. Res. Dev. 52, 449 (2008); [2] P. Zuliani et al., Solid State Electronics 111, 27 (2015)

**Mots clefs :** phase change material, *in situ* TEM, EDX

**SDM3-P15****ÉTUDE DES PROPRIÉTÉS PHYSIQUES DE COUCHES MINCES DE CrSi2 AMORPHE MODIFIÉES PAR IMPLANTATION IONIQUE****Study of the physical properties of amorphous CrSi2 thin films modified by ion implantation**

- **Mariana Timm** \* (mariana.timm@umontpellier.fr) / ICGM, Univ Montpellier, CNRS, ENSCM, Montpellier, France
- **Bárbara Konrad** / PPGCIMAT, Universidade Federal do Rio Grande do Sul (UFRGS), Porto Alegre, Brasil
- **Erwan Oliviero** / ICGM, Univ Montpellier, CNRS, ENSCM, Montpellier, France
- **Hugo Bouteiller** / Institut Pprime UPR3346, Université de Poitiers-CNRS-ENSMA, 86073 Poitiers, France
- **Jean-François Barbot** / Institut Pprime UPR3346, Université de Poitiers-CNRS-ENSMA, 86073 Poitiers, France
- **Jérémie Margueritat** / Institut Lumière Matière, UMR 5306, Université Lyon 1-CNRS, Université de Lyon, 69622 Villeurbanne, France
- **Paulo F.P. Fichtner** / Escola de Engenharia, Universidade Federal do Rio Grande do Sul (UFRGS), Porto Alegre, Brasil
- **Nicole Fréty** / ICGM, Univ Montpellier, CNRS, ENSCM, Montpellier, France

\* Auteur correspondant

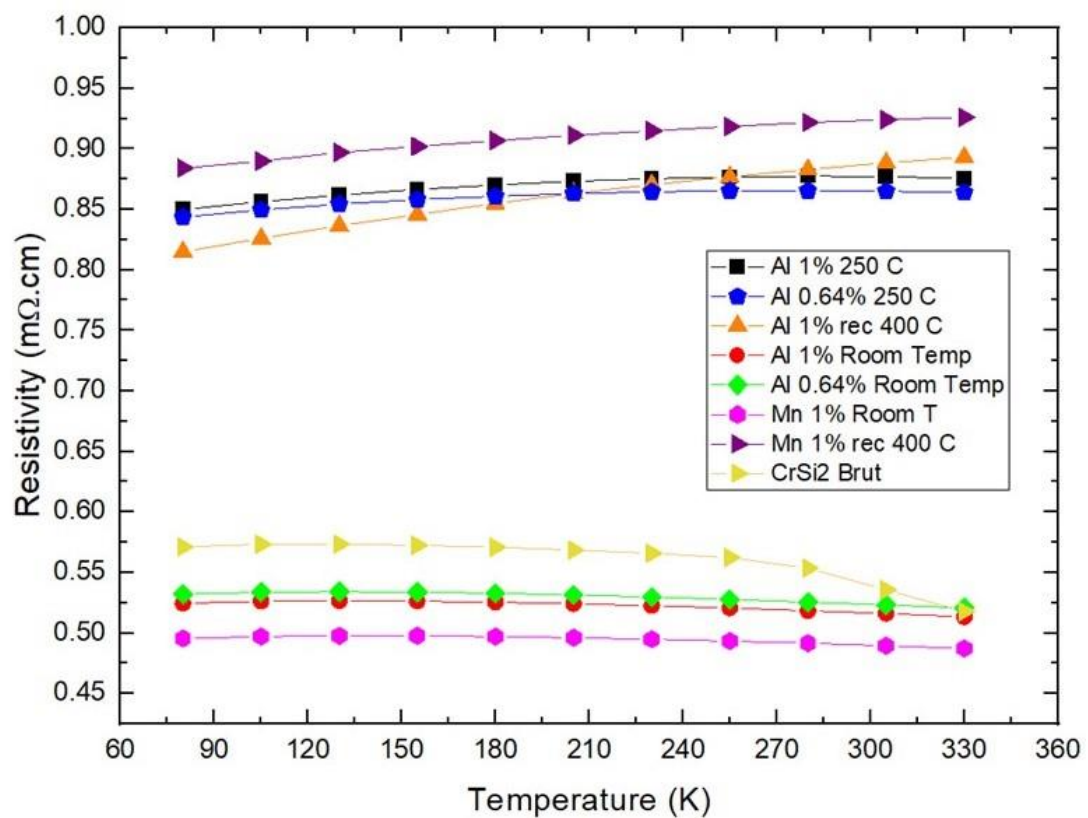
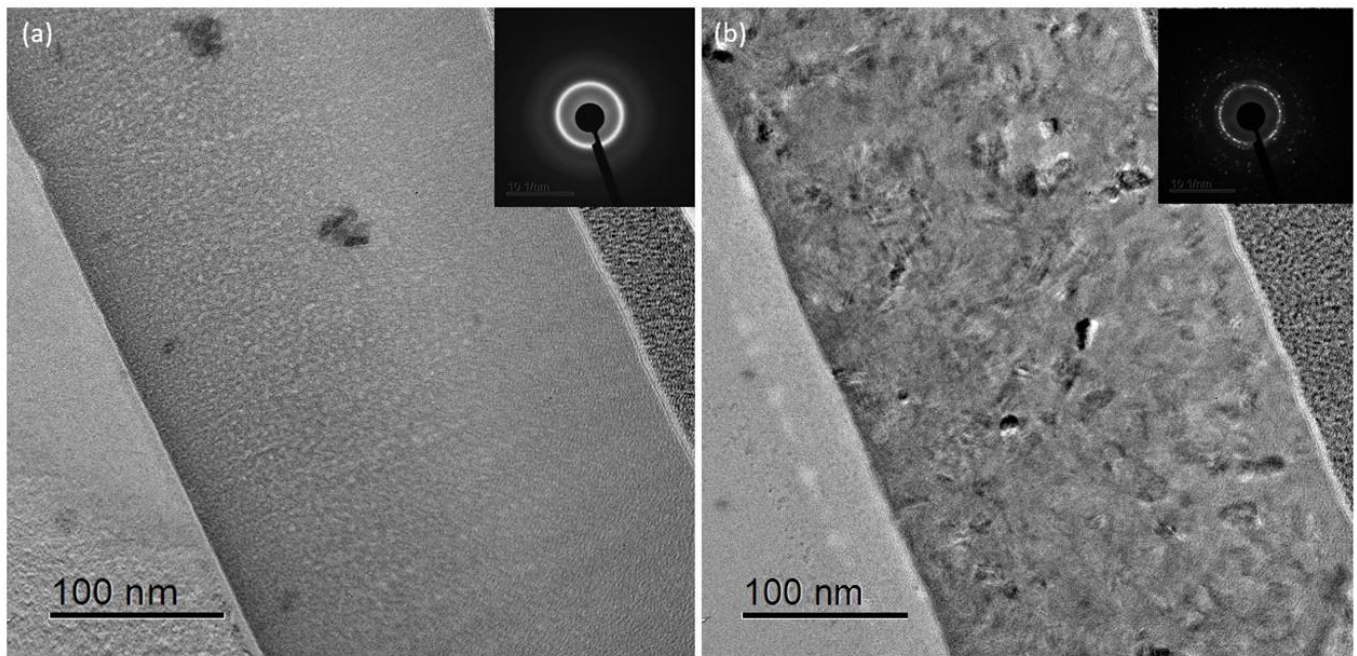
CrSi2 ((di)chromium silicide) is a potential thermoelectric material that has attracted attention in recent years due to its semiconducting properties and high thermal stability [1]. In this sense, the ion implantation technique can be used to adapt the physical properties of different materials and improve their semiconductor and/or thermoelectric performance [2]. This work investigates the influence of different ion species and implantation conditions on the microstructure, electrical resistivity and Seebeck coefficient/thermal conductivity behaviors in amorphous CrSi2 thin films.

CrSi2 films with a thickness of about 290 nm were produced by magnetron sputtering and deposited on a SiO<sub>2</sub>/Si substrate. The samples were implanted at room temperature and at 250 °C with Al or Mn ions, to form a concentration-depth plateau reaching a concentration of ≈ 0.008 at.%, ≈ (Al) 0.64 at.% (Al) and ≈ 1.0 at.-% (Al, Mn). TEM and STEM-EDX were used to characterize the microstructure and elemental distribution of the samples. The electrical resistivity was measured by the van der Pauw method, and the Seebeck coefficient was obtained with the Physical Property Measurement System (PPMS-TTO). Furthermore, the surface acoustic modes of the CrSi2 thin films were investigated by Brillouin Spectroscopy. The results obtained show that the Al and Mn implantations at room temperature cause the reduction of the electrical resistivity compared to the non-implanted film. On the other hand, the electrical resistivity values are significantly higher for Al and Mn implantations in heated and/or annealed substrates. The evolution of the microstructure and thermoelectrical behavior are discussed considering the effects of radiation damage and the formation of dense networks of nanocrystallites during the implantation process.

**Références**

- [1] T. Dasgupta et al. (2008) J Appl Phys., 103, 113536
- [2] I. R. Sanders et al (2002) Solid State Electron 20, pp: 703–707

**Mots clefs :** CrSi2, thin films, ion implantation



## SDM3-P16

### Influence de l'austénite sur le vieillissement de la ferrite des aciers inoxydables austéno-ferritiques

#### Influence of austenite on ferrite aging of austenitic-ferritic stainless steels

- **Jeffrey Renaux** \* (jeoffrey.renaux@univ-rouen.fr) / Groupe de Physique des Matériaux, CNRS, INSA, Université de Rouen, Saint-Étienne-du-Rouvray
- **Sébastien SAILLET** / EDF, Recherche et développement, département MMC, groupe métallurgique, Moret-sur-Loing
- **Romain Badyka** / EDF, Recherche et développement, département MMC, groupe métallurgique, Moret-sur-Loing .**Raphaël Pesci** / LEM3 UMR CNRS 7239, Metz
- **Samuel Jouen** / Groupe de Physique des Matériaux, CNRS, INSA, Université de Rouen, Saint-Étienne-du-Rouvray
- **Cristelle Pareige** / Groupe de Physique des Matériaux, CNRS, INSA, Université de Rouen, Saint-Étienne-du-Rouvray

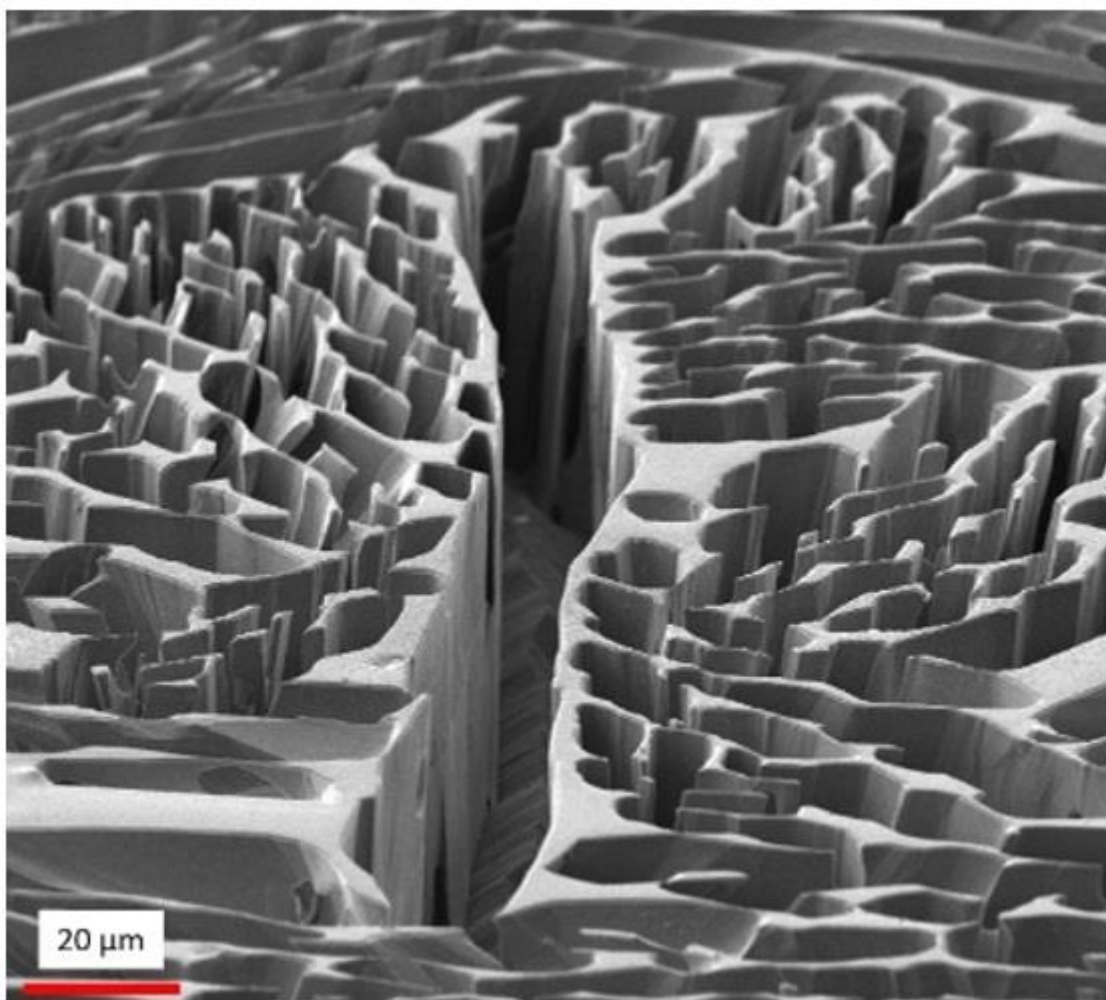
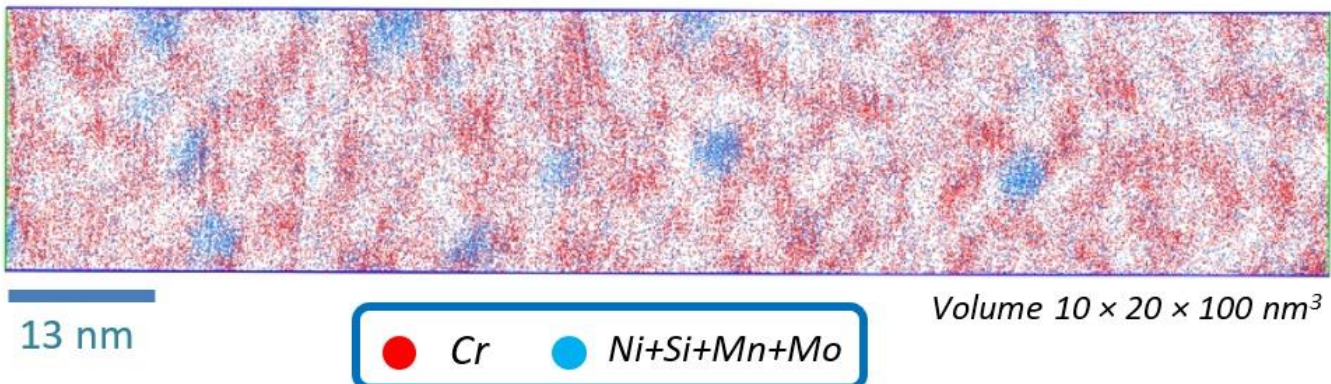
\* Auteur correspondant

Les aciers inoxydables austéno-ferritiques sont largement employés dans la conception des pièces de structure des centrales nucléaire de génération 2. Une problématique importante concerne la diminution de leurs propriétés mécaniques causées par l'évolution microstructurale de la ferrite aux températures de fonctionnement comprises entre 285 et 325 °C. À ces températures, la décomposition spinodale conduisant à l'apparition des phases  $\alpha$  (riche en Fe) et  $\alpha'$  (riche en Cr) est accompagnée par la précipitation de phase G, riche en Ni, Si, Mn et Mo (Figure 1). Des études antérieures [1,2] ont révélé que la ferrite des aciers duplex vieillit plus vite qu'une ferrite monphasée de même composition. Une des hypothèses avancées est la présence de contraintes résiduelles induites par l'austénite. Afin de tester cette hypothèse, nous avons entrepris l'étude du vieillissement de la ferrite avec et sans austénite par sonde atomique tomographique, le but étant de travailler avec des ferrites identiques en composition et morphologie. La préparation des échantillons étudiés a nécessité la dissolution sélective d'une région de l'échantillon par attaque électrochimique avant vieillissement, comme présenté sur la Figure 2. L'objectif est donc de réaliser une étude comparative du vieillissement par sonde atomique pour la ferrite sans austénite et la ferrite avec austénite afin d'identifier et quantifier les différences éventuelles liées à la présence de l'austénite. Les résultats obtenus montrent que plus que les contraintes résiduelles, ce sont les impuretés (P, Nb ...) qui semblent jouer un rôle significatif dans le vieillissement de la ferrite.

#### Références :

- [1] J.E. Brown, G.D.W. Smith, Atom probe studies of spinodal processes in duplex stainless steels and single- and dual-phase Fe-Cr-Ni alloys, *Surface Science*. 246 (1991) 285–291. [https://doi.org/10.1016/0039-6028\(91\)90428-U](https://doi.org/10.1016/0039-6028(91)90428-U). [2] R. Badyka, Influence des éléments d'alliage sur la cinétique de vieillissement de la ferrite d'aciers inoxydables austéno-ferritiques moulés, Normandie Université, 2018.

**Mots clefs** : vieillissement thermique, sonde atomique, aciers austéno-ferritiques, décomposition spinodale, phase G



## SDM3-P17

### Etude MET d'une vis fissurée de cloison-renfort d'un réacteur REP du parc français et irradiée jusqu'à 37 dpa

**TEM investigations of a cracked baffle-former bolt coming from a French PWR and irradiated up to 37 dpa**

- **Priscille CUVILLIER** \* (priscille.cuvillier@edf.fr) / EDF DI, CNPE de Chinon – BP 23 – 37420 Avoine, France
- **Eric DERNIAUX** / EDF DI, CNPE de Chinon – BP 23 – 37420 Avoine, France
- **Yannick THEBAULT** / EDF DI, CNPE de Chinon – BP 23 – 37420 Avoine, France
- **Maxime MISON** / EDF DI, 2 rue Ampère – 93206 Saint-Denis, France
- **Amélie LEDUC** / EDF UNIE, 1 place Pleyel – 93200 Saint-Denis, France
- **Virginie BOULAY** / EDF DT, 19 rue Pierre Bourdeix – 69007 Lyon, France

\* Auteur correspondant

A better understanding of degradation phenomena in nuclear reactor (i.e. ageing under neutrons irradiation or heating, corrosion under load, mechanical breaking, etc.) is needed in order to improve and guarantee the safety and the reliability of the exploitation, the maintenance strategies in the electricity production area and to reinforce the justification of the lifetime extension of reactors up to 60 years. The LIDEC laboratory based at EDF Chinon Nuclear Power Plant (NPP) is in charge of failure analysis on components from the French NPPs. Numerous CP0 plants series bolts have already been assessed by EDF ([1] – [7]). Here, this study concerns a cracked bolt (Figure 1) irradiated up to 37 dpa coming from the same NPP unit as uncracked bolt studied in [6] and with comparable irradiation level. Macroscopic examinations and preliminary TEM (FEI Tecnai Osiris) examinations were already performed on this cracked bolt [7] and confirmed a cracking mechanism due to Irradiation-Assisted Stress Corrosion Cracking (IASCC). FIB sample preparation was conducted in High Activity (HA) because of high irradiation levels, but TEM examinations are feasible out of HA cell afterwards ([8] – [10]) thanks to the negligible mass of a FIB sample. Here, after a brief reminder of the previous examinations, emphasis will be made on TEM investigations of the irradiation microstructure, the radiation-induced segregation at grain boundaries and the characterization of the crack and oxides at the tip ends (Figure 2). The main objective is to better understand the degradation mechanisms of materials at high level of irradiation and especially the Irradiation-Assisted Stress Corrosion racking (IASCC) mechanism.

#### References :

- [1] R. Cauvin et al., Fontevraud 3 (1994), p.54-65
- [2] G. Pironet et al., Fontevraud 4 (1998), p.195-206
- [3] C. Pokor et al., RGN, 6 (2007), p.31-37
- [4] C. Panait et al., Fontevraud 8 (2004)
- [5] L. Legras et al., Fontevraud 9 (2018)
- [6] É. Fargeas et al., Fontevraud 9 (2018)
- [7] P. Cuvillier et al., Fontevraud 10 (2022)
- [8] A. Assel et al., J. Nucl. Mater., 459 (2015), p.241-246
- [9] M.-H., Lee et al., J. Microsc., 261 (2016), p.243-248
- [10]L. Legras et al., EMC, 2016 (2016), p.443-444

**Mots clefs** : neutron irradiation, vessel internal structures, 316L, IASCC, TEM

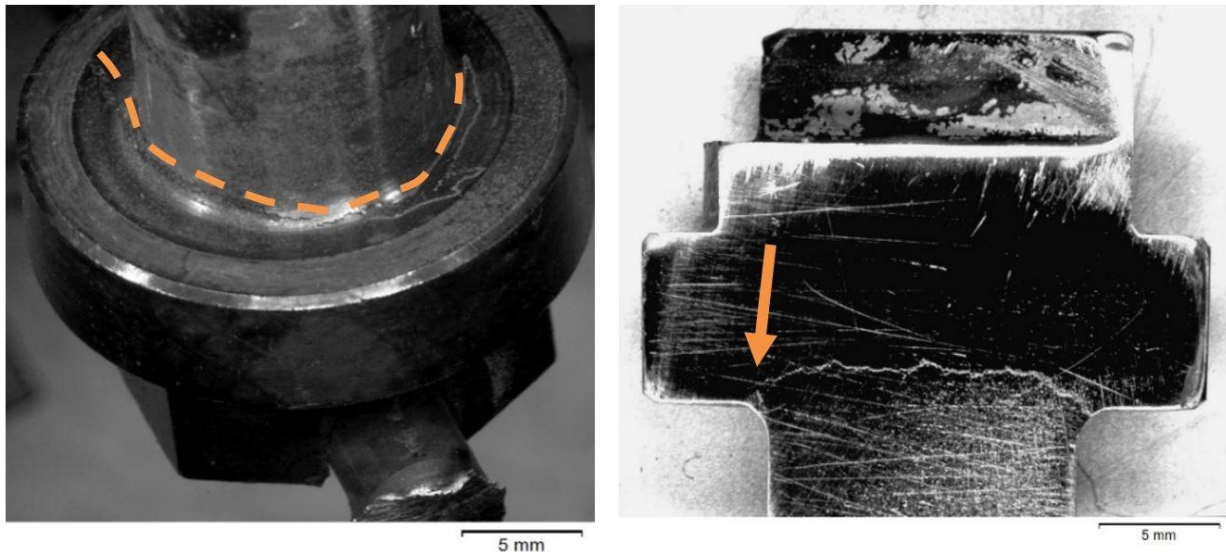


**Figure 1:** Visual examinations of the crack at the connecting fillet area between the head and the shank. Crack angular extent is about  $226^\circ$ . The crack almost reaches the opposite connecting fillet in the observation plan.

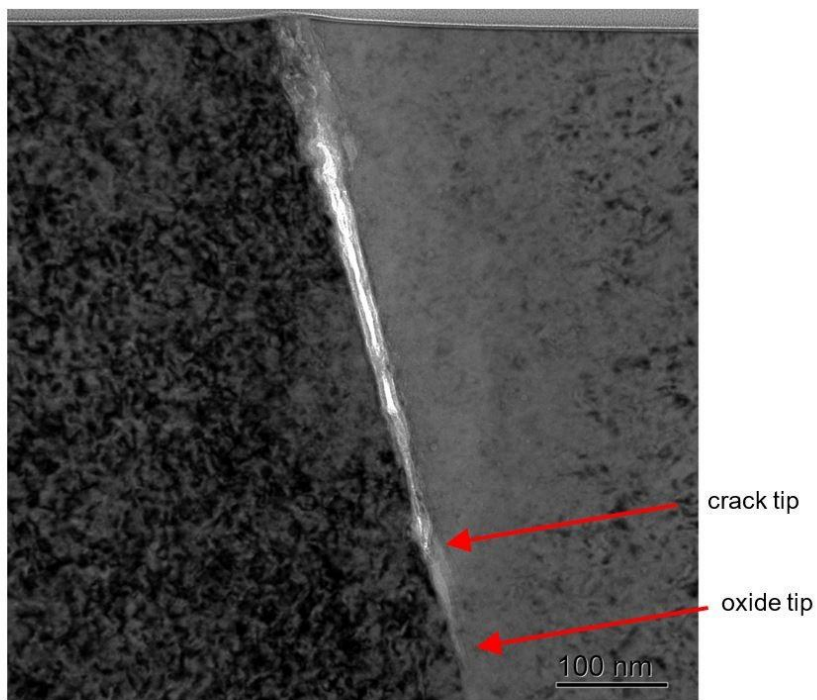


**Figure 2:** Bright field image of the crack. The crack tip is enriched in oxide.

## SDM3-P18

### Études par MET de l'influence de l'hydrogène et de la déformation sur la précipitation d'un alliage Al-Cu.

TEM investigations on the effects of hydrogen and deformation on the precipitation of an Al-Cu alloy.

- **Omar BOUKIR** \* (omar.boukir@univ-rouen.fr) / Univ Rouen Normandie, INSA Rouen Normandie, CNRS, Groupe de Physique des Matériaux UMR 6634, F-76000 Rouen, France
- **Xavier SAUVAGE** / Univ Rouen Normandie, INSA Rouen Normandie, CNRS, Groupe de Physique des Matériaux  
UMR 6634, F-76000 Rouen, France

\* Auteur correspondant

Hydrogen is becoming a key element of the energy transition worldwide, especially by using it as an energy carrier or directly as a fuel in automobiles and aircraft. Aluminium alloys are commonly used in the transportation industry due to their excellent strength-to-weight ratio [1]. Due to its small size and high mobility, hydrogen may however influence the mechanical properties of metals and alloys, leading to premature failure of structures and called hydrogen embrittlement (HE). The HE mechanisms are related to interactions between hydrogen and crystalline defects (dislocations, vacancies, grain boundaries and interfaces) [2]. So far, these mechanisms are not well understood, especially because H is difficult to localize using microscopy techniques. The aim of this work is to investigate the influence of H on phase transformation to collect, indirectly, information about the interactions of H with defects. Indeed, precipitation for example, is typically controlled by nucleation sites, atomic mobility and interface energies, all related to crystalline defects.

The Al-Cu model system was chosen for two reasons: 1) It exhibits an excellent STEM-HAADF contrast. 2) The precipitation sequence is well known: Super Saturated Solid Solution (SSSS) → Cu clustering → GP zones → Θ'' → Θ' → Θ [3].

The investigated material is a AA2011 commercial alloy (composition: (wt.%): 5.3%Cu-0.7%Fe-0.4%Si-0.3%Pb, Al balance). Samples were solubilized at 540°C for 1 hour, water quenched, and naturally aged at room temperature or in a furnace at 140°C. H charging was carried out in 0.1M NaOH solution during 5 hours. To modify the dislocation density, different strain levels were applied by cold rolling. STEM-HAADF images collected in various zone axes, demonstrate that hydrogen does not affect the precipitation sequence. The deformation promotes the nucleation and growth of the Θ' phase but H significantly slow down the kinetics.

References :

- [1] J.G. Kaufman, E.L. Rooy, Aluminum alloy castings : properties, processes, and applications, ASM Int. (2004).
- [2] A. Oudriss, J. Creus, J. Bouhattate, E. Conforto, C. Berziou, C. Savall, X. Feaugas, Acta Mater. 60 (19) (2012) 6814–6828.
- [3] Chunhui Liu, Ziyao Ma, Peipei Ma, Lihua Zhan, Minghui Huang. Materials Science & Engineering A 733 (2018) 28–38.

**Mots clefs** : Al-Cu alloys, Precipitation, Deformation, Scanning transmission electron microscopy

## SDM3-P19

### Caractérisation TEM d' hétéro-interfaces $\text{La}_{0.75}\text{Sr}_{0.25}\text{Cr}_{0.5}\text{Mn}_{0.5}\text{O}_3\text{-Ce}_{0.8}\text{Sm}_{0.2}\text{O}_2$ nanostructurées comme couches fonctionnelles entièrement céramiques pour les piles à combustible à oxyde solide

TEM Characterization of nanostructured  $\text{La}_{0.75}\text{Sr}_{0.25}\text{Cr}_{0.5}\text{Mn}_{0.5}\text{O}_3\text{-Ce}_{0.8}\text{Sm}_{0.2}\text{O}_2$  Heterointerfaces as All-Ceramic Functional Layers for Solid Oxide Fuel Cell

- **Iaetitia RAPENNE** \* (laetitia.rapenne@grenoble-INP.fr) / Univ. Grenoble Alpes, CNRS, Grenoble INP, LMGP, 38000 Grenoble, France
- **Juan DE DIOS SIRVENT** / Department of Advanced Materials for Energy, Catalonia Institute for Energy Research (IREC), Barcelona 08930, Spain
- **Albert CARMONA** \* (acarmonazpv@gmail.com) / Department of Advanced Materials for Energy, Catalonia Institute for Energy Research (IREC), Barcelona 08930, Spain
- **Francesco CHIABRERA, Alex MORATA** / Department of Advanced Materials for Energy, Catalonia Institute for Energy Research (IREC), Barcelona 08930, Spain
- **Mónica BURRIEL** / Univ. Grenoble Alpes, CNRS, Grenoble INP, LMGP, 38000 Grenoble, France
- **Federico BAIUTTI, Albert TARANCON** / Department of Advanced Materials for Energy, Catalonia Institute for Energy Research (IREC), Barcelona 08930, Spain

The use of nanostructured interfaces and advanced functional materials opens up a new playground in the field of solid oxide fuel cells (SOFCs).<sup>[1]</sup> In this work, we are <sup>[2]</sup>interested in two all-ceramic thin-film heterostructures based on samarium-doped ceria and lanthanum strontium chromite manganite as promising functional electrode layers. The films were fabricated by pulsed laser deposition on YSZ (100) single-crystal substrates. To prevent the formation of interface secondary phases, LSCrMn-containing films were grown with an additional  $\approx 10$  nm thick  $\text{Ce}_{0.8}\text{Gd}_{0.2}\text{O}_2$  buffer layer on top of YSZ. An enhancement of the electrochemical performance for the heterostructures with respect to single LSCrMn and SDC counterparts is highlighted under anodic conditions (area-specific resistance and in-plane conductivity), opening the possibility for using such thin-film-based heterointerfaces for catalyzing hydrogen oxidation in solid oxide cells. To better understand the functional properties improvement the microstructure of the two different thin-film heterostructures, namely an intermixed LSCrMn–SDC VAN-like nanocomposite and a bilayer composed of a thin layer of SDC deposited on top of the LSCrMn film, were investigated by TEM. The combination of HRTEM and STEM EDX reveals the formation of dense films with clear phase differentiation and a large degree of cationic intermixing in the case of the nanocomposite (Figure 1). Furthermore, to improve the inherent spatial phase identification at the nanometer scale, we employed automated crystal phase and orientation mapping (ACOM) with a precession system (ASTAR), which for the case of the nanocomposite layer, allowed to identify the presence of “boat-shape” isolated islands of rhombohedral LSCrMn within a predominant cubic fluorite phase (figure 2).

[1] M. Acosta, F. Baiutti, A. Tarancón, J. L. MacManus-Driscoll, *Adv. Mater. Interfaces* 2019, 6, 1.

[2] J. D. D. Sirvent, A. Carmona, L. Rapenne, F. Chiabrera, A. Morata, M. Burriel, F. Baiutti, A. Tarancón, *ACS Appl. Mater. Interfaces* 2022.

**Mots clefs :** Hétérostructures, Nanocomposites, Couches minces, ASTAR

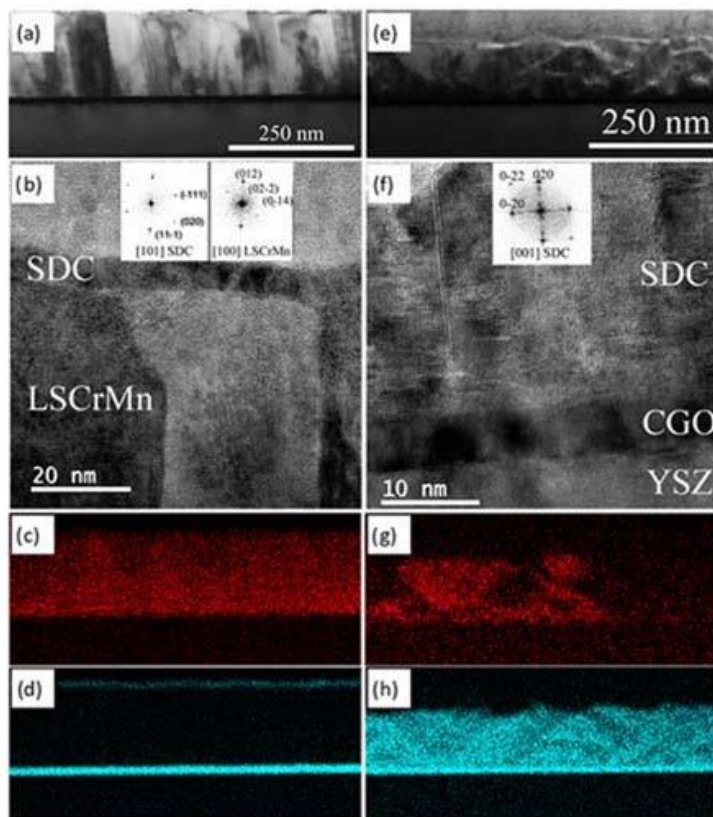


*Figure 1:* Cross-sectional characterization of the heterostructures studied:  
TEM and EDX mapping images (Sr- K signal in red, Ce- L in light blue) for  
LSCrMn- SDCBL (a- d) and LSCrMn- SDCNC (e- h). Insets in (b) and (f) show  
the related FT selected regions corresponding to each of the two phases.

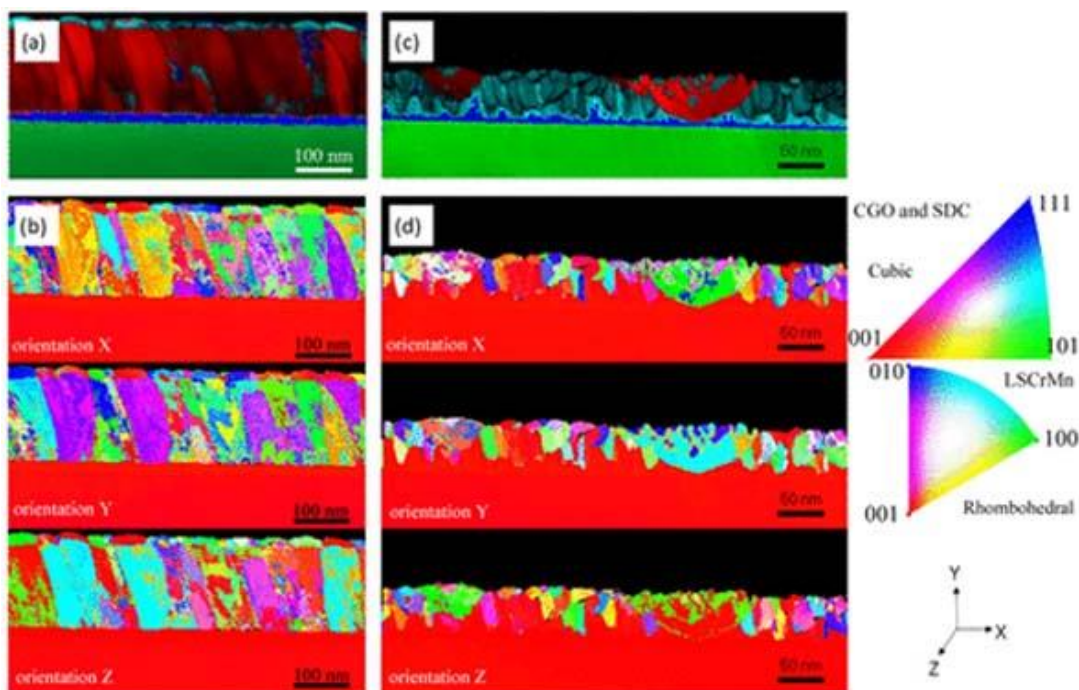


*Figure 2:* ASTAR phase and index analysis maps (top row) and corresponding orientation maps for each direction (bottom rows) of (a, b) LSCrMn- SDCBL and (c, d) LSCrMn- SDCNC films. Phase maps: YSZ in green, CGO in dark blue, LSCrMn in red, and SDC in light blue.

## SDM3-P20

### Mesure des contraintes résiduelles par imagerie MEB-FIB combinée à une technique de mesure de champs

Residual stress measurement by SEM-FIB imaging combined with a field measurement technique

- **Baptiste BOULET** \* (baptiste.boulet@insa-rouen.fr) / Univ Rouen Normandie, INSA Rouen Normandie, CNRS, Groupe de Physique des Matériaux UMR 6634, F-76000 Rouen, France
- **Alireza DASHTI** / Univ Rouen Normandie, INSA Rouen Normandie, CNRS, Groupe de Physique des Matériaux UMR 6634, F-76000 Rouen, France
- **Benoit VIEILLE** / Univ Rouen Normandie, INSA Rouen Normandie, CNRS, Groupe de Physique des Matériaux UMR 6634, F-76000 Rouen, France
- **Clément KELLER** / Laboratoire Génie de Production École Nationale d'Ingénieurs de Tarbes, 47 Avenue d'Azereix, 65000 Tarbes, France
- **Fabrice BARBE** / Univ Rouen Normandie, INSA Rouen Normandie, CNRS, Groupe de Physique des Matériaux UMR 6634, F-76000 Rouen, France
- **Ronan HENRY** / Univ Rouen Normandie, INSA Rouen Normandie, CNRS, Groupe de Physique des Matériaux UMR 6634, F-76000 Rouen, France

\* Auteur correspondant

Les contraintes résiduelles peuvent être bénéfiques (ex : amélioration de la résistance des revêtements) ou bien indésirables (ex : déformation des pièces en fabrication additive) et nécessitent donc d'être maîtrisées et quantifiées. Différentes techniques ont été définies pour les estimer, comme celle du perçage (ASTM E837) ou celle utilisant la diffraction des rayons X, applicable aux matériaux cristallins (EN15305). Pour d'autres matériaux et/ou pour réduire l'échelle de la mesure, certaines méthodes macroscopiques sont transposables à l'échelle microscopique grâce au MEB-FIB (Microscope Electronique à Balayage - Focused Ion Beam) [1]. Le MEB scanne la surface tandis que le FIB enlève progressivement la matière et relaxe ainsi graduellement les contraintes. La déformation résultante, pouvant être très faible et inférieure au pixel, est suivie par corrélation d'images numériques sur des points de repère en surface [2] (ex : micro-dépôts de platine). L'état de contraintes internes avant usinage est déduit par la loi de Hooke en considérant l'état asymptotique, i.e. au-delà d'une certaine profondeur d'usinage.

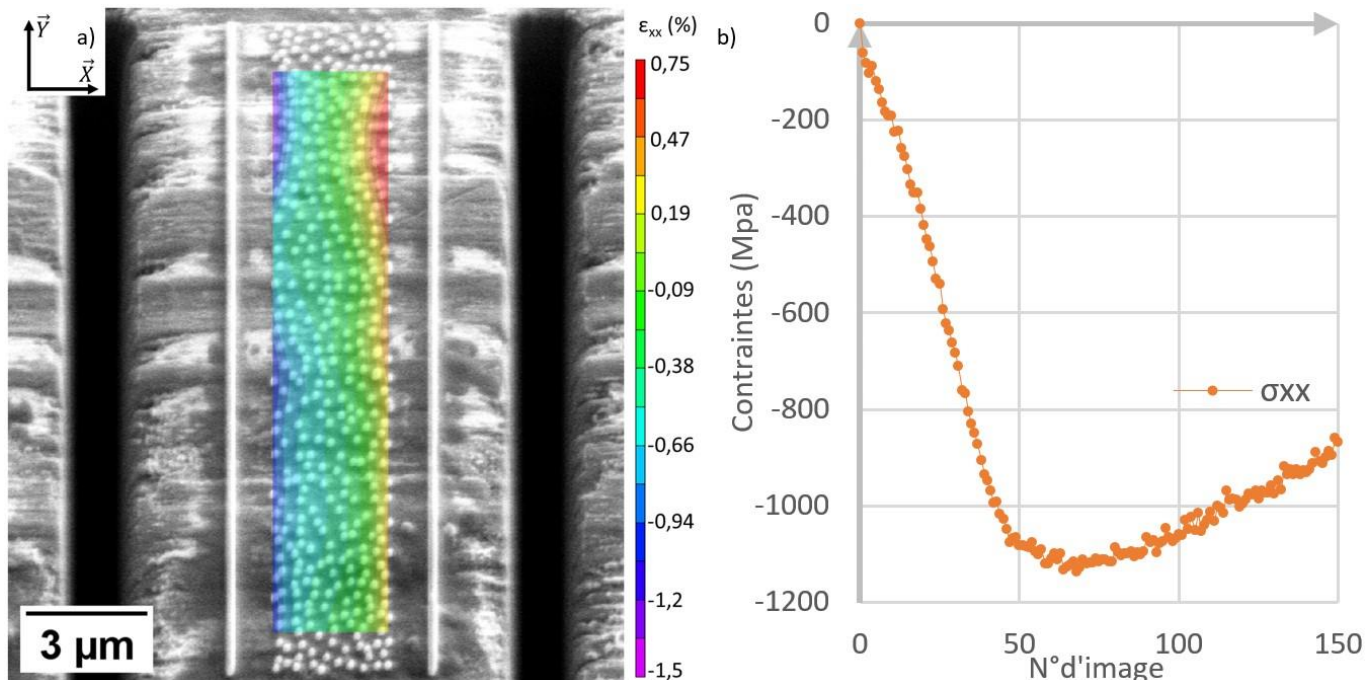
La précision de la méthode dépendant de la nature de l'échantillon, sa préparation (état de surface, forme...), des paramètres d'imagerie MEB (tension, contrastes, méthode de débruitage, détecteurs...) et des conditions d'usinage FIB (type d'ions (Xe, Ga), courant, redéposition [3]), cette étude s'applique à définir les paramètres à appliquer pour obtenir des résultats fiables. Afin de réaliser une étude paramétrique complète et d'estimer la fiabilité de la méthode, différents jeux d'images sont étudiés dans l'ordre suivant : images artificielles, issues de matériaux sans contraintes résiduelles, puis de matériaux dont l'état de contraintes résiduelles est connu. Après optimisation, cette méthode est appliquée sur différents matériaux d'intérêt, comme des métaux tréfilés (Figure 1), des alliages issus de fabrication additive ou encore des matériaux irradiés.

[1]A. M. Korsunsky et al. « Focused ion beam ring drilling for residual stress evaluation », Materials Letters, 63(2009), p.1961-1963.

[2]A. D. Kammers et al., « Small-scale patterning methods for digital image correlation under scanning electron microscopy », Meas.Sci. Technol., 22(2011).

[3]R. Guillon et al., « An Estimation of Local Residual Stresses in Amorphous and Crystallized Trivalent Chromium Coatings », Coatings, 13(2023), p.124.

**Mots clefs :** MEB-FIB, Corrélation d'images, Contraintes résiduelles



## SDM3-P21

### Influence de la préparation d'échantillon sur l'analyse MET de films minces Al-N-O-Cu synthétisés par pulvérisation magnétron

Influence of sample preparation on TEM analysis of nanostructured Al-N-O-Cu thin films synthesized by magnetron sputtering

- **Pierre Louis MARTIN** / Nantes université, CNRS, Institut des Matériaux de Nantes Jean Rouxel, IMN, F-44000 Nantes, France
- **Amina MERABET** / Nantes université, CNRS, Institut des Matériaux de Nantes Jean Rouxel, IMN, F-44000 Nantes, France
- **Nicolas GAUTIER** / Nantes université, CNRS, Institut des Matériaux de Nantes Jean Rouxel, IMN, F-44000 Nantes, France
- **Pierre Yves JOUAN** / Nantes université, CNRS, Institut des Matériaux de Nantes Jean Rouxel, IMN, F-44000 Nantes, France
- **Mireille RICHARD PLOUET** / Nantes université, CNRS, Institut des Matériaux de Nantes Jean Rouxel, IMN, F-44000 Nantes, France
- **Valérie BRIEN** \* (valerie.brien@cnrs-imn.fr) / Nantes université, CNRS, Institut des Matériaux de Nantes Jean Rouxel, IMN, F-44000 Nantes, France

\* Auteur correspondant

Whereas sulfides and oxides are usually known for their photocatalytic properties, metal doped nitrides recently showed a valuable potential[1].

In order to study the possibility to obtain various nanostructures of metal doped oxynitride by reactive magnetron sputtering, transmission electron microscopy (TEM) appears particularly suitable to determine the crystalline morphology, spatial localization of elements, and the nature of phases present in the films. Investigations were performed using a Thermo Fischer Scientific S/TEM Themis Z G3 microscope. Before studying the influence of process parameters, a preliminary work is performed to discard artefacts coming from sample preparation. So, the goal of this work was to prepare both cross sectional and plane views by different ways and compare them. Firstly, different thinning methods were performed on Al-N-O-Cu films deposited on (001) silicon. Whereas ultramicrotomy was discarded for high hardness of substrate, microcleavage (edge cleavage), ionic thinning by gallium ions thanks focused ion beam (FIB: on a Zeiss Crossbeam 550L) and thanks to argon ions in a precision ion polishing system (PIPS from Gatan) after conventional mechanical polishing have been achieved.

High resolution TEM (HRTEM) images, diffraction patterns, HR Fourier Fast Transform (FFT), inverse FFT, high-angle annular dark field scanning TEM (HAADF STEM), STEM-energy dispersive spectroscopy (STEM-EDS) and nanoscale TEM orientation mapping using nanobeam diffraction data were recorded. Comparison between preparation methods will be presented.

The nature of the grown films when a TEM carbon coated Au grid is used, will be elucidated, and will be compared to the one grown on silicon substrates.

#### References :

1. O. Baghrache, S. Rtimi, A. Zertal, C. Pulgarin, R. Sanjinés, and J. Kiwi, Applied Catalysis B: Environmental 174–175, 376 (2015).

**Mots clefs :** TEM, thin film, oxynitride, sample preparation

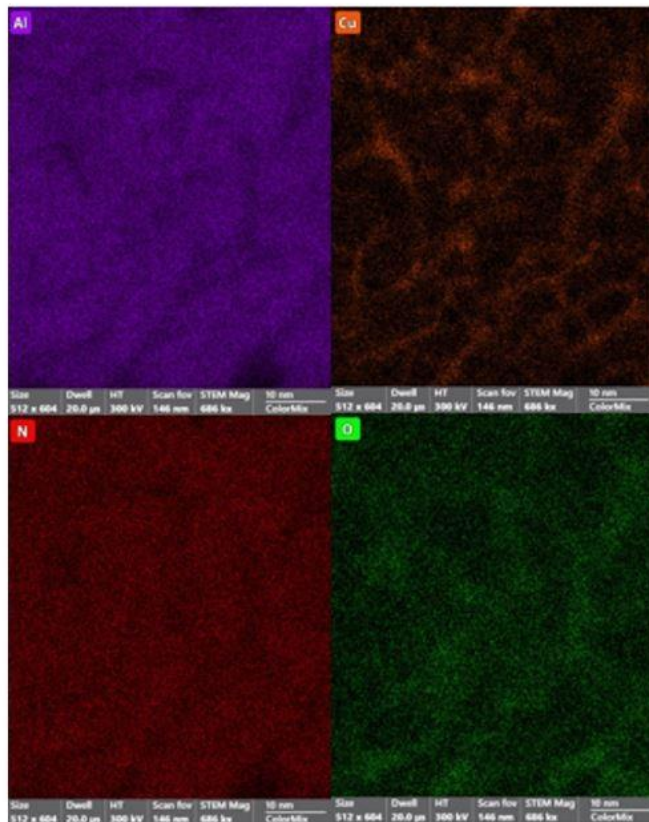


Figure 1: STEM-EDS plane view of Al-N-O-Cu deposited on (001) silicon thinned down by microcleavage

## SDM4-P1

### ANALYSE EELS DES PIQUES ELNES DU SEUIL SI-L2,3 DANS DES ÉCHANTILLONS PROVENANTS DE L'ASTEROÏDE RYUGU

#### EELS ANALYSIS OF THE ELNES PEAKS OF THE SI L2,3 EDGE IN SAMPLES FROM THE RYUGU ASTEROID

- **Mario PELAEZ FERNANDEZ** \* (pelaezfernandezmario@gmail.com) / 1 Unité Matériaux et Transformations (UMET UMR 8207), Univ Lille, Bâtiment C6, Cité Scientifique, 59650 Villeneuve d'Ascq, France 2 Laboratorio de Microscopías Avanzadas, Univ. Zaragoza, Zaragoza, Spain, 3 Instituto de Nanociencia y Materiales de
- **Maya MARINOVA** \* (maya.marinova@univ-lille.fr) / Univ. Lille, FR 2638-IMEC-Institut Michel-Eugène Chevreul, F-59000 Lille, France
- **Adrien TEURTRIE, Sylvain LAFORET, Corentin LE GUILLOU** / Unité Matériaux et Transformations (UMET UMR 8207), Univ Lille, Bâtiment C6, Cité Scientifique, 59650 Villeneuve d'Ascq, France
- **Hugues LEROUX** / 1-Unité Matériaux et Transformations (UMET UMR 8207), Univ Lille, Bâtiment C6, Cité Scientifique, 59650 Villeneuve d'Ascq, France, Univ. Lille, FR 2638-IMEC-Institut Michel-Eugène Chevreul, F-59000 Lille, 4-France
- **Francisco DE LA PEÑA** / Unité Matériaux et Transformations (UMET UMR 8207), Univ Lille, Bâtiment C6, Cité Scientifique, 59650 Villeneuve d'Ascq, France

\* Auteur correspondant

Grâce à la mission Hayabusa2 de l'Agence Japonaise pour l'Exploration Spatiale, des matériaux provenant de l'astéroïde Ryugu ont été ramenés sur Terre en 2020. Ces échantillons précieux contiennent de l'eau piégée au sein des phyllosilicates, comme en attestent les mesures infra-rouge à distance [1] et des nouveaux analyses de laboratoire [2]. Il existe deux familles de phyllosilicates avec des compositions chimiques et des structures crystallographiques différentes: des saponites et des serpentines.

La microscopie électronique est une candidate claire pour la caractérisation de ces phyllosilicates, qui sont mêlés à l'échelle nanométrique. Toutefois, la nature sensible de l'échantillon au faisceau d'électrons difficulte ce type d'études, autant des études STEM comme des études EDX; utilisées pour estimer ces compositions. Les études par 4DSTEM ont reçu pas mal d'intérêt vu la différente crystallographie des deux phyllosilicates mais restent toujours complexes.

Une autre façon de distinguer les phyllosilicates est à partir de leur signature ELNES, dépendante du phyllosilicate, déjà utilisée pour distinguer des différents états d'oxydation d'un élément quelconque dans un matériel spécifique[3, 4]. Au-delà, l'utilisation d'un détecteur d'électrons directe (MEDIPIX3), ainsi que les acquisitions multi-frame, rendent un signal sur bruit analysable en limitant l'endommagement, tout en donnant des analyses de ces échantillons pas possibles jusqu'à ce moment.

Cette étude caractérise la matrice phyllosilicatée de ces échantillons, en employant des techniques statistiques comme la décomposition NMF ou BSS dans les piques ELNES du seuil Si-L2,3.

Les résultats montrent deux composantes indépendantes qui gardent relation avec la présence des deux types différents de silicates.

Références:

- [1] Kitazato, K. et al, Science 364, no. 6437 (2019), p. 272–75.  
[2] Ito, M. et al, Nature Astronomy 6, no. 10 (2022), p. 1163–71.  
[3] de la Peña, F. et al, Ultramicroscopy 111, no. 2 (2011), p. 169–76. [4] Arenal, R., et al. Ultramicroscopy 109.1 (2008): 32-3

**Mots clefs** : EELS, ELNES, Sensitive materials, mineralogy, machine learning

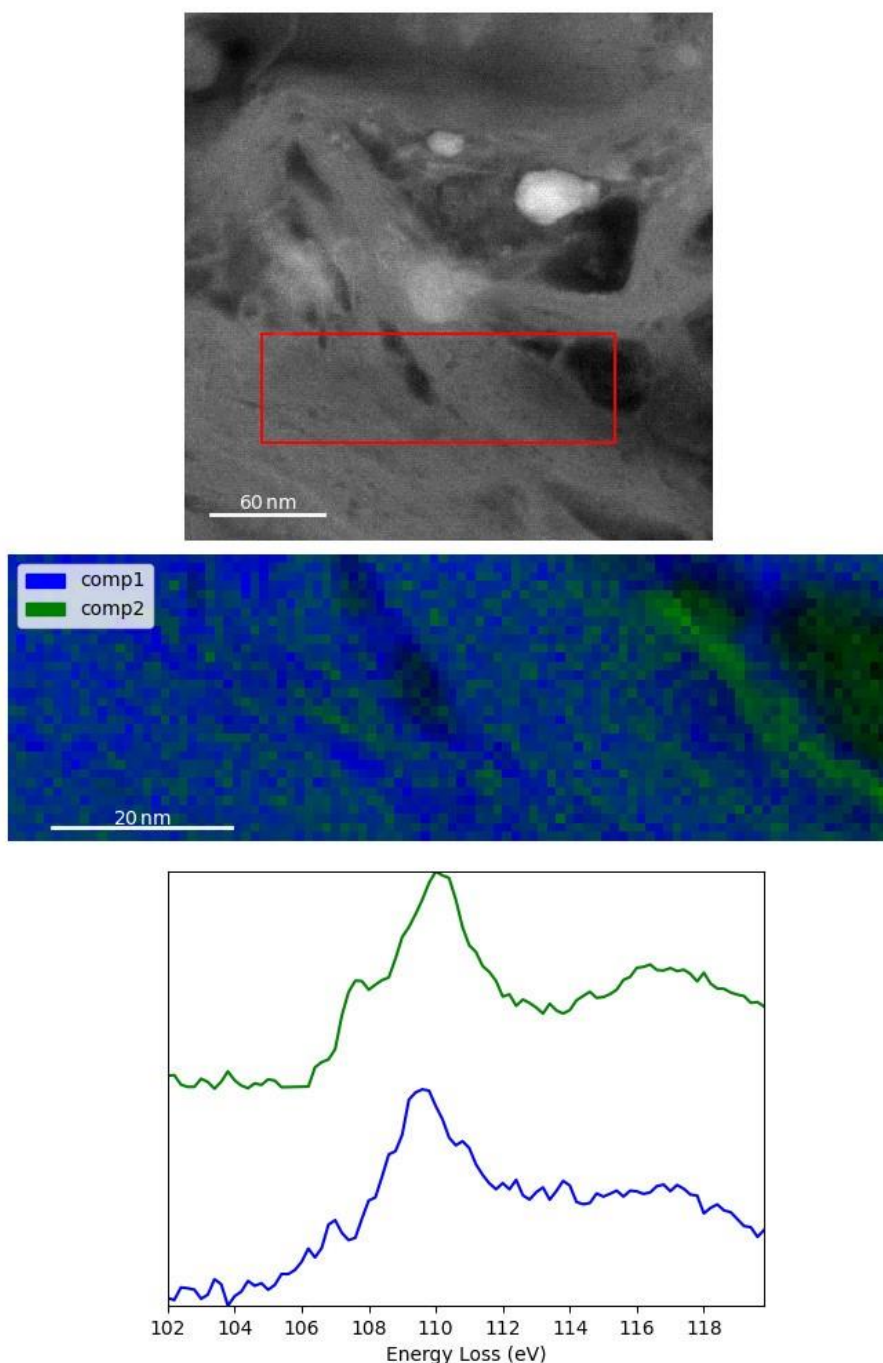


Figure 1: Etude des différents phyllosilicates dans un échantillon Ryugu en utilisant du NMF. Haut: image HAADF de l'échantillon en montrant la région à analyser. Centre: carte spectrale montrant les deux principales composantes trouvées par NMF. Bas: composantes spectrales correspondantes aux cartes mentionnées.

## SDM4-P2

### Source d'électrons lumineuse et ultrarapide en nanopointe LaB6

#### Bright and ultrafast electron point source made of LaB6 nanotip

- **Onkar Bhorade** \* (onkar.bhorade@univ-rouen.fr) / GPM, Université de Rouen
- **Bernard Deconihout** / GPM, Université de Rouen
- **Ivan Blum** / GPM, Université de Rouen
- **Jonathan Houard** / GPM, Université de Rouen
- **Simona Moldovan** / GPM, Université de Rouen
- **Angela Vella** / GPM, Université de Rouen

\* Auteur correspondant

As new frontiers in the study of complex material systems are reached, a shift from conventional techniques has become necessary. Time-resolved electron microscopy is one such tool which can help us gain fundamental understanding by pushing the present spatial and temporal scales. Stable and bright electron sources that can produce ultrafast electron bunches are imperative to the development of such microscopes. Recently Lanthanum hexaboride (LaB6) nanotips have shown high brightness and high emission stability when working in a continuous cold field emission mode. [1][2]

In the current work, we investigate the emission properties of his LaB6 nanotips under electrostatic fields (static emission) and femtosecond laser illumination (ultrafast emission). Using a high repetition rate laser in the infrared range, we present different field emission regimes as a function of extraction voltage and laser intensity. [3] The effect of change in applied voltage and laser intensity on emission pattern, energy spread, and current is also demonstrated. [4] The emission current is shown to be stable for several hours under static and ultrafast conditions with a low energy spread of electrons. Electron bunches can be controlled for achieving a few electrons per pulse to high brightness useful for several microscopic applications.

#### Références/References :

- [1] H. Zhang et al., *Nature Nanotech* 11, 273–279 (2016).
- [2] G. Singh et al., *Appl. Phys. Lett.* 113, 093101 (2018)
- [3] G. Herink et al. *Nature* 483, 190–193 (2012).
- [4] M. Borz et al., *Nanoscale*, 11, 6852– 6858 (2019)

**Mots clefs** : Ultrafast Microscopy, LaB6, Electron source

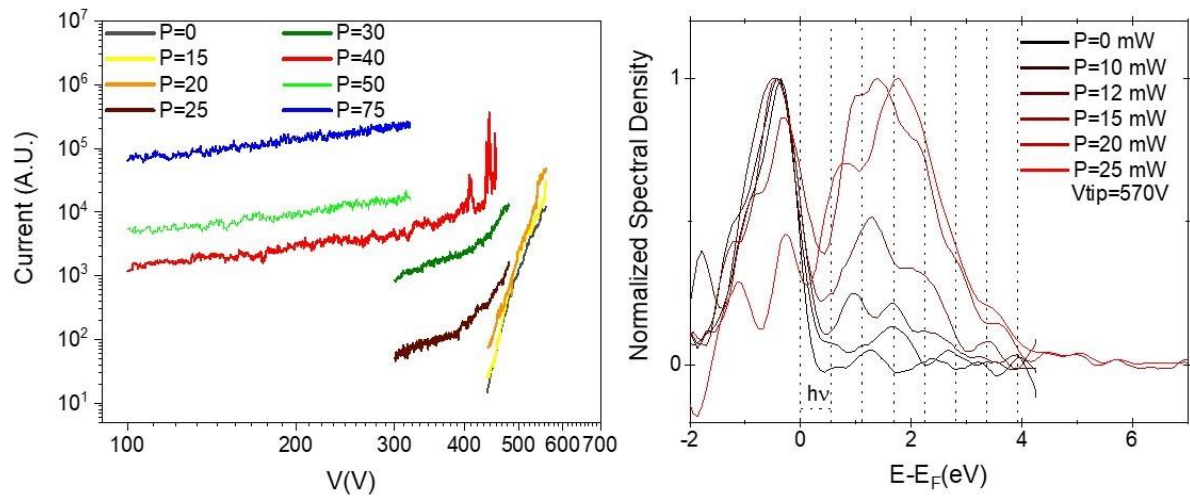


*Figure 1: a) I-V characteristics of electron emission from LaB6 nanotip b) Electron energy spectra under static and laser conditions*

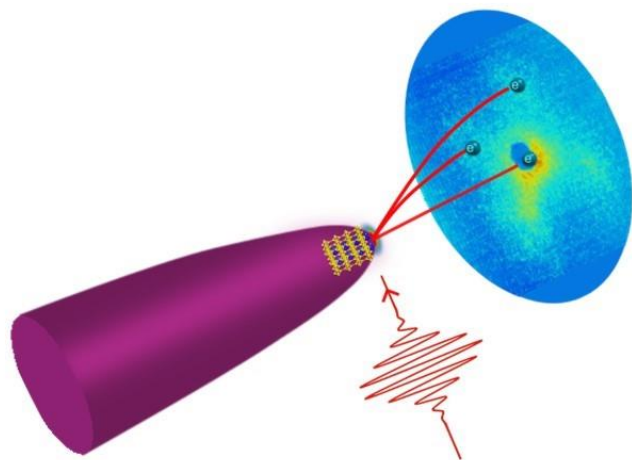


*Figure 2: Schematic of electron emission under laser illumination*  
 \*angela.vella@univ-rouen.fr

## SDM4-P3

### Caractérisation avancée par spectroscopie EELS de matériaux semiconducteurs dédiés à la microélectronique

Advanced EELS spectroscopy characterization of semiconductors materials for microelectronics

- **Estève DROUILLAS** \* (esteve.drouillas@st.com) / STMicroelectronics Crolles, Centre d'Elaboration de Matériaux et d'Etudes Structurales (CEMES), CNRS
- **Bénédicte WAROT-FONROSE** / Centre d'Elaboration de Matériaux et d'Etudes Structurales, CNRS, 29 rue Jeanne Marvig, BP 94347, 31055 Toulouse, France
- **Jean-Gabriel MATTEI** / STMicroelectronics Crolles, 850 Rue Jean Monnet, 38926 Crolles, France \*

Auteur correspondant

The complexification of new structures developed in microelectronic industries lead to the search for more advanced material characterization methods. Transmission Electron Microscopy (TEM) coupled with X-ray Energy-Dispersive Spectroscopy (XEDS) are already routinely employed in industries but mostly used for elemental analysis. Therefore, Electron Energy Loss Spectroscopy (EELS) is being developed for advanced elemental characterization using core edge energy-loss, answering a need to characterize light elements as well as providing information on the atoms chemical environment. Scanning TEM (STEM) and EELS were performed on a Cs-corrected JEOL Neo-ARM 200F equipped with a Cold-FEG and a Gatan GIF Continuum spectrometer with a 0.45 eV energy resolution.

STEM-HAADF (High-Angle Annular Dark Field) Spectrum Image [Fig. 1 (a)] displays a layer of nitrogen-doped GST (Germanium-Antimony-Tellurium) used for Phase Change Memory (PCM) devices surrounded by a layer of polycrystal titanium nitride (poly-TiN) (top layer) and an amorphous silicon nitride (a-SiN) (bottom layer). A poly-TiN heater (in grey in the bottom layer) is used to locally change the phase of GST from amorphous to crystal and vice versa to create binary system memory. An accurate knowledge of the dispersion of the nitrogen in the GST layer is essential to the modulation of the crystallization process [1] and will give leverage to optimize the cell performance and reliability. Relatively high energy dispersion in EELS allows to generate elemental mapping, especially for light elements such as nitrogen as illustrated in [Fig. 1 (b)]. Furthermore, the observation of the Near-Edge fine Structure (ELNES) of elements (typically nitrogen) provide information on the chemical environment [Fig. 1 (c)]. Otherwise, using post-treatment in the ELNES region such as Multiple Linear Least Squares (MLLS) fitting method allows to accurately identify and measure the thickness of oxide layer ( $\text{Al}_2\text{O}_3$ ) surrounded by metallic layers: Al in left and Ti in right [Fig. 2 (a) and (c)]. Comparisons of the aluminum K edge to references [2] tend to corroborate our observations [Fig. 2 (b)].

Références/References :

- [1]SM. Kim et al., Thin Solid Films, vol. 469–470 (2004), p. 322-326
- [2]P. Ewels et al., Microscopy and Microanalysis, vol. 22, no. 3 (2016), p. 717–724

**Mots clefs** : Transmission electron microscopy, EELS, ELNES, microelectronics

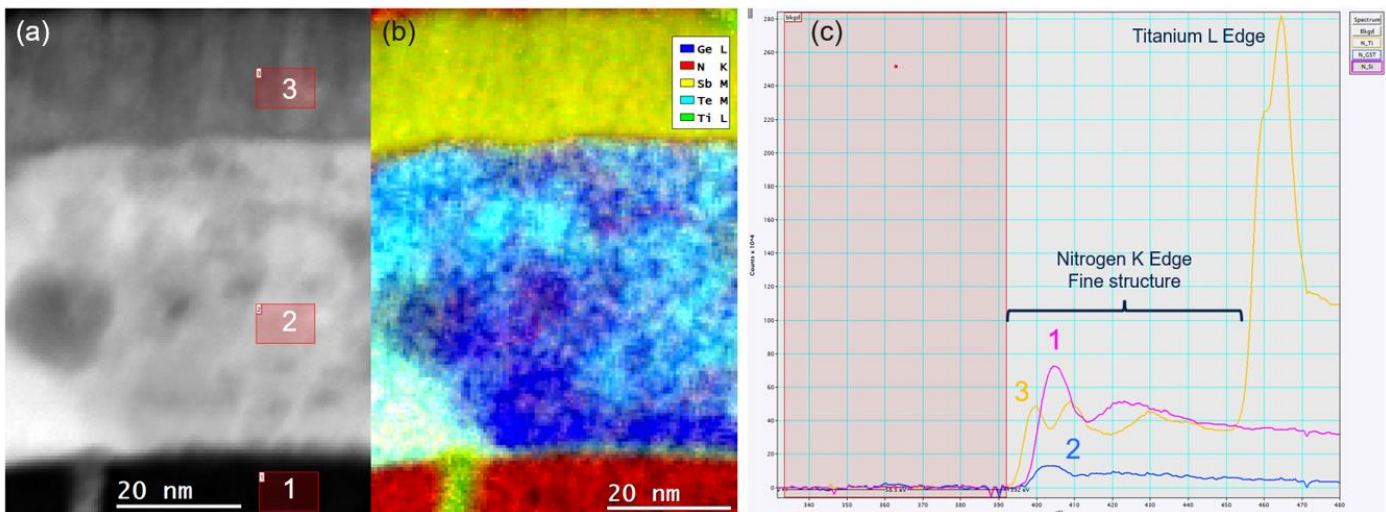


**Figure 1:** (a) STEM-HAADF Spectrum Image of a PCM Device in GST region (b) EELS elemental map of the Spectrum Image (c) Comparison of the EELS fine structure of the Nitrogen K edge with N bounded to Si, GST and Ti

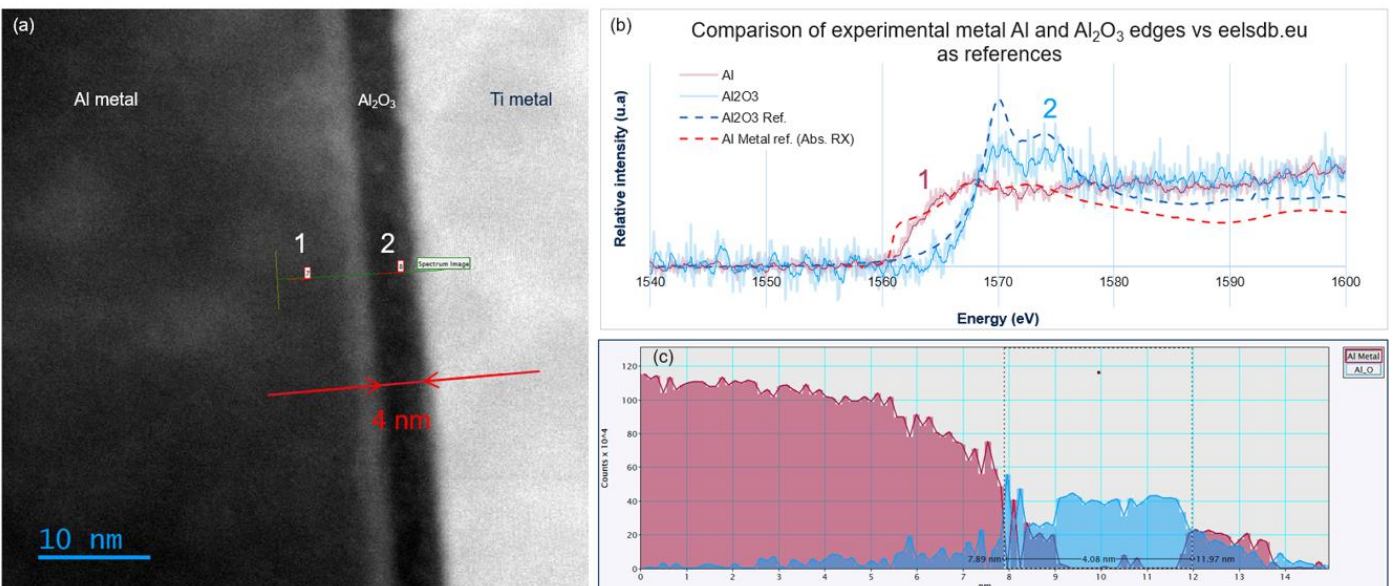


**Figure 2:** (a) STEM-HAADF Image. (b) Aluminum K edge for metal Al and Al oxide. (c) MLLS Fit Analysis from EELS Al K Edge along the line scan Spectrum Image

## SDV1-P1

### Septins: remodelage membranaire induit par des filaments sensibles à la courbe

#### Septins: membrane remodeling by curvature sensitive filaments

- **koyomi nakazawa** \* (koyomi.nakazawa@curie.fr) / institut Curie
- **michael trichet** / sorbonne université
- **stephanie mangenot** / MSCmed
- **Aurélie Bertin** \* (aurelie.bertin@curie.fr) / institut Curie

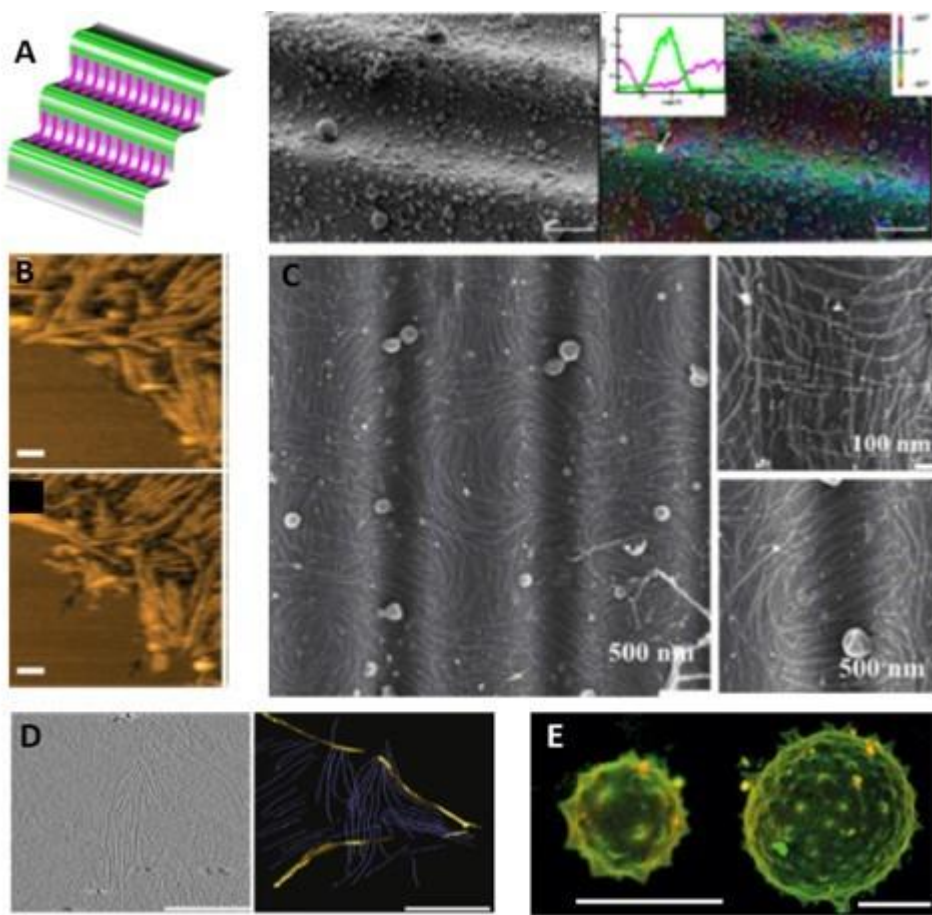
\* Auteur correspondant

Septins are ubiquitous cytoskeletal proteins essential for cell division which participate in the formation of diffusion barrier and might be involved in membrane deformation and rigidity. They polymerize into filamentous structures associated with the inner plasma membrane. We have used a combination of in vitro bottom approaches, various imaging methodologies (electron, atomic force and fluorescence microscopy) to analyze how the curvature sensitivity of budding yeast and human septins could induce membrane deformations [1-3]. We have compared how purified septin complexes arrange differently on positive or negative curvatures using scanning Electron Microscopy imaging on undulated PDMS substrates, cryo-electron microscopies/tomography or fluorescence imaging. Within in vitro reconstituted systems, we observe that human septins tend to organize within filamentous orthogonal arrays while yeast septins assemble into parallel arrays of filaments. Specific filamentous patterns are able to restrict the diffusion of membrane bound components, reshape membranes and tune their mechanical properties.

#### Références/References :

- [1] Alexandre Beber et al. Membrane reshaping by micrometric curvature sensitive septin filaments, Nat Commun.2019 Jan 24;10(1):420
- [2] Anthony Vial et al., Correlative AFM and fluorescence imaging demonstrates a nanoscale membrane remodelingand spontaneous ring-like and tubular structures formation by Septin, Nanoscale. 2021 Aug 7;13(29):12484-12493. [3] K. Nakazawa et al. A specific mesh-like organization of human septin octameric complex drives membrane reshaping and curvature sensitivity, Biorxiv 2022, doi.org/10.1101/2022.11.02.514824, under revision JCS.

**Mots clefs** : septin, membrane, cryo-EM, AFM, confocal microscopy, SEM



## SDV2-P1

### Observation directe des conformations de la formine au bout des brins barbés d'actine.

Direct observation of the conformational states of formin mDia1 at actin filament barbed ends.

- **Julien Maufront** \* (julien.maufront@curie.fr) / institut Curie
- **Antoine Jégou** / institut Jacques Monod
- **Guillaume Romet-Lemonne** / institut Jacques Monod
- **Aurélie Bertin** \* (aurelie.bertin@curie.fr) / institut Curie

\* Auteur correspondant

The fine regulation of actin polymerization is essential to control cell motility, architecture and to perform essential cellular functions. Formins are key regulators of actin filament assembly, known to processively elongate filament barbed ends and enhance their polymerization rate. Based on indirect observations, different models have been proposed to describe the molecular mechanism governing the processive motion of formin FH2 domains at polymerizing barbed ends. Using electron microscopy, we directly identified two conformations of the mDia1 formin FH2 domains in interaction with the barbed ends of actin filaments (Fig1). These conformations agree with the open and closed conformations of the "stair stepping" model proposed by Otomo and colleagues[1]. We observed the FH2 dimers to be in the open conformation for 79% of the data, interacting with the two terminal actin subunits of the barbed end, and with three actin subunits in the closed conformation. Further, our data reveal that the open state encompasses a continuum of states where the orientation of the leading FH2 domain with respect to the filament long axis varies from 108 to 135 degrees. In addition, we identified FH2 domains encircling the core of actin filaments, providing structural information for mDia1 away from the barbed end (Fig2). Based on these direct observations, we propose a model of the different conformations of formins in interaction with the actin filaments, where formins may transition from the barbed end to the core of the filament [2].

[1]Otomo, T. et al. Structural basis of actin filament nucleation and processive capping by a formin homology 2 domain, 2005, Nature 433, 488–494.

[2]J.Maufront et al., Direct observation of the conformational states of formin mDia1 at actin filament barbed ends and along the filament, 2022, Mol. Biol. Of the Cell, 34, 1, 1-12.

**Mots clefs :** actin, formin

## SDV2-P2

### Peut-on faire de la cryo SPA sans TEM cryo dédié ?

#### Is it possible to do cryo SPA on a non-dedicated TEM ?

- **Eric Gautron** \* (eric.gautron@cnrs-imn.fr) / Nantes Université, CNRS, Institut des Matériaux de Nantes Jean Rouxel, IMN, F-44000 Nantes, France
- **Philippe Moreau** / Nantes Université, CNRS, Institut des Matériaux de Nantes Jean Rouxel, IMN, F-44000 Nantes, France
- **Gildas Loussouarn** / L'unité de recherche de l'institut du thorax, Inserm UMR 1087/CNRS UMR 6291, IRS-UN - 8 quai Moncousu - BP 70721 44007 Nantes Cedex 1
- **Olga Sokolova** / Bioengineering department • Faculty of biology • Lomonosov Moscow State University • 119234, Russia, Moscow
- **Fayal Abderemane-Ali** / Department of Physiology, David Geffen School of Medicine, University of California, Los Angeles, 650 Charles E Young Dr Los Angeles, CA 90095

\* Auteur correspondant

Molecular structures resolution of biological objects has progressed considerably in recent years, thanks in particular to the development of dedicated microscopes and their improved performance, but also to the development of new technologies for image detection and processing. However, the configuration of the pole pieces, the vitrified grid insertion systems and the anti-contamination trap solutions of these dedicated microscopes make them not very versatile. This limits the range of applications for samples that can be characterised by this type of TEM and the analytical techniques that can be combined with imaging (e.g. EDX spectroscopic analysis).

In the case of TEMs dedicated to materials science, these are generally equipped with numerous "options" (S/TEM, spectroscopies, correctors, etc.). The use of side-entry cryo specimen holders allows cryo data collection keeping all the analysis possibilities offered by these TEMs. In cryo conditions, the rate of ice formation is relatively significant and often problematic in absence of an anti-contamination system. This is the case with the Themis Z (Thermo Fisher Scientific) at the Institut des Matériaux Jean Rouxel, due to the gap in the pole piece and the size of its 4 EDX detectors (Super-X system). Despite the absence of an anti-contamination trap, we were able to acquire images of apoferritin and chaperonin particles under conditions similar to those required for SPA (low dose, direct electron detection camera). The 3D reconstruction of the chaperonins (Fig.1) validates our experimental conditions (purity of the solution, preparation protocol, use of the Themis). We will compare it to that obtained with a Titan Krios. The ice growth rate and the means to limit it in the Themis Z will also be presented.

[1] Nakane T, et al. Single-particle cryo-EM at atomic resolution. *Nature*. 2020 Nov;587(7832):152-156. doi: 10.1038/s41586-020-2829-0.

[2] Schlossmacher, Peter, et al. "Nanoscale chemical compositional analysis with an innovative S/TEM-EDXsystem." *Microscopy and analysis* 5 (2010).

**Mots clefs :** cryo, SPA, ice growth

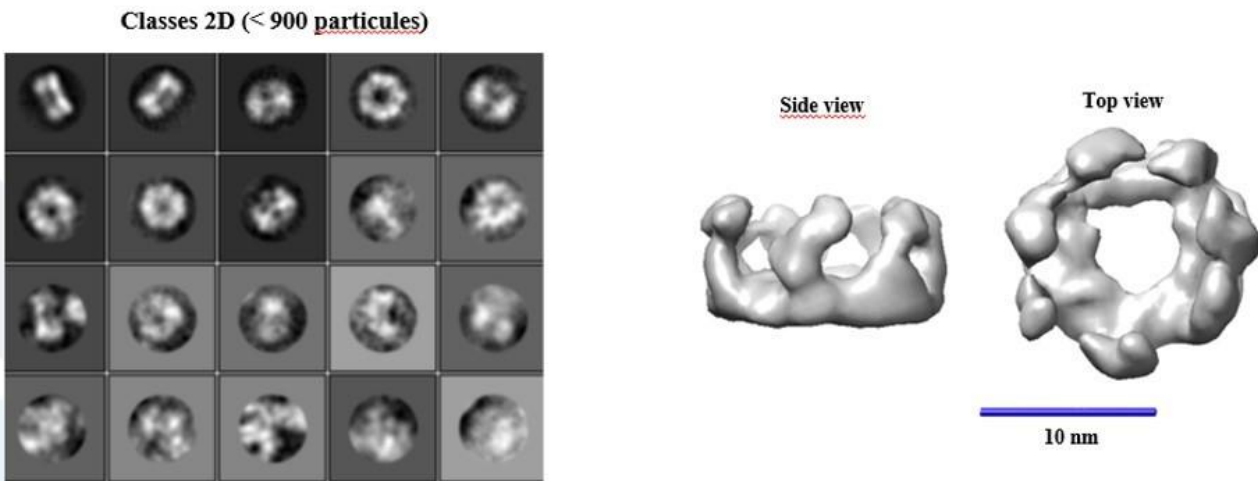


*Figure 1: 3D reconstruction of chaperonins. (Left) 2D classes : classes in two top rows were used for reconstruction, those in two bottom rows represent junk particles which were excluded. (right) side and top views after 3D reconstruction*

**SDV2-P3****CORRELATION ENTRE PROPRIETES PHYSICO-CHIMIQUES DE SOLUTIONS DE TENSIO-ACTIFS ET FORMATION DE FILMS MINCES POUR LA CRYO-MICROSCOPIE****ROLE OF SURFACTANTS IN ELECTRON CRYO-MICROSCOPY THIN FILM PREPARATION**

- **Amélie Leforestier** \* (amelie.leforestier@universite-paris-saclay.fr) / Université Paris-Saclay, CNRS, Laboratoire de Physique des Solides, Orsay, France
- **Baptiste Michon** / Université de Paris, Laboratoire de Biologie Physico-Chimique des Protéines Membranaires, CNRS, Paris, France
- **Uriel López-Sánchez** / Univ. Grenoble Alpes, CNRS, CEA, IBS, Grenoble, France
- **Hugues Nury** / Univ. Grenoble Alpes, CNRS, CEA, IBS, Grenoble, France
- **Jéril Degrouard** / Université Paris-Saclay, CNRS, Laboratoire de Physique des Solides, Orsay, France
- **Emmanuelle Rio** / Université Paris-Saclay, CNRS, Laboratoire de Physique des Solides, Orsay, France
- **Anniina Salonen** / Université Paris-Saclay, CNRS, Laboratoire de Physique des Solides, Orsay, France
- **Manuela Zoonens** / Université de Paris, Laboratoire de Biologie Physico-Chimique des Protéines Membranaires, CNRS, Paris, France

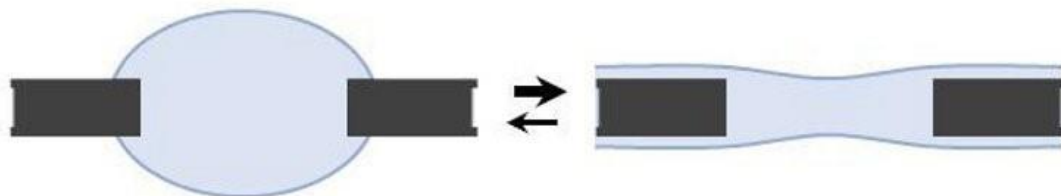
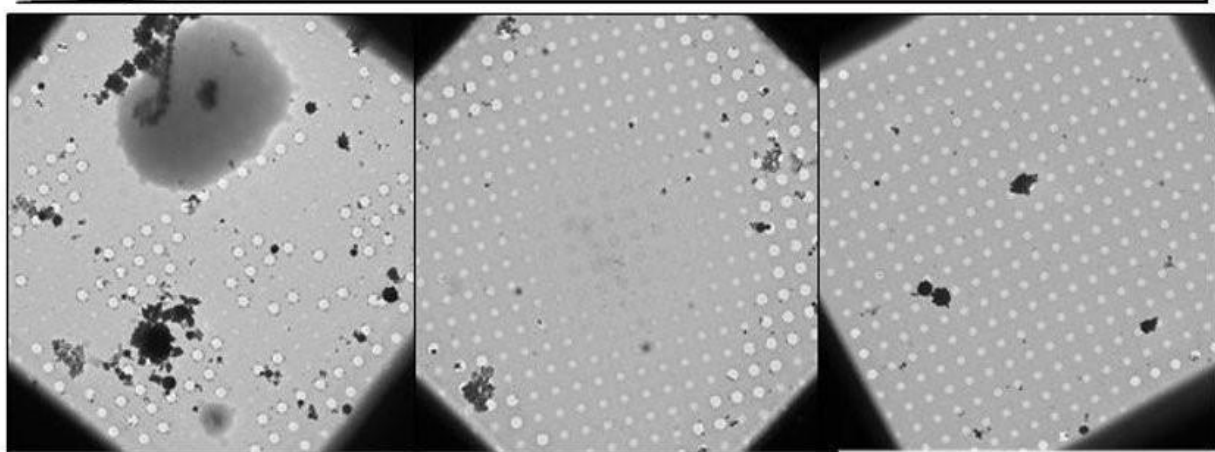
\* Auteur correspondant

Single-particle electron cryo-microscopy (cryo-EM) has become an effective and straightforward approach to determine the structure of membrane proteins (MPs). However, obtaining cryo-EM grids of sufficient quality for high-resolution structural analysis remains a major bottleneck. One of the difficulties arises from the presence of detergents, which often leads to a lack of control of the ice thickness. Amphiphatic polymers such as amphipols (APols) are detergent substitutes, which have proven to be valuable tools for cryo-EM studies.

We investigate the physico-chemical behavior of APol- and detergent-containing solutions and show a correlation with the properties of vitreous thin films in cryo-EM grids. The results suggest that the quality of cryo-EM specimens can be understood from a physico-chemical characterization of liquid films and interfaces to complement the empirical optimization of the grid preparation. We in particular provide new insight on the potential of APols, allowing a better control of ice thickness while limiting protein adsorption at the air-water interface, as shown with the full-length mouse serotonin 5-HT3A receptor whose structure is solved in APol. Our findings may speed up the process of grid optimization to obtain high-resolution structures of MPs.

**Mots clefs** : air-water interface, amphipol, detergent, ice thickness, membrane proteins, particle orientation

[polymer A8-35]



polymer A8-35 addition  
yields thinner,  
more stable ice layers

## SDV2-P4

### Influence des modulateurs d'assemblage sur la structure et la cinétique d'assemblage de la capsid du virus de l'hépatite B

#### Influence of assembly modulators on the structure and assembly kinetics of Hepatitis B virus capsid

- **Kalouna KRA** / Institut de Biologie Intégrative de la Cellule (I2BC), CNRS, Université Paris-Saclay, CEA, Saclay, France
- **Laetitia GARGOWITSCH** / Laboratoire de Physique des Solides (LPS), CNRS, Université Paris-Saclay, Orsay, France
- **Jéril DEGROUARD** \* (jeril.degrouard@universite-paris-saclay.fr) / Laboratoire de Physique des Solides (LPS), CNRS, Université Paris-Saclay, Orsay, France
- **Ana ARTENI** / Institut de Biologie Intégrative de la Cellule (I2BC), CNRS, Université Paris-Saclay, Gif-sur-Yvette, France
- **Javier PEREZ** / SOLEIL Synchrotron, Gif-sur-Yvette, France
- **Guillaume TRESSET** / Laboratoire de Physique des Solides (LPS), CNRS, Université Paris-Saclay, Orsay, France
- **Stéphane BRESSANELLI** / Institut de Biologie Intégrative de la Cellule (I2BC), CNRS, Université Paris-Saclay, CEA, Saclay, France

\* Auteur correspondant

Hepatitis B virus (HBV) is an enveloped virus with an icosahedral nucleocapsid. The constituent of the capsid, the Core protein, is a dimeric protein, which can self-assemble in vivo but also in vitro into capsids containing mainly 120 dimers. The CAMs (for capsid assembly modulators) that can disrupt HBV capsid assembly are antiviral molecules currently in clinical trials. They can either accelerate the assembly of seemingly normal, but empty, icosahedral capsids (CAM-E such as JNJ-632) or cause the formation of aberrant (larger and malformed) assemblies (CAM-A such as BAY 41-4107). Some CAM-A can also disrupt preformed capsids. However, the emergence of second- and third- generation CAMs with new mechanisms of action is redefining this classification.

Much of what is known about the mechanisms of action of CAMs comes from biochemical and structural work with recombinant, C-terminally truncated Core (Cp149). Here, we will present our characterization of the structures formed by Cp149 in the presence of several CAM-A and CAM-E, including well-known and newer compounds. We combine cryo-electron microscopy (cryo-EM) with time-resolved small-angle X-ray scattering (TR-SAXS) to characterize the structures and kinetics of formation of Cp149 assemblies at nanometer-to-atomic resolution. We establish that both the CAM-A and some CAM-E actually modify the structure and stoichiometry of assembled capsids, albeit in more subtle ways for CAM-E compounds. At equal concentration, not all CAM-E induce the same structural alterations. Some lead to mixtures of deformed and perfect capsids allowing atomic resolution reconstructions.

**Mots clefs :** Hepatitis B virus, capsid assembly, assembly modulators, kinetic modelling, time-resolved small-angle X-ray scattering, cryo-transmission electron microscopy

## SDV3-P1

### Décrypter le mode de vie intracellulaire de *Mycobacterium tuberculosis* dans les macrophages infectés par des approches de biologie structurale *in situ*.

#### Decipher *Mycobacterium tuberculosis* intracellular lifestyle within infected macrophages by *in situ* structural biology approaches

- **Camille Keck** \* (camille.keck@pasteur.fr) / Institut Pasteur
- **Léa Swistak** / Institut Pasteur
- **Stéphane Tachon** / Institut Pasteur
- **Anna Sartori-Rupp** / Institut Pasteur
- **Roland Brosch** / Institut Pasteur
- **Jost Enninga** / Institut Pasteur

\* Auteur correspondant

*Mycobacterium tuberculosis* (Mtb), the etiologic agent of tuberculosis, is an intracellular bacterium that was thought for a long time to be only an intraphagosomal pathogen. Indeed, the bacteria can subvert many host pathways to prevent phagosome acidification and maturation through effectors secreted by 5 distinct secretion systems (ESX-1 to ESX-5), which turn the environment of the phagosome into a more “friendly” one for replication and survival of the bacteria. However, the dogma of an exclusive intraphagosomal Mtb lifestyle has been challenged during the past decade with an increasing number of studies showing that the bacilli are able to access the cytosol of the host cell. The precise molecular processes involved in determining a vacuolar or cytosolic fate of the bacilli have remained debated, even though it is clear that the bacterial secretion system play a role.

To address this in a quantitative way, we created macrophage cell lines stably expressing fluorescent galectin 3 (Gal-3), a host galactoside-binding protein, to use it as a reporter for cytosolic access. This reporter does not only allow to count vacuolar damage at the single phagolysosome level, it also provides information whether membrane rupture occurs rather discretely, in an eruptive manner, or whether bacilli remain within damaged vacuoles. Using this reporter, we could score these different events, and we identified frequent early vacuolar damage events within the first 24 hours of bacterial infection, which contrasts with the previously late cytosolic access. We went on and implemented a cryo correlative light and electron tomography workflow to pinpoint at the ultrastructural level bacteria before, during and after phagolysosomal rupture. For this we infected our reporter cells with fluorescent bacteria (and mutant strains) on EM grids, prepared them for cryo fluorescence, thinned relevant regions to 100 nanometer-thick lamellae by cryo FIB milling, before obtaining cryo tomograms of *in situ* infection sites using a Titan Krios 300kV transmission microscope. Currently, we quantify difference in membrane damage in our cryo tomograms depending on the specific time points and bacterial strains. Our work will provide unprecedented insights into the intracellular niche formation of mycobacteria.

**Mots clefs :** *Mycobacterium tuberculosis*, macrophages, cryo-CLEM, tomographie

## SDV3-P2

### Optimisation de la cryo-tomographie de sections vitreuses pour l'imagerie de cellules et tissus

Optimization of cryo-tomography of vitreous sections for tissue and cell imaging

.Fatima Taiki \* (fatima.taiki@universite-paris-saclay.fr) / Université Paris-Saclay

\* Auteur correspondant

Cellular cryo-electron tomography (cryo-ET) explores tissue and cells in their unstained flash-frozen native state, revealing *in situ* the structure of macromolecules and their local environment and interactions with partners, also known as molecular sociology [1].

To obtain thin samples required for cryo-ET imaging (<250 nm), cryo-FIB milling of a lamella is nowadays the most popular method, with impressive successes. The alternative, cryo-ultramicrotomy [2], can provide larger surface areas and serial sections; in addition, it is devoid of ion beam damage leading to signal loss [3], and sample thickness can be tuned down to 30-50 nm, leading to a better signal-to-noise ratio, an advantage for small molecular complexes [4]. However, it is little used due to difficulty obtaining high-quality sections and inherent compression, which may complicate analyses.

This first difficulty is manifold: instabilities due to electrostatic perturbations during cutting, contamination by ice crystals, and poor adhesion to the support. Using a double manipulator [5] in a controlled dry environment ( $HR \leq 20\%$ ), which allows for pulling and collecting long (3mm) ribbons with little contamination, we tested several support films for optimal section adhesion and resistance to grid clipping required for data acquisition with high-end microscopes.

Optimizing these steps increased cryo-ET's throughput to equate with that of thin film cryo-tomography, leading reproducibly to the acquisition of several tens to hundreds of cryo-tomograms per grid. We thus reveal the complete landscape of the *Drosophila* embryo, with tomograms of diploid and polypliod nuclei, mitochondria, yolk granules, and more.

Thanks to high throughput cryo-ET of vitreous sections, we are now implementing cryo-correlative light and electron microscopy, with preliminary results of fluorescently labeled HP1 proteins targeting constitutive heterochromatin in the *Drosophila* embryonic brain.

**Mots clefs :** cryo-tomography; cryosectioning

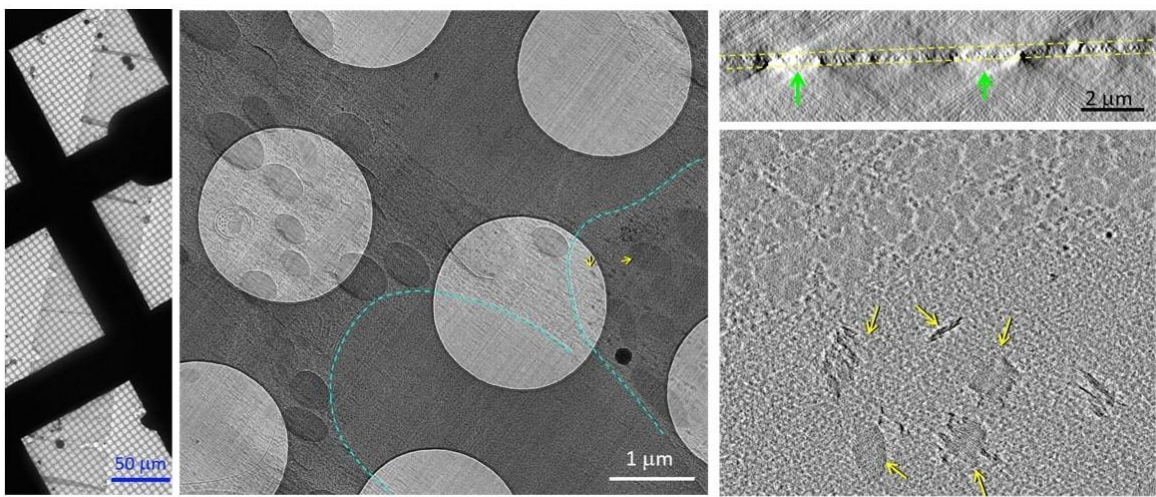


Figure 1: A. General view of a ribbon of serial cryosections. B. Detail of a cryosection of *Drosophila* embryo with many yolk granules (some are underlined in cyan dotted line). C. XZ view of a low magnification cryo-electron tomogram showing adhesion of the cryosection (dotted yellow line) on the holey film support visualized by its holes (green arrows). D. Virtual slice in a cryotomogram of a yolk granule in *Drosophila* embryo. Small crystalline inclusions are visible (yellow arrows).

**SDV3-P3****Localisation subcellulaire des N-glycoprotéines portant un noyau béta(1,2)-xylose chez la microalgue verte Chlamydomonas reinhardtii**

**Subcellular localization of N-glycoproteins bearing a core beta(1,2)-xylose in the green microalga Chlamydomonas reinhardtii**

- **Marc Ropitaux** \* (marc.ropitaux1@univ-rouen.fr) / Université de Rouen Normandie, Laboratoire GlycoMEV UR4358, SFR Normandie Végétal FED 4277, Innovation Chimie Carnot, F-76000 Rouen
- **Sophie Bernard** / Université de Rouen Normandie, Laboratoire GlycoMEV UR 4358, SFR Normandie Végétal FED 4277, Innovation Chimie Carnot, F-76000 Rouen
- **Isabelle Boulogne** / Université de Rouen Normandie, Laboratoire GlycoMEV UR 4358, SFR Normandie Végétal FED 4277, Innovation Chimie Carnot, F-76000 Rouen
- **Didier Goux** / Normandie University, UNICAEN, SFR ICORE, Plateau CMABio3, Caen, 14032
- **Jean-Claude Mollet** / Université de Rouen Normandie, Laboratoire GlycoMEV UR 4358, SFR Normandie Végétal FED 4277, Innovation Chimie Carnot, F-76000 Rouen
- **Patrice Lerouge** / Université de Rouen Normandie, Laboratoire GlycoMEV UR 4358, SFR Normandie Végétal FED 4277, Innovation Chimie Carnot, F-76000 Rouen
- **Muriel Bardor** / Université de Rouen Normandie, Laboratoire GlycoMEV UR 4358, SFR Normandie Végétal FED 4277, Innovation Chimie Carnot, F-76000 Rouen
- **Narimane Mati-Baouche** \* (narimane.mati@univ-rouen.fr) / Université de Rouen Normandie, Laboratoire GlycoMEV UR 4358, SFR Normandie Végétal FED 4277, Innovation Chimie Carnot, F-76000 Rouen

\* Auteur correspondant

The green microalgae *Chlamydomonas reinhardtii* synthesizes within the endoplasmic reticulum linear oligomannosides (Vanier et al., 2017; Lucas et al., 2018). Maturation of these oligomannosides in the Golgi apparatus results in N-glycans that are partially methylated and carry out one or two xylose residues. One xylose residue was demonstrated to be a core  $\beta$ (1,2)-xylose. Recently, the xylosyltransferase A (XTA) was demonstrated as responsible for the addition of the core  $\beta$ (1,2)-xylose (Schulze et al., 2018). Furthermore, another xylosyltransferase named XTB was reported to be also involved in the core xylosylation as well as in the addition of a second xylose residue (Lucas et al., 2020). Even if few information is available regarding the xylosylation pathway of *C. reinhardtii*, no data regarding the trafficking and subcellular localization of the N-glycosylated proteins bearing a core  $\beta$ (1,2)-xylose is available. In this work, subcellular immunolocalization of N-glycoproteins bearing the core  $\beta$ (1,2)-xylose epitope was conducted using transmission electron microscopy of wild type and IMXTAxIMXTB double mutant strains, allowing to identify specific organelles where the xylosylated glycoproteins are accumulated.

Acknowledgments: The authors thank the Region Normandie through the Normandy Plant Technologies (NPT) project (2019-2021), the GlycoMEV lab and the university of Rouen Normandie for their financial support.

**Mots clefs :** N-glycosylation, Localization, TEM, Microalgae

**SDV4-P1****AMELIORATION CONCOMITANTE DE LA RESOLUTION SPATIALE ET DE LA PRESERVATION DE L'ECHANTILLON EN UTILISANT DES STRATEGIES DE DUREE DE VIE DE FLUORESCENCE POUR L'IMAGERIE DES CELLULES VIVANTES****CONCOMITANT IMPROVEMENT OF SPATIAL RESOLUTION AND SAMPLE PRESERVATION WITH FLUORESCENCE LIFE-BASED STRATEGIES FOR LIVE-CELL IMAGING**

- **MAGALIE BENARD** \* (magalie.benard@univ-rouen.fr) / Univ Rouen Normandie, INSERM, CNRS, HeRacLeS US 51 UAR 2026, PRIMACEN, F-76000 Rouen, France
- **Damien SCHAPMAN** / Univ Rouen Normandie, INSERM, CNRS, HeRacLeS US 51 UAR 2026, PRIMACEN, F-76000 Rouen, France
- **Christophe CHAMOT** / Univ Rouen Normandie, INSERM, CNRS, HeRacLeS US 51 UAR 2026, PRIMACEN, F-76000 Rouen, France
- **Fatéméh DUBOIS** / ISTCT/CERVOxy group, CEA, CNRS, Université de Caen, CHU de Caen, GIP CYCERON, France
- **Alexis LEBON** / Univ Rouen Normandie, INSERM, CNRS, HeRacLeS US 51 UAR 2026, PRIMACEN, F-76000 Rouen, France
- **Guénaëlle LEVALLET** / ISTCT/CERVOxy group, CEA, CNRS, Université de Caen, CHU de Caen, GIP CYCERON, France
- **Hitoshi KOMURO** / Univ Rouen Normandie, INSERM, CNRS, HeRacLeS US 51 UAR 2026, PRIMACEN, F-76000 Rouen, France
- **Ludovic GALAS** / Univ Rouen Normandie, INSERM, CNRS, HeRacLeS US 51 UAR 2026, PRIMACEN, F-76000 Rouen, France

\* Auteur correspondant

Fluorescence microscopy is essential for detailed understanding of cellular processes and sample preservation is a matter of debate during live-cell imaging. Consequently, fluorescent probes for living cells, technological devices and methods for image processing should be carefully selected to obtain appropriate spectral, lifetime, spatial, and temporal resolutions notably through confocal light scanning microscopy (CLSM), fluorescence lifetime microscopy (FLIM), and STimulated-Emission Depletion (STED) nanoscopy. In this work, we firstly used spectral and lifetimes characteristics of red/near-infrared dyes to preserve living cells from visible radiation toxicity. Secondly, we combined 775 nm STED depletion laser with highly sensitive detectors (HyD), lifetime gate selection and image processing algorithms to promote high magnification/resolution images with low irradiance exposure. In these conditions, lateral resolution is improved from 492 +/- 8 nm (CLSM approach) to 259 +/- 16 nm (FLIM-STED approach) when mitochondria are observed in LBL-Dye M715-labeled living H28 cells and time-lapses can be performed due to reduction of light exposure. Thirdly, for multi-labeling experiments, we collected fluorescence signals simultaneously to limit light exposure of living cells and we analyzed fluorescence lifetimes ( $\tau$ ) through the Phasor plot to separate each dye through flexible and fast imaging. In particular, simultaneous activation of HyD detectors combined to FLIM enabled rapid acquisition and intensity overlay image of triple labeled living H28 cells after  $\tau$  separation of SPY620-DNA, SiR700-Actin and LBL-Dye M715. Therefore, combination of red/near-infrared dyes with lifetime-based strategies offers new perspectives for live-cell imaging with respect to sample preservation by reducing acquisition time and light exposure, allowing to perform long time-lapses with a minimum of stress for living cells.

Acknowledgments: This work was supported by the University of Rouen Normandy, Inserm, IRIB, Région Normandie (RIN plate-forme « 7D microscopy », RIN émergent « COMVOI »), the European Regional Development Fund (ERDF), the GIS IBiSA and the MESRI.

**Mots clefs :** FLIM; STED; living cells

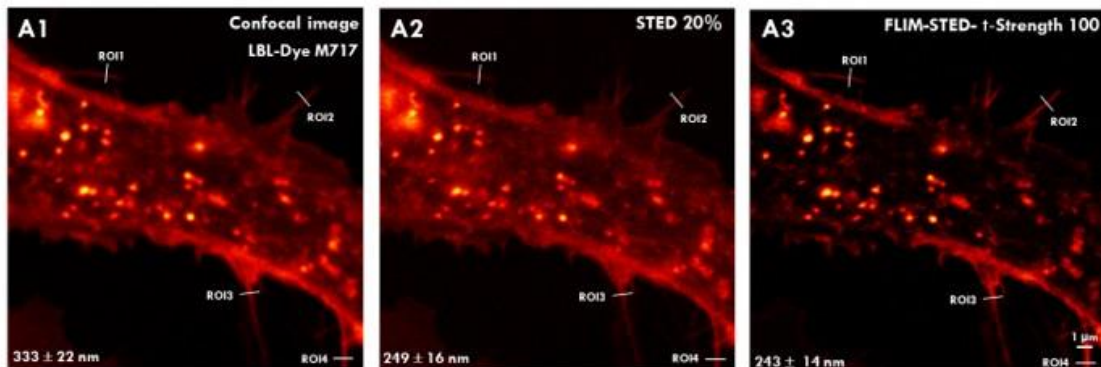


*Figure 1: FLIM-STED nanoscopy of living H28 cells labeled with LBL-Dye M717 near-infrared dyes. Confocal (A1), STED (20% 775-nm depletion laser, (A2) and FLIM-STED (A3) by using ex 690 nm, 3%, HyD-X imaging./*

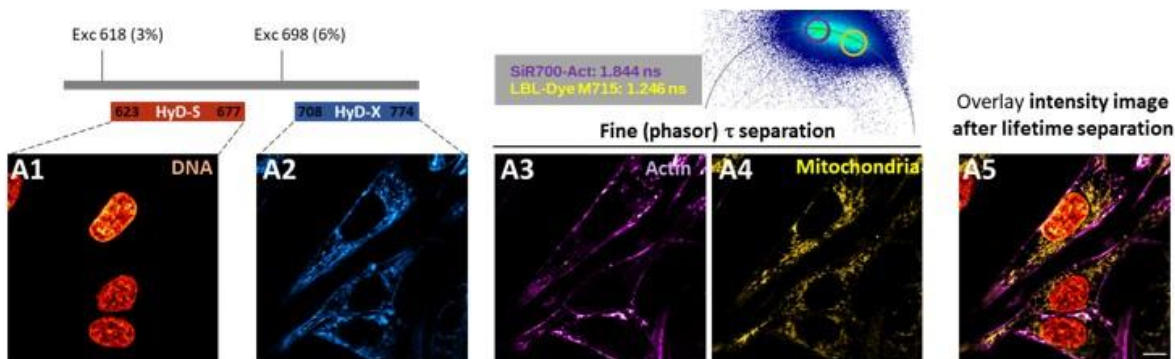


*Figure 2: Imaging of triple-stained 251 H28 cells in simultaneous mode. SPY620-DNA (ex 618 nm—HyD-S; A1) and SiR700-Actin with LBL-Dye M715 (ex 698 nm—HyD-X; A2) with fine Tau separation through phasor plot analysis after activation of FALCON module (A3–A4) and overlay of resulting imaging (A5). Low phototoxicity allowing time-lapse acquisition mode.*